

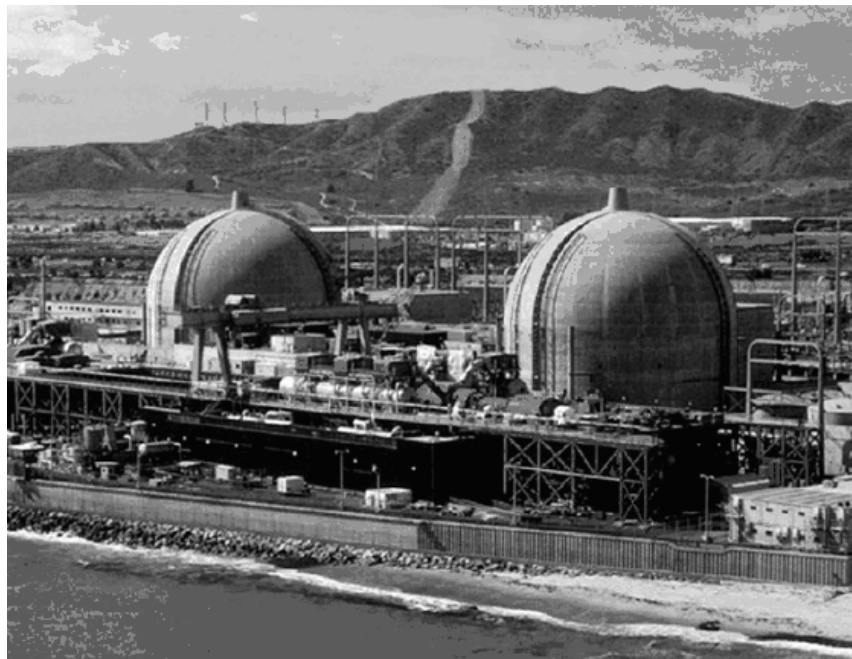
Leading the Way in Electricity



SOUTHERN CALIFORNIA
EDISON[®]

An *EDISON INTERNATIONAL*[®] Company

Southern California Edison's Evaluation of California Energy Commission AB 1632 Report Recommendations Appendices 1 through 9



February 2011

Appendix 1

**San Onofre Nuclear Generating Station 2010 Probabilistic Seismic Hazard Analysis
Report**

**SAN ONOFRE NUCLEAR GENERATING STATION
SEISMIC HAZARD ASSESSMENT PROGRAM
2010 PROBABILISTIC SEISMIC HAZARD ANALYSIS REPORT**

Prepared for
Southern California Edison

December 2010



PROBABILISTIC SEISMIC HAZARD ANALYSIS OUTLINE

1.0 INTRODUCTION

- 1.1 Purpose
- 1.2 Site Information
- 1.3 Approach
- 1.4 Acknowledgements

2.0 SEISMIC SOURCE CHARACTERIZATION

- 2.1 Strike-slip Seismic Source Characterization Model
- 2.2 Blind Thrust Seismic Source Characterization Model
- 2.3 Base-case Regional Fault Sources and Background Source Zones
- 2.4 Weighting of Alternative Models
 - 2.4.1 Discussion of Alternative Models
 - 2.4.2 Assigned Weights

3.0 PROBABILISTIC SEISMIC HAZARD ANALYSIS

- 3.1 PSHA Methodology
 - 3.1.1 General
 - 3.1.2 Attenuation Relationships
 - 3.1.3 Uncertainties
 - 3.1.3.1 GMPE Uncertainty
 - 3.1.3.2 Uncertainty Regarding Strike-Slip and Blind Thrust Sources
 - 3.1.3.3 Recurrence Relationships
- 3.2 PSHA Results
 - 3.2.1 Effects of Seismic Sources
 - 3.2.2 Deaggregation Results
 - 3.2.3 Comparison with 1995 PSHA Results

4.0 SUMMARY AND CONCLUSIONS

5.0 REFERENCES

- 5.1 Publicly Available Publications and Data
- 5.2 Personal Communication

6.0 GLOSSARY

APPENDIX A – SEISMIC SOURCE CHARACTERIZATION

APPENDIX B – 2010 PSHA GROUND MOTION CHARACTERIZATION

1.0 INTRODUCTION

1.1 Purpose

A seismic hazard analysis update was performed for the San Onofre Nuclear Generating Station (SONGS) to evaluate if the most recent or current available seismic, geologic, and ground motion information in the vicinity of SONGS has affected the seismic hazard at SONGS. The analysis specifically included the Uniform California Earthquake Rupture Forecast, Version 2 (UCERF 2) by the 2007 Working Group on California Earthquake Probabilities (WGCEP, 2008), which is the joint product of the Southern California Earthquake Center (SCEC), the California Geological Survey (CGS) and the United States Geological Survey (USGS).

1.2 Site Information

SONGS is located on the west coast of southern California in San Diego County, approximately 80 kilometers (km) northwest of the City of San Diego and 97 km southeast of Los Angeles, as seen in the map on Figure 1-1. The plant is located entirely within the Camp Pendleton Marine Corps Base (Base) near the northwest end of the Base's shoreline. Figure 1-1 also shows the general configuration of SONGS. The plant is currently operating Units 2 and 3, which, as seen on Figure 1-1, occupy about 21 hectare (ha) of the approximately 34 ha facility. The power block for both Units 2 and 3, and the station's switchyard cover about 11 ha with the remaining 10 ha providing parking, access areas, and other miscellaneous facilities.

Approximately 6 ha of SONGS, northwest of Unit 2, were previously occupied by Unit 1; the last of Unit 1 facilities was removed in 2008. This area is now called the "North Industrial Area," as shown on Figure 1-1.

1.3 Approach

This evaluation of the seismic hazard at SONGS utilizes a probabilistic seismic hazard analysis (PSHA) approach. The PSHA was used on the plant's established ground motion criteria to evaluate the implications of alternative active fault models based on the most recent or current seismic, geologic, and ground motion information in the vicinity of SONGS.

The analysis uses UCERF 2 (WGCEP, 2008), the National Seismic Hazards Mapping Program (NSHMP) (USGS, 2008), the current USGS implementation of UCERF 2 seismic source characterization (USGS, 2009, personal communication [PC]), and more recently available information regarding both the regional faults and the Newport-Inglewood/Rose Canyon (NI/RC) Fault Zone. The current USGS seismic source characterization roughly corresponds to the initial seismic source characterization used in the plant's licensing and in its two follow-on PSHAs (SCE, 1995 and 2001). These earlier seismic source characterizations and that used by the USGS (2008) lead to the conclusion that the active, right-lateral, strike-slip NI/RI Fault Zone is the largest contributor to the seismic hazard at SONGS.

A postulated active, regional low-angle thrust fault (the Oceanside Blind Thrust [OBT]) was proposed to extend beneath the coastline under SONGS and from offshore of Dana Point to the U.S./Mexican border by Rivero et al. (2000), Rivero (2004), Rivero and Shaw (2005), and Rivero and Shaw (2010, in press). The implication of this hypothesized OBT on SONGS' seismic hazard was first evaluated as part of the

SCE (2001) study through a PSHA approach using published and unpublished information available in 2001.

For this updated 2010 PSHA for SONGS, both a strike-slip end-member model, which includes the NI/RC Fault Zone source, and a blind thrust end-member model, which includes the OBT Fault source, were incorporated to reflect current alternative interpretations of the seismic source characteristics of active faults in the Inner Continental Borderland (ICB) near SONGS. For incorporation into this 2010 PSHA, a relative contribution, or relative weight, was assigned to each of these end-member models based on an assessment of the technical community's consensus on interpretation of data available in relevant publications and ongoing research.

The Next Generation Attenuation (NGA) relationships (NGA, 2008) were used in performing this PSHA. This seismic hazard evaluation was limited to annual frequencies of exceedance greater than 10^{-4} . A 10^{-4} annual frequency of exceedance is equivalent to a return period (RP) of 10,000 years. At annual frequencies of exceedance lower than 10^{-4} , some issues are to be addressed that potentially could affect the calculated seismic hazard results. These issues consist of those associated with dispersions, such as epistemic and aleatory uncertainties in seismic source characterization and ground motion characterization models including the ground motion predictive equation (GMPE) epistemic uncertainty, and those associated with nonlinear behavior of soils at the site. These issues will be addressed as part of the SONGS ongoing seismic hazard program.

In presenting the results of this SONGS seismic hazards analysis, this report is organized into six sections and two appendices.

Section 1 is this introductory section.

Section 2 describes the seismic source characterization used in this PSHA.

Section 3 presents a more detailed discussion of the methodology used in conducting the PSHA and the results of the PSHA.

Section 4 provides our conclusions regarding the SONGS seismic hazards assessment.

Section 5 lists the relevant references.

Section 6 provides a glossary.

The two appendices are:

- A. Seismic Source Characteristics, which provides a detailed summary of the currently available information regarding these seismic source characteristics including references and abstracts of the key sources of information (Attachment A-1).
- B. PSHA – Selected Issues, which provides a detailed summary of the methodology used and key issues with this current PSHA.

1.4 Acknowledgements

The overall project was sponsored by Southern California Edison (SCE). GeoPentech's effort was managed by Mr. John Barneich with the seismic source characterization work led by Mr. S. Thomas Freeman and the PSHA evaluation by Dr. Yoshi Moriwaki. Other GeoPentech team members were geoscientists Mr. Steven Duke (seismic source characterization support); Ms. Phuong Chau and Ms. Alexandra Sarmiento (geologic support); and engineers Dr. Phalkun Tan (PSHA) and Mr. Andrew Dinsick (logic tree development). Geoscientists Dr. Philip Hogan and Mr. Steven Varnell of Fugro West provided input on offshore fault characteristics from evaluations of available geophysical marine seismic surveys and other relevant sources of information. Ms. Kathryn Hanson of AMEC Geomatrix provided input, guidance, and reviews to the seismic source characterization effort, and Dr. Robert Youngs, also from AMEC Geomatrix, provided early input to the PSHA evaluation.

Mr. Freeman, Dr. Hogan, and Ms. Hanson served as a seismic source characterization integrator team in compiling the seismic source characterization models for the offshore area and ultimately developed the relative weights for these models that were used in this PSHA.

Several consultants were involved in the project, including Dr. John Shaw and Dr. Andreas Plesch of the Department of Earth and Planetary Sciences, Harvard University, who provided helpful input and reviews on the characteristics of the blind thrust fault models. Dr. Thomas Rockwell of San Diego State University contributed fault characterization input for the strike-slip fault model and provided helpful reviews. Dr. Peter Shearer and Dr. Neil Driscoll of the University of California at San Diego Scripps Institute, Dr. Lisa Grant of University of California at Irvine, and Dr. Roy Shlemon also provided timely input, guidance, and reviews on the source characterization effort.

Dr. Holly Ryan and Dr. Dan Ponti from the USGS are acknowledged for meeting with the seismic source characterization technical integrator team and sharing pre-publication data and information on the offshore faults and the onshore NI Fault, respectively, as well as providing helpful review comments.

Lastly, acknowledgement is given to the members of the Seismic Technical Advisory Board (STAB) for their comments and recommendations on the methods and presentation of this report: Dr. Clarence Allen, California Institute of Technology emeritus; Dr. Kevin Coppersmith, Coppersmith Consulting; Dr. Jan Rietman, consultant; Mr. Lloyd Cluff, consultant; Dr. Steven Day, San Diego State University; Dr. I.M. Idriss, consultant; and Dr. Norman Abrahamson, consultant.



2.0 SEISMIC SOURCE CHARACTERIZATION

Two variations have been proposed on the tectonic model explaining the crustal deformation currently occurring in the ICB offshore adjacent to SONGS.

One variation of the model, which has substantial support in the technical community (e.g., Moore, 1972; Fischer and Mills, 1991; Legg, 1991; Wright, 1991), assumes that active high-angle, right-lateral strike-slip faults, similar to what is observed on land, extend to seismogenic depth and are the primary source of large offshore earthquakes that might affect the plant. Figures 2-1a through 2c show the mapped surface traces of the active, right-lateral strike-slip faults and recorded earthquakes in the region surrounding SONGS. The closest of these right-lateral strike-slip faults to SONGS is the NI/RC Fault Zone, located 8 km offshore.

In this right-lateral strike-slip model, nearby shallow-dipping, active and non-active, normal, oblique, reverse, and thrust faults are subsidiary to the high-angle strike-slip fault (i.e., the NI/RC Fault Zone). The UCERF 2 (WGCEP, 2008) seismic source characterization model and the seismic source characterization model used in the 2008 National Seismic Hazard Mapping Program (USGS, 2008) and the current implementation of UCERF 2 by the USGS (2009, PC) are based on this strike-slip model. For this PSHA, a logic tree for the NI/RC Fault Zone was developed based on WGCEP (2008) and USGS (2008 and 2009, PC).

A brief overview of the seismic characteristics of the strike-slip dominated tectonic model used in this 2010 PSHA is provided in the following Section 2.1 with particular emphasis on the NI/RC Fault Zone, which is the closest fault source to SONGS. In addition, Dr. Tom Rockwell provides a more thorough discussion of the current understanding of the seismic characteristics of the NI/RC Fault Zone in Appendix A, Attachment A-2.

The other variation of the tectonic model was proposed by Rivero et al. (2000) in which regional blind thrust faults (reactivated Miocene detachment surfaces) also represent regional-scale active faults. These regionally extensive blind thrusts are inferred to interact at depth with high angle, strike-slip or oblique-slip faults, such as the NI/RC Fault Zone, yielding segmented fault geometries. This alternative model was further developed and described by Rivero (2004), Rivero and Shaw (2005), and Rivero and Shaw (2010, in press). Figure 2-2 provides a copy of the Community Fault Model (CFM) developed by Plesch et al. (2007), which illustrates the blind thrust faults included in this variation of the tectonic model. These postulated blind thrust fault sources were described in UCERF 2 (WGCEP, 2008) as being considered for future deformation model development, but they are not included in the current USGS source characterization model (USGS, 2009, PC).

Section 2.2 presents a brief overview of the seismic characteristics of the blind thrust variation to the tectonic model, in particular the OBT, the closest inferred blind thrust to SONGS. For this PSHA, Dr. Shaw and Dr. Plesch (2010, Appendix A, Attachment A-3) developed logic trees and segmentation models to assign seismic source characterization parameters for fault sources based on the blind thrust variations of the tectonic model as outlined by Rivero et al. (2000), Rivero (2004), Rivero and Shaw (2005), and Rivero and Shaw (2010, in press).

There are significant differences in the characterization of fault sources in the vicinity of SONGS based on these two variations of the tectonic model. As such, the alternative seismic source characterizations

that stem from these two models are considered end-member assessments, referred to as: (1) the strike-slip end-member seismic source characterization model and (2) the blind thrust end-member seismic source characterization model. Based on recent and ongoing interpretations of offshore and nearby onshore seismic and geologic data, other researchers (e.g., Grant et al., 2002; Grant and Rockwell, 2002; Grant and Shearer, 2004) have suggested modifications to the blind thrust model presented by Rivero et al. (2000) and Rivero (2004). The results of more recent studies (e.g., Ponti and Ehman, 2009; Ryan et al., 2009; Sorlien et al., 2009a; Conrad et al., 2010; Rockwell, 2010; and Rentz, 2010), which were not available or had not undergone sufficient peer-review at the time of preparing UCERF 2 (WGCEP, 2008), were incorporated in this study.

The seismic sources included in the PSHA for this current study are outlined in the following sections:

Section 2.1 provides an updated description of the NI/RC Fault Zone and its seismic source characterization parameters as part of the strike-slip end-member model.

Section 2.2 provides a summary of the seismic characterization parameters for alternative fault sources based on the blind thrust end-member seismic source characterization model.

Section 2.3 presents the time-independent seismic source characteristics of the more distant regional faults that were used in USGS (2009, PC) source characterization. These more distant faults in the region are included in both of the end-member models.

Section 2.4 provides discussions regarding the weights assigned to the two alternative end-member seismic source characterization models for incorporation in the PSHA based on information from previous studies and using more recent published and unpublished studies by other researchers in the technical community.

Summaries of the key publications and results and observations from past, recently completed, and ongoing research in the California Continental Borderland offshore SONGS that were used in this evaluation are provided in Attachment A-1 of Appendix A.

2.1 Strike-slip Seismic Source Characterization Model

In the strike-slip end-member seismic source characterization model used in this 2010 PSHA, the offshore portion of the high-angle, right-lateral NI/RC Fault Zone is the closest fault source to SONGS. The onshore NI/RC Fault Zone, including its numerous oil fields, has been extensively studied (Moody and Hill, 1956; Wilcox et al., 1973; Harding, 1973; and Yeats, 1973). These authors concluded that the subsidiary faulting is mechanically consistent with, and causally related to, dominant strike-slip faulting, and, parenthetically, the evidence is sufficiently strong that NI/RC Fault Zone has been sometimes cited as one of the classic examples of this so-called wrench tectonics mode of deformation. This theory explains and is compatible with the presence of shorter, shallower dipping, normal, and thrust subsidiary faults in a system dominated by a high-angle, through-going primary strike-slip fault.

During the 1970s, SCE, with the assistance of firms such as Fugro West, Western Geophysical, Woodward-Clyde Consultants, and other independent consultants, completed rigorous onshore and offshore investigations to evaluate the seismic source characteristics of the NI/RC Fault Zone. The conclusion from this work was that the faulting offshore of San Diego County is a continuation of the strike-slip dominated wrench faulting tectonics reflected in the northern onshore portion of the NI/RC

**SAN ONOFRE NUCLEAR GENERATING STATION
SEISMIC HAZARD ASSESSMENT PROGRAM
2010 PROBABILISTIC SEISMIC HAZARD ANALYSIS REPORT**

Fault Zone in the Los Angeles Basin. The characterization of the NI/RC Fault Zone as a strike-slip fault was the basis of deterministic ground motion analyses completed for the licensing of SONGS Units 2 and 3 and documented in the plant's Updated Final Safety Analysis Report (SCE, UFSAR). Little has changed in the geoscience community's overall understanding of the NI/RC Fault Zone's offshore characteristics since the original investigations for SCE's UFSAR. Some refinements were made in the mapped offshore traces of the fault by Fischer and Mills (1991), and slip rate estimates were improved for the on-shore portions of the NI/RC Fault Zone in Huntington Beach by Freeman et al. (1992), Law/Crandall, Inc. (1993), Grant et al. (1997), Shlemon et al. (1995), Franzen et al. (1998), and in Rose Canyon by Lindvall and Rockwell (1995). These changes in the NI/RC Fault Zone's seismic characteristics were incorporated in the source models used in the PSHAs for SONGS by SCE in 1995 and 2001, as well as in UCERF 2 (WGCEP, 2008), the NSHM (USGS, 2008), and in the current USGS implementation of UCERF 2 (2009, PC).

Further support for the strike-slip end-member model, with the high-angle NI/RC Fault Zone as the primary source fault closest to SONGS includes more recent research by Grant and Shearer (2004); Fisher (2009); Fisher et al. (2009a, 2009b); Lee et al. (2009); Ryan et al. (2009); Rockwell (2010); additional proprietary work completed offshore by Fugro West for the oil industry; and work currently underway by Dr. Dan Ponti of the USGS (Ponti, 2010, PC) along subsidiary traces of the onshore NI Fault north of Long Beach. The work completed by Ryan et al. (2009) is essentially an independent assessment of the available data reviewed during SCE's earlier work on the characteristics of the faults located offshore of SONGS, complemented by more recent seismic reflection data. Some of the proprietary marine geophysical survey data recently obtained by the USGS from WesternGeco and used by Ryan et al. (2009) was purchased by SCE years ago (Western Geophysical Company, 1972). Ryan (2010, PC) indicated that the results of the USGS independent assessment of the data are in general agreement with the results of SCE's previous investigations and analysis of the faulting offshore of SONGS.

UCERF 2 (WGCEP, 2008), the USGS (2008), and the current USGS implementation of UCERF 2 (2009, PC) characterize the NI/RC Fault Zone as a high-angle, right-lateral, strike-slip, primary seismic source, with relatively minor alternatives to its geometry onshore north of Long Beach. The map and logic tree used by the USGS (2008) for the NI/RC Fault Zone, with some minor changes to the seismic source characteristics based on USGS (2009, PC), are shown on Figures 2-3, 2-4, and 2-5. The same logic tree was utilized to represent the NI/RC seismic source model in this PSHA for SONGS.

Figures 2-3, 2-4, and 2-5 are an interpreted version of UCERF 2 (WGCEP, 2008), USGS (2008), and the current USGS implementation of UCERF 2 (2009, PC) seismic characterization of the NI/RC Fault Zone with a corresponding logic tree for that fault source. Further details regarding the earthquake recurrence model for the NI/RC Fault Zone used in this 2010 PSHA are presented in Section 3.1.3.3 of this report. Supporting the viability of the strike-slip end-member model is the possibility that the onshore and offshore segments of the NI/RC Fault Zone may be connected and capable of slipping together producing a significant magnitude earthquake. The sense of motion in the ICB offshore SONGS is dominantly NW-directed right-lateral shear at about 6 millimeters per year (mm/yr) based on recent global positioning system (GPS) data (Appendix A, Figure A-3), as discussed in more detail in Section 2.4. The dominance of right-lateral shear in the ICB has been in existence over the past approximately 20 Million Years (Ma) (Nicholson et al., 1994) as evidenced by the 250 km of strike-slip offsets of the Eocene Poway conglomerates from San Diego to the west end of the Channel Islands (Kies and Abbott, 1983; and Rockwell, 2010, PC). The initiation of this offset predates the inception of the San Andreas Fault (~5 Ma; Atwater, 1998). Furthermore, considering the kinematic motions in northern Baja

California, which projects into to ICB, there currently should be a small component of divergence in the Borderland offshore San Diego (Rockwell, 2010, PC). Observations of marine terraces along the coast of San Diego County and northern Baja California indicate that the uplift along this portion of the coast (~ 0.13 mm/yr) is regional in character, evenly distributed, and most likely driven by rift-shoulder uplift caused by the spreading of the Gulf of California (Mueller et al., 2009; and Rockwell, 2010, PC). This interpretation as to the cause of the evenly distributed, regionally persistent, uplifted terraces along the San Diego County/northern Baja California coast is further supported by the lack of folding in the Tertiary rocks beneath the terraces, except locally at the steps and bends in the strike-slip fault systems, such as the NI/RC Fault Zone through San Diego County and the Agua Blanca Fault in northern Baja California (Rockwell, 2010, PC).

Attachment A-2 of Appendix A presents Dr. Tom Rockwell's summary of current information concerning the NI/RC Fault Zone. This and other information form the basis for the weighting of the strike-slip end-member seismic source characterization model used in this study as discussed below in Section 2.4.

2.2 Blind Thrust Seismic Source Characterization Model

Reactivated Miocene detachment surfaces are the key elements of this blind thrust seismic source characterization model with the OBT being closest to SONGS. The OBT Fault was first proposed by Rivero et al. (2000) as an alternative primary active fault that could explain some of the deformation in the ICB region commonly associated with the strike-slip NI/RC Fault Zone. Rivero (2004) completed further assessments of the blind thrust fault systems (including the OBT and Thirtymile Bank Thrust Fault, TMBT) in his Ph.D. research, which was supervised by Professor John Shaw at Harvard University. Rivero et al. (2000), Rivero (2004), Rivero and Shaw (2005), and Rivero and Shaw (2010, in press) provide overviews of the evidence for active folding and blind-thrust faults induced by basin inversion processes in the southern ICB region and characterization of the OBT and TMBT as active fault sources. The OBT and TMBT are included in the CFM, developed by Dr. Andreas Plesch (a Research Associate at Harvard University) (Plesch et al., 2007). However, as noted above, the hypothesized active OBT and TMBT faults are not presently included as fault sources in UCERF 2 (WGCEP, 2008) or the USGS current implementation of UCERF 2 (2009, PC) seismic source characterization model. A focused summary of the seismic source characteristics of these postulated blind thrust fault sources and alternative models to explain the structural relationships among the active blind thrusts and strike-slip faults in the ICB region was prepared for SCE by Drs. Shaw and Plesch (2010, Appendix A, Attachment A-3), to reflect their current interpretation of the fault sources in the vicinity of SONGS.

The basis behind the OBT Fault model is Rivero's interpretation of paper copies of 1980s vintage oil industry digital deep-penetration 2D marine seismic reflection records (see Figures 2-6 and 2-7). Many of these records were proprietary at the time of Rivero's analyses, but have subsequently been released to the public and are being currently used by other researchers (e.g., Sorlien et al., 2009b and Ryan, 2010, PC).

Rivero et al. (2000) and Rivero (2004) formulated the models and sub-models presented on Figures 2-8, 2-9, and 2-10 and in Attachment A-3 of Appendix A based on the following:

- Based on balanced and restored cross-sections of the seismic reflection data, the recognition that compression has resulted in significant shortening of Plio-Pleistocene sediments into folds and faults;

- The 1986 Oceanside and Coronado Bank earthquake sequences;
- Regional uplift as evidenced by elevated onshore marine terraces; and
- To a very limited extent, GPS data.

Utilizing this data, Shaw and Plesch characterized the blind thrust fault sources (i.e., the OBT and TMBT) and their associated hanging wall and footwall subsidiary faults. Possible structural scenarios that represent potential interactions between the steeply-dipping strike-slip faults and the low-angle blind thrust fault sources are outlined in Figure A3-2A. Steeply-dipping, right-lateral strike-slip faults, such as the NI and RC, are incorporated into the blind thrust seismic source characterization model by Rivero (2004) and Rivero and Shaw (2010, in press). Preferred models for the interaction of these faults suggest that the strike-slip faults are segmented and offset at depth under the argument that continuous, through-going, strike-slip faults, as primary fault sources, are not kinematically compatible with the large amount of shortening documented on the OBT fault.

Shaw and Plesch (2010, Appendix A, Attachment A-3) qualitatively assigned weights to the four alternative models as shown on Figure 2-9 based on their observations and confidence in the available data. Utilizing the information developed by Rivero (2004), Rivero and Shaw (2005), and Rivero and Shaw (2010, in press), Shaw and Plesch (2010, Appendix A, Attachment A-3) developed the simplified rupture segmentation models as depicted on Figure 2-11 and depicted in the logic tree shown on Figure 2-12.

The map on Figure 2-11 and the logic tree on Figure 2-12 reflect the complex alternatives of the OBT Fault as the closest hypothesized fault to SONGS in the blind thrust fault end-member model. All of the alternative geometries of the OBT Fault with their single and combined segment rupture possibilities are addressed in this logic tree. The earthquake recurrence rates for these alternatives were calculated using the identified slip rates on Figure 2-12, and are discussed further in Section 3.1.3.3. Refer to the complete discussion by Shaw and Plesch (2010) in Appendix A, Attachment A-3 for additional details.

2.3 Base-case Regional Fault Sources and Background Source Zones

The more distant (with respect to SONGS) regional faults and background source zones used in the strike-slip and blind thrust end-member seismic source characterization models used in this 2010 PSHA are referred to as the base-case model. These base-case regional fault sources are shown on Figure 2-3 and their closest distances from the plant are listed in Table 2-1. The information presented in Table 2-1 is based on the time-independent characteristics of these seismic source faults used in the current implementation of UCERF 2 model provided by the USGS (2009, PC). Table 2-1 also lists non-designated faults (i.e., faults not presently included as seismic sources, but faults that WGCEP [2008] targeted for future consideration).

The use of time-independent characterization of seismic source faults in the PSHA for SONGS is justified by the observations that the seismic sources amenable to time-dependent modeling (such as the San Andreas Fault) are distant sources that are not the controlling sources for seismic hazard at SONGS, and there are uncertainties involved in evaluating time-dependency.

Following UCERF 2 (WGCEP, 2008), the seismic sources provided by the USGS (2009, PC) are designated as either a Type-A fault, a Type-B fault, or a Type-C zone, depending on the level of knowledge tied to

the specific seismic source. Type-A faults have known slip rates and paleoseismic recurrence interval estimates; Type-B faults have observed slip rates; and Type-C zones are areas of crustal shear that lack sufficient detailed knowledge to apportion slip onto specific faults. In southern California, Type-A faults include the San Andreas, San Jacinto, Elsinore, and Garlock faults. All other fault sources in southern California represented by the USGS (2009, PC) and used in this SONGS PSHA are designated Type-B faults. The Type-C zones in southern California include the Mojave or Eastern California shear zone, the San Gorgonio zone or “knot,” and the Brawley zone, or Imperial Valley zone (WGCEP, 2008; USGS, 2008). Figures 2-5 and 2-12 provide the key source characterization parameters for regional fault sources included in the SONGS PSHA. At a distance of about 38 km to the northeast, the Elsinore Fault is the Type-A designated fault closest to SONGS. The closest Type-B designated fault is the NI/RC Fault Zone, which lies about 8 km offshore to the west of SONGS. The characterization of the NI/RC Fault Zone source as a primary strike-slip fault end-member model is described in Section 2.1. Alternative geometries and slip rate estimates for the NI/RC Fault Zone source based on the blind thrust fault end-member model are presented in Section 2.2.

The next closest Type-B designated fault in UCERF 2 (WGCEP, 2008) is the Palos Verdes/Coronado Bank Fault, which is about 32 km west of SONGS. The San Diego Trough and San Clemente Faults, which lie at closest distances of 46 km and 94 km, respectively, are not presently characterized as fault sources by the USGS (2009, PC). The potential contribution of these faults to the seismic shaking hazard along the onshore portions of southern California, including SONGS, is judged to be negligible for several reasons including, but not exclusively, their location farther offshore, as shown on Figure 2-3, and their relatively low slip rates. These faults were included as fault sources in the SCE (1995, 2001) PSHA, and the results of these studies showed that neither the San Diego Trough nor San Clemente faults contribute significantly to the hazard at SONGS; thus these faults are not included in the PSHA for this study.

Of the three Type-C zones in southern California, the Eastern California Shear zone and Brawley zone are not significant contributors to the SONGS PSHA, due to their distances from SONGS (greater than 100 km), and thus were not included in the PSHA for this study. The San Gorgonio Type-C zone through Banning Pass, as shown on Figure 2-1b, is incorporated in the USGS (2009, PC) characterization as shown on Figure 2-3, as a low slip rate segment of the San Andreas Fault; this approach was followed in this PSHA.

The more distant regional faults listed in Table 2-1a, are included in both end-member seismic source characterization models for this PSHA. In the strike-slip end-member seismic source characterization model, the NI/RC Fault Zone, as characterized by UCERF 2 and USGS (2009, PC), is used; in the blind thrust end-member seismic source characterization model, the OBT and alternative characterizations of the NI and RC faults as defined by Shaw and Plesch (2010, Appendix A, Attachment A-3) are used.

In both end-member seismic source characterization models, the current SONGS PSHA incorporates a background seismicity zone(s) to account for additional seismicity not modeled by the seismic source faults using procedures similar to UCERF 2 (WGCEP, 2008) and the USGS’ current implementation of UCERF 2 (2009, PC).

2.4 Weighting of Alternative Models

Figures 2-1b, 2-2, 2-3, 2-6, and 2-8 in this report, and Figures A-7a through A-7f and A-17 in the accompanying Appendix A, present maps of the more recent alternative interpretations of the faulting in the ICB offshore of SONGS, as discussed above and in Appendix A. Figure 13a shows the nearby

location of the marine seismic reflection geophysical survey records that follow in Figures 13b through 13h. These geophysical records were used, in part, by Ryan et al. (2009), Sorlien et al. (2009b), and Rivero and Shaw (2010, in press) in their interpretations of the faulting offshore of SONGS. This sequence of figures is used to illustrate the similarity in these geophysical records and to illustrate the similarities and differences in these different researcher's interpretations of these records. This was accomplished by superimposing Ryan et al. (2009) and Rivero and Shaw (2010, in press) records over the Sorlien et al. (2009b) record, in both opaque and transparent overlays.

Generally, this exercise demonstrates that these different researchers are observing essentially the same geophysical record, but offer different interpretations as to what these records illustrate in regard to the location, geometry, and style of faulting in this area. Figure 14 is a consolidated sketch of the interpreted geophysical records based on Ryan et al. (2009), Sorlien et al. (2009b), and Rivero and Shaw (2010, in press). This sketch, and the following simplified sketches in Figure 15 of the two end-member fault models, illustrates the uncertainties in the different interpretations of these marine geophysical records. First, it is unclear how the principal faults interact with each other at depths greater than approximately 4 km. This uncertainty results in the question as to whether the blind thrust end-member model or the strike-slip end-member model is the primary nearby fault source to SONGS. Second, the apparent vertical displacement of the geophysical marker horizons across the inferred faults on these records may not reflect the actual slip and resulting slip rate across the faults in either of the two end-member models. For example, the apparent displacements of geophysical marker horizons inferred to be the top of the Pliocene, Pico or Repetto formations or the top of the basement rocks, across apparent faults, such as the San Mateo Thrust (SMT) Fault, may not reflect the amount of lateral displacement and thus not entirely representing the total amount and direction of slip across the fault. Further, in the area offshore of SONGS, the range in depth and age estimates placed on geophysical marker horizons, such as these, remains broad. This introduces uncertainty in estimates of the level of activity and slip rates on these faults based solely on the geophysical records, particularly uncertainty in the late Quaternary level of activity on these faults. This limitation in the geophysical survey records results in the need for a careful assessment of all available relevant information and the development of reasonable weightings, based on that information, as to which end-member fault model is the more likely the case driving the PSHA for SONGS.

2.4.1 Discussion of Alternative Models

The weights assigned to the two end-member alternative models for potential fault sources that pose the most significant seismic hazard to SONGS (i.e., the OBT and the NI/RC models) are based on available relevant evidence and information regarding their seismogenic potential. The data include their geometry and level of activity, as well as geologic and geodetic evidence that pertains to the style and rate of crustal deformation occurring in the present tectonic environment. The references utilized in this weighting assessment are summarized in Attachment A-1 of Appendix A.

The evidence supporting both the reactivation of parts of the Oceanside detachment (i.e., compressional folding and thrust/reverse faulting) and high-angle, right-lateral strike-slip along the NI/RC Fault Zone is generally unequivocal in the technical community. There is general agreement that detachment faults are present in eastern California, the Transverse Ranges, and portions of the Los Angeles Basin, and ICB. Fisher et al. (2009a) summarize the technical community's current understanding of the paleotectonics of southern California's Continental Borderland, stating: "A significant complication for hazards research is that during late Mesozoic and Cenozoic time, three

**SAN ONOFRE NUCLEAR GENERATING STATION
SEISMIC HAZARD ASSESSMENT PROGRAM
2010 PROBABILISTIC SEISMIC HAZARD ANALYSIS REPORT**

successive tectonic episodes affected this plate-boundary zone. Each episode imposed its unique structural imprint such that early-formed structures controlled, or at least influenced, the location and development of later ones.” Each episode was driven by changes in tectonic plate motion. During the first episode, in the Mesozoic, thrust faults developed in an accretionary wedge above an east-directed subduction zone. The second episode, during the Miocene, was transtensional in nature, resulting in the development of extensional detachment and normal faults concurrently with rotation and northward translation of the Western Transverse Ranges. The third episode, in Pliocene through Holocene time, was primarily transpressional, resulting in structural inversion of some of the Miocene normal faults as oblique reverse/strike-slip faults, and localized re-activation of low-angle detachment faults as thrust faults.

There is no direct evidence that clearly demonstrates that the Miocene detachment faults have been reactivated as blind thrust faults on a regional scale off of the San Diego County coast. At this time, based on more recent re-evaluations of existing data and more recently collected data, the specific characteristics and the seismogenic potential of these Miocene detachment faults remain in discussion. This led to conservatively considering both end-member seismic source characterization models as contributing to the ground motion hazard at SONGS rather than limiting the evaluation to a single dominate model. In accordance with Senior Seismic Hazard Analysis Committee (SSHAC) guidelines (Budnitz et al., 1997), the weighting of these two end-member seismic source models (i.e., dominated by the high-angle, strike-slip NI/RC or the low-angle OBT) is based on an assessment of the extent of the evidence supporting the respective interpretations and the current understanding of the technical community’s judgment regarding the tectonic setting of the region.

A low-angle detachment fault is visible in the marine seismic reflection records and has been recognized by the technical community as an east-northeast-dipping geologic structure beneath the ICB west of the mapped traces of the NI-RC Fault Zone (Bohannon and Geist, 1998; Crouch and Suppe, 1993; Ryan et al., 2009; Sorlien et al., 2009a, 2009b). Some geoscientists have interpreted this fault as having been reactivated on a regional scale in Pliocene through Holocene time as the OBT (Rivero 2004; Shaw and Plesch, 2010, Appendix A, Attachment A-3). However, their research by itself does not entirely resolve discrepancies between the strike-slip and blind thrust end-member models. The structural interaction of the detachment and high-angle faults cannot be resolved based on currently available marine seismic reflection records. More recent marine seismic reflection, coastal geomorphic, paleoseismic, and seismological research, previously not available to Rivero et al. (2000) and Rivero (2004), offer alternative interpretations of the lateral and down-dip extent of the OBT. Further, although the marine seismic reflection data supports Miocene extensional detachments and localized Pliocene through Holocene compressional activity, there is no direct evidence that clearly demonstrates Pleistocene or Holocene activity on the OBT as a major regional through-going thrust fault. Appropriate weight is given in this PSHA to the possibility that the OBT may be a capable seismic source based on the following data, observations, and interpretations:

- The wedge/thrust model developed by Rivero et al. (2000), Rivero and Shaw (2001), and Rivero (2004) to explain fold deformation along southern California’s offshore region is based on a systematic analysis and review of an extensive set of seismic data.
- This model provides an alternative explanation of the apparent discontinuity of post-Upper Miocene faulting in this region and explains the significant amounts of Pliocene and post-Pliocene crustal shortening exhibited by the folded strata at and seaward of the shelf break.

- Available seismic reflection data cannot resolve whether the high-angle, strike-slip faults along the NI/RC Fault Zone displace the postulated OBT.

The activity and seismogenic potential of the OBT, however, is not definitive. The evidence cited by Rivero et al. (2000), Rivero and Shaw (2001), and Rivero (2004) is based on their interpretation of:

- Geophysical evidence of post-Pliocene folding and faulting in the offshore region;
- A structural relationship between the San Joaquin Hills and a similar wedge/thrust structure in the offshore;
- Association of the 1986 Oceanside earthquake with a component of the ICB thrust belt system (the Thirtymile Bank blind thrust);
- Regional coastal uplift; and
- Geodetic measurement of contractional crustal strain.

Each of these items of evidence may have some viability for indicating the seismogenic capacity of the OBT, but, as noted below, they are also consistent with a predominantly strike-slip regime.

A stronger case is made in support of the model that characterizes the NI/RC Fault Zone as part of a system of through-going strike-slip faults. The primary data, observations, and interpretations supporting a higher weight given to the strike-slip model are:

- The dominance of strike-slip motions that has occurred on the faults in ICB since the Eocene.
- Marine 2D seismic reflection geophysical records, similar and in some cases the same as those used by Rivero et al. (2000) and by Rivero (2004), led to alternate interpretations by Moore (1972), Western Geophysical (1972), Fischer and Mills (1991), Sliter et al. (2001), Crouch and Suppe (1993), and more recently Legg et al. (2007), Ryan et al. (2009), Sorlien et al. (2009b), and Ryan (2010, PC) as to the relatively continuous zone of recently active en echelon fault traces offshore of southern Orange County and San Diego County linking the onshore traces of the NI Fault and RC Fault, and alternate configurations of the faults further offshore to the west.
- Evidence to support reactivation of the entire OBT in the current tectonic environment is not conclusive. Recent re-analysis of available deep seismic reflection data acquired in the 1970s (Ryan et al., 2009; Sorlien et al., 2009b) provides alternative interpretations that the OBT is not a continuous active tectonic structure, but is composed of smaller, separate segments, not all of which are active.
- Alternatively, late Pleistocene/Holocene faults and associated folding used to support the regionally continuous blind thrust model can also be explained by strain partitioning and contraction in the right-lateral NI/RC Fault Zone, in particular at en echelon left steps or bends in the fault trace. In addition, some compressional elements apparent in the available marine seismic reflection records may be relics of earlier Pliocene compression. Further, local apparent compressional folds and/or discontinuities evident in these marine seismic reflection records

also may be due to translation of sediments over inherited basement protrusions, as suggested by Wright (1991).

- Clockwise rotation of crustal blocks in the ICB, which was postulated in SCE (2001), has been emphasized by Ryan et al. (2009). Rotation of a large crustal block would be consistent with the local reactivation of northern portions of the OBT (i.e., late Quaternary compression on subsidiary reverse faults beneath the continental slope offshore of San Mateo Point west of the NI/RC Fault Zone), but would not require reactivation or rupture of the entire length or depth of the detachment. Late Quaternary inactivity of the OBT further south offshore of Carlsbad and extensional subsidiary fault activity on continental slopes west of the NI/RC between Carlsbad and La Jolla, as suggested by Sorlien et al. (2009b), are consistent with this block rotation model. Geodetic data on the neighboring Peninsula Range block shows similar clockwise rotation as detailed in Appendix A.
- Based on their analysis of the tectonics surrounding the Agua Blanca Fault in Baja California, Wetmore et al. (2010, in review) document evidence that the Agua Blanca Fault becomes transtensive as it transitions offshore into the Borderland. This interpretation is consistent with a current tectonic environment of transtension in the Borderlands offshore of southern California, and suggests that the current kinematic framework offshore is principally transtensional in nature. They state that "Major late Miocene normal faults form an important kinematic component of deformation in the southern half of the central domain, but extreme crustal thinning is partially compensated by north-south shortening associated with detachment folds and conjugate-slip faults." This suggests that the regionally extensive thrust faults in the southern portions of the Peninsular Ranges and the ICB inferred by Rivero et al (2000) may be inherited from the Pliocene before development of the through-going strike-slip faults of the Peninsular Ranges, such as the San Jacinto, Elsinore and NI/RC faults. However, the presence of local compressional folds and faults is not precluded (Rockwell, 2010, PC).
- Seismicity data show that the NI and RC faults are capable strike-slip faults (Hauksson, 1987; Hauksson and Gross, 1991; Astiz and Shearer, 2000; and Grant and Shearer, 2004). Based on discussions with Dr. Ryan of the USGS (2010, PC) regarding her recent assessment of high-resolution seismic reflection data (Conrad et al., 2010) and refined epicenter locations/focal mechanism analyses by Astiz and Shearer (2000), an alternate interpretation for the source behind the thrust mechanism of the 1986 Oceanside earthquake is strain partitioning and contraction in the a left-step in the right-lateral strike-slip San Diego Trough Fault. This interpretation further indicates that strike-slip faults extend to seismogenic depths and are the major seismic source faults in the ICB.
- Paleoseismic data demonstrates that the onshore NI and RC faults are strike-slip faults (Rockwell et al., 1991, 1992; Ponti and Ehman, 2009; Ponti, 2010, PC; and Rockwell, 2010, PC). A dominate long and continuous primary thrust fault between these two northern and southern right-lateral fault sections appears inconsistent with the current dominate tectonic framework of the Peninsular Ranges and the ICB, however, the local presence of blind thrust faults cannot be refuted.
- Regional coastal uplift, which is cited by Rivero et al. (2000) to indicate that the Oceanside and Thirtymile Bank thrusts are active over a region larger than the San Joaquin Hills (Grant et al.,

1999 and 2002) or Mount Soledad, (Rockwell, 2010) may be attributed to a large degree to other processes (e.g., rift shoulder thermal isostasy). Studies by Mueller et al. (2009) suggest that the uniform regional uplift observed in southern California may reflect the far-field effect of unloading and rift shoulder development associated with lithospheric thinning in the northern Gulf of California and the Salton Trough.

- There is no marked change in the pattern of coastal uplift across the segmentation boundary between the more shallow dipping northern OBT and the steeper dipping southern OBT as proposed by Rivero (2004), Rivero and Shaw (2010, in press), and Shaw and Plesch (2010, Appendix A, Attachment A-3). This suggests that either the coastal uplift is not directly linked to slip on the OBT, or the southern segment has a lower slip rate. Dr. T. Rockwell notes that there is no evidence for tilting or significant differential uplift along the coast as recorded by the Quaternary marine terraces and underlying Tertiary bedrock (Kern and Rockwell, 1992; Rockwell, 2001, PC and 2010, PC).
- The initiation of structural inversion and thrust faulting in the offshore, which is inferred to have begun in the Pliocene (Crouch and Suppe, 1993; Rivero et al., 2000; and Rivero and Shaw, 2001; Rivero, 2004; Rivero and Shaw, 2010, in press; and Shaw and Plesch, 2010, Appendix A, Attachment A-3), may significantly predate the initiation of coastal uplift as noted above. This suggests that coastal uplift is not directly linked with movement on the ICB thrust system. However, age estimates and correlation of stratigraphy across the fold belts in the offshore are not well constrained due to the paucity of offshore well control. Consequently, the initiation of folding could have been later than previously estimated.
- Geodetic data, as presented in Appendix A, shows that strain in the southern ICB is dominated by northwest directed shear subparallel to the overall North American/Pacific plate motion. Little or no convergence across the ICB normal to the plate boundary is observed in the vicinity of SONGS as detailed in Appendix A. In particular, the lack of significant convergence in the regional signal to the east of the OBT suggests there is not a regional “driving” force that would reactivate a through going seismogenic thrust (SCE, 2001).
- Some of the contractional deformation observed in the ICB could have occurred during the Pliocene or early Quaternary within a different stress regime. Based on geologic evidence that suggests coastal uplift in the San Diego region, as well as activity on the Elsinore Fault, was initiated approximately 0.9 to 1.0 Ma, Dr. Rockwell (2001, PC and 2010, PC) suggests that a reorientation of the plate vector may have occurred in the region during early to middle Quaternary. Dr. Ponti (2001 and 2010, PC) also suggests a change in the tectonic stress regime in that same time frame based on evidence for decreasing Late Quaternary slip rates compared to longer-term rates for some blind thrusts in the Los Angeles basin (e.g., the Compton-Los Alamitos and Las Cienegas faults).

2.4.2 Assigned Weights

Based on these observations and qualitative judgments, weights were assigned to the two alternative end-member seismic source fault characterization models by the seismic source characterization integrator team. The weights assigned reflect the team’s professional geoscience judgment as to the extent to which each end-member source fault model would find support from the currently available scientific evidence and best fit the engineering and scientific technical community’s current

**SAN ONOFRE NUCLEAR GENERATING STATION
SEISMIC HAZARD ASSESSMENT PROGRAM
2010 PROBABILISTIC SEISMIC HAZARD ANALYSIS REPORT**

understanding of the tectonic environment surrounding southern California, including SONGS. A 90% weight was assigned by two of the team members and a 85% weight was assigned by the third member to the strike-slip seismic source characterization model, which includes the through-going high-angle, right-lateral strike-slip, NI/RC Fault Zone as the nearest primary active fault system in the ICB offshore of SONGS. The blind thrust seismic source characterization model, which includes the postulated, regionally extensive OBT as the nearest primary fault system in the ICB offshore of SONGS, was assigned the remaining weight of 10 or 15%, respectively. For use in the 2010 PSHA, the weights assigned by the seismic source integrator team were numerically equal to 88% for the strike-slip end-member model and 12% for the blind thrust end-member model.

This weighting is supported by the following key points. First, there is little empirical evidence available to support that oblique slip with the ratio of strike-slip to dip-slip suggested by the available information regarding the OBT would occur on a fault plane dipping between 14 and 24 degrees. Second, recent assessments of offshore earthquakes relative to new mapped fault locations and geometry raise questions as to whether thrust focal mechanisms from recent earthquakes are tied to regionally persistent blind thrust faults or are generated by more local subsidiary blind thrust faults driven by strain partitioning in contractional left-steps or bends in the more dominate right-lateral strike-slip fault system. Finally, more current GPS records do not support a regionally persistent blind thrust model that would extend the full distance of the San Diego County coast line. Locally, there does appear to be indications of reactivation of low-angle Miocene detachment surfaces as thrust faults since late Pliocene time, but in the present tectonic environment, these thrust faults do not appear to make up a continuous, active tectonic structure on a regional scale.



**SAN ONOFRE NUCLEAR GENERATING STATION
SEISMIC HAZARD ASSESSMENT PROGRAM
2010 PROBABILISTIC SEISMIC HAZARD ANALYSIS REPORT**

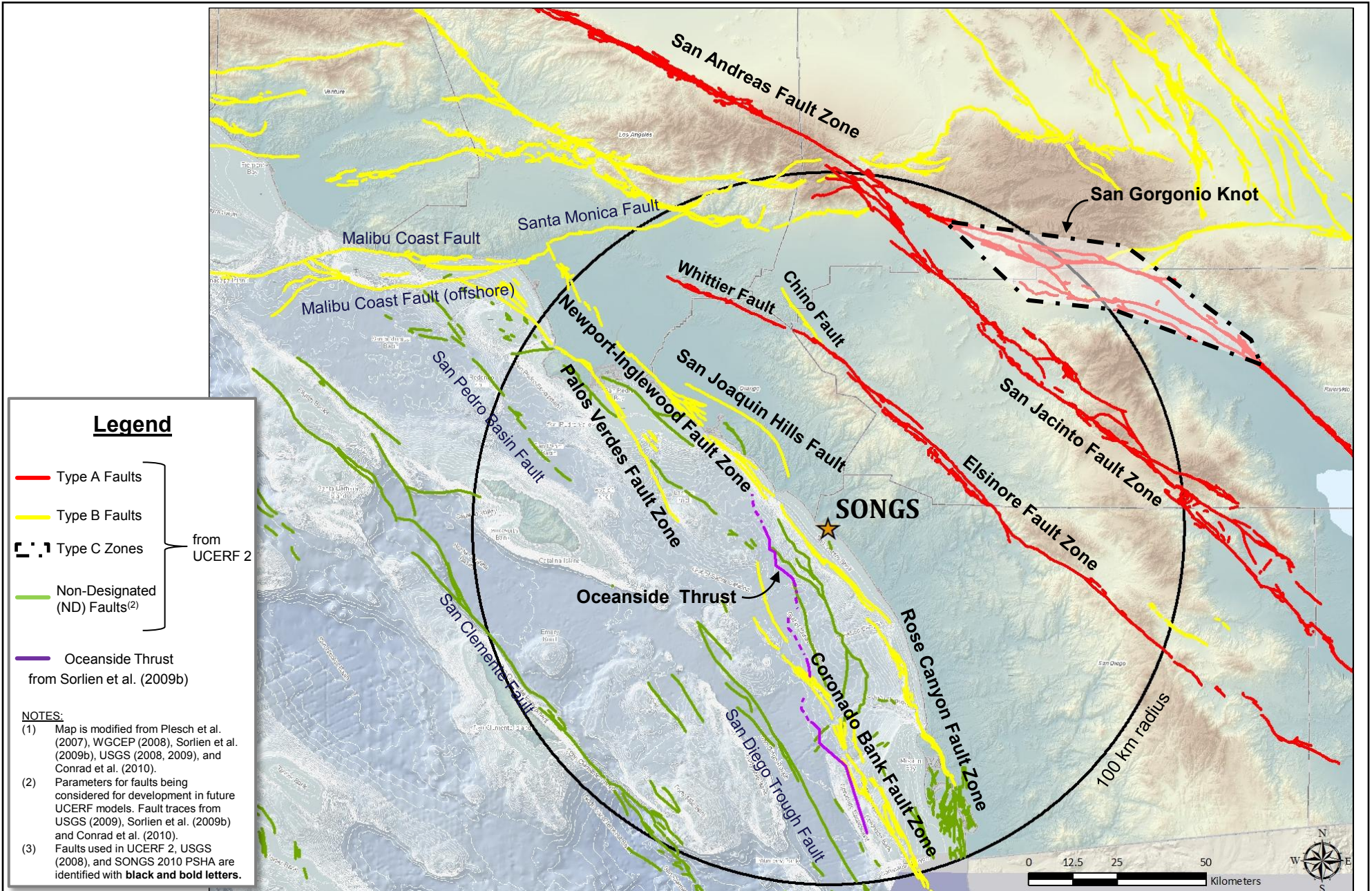
Table 2-1a: Type-A Faults and Type-B Faults

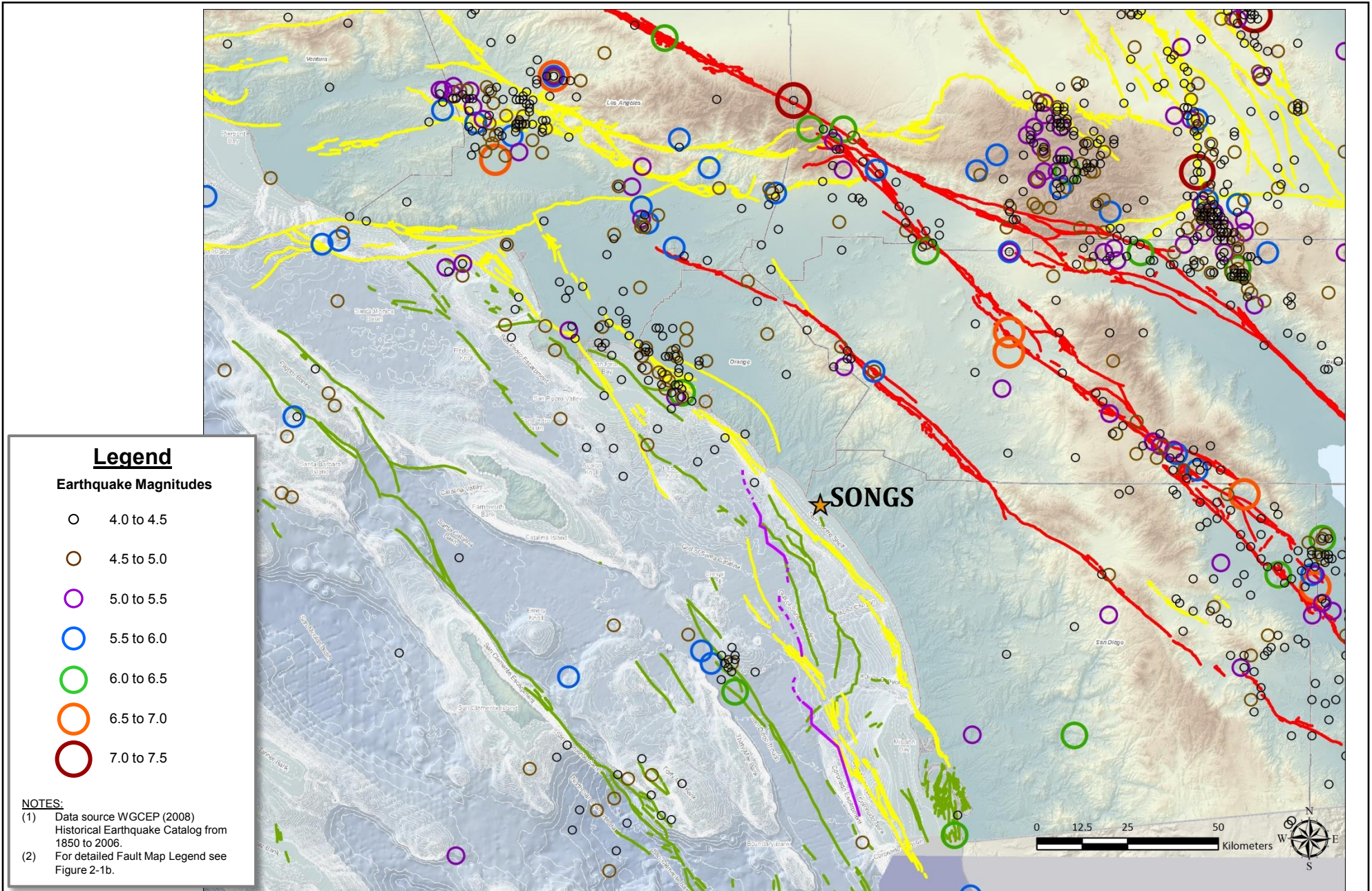
	Fault Name	Closest Distance from SONGS to Rupture Plane Rrup (km) ⁽⁵⁾
Type-A Faults⁽¹⁾	San Andreas ⁽³⁾	92
	San Jacinto ⁽³⁾	70
	Elsinore ⁽³⁾	38
Type-B Faults⁽¹⁾	Newport-Inglewood/Rose Canyon (NI/RC) ⁽³⁾	8
	Palos Verdes/Coronado Bank ⁽³⁾	32

Table 2-1b: Non-Designated Faults

	Fault Name	Closest Distance from SONGS to Rupture Plane Rrup (km) ⁽⁵⁾
Non-Designated Faults⁽²⁾	Oceanside Blind Thrust (OBT) ⁽⁴⁾	7
	San Diego Trough	46
	San Clemente	94

- (1) "Type" designated fault; parameters for fault listed in Table 1 of Appendix A in UCERF 2 and used in the current USGS implementation of UCERF 2 (2009, PC) and in this PSHA.
- (2) Non-designated fault; parameters for fault being considered for development by WGCEP (2008) as presented in Table 2 of Appendix A in UCERF 2.
- (3) Relevant faults models by the current USGS implementation of UCERF 2 (2009, PC) and used in this PSHA.
- (4) OBT Fault as hypothesized by Rivero et al. (2000) and Rivero (2004).
- (5) Distances taken from Figure 2-3.





Legend

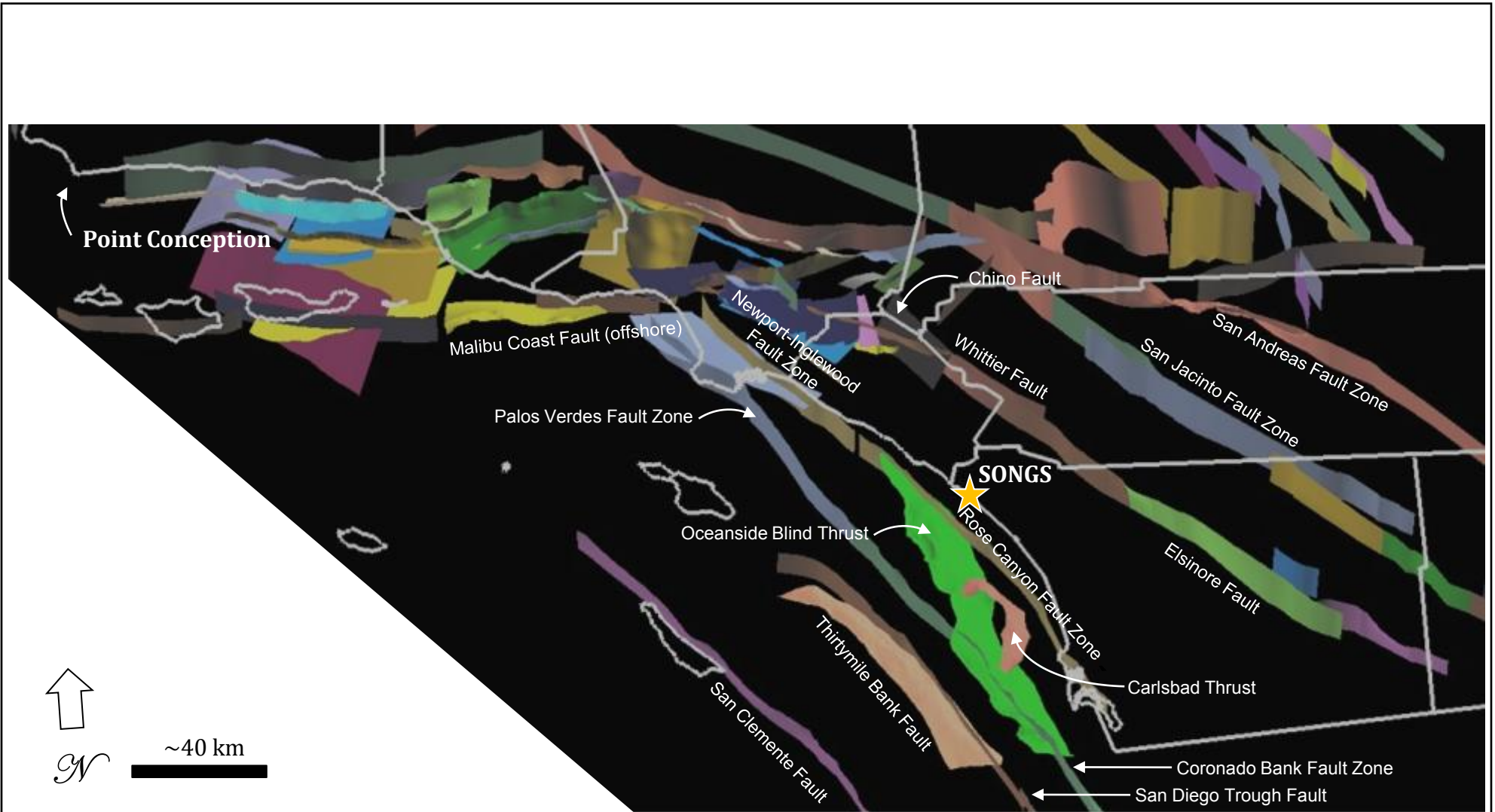
Earthquake Magnitudes

- 4.0 to 4.5
- 4.5 to 5.0
- 5.0 to 5.5
- 5.5 to 6.0
- 6.0 to 6.5
- 6.5 to 7.0
- 7.0 to 7.5

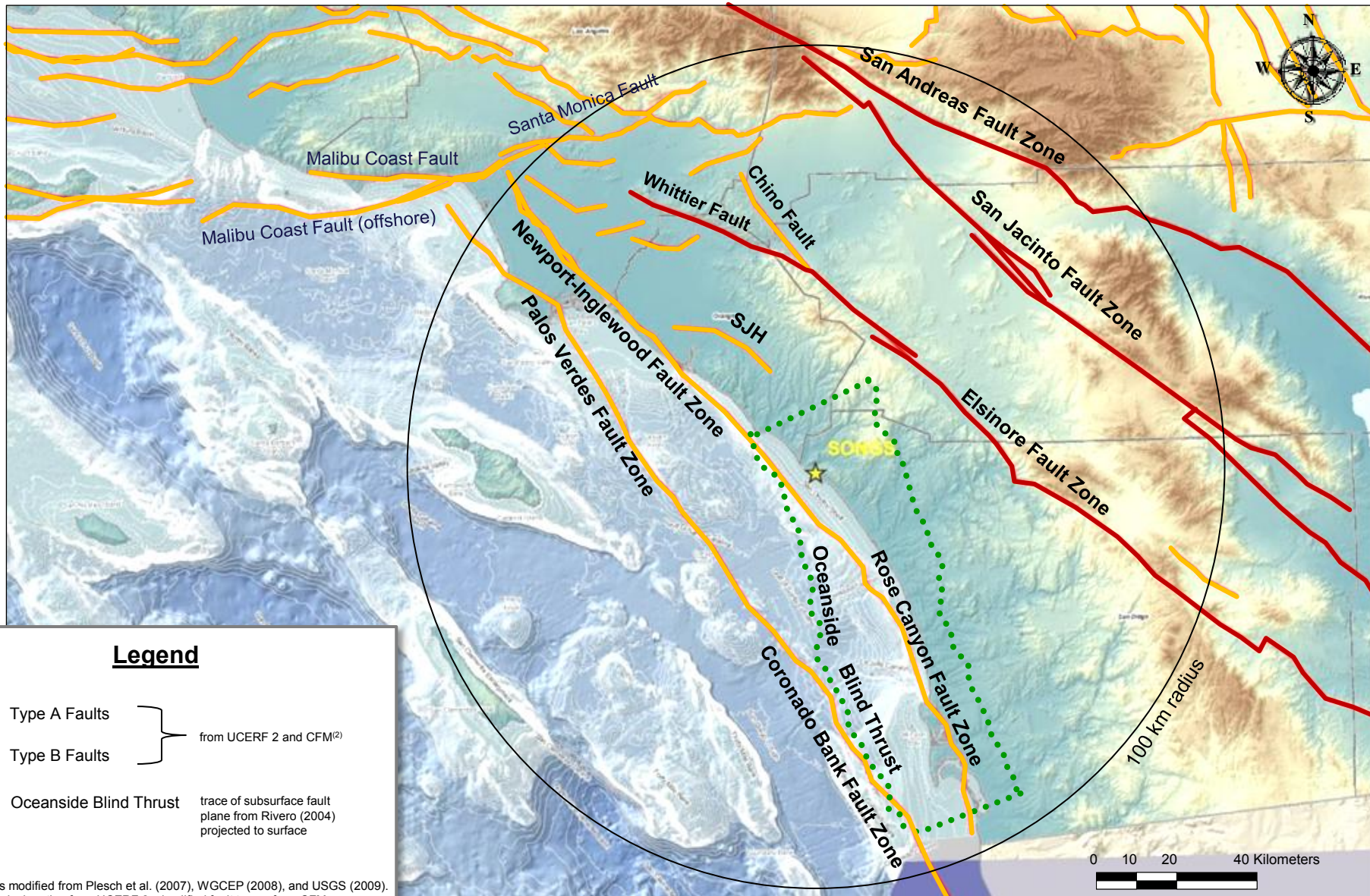
NOTES:

(1) Data source WGCEP (2008) Historical Earthquake Catalog from 1850 to 2006.

(2) For detailed Fault Map Legend see Figure 2-1b.

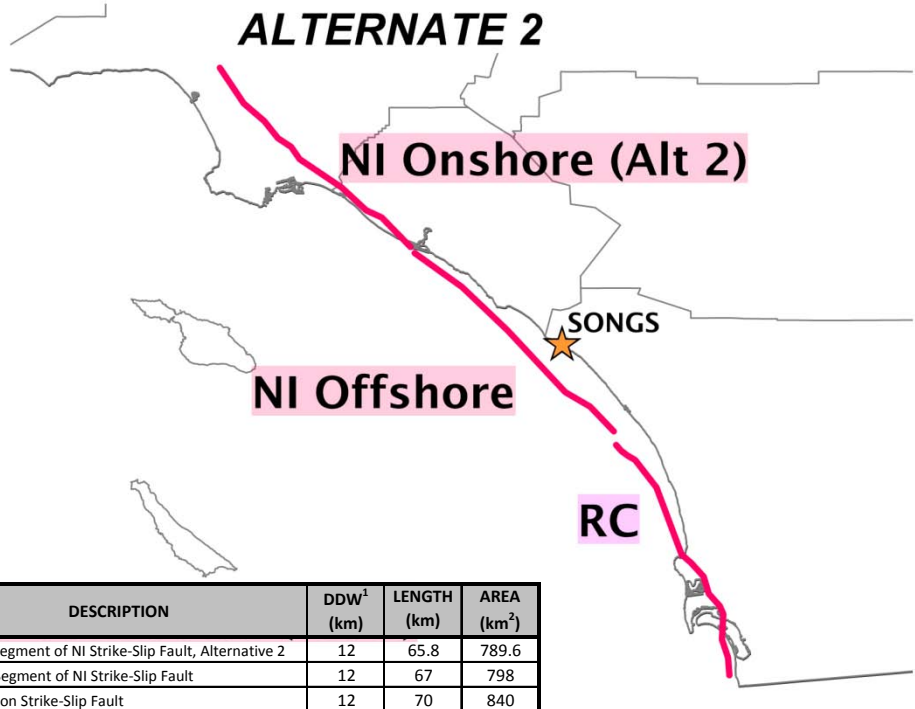
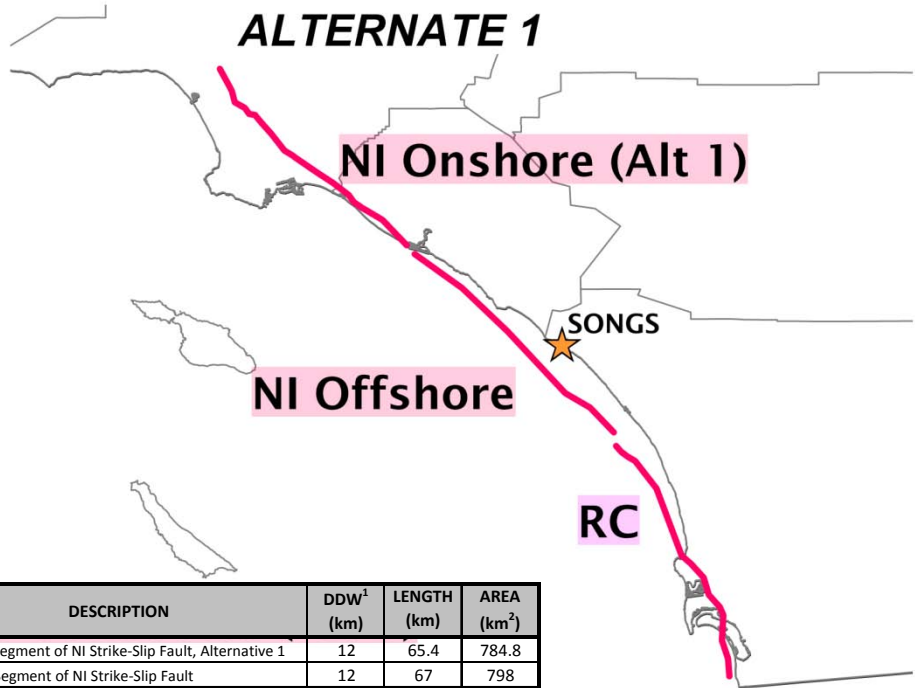


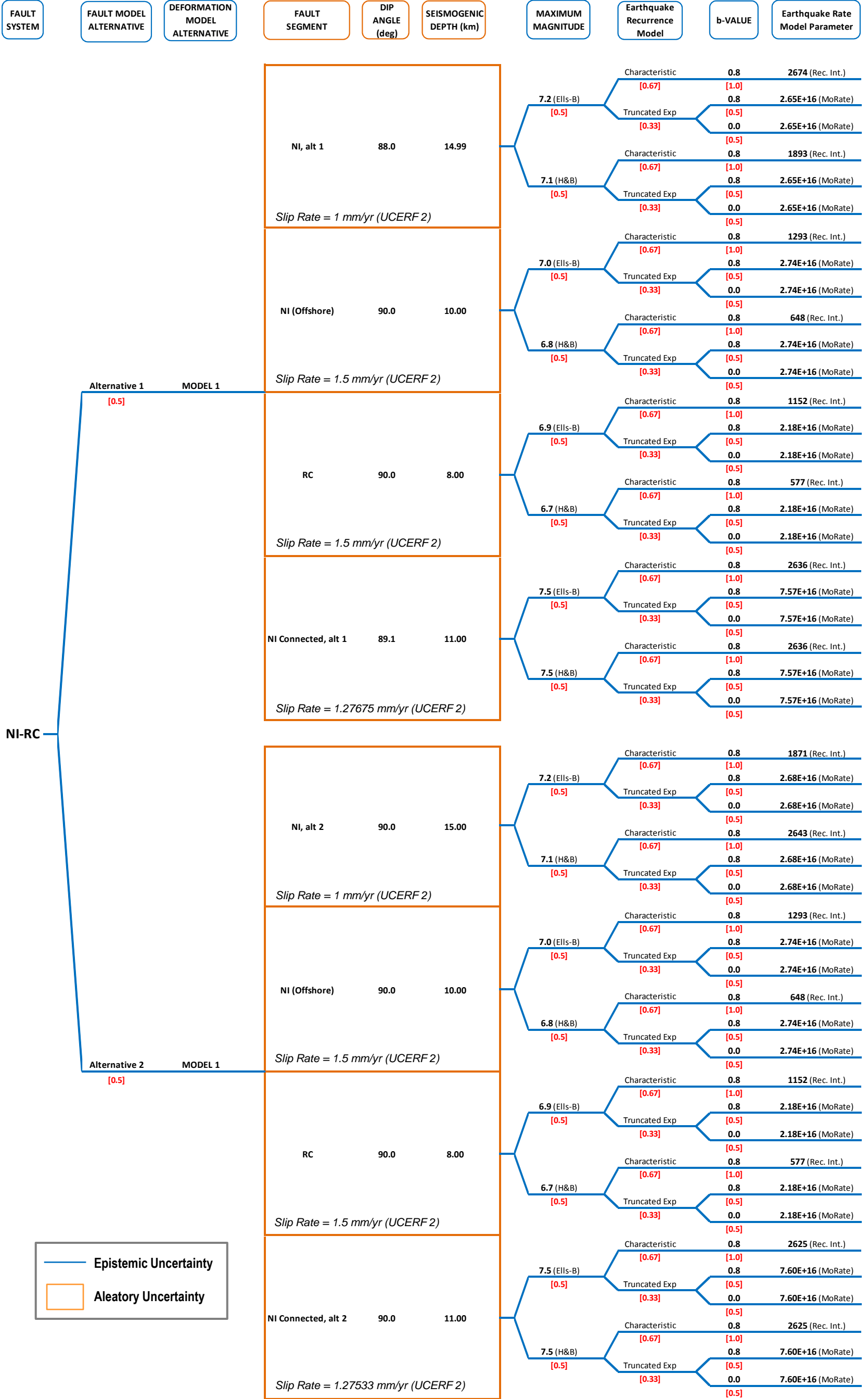
Modified from CFM (Plesch et al., 2007)



Notes:

¹ Assuming 5km to 17km Seismogenic Depth





— Epistemic Uncertainty
 □ Aleatory Uncertainty

NIRC 'LOGIC TREE' - 8 COMBINATIONS OF FAULT SEGMENT RUPTURE

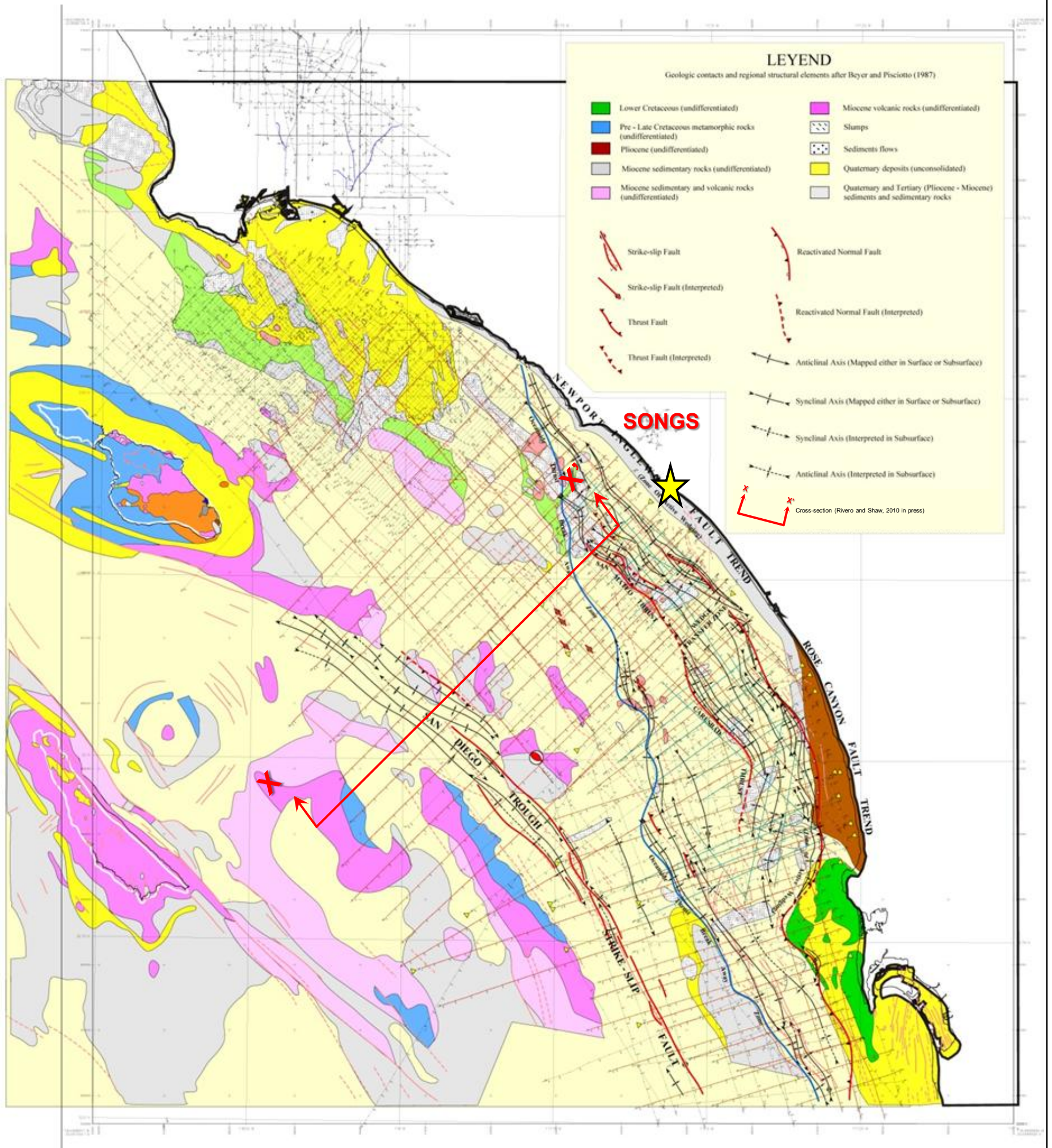
FIGURE 2-5



SAN ONOFRE NUCLEAR GENERATING STATION
 SEISMIC HAZARD ASSESSMENT PROGRAM

Seismic Reflection Data from Harvard University

Original data compiled from several petroleum industry sources



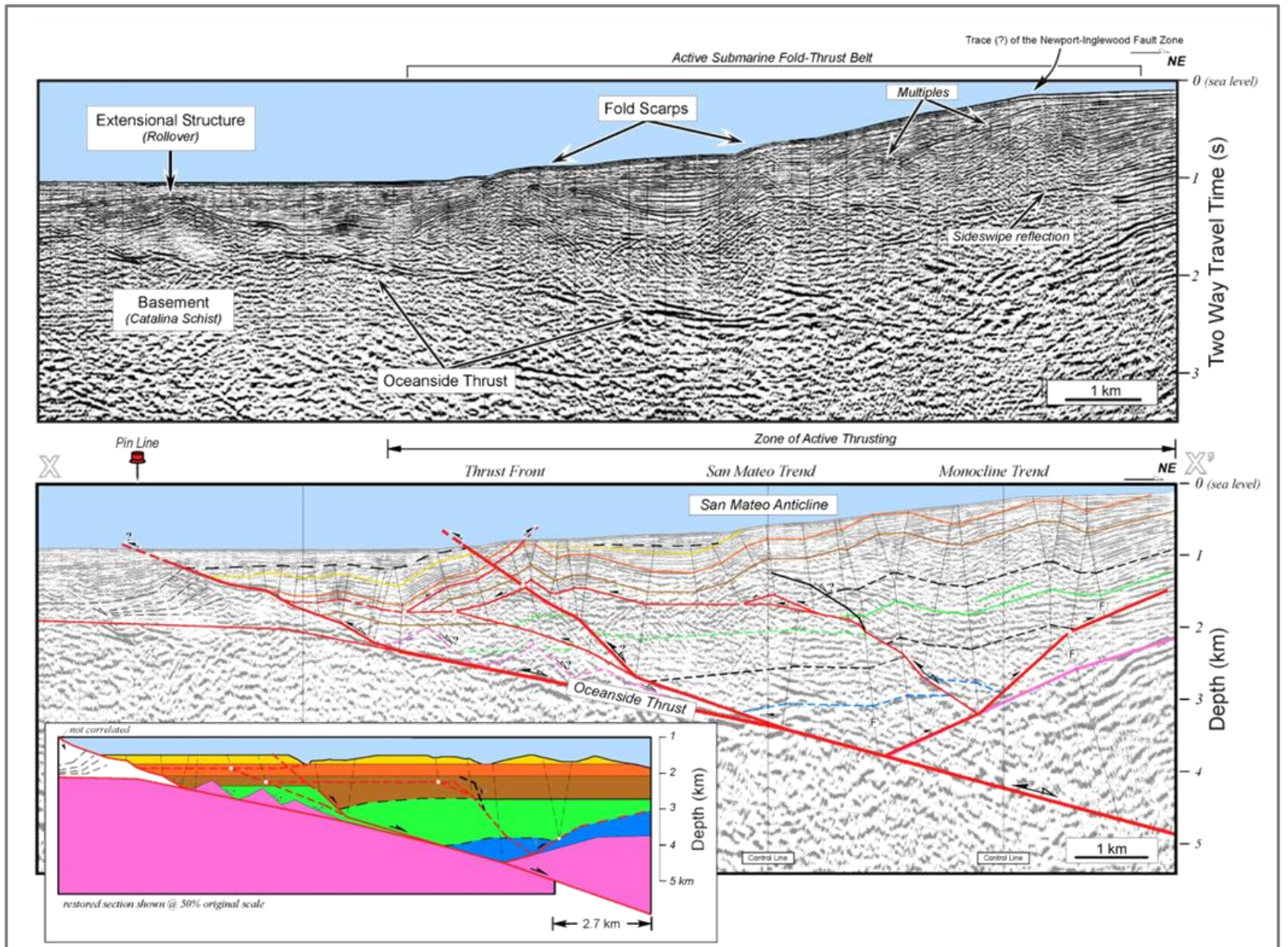
Modified from Rivero (2004)



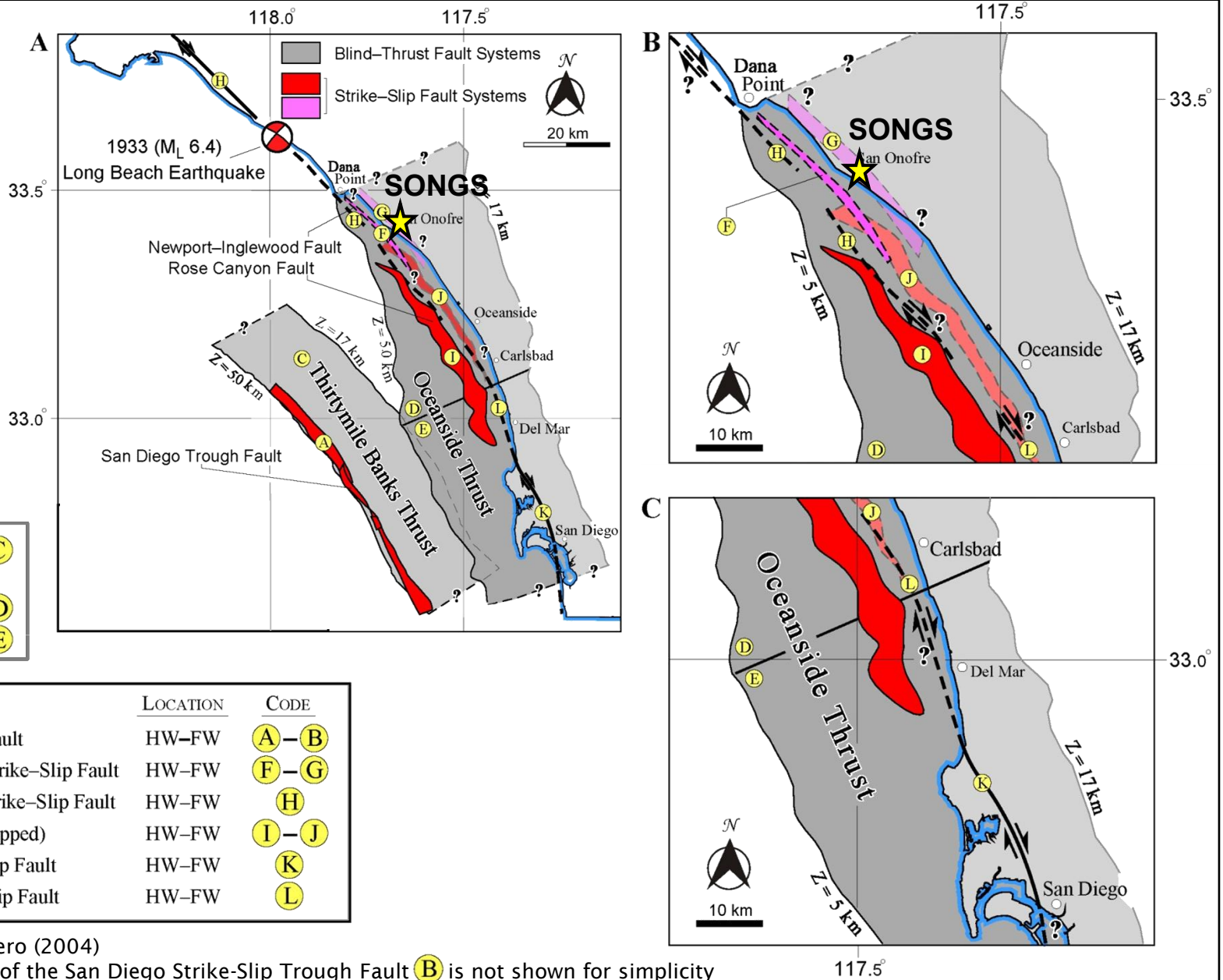
MARINE GEOLOGIC MAP

FIGURE 2-6

SAN ONOFRE NUCLEAR GENERATING STATION
SEISMIC HAZARD ASSESSMENT PROGRAM



Modified from
Rivero and Shaw
(2010, in press)

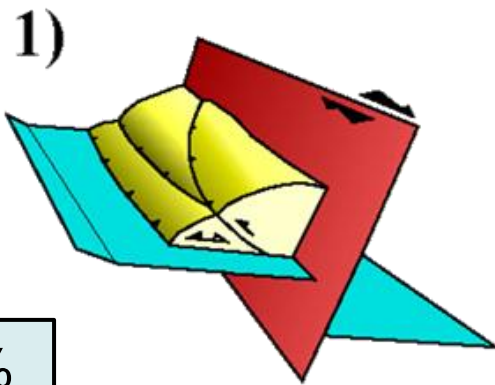


NOTES: (1) Modified from Rivero (2004)

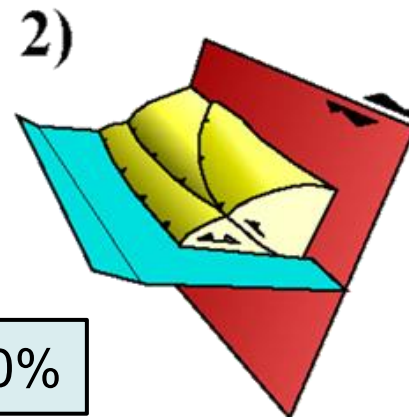
(2) Footwall segment of the San Diego Strike-Slip Trough Fault (B) is not shown for simplicity

(3) Latitude and longitude approximate

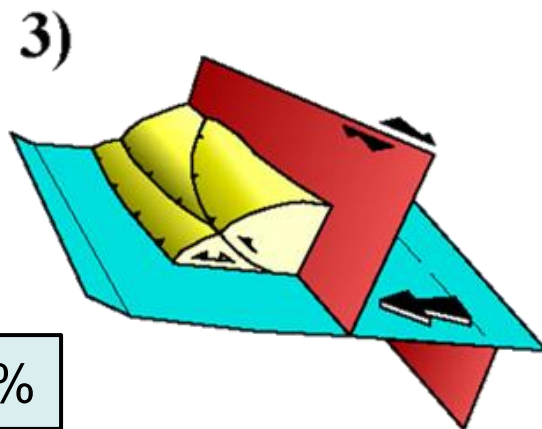
STRIKE-SLIP/THRUST FAULT INTERACTIONS



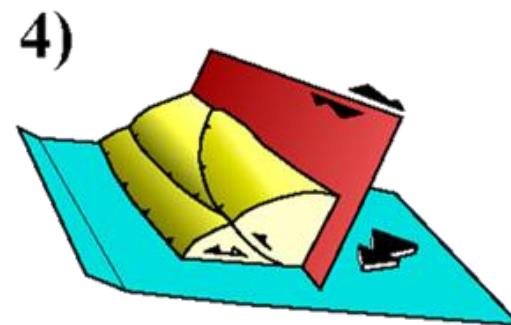
0%



10%



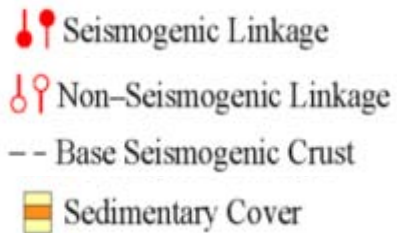
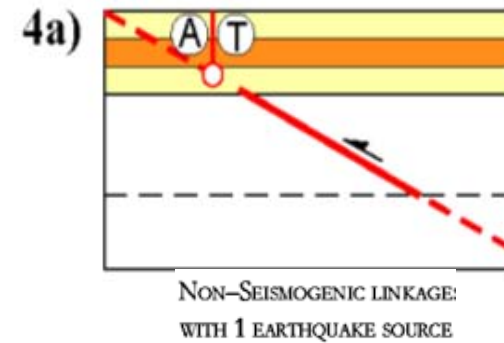
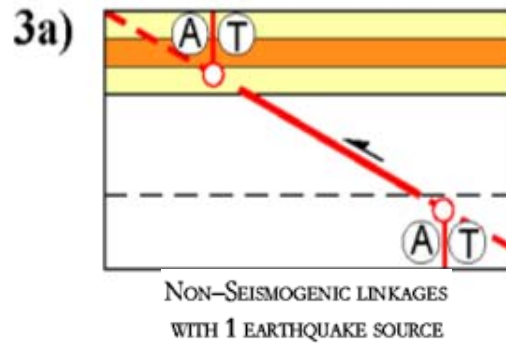
45%



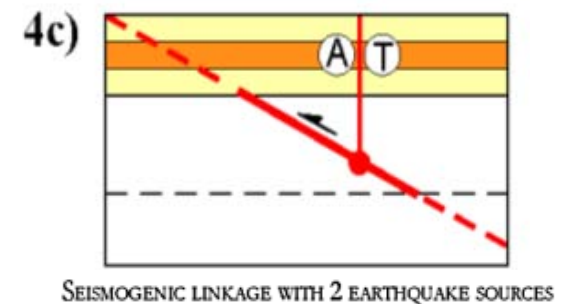
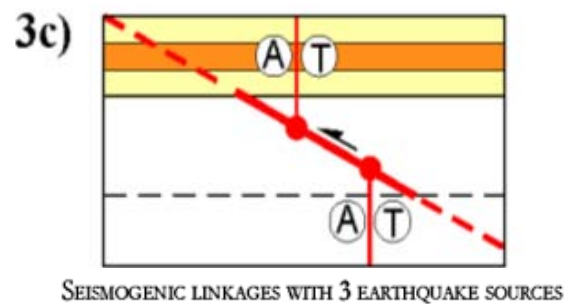
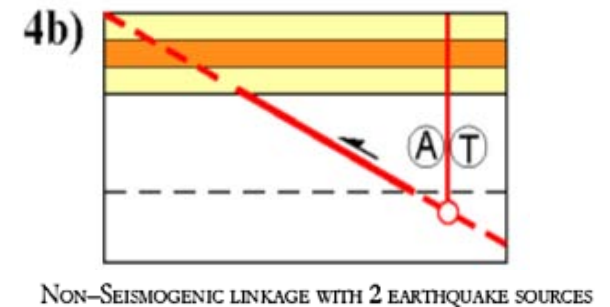
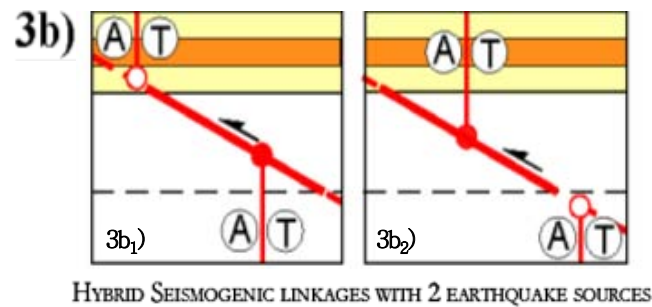
45%

Modified from Rivero (2004)

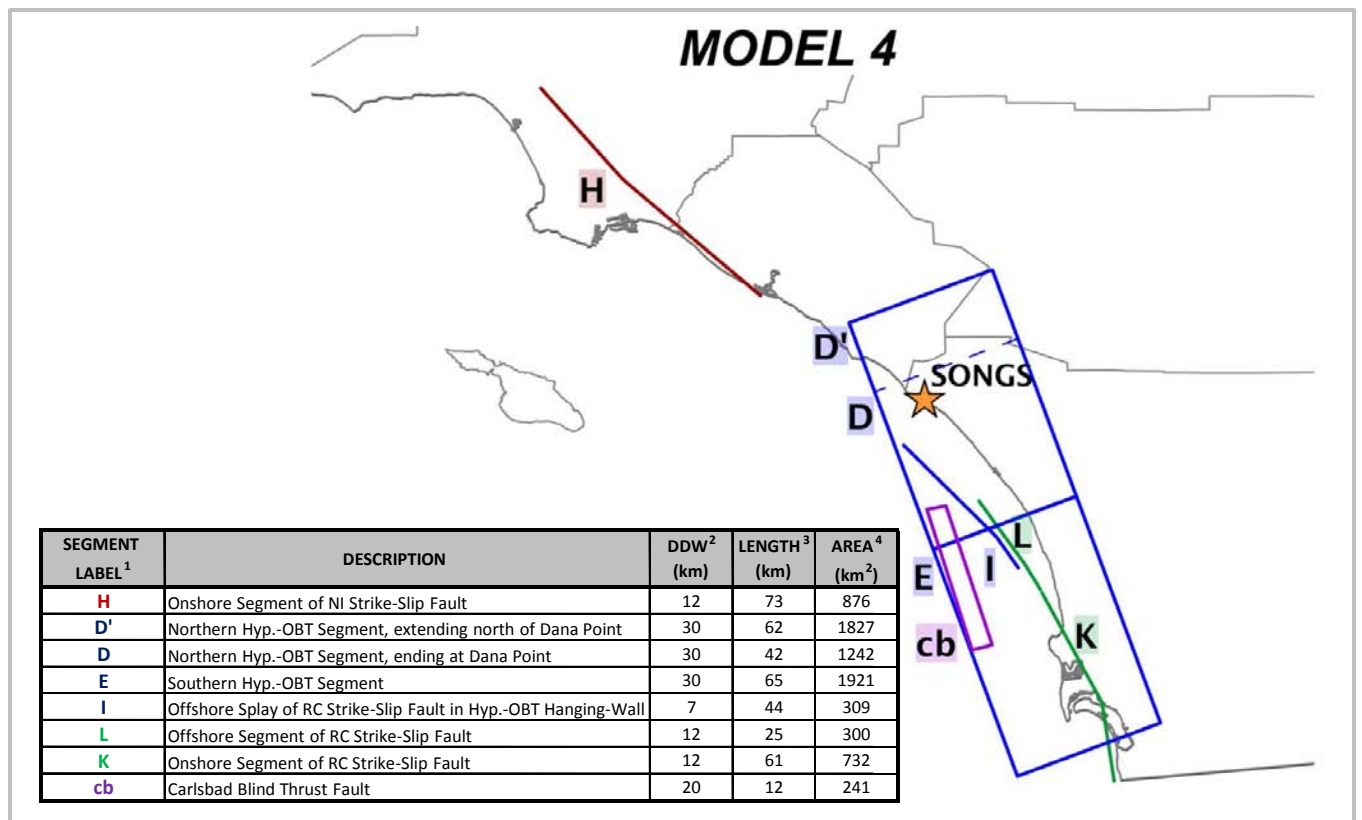
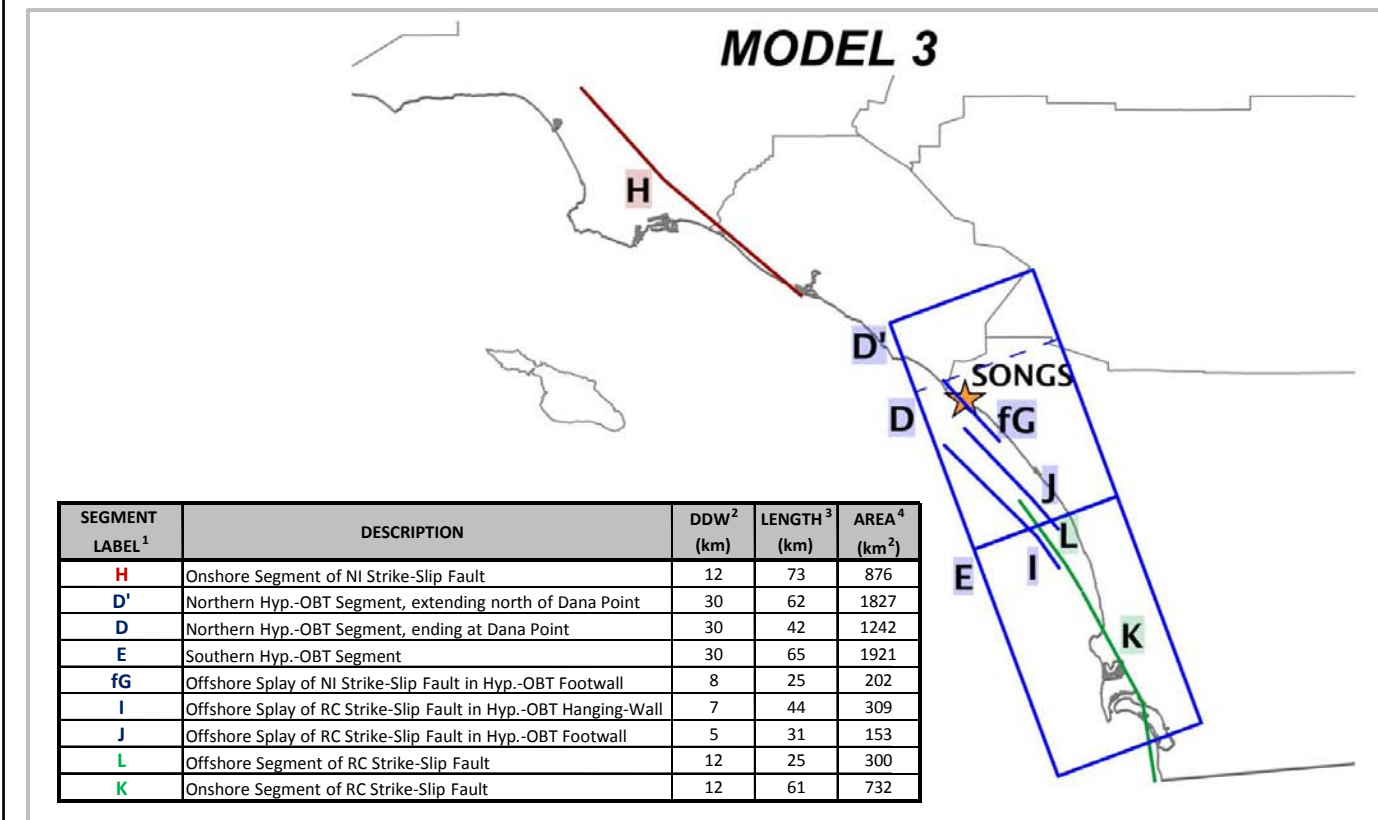
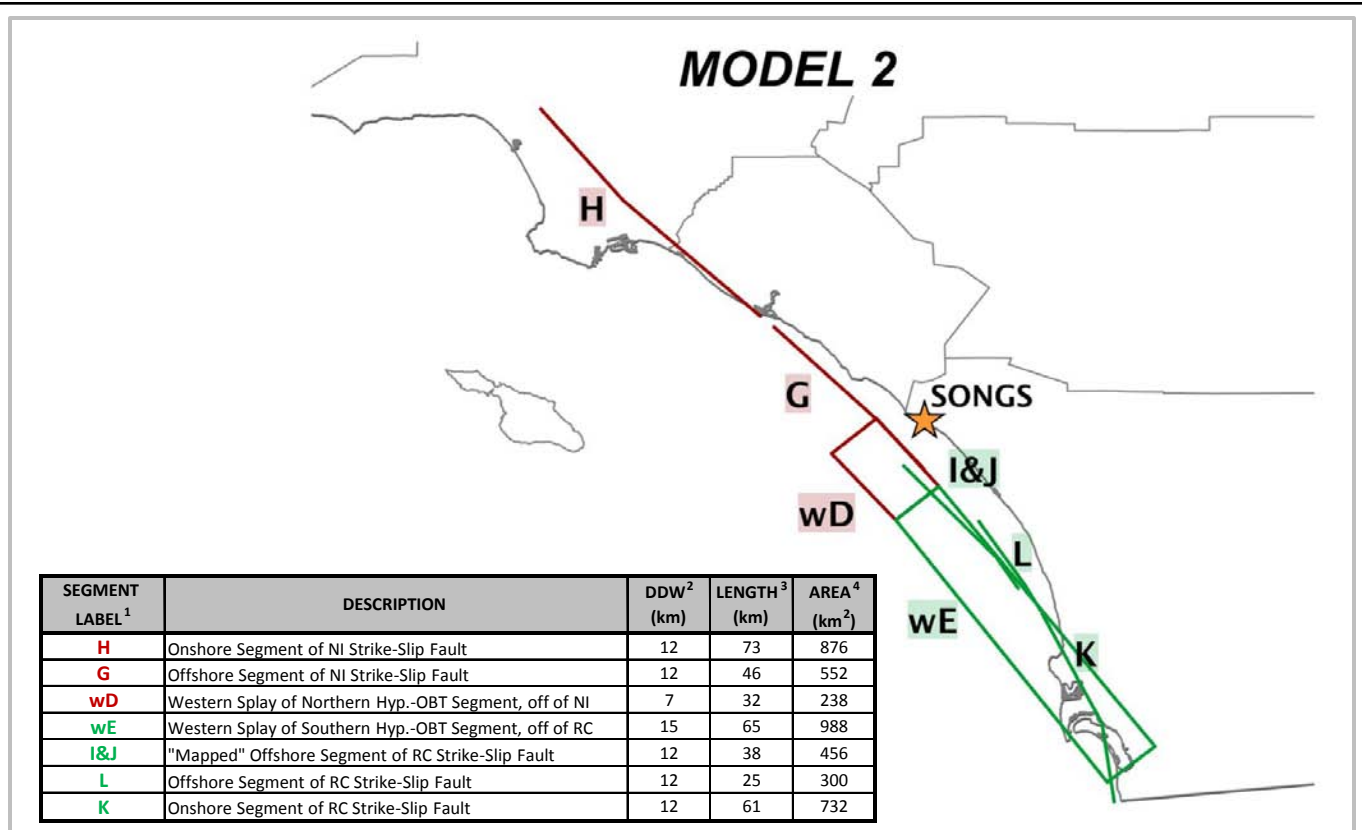
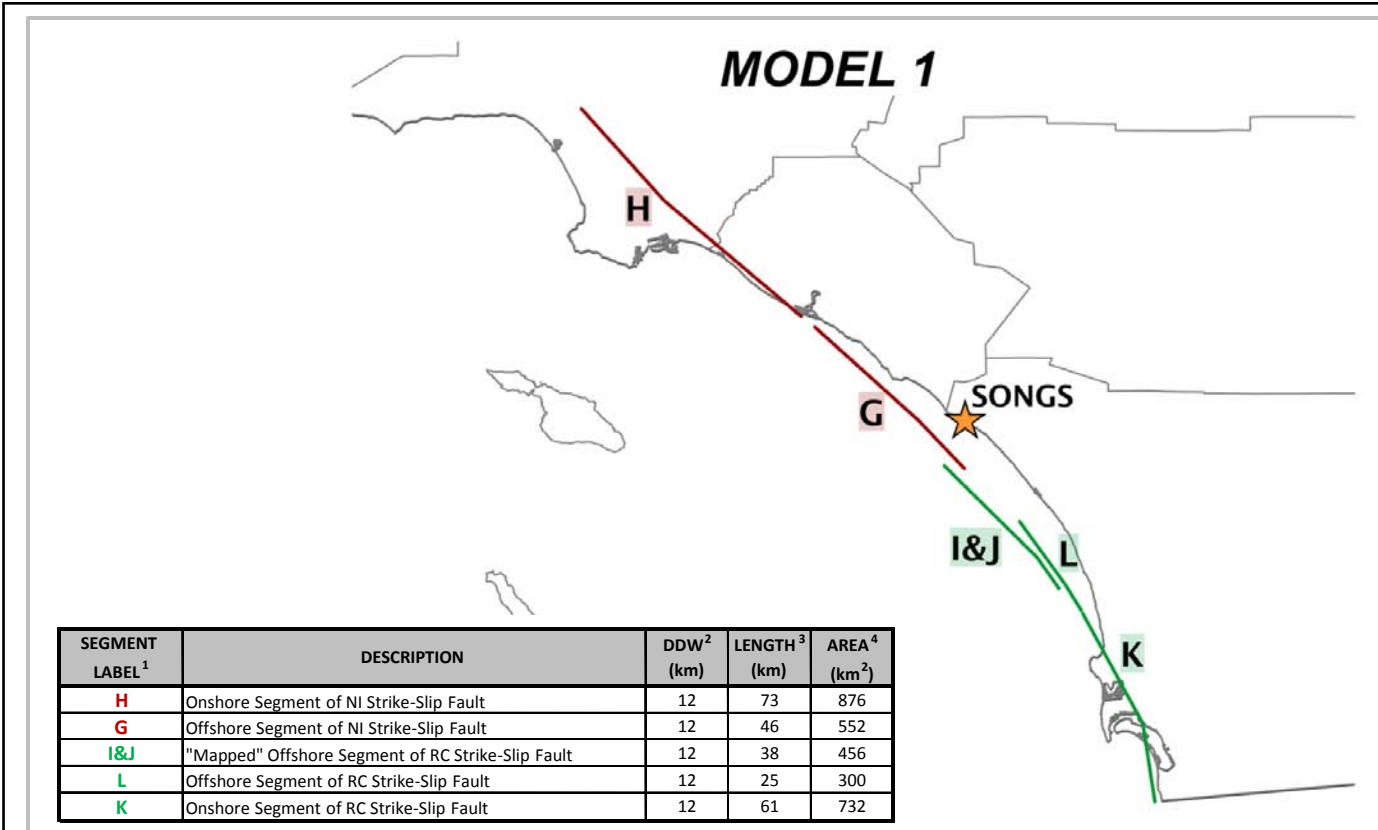
SINGLE EARTHQUAKE SOURCE



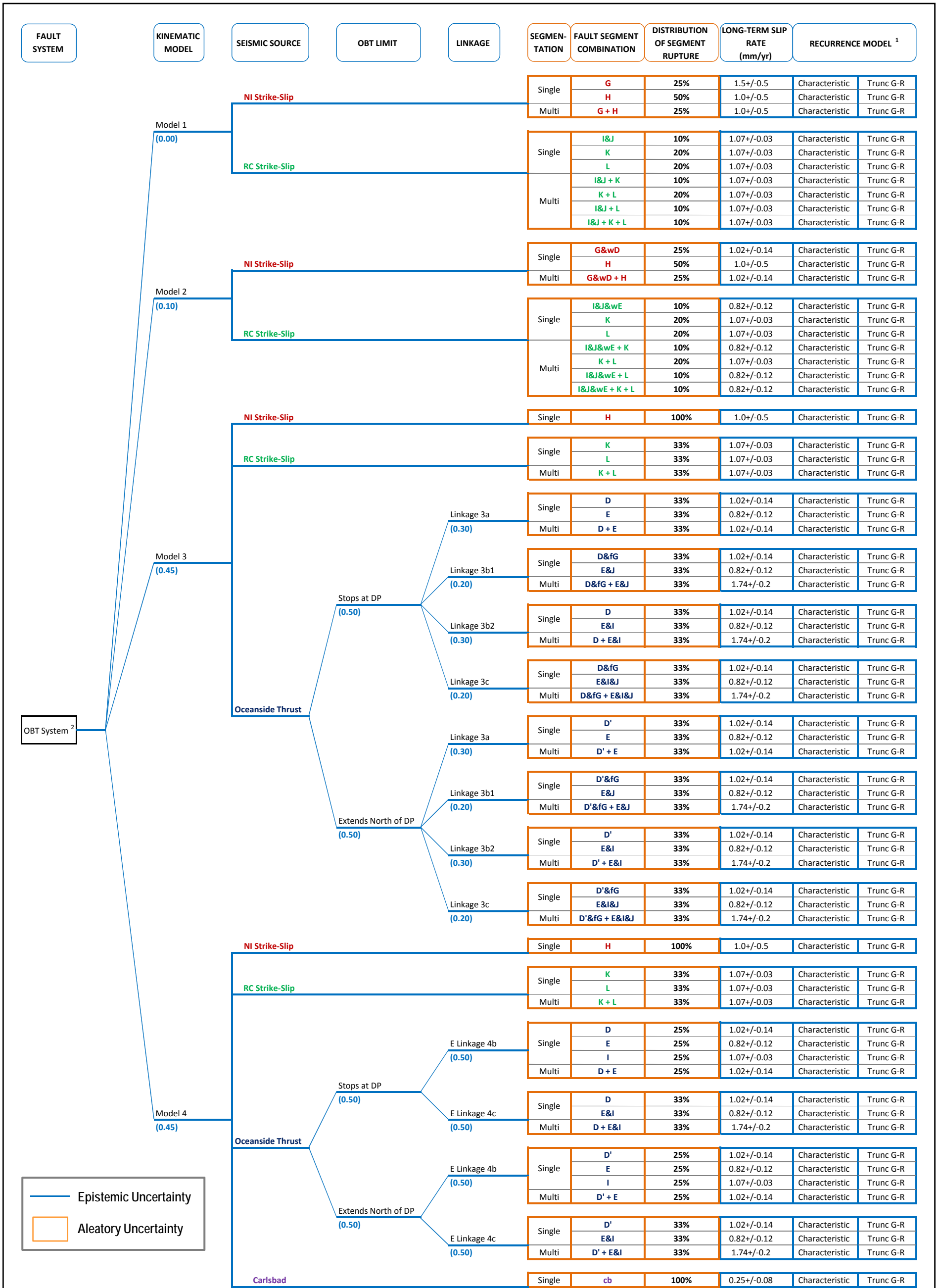
COMPLEX EARTHQUAKE SOURCES



Modified from Rivero and Shaw (2010, in press)



- Notes:
- ¹ Labels modified from Figure A-2-1
 - ² Assuming 5km to 17km Seismogenic Depth
 - ³ Based on Rivero (2004)
 - ⁴ Calculated based on DDW and Length
 - ⁵ See Appendix A, Attachment A-3 for details



Notes:
¹ Recurrence based on 2/3 Characteristic Model and 1/3 Truncated Gutenberg-Richter Distribution
² See Appendix A, Attachment A-3 for details

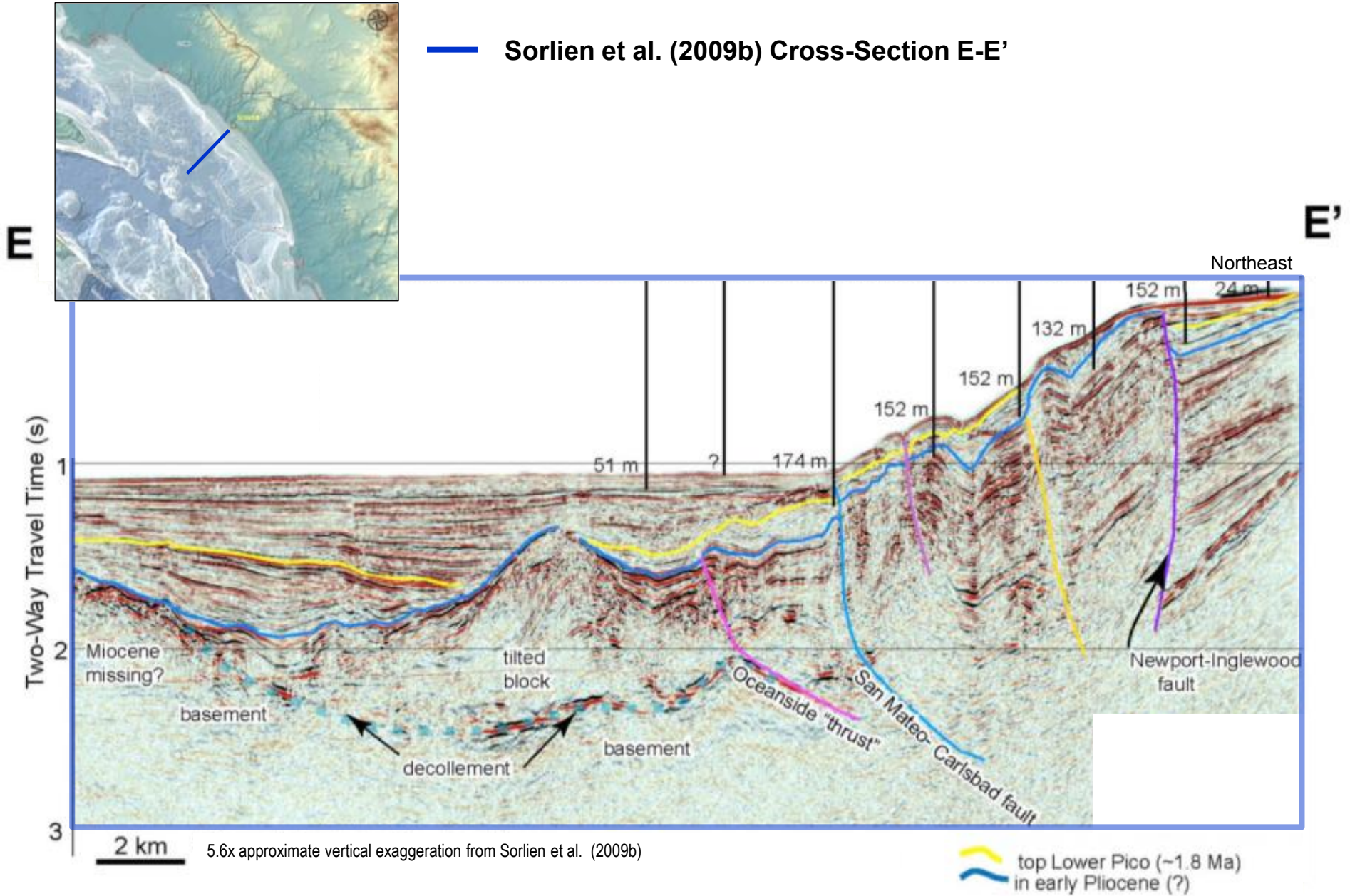
**HYPOTHESIZED - OBT 'LOGIC TREE' -
 73 COMBINATIONS OF FAULT SEGMENT RUPTURE**

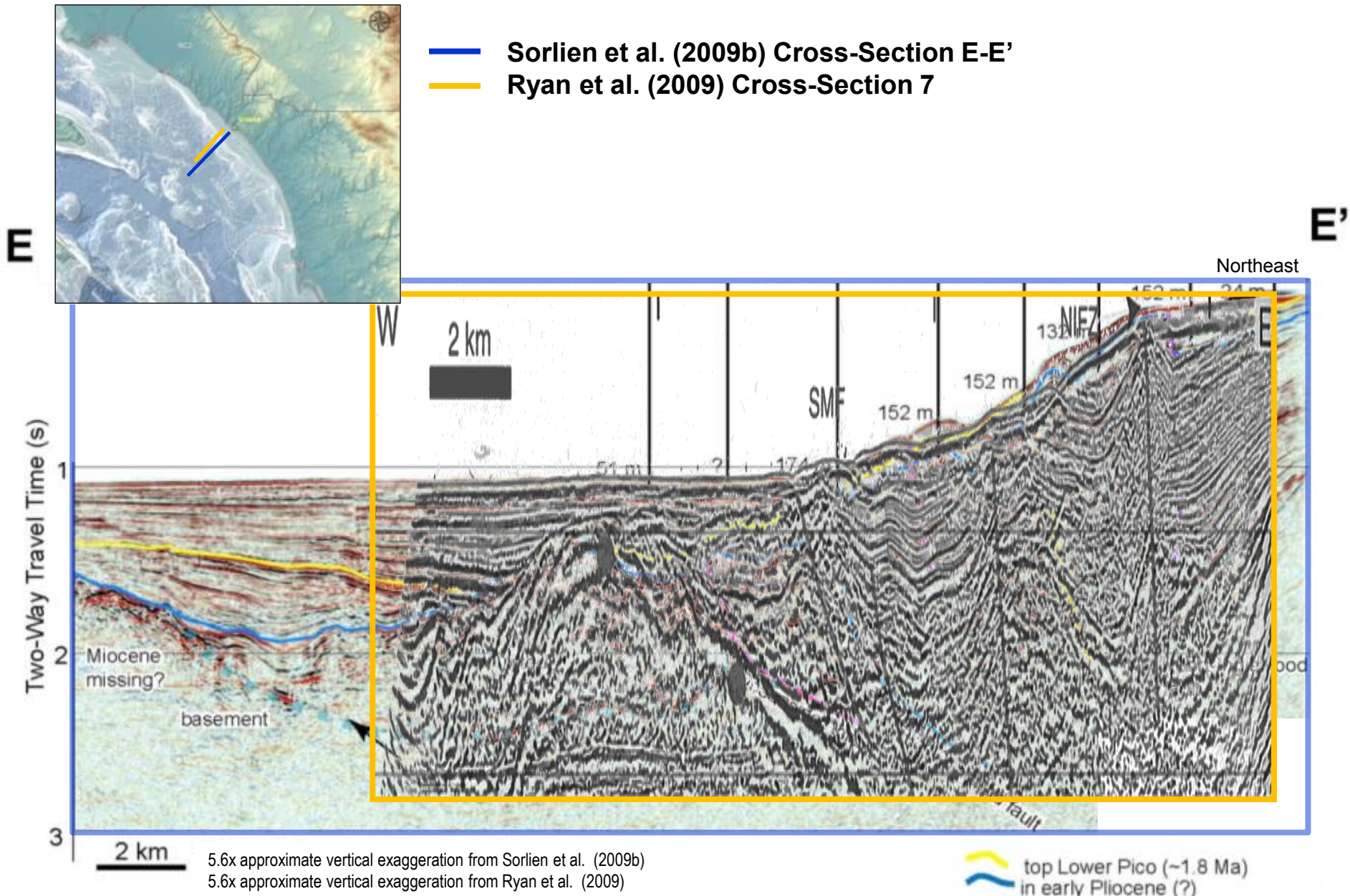
**FIGURE
 2-12**

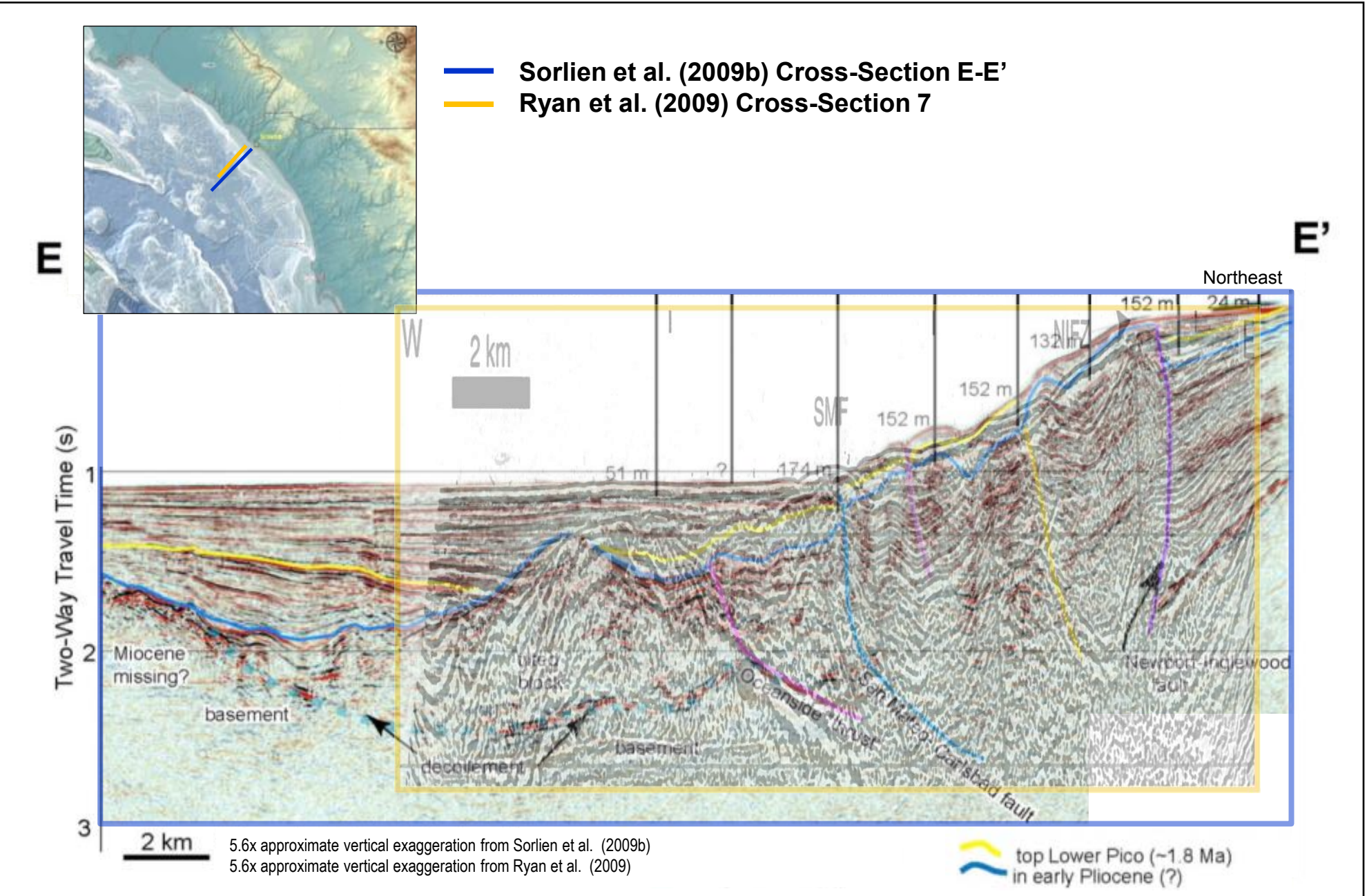


**SAN ONOFRE NUCLEAR GENERATING STATION
 SEISMIC HAZARD ASSESSMENT PROGRAM**

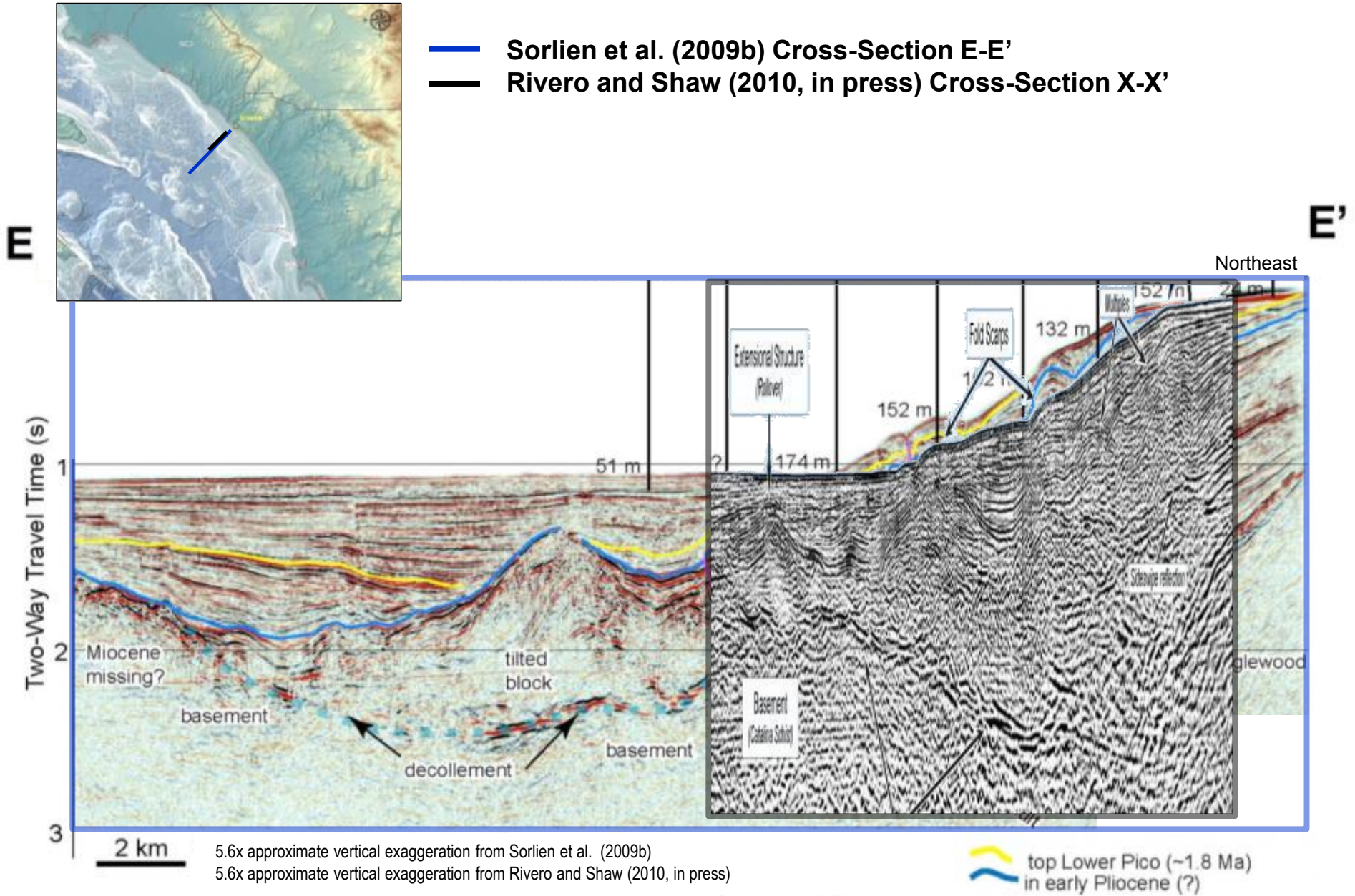
— Sorlien et al. (2009b) Cross-Section E-E'



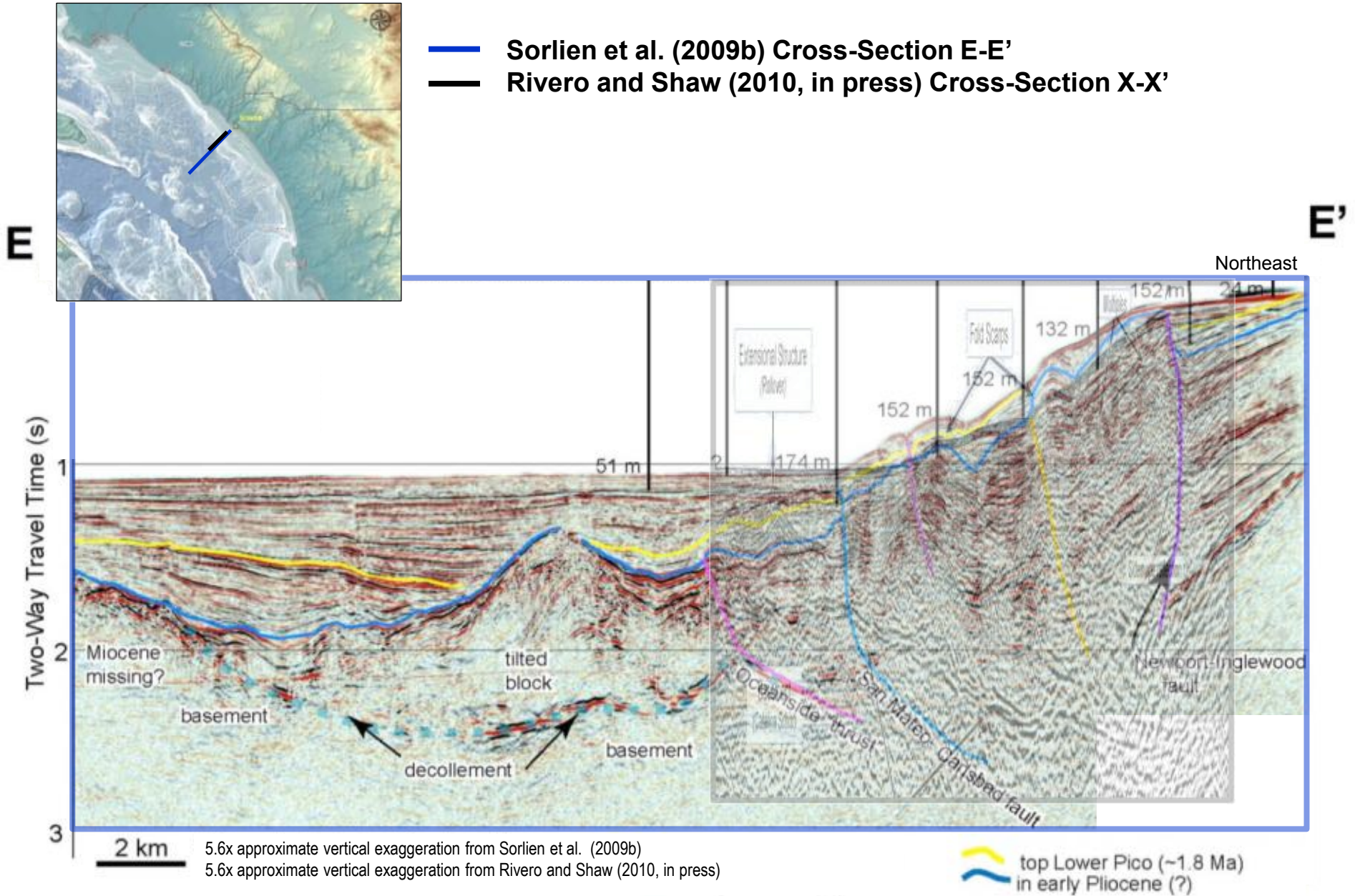




— Sorlien et al. (2009b) Cross-Section E-E'
— Rivero and Shaw (2010, in press) Cross-Section X-X'

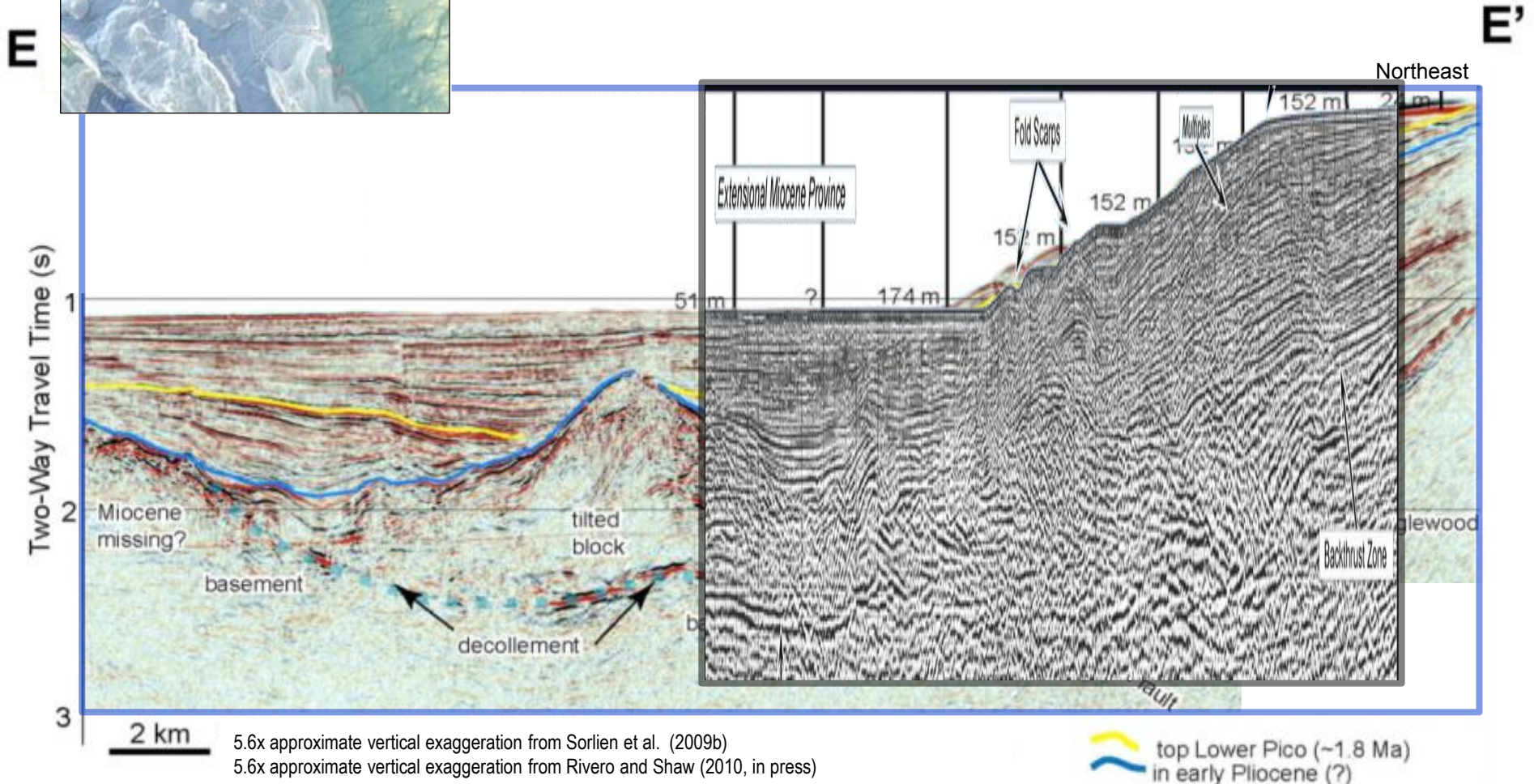


- Sorlien et al. (2009b) Cross-Section E-E'
- Rivero and Shaw (2010, in press) Cross-Section X-X'



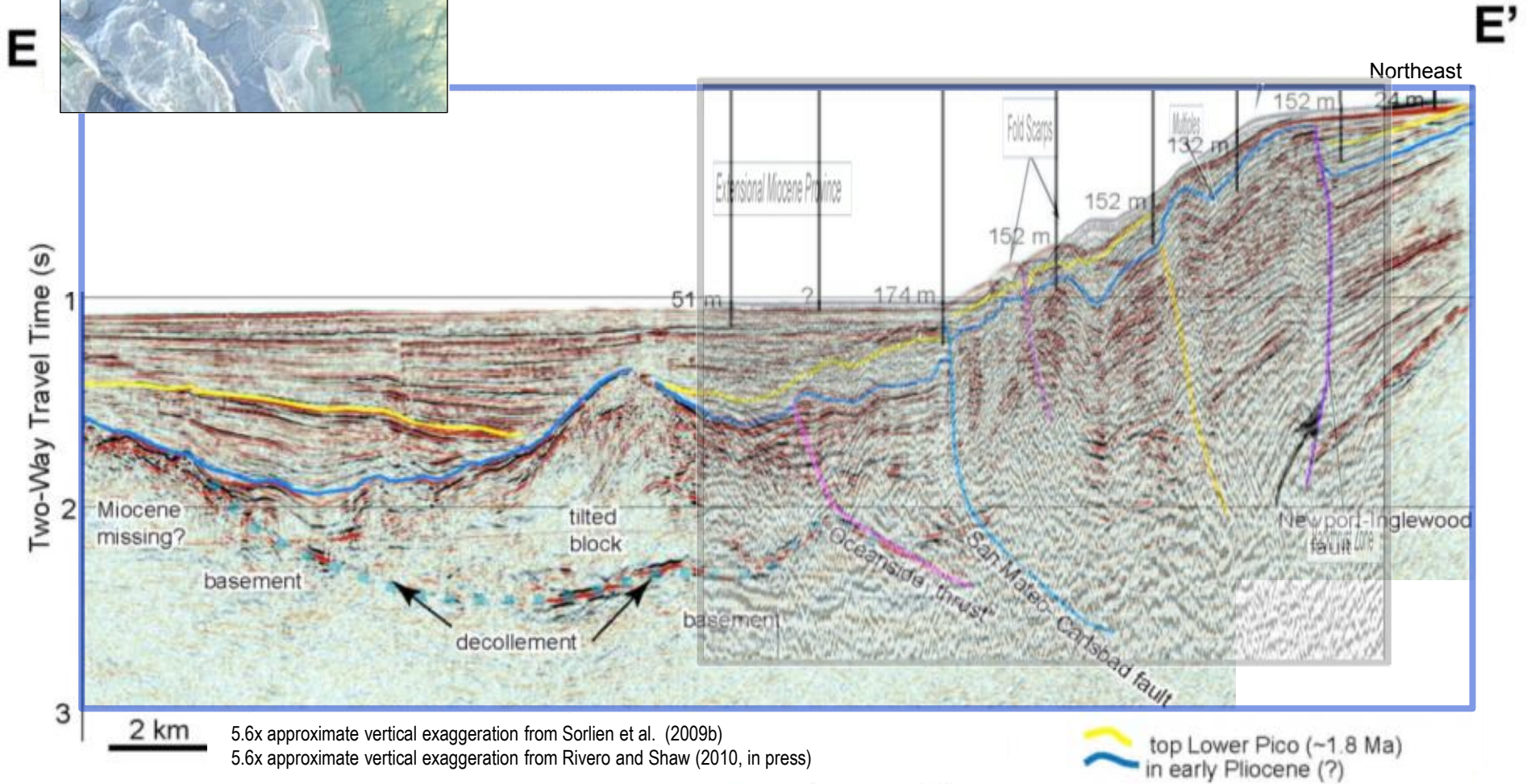


- Sorlien et al. (2009b) Cross-Section E-E'
- Rivero and Shaw (2010, in press) Cross-Section Y-Y'



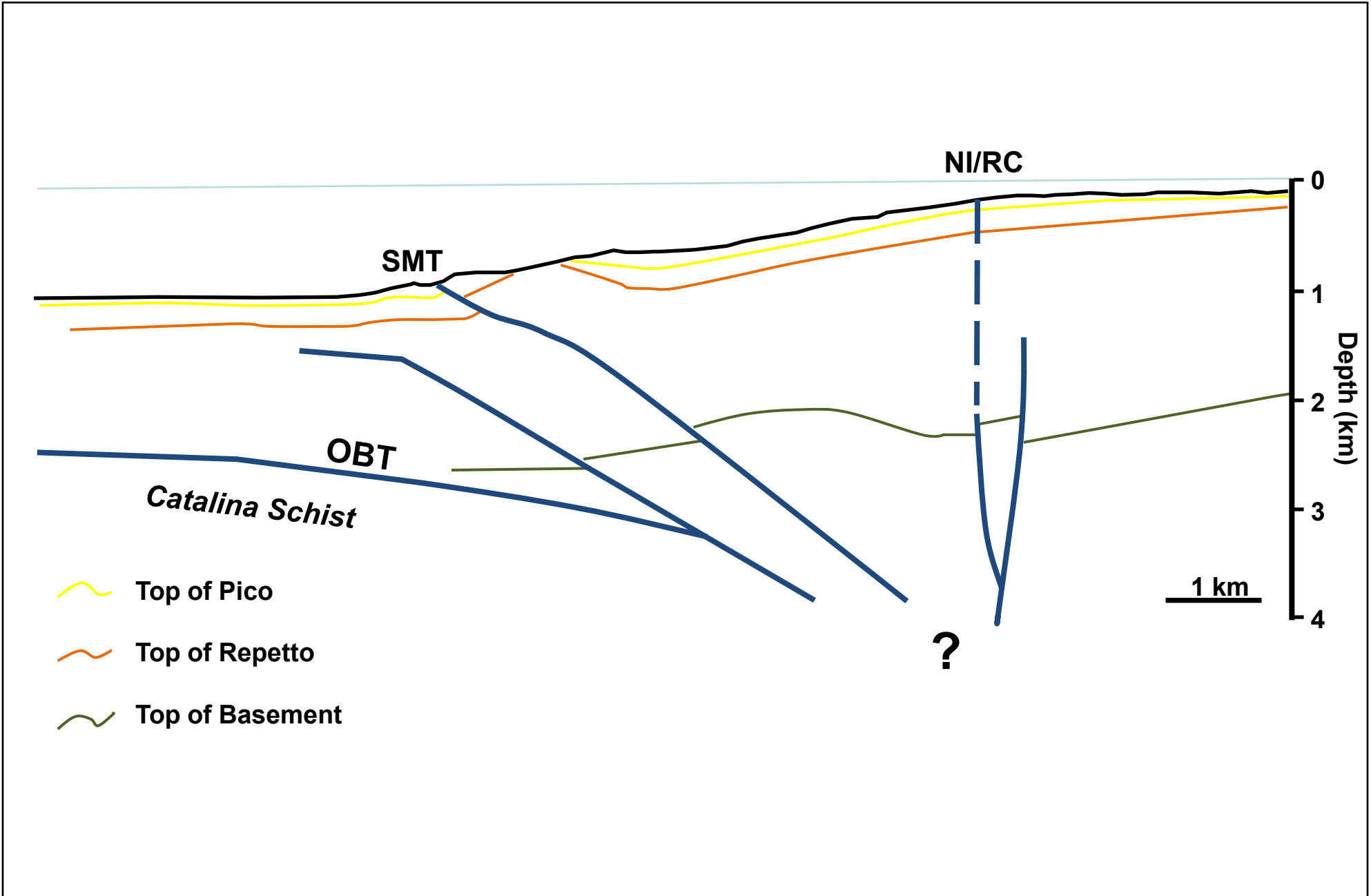


- Sorlien et al. (2009b) Cross-Section E-E'
- Rivero and Shaw (2010, in press) Cross-Section Y-Y'

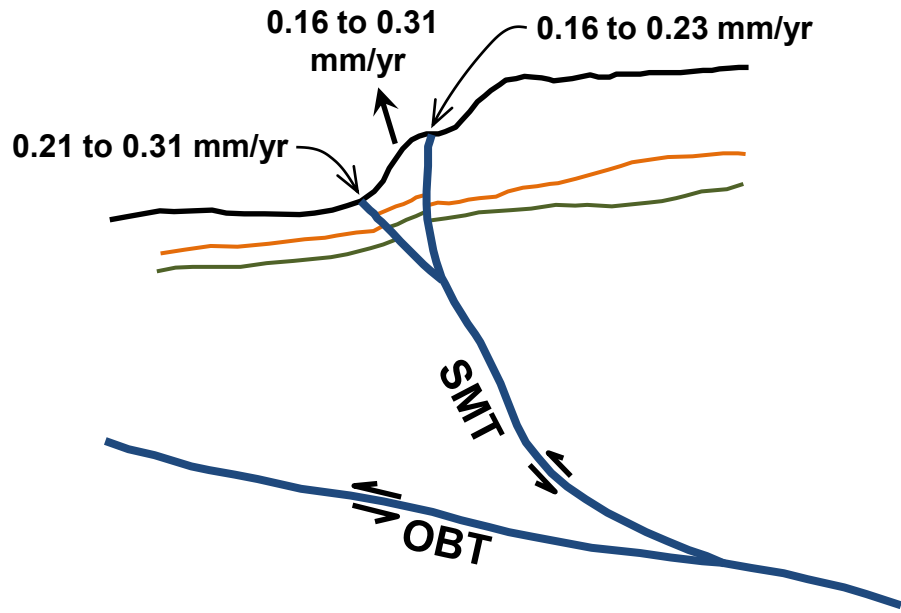


5.6x approximate vertical exaggeration from Sorlien et al. (2009b)
 5.6x approximate vertical exaggeration from Rivero and Shaw (2010, in press)

— top Lower Pico (~1.8 Ma) in early Pliocene (?)
— Sorlien et al. (2009b) Cross-Section E-E'

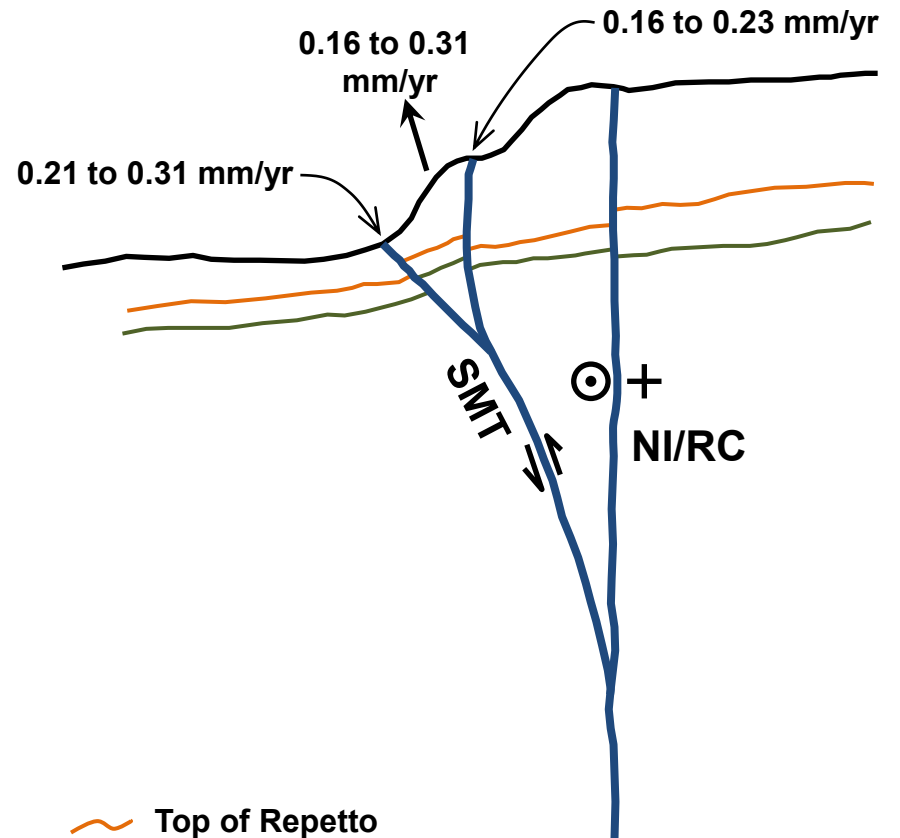


BLIND THRUST END MEMBER MODEL



- Top of Repetto
- Top of Basement

STRIKE-SLIP END MEMBER MODEL



- Top of Repetto
- Top of Basement

3.0 PROBABILISTIC SEISMIC HAZARD ANALYSIS

Spectral acceleration values for SONGS were obtained from the PSHA using the seismic sources discussed in Section 2.0. This SONGS 2010 PSHA followed the methods of the 1995 PSHA (SCE, 1995) and the 2001 PSHA (SCE, 2001). The 2001 PSHA results included both response spectral values and time histories, reflecting the effects of near-fault directivity and fling step. Unlike the 2001 PSHA results, the PSHA results reported here focus mainly on high frequency spectral accelerations and do not reflect the effects of near-fault directivity or fling step, which were found to be insignificant for SONGS. Based on the 2001 PSHA, the near-fault directivity and the fling steps only affect the low frequency range below about 1.5 Hertz (Hz), which is outside the frequencies of interest for structures and components at SONGS.

3.1 PSHA Methodology

3.1.1 General

The basic result of PSHA is a relationship between a ground motion parameter “Z” (peak ground acceleration [PGA] and spectral acceleration herein) and the mean number of seismic events per year in which “Z” at the site exceeds a specified value “z”. This relationship is called a "hazard curve." The mean number of seismic events per year is referred to as "annual frequency of exceedance" and designated " $\nu(Z \geq z)$ ". The inverse of this number is called the "return period" (RP) and is expressed in years. Once the relationships between appropriate parameters and annual frequency of exceedance are obtained, various probabilistic calculations can be made assuming a Poisson process. Details of PSHA are available elsewhere (e.g., SSHAC, 1997: <http://www.ce.memphis.edu/7137/>). Apart from the general discussions below, only the key pertinent topics will be discussed here with some further details presented in Appendix B.

The five major components in PSHA consist of the following:

- Characterization of Seismogenic Sources. The location, geometry, and characteristics of seismic sources (or earthquake generating faults) relative to the site are evaluated and specified. This component is addressed in Section 2.0
- Specification of Recurrence Relationship. In the PSHA, one of the most important characteristics of a seismic source is its recurrence relationship or the relationship showing the annual recurrence of earthquakes of various magnitudes up to the “maximum” magnitude. The recurrence relationship is used to provide the mean number of earthquakes per year having a particular magnitude “ m_j ” on a given seismic source, “ $\dot{N}_s(m_j)$ ”. Two types of recurrence relationships were used: the characteristic and the truncated exponential (Yongs and Coppersmith, 1985). These two recurrence models were selected to be consistent with the UCERF 2 (WGCEP, 2008).
- Evaluation of Probability of Distance to Rupture. Assuming that the typical earthquake generating fault rupture can occur anywhere along the plane of an active fault with an equal probability, the conditional probability is computed so that the rupture plane is at a specified distance, r_k , from the site for the given m_j . This probability is evaluated by considering the rupture plane’s dimensions and the distance definition used in the particular attenuation relationship being used.

- Calculation of Exceedance Using Attenuation Equation. The conditional probability that the ground motion parameter “Z” from the earthquake of a certain magnitude “ m_j ” occurring at a certain distance “ r_k ” on a particular seismic source fault will exceed a specified level “z” at the site is calculated based on the median and standard deviation of the ground motion given by the attenuation relationship.
- Calculation of Probabilistic Seismic Hazard. By combining the rate of occurrence of earthquakes of a given magnitude with the two conditional probability functions associated with steps 2 through 4 above, for each seismic source fault, the mean number of events per year (annual frequency of exceedance) resulting in “Z” being greater than “z” ($v(Z \geq z)$) at the site is computed for that particular seismic source fault. This process was repeated for each seismic source fault, and the contributions are added to obtain the total seismic hazard at the site for a given z. The complete hazard curve is obtained by repeating these computations for several levels of ground motion parameter z.

Once this mean number of events per year (annual frequency of exceedance) $v(Z \geq z)$ has been determined, the probability of the level of the seismic ground motion parameter being exceeded over a specified time period, t, is calculated by the following equation assuming the Poisson model for the earthquake occurrence:

$$Pr(Z \geq z) = 1 - \exp[-v(Z \geq z) \cdot t] \quad (3-1)$$

The results of the SONGS 2010 PSHA are presented here in terms of the mean number of events per year or annual frequency of exceedance, $v(Z \geq z)$. The results are presented from an annual frequency of exceedance of 10^{-2} to 10^{-4} corresponding to a RP of 100 to 10,000 years. The computer program Haz4.2 developed by Abrahamson (2010, PC) was used in completing this PSHA. The results of quality assurance/quality control (QA/QC) work performed on the program are summarized in Appendix B.

3.1.2 Attenuation Relationships

The attenuation relationships from the NGA project, which are now called GMPEs, were used in this PSHA and are listed in Table 3-1 along with key parameter values. These attenuation relationships are referred to herein as the "NGA relationships" and consist of the following:

- Abrahamson and Silva (2008)
- Boore and Atkinson (2008)
- Campbell and Bozorgnia (2008)
- Chiou and Youngs (2008)
- Idriss (2008)

Further details of these NGA relationships are provided in Appendix B.

3.1.3 Uncertainties

Two major types of uncertainties are addressed in PSHA. They are as follows:

- Aleatory Uncertainty. Uncertainties in the earthquake recurrence process and in the attenuation of ground motion are the major sources of the aleatory uncertainty in PSHA. This uncertainty is a reflection of the “randomness” inherent to the natural phenomenon of earthquake generation and ground motions. This uncertainty may be based in part on the limited scientific understanding of the natural phenomenon of earthquake generation and seismic wave propagation. This type of uncertainty, in theory, cannot be reduced when additional data or understanding of earthquakes and their effects become available.
- Epistemic Uncertainty. This uncertainty reflects limited available data, limited scientific understanding, and/or limitations in the utility of modeling earthquake and related processes. This type of uncertainty, in theory, can be reduced when additional data or understanding of earthquakes and their effects become available.

The PSHA methodology includes probability models for these two major types of uncertainty. For example, both aleatory uncertainty and epistemic uncertainty are reflected in the logic tree provided for the OBT seismic source fault shown on Figure 2-12 in Section 2.0. Two specific epistemic uncertainties considerations were addressed because of their pertinence to the current PSHA: one is associated with the GMPEs and the other is the NI/RC Fault Zone versus the OBT Fault as the primary seismic source fault.

3.1.3.1 GMPE Uncertainty

In using attenuation relationships, their epistemic uncertainty should be considered. In the past, this epistemic uncertainty was often accommodated by using multiple attenuation relationships. However, given the coordinated process used to develop the NGA relationships, it may not be adequate to address this epistemic uncertainty by just using multiple NGA relationships.

On the basis of the evaluation results presented in Appendix B, an epistemic GMPE uncertainty in addition to the five NGA relationships was used in the current PSHA. This additional uncertainty represents the difference between the GMPE uncertainty that the USGS (2008) is currently using with only three NGA relationships in their seismic hazard mapping program for the building code purposes and the epistemic uncertainty covered by the five NGA relationships and the GMPE uncertainty used in this PSHA.

3.1.3.2 Uncertainty Regarding Strike-slip and Blind Thrust Sources

As discussed in Sections 1 and 2, the seismic sources used in this PSHA consisted of the pertinent time-independent portion of the seismic source fault characterization in UCERF 2 (WGCEP, 2008). For SONGS, the most important seismic source fault in this PSHA’s base case set is the NI/RC source, which was also reflected in the 1995 PSHA (SCE, 1995) and a weighted NI/RC and OBT in the 2001 PSHA (SCE, 2001). Since the 2001 PSHA, the OBT has been re-characterized, and new weights have been assigned to the NI/RC (strike-slip) and OBT (blind thrust) models as recommended by the seismic source integration team. Based on the evaluation of the uncertainties associated with both models as discussed in Section 2, the numerically calculated average weights applied to the NI/RC model and the OBT model for use in the PSHA are: 88% and 12% for the strike-slip model and blind thrust end-member models, respectively. The PSHA utilized the above weights applied to the logic trees developed for the NI/RC model as shown

on Figure 2-5 and for the OBT as shown on Figure 2-12. These analysis results are, therefore, provided for a single case and referred to as the "2010 PSHA" results.

3.1.3.3 Recurrence Relationships

The recurrence relationships used for the NI/RC source followed UCERF 2 (WGCEP, 2008) and involved using the characteristic recurrence relationship of Youngs and Coppersmith (1985) with a 2/3 weight and the truncated exponential relationship of Molnar (1979) and Anderson (1979) with a 1/3 weight. For the hypothesized OBT source, a comparison of the recurrence model with the available seismicity data presented in Appendix B indicates that using only the characteristic recurrence relationship is more appropriate.

3.2 PSHA Results

The 2010 PSHA results are presented in terms of hazard curves relating spectral acceleration to annual frequency of exceedance on Figure 3-1 for PGA, 25 Hz, 10 Hz, and 5 Hz; similar results are presented on Figure 3-2 for 3.33 Hz, 2.5 Hz, 2 Hz, and 1 Hz. The 2010 PSHA results are also listed in Table 3-2.

3.2.1 Effects of Seismic Sources

The contributions to the total seismic hazard at the SONGS site from various seismic sources are presented for the 2010 PSHA results on Figures 3-3 and 3-4 corresponding to PGA and 1 Hz, respectively.

As shown on Figures 3-3 and 3-4 for the 2010 PSHA results, the NI/RC-OBT source contributes the most to the total hazard for annual frequency of exceedance less than about 10^{-3} for PGA and 1 Hz. For the higher annual frequency of exceedance, the San Jacinto source, the Southern San Andreas source, and, to a lesser degree, the Elsinore source start to contribute more than the NI/RC source.

3.2.2 Deaggregation Results

Figure 3-5 shows the results of deaggregation for the 2010 PSHA results for a RP of 475 years at PGA and 1 Hz; similarly, Figure 3-6 shows the results of deaggregation for a RP of 2,475 years at PGA and 1 Hz. The RP values of 475 and 2,475 years were selected to correspond to numbers often used in current building codes. For the 2010 PSHA results at 475 year RP, the PGA shaking at SONGS is primarily associated with the NI/RC-OBT source with moment magnitude falling in the 6.5 to 7.5 bin at a distance falling in the 5 to 10 km bin, whereas the 1 Hz shaking is somewhat more controlled by the San Jacinto, South San Andreas, and Elsinore faults with moment magnitude falling in the 7 to 8 bin at a distance falling in the 30 to 100 km bin. At 2,475 year RP, however, the ground motion at the SONGS site is dominated by the NI/RC-OBT source with moment magnitude falling in the 6.5 to 7.5 bin at a distance falling in the 5 to 10 km bin.

3.2.3 Comparison with 1995 PSHA Results

The "weighted hazard curve," presented previously (SCE, 1995 and 2001), shows the relationship between the weighted spectral acceleration values and annual frequency of exceedance. At each annual frequency of exceedance value evaluated, the weighted spectral values were obtained as follows: spectral accelerations at frequencies 1 Hz and 10 Hz are multiplied by $\frac{1}{2}$ and added to the sum of spectral accelerations at frequencies 5 Hz and 2.5 Hz with the resulting sum divided by 3.

**SAN ONOFRE NUCLEAR GENERATING STATION
SEISMIC HAZARD ASSESSMENT PROGRAM
2010 PROBABILISTIC SEISMIC HAZARD ANALYSIS REPORT**

The weighted hazard curves corresponding to the 2010 PSHA and 1995 PSHA results are presented on Figure 3-7. The results shown on Figure 3-7 indicate that the 2010 PSHA results are lower compared to the 1995 PSHA results throughout the range shown. These weighted hazard curves are also tabulated in Table 3-3.

Table 3-1: NGA Relationships and Related Parameters used in PSHA

NGA	Epistemic Weight	Subsurface Parameters [†]		
		V_{s30} [*]	$Z_{1.0\text{-km/s}}$ ^{**}	$Z_{2.5\text{-km/s}}$ ^{***}
Abrahamson & Silva (2008)	0.20	500-m/s ^{****}	0.31-km	3.35-km
Boore & Atkinson (2008)	0.20			
Campbell & Bozorgnia (2008)	0.20			
Chiou & Youngs (2008)	0.20			
Idriss (2008)	0.20			

Notes:

- [†] Used as needed in each NGA relationship.
- ^{*} V_{s30} is the average shear wave velocity in the upper 30 meters of a soil profile.
- ^{**} $Z_{1.0\text{-km/s}}$ is the depth at which the shear wave velocity is 1.0 kilometers per second (km/s).
- ^{***} $Z_{2.5\text{-km/s}}$ is the depth at which the shear wave velocity is 2.5 km/s.
- ^{****} m/s is meters per second.

Table 3-2: Mean Horizontal Ground Motions (g) at Various Frequencies of Exceedance for 2010 PSHA

Annual Frequency of Exceedance	Average Return Period	Spectral Acceleration - g*								Weighted**
		PGA	25-Hz	10-Hz	5-Hz	3.33-Hz	2.5-Hz	2-Hz	1-Hz	
1.00E-04	10,000	0.778	0.936	1.489	1.895	1.832	1.673	1.456	0.852	1.579
2.00E-04	5,000	0.618	0.736	1.178	1.477	1.413	1.284	1.131	0.661	1.227
5.00E-04	2,000	0.430	0.510	0.813	1.019	0.970	0.875	0.776	0.463	0.844
1.00E-03	1,000	0.318	0.372	0.593	0.746	0.716	0.638	0.576	0.353	0.619
2.00E-03	500	0.233	0.269	0.426	0.542	0.525	0.476	0.422	0.266	0.455
5.00E-03	200	0.152	0.176	0.272	0.356	0.348	0.314	0.280	0.176	0.298
1.00E-02	100	0.108	0.124	0.191	0.251	0.248	0.223	0.198	0.123	0.211
2.11E-03	475	0.227	0.263	0.415	0.530	0.515	0.464	0.413	0.261	0.444
4.04E-04	2,475	0.472	0.554	0.895	1.111	1.056	0.949	0.849	0.501	0.920

Notes: * Spectral Accelerations were interpolated at the provided annual frequencies of exceedance

** Weighted Spectral Acceleration (Sa) is determined as follows:

$$\text{Weighted Sa} = (0.5 * \text{Sa}_{10\text{-Hz}} + \text{Sa}_{5\text{-Hz}} + \text{Sa}_{2.5\text{-Hz}} + 0.5 * \text{Sa}_{1\text{-Hz}}) / 3$$

where $\text{Sa}_{x\text{-Hz}}$ is the spectral acceleration at x-Hz

**SAN ONOFRE NUCLEAR GENERATING STATION
SEISMIC HAZARD ASSESSMENT PROGRAM
2010 PROBABILISTIC SEISMIC HAZARD ANALYSIS REPORT**

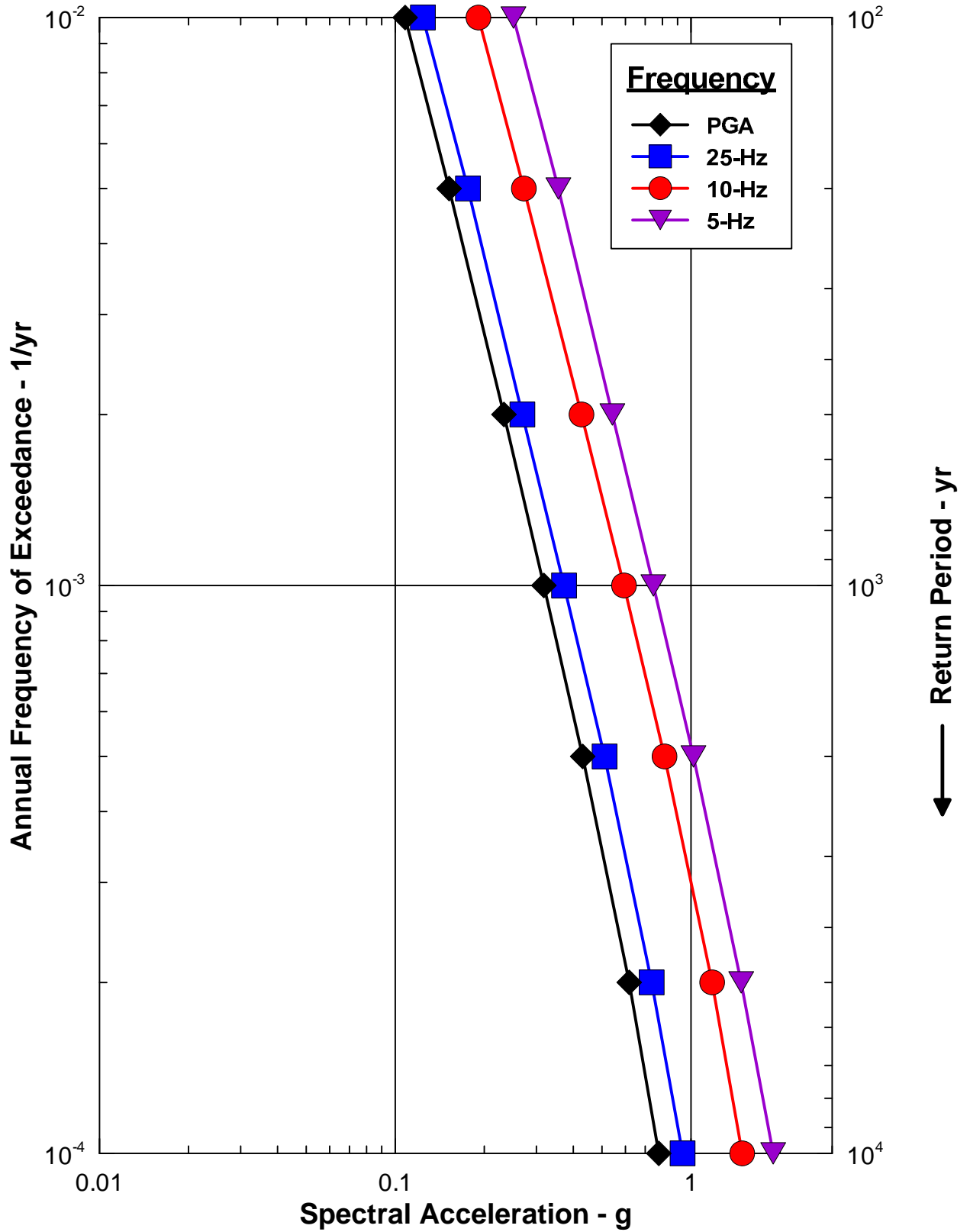
Table 3-3: Comparison of Weighted Hazard Curves 2010 PSHA and 1995 PSHA

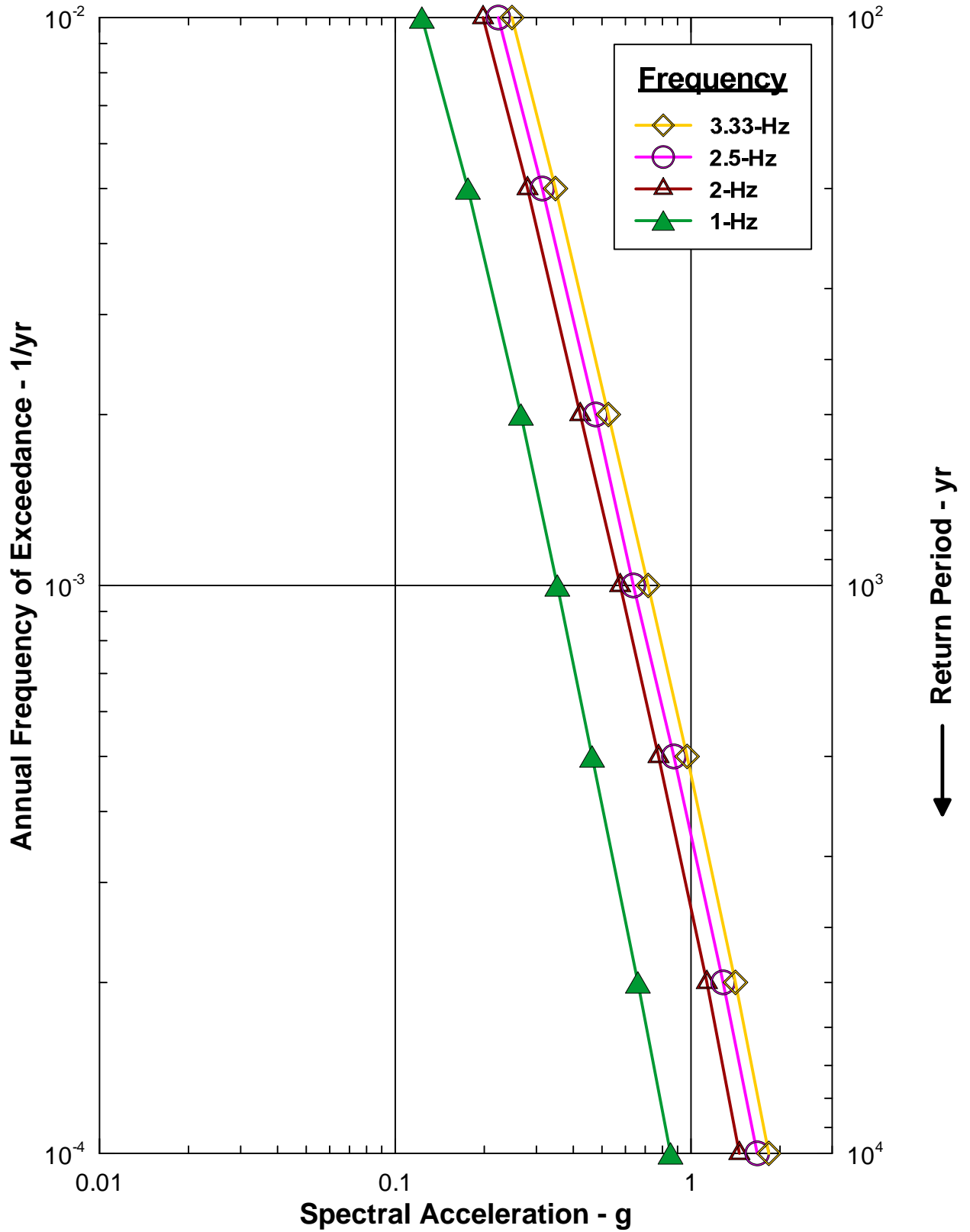
Annual Frequency of Exceedance*	Average Return Period	Weighted Spectral Acceleration – g**	
		2010 PSHA	1995 PSHA***
1.00E-04	10,000	1.579	1.656
2.00E-04	5,000	1.227	1.407
5.00E-04	2,000	0.844	1.015
1.00E-03	1,000	0.619	0.884
2.00E-03	500	0.455	0.675
5.00E-03	200	0.298	0.430
1.00E-02	100	0.211	0.310
2.11E-03	475	0.444	0.655
4.04E-04	2,475	0.920	1.077

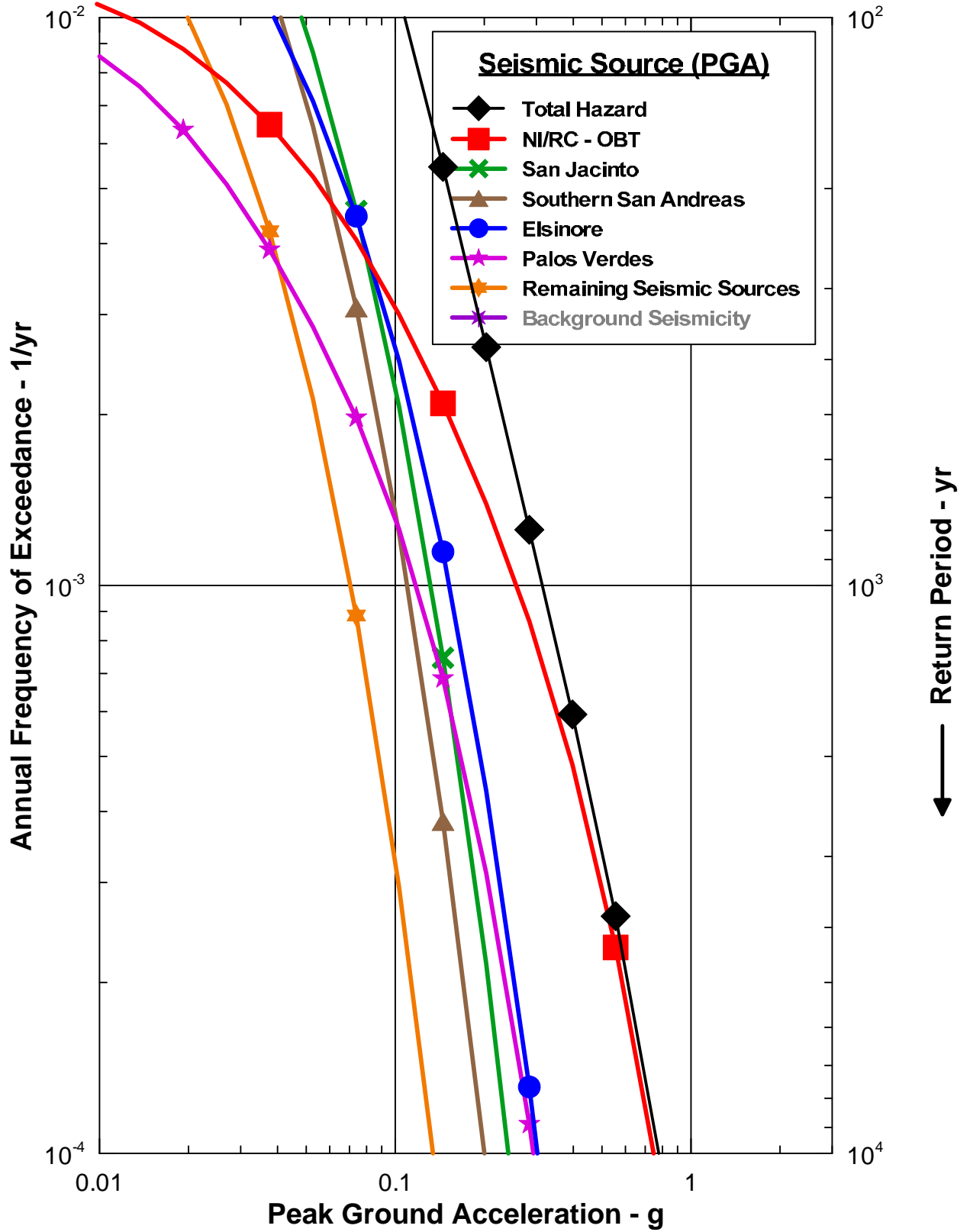
Notes:

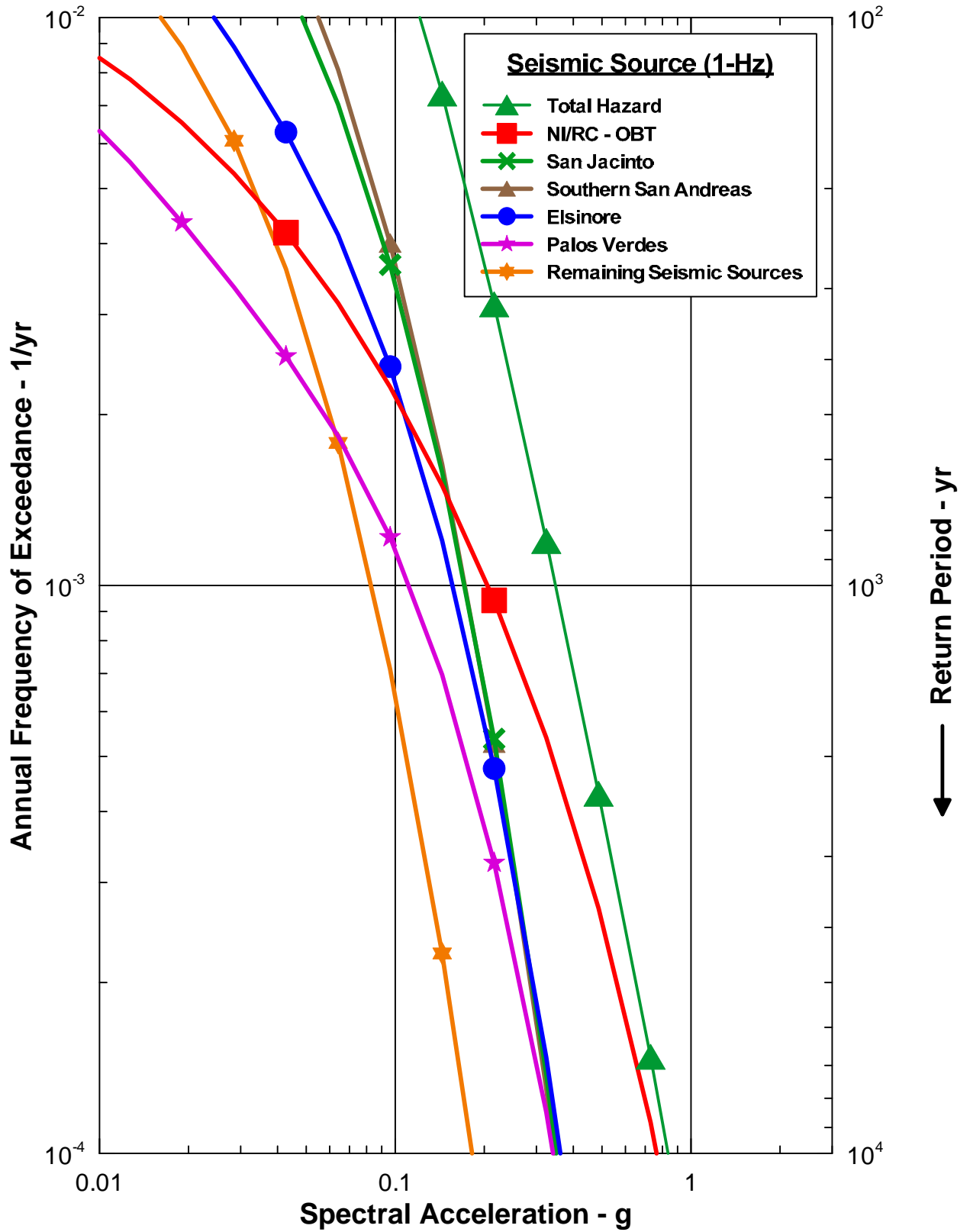
- * Spectral Accelerations were interpolated at the provided annual frequencies of exceedance
- ** Weighted Spectral Acceleration (Sa) is determined as follows:

$$\text{Weighted Sa} = (0.5 \cdot \text{Sa}_{10\text{-Hz}} + \text{Sa}_{5\text{-Hz}} + \text{Sa}_{2.5\text{-Hz}} + 0.5 \cdot \text{Sa}_{1\text{-Hz}}) / 3$$
 where $\text{Sa}_{x\text{-Hz}}$ is the spectral acceleration at x-Hz
- *** Spectral Acceleration not calculated for annual frequency of exceedance greater than 1.00E-02 in 1995 results.

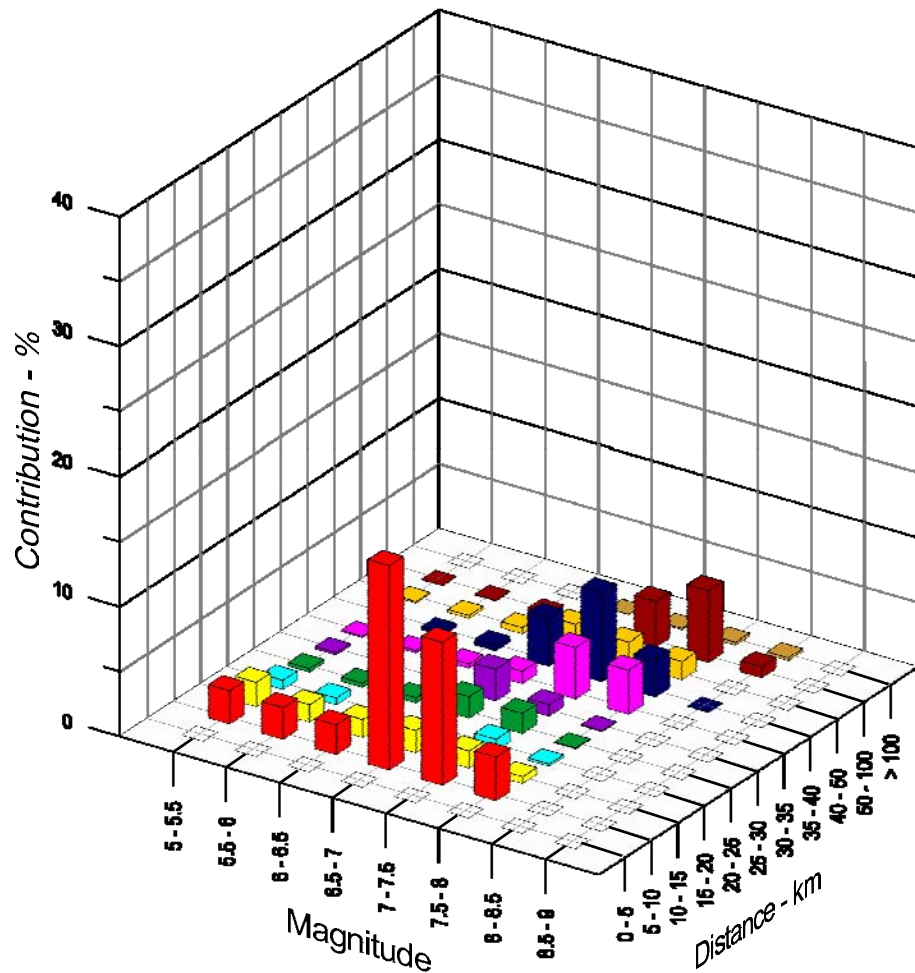




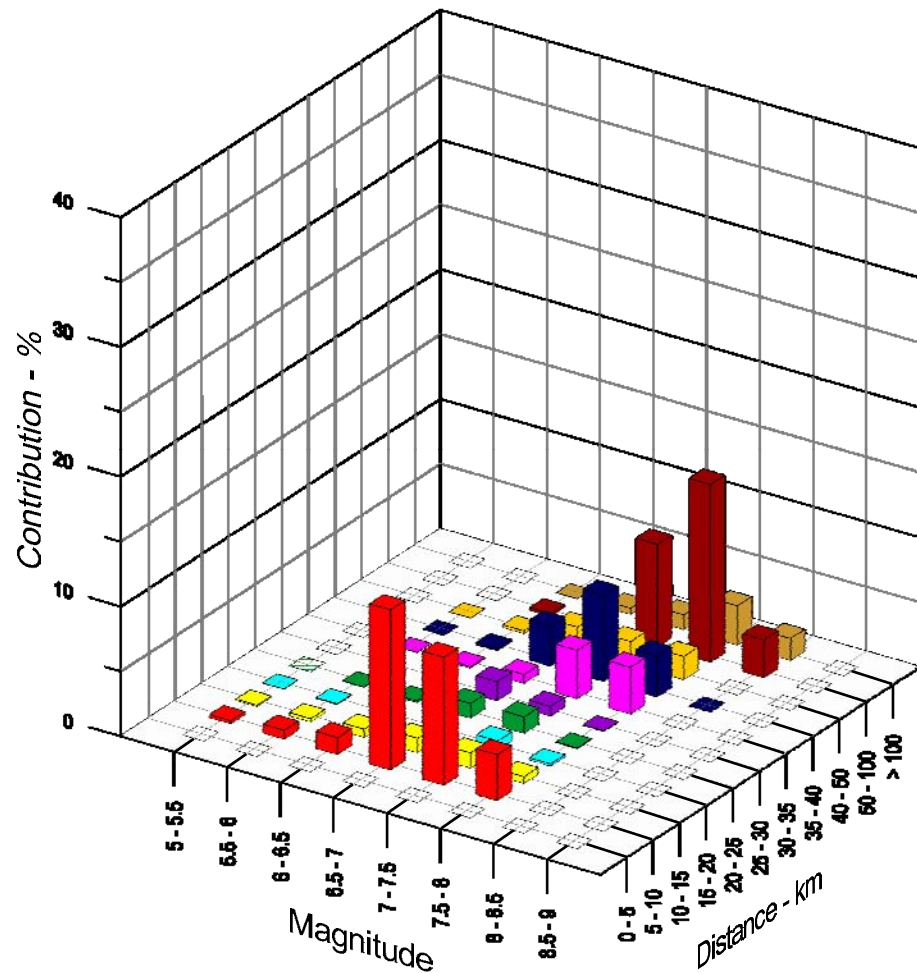




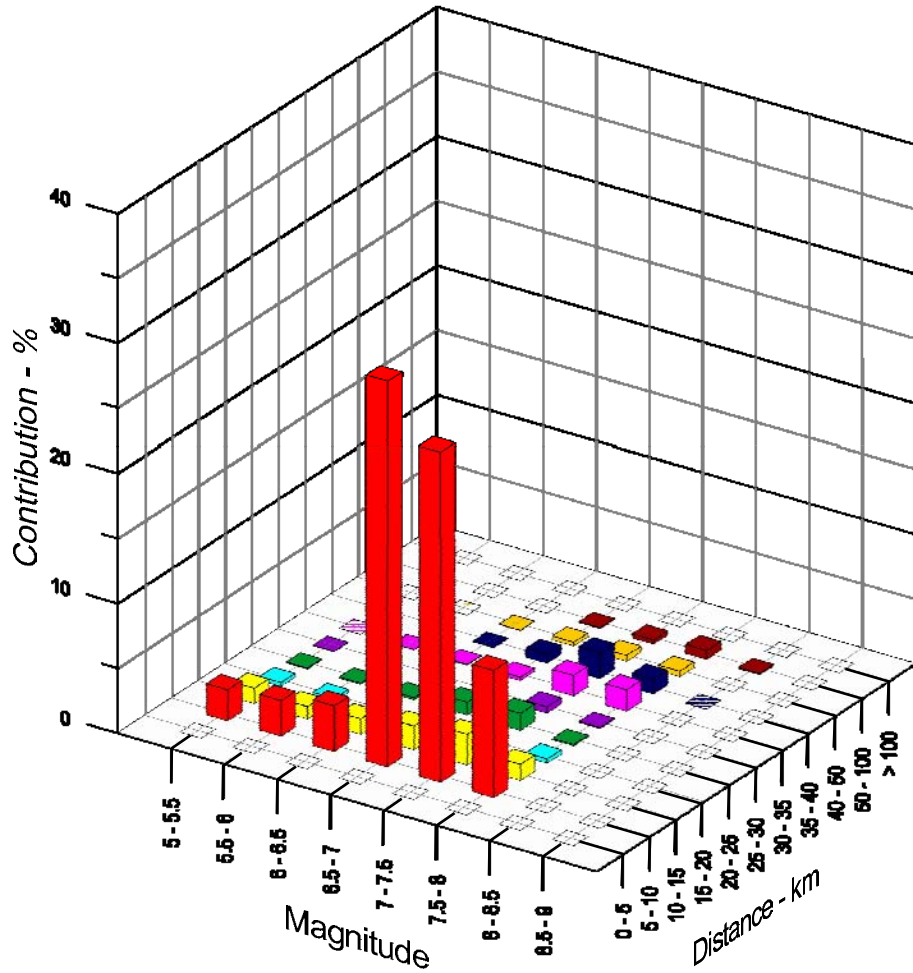
PGA



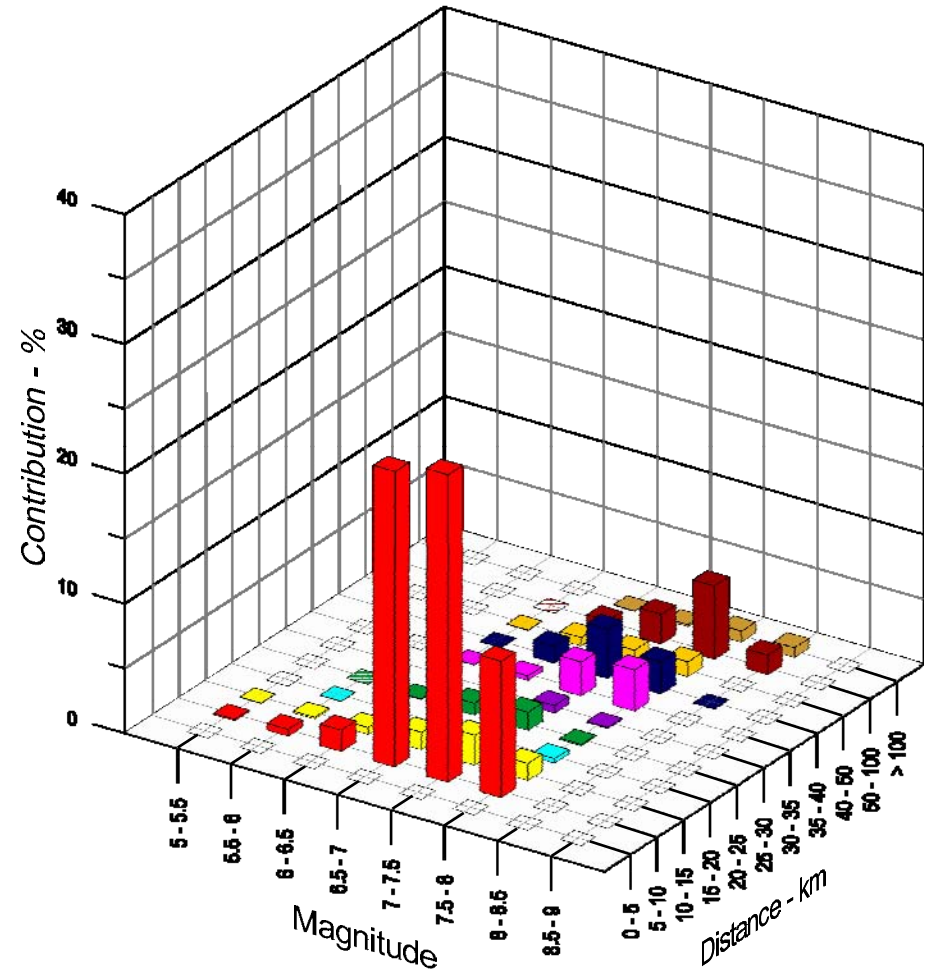
1-Hz

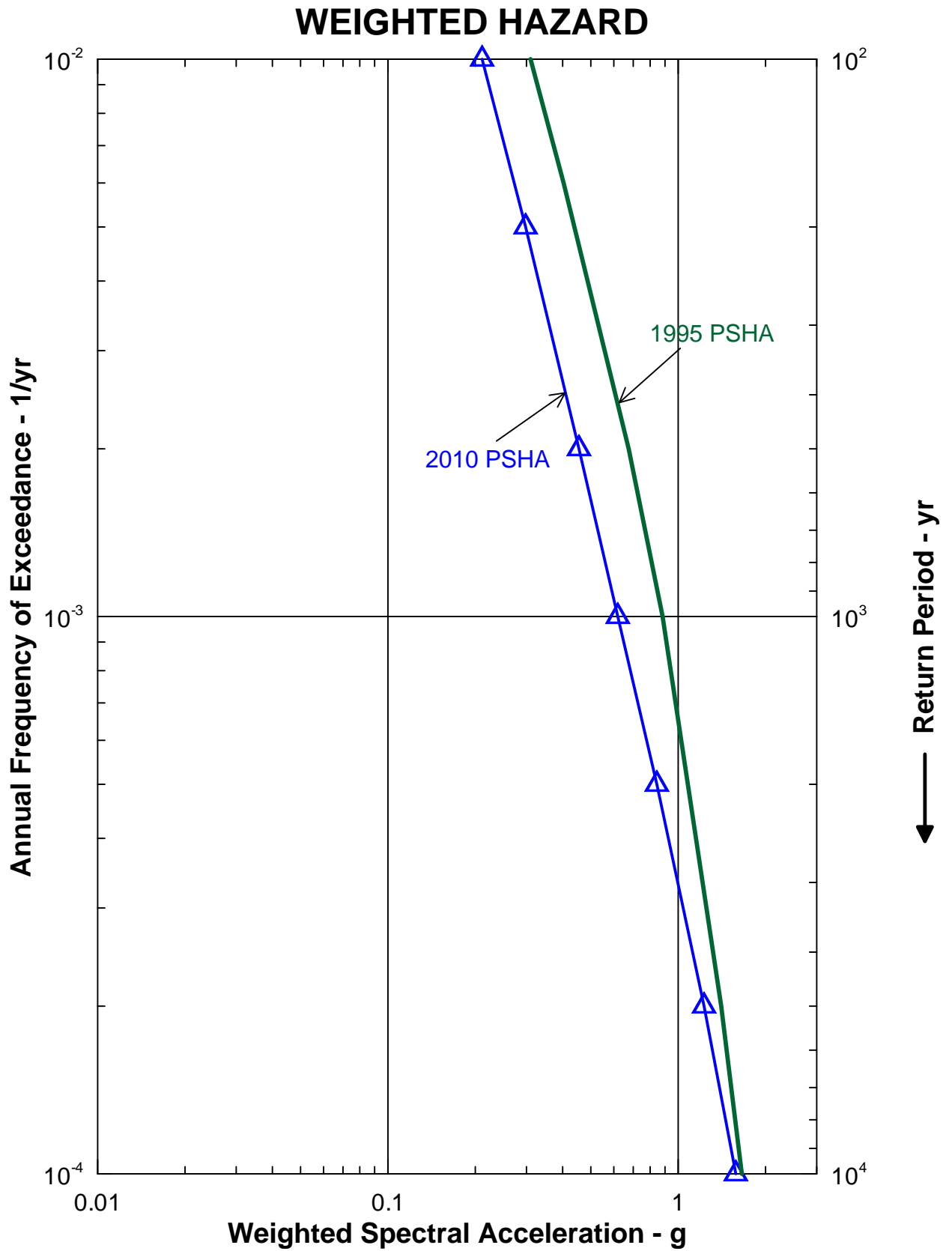


PGA



1-Hz





4.0 SUMMARY AND CONCLUSIONS

This seismic hazard assessment was completed to evaluate if recent available information has affected the seismic hazard at SONGS. A PSHA was performed utilizing available and regionally relevant seismic geology and seismology information (in particular, the recently released UCERF 2 [WGCEP, 2008], as well as discussions with current academic and USGS researchers) and the recently released five “Next Generation of Ground-Motion Attenuation Models” (NGA, 2008).

On the basis of this analysis, the following conclusions were reached:

- The two fault sources that contribute most to the ground motion hazard at SONGS are the NI/RC Fault Zone, which was the primary source fault governing the licensing of SONGS in the early 1980s, and the recently hypothesized OBT Fault of Rivero et al. (2000) and Rivero (2004). To appropriately represent the generally accepted NI/RC Fault Zone and the recently hypothesized OBT Fault in the 2010 PSHA, the end-member models associated with the NI/RC Fault Zone and OBT were evaluated as described in Section 2 of the report. The relative weights of 88% and 12% were assigned to the NI/RC Fault Zone and the hypothesized OBT, respectively, by the seismic source integration team. The weights are based on the consideration of a number of technical arguments given in the text.
- The mean seismic hazard curves presented on Figures 3-1 and 3-2 are assigned to the combined strike-slip and blind thrust end-member models. The NGA relationships (NGA, 2008) were used in performing this PSHA. This seismic hazard evaluation was limited to annual frequencies of exceedance greater than 10^{-4} . A 10^{-4} annual frequency of exceedance is equivalent to a RP of 10,000 years. At annual frequencies of exceedance lower than 10^{-4} , some issues are to be addressed that potentially could affect the calculated seismic hazard results. These issues consist of those associated with dispersions, i.e., epistemic and aleatory uncertainties in seismic source characterization and ground motion characterization models including the GMPE epistemic uncertainty; and those associated with nonlinear behavior of soils at the site. These issues will be addressed as part of the SONGS on-going seismic hazard program.
- The weighted hazard curves shown on Figure 3-7 indicate that the 2010 PSHA results are lower compared to the 1995 PSHA results throughout the range shown. These weighted hazard curves are also tabulated in Table 3-3.

5.0 REFERENCES

5.1 Publicly Available Publications and Data

Annotated bibliographies of pertinent publications provided in Appendix A, Attachment A-1, are denoted with an asterisk.

Abrahamson, N. and Silva, W., 2008, Summary of the Abrahamson & Silva NGA ground-motion relations: *Earthquake Spectra*, v. 24, no. 1, p. 67-97.

Allmendinger, R.W., 1998, Inverse and forward numerical modeling of trishear fault-propagation folds: *Tectonics*, v. 17, no. 4, p. 640-656.

Anderson, J.G., 1979, Estimating the seismicity from geological structure for seismic risk studies: *Bulletin of the Seismological Society of America*, v. 69, p. 135-158.

Argus, D.F., and Gordon, R.G., 1991, Current Sierra Nevada-North America motion from very long baseline interferometry: implications for the kinematics of the western United States: *Geology*, v. 19, p. 1085-1088.

*Astiz, L., and Shearer, P.M., 2000, Earthquake locations in the Inner Continental Borderland, offshore Southern California: *Bulletin of the Seismological Society of America*, v. 90, no. 2, p. 425-449.

Atwater, T., 1998, Plate tectonic history of southern California with emphasis on the western Transverse Ranges and Santa Rosa Island, *in* Weigand, P. W., ed., *Contributions to the geology of the Northern Channel Islands, Southern California: American Association of Petroleum Geologists, Pacific Section, MP 45*, p. 1-8.

Atwater, T., and Stock, J., 1998, Pacific-North America plate tectonics of the Neogene southwestern United States—an update: *International Geological Review*, v. 40, p. 375-402.

Axen, G J., and Fletcher, J.M., 1998, Late Miocene-Pleistocene extensional faulting, northern Gulf of California, Mexico and Salton Trough, California: *International Geological Review*, v. 40, p. 217-244.

Barrows, A.G., 1974, A review of the geology and earthquake history of the Newport–Inglewood Structural Zone, southern California, California Division of Mines and Geology, Special Report 114, 115 pp.

*Bender, E.E., 2000, Late Quaternary uplift and earthquake potential of the San Joaquin Hills, southern Los Angeles basin, California – COMMENT: *Geology*, v. 28, no. 4, p. 383.

Bennett, R.A., Rodi, W., and Reilinger, R.E., 1996 Global Positioning System constraints on fault slip rates in southern California and northern Baja, Mexico: *Journal of Geophysical Research*, v. 101, p. 21,943 – 21,960.

**SAN ONOFRE NUCLEAR GENERATING STATION
SEISMIC HAZARD ASSESSMENT PROGRAM
2010 PROBABILISTIC SEISMIC HAZARD ANALYSIS REPORT**

- *Bohannon, R.G., and Geist, E., 1998, Upper crustal structure and Neogene tectonic development of the California Continental Borderland: Geological Society of America Bulletin, v. 110, n. 6, p. 779-800.
- Boore, D.M., and Atkinson, G.M., 2008, Ground-motion prediction equations for the average horizontal component of PGA, PGV, and 5%-damped PSA at spectral periods between 0.01 s and 10.0 s: Earthquake Spectra, v. 24, no. 1, p. 99-138.
- Budnitz, R.J., Apostolakis, G., Boore, D.M., Cluff, L.S., Coppersmith, K.J., Cornell, C.A., and Morris, P.A., 1997, Recommendations for Probabilistic Seismic Hazard Analysis: Guidance on Uncertainty and Use of Experts, Report NUREG/CR-6372, Lawrence Livermore National Laboratory, sponsored by the US Nuclear Regulatory Commission, US Department of Energy, and Electric Power Research Institute, 888 pp.
- California Geological Survey (CGS), 2002a, California fault parameters-Interactive fault parameter map of California, [http://www.consrv.ca.gov/cgs/rghm/psha/fault_parameters/htm/Pages/index.aspx].
- California Geological Survey (CGS), 2002b, California geomorphic provinces, Note 36, December 2002, 4 pp.
- California Spatial Information Library (CaSIL), 2006, 1° x 1° Topography DEMs, [http://www.atlas.ca.gov/download.html] extract 1 March 2010.
- California State University Monterey Bay (CSUMB), 2010, Seafloor Mapping Lab data library, accessed June 2010 from SFML website, [http://seafloor.csumb.edu/SFMLwebDATA.htm].
- Campbell, K.W., and Bozorgnia, Y., 2008, NGA ground motion model for the geometric mean horizontal component of PGA, PGV, PGD and 5% damped linear elastic response spectra for periods ranging from 0.01 to 10 s: Earthquake Spectra, v. 24, no. 1, p. 139-171.
- *Campbell, B.A., Sorlien, C.C., Cormier, M., and Alward, W.S., 2009, Quaternary deformation related to 3D geometry of the Carlsbad fault, offshore San Clemente to San Diego [abstract]: Southern California Earthquake Center Proceedings and Abstracts, 12–16 September 2009, v. 19, p. 263.
- Cande, S.C., and Kent, D.V., 1995, Revised calibration of the geomagnetic polarity timescale for the late Cretaceous and Cenozoic: Journal of Geophysical Research, v. 100, no. B4, p. 6093-6095.
- Cao, T., Bryant, W.A., Rowshandel, B., Branum, D., and Wills, C.J., 2003, The revised 2002 California probabilistic seismic hazard maps June 2003: California Geological Survey, [http://www.consrv.ca.gov/cgs/rghm/psha/fault_parameters/pdf/2002_CA_Hazard_Maps.pdf].
- Chiou, B.S.-J., and Youngs, R.R., 2008, An NGA model for the average horizontal component of peak ground motion and response spectra: Earthquake Spectra, v. 24, no. 1, p. 173-215.
- Clark, M.M., 1972, Surface rupture along the Coyote Creek Fault: US Geological Survey Professional Paper 787, p. 55-86.

**SAN ONOFRE NUCLEAR GENERATING STATION
SEISMIC HAZARD ASSESSMENT PROGRAM
2010 PROBABILISTIC SEISMIC HAZARD ANALYSIS REPORT**

- Clark, D.H., Hall, N.T., Hamilton, D.H., and Heck, R.G., 1991. Structural analysis of late Neogene deformation in the central offshore Santa Maria Basin, California: *Journal of Geophysical Research*, v. 96, no.B4, p. 6435–6457.
- *Conrad, J.E., Ryan, H.F., and Sliter, R.W., 2010, Tracing active faulting in the Inner Continental Borderland, Southern California, using new high-resolution seismic reflection and bathymetric data [abstract]: *Seismological Society of America 2010 Annual Meeting, Seismological Research Letters*, v.81, no. 2, p. 347.
- *Crouch, J.K., and Suppe, J., 1993, Late Cenozoic tectonic evolution of the Los Angeles basin and Inner California Borderland: A model for core complex-like crustal extension: *Geological Society of America Bulletin*, v. 105, p. 1415-1434.
- Dames & Moore, 1970, Seismic and foundation studies, proposed units 2 and 3, San Onofre Nuclear Generating Station, for Southern California Edison, 15 April 1970.
- DeMets, C., and Dixon, T.H., 1999, New kinematic models for Pacific-North America motion from 3 Ma to present, I: evidence for steady motion and biases in the NUVEL-1A model: *Geophysical Research Letters*, v. 26, no. 13, p. 1921-1924.
- Dorsey, R.J., and Janecke, S.U., 2002, Late Miocene to Pleistocene West Salton detachment fault and basin evolution, southern California: new insights [abstract]: *Geological Society of America Abstracts with Programs*, v. 34, no. 248.
- *Ehlig, P.L., 1977, Geologic report on the area adjacent to the San Onofre Nuclear Generating Station northwestern San Diego County, CA, for Southern California Edison Company, 31 September 1977, 32 pp.
- Erslev, E., 1991, Trishear fault-propagation folding: *Geology*, v. 19, p. 617-620.
- Fialko, Y., 2006, Interseismic strain accumulation and the earthquake potential on the southern San Andreas fault system: *Nature*, v. 441, p. 968- 971, doi: 10.1038/nature04797.
- *Fischer, P.J. and Mills, G.I., 1991, The offshore Newport-Inglewood – Rose Canyon fault zone, California: structure, segmentation and tectonics *in* Abbott, P.L., and Elliott, W.J., eds., *Environmental Perils San Diego Region*: San Diego, San Diego Association of Geologists, p. 17-36.
- Fisher, M.A., 2009, Introduction to geologic hazards of offshore southern California *in* Lee, H.J., and Normark, W.R., eds., *Earth and Science in the Urban Ocean: The Southern California Continental Borderland*: Geological Society of America Special Paper 454, p. 227-228, doi: 10.1130/2009.2454(4.1).
- Fisher, M.A., Langenheim, V.E., Nicholson, C., Ryan, H.F., and Sliter, R.W., 2009a, Recent developments in understanding the tectonic evolution of the southern California offshore area: implications for earthquake-hazard analysis *in* Lee, H.J., and Normark, W.R., eds., *Earth and Science in the Urban Ocean: The Southern California Continental Borderland*: Geological Society of America Special Paper 454, p. 229-250, doi: 10.1130/2009.2454(4.2).

**SAN ONOFRE NUCLEAR GENERATING STATION
SEISMIC HAZARD ASSESSMENT PROGRAM
2010 PROBABILISTIC SEISMIC HAZARD ANALYSIS REPORT**

- Fisher, M.A., Sorlien, C.C., and Sliter, R.W., 2009b, Potential earthquake faults offshore southern California, from the eastern Santa Barbara Channel south to Dana Point *in* Lee, H.J., and Normark, W.R., eds., *Earth and Science in the Urban Ocean: The Southern California Continental Borderland: Geological Society of America Special Paper 454*, p. 271-290, doi: 10.1130/2009.2454(4.4).
- Franzen, S., Lew, M., and Elliott, P.J., 1998, Multiple investigation methods for fault rupture hazard evaluation, *in* Robertson, and Mayne, eds., *Geotechnical Site Characterization*, Balkema, Rotterdam, ISBN 90 5410 939 4, p. 139-144.
- Freeman, T.S., Heath, E.G., Guptill, P.D., and Waggoner, J.T., 1992, Seismic hazard assessment, Newport-Inglewood fault zone, *in* *Engineering Geology Practice in Southern California*, Special Publication, no. 4, Association of Engineering Geologists, Southern California Section, p. 211-231.
- Glover, E.S., 1876, Bird's Eye View of San Diego, California. Map published by Schneider and Kueppers, San Diego.
- *Grant, L.B., and Shearer, P.M., 2004, Activity of the offshore Newport-Inglewood Rose Canyon Fault Zone, coastal southern California, from relocated microseismicity: *Bulletin of the Seismological Society of America*, v. 94, no. 2, p. 747-752.
- *Grant, L.B., and Rockwell, T.K., 2002, A northward propagating earthquake sequence in coastal southern California?: *Seismological Research Letters*, v. 73, no. 4, p. 461-469.
- *Grant, L.B., Ballenger, L.J., and Runnerstrom, E.E., 2002, Coastal uplift of the San Joaquin Hills, southern Los Angeles basin, California, by a large earthquake since A.D. 1635: *Bulletin of the Seismological Society of America*, v. 92, no. 2, p. 590-599.
- *Grant, L.B., Mueller, K.J., Gath, E.M., and Munro, R., 2000, Late Quaternary uplift and earthquake potential of the San Joaquin Hills, southern Los Angeles basin, California – REPLY: *Geology*, v. 28, no. 4, p. 384.
- *Grant, L.B., Mueller, K.J., Gath, E.M., Cheng, H., Edwards, R.L., Munro, R., and Kennedy, G., 1999, Late Quaternary uplift and earthquake potential of the San Joaquin Hills, southern Los Angeles basin, California: *Geology*, v. 27, p. 1031-1034.
- Grant, L.B., Waggoner, J.T., Rockwell, T.K., and von Stein, C., 1997, Paleoseismicity of the north branch of the Newport-Inglewood fault zone in Huntington Beach, California, from Cone Penetrometer Test data: *Bulletin of the Seismological Society of America*, v. 94, no. 2, p. 277-293.
- Greene, H.G., Bailey, K.A., Clarke, S.H., Ziony, J.I., and Kennedy, M.P., 1979, Implications of fault patterns of the Inner California Continental Borderland between San Pedro and San Diego *in* Abbott, P.L., and Elliott, W.J., eds., *Earthquakes and Other Perils, San Diego Region*, San Diego Association of Geologists, p. 21-29.
- Hanks, T.C., and Kanamori, H., 1979, A moment magnitude scale: *Journal of Geophysical Research*, v. 84, no. B5, p. 2348-2350.



**SAN ONOFRE NUCLEAR GENERATING STATION
SEISMIC HAZARD ASSESSMENT PROGRAM
2010 PROBABILISTIC SEISMIC HAZARD ANALYSIS REPORT**

- Hanson, K.L., Angell, M., Foxall, W., and Rietman, J., 2002, Evaluation of seismic source characterization of models for the inner borderlands of southern California [abstract]: Eos (Transactions, American Geophysical Union) v. 83, no. 47, Fall Meeting Supplement, abstract S21A-0973, p. F1067.
- Harding, T.P., 1973, Newport-Inglewood trend, California – an example of wrenching style of deformation: American Association of Petroleum Geologists Bulletin, v. 57, no. 1, p. 97-116.
- *Hauksson, E., 1987, Seismotectonics of the Newport-Inglewood fault zone in the Los Angeles basin, southern California: Bulletin of the Seismological Society of America, v. 77, no. 2, p. 539-561.
- *Hauksson, E., and Gross, S., 1991, Source parameters of the 1933 Long Beach earthquake: Bulletin of the Seismological Society of America, v. 81, no. 1, p. 81-98.
- Hauksson, E., and Jones, L.M., 1988, The July 1986 Oceanside ($M_L = 5.3$) earthquake sequence in the Continental Borderland, southern California: Bulletin of the Seismological Society of America, v. 76, no. 6, p. 1885-1906.
- Idriss, I.M., 2008, An NGA empirical model for estimating the horizontal spectral values generated by shallow crustal earthquakes: Earthquake Spectra, v. 74, no. 1, p. 217-242.
- Jennings, C.W., 1994, Fault activity map of California and adjacent areas with location and ages of recent volcanic eruptions: California Department of Conservation, Division of Mines and Geology, Geologic Data Map Series, Map No. 6, map with explanatory text, 92 pp., scale 1:750,000.
- Kamerling, M.J., and Luyendyk, B.P., 1985, Paleomagnetism and Neogene tectonics of the northern Channel Islands, California: Journal of Geophysical Research, v. 90, p. 12,485-12,502.
- Kamerling, M.J., and Luyendyk, B.P., 1979, Tectonic rotations of the Santa Monica Mountains region, western Transverse Ranges, California, suggested by paleomagnetic vectors: Geological Society of America Bulletin, part I, v. 90, p. 331-337.
- Kennedy, M.P. and Clarke, S.H., 1996, Analysis of late Quaternary faulting in San Diego Bay and hazard to the Coronado Bridge, prepared for California Department of Transportation (Caltrans).
- Kern, J.P., 1977, Origin and history of upper Pleistocene marine terraces, San Diego, California, Geological Society of America Bulletin, v. 88, p. 1553-1566.
- *Kern, J.P., and Rockwell, T.K., 1992, Chronology and deformation of Quaternary marine shorelines, San Diego County, California *in* Kern, J.P., and Rockwell, T.K., eds., Quaternary Coasts of the United States: Marine and Lacustrine Systems, Special Publication no. 48, Society for Sedimentary Geology, 377-382.
- *Kier, G., and Mueller, K., 1999, Flexural modeling of the northern Gulf of California Rift: relating marine terrace uplift to the forebulge on a subsiding plate: Southern California Earthquake Center 1999 internship final report, 11 pp., [http://www.scec.org/education/college/internships/1999/99grant.pdf].

**SAN ONOFRE NUCLEAR GENERATING STATION
SEISMIC HAZARD ASSESSMENT PROGRAM
2010 PROBABILISTIC SEISMIC HAZARD ANALYSIS REPORT**

- Kies, R.P. and Abbott, P.L., 1983, Rhyolite clast populations and tectonics in the California continental borderland: *Journal of Sedimentary Research*, v. 53, no. 2, p. 461-475.
- Klinger, R.E. and Rockwell, T.K., 1989, Flexural-slip folding along the eastern Elmore Ranch fault in the Superstition Hills earthquake sequence of November 1987: *Bulletin of the Seismological Society of America*, v. 79, no. 2, p. 297-303.
- Lajoie, K.R., Ponti, D.J., Powell, C.L., Mathieson, S.A., and Sarna-Wojcicki, A.M., 1992, Emergent marine strandlines and associated sediments, coastal California: A record of Quaternary sea-level fluctuations, vertical tectonic movements, climatic changes and coastal processes, *in* Heath, E., and Lewis, L., eds., *The regressive Pleistocene shoreline in southern California*: Santa Ana, California, South Coast Geological Society annual Field Trip guidebook 20, p. 81-104.
- Law/Crandall, Inc., 1993, Report of potential fault displacements Wastewater Treatment Plant Number 2 Huntington Beach, California for County Sanitation Districts of Orange County, 2661.30140.0001, 16 September 1993, 10 pp, 7 plates.
- Lee, H.J., Greene, G.H., Edwards, B.D., Fisher, M.A., and Normark, W.R., 2009, Submarine landslides of the southern California Borderland Point *in* Lee, H.J. and Normark, W.R., eds., *Earth and Science in the Urban Ocean: The Southern California Continental Borderland*: Geological Society of America Special Paper 454, p. 251-269, doi: 10.1130/2009.2454(4.3).
- *Legg, M.R., 1991, Developments in understanding the tectonic evolution of the California Continental Borderland: Special Publication no. 46, *Society for Sedimentary Geology*, p. 291-312.
- *Legg, M.R., Goldfinger, C., Kamerling, M.J., Chaytor, J.D., and Einstein, D.E., 2007, Morphology, structure and evolution of California Continental Borderland restraining bends *in* Cunningham, W.D., and Mann, P., eds., *Tectonics of Strike-Slip Restraining and Releasing Bends*: Geological Society, London, Special Publications, 290, p. 143-168, doi: 10.1144/SP290.3.
- Legg, M.R., Kamerling, M.J., and Francis, R.D., 2004, Termination of strike-slip faults at convergence zones within continental transform boundaries: examples from the California Continental Borderland *in* Grocott, J., McCaffrey, K.J.W., Taylor, G., and Tikoff, B., eds., *Vertical Coupling and Decoupling in the Lithosphere*, Geological Society of London, p. 65-82.
- Leon, L.A., Dolan, J.F., Shaw, J.H., and Pratt, T.L., 2009, Evidence for large Holocene earthquakes on the Compton thrust fault, Los Angeles, California: *Journal of Geophysical Research*, v. 114, no. B12305, 14 pp., doi: 10.1029/2008JB006129.
- Lindvall, S.C., and Rockwell, T.K., 1995, Holocene activity of the Rose Canyon fault zone in San Diego, California: *Journal of Geophysical Research*, v. 100, no. B12, p. 24,121-24,132.
- Lutz, A.T.; Dorsey, R.J.; Housen, B.A.; and Janecke, S.U., 2006, Stratigraphic record of Pleistocene faulting and basin evolution in the Borrego Badlands, San Jacinto fault zone, southern California: *Geological Society of America Bulletin*, v. 118, p. 1377-1397.

**SAN ONOFRE NUCLEAR GENERATING STATION
SEISMIC HAZARD ASSESSMENT PROGRAM
2010 PROBABILISTIC SEISMIC HAZARD ANALYSIS REPORT**

- Medwedeff, D., 1992, Geometry and kinematics of an active, laterally propagating wedge thrust, Wheeler Ridge, California, *in* Mitra, S., and Fischer, G. W., eds., *Structural geology of fold and thrust belts*: Baltimore, Maryland, Johns Hopkins University Press, p 3-28.
- Minerals Management Services (MMS), 2001, Oil and gas resources in the Pacific outer continental shelf as of January 1, 1999: an expanded update to the 1995 National Assessment of United States Oil and Gas Resources: US Department of the Interior Minerals Management Services OCS Report MMS 2001-014, February 2001, 21 pp.
- Molnar, P., 1979, Earthquake recurrence intervals and plate tectonics: *Bulletin of the Seismological Society of America*, v. 69, p. 115-133.
- Morton, D.M., and Matti, J.C., 1993, Extension and contraction within an evolving divergent strike-slip fault complex: the San Andreas and San Jacinto fault zones at their convergence in southern California. *in* Powell, R.E. Weldon, R.J., and Matti, J.C., eds., *The San Andreas Fault system: displacement, palinspastic reconstruction, and geologic evolution*, Geological Society of America Memoirs, v. 178, p. 217-230.
- Moody, J.D., and Hill, M.J., 1956, Wrench-fault tectonics: *Geological Society of America Bulletin*, v. 67, p. 1207-1246.
- *Moore, G.W., 1972, Offshore extension of the Rose Canyon fault, San Diego, California: US Geological Survey Professional Paper 800-C, C113-C116.
- Moriwaki, Y., Tan, P., and Barneich, J.A., 2002, Evaluation of alternative seismic source models using SCIGN data [abstract]: *Eos (Transactions, American Geophysical Union)* v. 83, no. 47, Fall Meeting Supplement, 19 November 2002.
- Mount, V., Suppe, J., and Hook, S., 1990, A forward modeling strategy for balancing cross sections: *American Association of Petroleum Geologist Bulletin*, v. 74, p. 521-531.
- *Mueller, K., Kier, G., Rockwell, T., and Jones, C.H., 2009, Quaternary rift flank uplift of the Peninsular Ranges in Baja and southern California by removal of mantle lithosphere: *Tectonics*, v. 28, TC5003, doi:10.1029/2007TC002227.
- Mueller, K.J., Grant, L.B., and Gath, E., 1998, Late Quaternary growth of the San Joaquin Hills anticline—a new source of blind thrust earthquakes in the Los Angeles basin [abstract]: *Seismological Society of America 1998 Annual Meeting, Seismological Research Letters*, v. 69, no. 2, p. 161-162.
- NOAA, 2008, Geophysical Data System (GEODAS) bathymetry points, Volume 1, Version 5.0.11.
- NOAA, 2001, Geophysical Data System (GEODAS) bathymetry points, Volume 1, Version 4.1.
- NGA, 2008, *Earthquake Spectra*, v. 24, no. 1, p. 1-341.
- Nicholson, C., Sorlien, C.C., Atwater, T., Crowell, J.C., and Luyendyk, B.P., 1994, Microplate capture, rotation of the western Transverse Ranges, and initiation of the San Andreas transform as a low-

**SAN ONOFRE NUCLEAR GENERATING STATION
SEISMIC HAZARD ASSESSMENT PROGRAM
2010 PROBABILISTIC SEISMIC HAZARD ANALYSIS REPORT**

angle fault system: *Geology*, v. 22, p. 491-495.

Petersen, M.D., Bryant, W.A., Cramer, C.H., Cao, T., and Reichle, M., 1996, Probabilistic seismic hazard assessment for the State of California: U.S. Geological Survey Open File Report 96-706, 19 pp.

Plesch, A., Shaw, J.H., Benson, C., Bryant, W.A., Carena, S., Cooke, M., Dolan, J., Fuis, G., Gath, E., Grant, L., Hauksson, E., Jordan, T., Kamerling, M., Legg, M., Lindvall, S., Magistrale, H., Nicholson, C., Niemi, N., Oskin, M., Perry, S., Planansky, G., Rockwell, T., Shearer, P., Sorlien, C., Suss, M. P., Suppe, J., Treiman, J., and Yeats, R., 2007, Community Fault Model (CFM) for southern California: *Bulletin of the Seismological Society of America*, v. 97, no. 6, p. 1793-1802.

Ponti, D.J., 2010, USGS investigations of stratigraphy and neotectonics of the Los Angeles basin [abstract]: US Geological Survey, 5 pp.

*Ponti, D.J., 2001, Changing deformation rates through time: insights from new Quaternary stratigraphic studies in the Los Angeles basin, California [abstract]: American Geophysical Union 2001 Fall Meeting, 10–14 December 2001, abstract #S12E-11.

*Ponti, D.J., and Ehman, K.D., 2009, A 3-D sequence-based structural model for the Quaternary Los Angeles basin, California [abstract]: Southern California Earthquake Center Proceedings and Abstracts, 12–16 September 2009, vol. 19, p. 262-263.

Rentz, P., 2010, The influence of tectonics, sea level, and sediment supply on coastal morphology in the Oceanside littoral cell, CA, unpublished M.S. Thesis: University of California, San Diego.

*Rivero, C.A., 2004, Origin of active blind-thrust faults in the southern Inner California Borderlands, unpublished Ph.D. Dissertation: Harvard University, 146 pp.

*Rivero, C., and Shaw, J.H., 2010, in press, Active folding and blind-thrust faulting induced by basin inversion processes, Inner California Borderlands: Tectonics, submitted for consideration of publication 2010, 45 pp.

*Rivero, C., and Shaw, J.H., 2005, Fault-related folding in reactivated offshore basins, California *in* Interpretations of Contractual Fault-Related Folds, An American Association of Petroleum Geologists Seismic Atlas, Studies in Geology, No. 53, Department of Earth and Planetary Sciences: Harvard University, Cambridge, MA, 3 pp.

*Rivero, C., and Shaw, J.H., 2001, 3D geometry and seismogenic potential of the Inner California Borderland blind thrusts system [abstract]: Southern California Earthquake Center Proceedings and Abstracts, 23–26 September 2001, p. 105-106.

*Rivero, C., Shaw, J.H., and Mueller, K., 2000, Oceanside and Thirtymile Bank blind thrusts: implications for earthquake hazards in coastal southern California: *Geology*, v. 28, no. 10, p. 891-894.

Rockwell, T., 2010a, The Rose Canyon Fault Zone in San Diego; Proceeding of Fifth International Conference on Recent Advances in Geotechnical Earthquake Engineering and Soil Dynamics and Symposium in Honor of Professor I.M. Idriss; Paper No. 7.06c, 9pgs.

**SAN ONOFRE NUCLEAR GENERATING STATION
SEISMIC HAZARD ASSESSMENT PROGRAM
2010 PROBABILISTIC SEISMIC HAZARD ANALYSIS REPORT**

- Rockwell, T., 2010b, The non-regularity of earthquake recurrence in California: Lessons from long paleoseismic records from the San Andreas and San Jacinto faults in southern California, and the north Anatolian fault in turkey, Proceeding of Fifth International Conference on Recent Advances *in* Geotechnical Earthquake Engineering and Soil Dynamics and Symposium in Honor of Professor I.M. Idriss, Paper No. EQ 5, 9 pp.
- Rockwell, T., 2010c, Fault hazard characterization for a transportation tunnel project in Coronado, California *in* Geotechnical Earthquake Engineering and Soil Dynamics and Symposium in Honor of Professor I.M. Idriss, Paper No. 7.02c, 13 pp.
- Rockwell, T.K. and Murbach, M., 1999, Holocene earthquake history of the Rose Canyon fault zone. USGS Award No. 1434-95-G-2613 Final Technical Report 36 pp (plus appendix).
- *Rockwell, T.K., Lindvall, S.C., Haraden, C.C., Hirabayashi, C.K., and Baker, E., 1992, Minimum Holocene slip rate for the Rose Canyon fault in San Diego, California, *in* Heath, E.G., and Lewis, W.L., eds., The Regressive Pleistocene Shoreline Coastal Southern California: South Coast Geological Society, Inc., 1992 Annual field Trip Guide Book No. 20, p. 55-64.
- Rockwell, T.K., Lindvall, S.C., Haraden, C.C., Hirabayashi, C.K., and Baker, E., 1991, Minimum Holocene slip rate for the Rose Canyon fault in San Diego, California *in* Abbott, P.L., and Elliott, W.J., eds., Environmental Perils San Diego Region: San Diego, San Diego Association of Geologists, p. 37-46.
- *Ryan, H.F., Legg, M.R., Conrad, J.E., and Sliter, R.W., 2009, Recent faulting in the Gulf of Santa Catalina: San Diego to Dana Point *in* Lee, H.J., and Normark, W.R., eds., Earth and Science in the Urban Ocean: The Southern California Continental Borderland: Geological Society of America Special Paper 454, p. 291-315, doi: 10.1130/2009.2454(4.5).
- SCE, UFSAR, San Onofre Nuclear Generating Station, Units 2 & 3, Updated Final Safety Analysis Report, submitted to the U.S. Nuclear Regulatory Commission (NRC).
- SCE, 2001, San Onofre Nuclear Generating Station Units 2 and 3 Seismic Hazard Study of Postulated Blind Thrust Faults, prepared by Geomatrix Consultants, GeoPentech, and Southern California Edison for the Nuclear Regulatory Commission, 26 December 2001, 165 pp.
- SCE, 1995, Seismic Hazard at San Onofre Nuclear Generating Station, prepared by Risk Engineering, Inc. for Southern California Edison Co., 2244 Walnut Grove Avenue, Rosemead, California 91770, 25 August 1995, 340 pp.
- SCE, 1979, Report of the Evaluation of Maximum Earthquake and Site Ground Motion Parameters Associated with the Offshore Zone of Deformation San Onofre Nuclear Generating Station, prepared by Woodward-Clyde Consultants for Southern California Edison, P.O. Box 800, Rosemead, California 91770, June 1979, 243 pp.
- SSHAC, 1997, Recommendations for probabilistic seismic hazard analysis: Guidance on uncertainty and use of experts, prepared by Senior Seismic Hazard Analysis Committee, Lawrence Livermore National Laboratory, Volume 1, Main Report, NUREG/CR-6372, UCRL-ID-122160, 280 pp.

**SAN ONOFRE NUCLEAR GENERATING STATION
SEISMIC HAZARD ASSESSMENT PROGRAM
2010 PROBABILISTIC SEISMIC HAZARD ANALYSIS REPORT**

- Schneider, C.L., Hummon, C., Yeats, R.S., and Huftile, G.L., 1996, Structural evolution of the northern Los Angeles basin, California, based on growth strata: *Tectonics*, v. 15, no. 2, p. 341-355.
- Scripps Orbit and Permanent Array Center (SOPAC), 2010, SOPAC refined velocities, accessed June 2010, from SOPAC website, [<http://sopac.ucsd.edu/cgi-bin/refinedModelVelocities.cgi>].
- Seeber, L. and Sorlien, C.C., 2000, Listric thrusts in the western Transverse Ranges, California: *Geological Society of America Bulletin*, v. 112, p. 1067-1079.
- Shaw, J., and Suppe, J., 1996, Earthquake hazards of active blind-thrust faults under the central Los Angeles basin, California: *Journal of Geophysical Research*, v. 101, no. B4, p. 8623-8642.
- Shlemon, R.J., 1987, The Cristianitos fault and Quaternary geology, San Onofre State Beach, California *in* *Geological Society of America Continental Field Guide—Cordilleran Section*, p. I126-I129.
- Shlemon, R.J., 1978, Late Quaternary rates of deformation Laguna Beach—San Onofre State Beach Orange and San Diego Counties, California, prepared by Roy J. Shlemon & Assoc. for Southern California Edison Company and San Diego Gas & Electric Company, October 1978, 31 pp.
- Shlemon, R.J., Elliott, P., and Franzen, S., 1995, Holocene displacement history of the Newport-Inglewood, north branch fault splays, Santa Ana River floodplain, Huntington Beach, California [abstract]: *Geological Society of America Abstracts with Programs 1995 Annual Meeting*, 6–9 November 1995, v. 27, no. 6, p. A-375.
- *Sliter, R.W., Ryan, H.F., and Normark, W.R., 2001, Does recent deformation at the base of slope provide evidence of a connection between the Newport-Inglewood and the Rose Canyon fault zones offshore southern California? [abstract]: *American Geophysical Union 2001 Fall Meeting*, 10–14 December 2001, abstract #S11A-0531.
- *Sorlien, C.C., Campbell, B.A., Alward, W.S., Seeber, L., Legg, M.R., and Cormier, M., 2009a, Transpression along strike-slip restraining segments vs. regional thrusting in the Inner California Continental Borderland [abstract]: *Southern California Earthquake Center Proceedings and Abstracts*, 12–16 September 2009, v. 19, p. 264.
- *Sorlien, C.C., Campbell, B.A., and Seeber, L., 2009b, Geometry, kinematics, and activity of a young mainland-dipping fold and thrust belt: Newport Beach to San Clemente, California, USDI/USGS Award No. 08HQGR0103 Final Technical Report, 25 pp.
- Sorlien, C.C., Kamerling, M.J., and Mayerson, D., 1999, Block rotation and termination of the Hosgri strike-slip fault system, California, from 3-D map restoration: *Geology*, v. 27, p. 1039-1042.
- Suppe, J., 1983. Geometry and kinematics of fault bend folding: *American Journal of Science*, v. 283, p. 684–721.
- Suppe, J., and Medwedeff, D.A., 1990, Geometry and kinematics of fault-propagation folding: *Eclogae Geologicae Helvetiae*, v. 83, p. 409-454.

**SAN ONOFRE NUCLEAR GENERATING STATION
SEISMIC HAZARD ASSESSMENT PROGRAM
2010 PROBABILISTIC SEISMIC HAZARD ANALYSIS REPORT**

- Thomas, P., Wong, I., and Abrahamson, N., 2010, Verification of probabilistic seismic hazard analysis computer programs: PEER Report 2010/106, Pacific Earthquake Engineering Research Center, College of Engineering, University of California, Berkeley, May 2010, 176 pp.
- Treiman, J., 1993, The Rose Canyon fault zone, southern California: California Division of Mines and Geology, Open File Report 93-02, 45 pp.
- USGS, 2009, Quaternary fault and fold database for the United States, accessed 25 October 2010, from USGS website, [<http://earthquakes.usgs.gov/regional/qfaults/>].
- USGS, 2008, Documentation for the 2008 update of the United States National Seismic Hazard Maps, prepared by Petersen, M. D., Frankel, A. D., Harmsen, S. C., Mueller, C. S., Hallar, K. M., Wheeler, R. L.,
- Wesson, R. L., Zeng, Y., Boyd, O. S., Perkins, D. M., Luco, N., Field, E. H., Wills, C. J., and Rukstales, K. S., U.S. Geological Survey Open File Report 2008-1128, 128 pp.
- WGCEP, 2008, The Uniform California Earthquake Rupture Forecast, Version 2 (UCERF 2), prepared by 2007 Working Group on California Earthquake Probabilities: US Geological Survey Open File Report 2007-1437 and California Geological Survey Special Report 203, [<http://pubs.usgs.gov/of/2007/1497/>].
- WGCEP, 1995, Seismic hazards in southern California: probable earthquakes, 1994-2024: Bulletin of the Seismological Society of America, v. 85, p. 379-439.
- Weichert, D.H., 1980, Estimation of the earthquake recurrence parameters for unequal observation periods for different magnitudes: Bulletin of the Seismological Society of America, v. 70, no. 4, p. 1337-1346.
- Wells, D.L., and Coppersmith, K. J., 1994, New empirical relationships among the magnitude, rupture length, rupture width, rupture area, and surface displacement: Bulletin of the Seismological Society of America, v. 84, p. 974-1002.
- Wentworth, C.M., 1990, Structure of the Coalinga region and thrust origin of the earthquake, in The Coalinga, California earthquake of May 2, 1983: US Geological Survey Professional Paper 1487, p. 41-68.
- Wesnousky, S.G., 2008, Displacement and geometrical characteristics of earthquake surface ruptures: Issues and implications for seismic-hazard analysis and the process of earthquake rupture: Bulletin of the Seismological Society of America, v. 98, p. 1609-1632.
- Western Geophysical Company, 1972, Final Report: San Onofre Offshore Investigations, in SCE, 2001, SONGS Units 2 and 3 Seismic Hazard Study of Postulated Blind Thrust Faults, offshore marine reflection seismic data, Plate 2-3, 26 December 2001.
- Weston Geophysical, 1971, Seismic Velocity Measurements, San Onofre Nuclear Generating Station, in Woodward-McNeill and Associates, 1972, Material Property Studies, San Onofre Nuclear Generating Station, Appendix C, 15 March 1972.

- *Wetmore, P.H., Malservisi, R., Fletcher, J., Alsleben, H., Callihan, S., Springer, A., and González-Yajimovich, O., 2010, in review, Transtension within a restraining bend domain of a transform plate boundary: the role of block rotations and the reactivation of preexisting crustal structures: Geological Society of America Lithosphere, submitted for consideration of publication 2010, 17 pp.
- Wilcox, R.E., Harding, T.P., Seely, D.R., 1973, Basic Wrench Tectonics: American Association of Petroleum Geologists Bulletin, v. 57, no.1, p. 74-96.
- Woodward-Clyde Consultants, 1980, Response to NRC Questions San Onofre 2 & 3, Question 361.61, 4 pp., 3 figures, April 1980.
- Woodward-McNeill and Associates, 1972, Material Property Studies, San Onofre Nuclear Generating Station, Appendix E, 15 March 1972, 8 pp.
- *Wright, T.L., 1991, Structural geology and tectonic evolution of the Los Angeles basin, California *in* Biddle, K.T., ed., Active margin basins: American Association of Petroleum Geologists Memoir 52, p. 35–134.
- Yeats, R.S., 1987, Late Cenozoic structure of the Santa Susana fault zone, California: U.S. Geological Survey Professional Paper 1339, p. 137-160.
- Yeats, R.S., 1973, Newport-Inglewood fault zone, Los Angeles basin, California: American Association of Petroleum Geologists Bulletin, v. 57, no. 1, p. 117-135.
- Yerkes, R.F., 1990, Tectonic setting, in The Coalinga, California earthquake of May 2, 1983: US Geological Survey Professional Paper 1487, p. 13-22.
- Youngs, R.R., and Coppersmith, K.J., 1985, Implications of fault slip rates and earthquake recurrence models to probabilistic seismic hazard analysis: Bulletin of the Seismological Society of America, v. 75, no. 4, p. 939-964.

5.2 Personal Communication

Details of personal communication summarized in Appendix A, Attachment A-1, are denoted with an asterisk.

Abrahamson, N., 2010, personal communication.

*Ponti, D., 2010, personal communication.

*Rockwell, T., 2010, personal communication.

Rockwell, T., 2001, personal communication.

*Ryan, H., 2010, personal communication.

USGS, 2009, Harmsen, S., personal communication on 20 October 2009.

USGS, 2007, Kendrick, C., personal communication.

6.0 GLOSSARY

ALEATORY UNCERTAINTY: Uncertainty arising from or associated with the inherent, irreducible, natural randomness of a system or process

ANNUAL FREQUENCY OF EXCEEDANCE: Mean number of seismic events per year exceeding a specified value

BASE: United States Marine Corps Base at Camp Pendleton

CFM: Community Fault Model of southern California developed by Plesch et al. (2007)¹

CGS: California Geological Survey

CPT: Cone Penetration Test

d_{gnd}: The median or spectral acceleration uncertainty for any given attenuation relationship

EPISTEMIC UNCERTAINTY: Uncertainty associated with a model of a system or process and its parameters that arises from limitations of the data available or on causal understanding

GMPEs: Ground motion prediction equations

GPS: Global Positioning System

HAZ4.2: PSHA computer program developed by Dr. Norman Abrahamson (2010, PC)¹

HAZARD CURVE: Plot of the relationship between a ground motion parameter and the mean number of seismic events per year in which the ground motion parameter at the site exceeds a specified value; herein, the ground motion parameters of interest are the peak ground acceleration and spectral acceleration

HECTARE: Unit of surface area equal to 10,000 square meters (i.e., 100 meters by 100 meters); also equal to 2.47 acres

Hz: Hertz

ICB: Inner Continental Borderland

InSAR: Interferometric Synthetic Aperture Radar

ka: Thousand years ago

km: Kilometers

km/s: Kilometers per second

SAN ONOFRE NUCLEAR GENERATING STATION
SEISMIC HAZARD ASSESSMENT PROGRAM
2010 PROBABILISTIC SEISMIC HAZARD ANALYSIS REPORT

Ma: Million years ago

MIS 5e/5a: Marine Isotope Stages 5e/5a; part of a series of stages 1 through 6

MMS: Minerals Management Services

mm/yr: Millimeters per year

m_j : A variable used in PSHA calculations representing an earthquake of a particular magnitude

m/s: Meters per second

M: A quantity characteristic of the total energy released by an earthquake

M_L : Local magnitude scale developed by Richter in the 1930s

M_w : Moment magnitude scale as presented by Hanks and Kanamori (1979)¹

NGA: Next Generation Attenuation relationships presented as part of the NGA Relations Project, a five year research program designed to improve earthquake ground motion attenuation relationships for shallow crustal earthquakes in the western United States¹

NI: Newport-Inglewood (Fault)

NI/RC: Newport-Inglewood/Rose Canyon Fault Zone

NSHM: National Seismic Hazard Maps as presented by USGS (2008; 2009, PC)¹

$\dot{N}_s(m_j)$: A variable used in PSHA calculations representing the mean number of earthquakes per year having an earthquake magnitude m_j

OBT: Oceanside Blind Thrust Fault as characterized by Rivero et al. (2000)¹, Rivero and Shaw (2001)¹, Rivero (2004)¹, Rivero and Shaw (2005)¹, and Rivero and Shaw (2010, in press)¹

OZD: Offshore Zone of Deformation

PC: Personal communication

PEER: Pacific Earthquake Engineering Research

PGA: Peak ground acceleration

PSHA: Probabilistic Seismic Hazard Analysis

POISSON PROCESS: A random function which describes the number of random events in a specified interval of time or space; the random events have the following properties: (i) the probability of more

SAN ONOFRE NUCLEAR GENERATING STATION
SEISMIC HAZARD ASSESSMENT PROGRAM
2010 PROBABILISTIC SEISMIC HAZARD ANALYSIS REPORT

than one event during the specified time interval is negligible; (ii) the probability of an event during the specified time interval does not depend on what happened prior to the specified time

QA/QC: Quality Assurance/Quality Control

RC: Rose Canyon (Fault)

RP: Return Period in years; inverse of annual frequency of exceedance value

RECURRENCE RELATIONSHIP: Relationship showing the annual recurrence of earthquakes of various magnitudes up to a maximum magnitude; used to determine the mean number of earthquakes per year

r_g : A variable used in PSHA calculations representing the distance between the site and a fault rupture plane

SA: Spectral Acceleration

SCE: Southern California Edison

SCOZD: South Coast Offshore Zone of Deformation

SDT: San Diego Trough

SONGS: San Onofre Nuclear Generating Station

SOPAC: Scripps Orbit and Permanent Array Center

SSHAC: Senior Seismic Hazard Analysis Committee

STAB: Seismic Technical Advisory Board for SONGS Seismic Hazard Analysis

TMBT: Thirtymile Bank Blind Thrust Fault as characterized by Rivero (2004)¹ and Plesch et al. (2007)¹

TECHNICAL COMMUNITY: As used in this report, this term refers to geoscientists and engineers that have demonstrated expertise in relevant ground motion and seismotectonic fields of study in the area around SONGS

TYPE-A FAULT: Seismic sources with detailed earthquake recurrence models where the timing of past events and event displacements are available; earthquakes on Type-A Faults are modeled as characteristic earthquakes; faults as presented by WGCEP (2008)¹ and USGS (2008)¹

TYPE-B FAULT: Seismic sources with measurable slip rates but lacking information of the timing of past events, fault segmentation, and/or event displacements; earthquakes on Type-B Faults are modeled as characteristic earthquakes that rupture the full fault length; faults as presented by WGCEP (2008)¹ and USGS (2008)¹

**SAN ONOFRE NUCLEAR GENERATING STATION
SEISMIC HAZARD ASSESSMENT PROGRAM
2010 PROBABILISTIC SEISMIC HAZARD ANALYSIS REPORT**

TYPE-C ZONE: Regions of distributed shear in which overall rate and style of deformation are unknown; zones as presented by WGCEP (2008)¹ and USGS (2008)¹

UCERF 2: Uniform California Earthquake Rupture Forecast, Version 2 as developed by the 2007 WGCEP (WGCEP, 2008)¹

UFSAR: Updated Final Safety Analysis Report

V_{s30} : A variable used in the NGA relationships for the average shear wave velocity from the ground surface to a depth of 30 m

$v(Z \geq z)$: A function used in PSHA calculations representing the annual frequency of exceedance

USGS: United States Geological Survey

WGCEP: Working Group(s) on California Earthquake Probabilities

WEIGHTS: A weight as used in this report is a number between zero and one assigned to a branch of logic trees in such a way that the sum of the weights assigned to the branches associated with any single branching point (a point from which all the branches under considerations are shown) is one. A weight assigned to a branch usually represents the assigner's or assigners' combined judgment regarding how that branch should be counted with respect to the other branches associated with that branching point in the analysis of the probabilistic model represented by the entire logic tree.

Z : A variable used in PSHA calculations representing the ground motion parameters peak ground acceleration (PGA) and spectral acceleration (SA)

z : A variable used in PSHA calculations representing a specified ground motion parameter threshold

$Z_{1.0}$: A variable used in the NGA relationships for the approximate depth to 1.0 km/s shear wave velocity material

$Z_{2.5}$: A variable used in the NGA relationships for the approximate depth to 2.5 km/s shear wave velocity material

¹ Citation contained in Section 5.0 References

APPENDIX A

SEISMIC SOURCE CHARACTERIZATION



APPENDIX A OUTLINE

A1.0 INTRODUCTION

A2.0 CHRONOLOGY OF PREVIOUS RELEVANT SEISMIC HAZARD ASSESSMENTS

A3.0 TECTONIC AND GEOLOGIC SETTING

A3.1 Physiographic Provinces in the Study Region

A3.2 Tectonic History of the Inner Continental Borderland and Transverse Ranges

A3.2.1 Phase 1 - Collision and Subduction

A3.2.2 Phase 2 - Oblique Extension

A3.2.3 Phase 3 - Transform Plate Boundary (Present)

A4.0 DATA AND OBSERVATIONS SUPPORTING THE NI/RC AS THE PRIMARY FAULT SOURCE

A4.1 Geometry and Structural Analyses

A4.2 Evidence for Activity

A4.2.1 Paleoseismicity

A4.2.2 Geomorphology

A4.2.3 Seismology

A4.2.4 GPS

A5.0 DATA AND OBSERVATIONS SUPPORTING THE OBT AS THE PRIMARY FAULT SOURCE

A5.1 Geometry and Structural Analysis

A5.1.1 Geometry

A5.1.2 Structural Analysis

A5.2 Evidence for Activity

A5.2.1 Paleoseismicity

A5.2.2 Geomorphology

A5.2.3 Seismology

A5.2.4 GPS

ATTACHMENT A-1 – ANNOTATED BIBLOGRAPHIES

ATTACHMENT A-2 – SEISMIC SOURCE CHARACTERISTICS OF NI/RC FAULT SYSTEM

ATTACHMENT A-3 – SEISMIC SOURCE CHARACTERISTICS OF OBT SYSTEM

APPENDIX A

SEISMIC SOURCE CHARACTERIZATION

A1.0 INTRODUCTION

This Appendix provides additional background information to support the judgments regarding the weights assigned to the alternative strike-slip and blind thrust end-member seismic source characterization models discussed in Section 2.0 of the main report. Brief summaries of key seismic hazard assessments that have been conducted specifically for the SONGS Units 2 and 3 and of the current community seismic source characterization model are given in Section A-2. Section A-3 outlines the geologic and tectonic setting and history of the study region. Sections A-4 and A-5 provide additional discussion of the data and studies supporting the strike-slip fault source model (NI/RC as the primary fault source) and the blind thrust fault source model (OBT as the primary fault source), respectively. The following three Attachments are included in this Appendix and provide additional background information:

- A-1 Annotated Bibliographies, which contain abstract summaries of selected references.
- A-2 Seismic Source Characterization of Onshore RC Fault by Dr. Thomas Rockwell of San Diego State University.
- A-3 Seismic Source Characteristics of Inner California Borderland's Blind Thrust Fault Systems by Dr. John Shaw and Dr. Andreas Plesch of Harvard University.

A2.0 CHRONOLOGY OF PREVIOUS RELEVANT SEISMIC HAZARD ASSESSMENTS

During the 1970s and early 1980s, SCE, with the assistance of firms such as Dames & Moore, Fugro, Western Geophysical, Woodward-Clyde Consultants, and several independent consultants completed rigorous onshore and offshore investigations to identify and characterize nearby fault sources and to evaluate their impact on potential earthquake ground motion and tsunami hazards for licensing SONGS Units 2 and 3 (SCE, UFSAR). During these SCE licensing investigations, what was referred to then as the Offshore Zone of Deformation (OZD), was part of a system of faults that included the onshore NI to the north, the offshore South Coast Offshore Zone of Deformation (SCOZD) in the middle, and the RC Fault to the south as illustrated on Figure A-1a. The SCOZD, the closest of these OZD source faults, is located offshore about 8 km southwest of SONGS. This system of faults was identified as the controlling earthquake source in the deterministic assessment of earthquake ground motions completed at that time.

The Cristianitos Fault, which is the closest mapped fault (refer to Figures A-1a, b, and c), is exposed in the sea cliff 915 m southeast of SONGS. Based on this exposure, the Cristianitos Fault was found by SCE (UFSAR) and Shlemon (1987) to have not displaced a 125 ka old marine terrace platform. Therefore, the Cristianitos Fault was not considered to be a fault source in the licensing earthquake ground motion assessment (SCE, UFSAR).

Other fault sources considered during the licensing of Units 1 and 2 to be capable of producing significant earthquake ground motions at SONGS included the onshore San Andreas, San Jacinto, and

**SAN ONOFRE NUCLEAR GENERATING STATION
SEISMIC HAZARD ASSESSMENT PROGRAM
2010 PROBABILISTIC SEISMIC HAZARD ANALYSIS REPORT**

the Elsinore fault zones, and the offshore Palos Verdes, Coronado Banks, Santa Catalina, San Diego Trough, and San Clement faults, as illustrated in Figures A-1a and b.

An updated seismic hazard assessment was conducted by SCE in 1995, with the assistance of Geomatrix Consultants, Risk Engineering, and Woodward-Clyde Consultants. During the 1995 PSHA (SCE, 1995), offshore and onshore data relevant to the OZD, in particular the SCOZD, that had become available since the preparation of the SCE UFSAR, were evaluated. The results of a PSHA, which was completed in this study, also showed that the NI, the SCOZD, and the RC fault sources were the controlling sources for seismic hazard at SONGS.

In 2001, with the assistance of Fugro West, Geomatrix Consultants, and GeoPentech, SCE completed a re-assessment of the seismic source characteristics of the NI/SCOZD/RC and conducted a PSHA that specifically addressed the newly postulated blind fault sources in the vicinity of SONGS. Alternative source characterizations for this 2001 seismic hazard analysis were developed to capture the range of plausible fault geometries and interactions between postulated thrusts, including the OBT (Rivero et al., 2000) and the San Joaquin Hills Blind Fault (SJBF) (Grant et al., 1999 and 2000), and strike-slip faults, including the NI/SCOZD/RC faults. Analysis of geodetic GPS data conducted as part of this assessment showed relative motion more consistent with north-northwest shear with little or no convergence across the ICB Province, or evidence of a regional “driving” force that would reactivate a large seismogenic thrust fault (SCE, 2001; Hanson et al., 2002; Moriwaki et al., 2002). Quaternary slip rates assigned to offshore blind thrust fault sources were modified from postulated higher long-term post-Pliocene slip rates (Rivero et al., 2000) to reflect constraints provided by the geodetic data and coastal marine terrace uplift rates.

UCERF 2, which was published by the 2007 WGCEP in 2008, represents the USGS current seismic source model for the southern California region. UCERF 2 primarily updated the state of knowledge on the southern California portion of the San Andreas Fault and the San Jacinto and Elsinore faults over what had previously been reported by a WGCEP in 1995. Postulated onshore blind thrust faults, such as the SJBF (Grant et al., 1999) were included in UCERF 2. However, postulated blind thrust faults in the ICB Province are not included in the source model used in UCERF 2, but were flagged by the authors of UCERF 2 as potential sources for future consideration.

There is ongoing debate within the technical community (e.g., Rivero and Shaw, 2001; Grant et al., 2002; Grant and Rockwell, 2002; Rivero, 2004; Grant and Shearer, 2004; Rivero and Shaw, 2005; Ryan et al., 2009; Sorlien et al., 2009b; Rentz, 2010; Rivero and Shaw, 2010, in press; and many others) as to whether high-angle strike-slip faults or low angle reverse or thrust faults are the primary tectonic structures or faults accommodating the crustal motions in the vicinity of SONGS. The present study utilizes two end-member tectonic structural models (referred to as the strike-slip and blind thrust system models) to facilitate the characterization of the closest offshore faults that have been demonstrated to dominate the earthquake shaking hazard for SONGS. UCERF 2 was selected as the basis or reference for one end-member model because it represents the most recent technical community's consensus seismic source characterization model for California faults. In this strike-slip end-member model, the NI/RC Fault Zone is characterized as the closest, active, primary strike-slip fault to SONGS. The source parameters from UCERF 2 used to characterize the NI/RC Fault Zone in the USGS (2008) and USGS (2009, PC) seismic hazard mapping studies are used in this study. For the blind thrust end-member model, the OBT is characterized as the primary contributing seismic source for SONGS. The OBT is

included in the CFM (Plesch et al., 2007) and is identified in UCERF 2 as a potential fault source that should be given future consideration.

A3.0 TECTONIC AND GEOLOGIC SETTING

Southern California is divided into several physiographic regions, or provinces based on the makeup of their geologic and tectonic characteristics. Refer to Figure 2-1 in the main portion of this report and Figures A-2a, b, c, and d for the location of these provinces relative to SONGS and illustrations of their long and complex tectonic evolution. SONGS is located in the Peninsular Ranges Province, just east of its boundary with the ICB Province and to the south of the Transverse Ranges Province.

A summary of the geologic and tectonic characteristics of these physiographic provinces (Section A3.1) and a tectonic history that outlines the development of their key geologic and tectonic structures (Section A3.2 and Figures A-2a, b, c, and d) provide additional perspectives on the relationships between strike-slip and thrust faults in the region.

A3.1 Physiographic Provinces in the Study Region

As seen on Figure A-2a, the Peninsular Ranges Province extends from Colorado Desert Province in Coachella/Imperial Valley on the east, well into Baja California on the south, and to the Transverse Ranges Province on the north. To the west, the ICB Province is almost entirely offshore, including Santa Catalina and San Clemente Islands. This province also includes the Palos Verdes Peninsula and the western portion of the Los Angeles (LA) Basin. Similar to the Peninsular Ranges Province, the ICB Province is also bounded on the north by the Transverse Ranges Province and also extends to the south offshore of Baja California. The Outer Continental Borderland Province (MMS, 2001 and Crouch and Suppe, 1993) bounds the ICB Province on the west.

The Peninsular Ranges and ICB provinces are dominated by northwest-southeast trending mountain ranges and intervening basins that extend from within Baja California to the southern border of the Transverse Ranges Province (CGS, 2002b). The Transverse Ranges province is dominated by east-west trending mountain ranges and intervening basins that extend from the Twenty-Nine Palms/Palm Springs area on the east to offshore of Point Conception and the Channel Islands on the west. The basins and ranges in the Peninsular Ranges, ICB, and Transverse Ranges Provinces are commonly separated by fault zones that trend parallel to the ranges and valleys. The LA Basin, located at the juncture of these three physiographic provinces, includes faults and folds with differing orientations resulting from the complex interaction between the northwest-trending Peninsular Ranges and ICB Provinces and the east-west-trending Transverse Ranges Provinces.

As mentioned above, the physiography of both the ICB and the Peninsular Ranges provinces are composed of generally similar northwest-oriented faulted ridges and basins, with relatively steep slopes on the flanks of the uplifted ridges. However, there are distinct differences between the ICB and Peninsular Ranges provinces in their underlying basement rock composition and their structural relief their overlying sedimentary rocks, which suggest that it is appropriate to keep these two provinces separated. The ICB Province is underlain by the Catalina Schist basement rock complex and the Peninsular Ranges Province is underlain by a batholithic and older basement rock complex, as illustrated on Figures A-2c and A-2d. The ICB Province is bounded on the east by the NI/RC Fault Zone near the coast. The East Santa Cruz Basin Fault bounds the ICB Province on the west. The Peninsular Ranges

Province is bound on the west by the NI/RC Fault Zone and on the east by the Coachella and Imperial valleys with their San Andreas Fault System (refer to Figures A-2a and A-3).

A3.2 Tectonic History of the Inner Continental Borderland and Transverse Ranges

Southern California's current complex tectonic and geologic setting resulted from a long and complicated history in crustal plate interaction that has culminated in today's San Andreas Fault being the dominate player in the predominate right-lateral strike-slip boundary between the Pacific and North American crustal plates (Figures A-2b and 2c) (Atwater, 1998; Nicholson et al., 1994; Bohannon and Geist, 1998; Fisher 2009; and Fisher et al., 2009a). This complex deformational history and resulting tectonic setting form the basis for interpreting the stratigraphy, faults and folds, and present seismotectonic setting of the Peninsular Ranges and ICB provinces in the area around SONGS. Essentially, there have been three different phases of the crustal deformation, each with a distinct style and pattern of deformation and resulting geology.

A3.2.1 Phase 1 - Collision and Subduction

In the Cretaceous and early Tertiary, the western side of the Continental Borderland was a convergent (subduction) plate boundary (Figure A-2b). During Cretaceous and Paleogene time (>24 Ma), the oceanic Farallon plate was subducting beneath the continental crust of western North America, resulting in a continental margin arc-trench system. The subduction-related geology of California, when reconstructed, includes the Sierra Nevada granitic batholith that formed the roots of a magmatic arc, the metamorphic rocks along the arc front that form the foothills belt of the Sierra Nevada, the Great Valley Sequence of marine sedimentary rocks formed in the submarine fore-arc basin, the Coast Range ophiolite that was the oceanic floor of the fore-arc basin, and the Franciscan complex of accreted terrain metamorphic rocks formed in the accretionary wedge at the subduction front. These major geologic units are still recognizable in southern California, but, as illustrated on Figures A-2c and 2d, they have been broken up and re-organized by subsequent tectonic events (Atwater, 1998; Nicholson et al., 1994; Bohannon and Geist, 1998; Fischer, 2009; and Fisher et al., 2009a).

A3.2.2 Phase 2 - Oblique Extension

Beginning in the late Oligocene and early Miocene (17 to 24 Ma), subduction gradually ceased along the western margin of North America when the East Pacific Rise (source of the Farallon and Pacific Plates) encountered the continental margin and, along with the Farallon Plate, was, in turn, subducted beneath North America (Figure A-2b). A new plate boundary configuration resulted with the Pacific Plate in direct contact with the North American Plate along the strike-slip San Andreas Fault. The relative motion between the Pacific and North American Plates was no longer convergent, but rather largely right-lateral translational in nature.

During the Miocene (5 to 24 Ma), various crustal blocks along the North American margin became attached to the northward-moving Pacific Plate (Atwater, 1998). This microplate capture led to extensional deformation of the upper plate of the subduction zone, rotation and translation of large crustal blocks, normal faulting, widespread Middle Miocene Volcanism, and a zone of oblique extension (transtension) in the Borderland (Kamerling and Luyendyk, 1979 and 1985; Wright, 1991; Nicholson et al., 1994; Fisher, 2009; and Fisher et al., 2009a). This oblique extension continued into the middle Pliocene (~4 Ma) and caused extensive ridge and basin (horst and graben) morphology (similar to block

faulting in the Basin and Range Province) to occur in the ICB. This formed many of the generally northwest-trending basins and ridges of the ICB that are apparent today.

As schematically illustrated by Nicholson et al. (1994) in the sequence of maps shown on Figure A-2b, the western Transverse Ranges Province was one of these several captured rotating crustal blocks. These blocks, while simultaneously being translated northward, were also rotated as much as 90 to 110 degrees in a clockwise direction (also refer to Figure A-2c) forming the east-west trending, western portion of the Transverse Ranges Province (Kamerling and Luyendyk, 1985; Crouch and Suppe 1993; and Bohannon and Geist, 1998). As the Transverse Ranges Province moved northward and rotated into its present position and the transform plate boundary continued to develop along the eastern edge of the rotating block, significant extension occurred in the Los Angeles Basin and ICB Province resulting in rapid basin subsidence and sedimentation accumulation during the Miocene and early Pliocene. Approximately 4 to 5 Ma (during the early Pliocene), another reorientation of the plate boundary in southern California and northern Mexico occurred. The plate boundary south of the Borderland and west of Baja California migrated eastward, splitting Baja California and coastal southern California off from the rest of North America, attaching these crustal blocks to the Pacific Plate (Figure A-2b). Since that time (about 5 Ma), the relative plate motion vector between the North American and Pacific Plates has been oriented approximately N37°W (Cande et al., 1995; Atwater and Stock, 1998). The southern San Andreas Fault was the manifestation of this new shift eastward of the plate boundary in southern California. The southern San Andreas and the northern San Andreas are now connected through the well-known, large left restraining bend in the fault trace, (now referred to as the Mojave segment) thereby producing convergence across a wide area of the southern California, expressed most proximately in the Transverse Ranges Province (Clark et al., 1991; Wright, 1991; Schneider et al., 1996; Sorlien et al., 1999; and Seeber and Sorlien, 2000).

Thus, overall, the tectonic setting in this portion of southern California changed in the Pliocene from predominately transtensional to predominately transpressional. The increased convergence commonly resulted in diversely-striking Miocene normal faults being reactivated as reverse faults, and inversion of half-graben basins into anticlines (Yeats, 1987; Clark et al., 1991; Seeber and Sorlien, 2000). Significant transpression occurred across the newly-developing Transverse Ranges and portions of the LA Basin on numerous oblique reverse and blind faults, many of which are inverted normal faults (Pasadenan orogeny). Large scale, rapid uplift of crustal blocks north of the LA Basin occurred concurrently with gradual uplift of the Palos Verdes Peninsula and the San Joaquin Hills, and subsidence and rapid sedimentation in the LA Basin (Wright, 1991).

A3.2.3 Phase 3 - Transform Plate Boundary (Present)

The present-day Pacific-North American Plate boundary south of the Transverse Ranges Province in southern California is dominated by a broad zone of distributed right-lateral strike-slip motion. This motion affects an area extending from the San Andreas Fault in the east to the offshore San Clemente Fault in the west (Figure A-1a).

Various studies have estimated that approximately 48 to 52 millimeters per year (mm/yr) of right-lateral shear occurs across southern California (Bennett et al., 1996; DeMets and Dixon, 1999). The San Andreas Fault and several other strike-slip fault zones accommodate most of the slip across the plate boundary (Jennings, 1994; Petersen et al., 1996). The Eastern California Shear Zone (east of San Andreas Fault) is believed to accommodate about 10 mm/yr of right-lateral slip (Bennett et al., 1996). The slip

rate on the San Andreas Fault is variable, but ranges from about 10 to 35 mm/yr in southern California. The most recent information from paleoseismic studies suggests that the San Jacinto Fault has a slip rate of about 15 to 20 mm/yr (C. Kendrick, USGS, 2007, PC), which exceeds the 12 mm/yr reported by the CGS and the SCEC. Geologic data suggest that the Whittier-Elsinore, NI onshore, and Palos Verdes faults have slip rates of about 5, 1, and 3 mm/yr, respectively (Cao et al., 2003).

Quaternary to Holocene offsets on the major fault zones within the Continental Borderland are interpreted to be primarily right-lateral strike-slip faults with a lesser vertical slip component, commonly referred to as oblique-slip faults. The San Pedro Basin Fault and the San Clemente Fault are two of the most active faults in the Borderland, but their slip-rates are largely unknown. Based on regional slip budgets and offsets of Miocene volcanic rocks, estimates of the slip-rates of the key faults in the ICB are as follows: the San Pedro Basin Fault has a slip-rate of 1 to 2 mm/yr and individual splays of the San Clemente Fault Zone (including the Santa Cruz-Catalina Ridge and Pilgrim Banks-Santa Barbara Island faults) have slip-rates of 1 to 4 mm/yr. GPS observations between 1986 and 1995 indicate that the total relative slip between the North American and Pacific plates is 49 ± 3 mm/yr. The estimated total relative slip-rate between the North American and Pacific Plates is reported by DeMets and Dixon (1999) to be about 52 mm/yr. While there are no permanent GPS stations on the eastern edge of the Pacific Plate, stations on Santa Catalina, San Clemente and San Nicolas Islands have shown 45.5, 47.5 and 48.5 mm/yr of slip with respect to stable North America, respectively (SOPAC, 2010). As shown in Figure A-3, the station on San Clemente Island, *scip*, is moving at a rate of 6 mm/yr with an azimuth of 41 degrees west of north relative to station, *scms*, in San Clemente (11 miles northeast of SONGS). These GPS velocities would suggest that the upper limit of postulated slip-rates for the offshore right-lateral strike-slip faults is slightly overestimated.

Using this more regional perspective and stepping closer to the area surrounding SONGS, two end models were utilized to facilitate the characterization of the closest offshore faults that have been demonstrated to dominate the seismic shaking hazard for SONGS. In this regard, UCERF 2 was selected as the basis for reference because it represents the most recent regionally documented seismic source characterization for California faults. Therefore, for the first end-member model, the NI/RC Fault Zone was selected because it was the only UCERF 2 model utilized by the USGS (2008) and USGS (2009, PC) in developing the seismic hazard maps for the building code that applies to the area near SONGS. Similarly, the other end-member model selected was the OBT because of its postulated ability to generate large magnitude earthquakes on a fault plane that was proposed to extend eastward, under the coastline and beneath SONGS.

A4.0 DATA AND OBSERVATIONS SUPPORTING THE NI/RC AS THE PRIMARY FAULT SOURCE

This section provides more detailed discussion of the available and relevant structural, geomorphology, paleoseismicity, seismology and GPS information that have been used to identify and characterize the NI/RC Fault Zone as a predominantly high-angle, right-lateral, strike-slip fault. The NI/RC Fault Zone is the closest primary seismic source fault to SONGS in the strike-slip end-member seismic source model included in this 2010 PSHA. Attachment A-2 presents Dr. Tom Rockwell's summary of current information concerning the NI/RC Fault Zone.

A4.1 Geometry and Structural Analyses

The geometry of a fault, as well as its flanking lithology, provide the geologic and tectonic structural information for estimating how that fault will rupture in the future; this information in turn is needed to

**SAN ONOFRE NUCLEAR GENERATING STATION
SEISMIC HAZARD ASSESSMENT PROGRAM
2010 PROBABILISTIC SEISMIC HAZARD ANALYSIS REPORT**

model the resulting earthquake ground motions that will impact facilities, such as SONGS. In addition to geometry and structural geologic information about the San Andreas Fault and other active strike-slip faults in the world, subsurface data from the oil fields under the LA Basin along the onshore NI portion of the NI/RC Fault Zone lead to the development of the classic theory of wrench fault tectonics (Moody and Hill, 1956; Wilcox et al., 1973; Harding, 1973; Yeats, 1973; Barrows, 1974; Harding 1985). In simplistic terms, as illustrated on Figure A-4a, the primary principal behind wrench fault theory is that, as high-angle, crustal-through-going, strike-slip faults progressively propagate through overlying more recently deposited sediments, they initially form a broad, near-surface zone of subsidiary faults in a flower-like pattern (refer to Figure A-4b). The orientation of these subsidiary faults is at oblique angles to the primary strike-slip fault and the direction of crustal deformation. These conjugate subsidiary faults vary in their geometry and style of faulting (i.e., normal, reverse, thrust, strike-slip, or oblique-slip) depending on their orientations relative to the strike and dip of the primary strike-slip fault. As the displacement of these more recently deposited sediments increases, the broad, flower-like pattern progressively narrows into the primary trace of the fault. The subsidiary fault patterns are most prominent in en echelon step-overs or bends in the trace of the primary, high-angle, strike-slip fault. As illustrated on Figures A-4a and A-4b, for right-lateral strike-slip faults right step-overs produce localized zones of tension expressed in subsiding blocks bracketed by normal or transtensional oblique slip faults. Examples of the en echelon right step-overs along the NI/RC Fault Zone are the subsiding San Diego Bay and Bolsa Chica and Anaheim Bay wetlands. Left step-overs produce localized zones of compression expressed in rising blocks bracketed by thrust, reverse, or transpressional oblique slip faults. Examples of these left step-overs along the NI/RC Fault Zone are Mount Soledad, Signal Hill, Domingues Hills, and Baldwin Hills.

SCE (UFSAR), with the assistance of Woodward-Clyde Consultants (1980), completed a thorough re-analysis of the oil well records and available geologic data from the oil fields between Newport Beach and Westwood (an example is provided on Figure A-5). This independent assessment concluded that the oil field data supported the wrench fault model and that a high-angle, right-lateral strike-slip fault dominated by the NI Fault Zone, and estimated that the long term slip rate on the fault was about 0.5 mm/yr. More recent work in examining oil well and groundwater well data from western Los Angeles County by Dr. Dan Ponti of the USGS (2010, PC) further supports the dominance of the high-angle strike-slip fault in the NI Fault Zone as illustrated in Figure A-6.

Data supporting the characteristics of the offshore part of the NI/RC Fault Zone are more limited. The continuity of the NI/RC Fault Zone, between its southern onshore trace near La Jolla and its onshore traces north of Newport Beach was first suggested by Moore (1972). SCE (UFSAR), through Western Geophysical Company, completed rigorous offshore marine seismic reflection surveys to assess potential faulting offshore of SONGS (Western Geophysical Company, 1972). Track lines of these surveys and their interpreted faults are shown on Figure A-7a. This offshore work supported the conclusion that the closest primary seismic source fault to SONGS is the offshore continuation of the high-angle, right-lateral, strike-slip NI/RC Fault Zone, whose characteristics are reflected in the wrench fault style of tectonics present in the northern and southern onshore portions of the fault zone.

Little has changed in the geoscience community's overall assessment of the NI/RC Fault Zone characterization as a strike-slip fault zone since the SCE's original investigations were completed. Some refinements were made in the mapped offshore traces of the faults by Fischer and Mills (1991) (Figure A-7b); Ryan et al. (2009) (Figure A-7c); Sorlien et al. (2009b) (Figure A-7d); and Conrad et al. (2010) (Figure A-7e). Figure A-7f illustrates a map containing the USGS (2009) Quaternary Fault and Fold

**SAN ONOFRE NUCLEAR GENERATING STATION
SEISMIC HAZARD ASSESSMENT PROGRAM
2010 PROBABILISTIC SEISMIC HAZARD ANALYSIS REPORT**

Database in the ICB. The changes in the NI/RC Fault Zone's seismic characteristics by Fischer and Mills (1991) were incorporated in the source models used in SCE (1995 and 2001) and those by Ryan et al. (2009), Sorlien et al. (2009b), and Conrad et al. (2010) were considered in this PSHA. Other research, including Grant and Shearer (2004), Fisher (2009), Fisher et al. (2009a), Fisher et al. (2009b), Lee et al. (2009), Rockwell (2010a and 2010c), proprietary work completed by Fugro, Inc., and work currently underway by Dr. Dan Ponti of the USGS along the onshore NI Fault and its subsidiary traces north of Long Beach, further supports the weights assigned herein to a high-angle, strike-slip characterization of the NI/RC Fault Zone as the closest primary source fault to SONGS in the strike-slip end-member model incorporated into this PSHA.

Most notable of this more recent research is the work completed by Ryan et al. (2009), which essentially is an independent assessment of the available data reviewed during SCE's earlier work (Western Geophysical Company, 1972) on the characteristics of the faults located offshore of SONGS. Some of the proprietary marine geophysical survey data recently obtained by the USGS from WesternGeco and used by Ryan et al. (2009) was purchased by SCE years ago. Ryan (2010, PC) indicated that the results of the USGS's independent assessment of the data are in general agreement with the results of SCE's previous investigations and analysis of the faulting off-shore of SONGS, as seen by comparing Figure A-7a and A-7c.

USGS (2009) considers the NI/RC Fault Zone to be a primary, high-angle, right-lateral, strike-slip seismic source fault, with relatively minor alternatives to its most northern on-shore geometry.

A4.2 Evidence for Activity

A4.2.1 Paleoseismicity

The results of the SCE (UFSAR) (Woodward-Clyde) analysis of the oil field data (see example on Figure A-5 from Freeman et al., 1992) showed that, although the quality of the data varied between the different oil fields, the best fit of that data indicated about 0.5 mm/yr of strike-slip displacement across the main trace of the NI Fault. Slip rate estimates for the northern on-shore part of the NI/RC Fault Zone have been made by Fischer and Mills (1991), Freeman et al. (1992), Law/Crandall, Inc. (1993), Shlemon et al. (1995), Grant et al. (1997), and Franzen and Elliott (1998). In combination, these estimates suggest a wide range in slip-rate between 0.4 to 3.0 mm/yr for the onshore RC segment. More thorough and extensive paleoseismic investigations conducted by Lindvall and Rockwell (1995) and Rockwell (2010a and 2010c) support seismic source characteristics assigned to the southern onshore portion of the NI/RC Fault Zone in the San Diego area (summarized in Attachment A-2). Detailed 3D fault trenching in that work further supports the dominate high-angle, right-lateral, strike-slip style of faulting along the NI/RC Fault Zone with slip-rates estimated to be between 1.5 and 2.5 mm/yr. Offshore the paleoseismic data along the NI/RC Fault Zone has been more limited. Fischer and Mills (1991), based on their re-assessment of seismic reflection data available at that time, estimated a slip-rate of about 0.8 mm/yr, but were careful to qualify their estimate based on the limitations of their available data. Recent, high resolution marine geophysical surveys, like the USGS (Conrad et al., 2010) survey over the San Diego Trough Fault and the Rentz (2010) survey off the coast over the inner shelf between Dana Point and Carlsbad (refer to Figure A-8a), are providing more useable data to assess the paleoseismic record beneath the ICB.

High-resolution seismic data on the inner shelf has been used to constrain the recency of displacement on the Cristianitos Fault. Using this data, which is illustrated on Figure 8b, Rentz (2010) notes that what

subtle surface relief is observed locally on the inner shelf is of eroded, partially buried, bedrock remnants of "...adjacent geologic formations with different erosive properties." As Rentz (2010) suggests, "this differential erosion may be responsible for the trend of the San Mateo promontory, the highstand relief in the seismic profiles, and the ~9.6 km wide shelf," off of the coast between Dana Point and Carlsbad. Further, they conclude that in the area of their survey, "There is no observed offset of the overlying Holocene sediment packages, which would be expected if deformation was ongoing"; further supporting the SCE (UFSAR) conclusion that the Cristianitos Fault is inactive.

A4.2.2 Geomorphology

The geomorphology along the onshore parts of the NI/RC Fault Zone clearly supports the dominance of a high-angle strike-slip fault. As Dr. Rockwell presents in more detail in Attachment A-2, displaced stream channels in RC Fault are predominately offset right-laterally. Although the location and geomorphology defined by the NI/RC Fault Zone is less obvious in other parts of San Diego due to urban development, Dr. Rockwell presents in Attachment A-2, a late 19th century cartographer's sketch that shows a linear topographic lineament, which correlates with the present known location of the NI/RC Fault Zone. The pattern of this lineament across San Diego's hilly terrain supports the presence of an active near-vertical, right-lateral fault plane along this trace of the NI/RC Fault Zone.

The linear surface trace of the NI/RC Fault Zone through the western part of the LA Basin, particularly between Newport Beach and Long Beach, and the presence of localized uplifted hills and plateaus and intervening subsiding lowlands and wetlands is consistent with the presence of an underlying strike-slip dominated wrench fault system.

Between Newport Beach and La Jolla, the onshore geomorphology is characterized by a flight of emergent marine terraces (Figure A-9). The relatively uniform altitude of these surfaces suggests uniform uplift that does not appear to be consistent with the varying dips and long-term rates of slip postulated for the OBT. The sequence of emergent marine terraces have been mapped and described by Shlemon (1978), Kern and Rockwell (1992), Lajoie et al. (1992), and Grant et al. (1999) (refer to Figure A-9). Dating of the emergent MIS 5e/5a marine terraces at 125/80 ka by these authors, suggests regionally uniform coast uplift at a rate of about 0.13 to 0.14 mm/yr. Along the coastal San Joaquin Hills, the uplift rate may be as high as 0.21 to 0.27 mm/yr (Grant et al., 1999).

The presence and regionally persistent elevations of these onshore marine terraces, which are subparallel with the trend of the NI/RC Fault Zone, are more in concert with a nearby strike-slip faulting rather than a regionally persistent underlying thrust fault with changing dip angles, as proposed by Rivero et al. (2000) and Rivero (2004). As suggested by Mueller et al. (2009), the uniform uplift of these late Pleistocene uplifted marine terraces is more likely tied to regional tilting or "flexure of the crust driven largely by heating and thinning of the upper mantle beneath the Gulf of California and eastern Peninsular Ranges." Locally, this regional uplift is amplified by transpressional bends and en echelon step overs in the NI/RC Fault Zone leading to the higher uplift rates such as those tied of the San Joaquin Hills (Grant et al., 1999, 2000, and 2002) and Mount Soledad (Rockwell, 2010).

A relatively low-relief offshore continental shelf and the consistent 400-foot depth of its shelf break, is evident in the bathymetry extending along the coast between Palos Verde Peninsula to the Mexican Border, as illustrated in Figure A-10. This geomorphology also is inconsistent with a regionally persistent underlying thrust fault with changing dip angles, as proposed by Rivero et al. (2000) and Rivero (2004).

This uniform low-relief surface, which correlates to the last glacial maximum sea level low-stand at approximately 19 to 21 ka, is more consistent with a through-going strike-slip fault, such as the NI/RC.

Recent marine geophysical surveys along this shelf by Rentz (2010) are consistent with this conclusion by associating the wider shelf offshore between Dana Point and Carlsbad Canyon, in contrast to the width of the rest of the self between Newport Beach and Dana Point and between Carlsbad Canyon and La Jolla, to more erosion resistant bedrock formations. However, agreeing that the width of the shelf is at least in part is controlled by erosion patterns, based on new multibeam data acquired by the USGS in November 2010, Dr. Ryan (2010, PC) notes that there are major changes in erosion patterns across the San Mateo Point area and suggest that the San Mateo fold and thrust belt, located to the west of the NI/RC Fault Zone, does contribute to the shelf width. She also noted that the shelf morphology would be primarily controlled by sea level cycles, especially considering the low slip rate estimates for the offshore reverse and thrust faults.

A4.2.3 Seismology

Seismology data from the ICB, as a tool to help resolve the location and geometry of faults in this province, has limitations due to the paucity of nearby stations, limited azimuthal coverage, and uncertainties in the underlying velocity structure. Recognizing these limitations, Astiz and Shearer (2000) used improved methods to refine the locations of earthquakes that occurred in the Borderland between 1981 and 1997. Rivero et al. (2000) and Rivero (2004) utilized Astiz and Shearer (2000), in particular the 1986 M_L 5.3 Oceanside Earthquake, to support the offshore thrust fault models as discussed below in Section A-5.

Grant and Shearer (2004) also re-analyzed the 1981 M <3.0 cluster of earthquakes located about 10 km northwest of Oceanside and a 2,000 cluster of seismic events offshore of Newport Beach (refer to Figure A-11). Their work, especially the analysis of earthquakes northwest of Oceanside, supports a high-angle fault plane at depths of 12.5 to 13 km. This orientation of hypocenters and their depth suggest the presence of a deep-rooted, high-angle, strike-slip fault (i.e., the NI/RC Fault Zone), rather than a low-angle reverse or thrust fault (i.e., the OBT). This supports the high-angle, strike-slip, end-member model containing the NI/RC Fault Zone as the closest primary seismic source fault to SONGS.

The 2,000 cluster of earthquakes offshore of Newport Beach also indicate a high-angle fault, such as the NI/RC Fault Zone, but this cluster is located west of the surface trace of the NI/RC Fault Zone and occurs at a depth of 6.5 to 7 km. The shallow depth of these earthquakes, however, does not preclude the possible presence of a seismogenic thrust fault plane passing beneath the high-angle structure.

Marrying the epicenter data from the M 5.3, 1986 Oceanside Earthquake with the new trace of the San Diego Trough Fault, recently re-located by new USGS offshore marine geophysical surveys (Conrad et al., 2010 and Ryan, 2010, PC) is in contrast with the thrust mechanism of that event being correlated with the Thirtymile Bank Blind Thrust (TMBT) as suggested by Rivero et al. (2000) and Rivero (2004). As seen on Figure A-12, the Oceanside event occurred near the San Diego Trough Fault at a left bend in that fault's trace. This relationship supports the occurrence of a thrust event within a high-angle, right-lateral, strike-slip fault system and not the occurrence of a thrust event on a regionally persistent underlying blind thrust fault.

A4.2.4 GPS

Clockwise rotation of crustal blocks in the ICB Province, suggested in SCE (2001), has been emphasized by Ryan et al. (2009). The rotating block proposed by Ryan et al. (2009) has been plotted along with geodetic data on Figure A-13 to qualitatively analyze whether geodetic data collected in southern California supports possible block rotation. Figure A-13 shows the best estimate of long-term velocities for permanent continuous GPS stations with respect to station ID *scms* in San Clemente. As shown on Figure A-13, stations in the southern portion of the Peninsula Range crustal block (shown in purple) appear to show slight clockwise rotation about the *scms* reference station. It is noted that the velocity vectors are presented in an exaggerated scale (1 inch equals 15 mm/yr) for effect. The tension and compression caused by this block rotation would likely lead to the reactivation of some portions of the Oceanside detachment as thrust faults and some portions as normal faults. Some portions would likely remain inactive, making it kinematically incompatible with the postulated through-going, regional thrust model. Conversely, Late Quaternary inactivity of the OBT fault offshore of Carlsbad and La Jolla, as suggested by Sorlien et al. (2009b), is consistent with this block rotation model.

Similarly, a qualitative analysis of geodetic data was prepared with respect to San Clemente Island as previously shown in Figure A-3. The visual trend of the relative velocities presented on Figure A-3 is in strong agreement with the strike-slip end-member seismic source characterization model for the ICB Province. It is noted that the velocities are presented in a smaller scale than in the previous figure (1 inch equals 5 mm/yr). In a qualitative sense, no tension or compression is observed in the relative velocities between Santa Catalina or San Clemente Islands and the Peninsula Range as would be expected in the blind thrust end-member model. The geodetic data (velocities and uncertainties) presented on Figures A-3 and A-13 are based on the public archive preserved by the Scripps Orbit and Permanent Array Center (SOPAC) and includes all permanent continuous GPS stations installed in southern California between 1995 and 2008 with at least 1.5 years of data collected.

A5.0 DATA AND OBSERVATIONS SUPPORTING THE OBT AS THE PRIMARY FAULT SOURCE

This section provides more detailed discussion of the available and relevant structural, geomorphology, paleoseismicity, seismology and GPS information that have been used to identify and characterize the OBT as the closest primary seismic source fault to SONGS. This summary is based primarily on Rivero (2004), Rivero and Shaw (2005), and Rivero and Shaw (2010, in press). Attachment A-3 presents Dr. John Shaw's and Dr. Andreas Plesch's assessment of the seismic source characteristics and current information concerning the OBT Fault based primarily on the work summarized in these publications. Figures A-14 through A-27 present illustrations supporting the data and observations described in this section of Appendix A. This information forms the basis for the blind thrust seismic source characterization end-member model used in the 2010 PHSA.

The OBT model is based on recognition of an extensive offshore low-angle fault by previous workers (Fischer and Mills, 1991; Crouch and Suppe, 1993; Rivero et al., 2000; Rivero and Shaw, 2010, in press). Rivero et al. (2000) first postulated that regional offshore thrust faults are primary, regional-scale active faults. These workers suggest that Mesozoic subduction zones (Phase 1) were reactivated as detachment surfaces during rotation of the Transverse Ranges in the Miocene (Phase 2), and that subsequent transpression in the Pliocene and Quaternary has resulted in structural inversion (Phase 3). According to Rivero et al. (2000) the OBT forms a regionally continuous fault extending from Laguna Beach to at least the US-Mexican Border. Fault rupture scenarios by Rivero et al. (2000) suggest the

potential to generate large (M_w 7.1-7.6) earthquakes that would control seismic hazards in the adjacent coastal area.

These regionally extensive blind thrusts are inferred to interact at depth coevally with displaced high angle, strike-slip or oblique-slip faults, such as the NI/RC Fault Zone and the other high-angle, strike-slip faults in the ICB, which are illustrated in Figure A-14. This blind thrust system model was further developed and described by Rivero (2004), Rivero and Shaw (2005), and Rivero and Shaw (2010, in press). Figure 2-2 in the main text provides a copy of the CFM developed by Plesch et al. (2007), which illustrates the OBT and TMBT fault sources included in this alternative seismic source model. These postulated blind thrust fault sources were addressed in UCERF 2 (WGCEP, 2008) as being considered for future deformation model development, but they are not in the current USGS source characterization model (USGS, 2009, PC).

Utilizing available seismic data Rivero and Shaw (2010, in press) and Shaw and Plesch (Attachment A-3) characterized the blind thrust fault sources (i.e., the OBT and TMBT) and associated hanging wall and footwall subsidiary faults. Possible structural scenarios that represent potential interactions between the steeply-dipping strike-slip faults and the low-angle blind thrust fault sources are outlined in Figure A3-2. Steeply-dipping, right-lateral strike-slip faults, such as the NI and RC, are incorporated into Rivero's (2004) blind thrust seismic source characterization model as highly segmented and offset faults under the argument that continuous, through-going, strike-slip faults, as primary fault sources are not kinematically compatible with the several km of shortening documented on the OBT Fault.

The key data and analyses that Rivero (2004), Rivero and Shaw (2005), and Rivero and Shaw (2010, in press) present in support of the OBT as a primary regional-scale active blind thrust are discussed in the following sections.

A5.1 Geometry and Structural Analysis

A5.1.1 Geometry

The geometry and style of faulting associated with the OBT are less well understood than for many other faults in southern California. Until recently, studies of blind faults and large oblique reverse faults in southern California focused primarily on the Transverse Ranges Province and the LA Basin where higher rates of contractional strain were expected. The work of Shaw and Suppe (1996) identified the Compton blind thrust as part of an active regional fault bend fold system in the western LA Basin. The OBT may be inferred to be an analog and possible extension of this system further to the southeast into the ICB Province. Although the offshore setting of the ICB Province poses challenges to the identification and characterization of blind thrust faults, the Oceanside detachment surface that is interpreted to be the OBT is clearly imaged in many offshore seismic reflection profiles.

The prominent reflector in the seismic data, now interpreted to be the OBT, originally was mapped by Western Geophysical Company (1972). Western Geophysical mapped a regional unconformity or disconformity at the top of acoustical basement, and mapped faults in 'cover sediments' offsetting upper Miocene strata above this surface (Figure A-7a). Subsequent studies described the regional disconformity as an extensional breakaway detachment fault surface (Figure A-2a-d), and identified it throughout much of the ICB Province (e.g., Crouch and Suppe, 1993 and Bohannon and Geist, 1998). The exposed detachment surface became an erosional unconformity that was subsequently covered by Miocene and younger sediments.

Rivero (2004) presents a detailed map (Figure 2-6) showing the locations of seismic profile data used to constrain the location and geometry of the OBT as developed by Rivero et al. (2000) and described by Rivero and Shaw (2005), and Rivero and Shaw (2010, in press). More than 10,000 km of industry seismic reflection profiles, well data, seismicity, and seafloor geologic maps were analyzed. The structural analysis employed kinematic and forward modeling techniques based on quantitative structural relationships between fold shape and fault geometry (Suppe, 1983; Suppe and Medwedeff, 1990; Mount et al., 1990; Erslev, 1991; and Almendinger, 1998). Advanced three-dimensional modeling techniques were used to generate full representations of fault surfaces and key stratigraphic markers. The lateral extent and geometric segmentation of the active blind-thrust ramps were determined by mapping of direct fault plane reflections and associated fold trends throughout the basin areas covered by the seismic grid. The three-dimensional modeling also was used to quantify the distribution of dip slip on the active fault system, and to further constrain the geometrical analysis (Rivero, 2004).

The geometry of the two segments of the OBT as represented in the CFM (Plesch et al., 2007), which is used to characterize the OBT for this study, therefore, is based on a systematic and comprehensive analysis of offshore deep seismic reflection data.

The geometry of the OBT as mapped by Rivero and Shaw consists of two segments of differing sizes and dips. The OBT has been mapped over an area of more than 1800 km², and extends to the south beyond the mapped limits of the fault at the US-Mexican Border. The northern segment averages 14 degree dip, and the southern segment averages 25 degree dip (Rivero et al., 2000). The geometry of the OBT is described in greater detail in Attachment A-3 and Rivero (2004).

A5.1.2 Structural Analysis

Rivero (2004) presents a comprehensive structural analysis of faults in the ICB, focusing on the tectonic reactivation of the Oceanside and Thirtymile detachments as blind-thrust faults. As an outgrowth of the studies presented in Rivero et al. (2000), this analysis generated more precise three-dimensional representations of the faults and estimates of long-term slip rates. More advanced three-dimensional modeling techniques and fault-related fold theories were employed to identify and to describe active blind-thrust faulting and folding induced by the reactivation of the OBT and the TMBT in the Dana Point, Carlsbad and TMBT regions. Over 10,000 km of industry seismic reflection profiles, well data, seismicity, and geologic maps were used. Rivero (2004) performed kinematic and forward modeling structural analysis techniques based on quantitative structural relationships between fold shape and fault geometry. He also used advanced 3D modeling techniques to generate full representations of fault surfaces and key stratigraphic horizons, and provided evidence for present day strain partitioning produced by the interaction of the low-angle thrusts and vertical strike-slip faults (Figures A-16, A-18 through A-20, A-22, and A-26).

The structural analysis led Rivero and Shaw to postulate Pliocene and Quaternary oblique compression and structural reactivation processes as the originating mechanism of the regional blind-thrust fault system (Rivero and Shaw, 2010, in press). This reactivation generated regional structural wedges cored by faulted basement blocks that inverted sedimentary basins (Figures A-15 and A-16) in the hanging wall of the Miocene detachments (Rivero, 2004). The Miocene detachment break-away zone and Pliocene through Quaternary reactivated blind thrust, as well as emergent thrust faults such as the San Onofre Thrust, located in the hanging wall of the OBT, were mapped (Figures A-17 through A-20). From these results, earthquake scenarios based on the structural interaction of active blind-thrust faults and major

strike-slip faults were developed for the ICB Province (see discussion in Attachment A-3). By defining new long-term slip rates, Rivero (2004) concluded that simple and complex earthquake sources could produce large earthquakes (M 7.0 to M 7.6) with recurrence intervals from 970 to 1,810 years (Attachment A-3).

Rivero (2004) notes that it is not possible to directly measure the long-term amount of contractional slip on the OBT because it is generally blind. However, since the location of the OBT is constrained in the region, he used area balancing methods to constrain fault slip. He also evaluated alternative slip values derived from balanced structural interpretations located across several of the major contractional trends observed in the study area as an additional constraint. Excess-area balancing methods were modified and used to invert for the amount of contractional slip consumed by the OBT (Figures A-24 and A-25), since the spatial location and geometry (dip value) of this fault were assumed by Rivero 2004 to be well-known in the study region.

Balanced and restored cross sections based on available seismic data and well data suggest approximately 2.2 to 2.7 km of shortening across the OBT during the last 1.8 to 2.4 Ma (Rivero and Shaw, 2010, in press; Attachment A-3). This suggests an average slip rate of about 1 mm/yr on the OBT, although shortening rate estimates vary significantly along strike (Figures A-24 and A-25).

A5.2 Evidence for Activity

Blind thrusts by definition do not extend to the surface and thus cannot be observed directly. Secondary deformation related to folding and faulting in the hanging wall of the blind thrust is used to identify and characterize recent movement on such fault sources. The following two subsections (4.2.1 Paleoseismicity and 4.2.2 Geomorphology) describe evidence and methods used to evaluate evidence for activity and provide constraints slip rates for the OBT and related structures.

A5.2.1 Paleoseismicity

Fault trenching or other paleoseismic data are not available for the OBT. The offshore location of the near-surface projected traces of the main thrust and back thrusts mapped by Rivero (2004) precludes direct observation of the surface deformation that may be associated with these tectonic structures. The Compton blind thrust, which is postulated to be an onshore equivalent of the OBT, may provide an analog to the OBT.

Leon et al. (2008) employed a multidisciplinary methodology that uses a combination of high-resolution seismic reflection profiles and borehole excavations to suggest a link between blind faulting on the Compton thrust at seismogenic depths directly to near-surface folding. They concluded from these studies that the Compton blind thrust fault is active and has generated at least six large-magnitude earthquakes (M_w 7.0 to 7.4) during the past 14,000 years that deformed the Holocene strata record. Growth strata (discrete sequences that thicken sequentially across a series of buried fold scarps) are interpreted to be associated with uplift events on the underlying Compton thrust ramp.

Rivero et al. (2000) interpret the San Joaquin Hills Blind Thrust (SJHBT) as a backthrust to the OBT. Rivero (2004) estimates that M 7.1 and M 7.3 events would occur on average every 1,070 to 1,430 and 1,480 to 1,960 years, respectively, on the OBT where the SJHBT is linked with the OBT. Grant et al. (1999) also suggest that a backthrust that soles into the OBT is a viable structural model, although less preferred than one in which movement of the SJHB is the product of partitioned strike-slip and

compressive shortening across the NI/RC Fault Zone. They calculated average recurrence times of 1,650 to 3,100 years for moderate-magnitude earthquakes (based on an average uplift event of 1.3 m; Grant et al., 2002).

A5.2.2 Geomorphology

Rivero et al. (2000) provides a viable structural model that explains the localized uplift of the San Joaquin Hills as a backthrust in the hanging wall of the OBT (Figure A-21). They interpret an offshore extension of this structure that is imaged in seismic data as forming above a shallow blind thrust ("Shelf Monocline Trend" on Figure A-21) with an average southwest dip value of 23 degrees. This shallow fault is restricted to the hanging wall of the OBT at depth, and they interpret that this shallow fault soles into the OBT forming a structural wedge (Medwedeff, 1992; Mueller et al., 1998 and Rivero, 2004) (Figure A-21 and A-26). Quaternary uplift of the San Joaquin Hills as manifested by emergent marine terraces, therefore, is interpreted as evidence of Quaternary reactivation of the OBT (Figure A-23).

On a more regional scale, Rivero and Shaw suggest that emergent marine terraces along the entire coast between southern Orange County and northern Baja California show evidence for regional uplift of approximately 0.13 to 0.14 mm/yr (Kern and Rockwell, 1992), and may be the surface manifestation of Quaternary uplift in the hanging wall to the OBT (Rivero et al., 2000 and Rivero, 2004; Attachment A-3).

Seafloor fold and fault scarps associated with the OBT (Figures A-4b, A-16, A-18, A-19, and A-20) also suggest recent contractional activity (Rivero et al., 2000 and Rivero, 2004). Structural inversion and associated reactivation of normal faults commonly produce broad regions of positive structural relief characterized by the development of broad anticlines located directly on top of extensional rollovers and syn-extensional stratigraphic wedges (Figure A-15). Rivero (2004) concludes that thrust motion on the OBT generated four prominent contractional fold trends. Three of these trends are foreland-directed structures, namely the San Mateo, the San Onofre and the Carlsbad trends (Figures A-17 through A-20). These active structures are characterized by thrust sheets that extend laterally for 10 to 20 km, and produce prominent fold and fault scarps on the sea floor. The fourth trend is characterized by hinterland thrusting, which is manifested in a laterally continuous monocline that controls the relief and bathymetric expression of the continental shelf. This monocline is interpreted to result from the interaction between a shallow west-dipping back thrust system and the deep-seated, east-dipping OBT.

Geomorphically, youthful seafloor scarps and folds above fault tiplines have been documented on multibeam bathymetry data and seismic reflection data. Growth folding and offset of Late Quaternary strata are locally apparent on the seismic records, documenting active seafloor uplift on the continental slope in the vicinity of the San Mateo, San Onofre, and Carlsbad faults (Sorlien et al., 2009b; Ryan et al., 2009 and Rivero and Shaw, 2010, in press).

A5.2.3 Seismology

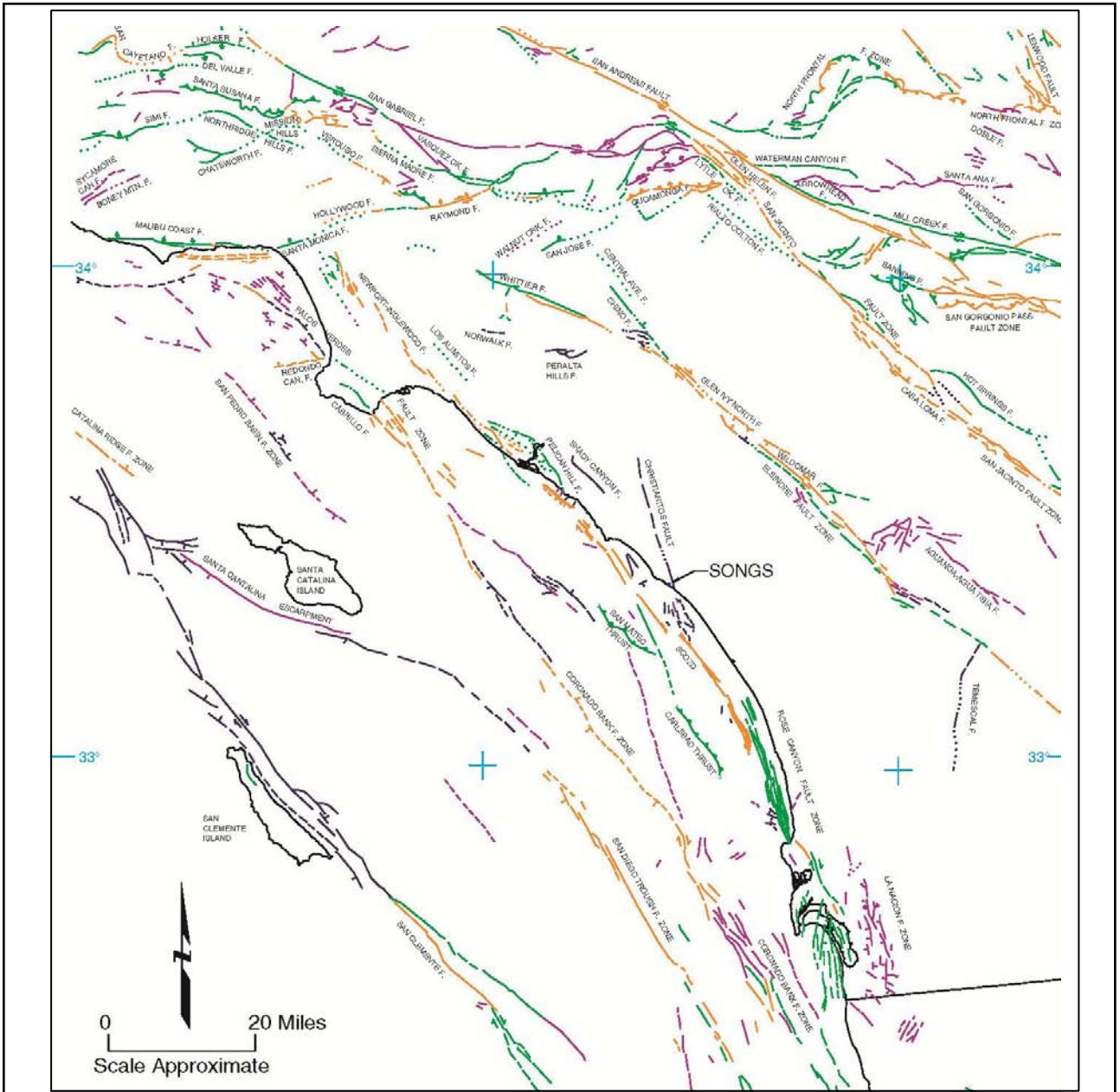
Seismicity in the offshore region is generally diffuse and scattered as compared to more spatially correlated patterns associated with many strike-slip active faults in the Peninsular Ranges on the mainland (Astiz and Shearer, 2000). The focal mechanism of the 1986 M_L 5.6 Oceanside event suggests that the main shock during that event had reverse motion (Hauksson and Jones, 1988). Most importantly, Astiz and Shearer (2000) document a shallow, east-dipping plane of seismicity at a depth of between 10 and 15 km beneath the continental slope and shelf west of San Diego based on relocation of

1981–1997 earthquakes (Figure A-27). The standard errors associated with these earthquake locations are less than 1.5 km. Astiz and Shearer (2000) suggest that these focal mechanisms document the existence of an active, low-angle east-dipping fault in the Coronado Banks Region that may be part of a larger system of offshore thrust faults like the OBT. Rivero (2004) cites this low angle plane of seismicity as evidence for contractional activity on the OBT.

A5.2.4 GPS

As previously noted, the geodetic data (velocities and uncertainties) presented on Figures A-3 and A-13 are based on the public archive preserved by the Scripps Orbit and Permanent Array Center (SOPAC) and includes all permanent continuous GPS stations installed in southern California between 1995 and 2008 with at least 1.5 years of data collected. The GPS data collected to date generally does not support regional compression or extension normal to the postulated OBT. However, it is noted that the current status of geodetic data can be considered inconclusive due to the following:

- Data reduction has quantitative limitations due to the uncertainty caused by locking effects that are dependent upon the characterization of major strike-slip faults in the Continental Borderlands.
- Currently, GPS stations in the vicinity of SONGS are either located on what would be the locked part of the OBT where resolution of low postulated slip rates are within the uncertainty of the GPS measurements or they are located too close to the Elsinore Fault to show any gradient of shortening across the area in question.
- There are very few GPS stations in the vicinity of SONGS and even fewer in the offshore region of the Continental Borderlands; one continuous station exists on San Clemente Island and two on Catalina Island.
- There are many sources with unknown slip-rates in the ICB Province making it difficult to resolve the low magnitude of slip postulated on either the OBT or the NI/RC Fault Zone system.



FAULT REACTIVITY CLASSIFICATION

- Faults that displace Holocene (~ 10 ka) or latest Pleistocene (~ 20 ka) deposits or geomorphic surfaces.
- Faults that displace late Quaternary (~ 780 ka) deposits or geomorphic surfaces
- Quaternary faults (1.8 Ma)
- Faults that displace pre-Quaternary deposits. Reactivity of last displacement for offshore faults generally not known. Only selected faults from Jennings (1992) are shown.

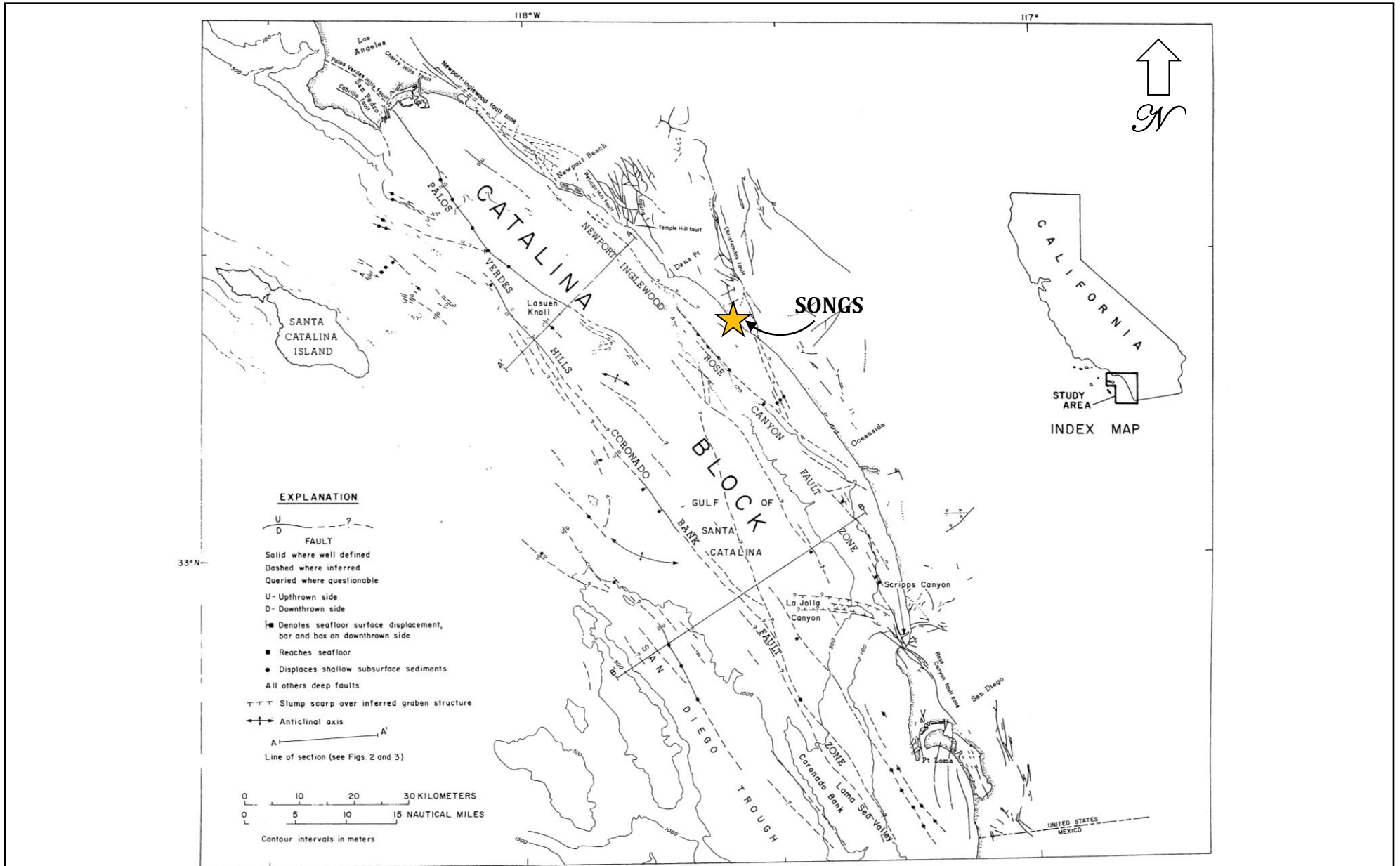


SCE (2001) QUATERNARY FAULT MAP

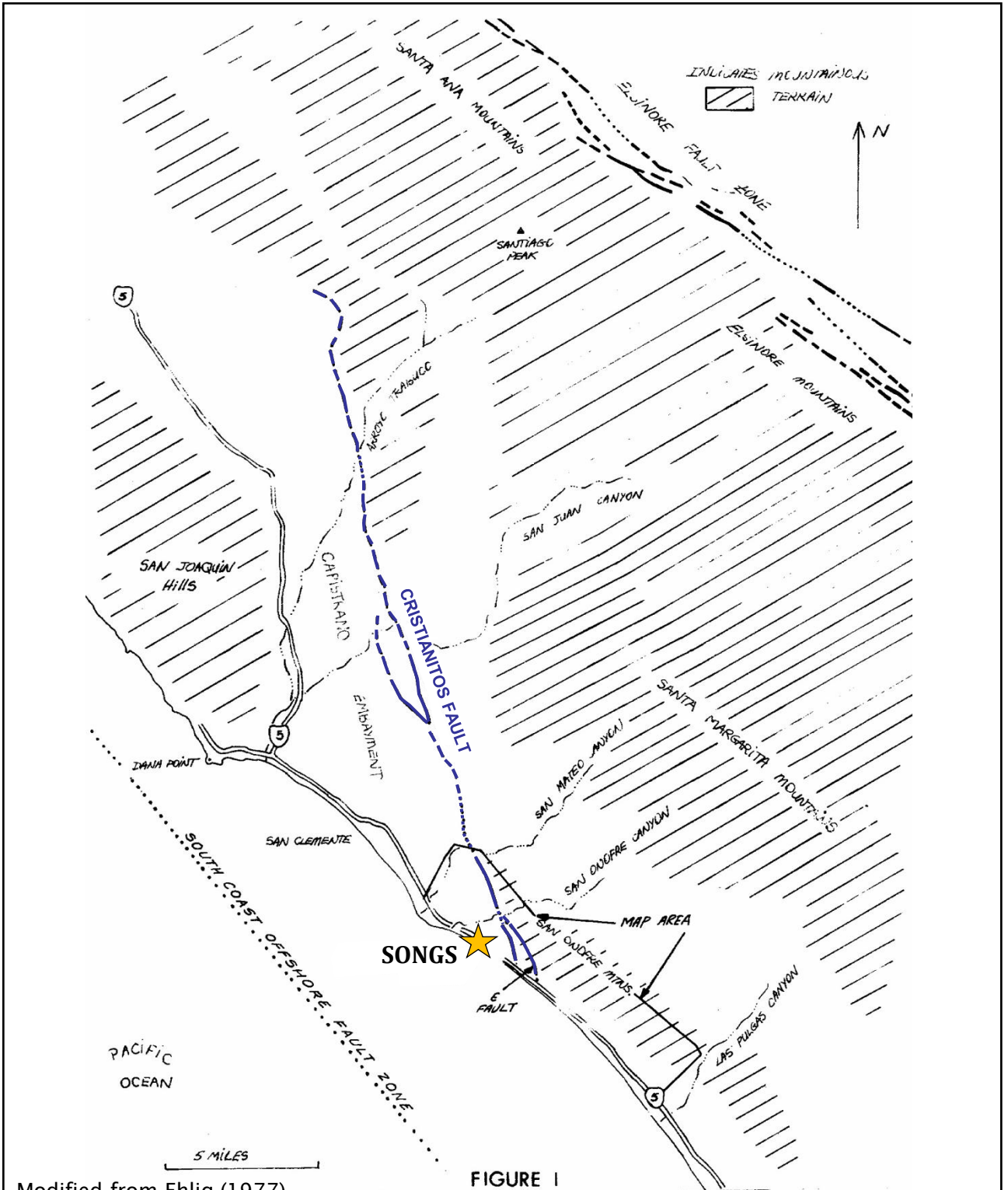
SAN ONOFRE NUCLEAR GENERATING STATION

SEISMIC HAZARD ASSESSMENT PROGRAM

FIGURE
A-1a

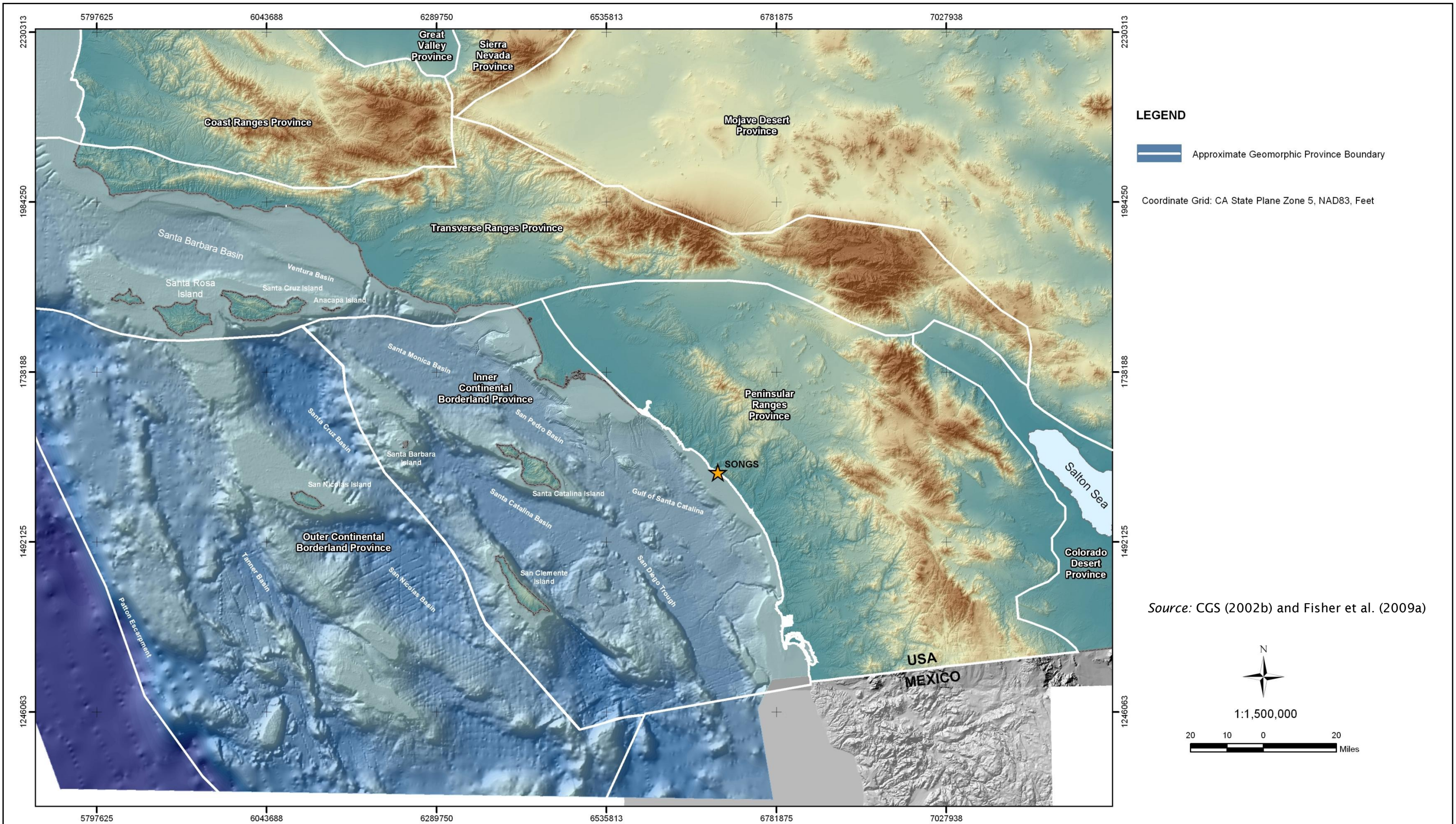


Modified from Greene et al. (1979)



Modified from Ehlig (1977)

 <p>GeoPentech Geotechnical & Geoscience Consultants</p>	<p>MAP OF CRISTIANITOS FAULT ZONE</p>	<p>FIGURE A-1c</p>
	<p>SAN ONOFRE NUCLEAR GENERATING STATION</p> <p>SEISMIC HAZARD ASSESSMENT PROGRAM</p>	

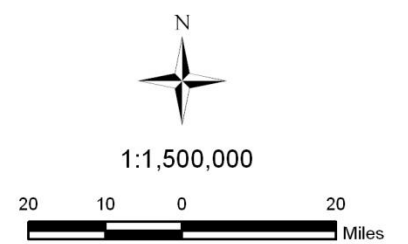


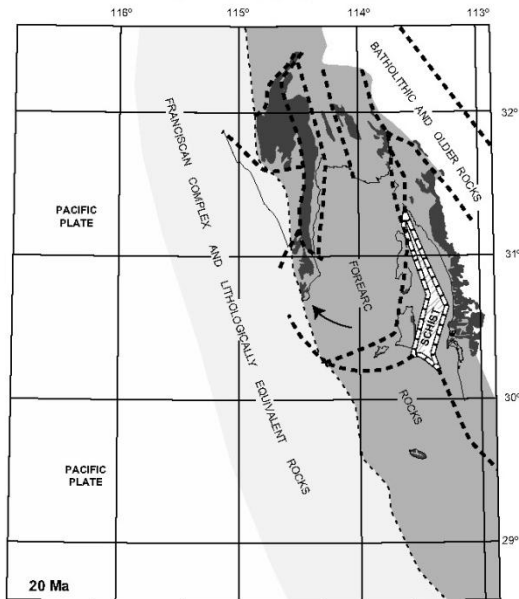
LEGEND

 Approximate Geomorphic Province Boundary

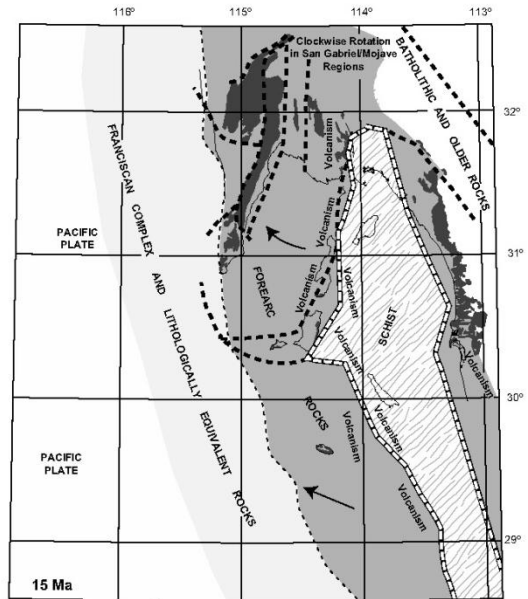
Coordinate Grid: CA State Plane Zone 5, NAD83, Feet

Source: CGS (2002b) and Fisher et al. (2009a)

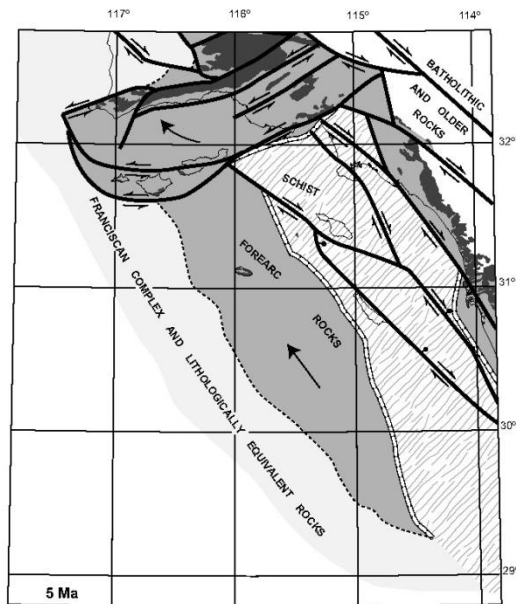




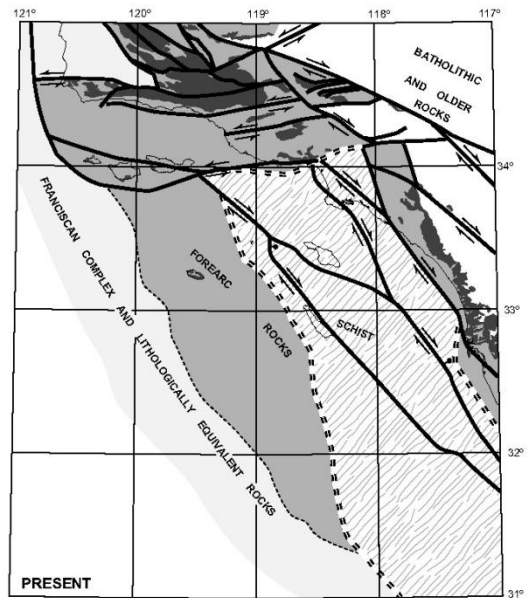
A



B



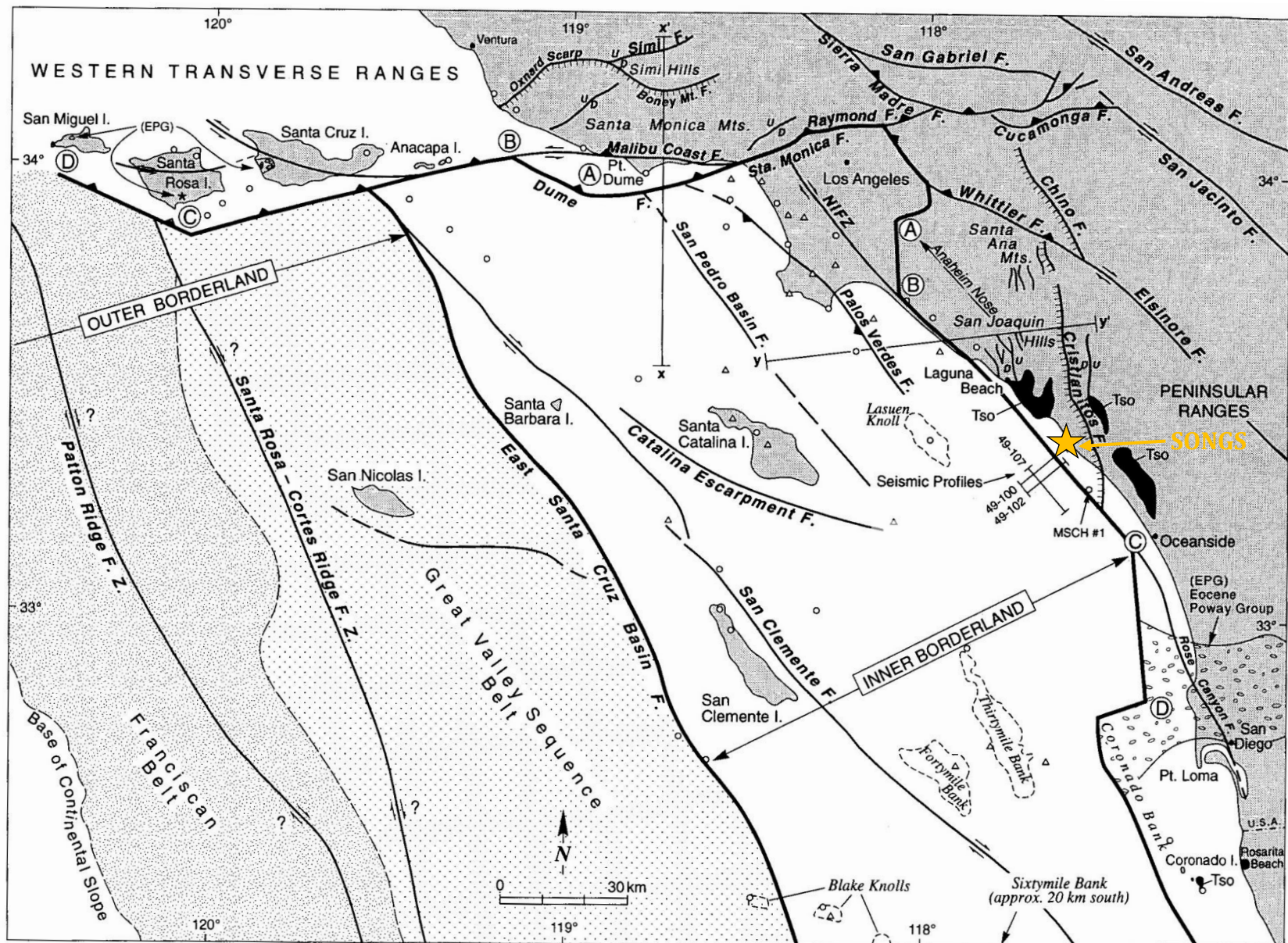
C



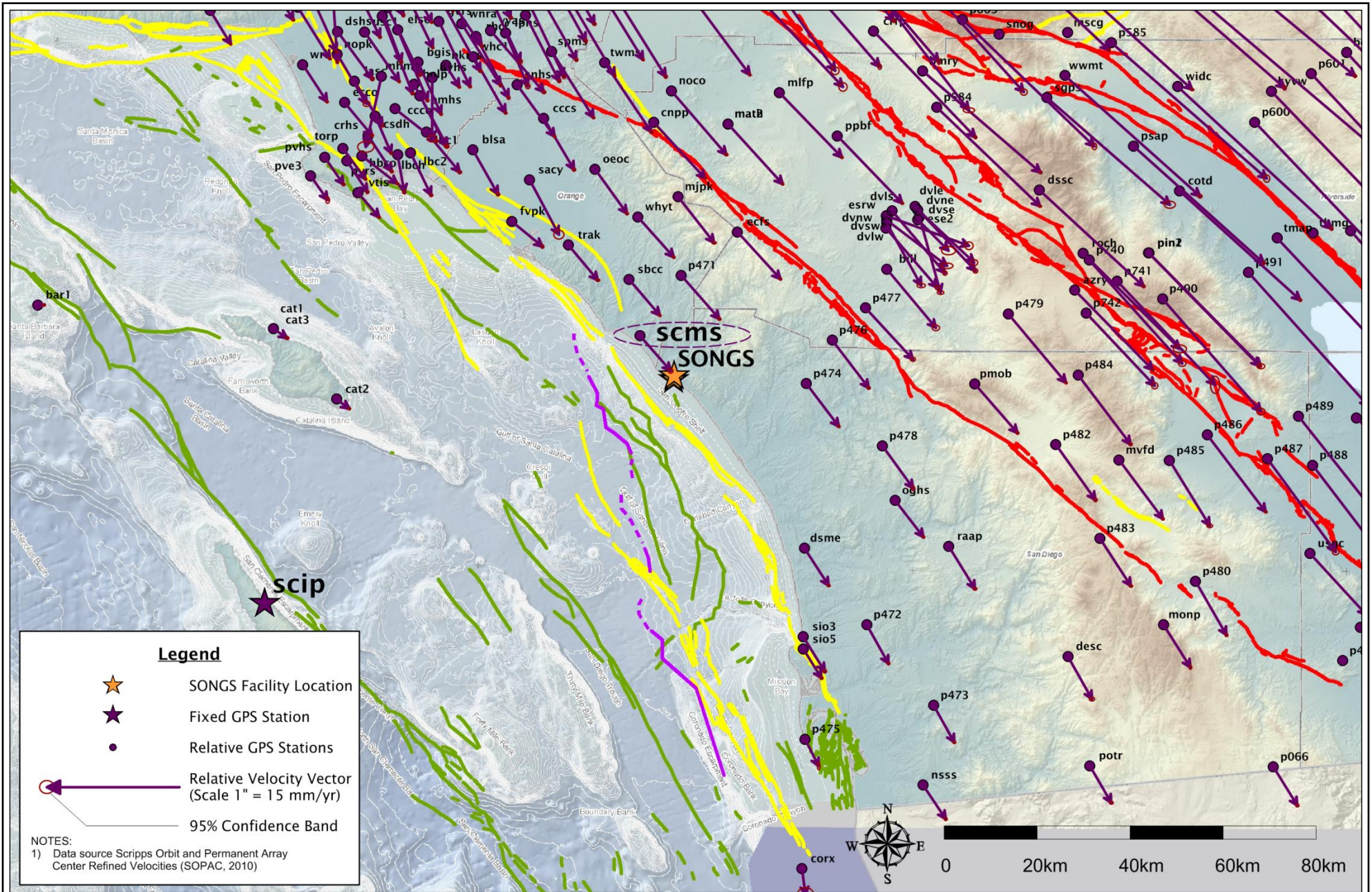
D

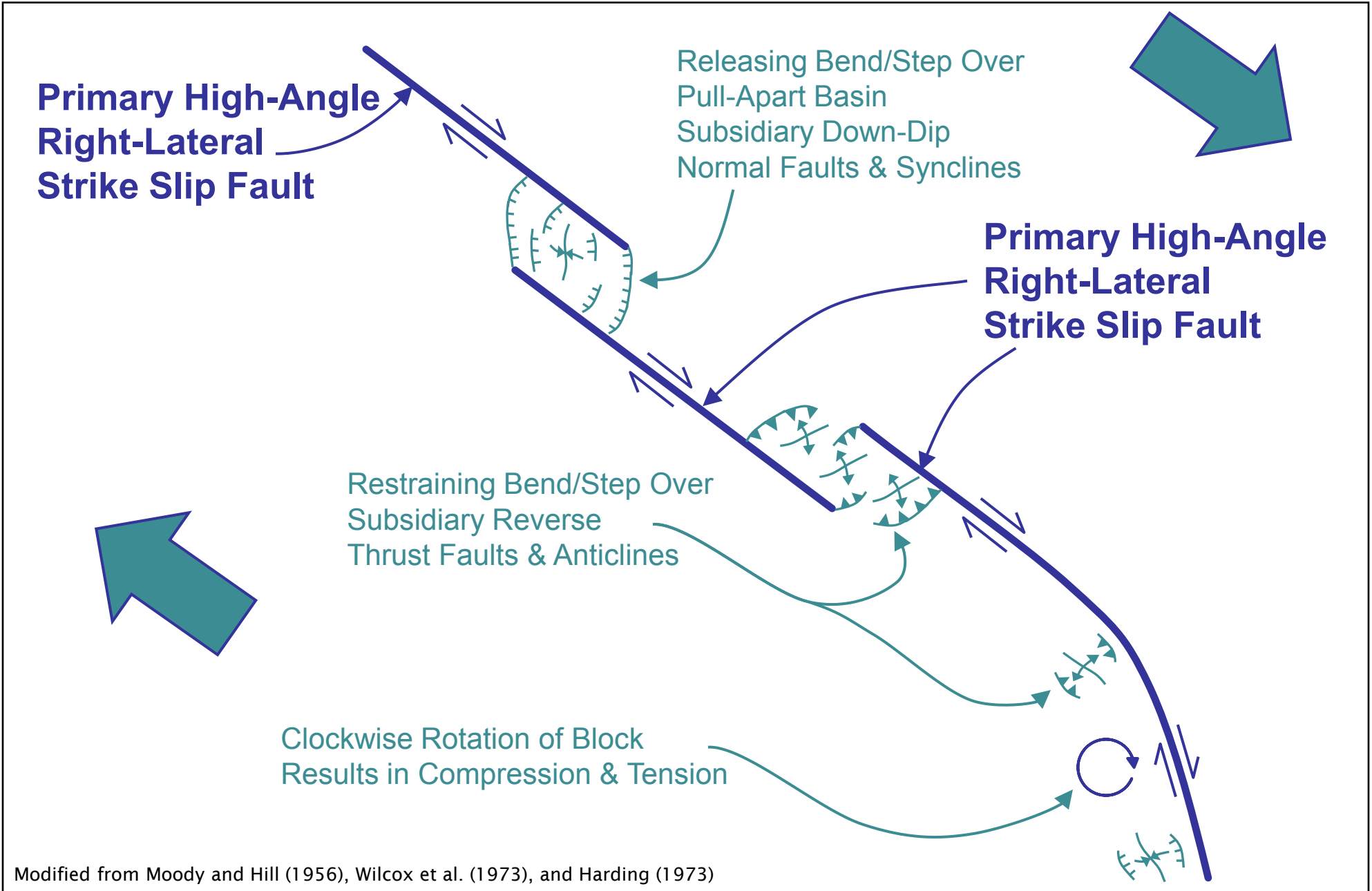
Palinspastic maps of California continental borderland and adjacent regions for past 20 m.y. Light gray areas are accretionary rocks of Franciscan Complex or belts that are lithologically similar to that complex. Medium gray areas are underlain by forearc strata. Dark gray areas are known outcrops of forearc strata. Area in wavy lined pattern is Catalina Schist belt. White areas are floored by batholithic basement rocks. Fine line is modern shoreline and island configuration, shown deformed and displaced for reference in earlier models. Heavy lines are major faults that are thought to be active during time represented. Dashed double line is fault-bounded margin of Catalina Schist belt. Dashed boxed line is active margin of extending region within Catalina Schist belt. Arrows show approximate trajectories of areas with respect to North America. (A) 20 Ma; time period prior to most of the deformation. (B) 15 Ma; time period in migrating-hinge phase of extension. (C) 5 Ma; time period in dispersed right-normal-slip phase of extension. (D) Present-day configuration.

Source: Bohannon and Geist (1998)



NOTES: (1) Modified from Crouch and Suppe (1993)
 (2) Presented in SCE (2001)



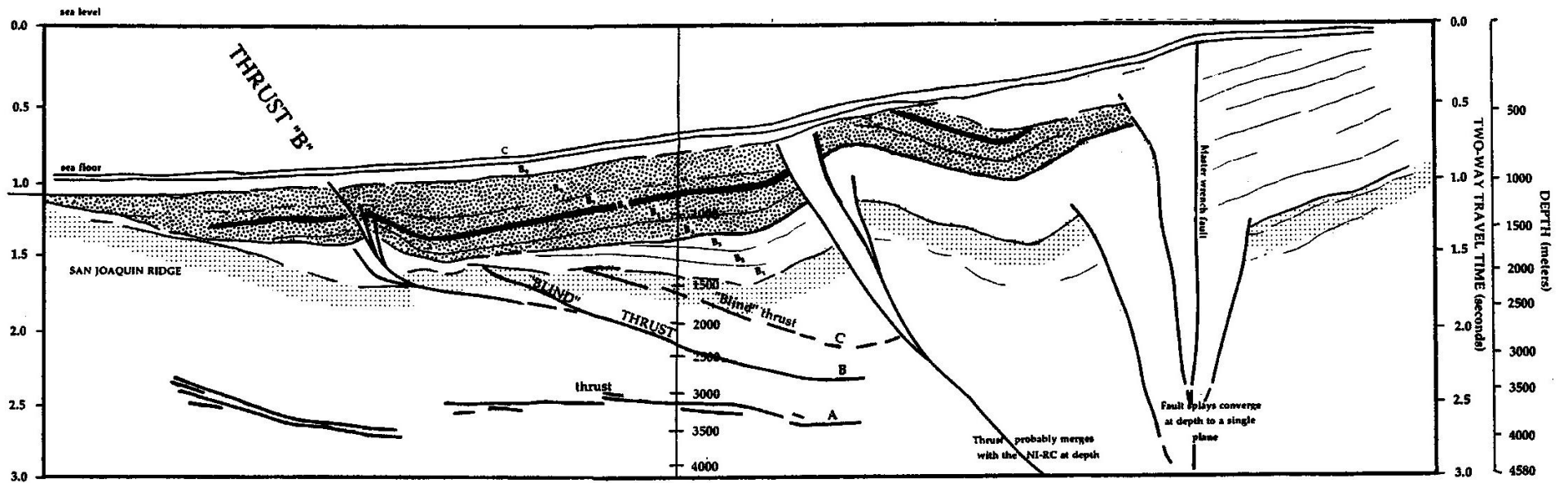


Modified from Moody and Hill (1956), Wilcox et al. (1973), and Harding (1973)

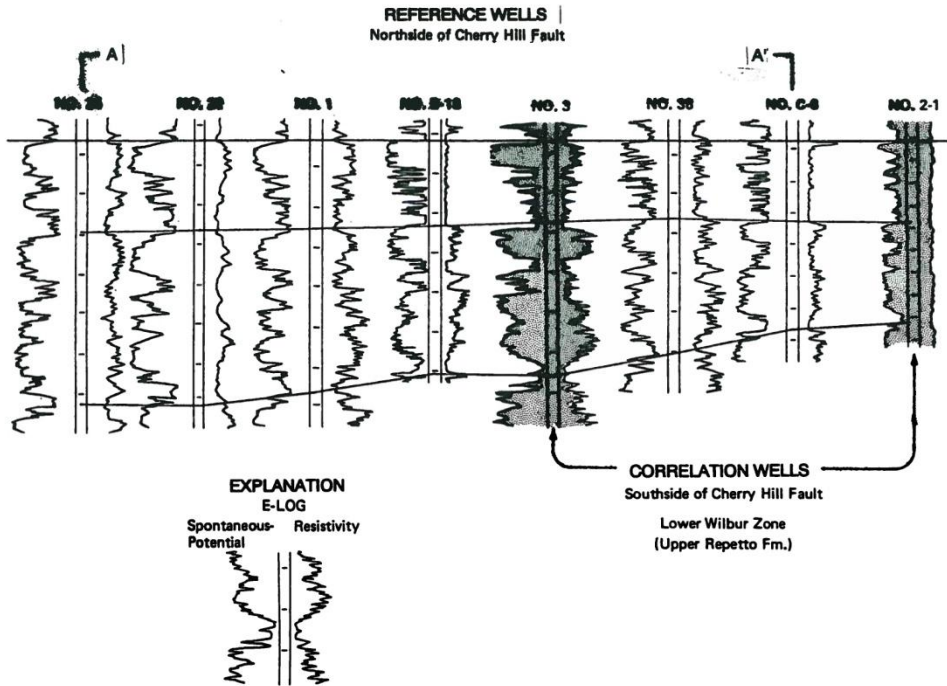
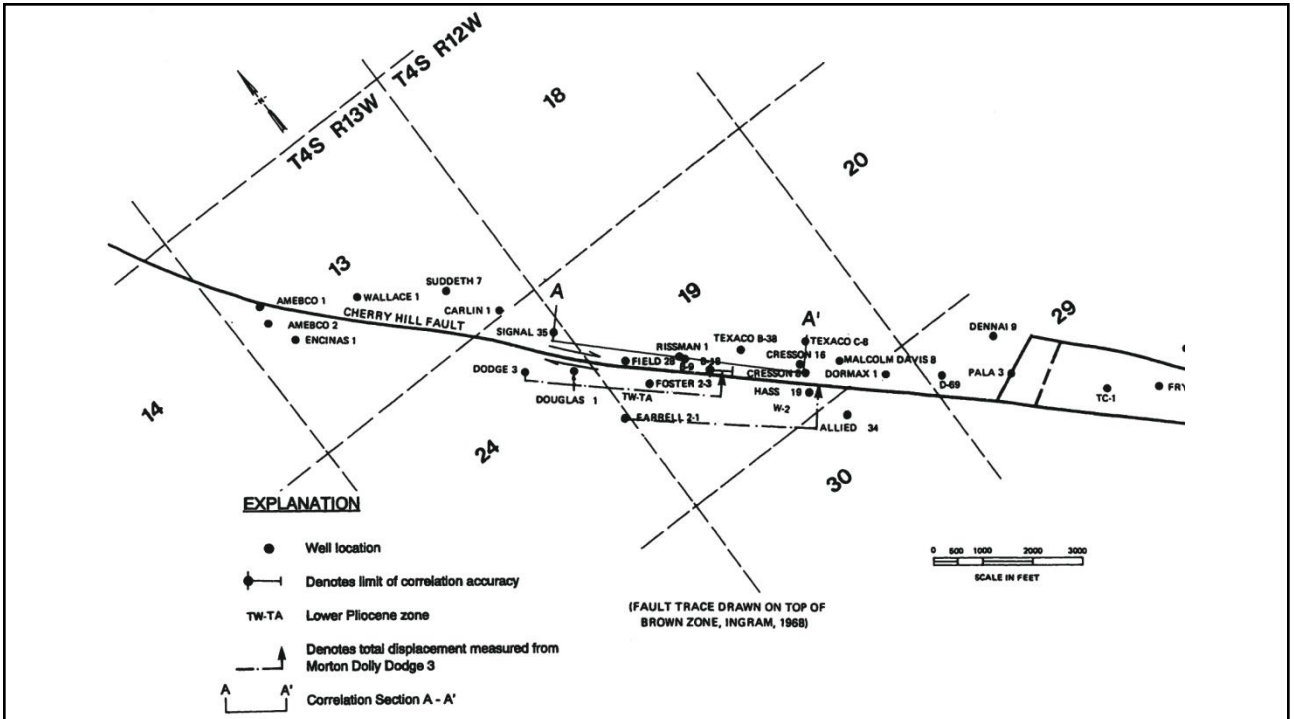
OUTER THRUST-FOLD COMPLEX

**SAN MATEO ANTICLINE /
FOLD COMPLEX**

**POSITIVE
FLOWER
STRUCTURE**

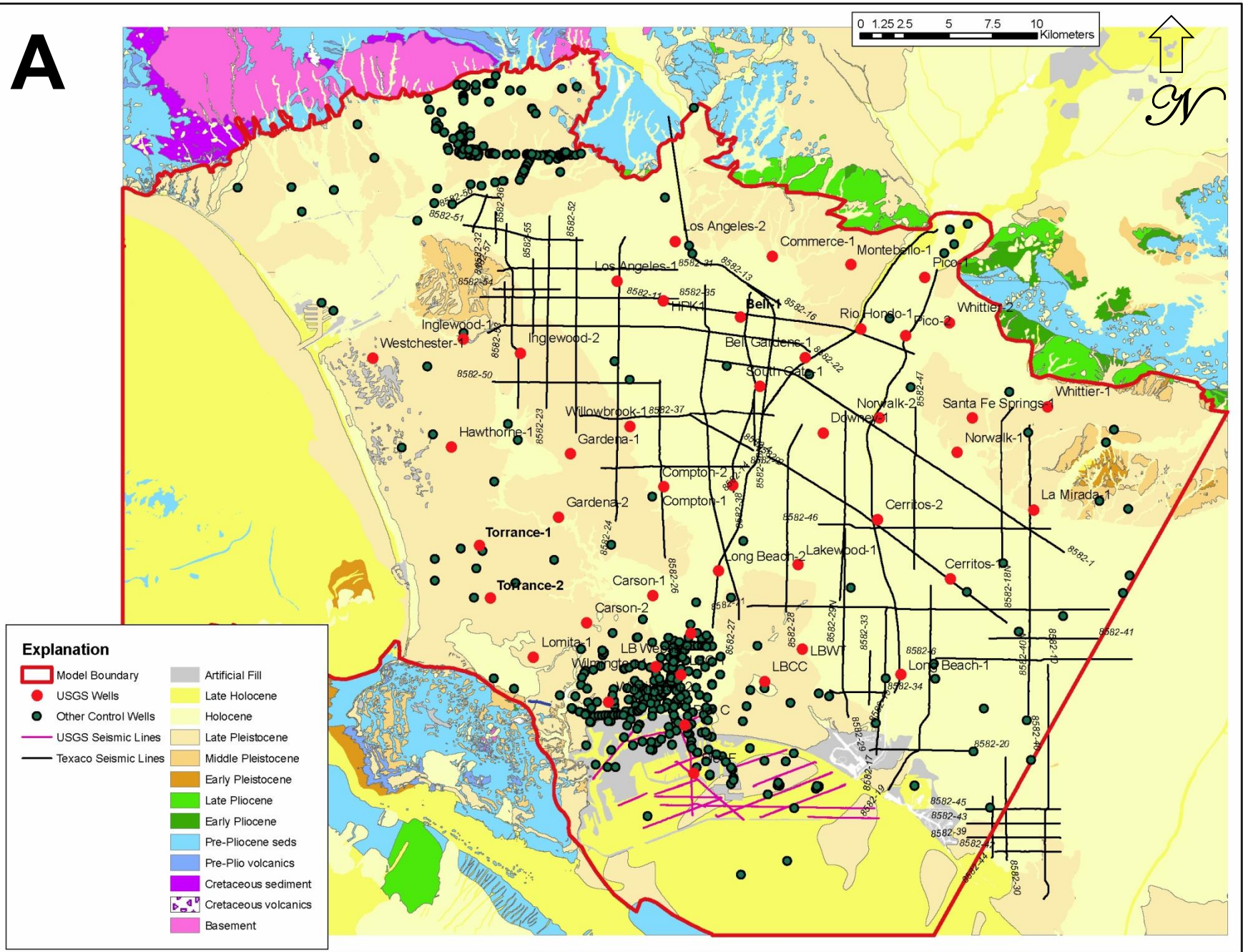


NOTES: (1) Modified from Fischer and Mills (1991)
(2) Presented in SCE (2001)

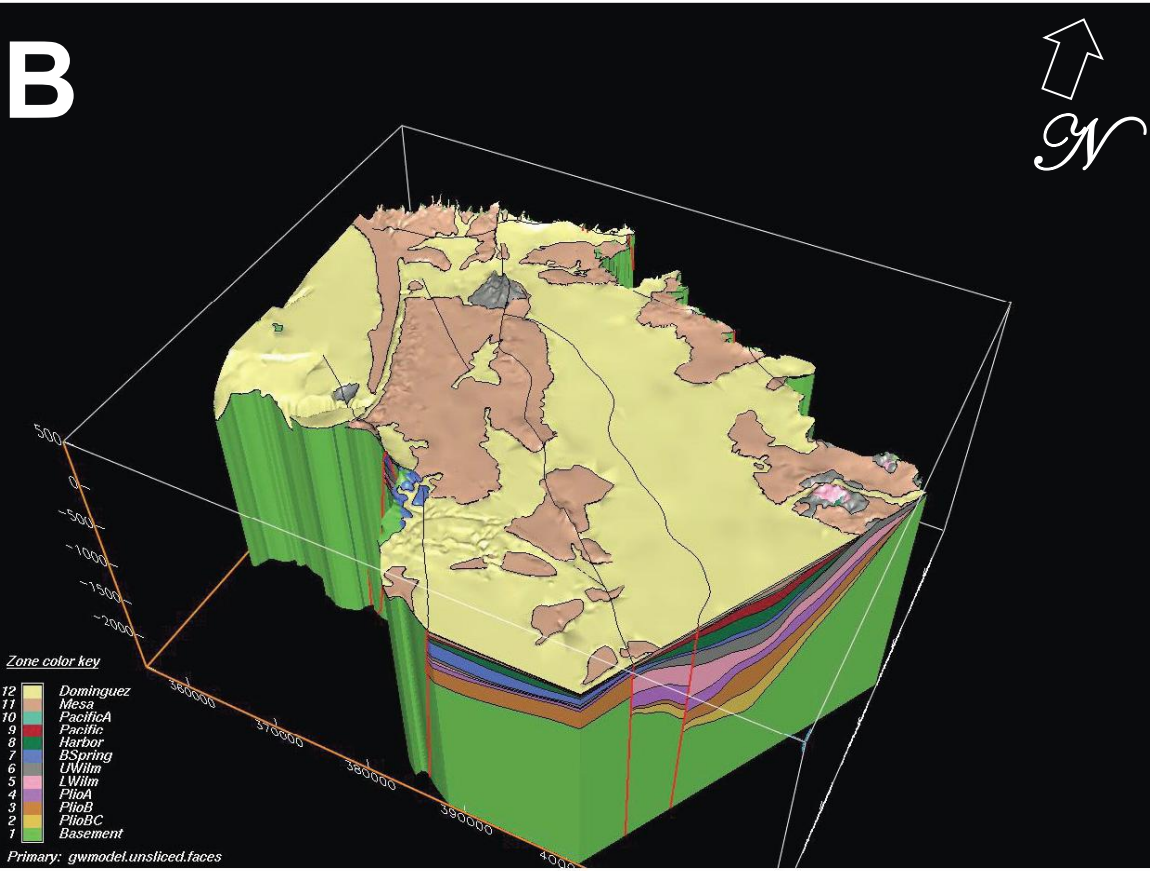


Source: Freeman et al. (1992)

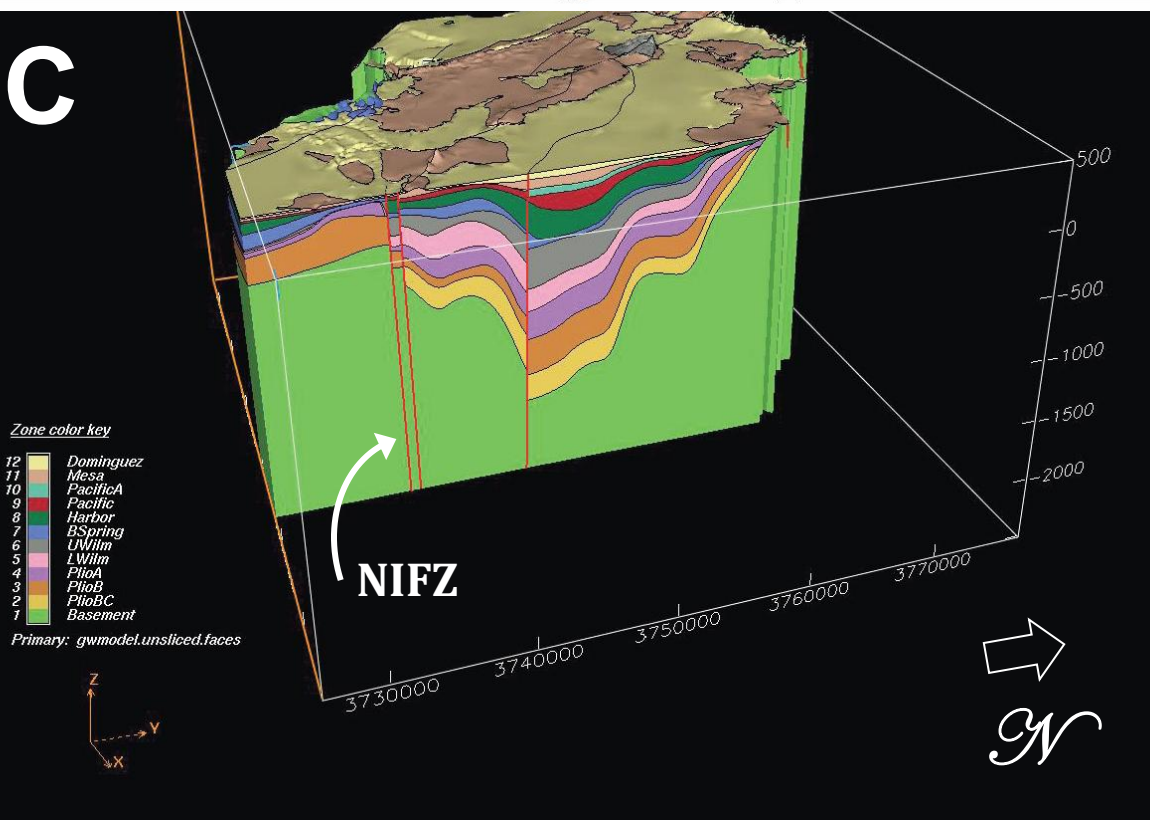
A



B



C



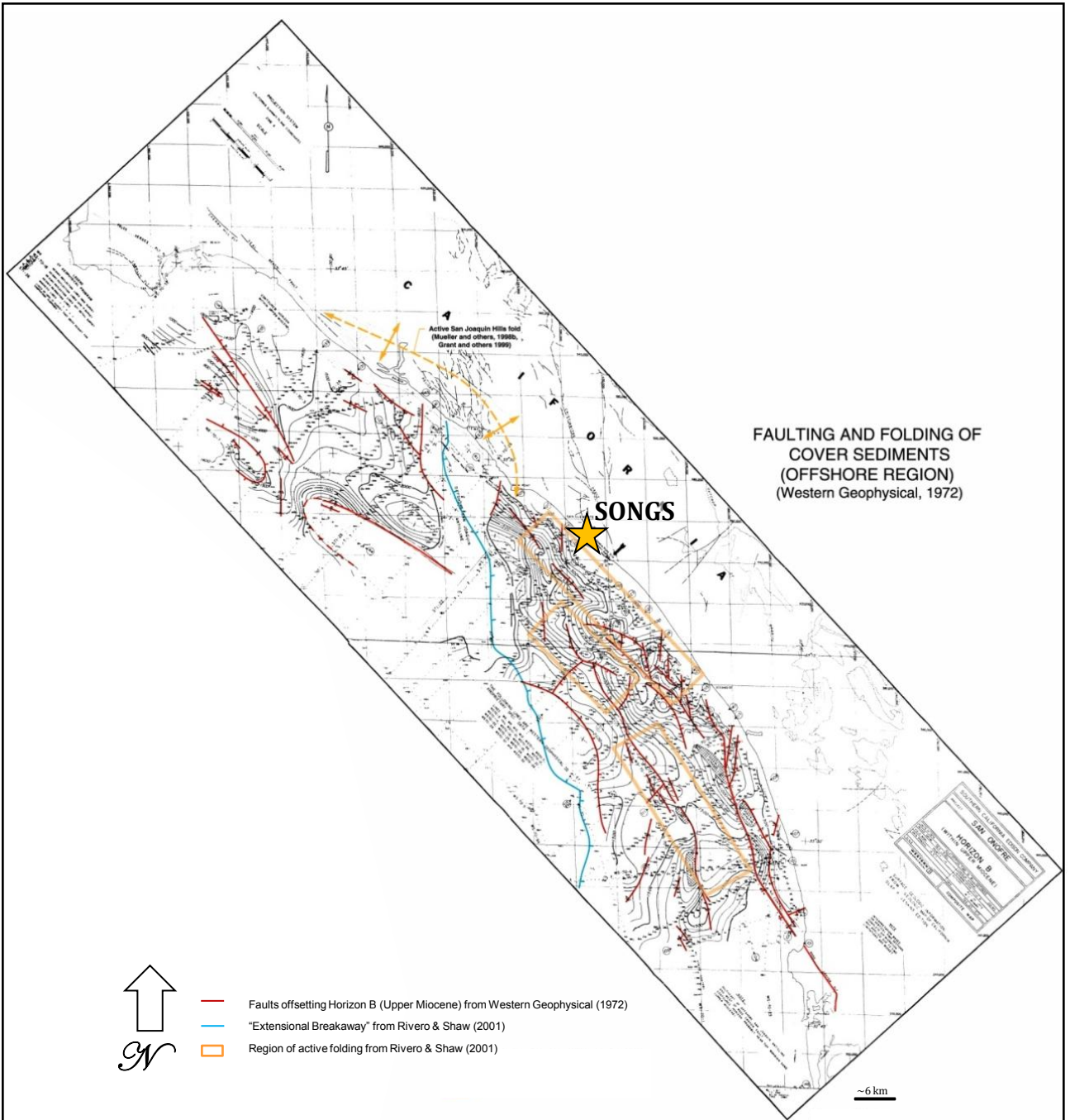
Modified from Ponti (2010)



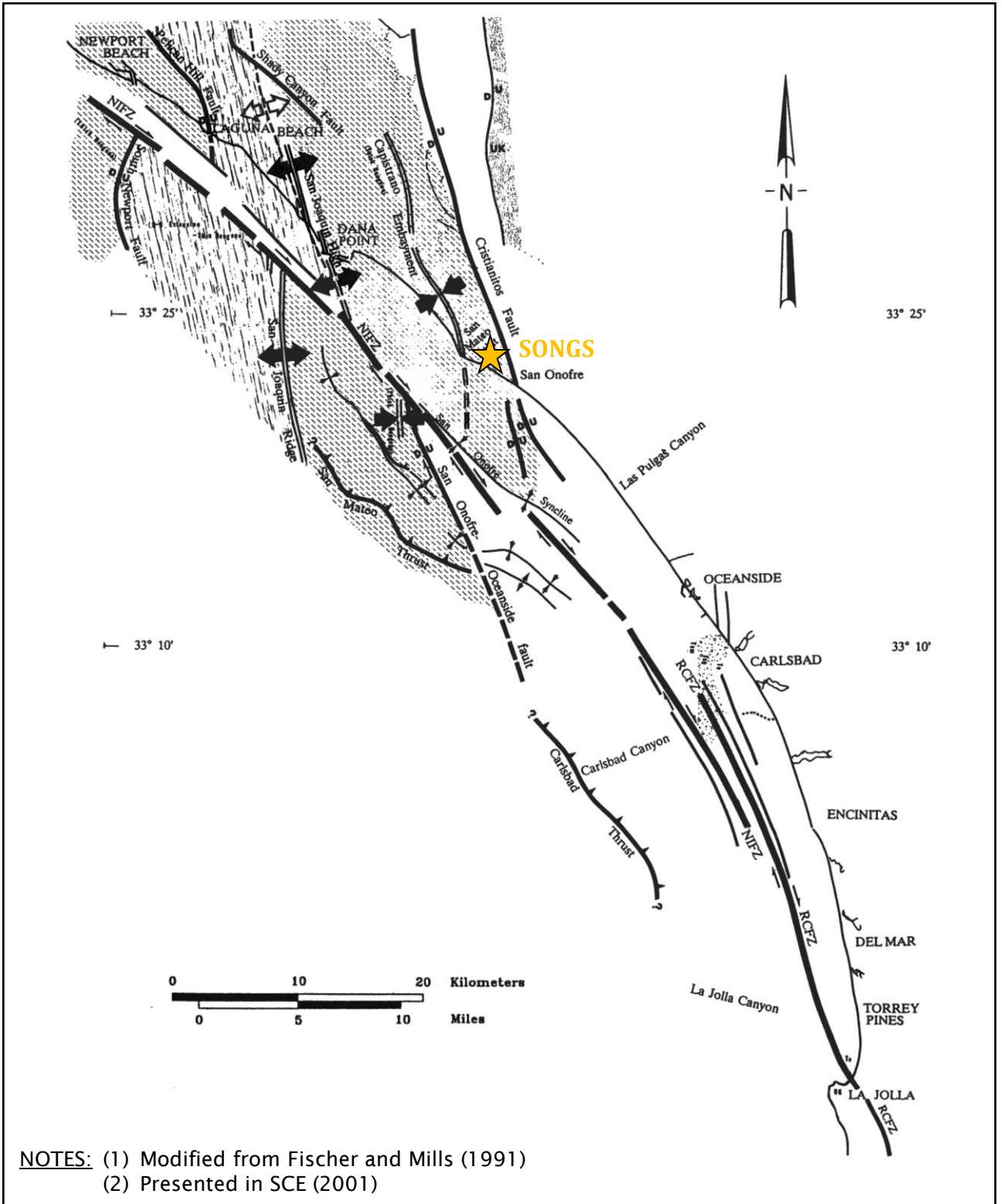
SAN ONOFRE NUCLEAR GENERATING STATION
SEISMIC HAZARD ASSESSMENT PROGRAM

MAP AND 3D STRUCTURAL MODEL OF THE LA BASIN

FIGURE A-6



NOTES: (1) Modified from Western Geophysical (1972) and Rivero and Shaw (2001)
 (2) Presented in SCE (2001)

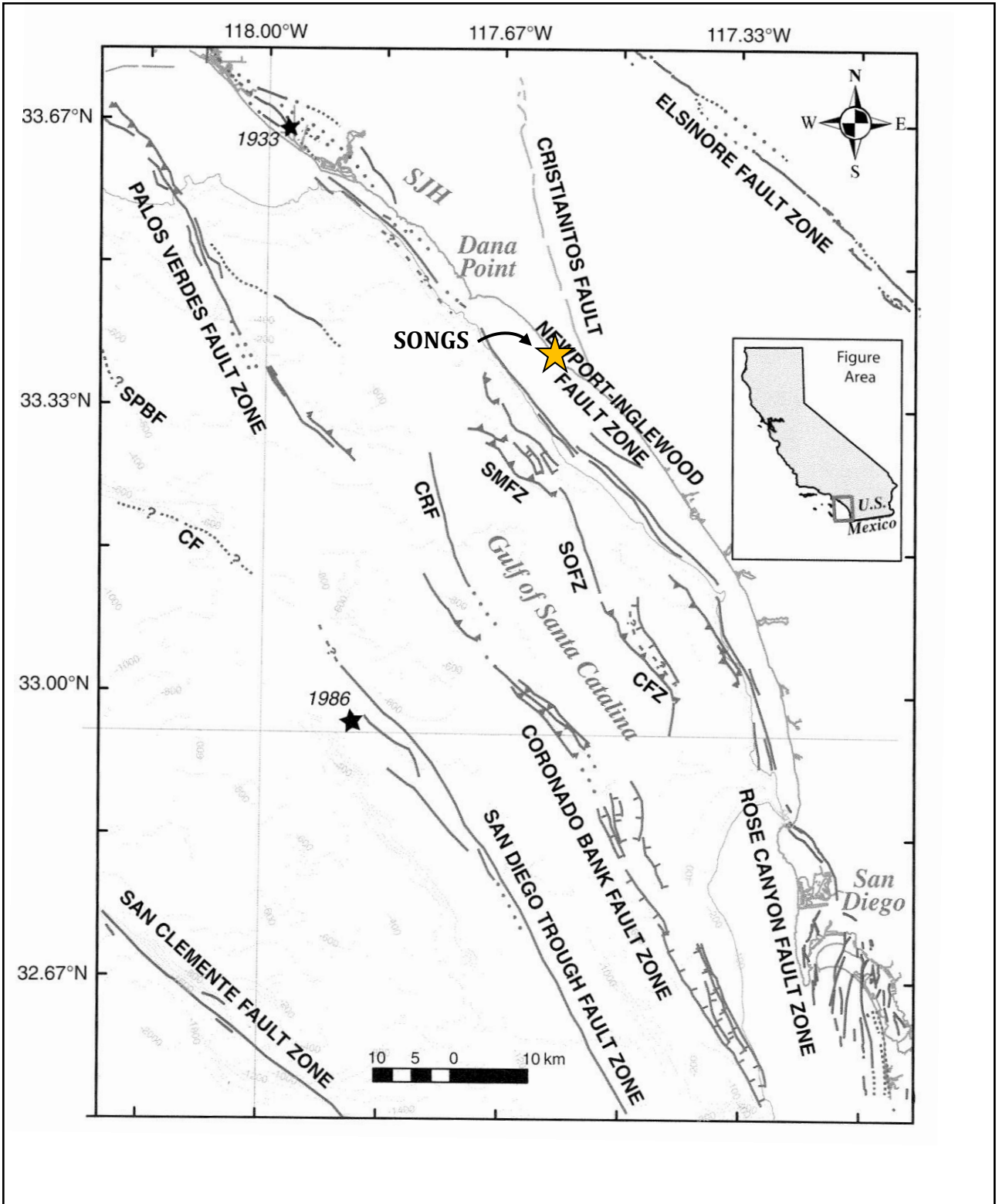


FAULT AND FOLD MAP OF THE INNER CONTINENTAL BORDERLAND AND COASTAL REGION

FIGURE A-7b

SAN ONOFRE NUCLEAR GENERATING STATION

SEISMIC HAZARD ASSESSMENT PROGRAM

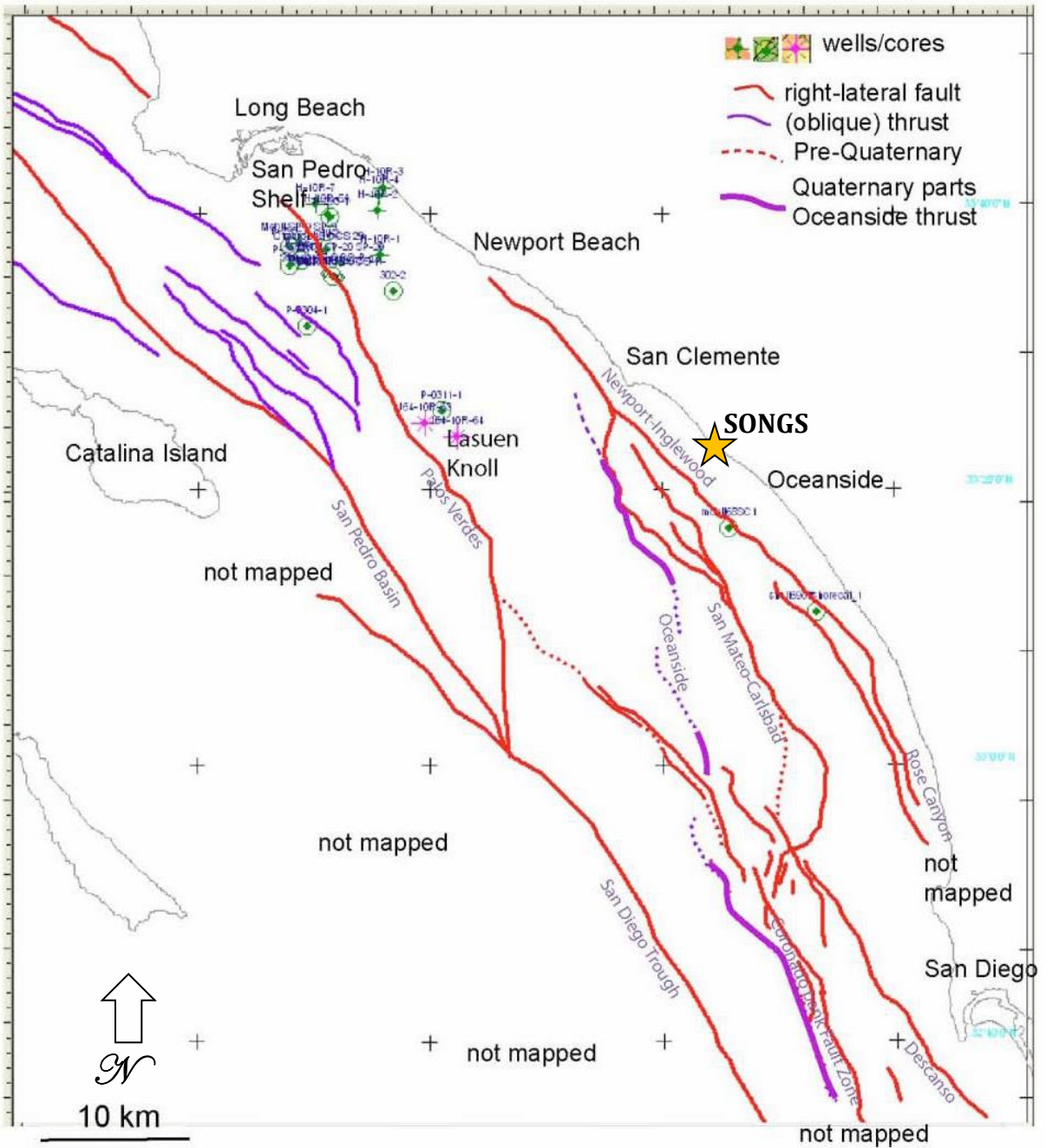


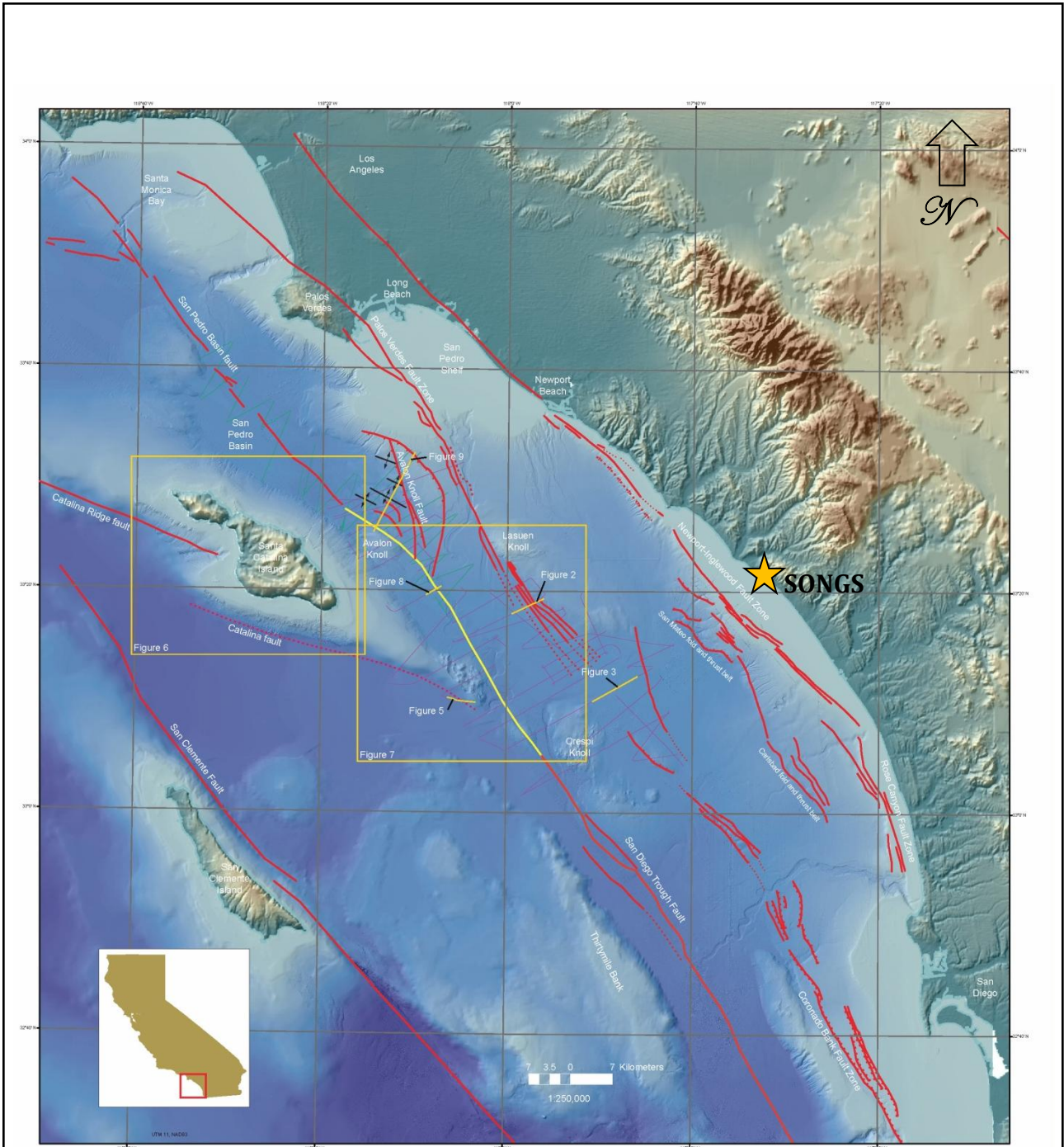
OFFSHORE FAULT MAP BY RYAN ET AL. (2009)

FIGURE A-7c



SAN ONOFRE NUCLEAR GENERATING STATION
SEISMIC HAZARD ASSESSMENT PROGRAM



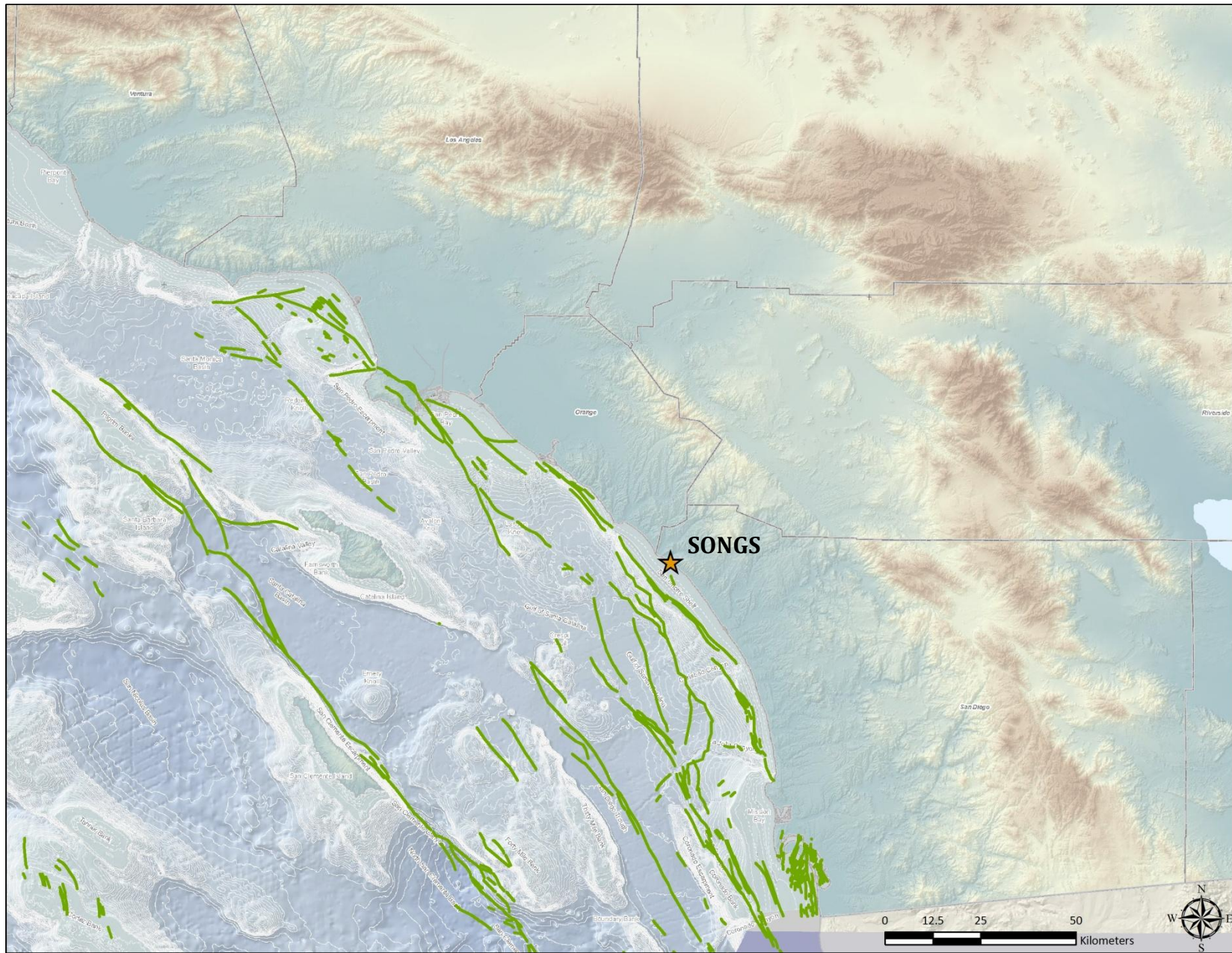


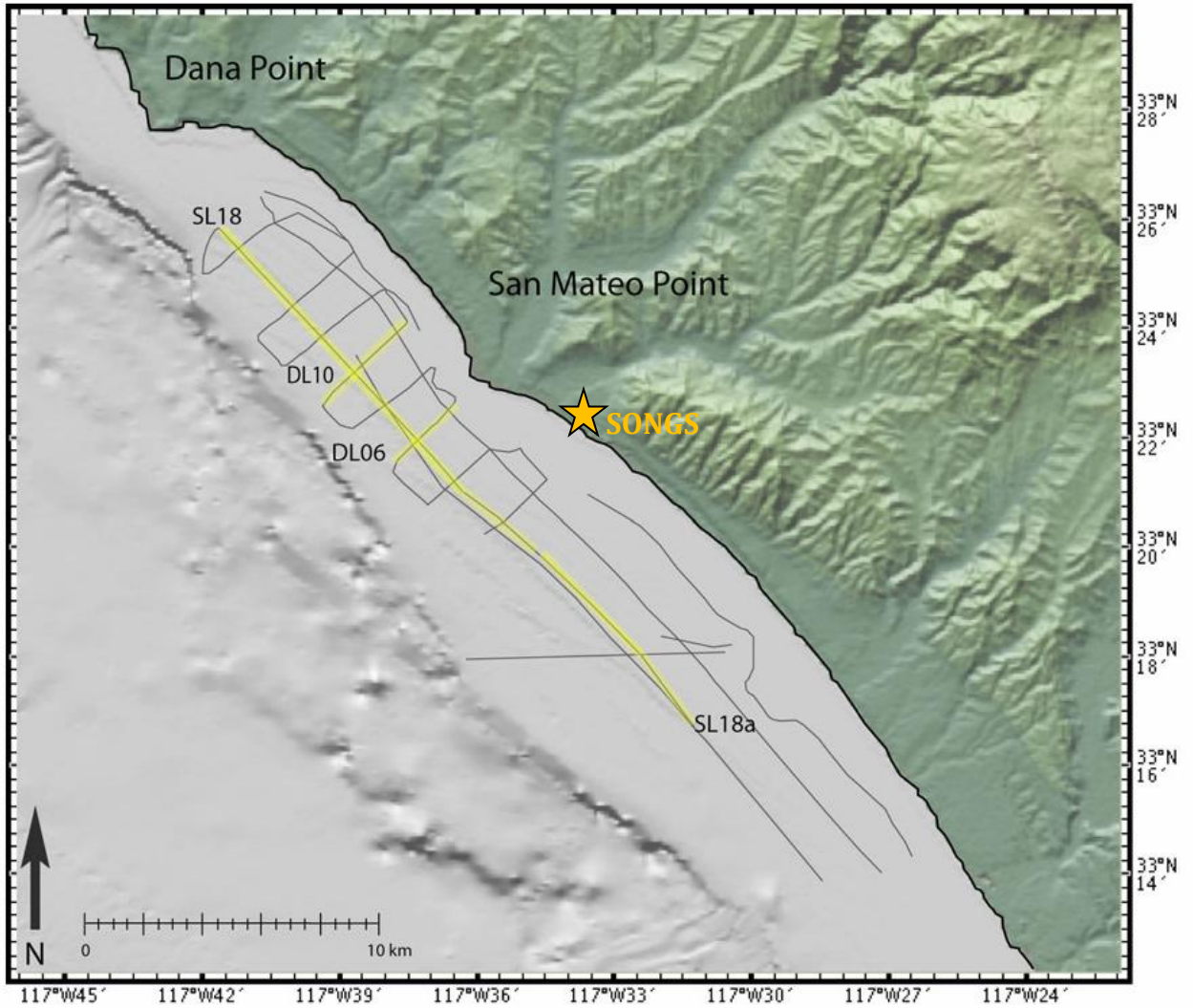
OFFSHORE FAULT MAP BY CONRAD ET AL. (2010)

FIGURE A-7e



SAN ONOFRE NUCLEAR GENERATING STATION
SEISMIC HAZARD ASSESSMENT PROGRAM





NOTE: Based on Rentz (2010)

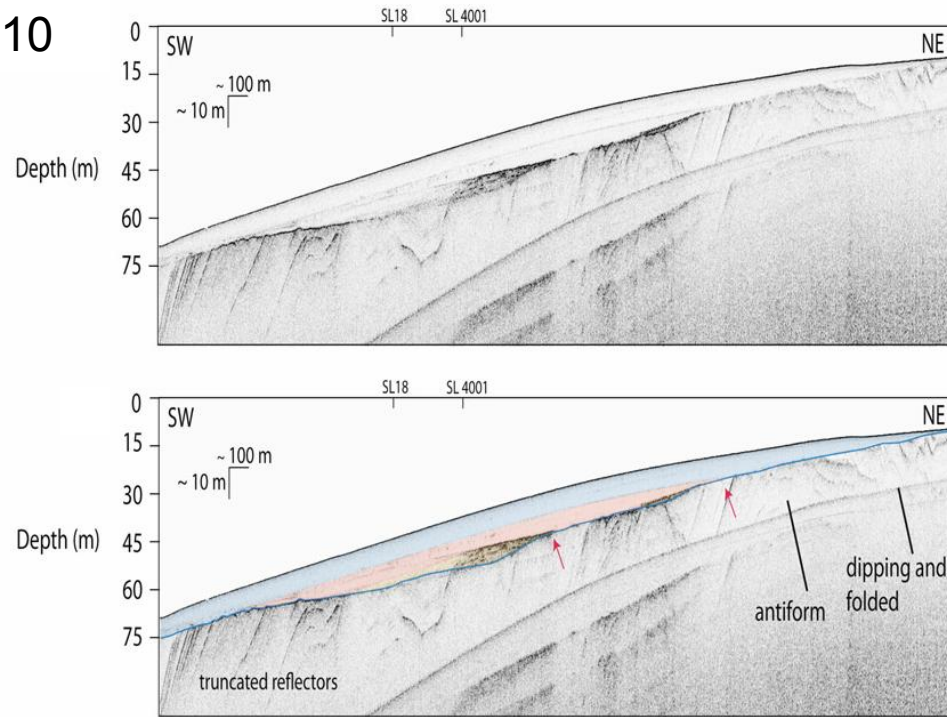


SEISMIC LINE INTERPRETATIONS

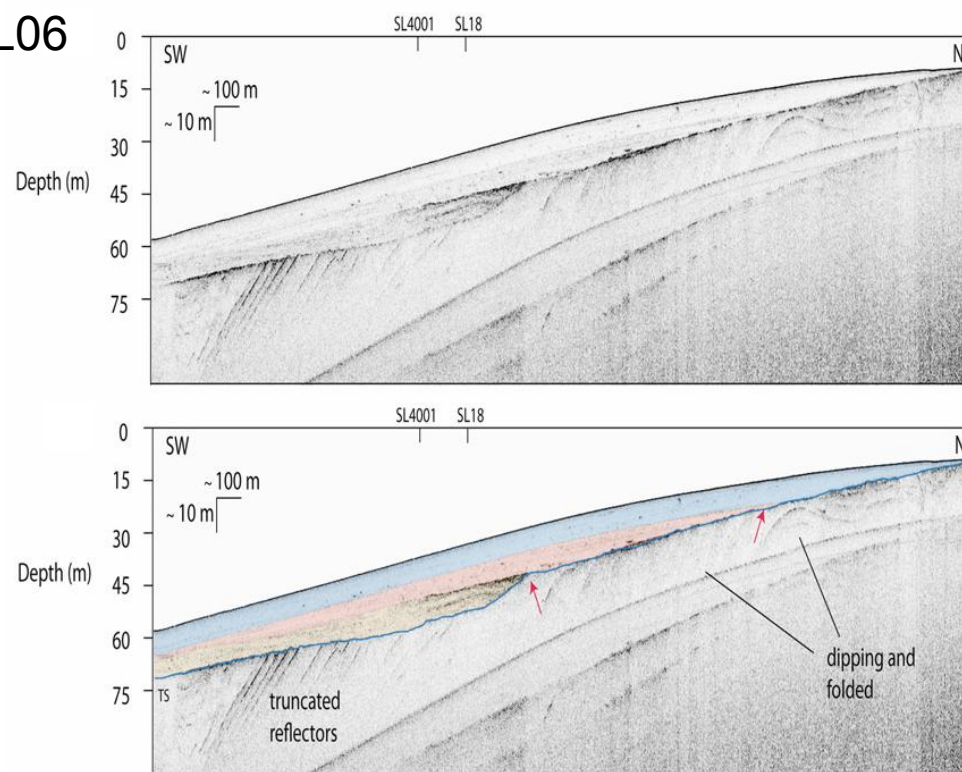
**FIGURE
A-8a**

**SAN ONOFRE NUCLEAR GENERATING STATION
SEISMIC HAZARD ASSESSMENT PROGRAM**

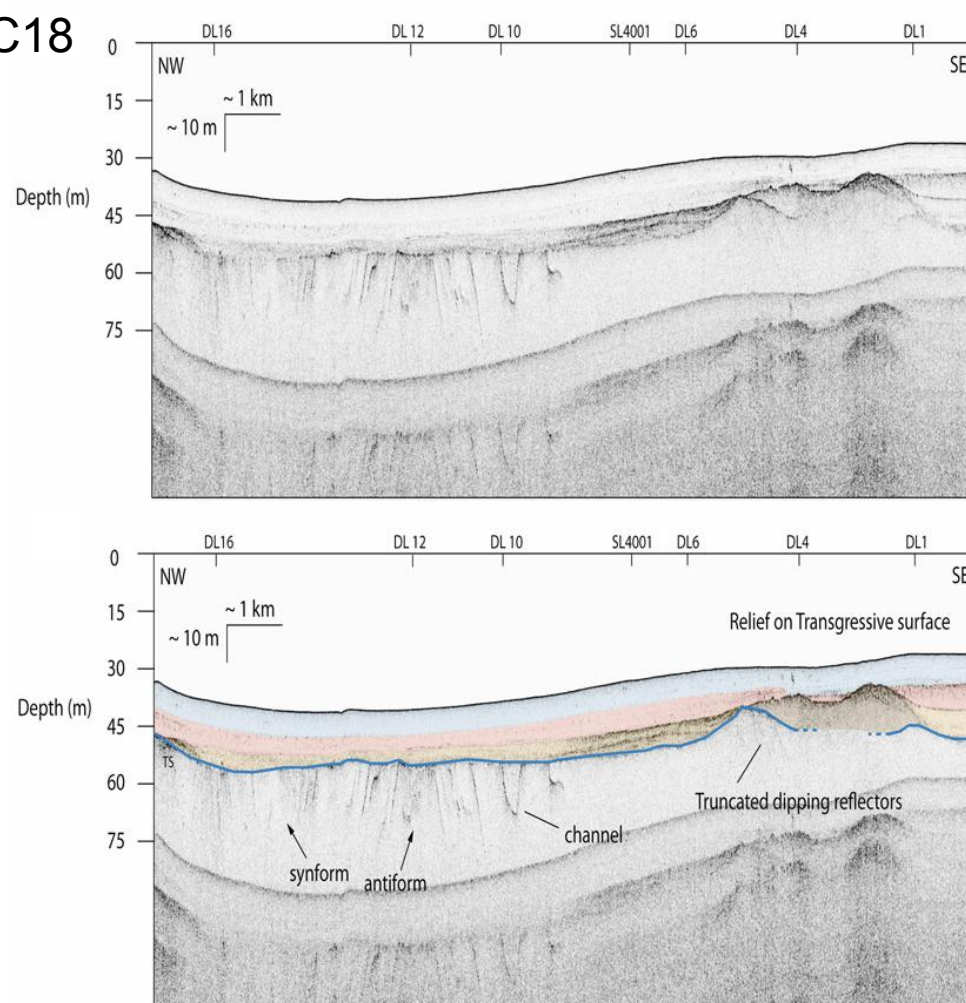
LINE DL10



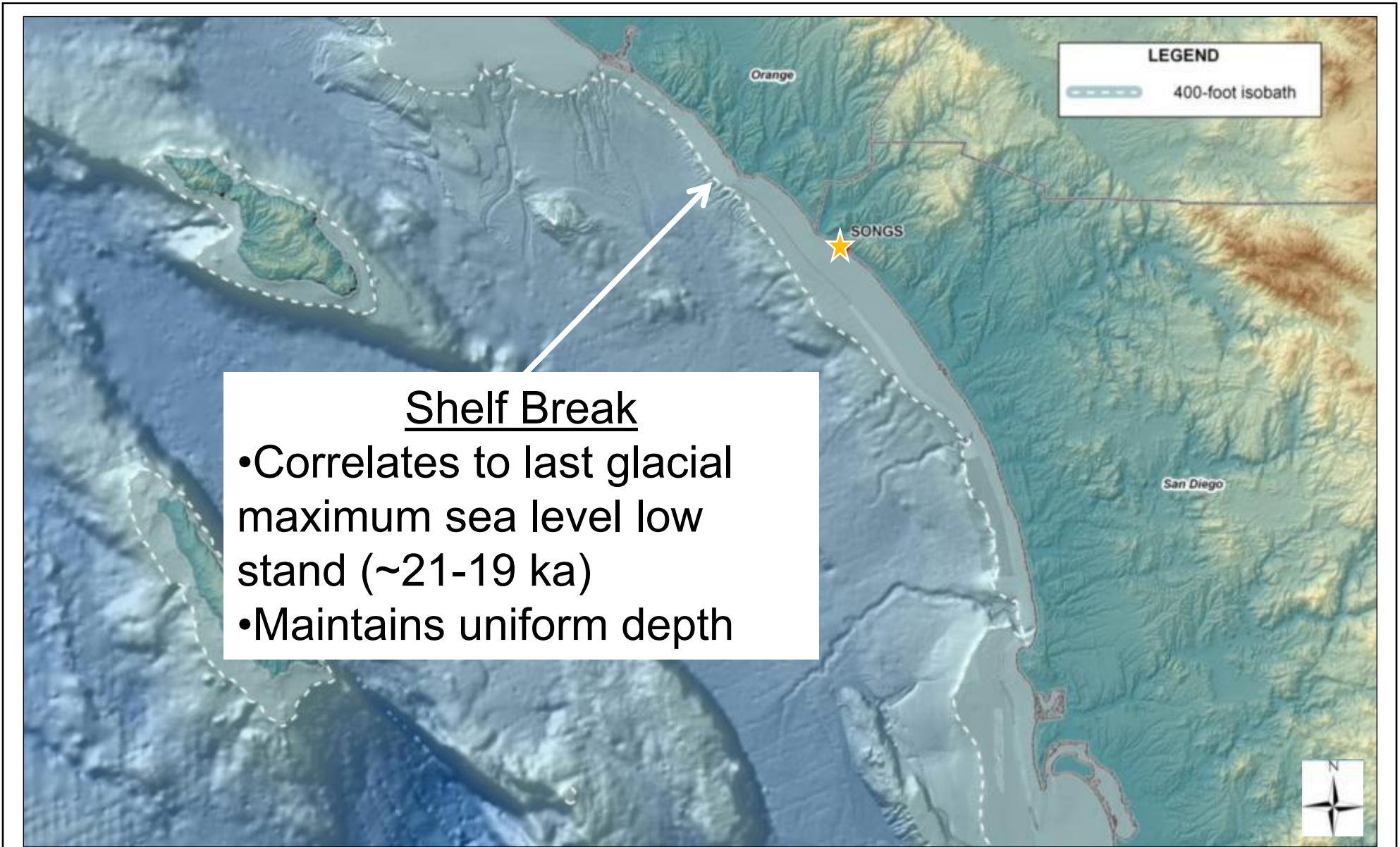
LINE DL06



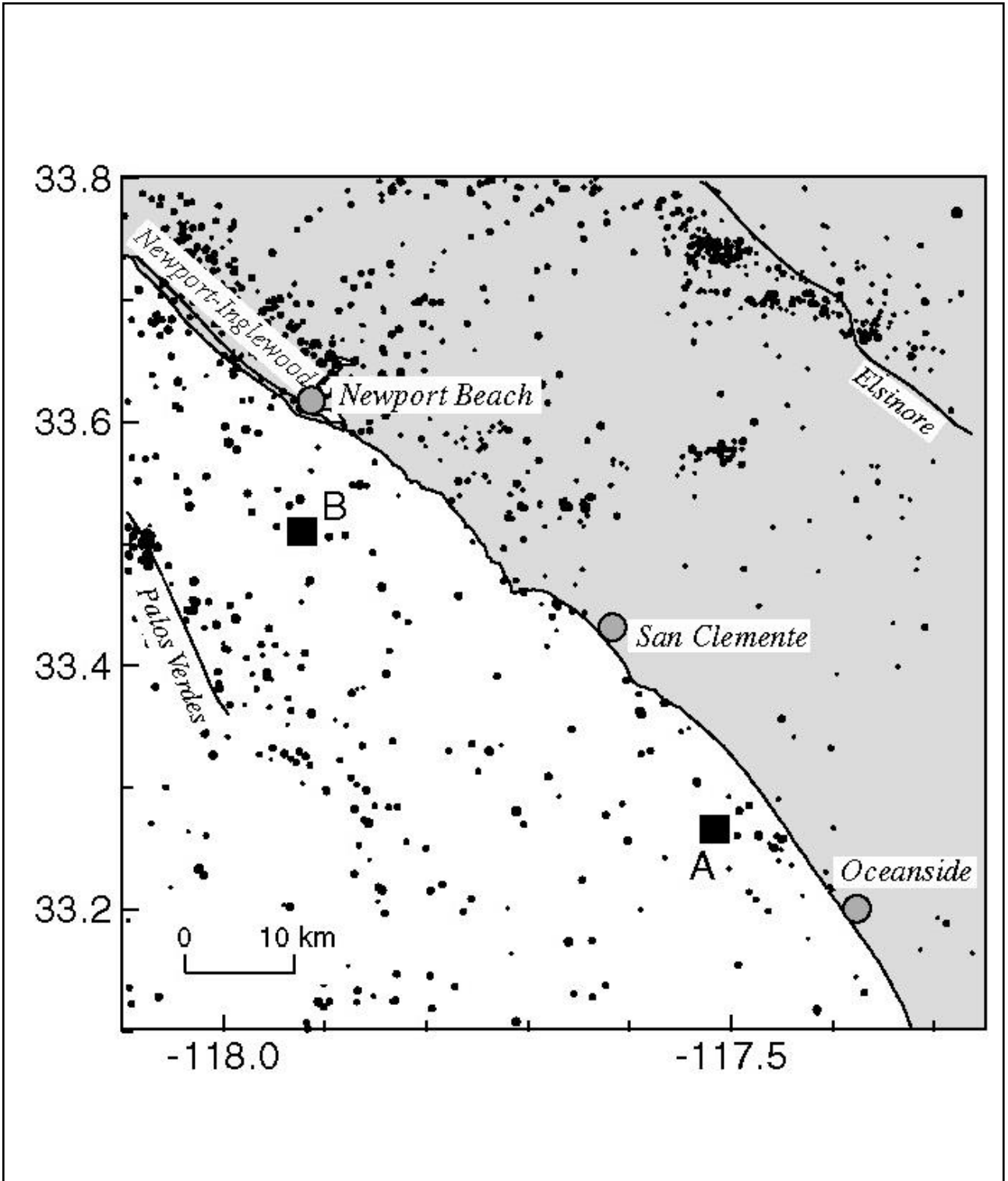
LINE SC18



NOTES: (1) Based on Rentz (2010)
 (2) Locations of seismic lines shown in Figure 8a



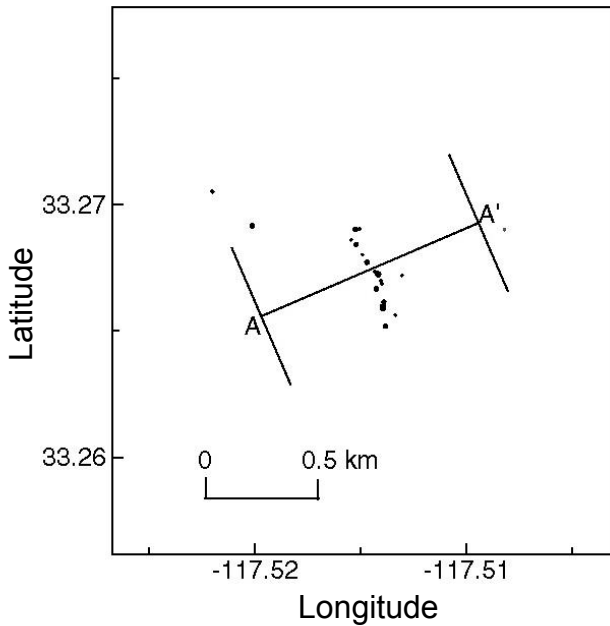
Modified from NOAA (2001, 2008), CSUMB (2010), and CaSIL (2006)



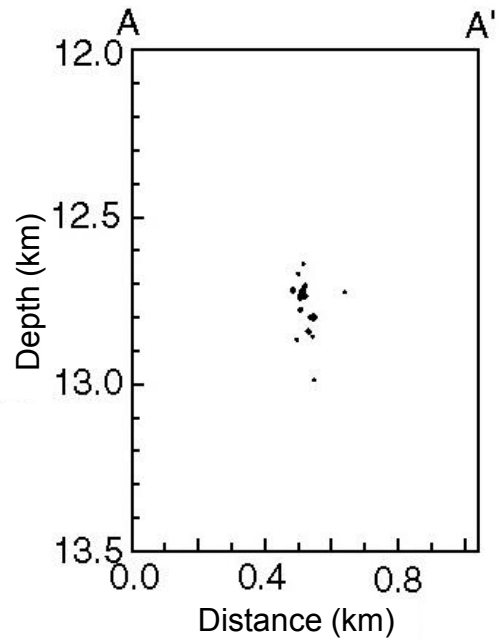
Source: Grant and Shearer (2004)

 <p>GeoPentech Geotechnical & Geoscience Consultants</p>	<p>RELOCATED EPICENTERS FROM THE 1981 OCEANSIDE AND 2000 NEWPORT BEACH EARTHQUAKE CLUSTERS</p> <p>SAN ONOFRE NUCLEAR GENERATING STATION</p> <p>SEISMIC HAZARD ASSESSMENT PROGRAM</p>	<p>FIGURE A-11a</p>
---	---	---------------------

LOCATION A

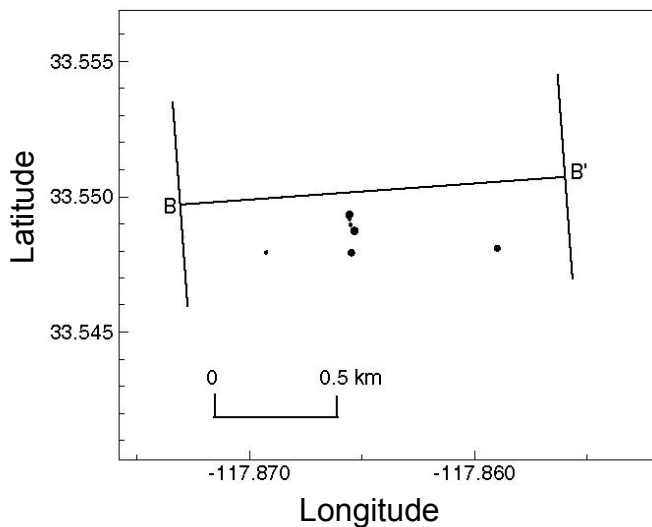


PLAN VIEW

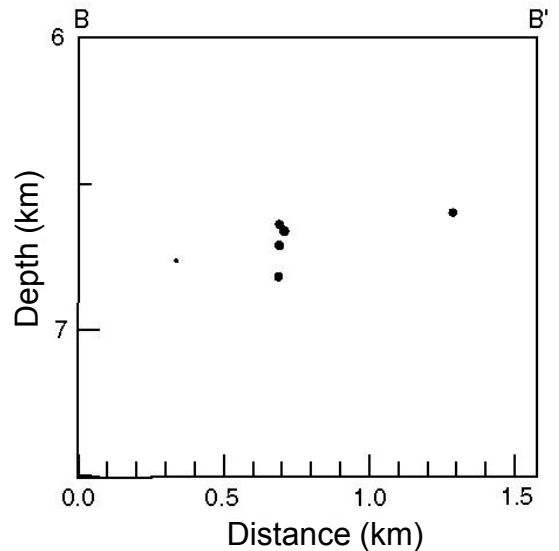


PROFILE VIEW

LOCATION B

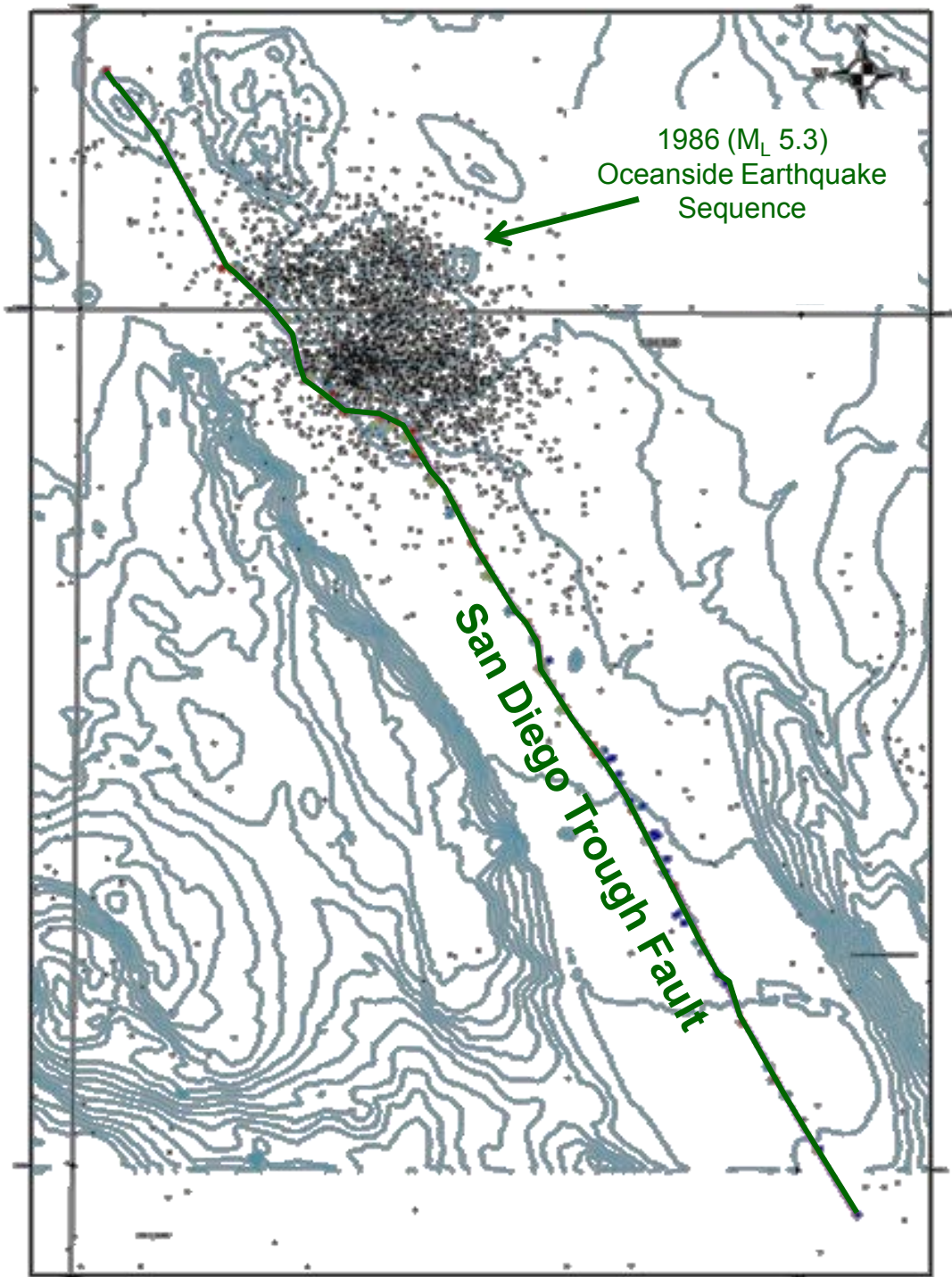


PLAN VIEW

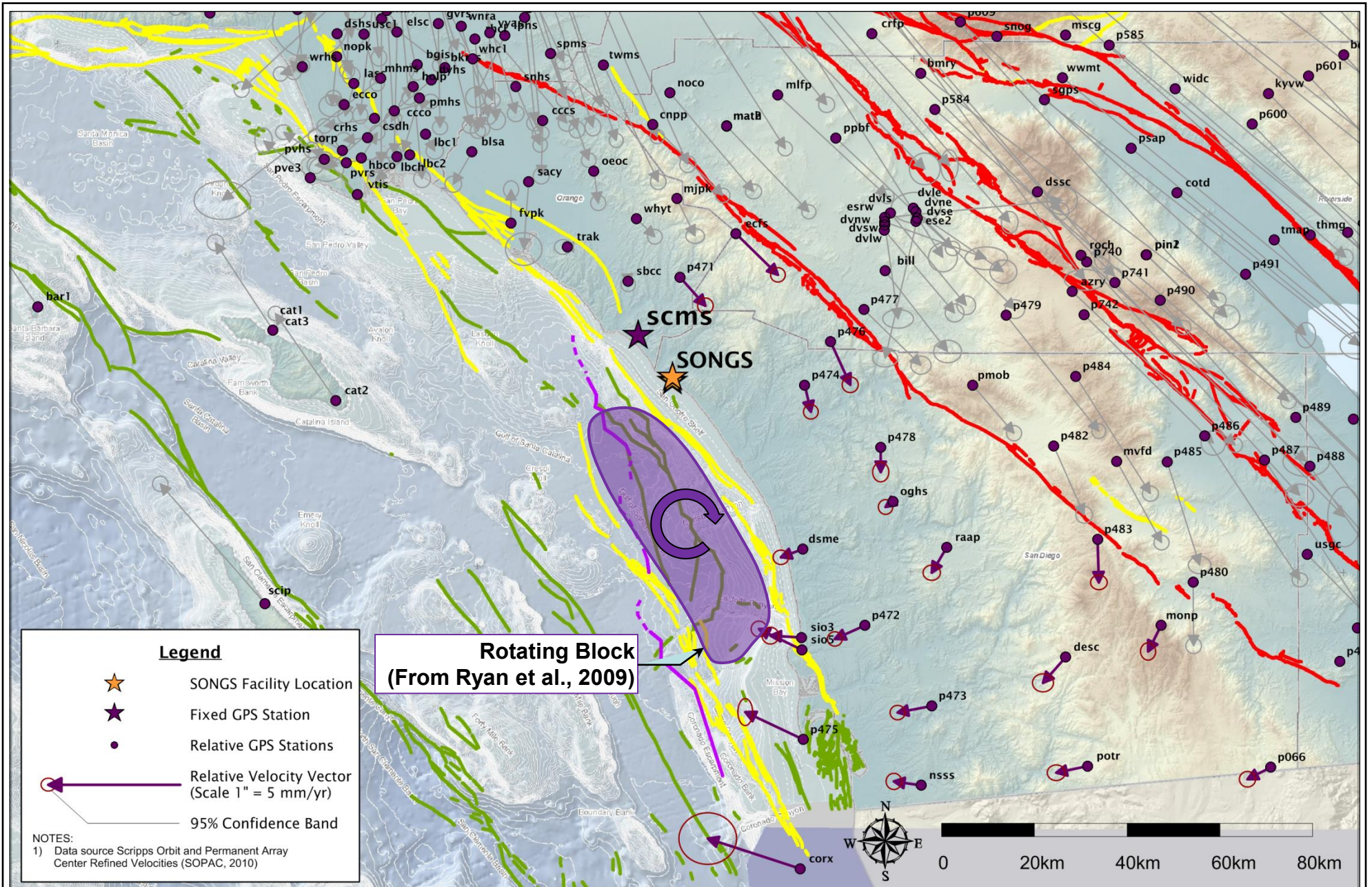


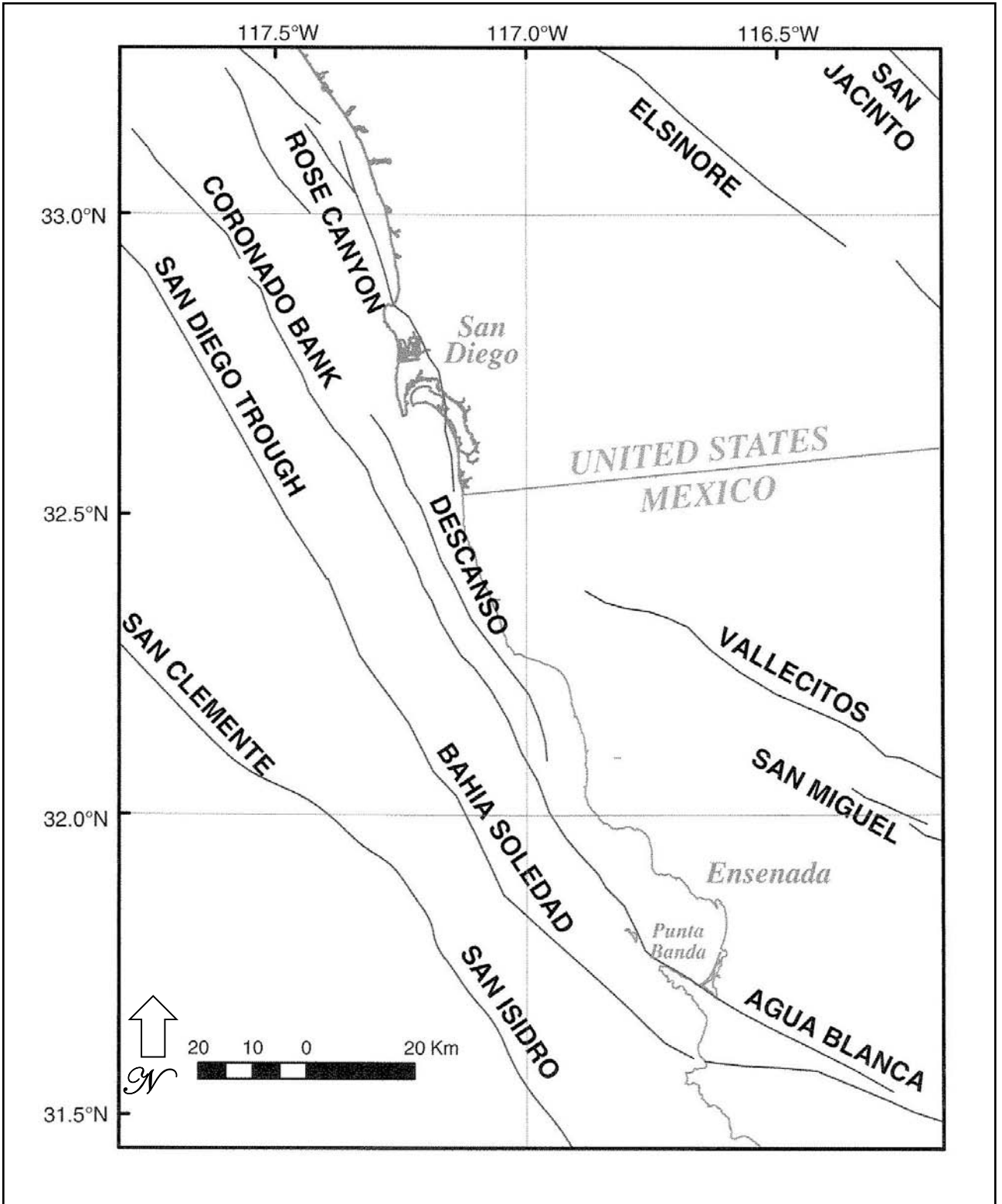
PROFILE VIEW

NOTES: (1) Modified from Grant and Shearer (2004)
 (2) Locations of "A" and "B" shown in Figure A-11a



NOTE: Based on Ryan (2010, personal communication)





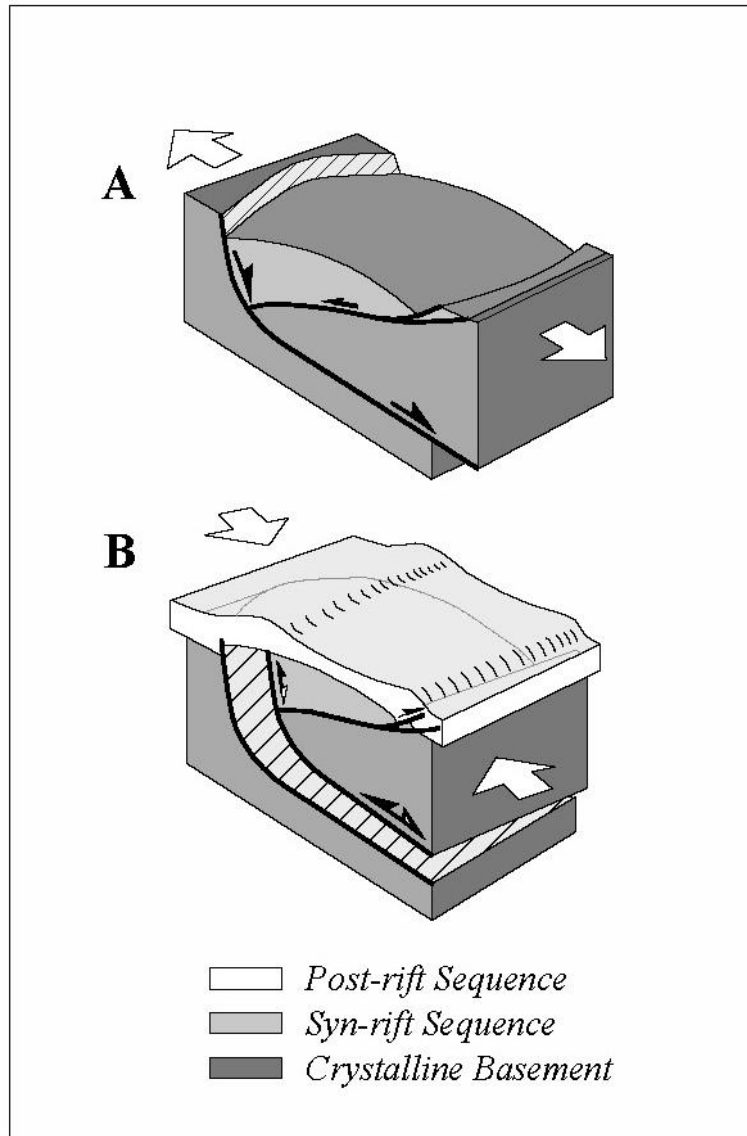
SIMPLIFIED FAULT MAP FOR BAJA CALIFORNIA, MEXICO REGION BY RYAN ET AL. (2009)

FIGURE A-14



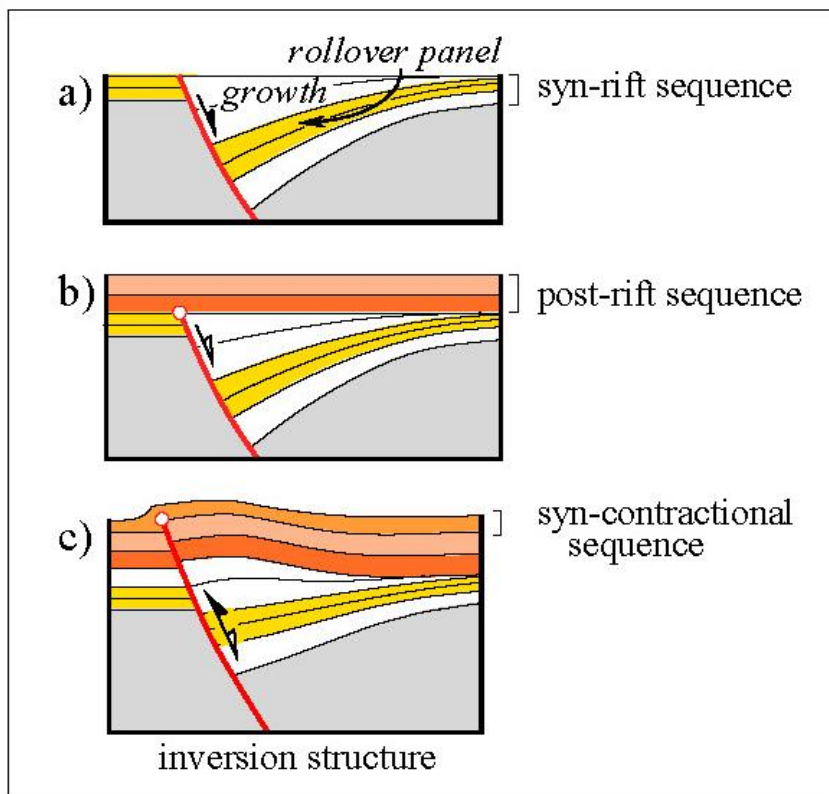
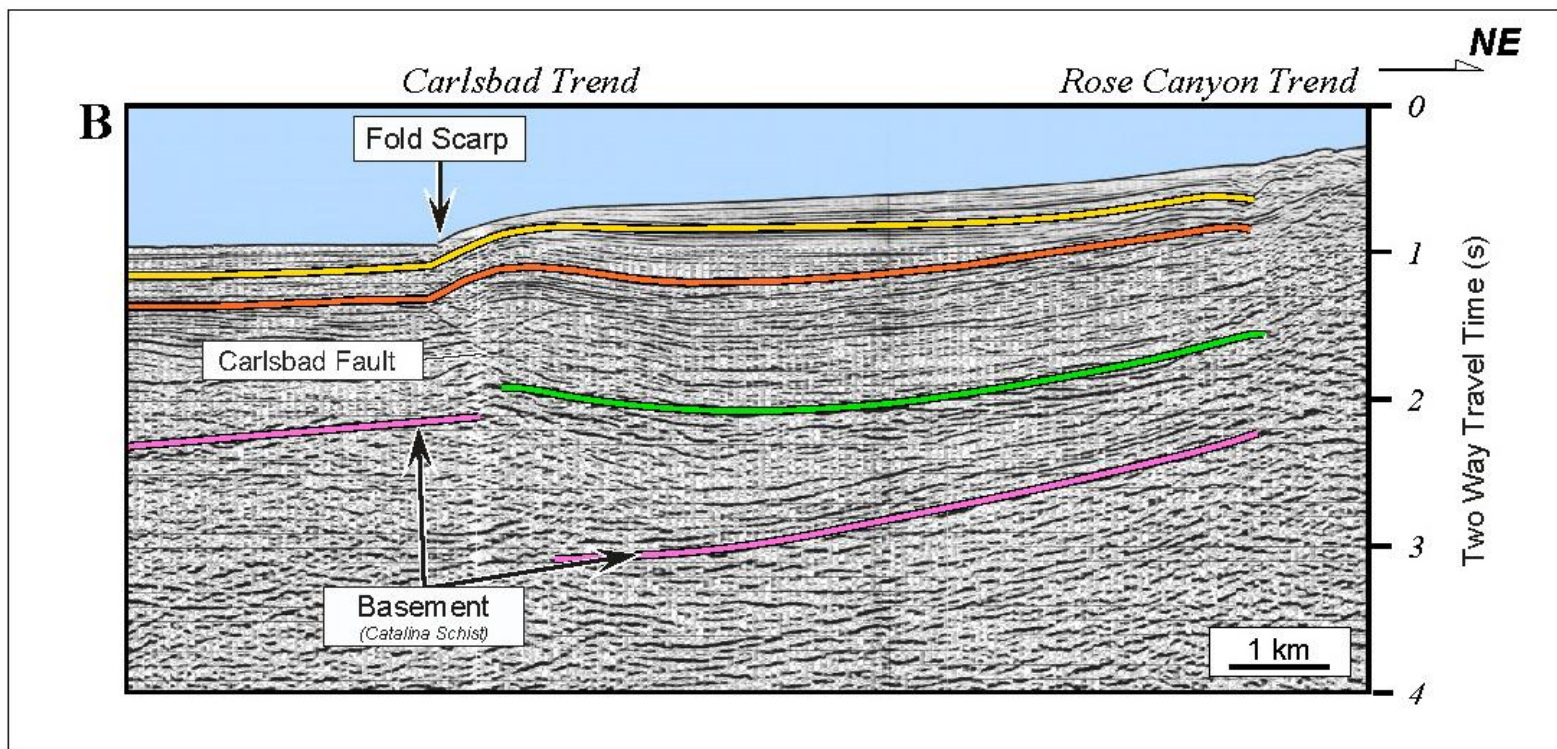
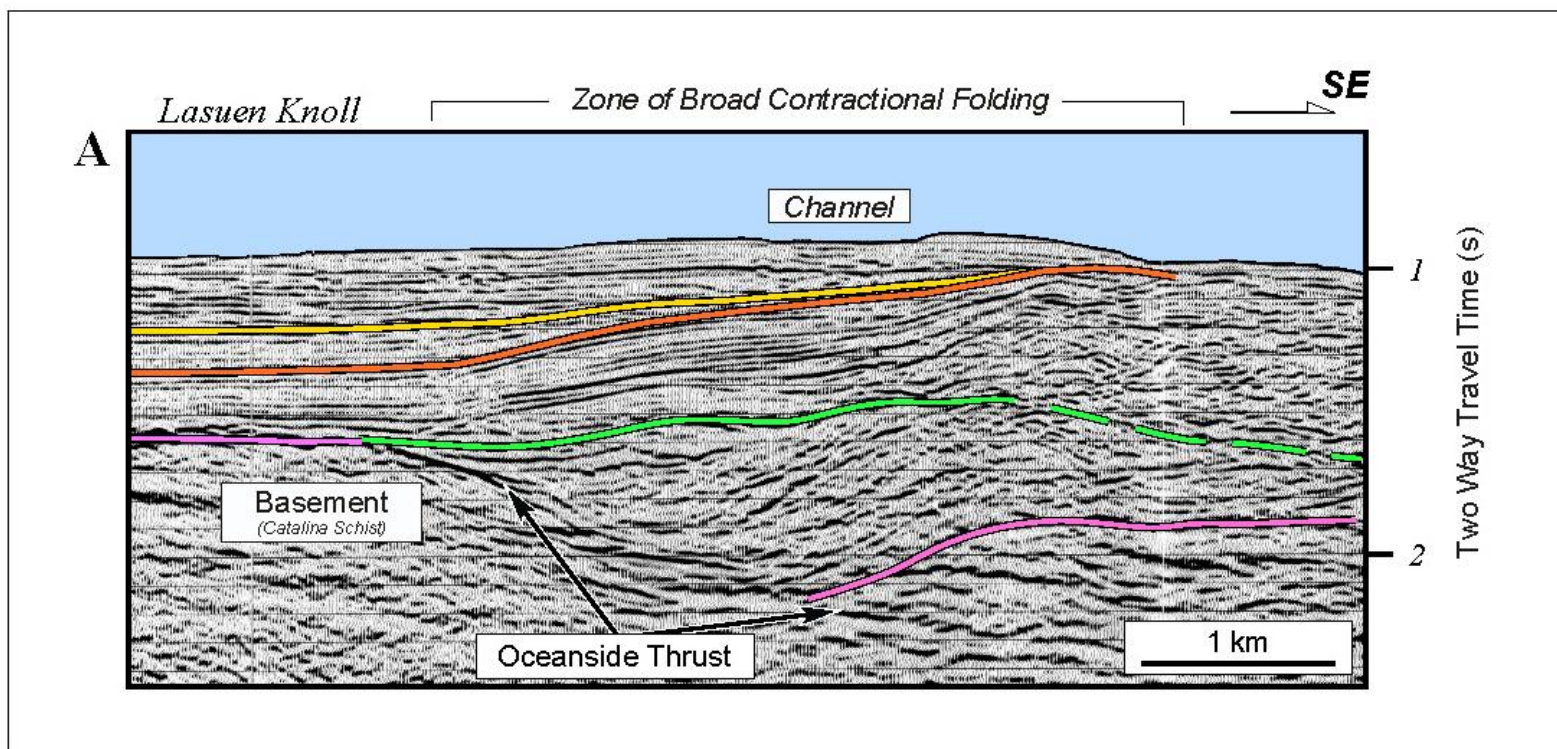
GeoPentech
Geotechnical & Geoscience Consultants

SAN ONOFRE NUCLEAR GENERATING STATION
SEISMIC HAZARD ASSESSMENT PROGRAM



Conceptual model of basin inversion of a half-graben structure due to transpressional tectonics and wedging [modified after Bally, 1984]. **(A)** Development of the half-graben and associated roll-over structure by normal slip on an extensional detachment **(B)** Basin inversion phase characterized by development of a hanging-wall wedge and asymmetrical contractional folds due to the reactivation of the extensional detachment.

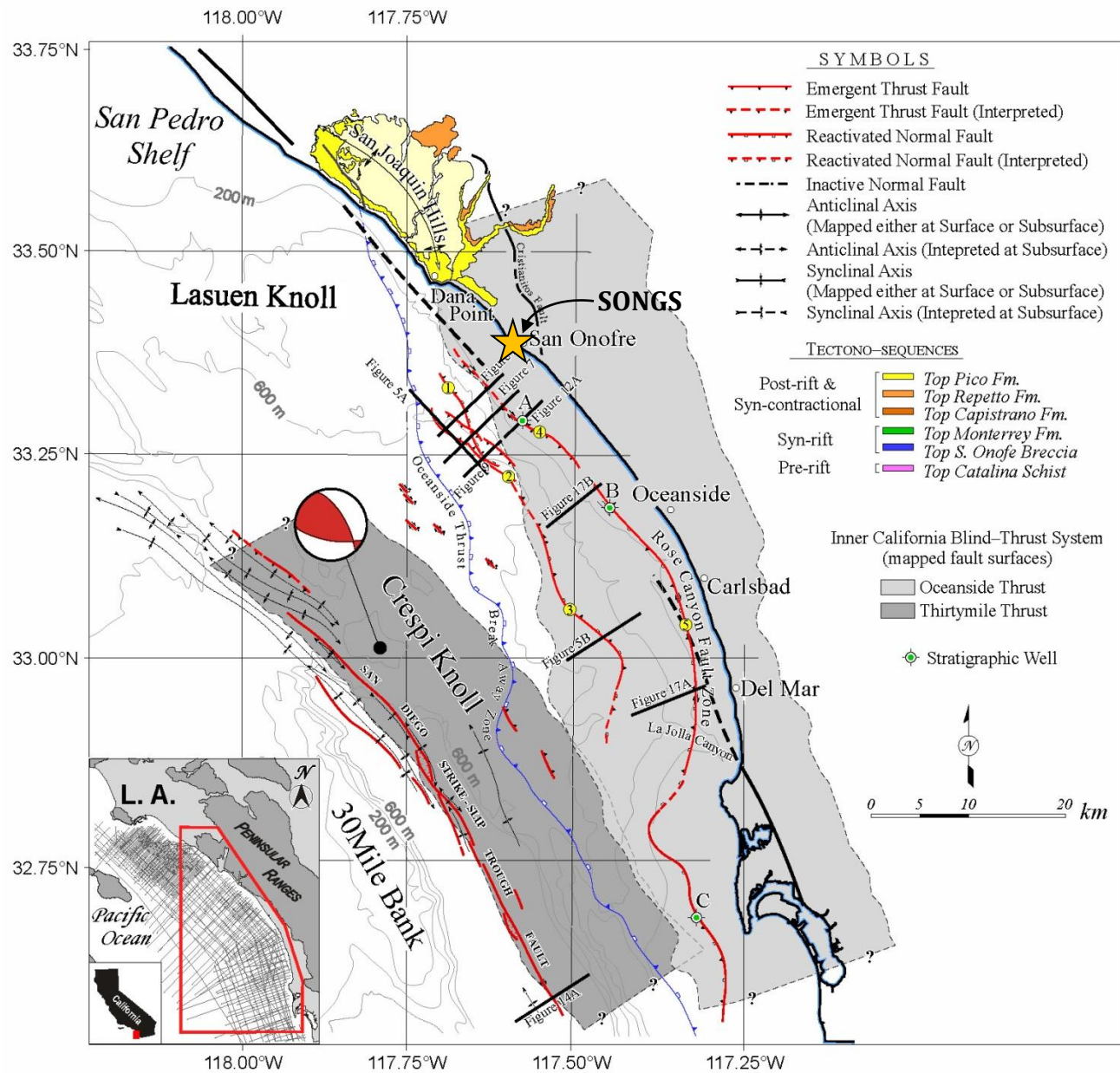
Source: Rivero (2004)

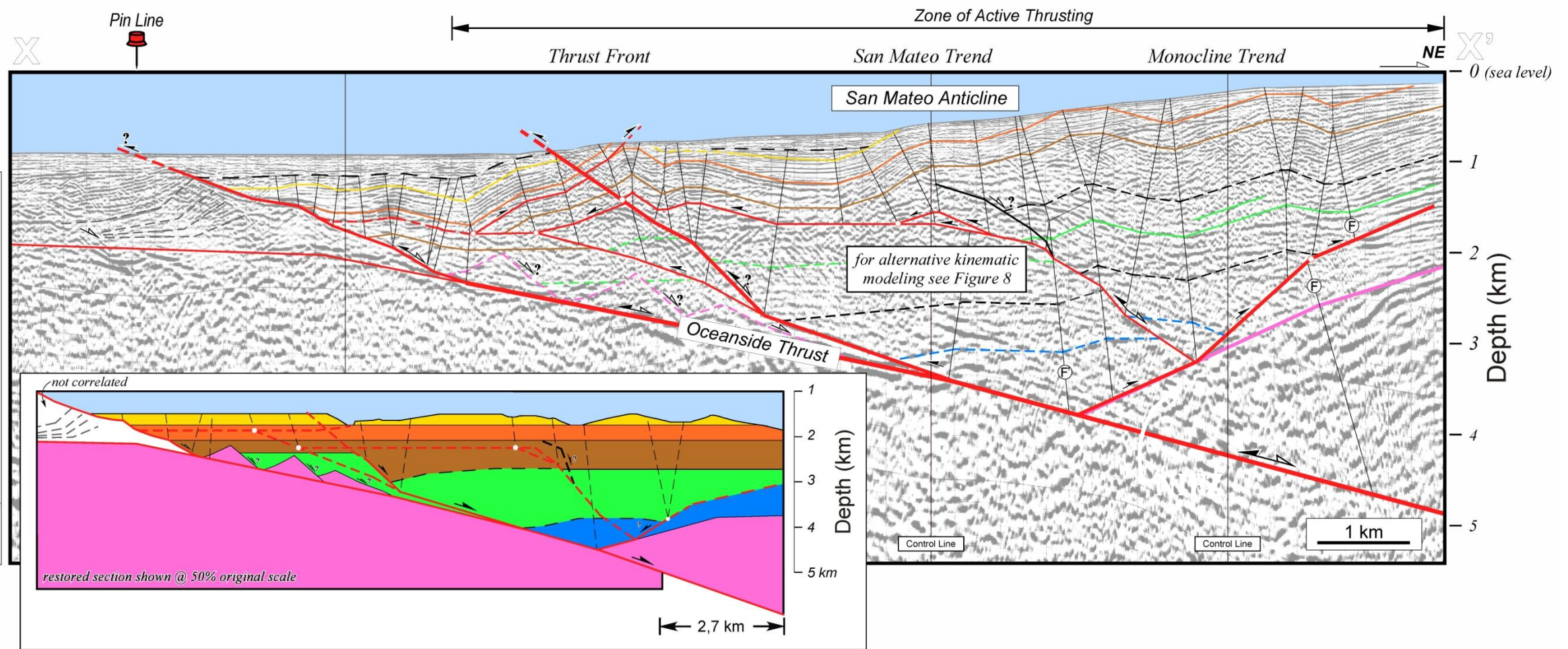
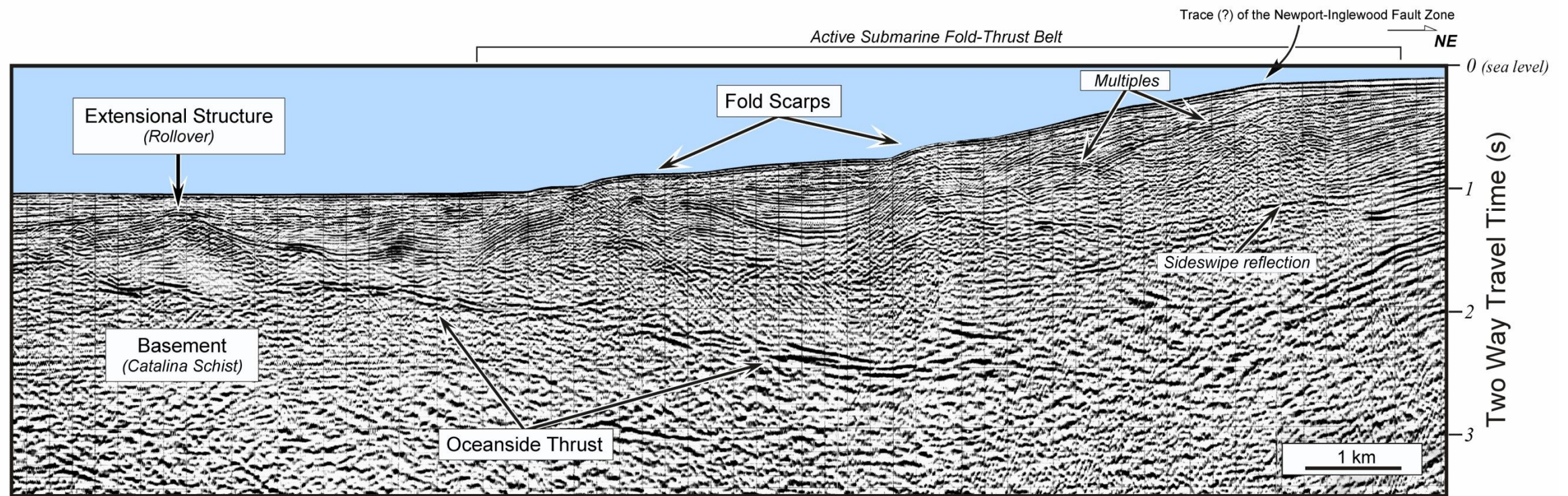


P	Top Pico Fm.]	Pliocene
R	Top Repetto Fm.]	Miocene
M	Top Monterrey Fm.]	
S	Top Catalina Schist]	Mesozoic

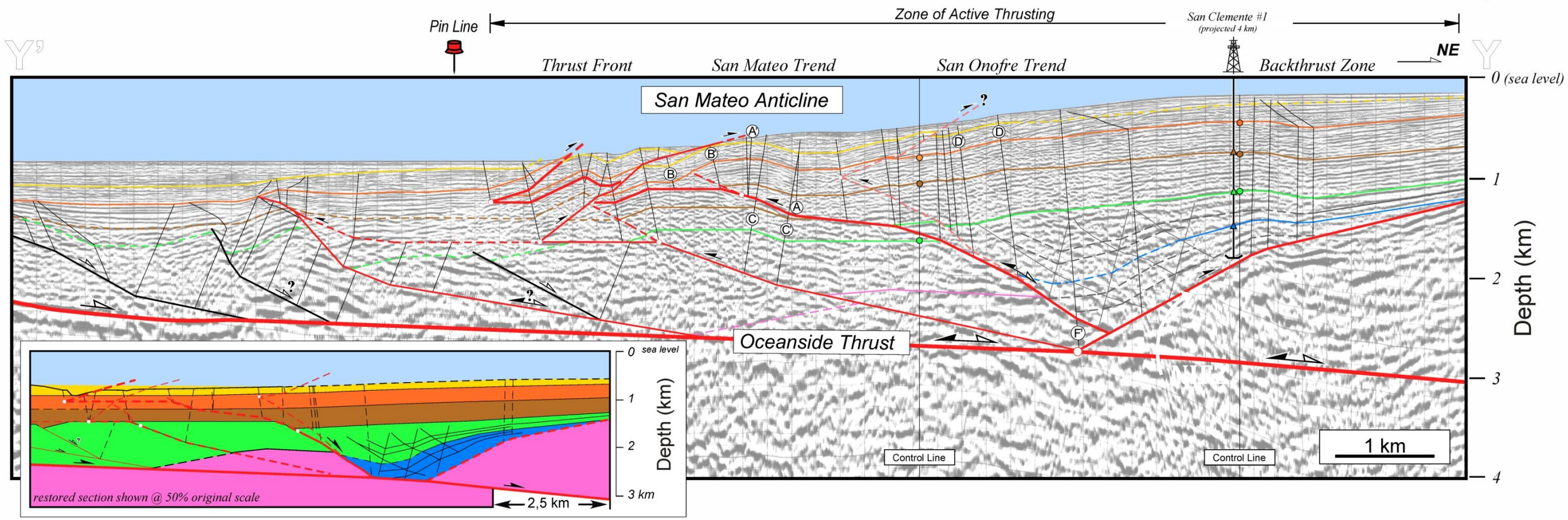
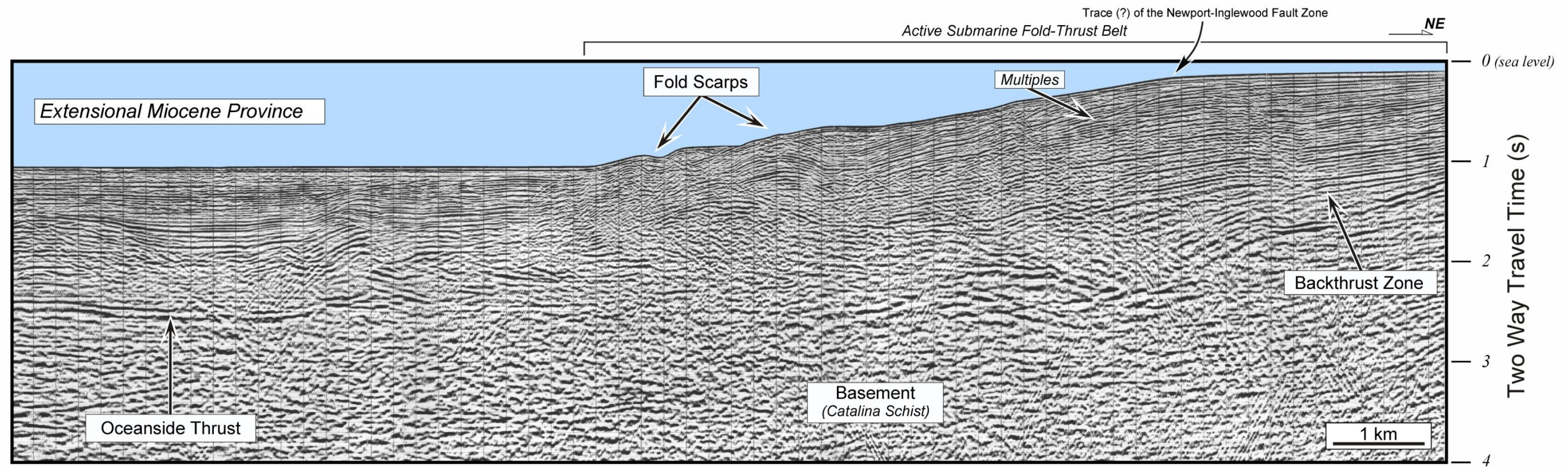
Seismic examples of basin inversion structures associated with activity of the Oceanside Thrust. **(A)** Half-graben reactivation along a lateral ramp of the Oceanside Thrust. **(B)** Tip-fold structure developed by contractional reactivation of the Carlsbad fault, which is located within the hanging wall block of the Oceanside Thrust. In both cases divergent termination of the seismic reflections within the Monterrey Fm. define the stratigraphic expansion of the syn-rift sequence. Similarly, the phase of basin inversion is well recorded by the contractional geometry, internal onlap terminations, and general thinning of the syn-contractional Pico Fm. on the crest of the anticlines. **Inset:** Conceptual model of basin inversion after Bally [1984] and Letouzey [1990]. **(a)** Development of the extensional half-graben and associated rollover structure, **(b)** Period of quiescence and sedimentation of the post-rift sediments, **(c)** Reactivation of the normal fault with development of asymmetrical contractional fold. The model highlights the stratigraphic relationships between the three main tectonosequences characteristics of basin inversion. Location of the seismic lines is shown in Figure 3.5.

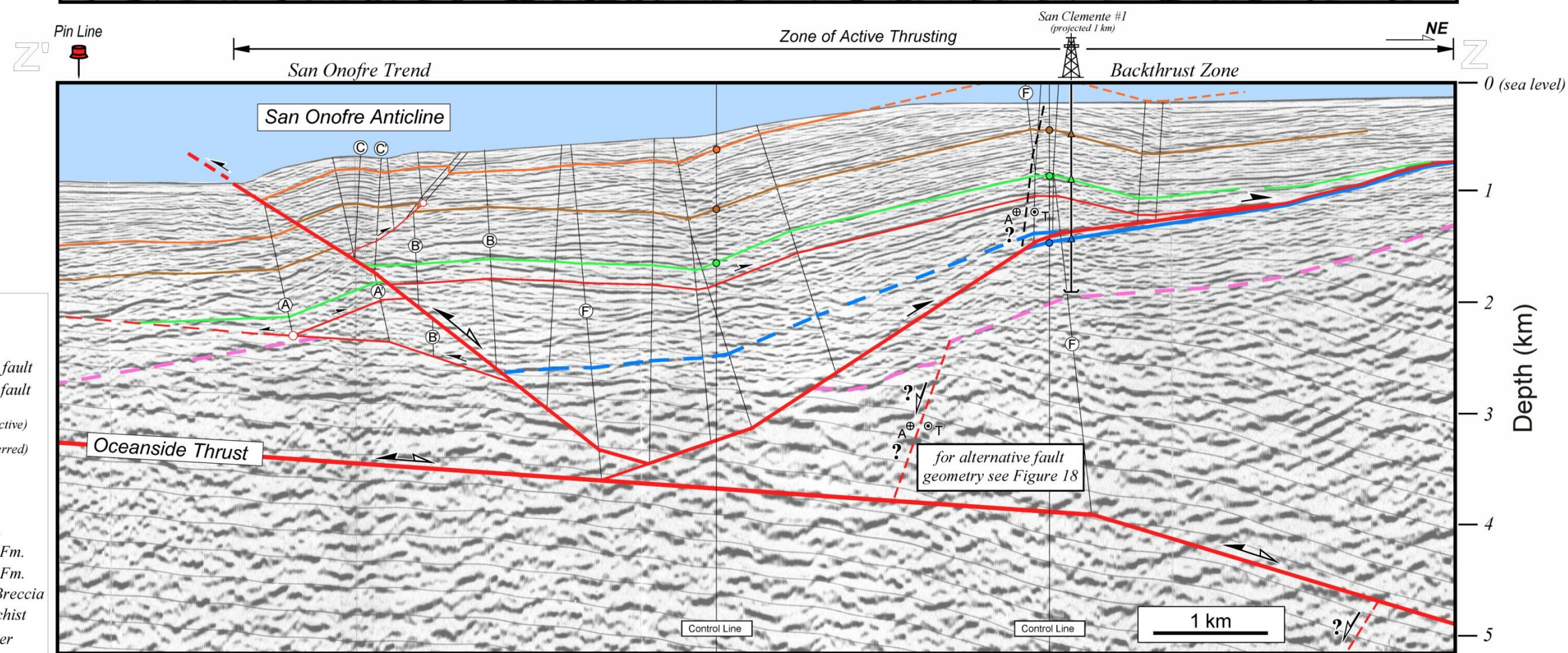
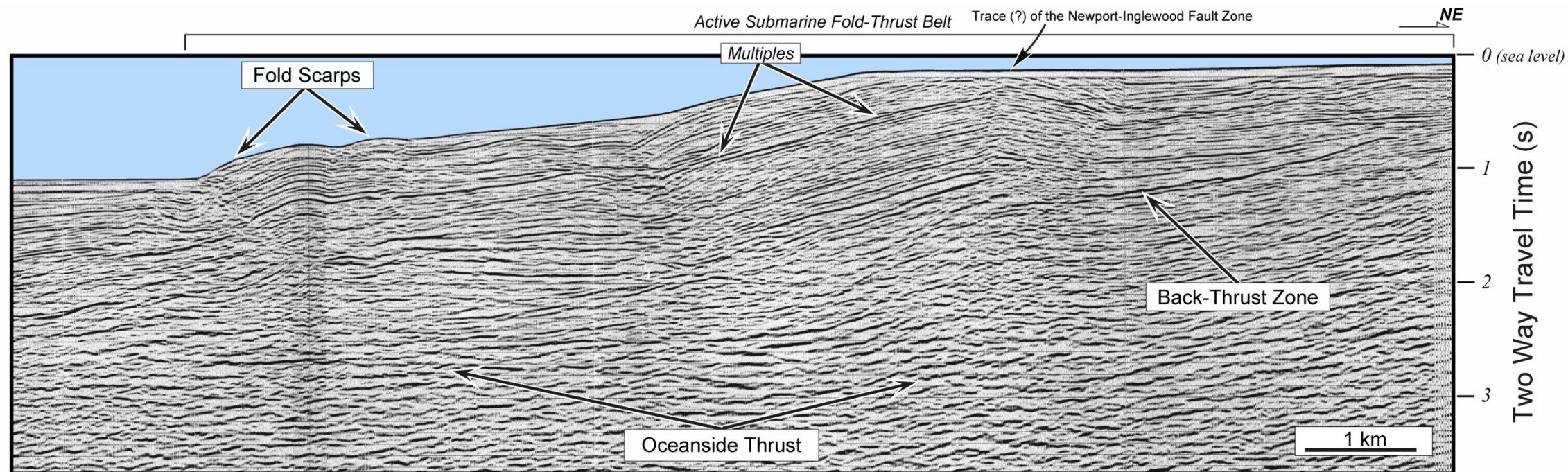
tions, and general thinning of the syn-contractional Pico Fm. on the crest of the anticlines. **Inset:** Conceptual model of basin inversion after Bally [1984] and Letouzey [1990]. **(a)** Development of the extensional half-graben and associated rollover structure, **(b)** Period of quiescence and sedimentation of the post-rift sediments, **(c)** Reactivation of the normal fault with development of asymmetrical contractional fold. The model highlights the stratigraphic relationships between the three main tectonosequences characteristics of basin inversion. Location of the seismic lines is shown in Figure 3.5.

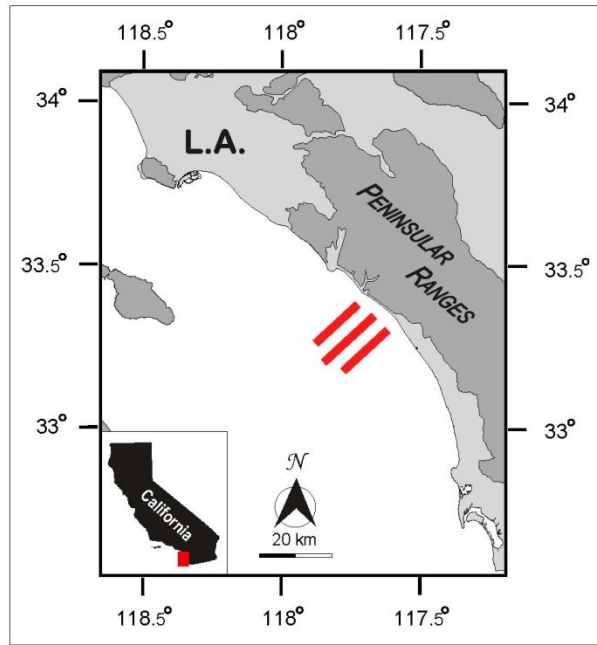




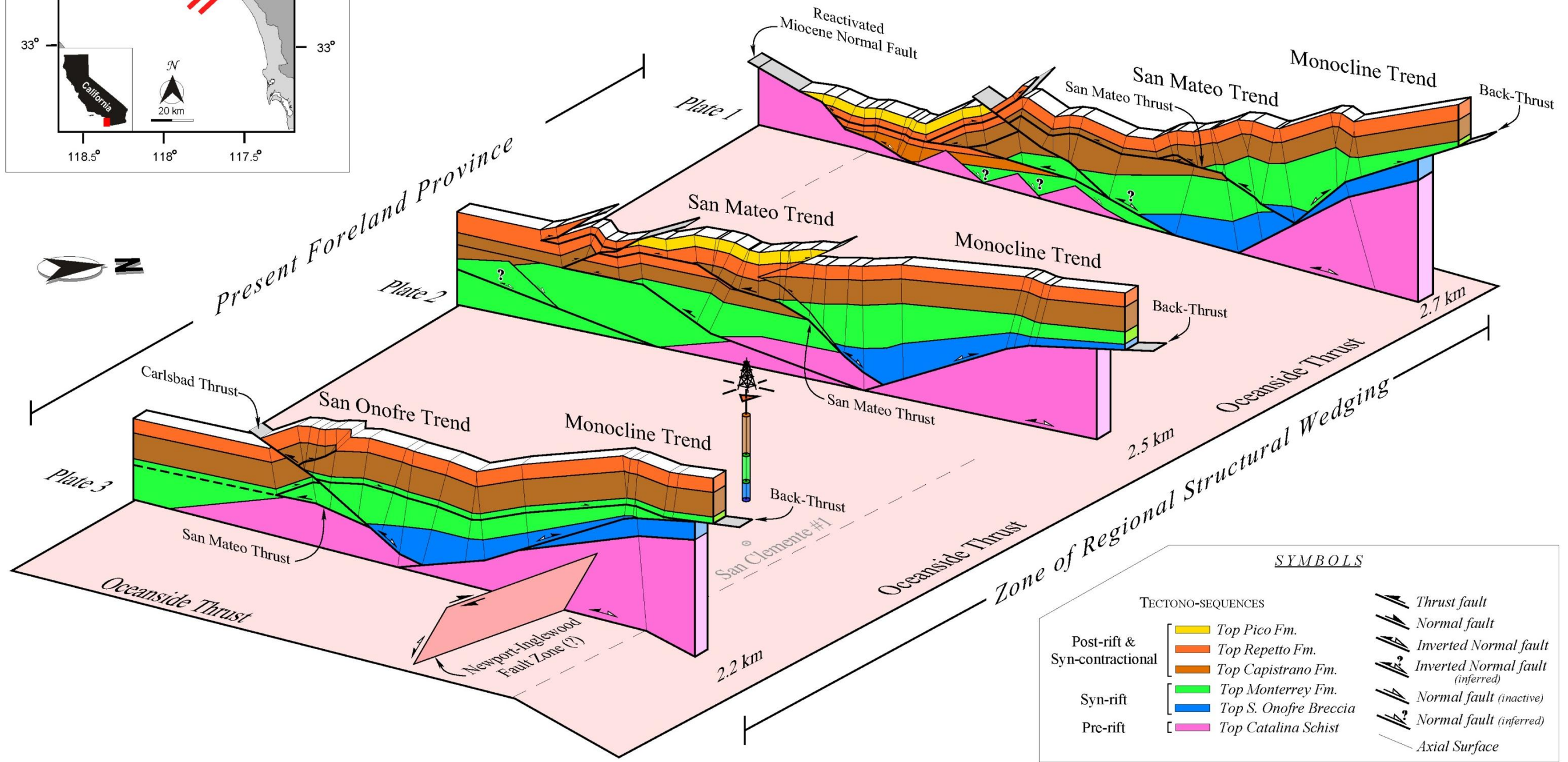
- SYMBOLS**
- Thrust fault
 - Normal fault
 - Inverted Normal fault
 - Inverted Normal fault (inferred)
 - Normal fault (inactive)
 - Normal fault (inferred)
 - Axial Surface
- Top Pico Fm.
 - Top Repetto Fm.
 - Top Capistrano Fm.
 - Top Monterey Fm.
 - Top S. Onofre Breccia
 - Top Catalina Schist
 - Arbitrary Marker



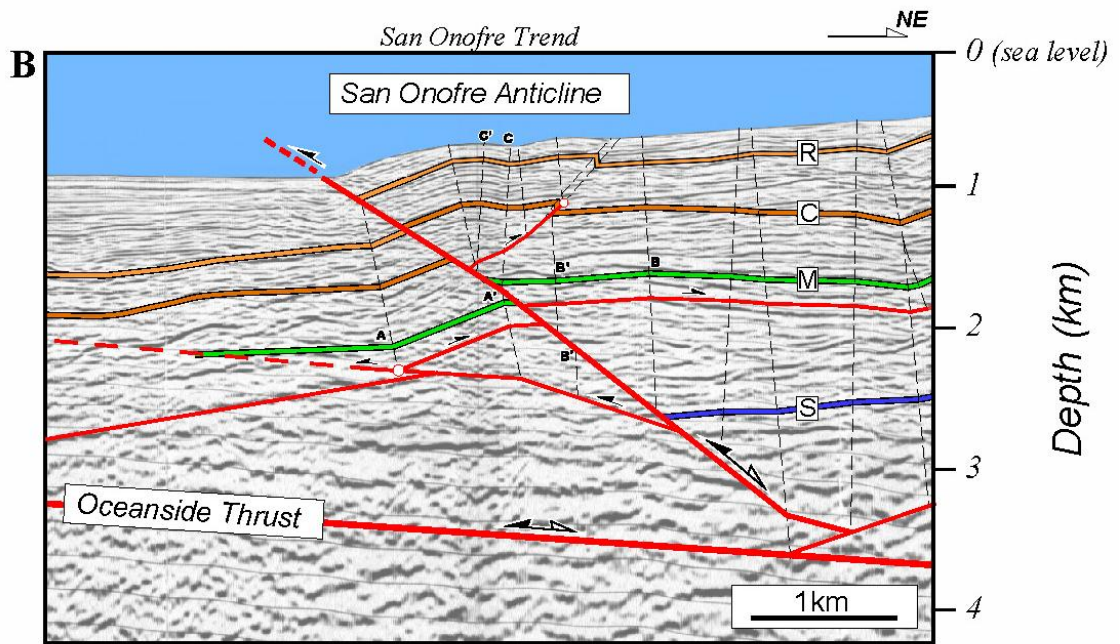
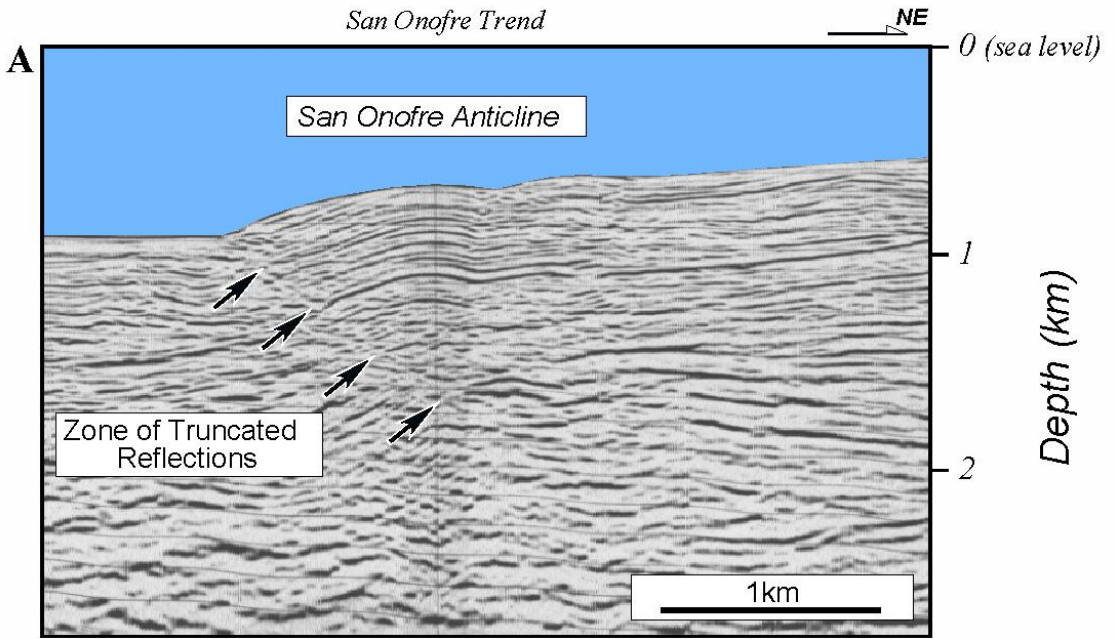




Diagrammatic representation of the main structural elements and trends observed along transects X-X', Y-Y', and Z-Z'. The representation illustrates the lateral continuity of the offshore-dipping monocline, and the role of the Oceanside thrust as a regional basal detachment level. The diagram also highlights the complex arrangements of the modern contractional trends within the active submarine fold-thrust belt, and the control induced by the Miocene normal fault system and the propagating structural wedge in their location. A common pitfall in structural interpretation is also evident, the most important fold structure in a profile do not necessarily correlates across the trends (i.e. observed the transition of the San Mateo and San Onofre anticlines between profiles 2 and 3). Several basement riders located on top of the Oceanside thrust have been identified based on local seismic expression. Some geometries have been simplified for clarity. The presence of the Newport-Inglewood strike-slip fault is inferred as restricted to the monocline location on Plate 3. Some modest amounts of dextral movement in the contractional trends is compatible with the interpretation and cannot be completely ruled out.



Modified from Rivero (2004)



- R Top Repetto Fm.
- C Top Capistrano Fm.
- M Top Monterrey Fm.
- S Top San Onofre Breccia

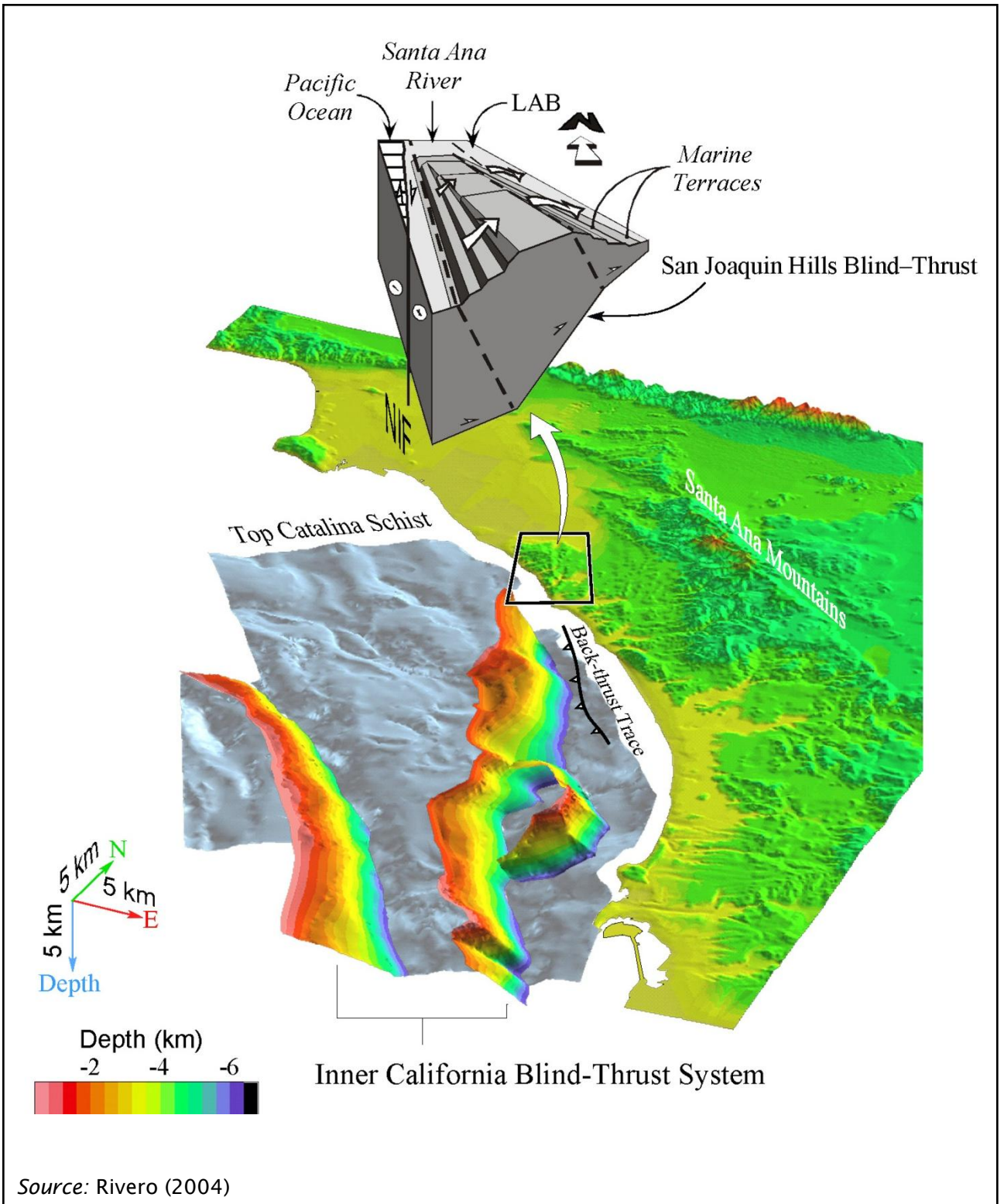
SEISMIC REFLECTION PROFILE AND INTERPRETATION OF THE SAN ONOFRE TREND FROM RIVERO (2004)

FIGURE A-22



GeoPentech
Geotechnical & Geoscience Consultants

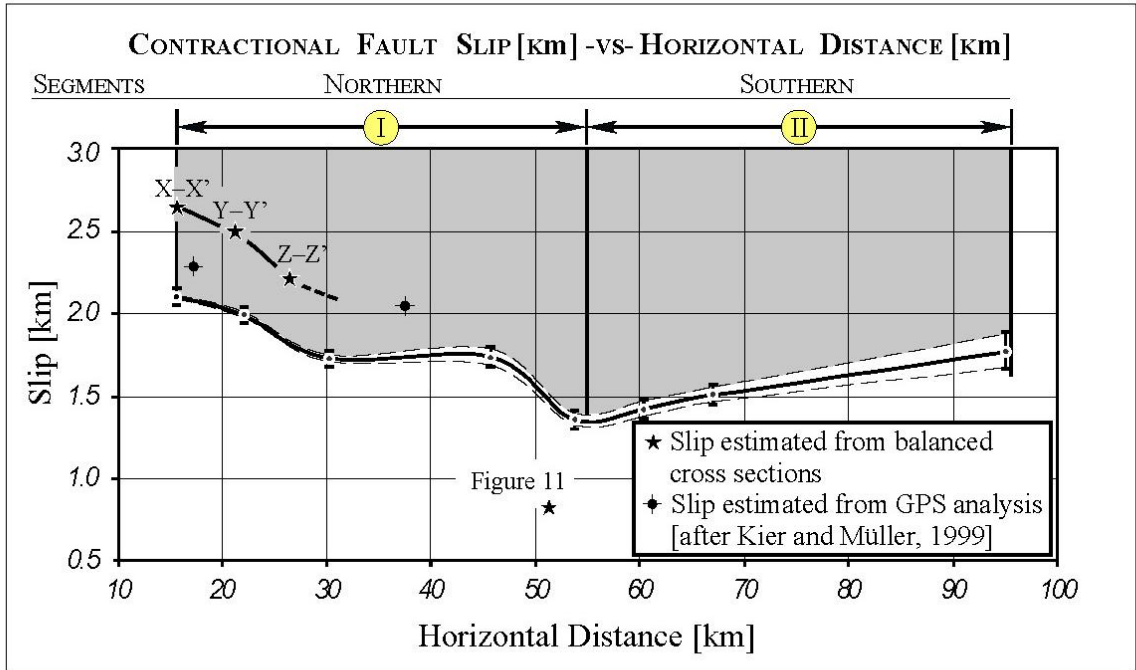
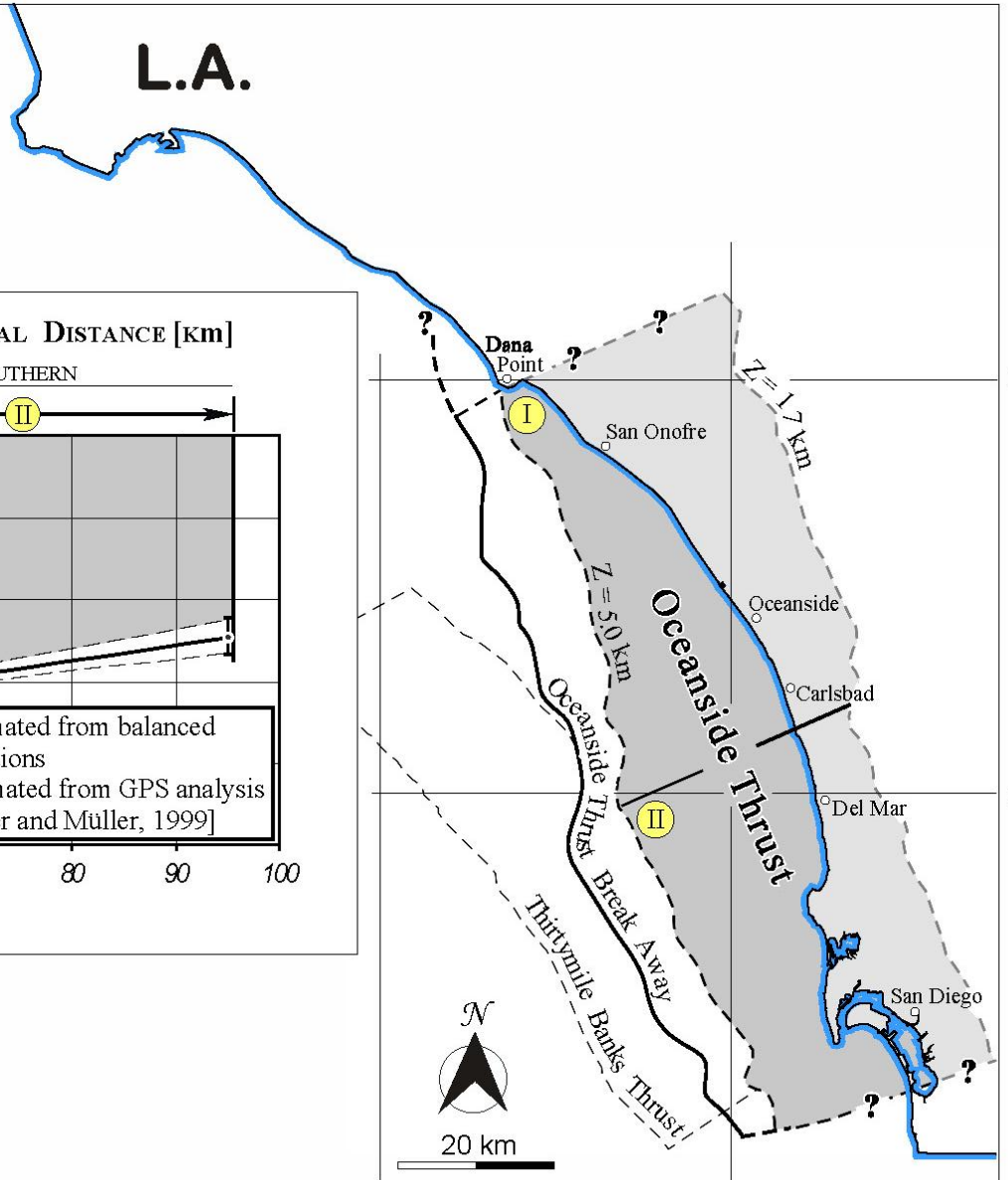
SAN ONOFRE NUCLEAR GENERATING STATION
SEISMIC HAZARD ASSESSMENT PROGRAM



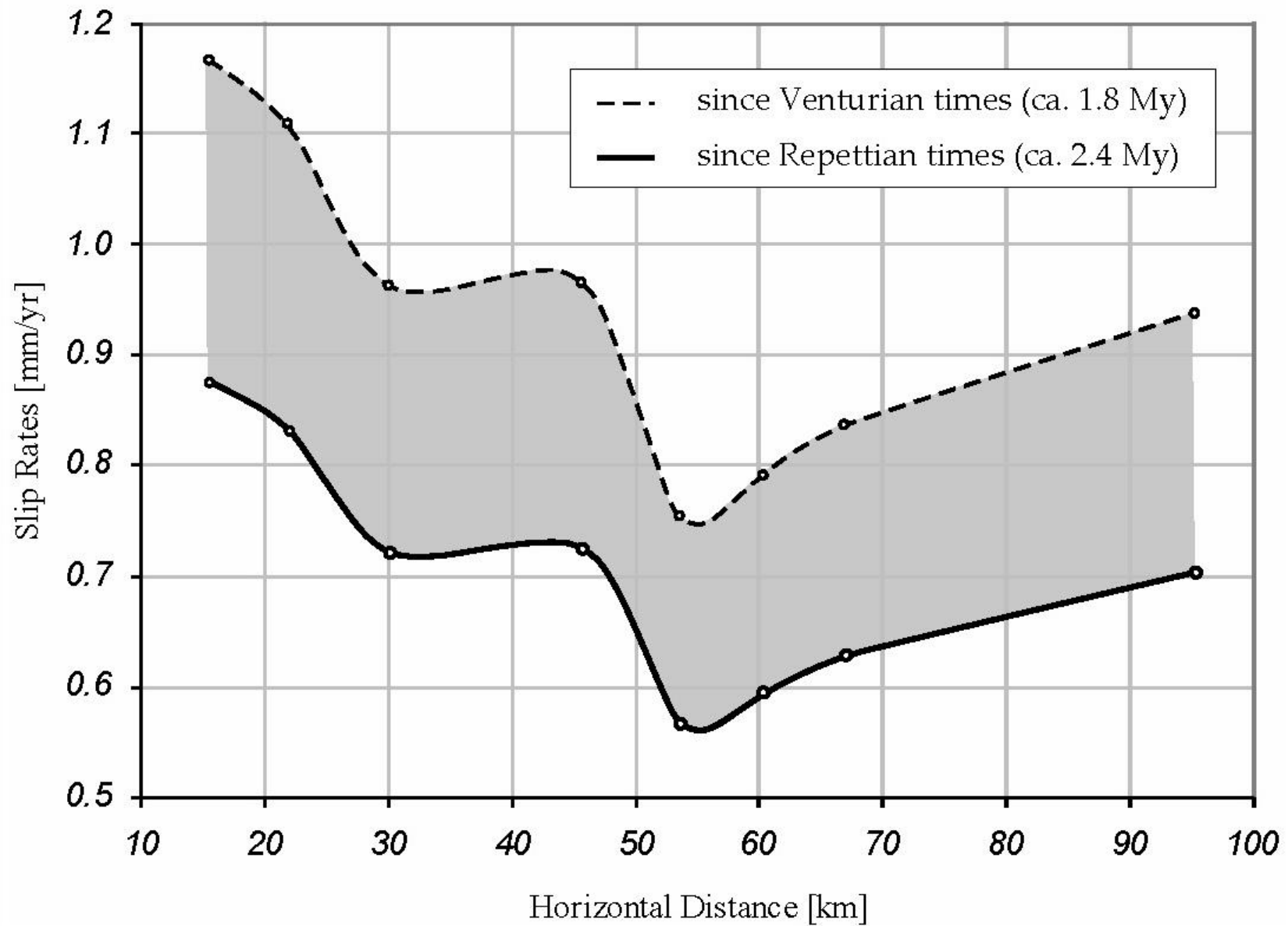
Source: Rivero (2004)

 <p>GeoPentech Geotechnical & Geoscience Consultants</p>	<p>SCHEMATIC DIAGRAM RELATING THE INNER CALIFORNIA BLIND THRUST SYSTEM TO THE SAN JOAQUIN HILLS</p>	<p>FIGURE A-23</p>
	<p>SAN ONOFRE NUCLEAR GENERATING STATION SEISMIC HAZARD ASSESSMENT PROGRAM</p>	

Computed contractional slip on the Oceanside Thrust derived using the excess-area method discussed in Appendix B. Dashed lines represent maximum and minimum values yielded by the method, when accounting for uncertainties on the geometry of the Oceanside Thrust, and on the depth-conversion process. Fault slip measurements derived from balanced structural interpretations (Plates 1 to 3, and Figure 3.11), and slip estimates derived from GPS analysis [Kier and Mueller, 1999] are also shown.

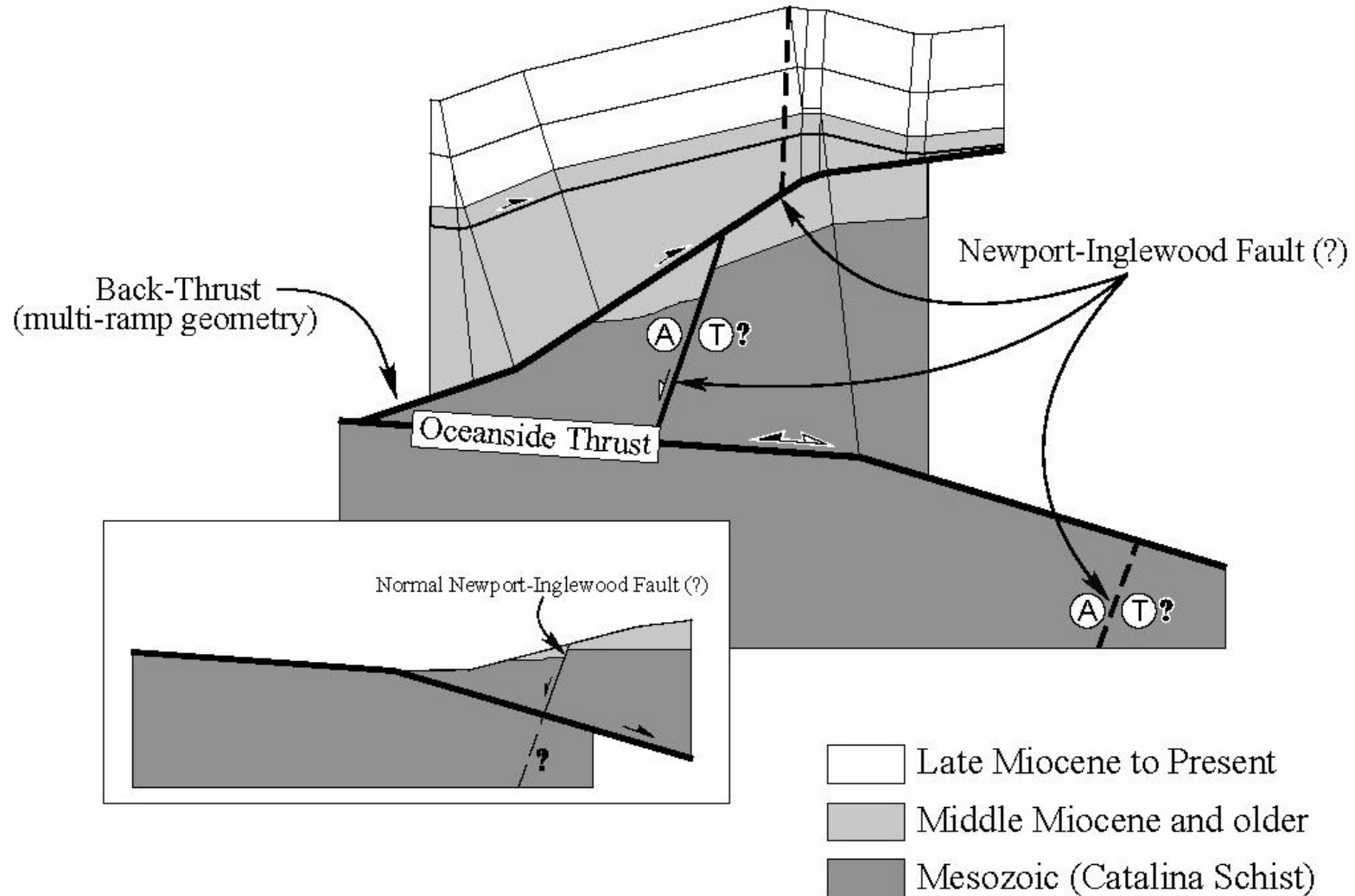


SEISMOGENIC AREAS
 Segment I: 1,242.0 km²
 Segment II: 1,921.3 km²
 Total Area (Segment I + II): 3,163.5 km²

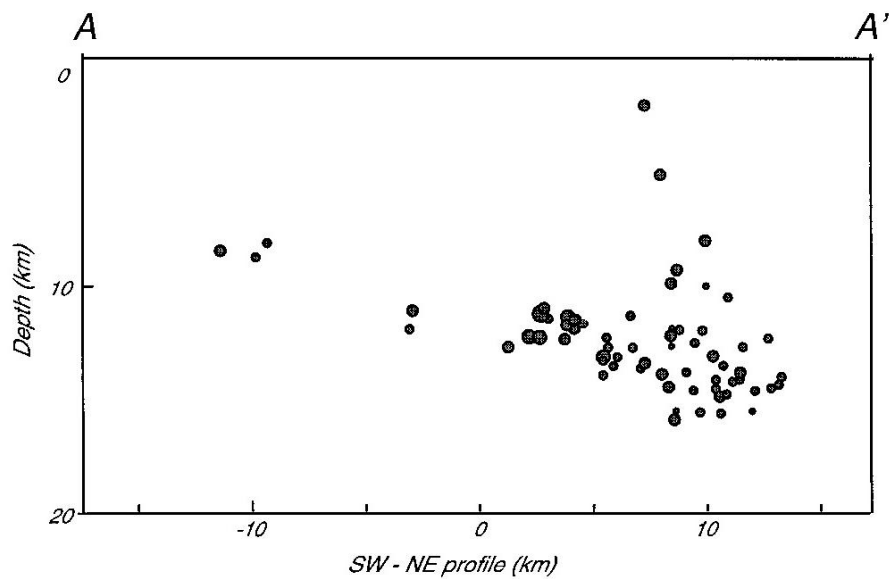
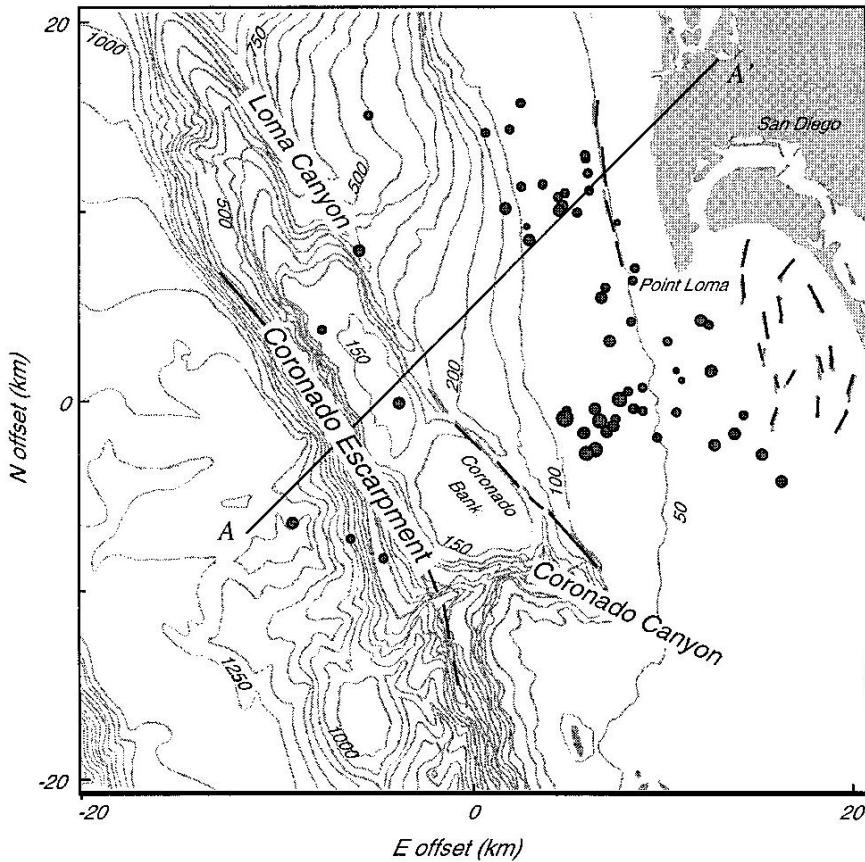


NE

Monocline Trend



Source: Rivero (2004)



Source: Astiz and Shearer (2000)

APPENDIX A – ATTACHMENT A-1

ANNOTATED BIBLIOGRAPHIES

INTRODUCTION

The following references were considered in determining the weights for the end-member models discussed in Section 2.4. These references, in whole or in part, address the seismotectonic setting of southern California and the Continental Borderlands. Specifically, these authors offer information bearing on the structural, seismologic, paleoseismic, geomorphic, and/or geodetic character of the region. For convenience, the annotated bibliographies are subdivided into these same character categories.

ANNOTATED BIBLIOGRAPHIES

Moore, G.W., 1972, Offshore extension of the Rose Canyon fault, San Diego, California: US Geological Survey Professional Paper 800-C, C113-C116.

STRUCTURAL

- First suggested possible offshore extension of Holocene active traces of the Rose Canyon Fault Zone based on “a net of subbottom acoustic profiles spaced about 5 km apart.” The survey completed by the USGS and Scripps Institution extending from La Jolla into Camp Pendleton (up to latitude 33° 20’).
- Pointed out that straight sections are relatively narrow (0.5 km wide) with wider reaches “as much as 2 km wide at curves.”
- Indicated that “...Cretaceous and Tertiary sedimentary rocks that are generally nearly flat lying but dip moderately to steeply within and near the fault zone...”
- “The greatest local uplift lies adjacent to an S-shaped bend in the Rose Canyon fault...”
- “This uplift is believed to have resulted from compression there as a consequence of right-lateral strike-slip movement along the fault.”
- Further stated that “Corey (1954) and the other previously cited investigations that extrapolated the Rose Canyon fault to the northwest connected it with the Newport-Inglewood fault zone, near which the 1933 Long Beach earthquake of magnitude 6.3 occurred. The offshore evidence of the present study agrees with such a projection, at least as far north as Camp Pendleton.”

Ehlig, P.L., 1977, Geologic report on the area adjacent to the San Onofre Nuclear Generating Station northwestern San Diego County, CA, for Southern California Edison Company, 31 September 1977, 32 pp.

STRUCTURAL

- Marine terraces near SONGS "do not appear to be deformed or tilted."

Hauksson, E., 1987, Seismotectonics of the Newport-Inglewood fault zone in the Los Angeles basin, southern California: Bulletin of the Seismological Society of America, v. 77, no. 2, p. 539-561.

SEISMOLOGY

- Shows focal mechanism solutions for 37 earthquakes along and near the onshore portion of the NI in Los Angeles and Orange Counties. Seventy-eight percent (78%) of these solutions are predominately strike-slip events; most of these are located along the main trace of the fault. The reverse or thrust events are mostly situated northeast or southwest of the main trace, most pronounced being along the Compton-Los Alamitos Fault to the northeast, but parallel to the trend of the of the NI.

Fischer, P.J. and Mills, G.I., 1991, The offshore Newport-Inglewood – Rose Canyon fault zone, California: structure, segmentation and tectonics *in* Abbott, P.L., and Elliott, W.J., eds., Environmental Perils San Diego Region: San Diego, San Diego Association of Geologists, p. 17-36.

STRUCTURAL

- “We used new (1989) digitally processed seismic reflection data with an average spacing of 1.5 km, in conjunction with older digital data and a grid of closely spaced, high resolution analog profiles, to map the geology of the inner margin.” Three major fault segments of the offshore NI/RC zone between Newport Beach and La Jolla and their geology are described
- Dana Point segment between Newport Beach and Las Pulgas Canyon is 43 km long, Oceanside segment between Las Pulgas Canyon and Encinitas is 32 km long, and Del Mar segment from Carlsbad to La Jolla is 34 km long.
- “Piercing points between Newport Beach and the correlative Cristianitos-San Onofre-Oceanside faults indicate that an average of 7 km of right-lateral displacement has occurred along the NIZ since early Pliocene time.”
- “Between San Mateo Point and Oceanside, multiple thrust faults and thrust generated folds or fault-propagation folds were mapped along the slope of the inner margin, west of the NI-RC fault zone...They may be separated into an inner thrust fault-fold complex that is probably a part of the flower structure of the NIFZ, and an outer thrust-fold complex. The inner thrust fault complex is located near mid-slope, about at the 500 m isobath while the outer thrust complex follows the base of the slope near the 700 m isobath.”
- The main thrust fault of the inner thrust-fold complex is between 3 and 4 km beyond the shelf-break and dips 20-30 degrees east.
- “The main thrust of the outer thrust-fold complex trends southeast along the base of the slope of the inner margin. It is southwest-vergent and dips about 9 degrees east shoreward of the thrust ramp.”
- “At this time, a most probable slip rate of 1 mm/yr for the NI-RC zone is suggested.”
- “At this time, it appears that the most probable horizontal slip rate for the NI-RC zone is between 1.3 mm/yr and 2.1 mm/yr. If the Quaternary slip rates are emphasized the most probable modern (?) slip rate is between 0.8 and 1.3 mm/yr, or about 1 mm/yr.”
- “The thrust faults along the inner margin are active, as is evidenced by their surficial topographic expression and the displacement of Quaternary reflectors.”

- “A potential seismic hazard, that has not been considered along the inner margin south of Dana Point, is posed by the thrust faults mapped off San Mateo Point-San Onofre to Oceanside and possible south to Encinitas.”

SEISMOLOGY

- “The focal mechanisms are in general agreement with right-lateral, strike-slip faulting along the northwest trending NI-RC zone.”

Hauksson, E., and Gross, S., 1991, Source parameters of the 1933 Long Beach earthquake: Bulletin of the Seismological Society of America, v. 81, no. 1, p. 81-98.

STRUCTURAL

- “The existence of a small normal component in the mechanism and in the geological cross sections suggests that the southwestern block of the Los Angeles basin is still subsiding.”
- Recent data suggests that “most geological structures adjacent to the NIF are not secondary features resulting from wrench faulting (Wright, 1990 [sic]) but are rather primary structures resulting from north-south compression of the basin (Hauksson, 1990).”
- “[A]bsence of a thrust component is consistent with the slip partitioning model of the seismotectonics of the Los Angeles basin by Hauksson (1990).”
- In the slip partitioning model by Hauksson (1990), “strike-slip faulting on vertical faults and thrust faults on gently dipping faults replace a system of oblique faulting...[t]he almost pure strike-slip mechanism of the 1933 earthquake and the pure thrust mechanism for the 1987 ($M_L=5.9$) Whittier Narrows earthquake are consistent with this slip partitioning model.”

SEISMOLOGY

- Relocated 1933 (M_W 6.4) mainshock “showed right-lateral motion along the NIF [Newport-Inglewood Fault] with a small normal component.”
- The “centroidal depth [of the mainshock] was 10 ± 2 km.”
- The “best fitting focal mechanism shows right-lateral strike-slip motion with a minor normal component.”
- “Both the focal mechanism of the 1933 main shock and the spatial distribution of aftershocks indicate that the earthquake occurred on the NIF.”
- Woodward-Clyde (1979) determined a different focal mechanism for the main shock based on first motion polarities and suggested the earthquake was not on the Newport-Inglewood Fault; this study by Hauksson is more accurate because it is based on fitting the whole teleseismic waveforms.
- The “rupture initiated near the Huntington Beach–Newport Beach City boundary and extended unilaterally to the northwest to a distance of 13 to 16 km.”
- “[N]o reliable surface rupture was reported.”
- “The main shock caused 85–120 cm of slip at depth.”

GEOLOGY

- “[P]rominent surface expression [of the Newport-Inglewood Fault] may be a manifestation of the basement boundary rather than being primarily caused by the right-lateral offset,”

(i.e., metamorphic basement on the west juxtaposed against metaseds and volcanic on the east).

Legg, M.R., 1991, Developments in understanding the tectonic evolution of the California Continental Borderland: Special Publication no. 46, Society for Sedimentary Geology, p. 291-312.

STRUCTURAL

- "[T]ranspressional structure along the offshore NI fault zone and prominent northwest-trending thrust faults at the base of the continental slope west of Newport and San Juan Capistrano suggest northeast-southwest convergence in this area."
- Post-Miocene north-south/northeast-southwest shortening in northern Borderland, extension or transtension on inner Borderland faults from latitude of San Diego southward.
- Palos Verdes Hills Fault is "recognized to have significant thrust or oblique-dextral reverse slip components."

SEISMOLOGY

- "[S]hortening in northeastern Borderland is manifested by the numerous earthquakes with reverse-faulting mechanisms."
- "[T]hrust-fault earthquake mechanisms have been observed as far south as the northern end of the San Diego trough."

Wright, T.L., 1991, Structural geology and tectonic evolution of the Los Angeles basin, California *in* Biddle, K.T., ed., Active margin basins: American Association of Petroleum Geologists Memoir 52, p. 35–134.

STRUCTURAL

- "The Newport-Inglewood fault zone (NIFZ) is the best known structural feature of the Los Angeles basin (Figure 7)."
- "The zone has long been considered a classical example of the development of an echelon folds and faults along a deep-seated-strike-slip fault...."
- Numerous examples are provided of the dominance of Pliocene and later strike slip displacements and the significant variations in their corresponding vertical displacements.
- "Harding concluded that the structures within the zone "may be taken as a unit and related dynamically to one type of deformation – wrenching."
- "There are dissenting views to this interpretation. Yeats (1973) found it satisfactory for the late Pliocene and Quaternary history of the Newport-Inglewood zone, but too simple for the late Miocene and early Pliocene. It does not account for the fact that most of the more diversely oriented normal and reverse faults (except for Inglewood oil field) became inactive during the Pliocene whereas the en echelon right-lateral slip faults of the Newport-Inglewood zone continued to be active through the Pleistocene."
- "Each of the Neogene episodes has probably involved regional right-lateral simple shear, but along the NIFZ itself, total right-lateral slip since the middle Miocene has not exceeded 3km (Yeats, 1973) or about 1-2 mi. Evidence of this from the subsurface is compatible with the



- estimate of 0.5 mm/year during the past 5 m.y. (Guptill and Heath, 1981) and 0.4-0.8 mm/year (Bird and Rosenstock, 1984)."
- "Classic wrench-fault deformation, however, is not the primary cause of most of the anticlinal features along the NIFZ. In the preceding discussion we have seen that many of these structures do not conform to a pattern of en echelon folding, but are related to local basement geometry and perhaps to a wide zone of pervasive shear within the basement. Along the southern NIFZ, the Long Beach, Seal Beach, and Huntington Beach (onshore) structures are block-edged force folds (Harding and Tuminas, 1988) forced along the middle to late Miocene block boundary. Offshore Huntington Beach has been constricted against the Offshore Newport ridge. Dominguez is a part of the El Segundo-Lawndale-Alondra fold trend, complicated by offset on the NIFZ. Inglewood (and perhaps Potero) formed in concert with uplift of the Las Cienegas block that buckled the sedimentary wedge against shallow basement of the western shelf (Wright, 1987d)."
 - Although Hazenbush and Allen 1958 implied a 0.5mm/yr to 1.0mm/yr slip rate since mid-Miocene on the NIFZ in Huntington Beach, "detailed subsurface mapping of oil fields along the NIFZ has revealed a variety of structural patterns and histories, and many of these cannot easily be reconciled with a pure strike-slip origin."
 - "Faults within the San Andreas transform system may utilize relict zones of crustal weakness formed during earlier terrane accretion."
 - "In analyzing Pasadenan deformation, the flake-tectonics model is more appropriate than the fold-and-thrust-belt model, although both models incorporate aseismic detachment at midcrustal depths. The flake-tectonics model is valid for all phases of Neogene deformation, both transtensional and transpressive, in the Los Angeles region."
 - "The transition between the strong compressive shortening of the Transverse Ranges and the moderate right slip of the Peninsular Ranges blocks occurs systematically across the Los Angeles basin. Those relationships... show contrasting structural styles on the two sides of the basin. The northeast flank is dominated by blind thrusts of the Transverse Ranges system that flatten with depth. The southwest flank features right-oblique faults of the Peninsular Ranges system that steepen into near-vertical zones of active seismicity."; "Viewed south to north (GG' to AA'), these cross sections confirm the gradual change from extension at the southern end of the basin to compressive shortening at the northern end...."
 - "Relative motion between crustal flakes may involve rifting and separation, transform movement, or collision and shortening, combinations of these, and superposition of several modes over time. Local structures are shaped not by regional stress fields embracing areas hundreds of miles across but by the interaction of adjacent tectonic flakes, creating basement blocks and sedimentary wedges that may differ significantly in their densities, ductilities, and thermal characteristics."; "In shaping local structure, the influence of these internal features of the shallow crust may be as important as the orientation of the stresses being applied."
 - "In forming a structure, the shape of the mold counts for as much as how the hammer is swung."
 - "All of those structures developed within a wide region of pervasive right slip associated with the evolving San Andreas transform zone. Nevertheless, strike-slip folding caused by displacement along an individual fault is not a dominant factor in the genesis of structures in the Los Angeles basin, though it may well have contributed to deformation along the

**SAN ONOFRE NUCLEAR GENERATING STATION
SEISMIC HAZARD ASSESSMENT PROGRAM
2010 PROBABILISTIC SEISMIC HAZARD ANALYSIS REPORT**

northern NIFZ (Figure 9) and perhaps the deformation along the Santa Monica fault (by left slip). That mechanism and other classic patterns of fold and fault development have been nullified by the effects of preexisting basement blocks and sedimentary wedges.”

Kern, J.P., and Rockwell, T.K., 1992, Chronology and deformation of Quaternary marine shorelines, San Diego County, California *in* Kern, J.P., and Rockwell, T.K., eds., Quaternary Coasts of the United States: Marine and Lacustrine Systems, Special Publication no. 48, Society for Sedimentary Geology, 377-382.

STRUCTURAL

- Mapping of shorelines provides evidence for uniform uplift of the entire coastal zone in San Diego County (downtown San Diego to Oceanside) at a rate of 0.13 to 0.14 m/kyr during the Quaternary with exception of areas deformed locally by the Rose Canyon Fault Zone.
- Both higher and lower uplift rates are observed along the Rose Canyon Fault Zone, which is shown by its effects on shoreline configurations to have been active for at least the past million years.
- The average long-term uplift rate for the San Diego region is similar to those for other areas of coastal California that are dominated by strike-slip tectonics.

GEOFORMOLOGY

- Shoreline angle elevations are estimated for 16 shorelines estimated to range in age from 80 ka to perhaps as old as 1.29 Ma.
- Shoreline geometry is modified both by regional uplift and by extensive faulting in the right-slip wrench system of the Rose Canyon Fault Zone.

Rockwell, T.K., Lindvall, S.C., Haraden, C.C., Hirabayashi, C.K., and Baker, E., 1992, Minimum Holocene slip rate for the Rose Canyon fault in San Diego, California, *in* Heath, E.G., and Lewis, W.L., eds., The Regressive Pleistocene Shoreline Coastal Southern California: South Coast Geological Society, Inc., 1992 Annual field Trip Guide Book No. 20, p. 55-64.

STRUCTURAL

- “Rose Canyon fault appears to feed directly into the Newport-Inglewood fault zone to the northwest. Although the Coronado Bank fault may also feed slip into the Newport-Inglewood fault zone, the rate determined for the Rose Canyon fault in this study also provides a minimum slip rate for [the offshore NI/RC].”

PALEOSEISMOLOGY

- Rose Canyon Fault is Holocene active based on radiocarbon dates obtained from charcoal deposited stratigraphically below a tectonically offset channel.
- Authors demonstrate offset of channel is likely all or mostly tectonic with no or very minimal deflection.
- Minimum slip rate of the Rose Canyon Fault of ~1 mm/yr is afforded from the trenching, presuming 8.7 m of brittle slip in ~8150 years.

**SAN ONOFRE NUCLEAR GENERATING STATION
SEISMIC HAZARD ASSESSMENT PROGRAM
2010 PROBABILISTIC SEISMIC HAZARD ANALYSIS REPORT**

- The “actual rate could be substantially higher if the age of the [tectonically offset] channel is as much as 1000 years younger than the age of [the radiocarbon date obtained from the charcoal].”

GEOPMORPHOLOGY

- Rose Canyon Fault is late Pleistocene active based on a 17–28 ka terrace riser offset 33–35 m.
- Maximum slip rate of the Rose Canyon Fault of ~2 mm/yr is based on the maximum offset of the terrace riser (35 m) in the minimum amount of time (17 ka).

Crouch, J.K., and Suppe, J., 1993, Late Cenozoic tectonic evolution of the Los Angeles basin and Inner California Borderland: A model for core complex-like crustal extension: Geological Society of America Bulletin, v. 105, p. 1415-1434.

STRUCTURAL

- Propose large magnitude (>200 km) crustal extension formed LA Basin, Inner California Borderlands, and Southern California Borderlands in major late Cenozoic rifting.
- Several current right lateral strike slip structures originated as high-angle normal faults prior to Pliocene.
- “Faults such as the Newport-Inglewood and Whittier-Elsinore originated as high-angle, hanging-wall normal faults above detachments and hence, modern strike slip along these faults may end downward against the detachments.”
- Image detachment fault over regional extent, from ~San Clemente to Oceanside.
- From San Clement to Oceanside, “30-km-long fold and thrust belt underlies the continental slope seaward of the Newport-Inglewood fault zone.”
- “[The] detachment fault has become reactivated in places and now accommodates northeast-southwest-directed contraction that has formed the overlying fold and thrust belt.”
- “Crustal shortening, which began in Pliocene time, appears to still be active.”
- “Thrust faults within this belt appear to be rooted into the former detachment, and crustal shortening has structurally inverted (uplifted and folded) a former sediment-filled trough situated along the Newport-Inglewood fault zone.”

Bohannon, R.G., and Geist, E., 1998, Upper crustal structure and Neogene tectonic development of the California Continental Borderland: Geological Society of America Bulletin, v. 110, n. 6, p. 779-800.

STRUCTURAL

- “The California continental borderland structural province offshore of the southwestern United States and northwestern Mexico is nearly as wide as the Basin and Range province, but it is less well known....”
- “[P]late interactions are generally thought to have caused the borderland deformation, but the specific history and style of tectonism has been debated.”
- “Luyendyk et al. (1980) used paleomagnetic evidence to argue that the western Transverse Ranges had undergone 90°–105° of clockwise rotations, about vertical axes, mostly during middle to late Miocene time. Numerous way have been proposed to explain the clockwise

- rotation and most of these link the rotation with large amounts of strike slip in the adjacent nonrotated regions to the north and south.”
- “The linked rotation–strike-slip models do not explain the most pronounced lithotectonic abnormality—the regional occurrence of the Catalina Schist that forms the basement of the inner continental borderland and the western part of the Los Angeles basin.”
 - Other authors have suggested “that the Catalina Schist was exposed, from an undetermined depth, through a process of tectonic unroofing in a large inner continental borderland rift that developed behind the clockwise-rotating beam of the western Transverse Ranges.”
 - “The Peninsular Ranges and Catalina Schist boundary has commonly been drawn at the near-vertical Newport-Inglewood and Rose Canyon fault system (e.g., Vedder, 1987). However, Crouch and Suppe (1993) described the boundary as a detachment- fault surface that dips gently to the east in the subsurface north of Oceanside. They used industry seismic-reflection data to support their view. Our data corroborate the findings of Crouch and Suppe (1993) in that the Newport-Inglewood and Rose Canyon fault system is entirely within sedimentary rocks of the Peninsular Ranges belt on line 120 (Fig. 6), and we imaged a similar deeply buried, low-angle fault having an east dip at about the same depth and position as Crouch and Suppe’s (1993) detachment fault. We think that the entire Peninsular Ranges–Catalina Schist boundary is along a low-angle detachment fault, which we call the Oceanside detachment fault.”
 - “The Oceanside detachment fault is defined in the seismic data by several aligned, high-amplitude reflections with gentle apparent east.... These project eastward to an indistinct east-dipping reflection beneath the shelf...and they project westward and upward, through a zone of discontinuous, short reflections, to a series of east-dipping reflections...beneath the western part of the gulf.... We locate the breakaway zone of the detachment fault at the inclined reflections beneath the western part of the gulf.”
 - “Numerous fault zones interrupt the coherency of the reflections that makes up the upper plate of the Oceanside detachment fault and some of these appear to disturb the sea floor.”
 - “The Newport-Inglewood zone is inclined steeply east and it penetrates the entire reflective sequence, including the sea floor. The fault may have a strong normal component of offset. Most of the lesser steep faults appear either to merge downward with the detachment or they truncate at it. This could also be true of the Newport-Inglewood fault zone, although clear documentation is lacking in our data.”
 - “Between the Gulf of Santa Catalina and the San Clemente Island region, there are several small fault-bounded and internally faulted basins....Much of the fill is probably syntectonic....It is not possible to determine the age of the basin fill.”
 - “The San Clemente Island–Cortes Bank region is within the Nicolas forearc belt....Overall deformation within the Nicolas forearc belt is slight and most of the belt remains intact. There are numerous small structural basins, filled with middle Miocene and younger strata, that are bounded by young faults with pronounced normal separations, and these indicate that the belt was deformed by an episode of extensional and possibly strike-slip tectonism.”
 - “The boundary between the Nicolas forearc and Catalina Schist belts is a prominent west-dipping fault...that has been called the East Santa Cruz basin fault.”
 - “It is not possible to determine the magnitude and sense of slip from the seismic data, but the East Santa Cruz basin fault is assumed to have a large amount of right slip.... It probably also has incurred a large, but unknown, amount of normal displacement....The fault appears to break through to the surface....”

**SAN ONOFRE NUCLEAR GENERATING STATION
SEISMIC HAZARD ASSESSMENT PROGRAM
2010 PROBABILISTIC SEISMIC HAZARD ANALYSIS REPORT**

- “The East Santa Cruz basin fault may splay into a group of west-dipping faults on north and west flanks of Sixtymile Bank...and between the East Cortes basin and the Blake Knolls.”
- “The boundary between the Nicolas forearc and western Transverse Ranges belts is just south of the northern Channel Islands....[C]ontinuous reflectors...end abruptly at a steep fault that penetrates the seismic section to all depths. We call this the Channel Island fault zone.”
- “The extensional basins, which serve to define the borderland structural province, formed during Miocene to Pliocene time.”
- “Many of the largest basin-bounding faults...might still be active.”
- “Most of the large northwest-oriented, basin-bounding faults exhibit characteristics that are consistent with a strong strike-slip component in addition to the large vertical separations that can be documented....They have long and straight fault traces and commonly have opposing down-thrown sides along the same fault trace....”
- “We think that the Oceanside detachment fault...is the primary structure upon which the schist basement was uplifted relative to the Peninsular Ranges batholithic basement along the east side of the Catalina Schist belt.”
- “We propose a two-stage model of upper crustal extension. The inner borderland rift formed during the early stage, beginning in early Miocene time when the western Transverse Range belt was oriented more or less north-south. The Catalina Schist was uplifted from middle crustal levels and exposed in the rift as the western Transverse Ranges began to rotate and the Nicolas forearc belt began to be displaced to the west. Most of the modern borderland physiography formed in the later stage, which began at the end of middle Miocene time. The later stage occurred in conjunction with the bulk of the rotation of the western Transverse Ranges. The later stage is primarily one of right-normal faulting in the borderland. Some parts of the borderland may still be in a right-normal slip regime.”
- “[T]here has been approximately 100 km of extension across the part of the borderland...About 60 km of that extension took place during the early stage as the result of a migrating hinge of localized uplift and extension. About 40 km of extension occurred during the later stage as the result of distributed faulting on right-normal faults having northwest orientations.”
- “We speculate that, after 15 Ma, the pattern of borderland deformation changed from localized extension (migrating hinge-flexural uplift model) to more distributed shear on right-normal slip on faults with north-northwest trends.”
- “The Channel Island fault zone and the Santa Cruz Island and related faults, which also probably have curved traces...are viewed as left-slip zones that compensate for differences between the southwest end of the rotating western Transverse Ranges....”

SEISMOLOGY

- “Patterns of seismicity (Legg, 1985) suggest that...the San Clemente, Coronado Bank, San Diego Trough, and Palos Verdes Hills faults, may be active.”

**SAN ONOFRE NUCLEAR GENERATING STATION
SEISMIC HAZARD ASSESSMENT PROGRAM
2010 PROBABILISTIC SEISMIC HAZARD ANALYSIS REPORT**

Kier, G., and Mueller, K., 1999, Flexural modeling of the northern Gulf of California Rift: relating marine terrace uplift to the forebulge on a subsiding plate: Southern California Earthquake Center 1999 internship final report, 11 pp., [<http://www.scec.org/education/college/internships/1999/99grant.pdf>].

STRUCTURAL

- "Therefore, shortening must occur between 0.89 and 2.39 m/ka to achieve between 14 ± 0.03 and 0.25 ± 0.03 m/ka vertical uplift on a fault dipping 6-9 degrees. Using standard vector analysis we rotated the coordinate axes of the regional velocity field to calculate the component normal to the strike of the Oceanside fault as shown in figure 1 (SCEC Data Center, 1999). We then compare the regional surface velocity normal to the fault to the velocity required for current terrace uplift rates. This shows that the current surface shortening is within the range that would generate current uplift patterns but relies on the assumption that velocities at depth are consistent with surface velocities. The northern and southern terminations of the Oceanside fault are at approximately the San Joaquin Hills and the U.S. Mexican border respectively (John Shaw, work in progress)."
- "Of the three models tested in this project, uplift due to forebulging on a subsiding plate provides the best fit model for the observed uplift of marine terraces."

Grant, L.B., Mueller, K.J., Gath, E.M., Cheng, H., Edwards, R.L., Munro, R., and Kennedy, G., 1999, Late Quaternary uplift and earthquake potential of the San Joaquin Hills, southern Los Angeles basin, California: *Geology*, v. 27, p. 1031-1034.

STRUCTURAL

- "Indications of late Quaternary folding are present in the San Joaquin Hills at the southern margin of the Los Angeles basin."
- "The San Joaquin Hills are the topographic expression of a northwest-trending anticlines between San Juan Capistrano and Huntington Mesa."
- "Uplift of the San Joaquin Hills began in the early Pleistocene."
- "Analysis of emergent marine terraces in the San Joaquin Hills...and ²³⁰Th dating of solitary corals from the lowest terraces reveal that the San Joaquin Hills have risen at a rate of 0.21–0.27 m/k.y. during the past 122 k.y."
- "The location and thickness of Holocene sediments in the San Joaquin Hills suggest that tectonic uplift continued during the middle to late Holocene."
- "[W]e do not have direct evidence for Holocene activity of the San Joaquin Hills thrust."
- "A fault-bend fold model with movement on a northwest-vergent thrust fault best explains the elevations of marine terraces..."
- "In [one] interpretation the San Joaquin Hills thrust is a backthrust that soles into the Oceanside detachment (Bohannon and Geist, 1998) as part of a wedge-thrust structure."
- "We prefer to interpret movement of the San Joaquin Hills blind thrust to be the product of partitioned strike slip and compressive shortening across the Newport-Inglewood fault zone."

Bender, E.E., 2000, Late Quaternary uplift and earthquake potential of the San Joaquin Hills, southern Los Angeles basin, California – COMMENT: *Geology*, v. 28, no. 4, p. 383.

STRUCTURAL

- “Grant and et al. (1999) [sic] rather unequivocally demonstrated that the San Joaquin Hills...have risen at a rate of 0.021–0.027 mm/yr over the past 122 k.y. Based largely on geomorphic evidence, they attribute this uplift as a fault-bend fold above a southwest-dipping blind thrust fault.”
- Flower structures “have been shown to exist along the Newport-Inglewood fault zone (Harding, 1979; Wright, 1991), and the extensive, nearly vertical faulting observed in the San Joaquin Hills is suggestive of such a structure extending off of the fault zone.”
- “It appears more likely, on geologic grounds, to suggest that the uplift within the San Joaquin Hills is generated by squeezing upward along the Newport-Inglewood fault zone in shortening deformation accompanying northwest-southeast horizontal shear or transpression.”

Grant, L.B., Mueller, K.J., Gath, E.M., and Munro, R., 2000, Late Quaternary uplift and earthquake potential of the San Joaquin Hills, southern Los Angeles basin, California – REPLY: *Geology*, v. 28, no. 4, p. 384.

STRUCTURAL

- “Bender’s conclusion that uplift within the San Joaquin Hills is generated by squeezing upward along the Newport-Inglewood fault zone by shortening that accompanies northwest-southeast horizontal shear (i.e., transpression) agrees with our statement that, ‘We prefer to interpret movement of the San Joaquin Hills blind thrust to be the product of partitioned strike-slip and compressive shortening across the southern Newport-Inglewood fault zone,’ (p. 1034, Grant et al., 1999).”
- “However, we disagree with Bender’s assertion that the structure of the San Joaquin Hills and proximity to the Newport-Inglewood fault make a blind thrust model unattractive.”
- The “San Andreas fault in central California [is described by Wilcox et al. (1973)] as an example of a wrench fault with a series of en echelon folds on the eastern side of the fault. These folds (anticlines) are now known to be underlain by seismogenic blind thrust faults (Stein and Yeats, 1989; Stein and Ekstrom, 1992) created by transpressive strain partitioned across western California (Lettis and Hanson, 1991). A similar structural relationship probably exists between the Newport-Inglewood fault zone and the San Joaquin Hills.”
- “Our data do provide strong evidence that the San Joaquin Hills are rising in response to a potentially seismogenic, underlying blind fault, and we suggest that this potential earthquake source should be included in regional seismic hazard models.”



Astiz, L., and Shearer, P.M., 2000, Earthquake locations in the Inner Continental Borderland, offshore Southern California: Bulletin of the Seismological Society of America, v. 90, no. 2, p. 425-449.

STRUCTURAL

- Evidence in article forms the basis of several arguments regarding the location, geometry, and style of faulting in the offshore structural models.

SEISMOLOGY

- “[F]ault geometries in this complex region [referring to offshore southern California] are often poorly constrained due to lack of surface observations and uncertainties in earthquake locations and focal mechanisms. To improve the accuracy of event locations in this area, we apply new location methods to 4312 offshore seismic events that occurred between 1981 and 1997 in seven different regions within the Borderland.”
- “Obtaining accurate locations for these events is difficult, due to the lack of nearby stations, the limited azimuthal coverage, and uncertainties in the velocity structure for this area.”
- “In general, our relocated events have small estimated relative location errors and the events are more clustered than the SCSN catalog locations”; “...under ideal conditions offshore events can be located to within 1 to 2 km of their true locations.”
- “Our final locations for most clusters are well correlated with known local tectonic features.”
- “We can relate the 1981 Santa Barbara Island (ML =5.3) earthquake with the Santa Cruz fault, the 13 July 1986 Oceanside (ML = 5.3) sequence with the San Diego Trough fault zone, and events near San Clemente Island with known trace of the San Clemente fault zone.”
- “Our locations define a northeast-dipping fault plane for the Oceanside sequence, but in cross-section the events are scattered over a broad zone (about 4 km thick)...This could either be an expression of fault complexity or location errors due to unaccounted for variations in the velocity structure.”
- “104 Events recorded between 1981 and 1997 that occur near Coronado Bank in the SCSN catalog, are relocated closer to the San Diego coast and suggest a shallow-angle, northeast-dipping fault plane at 10 to 15 km depth.”
- “We plot 65 events, those with standard errors less than 1.5 km.... Locations for events near the Coronado Bank region...occur at 10 to 15 km depth along an apparent northeast dipping fault close to the San Diego Coast.”
- “It is possible that these faults are shallow-angle thrust or detachment faults seen in seismic reflection data...to mark the boundary between the Peninsular Ranges to the east and the Catalina Schist best to the west”
- “If the Oceanside and/or Coronado events indeed occur on portions of a much larger system of offshore thrust faults, this would have important implications because it would establish that these faults are seismically active and a potential source of large future offshore events.”



Rivero, C., Shaw, J.H., and Mueller, K., 2000, Oceanside and Thirtymile Bank blind thrusts: implications for earthquake hazards in coastal southern California: *Geology*, v. 28, no. 10, p. 891-894.

STRUCTURAL

- Oblique convergent slip at depth may be partitioned separately onto NI/RC and OBT (model "D").
- "San Joaquin Hills are formed by northeast-vergent anticline that uplifts and defines marine terraces...[offshore imaging confirms] it formed above a shallow blind thrust [dipping $\sim 23^\circ$ southwest that is] restricted to the hangingwall of the [OBT]; at depth, we interpret that this shallow fault soles into the [OBT]."

SEISMOLOGY

- From seismology (i.e. 1986 Oceanside earthquakes), interpretation suggests Thirtymile Bank Thrust is through-going and not cut by San Diego Trough; if logic is extrapolated to OBT, then OBT is through-going and not cut by NI/RC Fault.
- "[R]elocated mainshock and aftershocks of [1986] Oceanside earthquake [are] clustered at ~ 8 km depth and [define] a $25\text{-}30^\circ$ east-dipping surface" consistent with slip on Thirtymile Bank Thrust fault plane and an epicenter $\sim 14\text{-}17$ km east of San Diego Trough Fault.

GEOPMORPHOLOGY

- Imaged thrusts are "commonly associated with pronounced seafloor fold scarps."

GEODETTIC

- Geodetic observations from Kier & Mueller (1999) indicate "as much as 2 mm/yr of NE-SW convergence between Catalina Island and the coast."

Ponti, D.J., 2001, Changing deformation rates through time: insights from new Quaternary stratigraphic studies in the Los Angeles basin, California [abstract]: American Geophysical Union 2001 Fall Meeting, 10–14 December 2001, abstract #S12E-11.

STRUCTURAL

- Geologically-derived fault slip and fold deformation rates may only be applicable when rate of deformation is constant over time.
- "[S]tratigraphic analysis of Quaternary deposits in [the LA Basin] show [the rate of] fold growth has not been constant during the last ~ 1 Ma."
- "[C]onstant deformation should not be broadly presumed without specific supporting evidence."



Rivero, C., and Shaw, J.H., 2001, 3D geometry and seismogenic potential of the Inner California Borderland blind thrusts system [abstract]: Southern California Earthquake Center Proceedings and Abstracts, 23–26 September 2001, p. 105-106.

STRUCTURAL

- “Inner Continental Borderland blind-thrust system includes a pair of inverted Miocene extensional detachments...reactivated as low-angle thrust faults during the Pliocene.”
- “Thrust motions on these detachments produced several trends of contractional fault-related folds (e.g., San Mateo and Carlsbad structures) that partition oblique convergence with regional strike-slip systems.”

SEISMOLOGY

- “Earthquake hypocenters...suggest that the Inner California blind thrust system is active and seismogenic.”

Sliter, R.W., Ryan, H.F., and Normark, W.R., 2001, Does recent deformation at the base of slope provide evidence of a connection between the Newport-Inglewood and the Rose Canyon fault zones offshore southern California? [abstract], American Geophysical Union 2001 Fall Meeting, 10–14 December 2001, abstract #S11A-0531.

STRUCTURAL

- Previous work by others suggests NIFZ and RCFZ connect along the continental shelf “with the main deformation occurring near the shelf edge.”
- “[O]bserve sediments at the seafloor deformed near the base of the slope at water depths of about 700 m on [multichannel seismic reflection] data between Dana Point and Oceanside.”
- Observe folding of seafloor between Oceanside and Carlsbad at 300 m depth.
- “[D]ata show recent faulting on the shelf (< 100 m water depth) associated with the Rose Canyon fault from Carlsbad to La Jolla.”
- “[I]nterpret the base of the slope faulting to be related to a strand of the NIFZ...that may connect with the RCFZ by a left step near Carlsbad, as evidenced by recent folding of the seafloor.”

Grant, L.B., and Rockwell, T.K., 2002, A northward propagating earthquake sequence in coastal southern California?: Seismological Research Letters, v. 73, no. 4, p. 461-469.

STRUCTURAL

- Faults within the Coastal Fault Zone (>300 km in length) “appear to be kinematical linked.”
- “At a minimum, the Coastal Fault Zone extends from Beverly Hills, California (USA) southeast to the Punta Banda peninsula in Baja California (Mexico) and includes both [the] onshore and offshore...NIFZ (northern and southern segments), the offshore NIFZ, the Rose Canyon Fault, the Descanso strand of the offshore Coronado Bank Fault, and the Agua Blanca Fault.”
- “The offshore NIFZ is a structurally complex zone of folds and faults.”

- “Continuity of the offshore and southern NIFZ was debated. Several studies (e.g., Barrows, 1974; Fischer and Mills, 1991) have concluded that they are continuous or kinematically linked, and therefore the offshore NIFZ is assumed to be seismogenic.”
- “An upper bound slip rate of 3.5 m/yr has been estimated (Fischer, 1992) based on total offset with an estimated age of 2 Ma (Crouch and Bachman, 1989), but the Holocene slip rate is probably lower.”
- “Fischer and Mills (1991) report a seismically active positive flower structure and thrust complex approximately 240 km long.”
- “Several high-angle faults in the [San Joaquin Hills (SJH)] may be strands of the ancestral NIFZ (Bender, 2000) and show evidence of Quaternary surface rupture (Grant et al., 2000). Based on measurements of late Quaternary and Holocene uplift, the SJH have been interpreted to be underlain by an active blind thrust fault (Grant et al., 1999, 2000, 2002). Movement of the SJH blind fault may be kinematically linked to the NIFZ (Grant et al., 1999, 2000), the offshore Oceanside Fault (Rivero et al., 2000), or both.”

SEISMOLOGY

- “Scattered seismicity occurs along the [NIFZ], although events are difficult to locate accurately due to poor station coverage.”
- “The date of most recent rupture of the offshore NIFZ is not known [sic], although seismic-reflection observations and microseismicity indicate that it was during the Holocene.”
- “Toppozada et al. (1981) estimated a $M \geq 6.5$ [earthquake] and proposed a coastal or offshore location for the 1800 earthquake. If this interpretation is correct, the earthquake could have occurred on the offshore NIFZ.”
- The onshore NIFZ northern and southern segments “have been seismically active during the historic period.”
- “Despite relatively high historic levels of microseismicity, the northern NIFZ may be a seismic gap.”
- “The recent seismicity suggest that the northern NIFZ might be in the latter stages of its seismic cycle.”

PALEOSEISMOLOGY

- “[R]ecently published fault investigations in the northern Baja California peninsula (Mexico) and coastal southern California (USA) reveal evidence for geologically contemporaneous or sequential earthquakes along a >300-km-length, predominantly strike-slip seismic zone [which] includes structures previously mapped as the Agua Blanca, Rose Canyon, San Joaquin Hills, and southern Newport-Inglewood Fault zones.”
- “The historic and paleoseismic records indicate that the Coastal Fault Zone has ruptures from the Agua Blanca to the southern NIFZ within the last few centuries, with the possible exception of the northern NIFZ and portions of the offshore NIFZ.”
- “The date of the last surface rupture of the northern NIFZ is not known.”
- “[T]he paleoseismic data and historic observations suggest that the northern NIFZ has not ruptured as recently as other sections of the Coastal Fault Zone.”

GEODETTIC

- “GPS measurements indicate that approximately 14% of the total Pacific-North America Plate motion occurs west of the Elsinore Fault, most likely distributed across the San

Clemente, Newport-Inglewood, Rose Canyon, and other coastal or offshore faults (Bennett et al., 1996).”

OTHER

- “Seismic hazard associated with [the Coastal Fault Zone] has been recognized for decades...but is still poorly quantified...due, in part, to the difficulty of integrating observations onshore and offshore.”
- “[T]he coastal faults have lower slip rates and longer recurrence intervals than many onshore faults and therefore are calculated to represent relatively low hazard...[h]owever, if we examine the entire zone, we find that it ruptured most recently in a temporal cluster or propagating sequence of large earthquakes. Therefore the hazard may be high if the sequence or cluster is still in progress.”
- “The southern California coastal fault zone [sic] might be in the later stages of [a] multicentury failure sequence.”

Grant, L.B., Ballenger, L.J., and Runnerstrom, E.E., 2002, Coastal uplift of the San Joaquin Hills, southern Los Angeles basin, California, by a large earthquake since A.D. 1635: Bulletin of the Seismological Society of America, v. 92, no. 2, p. 590-599.

STRUCTURAL

- “The San Joaquin Hills...are the surficial expression of a faulted anticline parallel to the active Newport-Inglewood fault zone....”
- “Grant et al. (1999, 2000) proposed that uplift was generated by movement on an underlying blind thrust fault due to partitioned strike-slip and compressive shortening across the southern Newport-Inglewood fault zone.”
- Study of marsh deposits in Newport Bay, “a late Pleistocene erosional gap between the northern San Joaquin Hills and Newport Mesa.”
- Prior work by Stevenson (1954) suggested “the marsh bench was created by emergence of late Holocene marshland and subsequent death of the elevated marsh community. Stevenson (1954) hypothesized that ‘the greater height of the ‘marsh bench’ in the central area is probably the result of movement during Recent time of a major anticline and fault system which cut through the Bay in a NW–SE direction.’”
- “The pattern of uplift reported by Stevenson (1954) is consistent with both the geomorphic expression of the San Joaquin Hills and the expected vertical displacement field that would be generated by coseismic growth of the San Joaquin Hills.”
- “Our data agree with Stevenson’s (1954) hypothesis that the marsh bench emerged due to tectonic uplift of the San Joaquin Hills.”
- “The spatial pattern of emergent shorelines and marsh deposits roughly mimics the topographic expression of the San Joaquin Hills and is consistent with a tectonic origin.”
- “The marsh bench and coastal benches could not have formed solely by erosion or deposition due to a sea level highstand because the elevations are different at different locations and the average elevations are different on each side of Newport Bay and along the open coast. Therefore, the most plausible mechanism for creating both the marsh bench and coastal platforms is emergence by tectonic uplift.”

- “The age of the marsh bench is constrained by radiocarbon dating.... Active marsh deposition and growth must have ceased on the marsh bench sometime after our samples were deposited.”
- “Uplift of the San Joaquin Hills must have occurred after A.D. 1635, the earliest plausible age of the marsh bench.”
- “Several fault models have been proposed to explain uplift and folding of the San Joaquin Hills. Grant et al. (1999) developed a model of a blind thrust fault dipping 30° to the southwest. Bender (2000) proposed that uplift is occurring in response to movement of the steeply dipping, strike-slip Newport–Inglewood fault system. Both types of faults may have contributed to uplift during the late Quaternary (Grant et al., 2000). A third model proposed by Rivero et al. (2000) attributes uplift to movement of a large regional thrust, the northeast-dipping Oceanside fault extending offshore of the San Joaquin Hills south to Oceanside and San Diego.”
- “Several observations suggest that the San Joaquin Hills are underlain by a fault that is distinct from the NIFZ, although they may be linked kinematically.”
- “Other topographically prominent anticlines, such as Signal Hill, are located within the structurally complex NIFZ and are associated with step-overs (Barrows, 1974). In contrast, the San Joaquin Hills anticline is east of the main NIFZ, and there is a releasing bend at the mouth of the Santa Ana River where the fault goes offshore (Morton and Miller, 1981) near the northern San Joaquin Hills.”

SEISMOLOGY

- The 28 July 1769 historic earthquake is “a good candidate for the most recent earthquake that raised the San Joaquin Hills coastline.”
- “Other candidates for the San Joaquin Hills earthquake occurred on 22 November 1800 and 10 July 1855.”
- “There are no other documented earthquakes that could have generated more than 1 –m uplift of the San Joaquin Hills after 1855, so we conclude that uplift and the causative earthquake occurred between A.D. 1635 and 1855.”
- “Based on our interpretations of the data, this region was more seismically active in the preinstrumental period.”

GЕOMORPHOLOGY

- “In the San Joaquin Hills, wave erosion and coastal processes have formed a suite of shore platforms extending from the modern shoreline up to an elevation of greater than 300 m above sea level, indicating late Quaternary tectonic uplift.”
- “[T]here is common agreement that modern and ancient shorelines are geomorphic indicators of sea level relative to land.”
- “Along the open coast of the San Joaquin Hills, the lower emergent platform and shoreline are a few meters above the lowest (modern) wave-cut platform and several meters below any previously mapped or dated shoreline.... Based on position between the modern shoreline and dated shorelines at higher elevation, the lower emergent shoreline should be younger than 83 ka (stage 5a sea level highstand).... Therefore, the lowest emergent platform and shoreline...are most likely Holocene age (stage 1 sea level highstand).”
- “Most emergent Holocene shorelines in tectonically active areas are less than 6000 yr old and reflect coseismic uplift rather than sea level fluctuation or large storms.”



- “Changes in pollen types, as well as sedimentation, reported from a core of San Joaquin Marsh (Davis, 1992) are consistent with an interpretation of latest Holocene tectonic uplift of the San Joaquin Hills. San Joaquin Marsh is currently a freshwater marsh located between the city of Irvine and upper Newport Bay.... Radiocarbon dates and analysis of pollen from core sediments show that San Joaquin marsh responded to changes in relative sea level during the Holocene (Davis, 1992). After approximately 4500 yr B.P., freshwater pollen types were replaced with salt marsh types as marsh flora responded to the Holocene sea level highstand (Davis, 1992). Freshwater conditions returned briefly circa 3800, 2800, 2300, and after 560 yr. B.P.”
- A “possible explanation is that tectonic uplift of the San Joaquin Hills elevated San Joaquin Marsh above sea level, causing a return to freshwater conditions.”

Grant, L.B., and Shearer, P.M., 2004, Activity of the offshore Newport-Inglewood Rose Canyon Fault Zone, coastal southern California, from relocated microseismicity: Bulletin of the Seismological Society of America, v. 94, no. 2, p. 747-752.

STRUCTURAL

- Structure of offshore NI/RC may be like onshore Newport-Inglewood Fault, with multiple strike-slip strands.

SEISMOLOGY

- Relocated two microearthquake clusters associated with offshore NI/RC: 1981 Oceanside cluster (19 events) and 2000 Newport Beach cluster (7 events).
- 1981 Oceanside cluster not associated with 1986 Oceanside earthquake sequence.
- The “events [in the 1981 Oceanside cluster] align along a north-northwest trend about 0.5 km long...[and] define a nearly vertical plane between 12.5 and 13.0 km depth” and are “approximately parallel to the fault zone.”
- The “strike, dip, and location of a plane fit by these events are consistent with active strike-slip faulting” on the offshore NI/RC Fault Zone.
- Composite waveform polarities “are consistent with a right-lateral strike-slip focal mechanism,” but “cannot eliminate other possible focal mechanisms.”
- “[F]ive of seven events [in the 2000 Newport Beach cluster] are aligned in a pattern consistent with a shallow (7 km) north-northwest-striking, vertical or steeply dipping active fault,” but polarities are too small for focal mechanism solutions.
- Overall, dataset too sparse to determine if there is (or is not) a through-going strike-slip fault zone.
- The “location and ~13 km depth of the Oceanside cluster suggests that the [OBT] is terminated by active strike-slip faults.”

**SAN ONOFRE NUCLEAR GENERATING STATION
SEISMIC HAZARD ASSESSMENT PROGRAM
2010 PROBABILISTIC SEISMIC HAZARD ANALYSIS REPORT**

Rivero, C.A., 2004, Origin of active blind-thrust faults in the southern Inner California Borderlands, unpublished Ph.D. Dissertation: Harvard University, 146 pp.

STRUCTURAL

- "Several of [the] contractional and extensional structures [offshore Dana Point] were previously interpreted as wrench-related thrusts and folds, and as 'flower structures' produced by active offshore segments of the Newport-Inglewood."
- "[I]nterpret most of the contractional trends sole into, and do not cross, the [OBT]."
- Complex faulting in basin inversions may be "prone to be confused with flower structure."
- "Shallow slip partitioning is the most likely description of the structural relationship between the Thirtymile Bank and San Diego Trough faults."
- "In many cases, seismic reflection data indicate previously interpreted strike-slip fault splays correspond with active hinges of contractional anticlines produced by...motion on a deep structural wedge."
- OBT Segment I (Dana Point to south of Carlsbad) slip rate 0.88–1.17 mm/yr; M 7.1 → return interval (RI) = 1070–1430 yrs; M 7.3 → RI = 1480–1960 yrs.
- OBT Segment II (south of Carlsbad to south of San Diego) slip rate 0.70–0.94 mm/yr; M 7.3 → RI = 1840–2470 yrs.
- OBT full length, M 7.5 → RI = 2030–3390 yrs.

GEOPMORPHOLOGY

- "[L]ocal asymmetric anticlines with bathymetric expression, sitting on top of regional rollovers" are associated with mapped structures (proposed thrust systems).
- "Structural wedge system above the [OBT] shows a spatial correlation with the occurrence of Quaternary uplift in adjacent coastal areas," e.g. San Joaquin Hills, and marine terraces and strand lines along coastal Orange and San Diego Counties.

Rivero, C., and Shaw, J.H., 2005, Fault-related folding in reactivated offshore basins, California *in* Interpretations of Contractual Fault-Related Folds, An American Association of Petroleum Geologists Seismic Atlas, Studies in Geology, No. 53, Department of Earth and Planetary Sciences: Harvard University, Cambridge, MA, 3 pp.

STRUCTURAL

- "The San Mateo anticline developed by the upward propagation of reverse slip during the inversion of Miocene half-grabens."
- Oceanside detachment "is not folded by the contractional structures; thus we interpret that the San Mateo Anticline is formed by thrusting ramping up from this detachment surface."
- San Mateo ramp is also folded by a younger, deeper thrust.
- San Mateo thrust and underlying thrust "terminate in structural wedges...that propagate slip back to the hinterland...as no foreland structures that could account for the transfer of slip exist beyond the San Mateo anticline."
- "[I]nterpret the San Mateo Anticline as an imbricated fault-bend fold produced by the upward propagation of contractional slip from an inverted normal fault into multiple detachment levels."

- “The back-limb geometry...indicates the presence of a deeper structure [that] refolds the shallow thrust sheet of the San Mateo Anticline in a way consistent with a break-forward system.”
- Estimated total shortening offshore the San Clemente region is 2.5 km.
- “The San Mateo anticline is an imbricated fault-bend fold originated by basin inversion processes” along a thrust that “reactivated a segment of a northeast-dipping Miocene normal fault.”
- “The phase of basin inversion also reactivated a Miocene low-angle detachment as the [OBT]” and the OBT “transferred contractional slip to associated synthetic and antithetic normal structures, inverting a major graben-boundary fault, and generating a regional structural wedge [that] controls the location of a prominent monocline with bathymetric expression.”

Legg, M.R., Goldfinger, C., Kamerling, M.J., Chaytor, J.D., and Einstein, D.E., 2007, Morphology, structure and evolution of California Continental Borderland restraining bends *in* Cunningham, W.D., and Mann, P., eds., *Tectonics of Strike-Slip Restraining and Releasing Bends*: Geological Society, London, Special Publications, 290, p. 143-168, doi: 10.1144/SP290.3.

STRUCTURAL

- A “restraining bend exists where the fault curves or steps to the left when following the fault trace. Crowding of crustal material by lateral movement into the fault bend produces uplift and crustal thickening....”
- “Right-slip on irregular fault traces in the California Continental Borderland “has produced numerous restraining bend pop-ups that exhibit distinctive seafloor morphology.”
- “The submarine basins of the Borderland range in depth from a few hundred metres to more than 2000 m...erosion is greatly diminished in these deep basins compared with subaerial regions, so that pop-up morphology is well preserved on the seafloor.”
- “The San Clemente fault zone includes a 60-km-long restraining bend that exhibits prominent seafloor uplift in the 1300-m deep Descanso Plain offshore of northwest Baja California....”
- San Clemente Fault bed region minimum uplift rate is 0.47 to 0.70 m/ka.
- “The Catalina Fault forms an 80-km-long restraining double bend (cf. Crowell 1974) between the Santa Cruz-Catalina Ridge and San Diego Trough fault zones. Uplift due to oblique convergence along this transpressional fault has produced Santa Catalina Island and the wide submerged shelf and slope surrounding the island.”
- Model for restraining bend evolution:
 - “First, the strike of the principal displacement zone (PDZ) in the major restraining bends is parallel to the Miocene Pacific-North America (PAC-NOAM) relative motion vector(s).”
 - “Second, the major faults within the restraining bend pop-up have very steep to vertical dips.”
 - “Third, the pop-up structures for the major restraining bends have structurally inverted Miocene basins.”
 - “Fourth, there is an overall right-stepping en echelon character to the major right-slip fault pattern of the Borderland.”

**SAN ONOFRE NUCLEAR GENERATING STATION
SEISMIC HAZARD ASSESSMENT PROGRAM
2010 PROBABILISTIC SEISMIC HAZARD ANALYSIS REPORT**

Campbell, B.A., Sorlien, C.C., Cormier, M., and Alward, W.S., 2009, Quaternary deformation related to 3D geometry of the Carlsbad fault, offshore San Clemente to San Diego [abstract], Southern California Earthquake Center Proceedings and Abstracts, 12–16 September 2009, v. 19, p. 263.

STRUCTURAL

- Parts of Carlsbad-Coronado fault system coincide with the SCEC CFM OBT.

Mueller, K., Kier, G., Rockwell, T., and Jones, C.H., 2009, Quaternary rift flank uplift of the Peninsular Ranges in Baja and southern California by removal of mantle lithosphere: Tectonics, v. 28, TC5003, doi:10.1029/2007TC002227.

STRUCTURAL

- Presents argument for the model that the elevated terraces along the Pacific coast of northern Baja California and southern California are the result of the distal effect of “flexure of the elastic lithosphere driven largely by heating and thinning of the upper mantle beneath the Gulf of California (and the Salton Trough) and eastern Peninsular Ranges.”
- “Pliocene strata deposited at sea level along the Pacific coastline in southern California have not been uplifted significantly above Quaternary marine terrace deposits.”

Ponti, D.J., and Ehman, K.D., 2009, A 3-D sequence-based structural model for the Quaternary Los Angeles basin, California [abstract]: Southern California Earthquake Center Proceedings and Abstracts, 12–16 September 2009, vol. 19, p. 262-263.

STRUCTURAL

- “A 3-D sequence-based structural/stratigraphic model for the Los Angeles Basin is being developed by the USGS for use in earthquake hazards and groundwater resources research.”
- “The Quaternary section reaches a maximum thickness of more than 1280 m in the Lynwood area east of the Newport-Inglewood (N-I) fault zone. In the west basin, the Quaternary section reaches its greatest thickness (>410 m) in San Pedro Bay just east of the Palos Verdes fault. Of the inter-basin structures that impact the Quaternary section, the Compton-Alamitos fault (Wright, 1991) is the most prominent. Discreet faulting of mid-late Pleistocene deposits and structural relief of up to 300 m is suggested by the seismic data and by anomalous water levels near Los Alamitos. West of the N-I fault, two W-NW-trending inter-basin faults offset mid-late Pleistocene sediments and may serve to consume slip from the N-I. The M4.7 Hawthorne earthquake of May 18, 2009 was located near the northernmost of these structures and has a fault-plane solution consistent with the geometry and kinematics of this fault as evidenced in the geology.”

Ryan, H.F., Legg, M.R., Conrad, J.E., and Sliter, R.W., 2009, Recent faulting in the Gulf of Santa Catalina: San Diego to Dana Point *in* Lee, H.J., and Normark, W.R., eds., *Earth and Science in the Urban Ocean: The Southern California Continental Borderland: Geological Society of America Special Paper 454*, p. 291-315, doi: 10.1130/2009.2454(4.5).

STRUCTURAL

- Where the Rose Canyon FZ "is imaged on industry MCS records, [it] forms a complex flower structure near the shelf break" (offshore Encinitas).
- "[M]ain strand of [offshore] Newport-Inglewood FZ forms a prominent positive flower structure" (offshore San Onofre).
- NI/RC bend/connection "is accommodated by reverse faulting...faulting dies off rapidly [away from bend/connection], however folding continues [from] Carlsbad Canyon [to] near the left step [in] Newport-Inglewood FZ."
- "[I]ndustry seismic reflection profiles suggest the [OBT] might not be continuous," and it is "uncertain [whether OBT] offsets San Onofre FZ south of San Mateo Point."
- "[L]ack sufficient data] to determine whether or not [OBT] intersects and offsets Newport-Inglewood FZ."
- "[S]outh of La Jolla Fan Valley...little evidence for shortening associated with [OBT]."
- Of the main, through-going offshore faults, the "more northerly...tend to be transtensional and the more westerly [tend to be] transpressional."
- Key issue of San Mateo FZ and Carlsbad FZ: are these reverse faults "indicative of broad scale contraction...related to the reactivation of the Oceanside detachment as a blind thrust...or related to more localized complexities associated with slip partitioning along Newport-Inglewood FZ."
- "[U]plift of marine terraces along much of the coastline between Newport Beach and La Jolla provides possible evidence for the large-scale reactivation of the entire Oceanside detachment surface as a blind thrust"..."however, uplift of terraces could also be explained by transpression along Newport-Inglewood FZ."
- "[A]lthough a low-angle detachment surface is imaged...throughout much of the offshore Gulf of Santa Catalina, there is not unequivocal evidence that it has been reactivated as an uninterrupted active thrust fault."

Sorlien, C.C., Campbell, B.A., Alward, W.S., Seeber, L., Legg, M.R., and Cormier, M., 2009a, Transpression along strike-slip restraining segments vs. regional thrusting in the Inner California Continental Borderland [abstract]: *Southern California Earthquake Center Proceedings and Abstracts*, 12–16 September 2009, v. 19, p. 264.

STRUCTURAL

- The OBT "has little effect on the ~2.5 Ma horizon above [it], and a regional anticline expected due to deeper blind thrust slip beneath the Gulf of Santa Catalina is lacking."
- "Significant Plio-Quaternary folding is only present where the [OBT] bends to merge with the Carlsbad fault."
- Carlsbad Fault is oblique-right reverse, "SW-verging thrust slip [on it] contributes to uplifting continental shelf...and San Joaquin Hills."

Sorlien, C.C., Campbell, B.A., and Seeber, L., 2009b, Geometry, kinematics, and activity of a young mainland-dipping fold and thrust belt: Newport Beach to San Clemente, California, USDI/USGS Award No. 08HQGR0103 Final Technical Report, 25 pp.

STRUCTURAL

- "[R]ight lateral NI fault [is] part of a larger 3D system of oblique-right reverse faults."
- The central OBT does not deform early Quaternary seds and has "normal separation near [the] base of [the] Pliocene horizon."
- Northwest OBT coincides with San Mateo/Carlsbad Fault; progressive tilting in hangingwall forelimb indicates subsidence; Newport Beach/Oceanside slope and shelf and San Joaquin Hills being uplifted on San Mateo/Carlsbad Fault.
- Southeast OBT coincides with Coronado Bank Fault, locally pure right lateral.

Conrad, J.E., Ryan, H.F., and Sliter, R.W., 2010, Tracing active faulting in the Inner Continental Borderland, Southern California, using new high-resolution seismic reflection and bathymetric data [abstract]: Seismological Society of America 2010 Annual Meeting, Seismological Research Letters, v.81, no. 2, p. 347.

STRUCTURAL

- Based on recent high resolution seismic and bathymetric surveys, the mapped traces of the Palos Verde, Coronado Bank, San Diego Trough, and San Pedro Faults have been significantly altered.
- Indicate that the Avalon Knoll Fault also shows evidence of recent offsets and "these faults are thought to accommodate about 5-8 mm/yr of slip but it is not clear how slip on these faults is distributed...."
- Re-defined the Catalina Fault as inactive and report the Catalina Island is subsiding rather than rising.
- Presented the USGS's latest map of the NI/RC fault system, but do not discuss it specifically.
- The key value is the more accurate map of the San Diego Trough Fault and correlating this more location and mapped configuration with its associated step-overs and the 1986 Oceanside earthquake (See Ryan, 2010, personal communication).

Ponti, D., 2010, personal communication.

STRUCTURAL

- Amplifying on Ponti, D.J. and Ehman, K.D. (2009), "At present, faults are highly simplified in the model; we have not accounted for every known structure in the basin, but instead have focused on modeling faults that have an apparent impact on groundwater flow... Vertical terminations of the faults have also not yet been tightly constrained."

SEISMOLOGY

- "The Charnock fault, originally proposed by Poland and others (1959) to explain groundwater anomalies within Pleistocene sediment, may in fact correspond with a more

NW-trending structure identified by Wright (1991) that appears associated with a trend of seismicity evident in recent relocations. The M4.7 Inglewood earthquake of May 18, 2009 was located near the southern end of this seismicity tren(d) and has a fault-plane solution consistent with the geometry and kinematics of this fault as evident in the geology.”

Rivero, C., and Shaw, J.H., 2010, in press, Active folding and blind-thrust faulting induced by basin inversion processes, Inner California Borderlands: Tectonics, submitted for consideration of publication 2010, 45 pp.

STRUCTURAL

- “We evaluate several different styles of geometric and kinematic interactions between high-angle strike-slip faults and the low-angle detachments, and favor interpretations where deep oblique slip is partitioned at shallow crustal levels into thrusting and right-lateral strike-slip faulting. “
- “Restored and Balanced cross-sections provide a minimum SW-directed slip of 2.2-2.7 km on the Oceanside Thrust, and illustrate the role of this detachment in controlling the process of basin inversion and the development of the overlying fold-and-thrust belt.”
- “Interpret observations to reflect a complex mixture of strike-slip and blind-thrust faulting in the Inner Borderlands that is similar to the style of deformation in the onshore LA basin.”
- “Miocene low-angle normal (detachment) faults... that were reactivated by basin inversion processes initiated in the Late Pliocene, during the onset of the modern transpressional regime.”
- “[N]ew geometric representations of the offshore Newport-Inglewood, Rose Canyon, and San Diego Trough fault zones...consistent with basin inversion processes and the presence of both active blind-thrust and strike-slip faults in the southern Inner California Borderlands.”
- “[P]rovide insight into the subsurface geometries of complex zones where coeval active strike-slip and thrust faults interact. Both types of fault systems are deemed likely to be active, and should be considered in the context of regional earthquake hazards assessment.”
- “[M]otion on the Oceanside Thrust generated four prominent contractional fold trends. Three of these are foreland-directed structures (San Mateo, San Onofre, and Carlsbad Trends) that produce prominent fold scarps at the seafloor...suggesting Quaternary activity. The fourth is a backthrust (hinterland-directed) system...manifested in a laterally continuous monocline that controls the relief and bathymetric expression of the shelf.”
- “[C]ontractional and extensional structures represent local restraining and releasing bends along the offshore extension of the Rose Canyon strike-slip fault. At depth, the NI and RC strike-slip fault zones intersect with the Oceanside Thrust...at relatively shallow levels of ~4km in the north and deeper ~10 km in the south. Data are insufficient to uniquely define the manner in which these two fault systems interact. Scenarios where the two fault systems interact at depth in a manner consistent with their coeval activity are favored.”

SEISMOLOGY

- “The Inner Borderlands do not display the apparent spatial correlation between EQ activity and regional strike-slip fault zones that is observed around the onshore region of the Peninsular Ranges...Seismicity in this area is diffuse and scattered.”

Rockwell, T., 2010, personal communication.

GEOPMORPHOLOGY

- 3-D trenching and “Paleoseismic work along the onshore Rose Canyon fault zone in the City of San Diego clearly demonstrates that the fault has sustained recurrent Holocene activity ...”
- “Considering that the surface soil represents a long period of stability, it is not possible to simply space the timing of all six events equally for the past 9.3 ka. In fact, if the interpretation is correct that the surface soils represent at least 5 ka of development, then five of these events occurred as a cluster in the period between about 9.3 and 5 ka, with an average interval of recurrence of less than 1 ka.”
- “If the fault principally behaves in a clustered seismicity mode, and if the five early Holocene events represent such a cluster, then one must consider the possibility that the recent earthquake of ca. AD 1650 represents a return to activity and is possibly the first in the next cluster of large earthquakes.”

Rockwell, T.K., 2010, Appendix A, Attachment A-2, Seismic source characteristics of onshore Rose Canyon fault, for GeoPentech, Inc., 14 pp.

STRUCTURAL

- “Marine terraces on the southwest flank of the uplift (Kern, 1977; Kern and Rockwell, 1992), along with the presence of the Linda Vista Formation marine terrace alluvium capping Mount Soledad, attest to the higher rate of uplift of the restraining bend area (0.25 mm/yr) relative to the surrounding coastal plain (0.13 mm/yr) (Kern and Rockwell, 1992), with the background regional uplift attributed to rift-flank uplift from extension in the Gulf (Mueller et.al., 2009).”
- The combination of the releasing step plus a change in fault strike make the Oceanside step a likely (northern) termination zone for ruptures, although a through-going rupture cannot be precluded.”
- “However, the San Joaquin Hills may represent uplift associated with a step from the northern termination of the Rose Canyon to the Newport-Inglewood fault zone.”
- “If the Oceanside step-over is a barrier to rupture propagation, it would divide the Rose Canyon fault into two roughly similar-length sections: a 65 km segment from San Diego Bay to Oceanside, and a 55 km segment from Oceanside to the San Joaquin Hills...one cannot preclude rupture of the entire Rose Canyon fault for a distance of more than 100 km. However, I consider this model a lower likelihood than rupture of individual segments and weight it a 25%, versus 75% for the more segmented rupture behavior.”

PALEOSEISMOLOGY

- The “most recent earthquake occurred sometime between AD 1523 and 1769. These 3-D trenching data further suggest that about 3 m of right lateral, strike-slip displacement occurred during this event, with a 1:10 ratio of vertical to horizontal displacement.”

- “In particular, the onshore data supports the argument that the high-angle, right-lateral, strike-slip as NI/RC Fault System is a primary seismic source fault whereas the nearby, shallow-dipping normal, oblique, and reverse faults are subsidiary.”
- Paleoseismic data further suggest a termination zone near the San Joaquin Hills and “that the San Joaquin uplift is structurally tied to the coastal system of strike-slip faults.”

GEOPMORPHOLOGY

- “The level of activity is indicated by both the relatively large lateral deflections of stream channels that are incised into low marine terraces (Figure A-4-4), and by the results of the three-dimensional trenching. These observations suggest a lateral slip rate of about 2 mm/yr during the late Quaternary (Rockwell, 2010a).”
- “For the southern termination, the right-step between the Rose Canyon and Descanso faults forms the depression occupied by San Diego Bay (Figure A-4-1, and is likely large enough (>5 km) to arrest dynamic slip.”

OTHER

- “... I suggest using the maximum slip rate range of 1.1 to 2.5 mm/yr, with the best estimate of 1.5-2.5 mm/yr, with the following weights: 0.5 (0% weight), 1.0 (10% weight), 1.5 (30% weight), 2.0 (40% weight), 2.5 (20% weight), and 3.0 (0% weight).” In order to accommodate the possibility of clustering “I would suggest using the long-term rate (the above) with an 80% weight, and consider using an alternate weighting scheme for slip rate (in mm/yr) with a 20% overall weight as follows: 0.5 (0% weight), 1.0 (10% weight), 1.5 (30% weight), 2.0 (30% weight), 2.5 (20% weight), and 3.0 (10% weight).”

Ryan, H., 2010, personal communication.

STRUCTURAL

- Does not see OBT as single large structure, but rather small segments reactivated, possibly by block rotation and localized transpression in the San Diego Trough/Gulf of Santa Catalina region.
- San Diego Trough Fault connects in north with San Pedro Basin Fault, rather than Catalina Ridge.
- At the behest of the California Geological Survey, the extent of the OBT was mapped using industry MCS data available at the USGS NAMSS web site. The main OBT reflector is quite strong and well imaged off of San Mateo point (e.g., Crouch and Suppe, 1993). Following this prominent reflector on strike lines that extend along most of the Gulf of Catalina, it was not possible to tie the reflector to the OBT mapped south of the area around San Mateo Point. Hence, it is difficult to justify a pervasive areal extent of the OBT.
- High-resolution reflection profiles imaging folds within the hanging wall of the OBT show reflectors with increasing tilt with depth behind one of the prominent folds. Although this may indicate active folding/uplift, it is not possible to preclude the possibility that the progressively tilted beds are from sediment waves, which are pervasive in the area owing to the close proximity of the San Mateo channel and fan system.
- Notes no evidence for Holocene connection between Coronado Banks Fault and Palos Verdes Fault, contrary to what is depicted in UCERF 2 and the CFM.



- New USGS surveys planned for spring and summer of 2010.

SEISMOLOGY

- Comparison of the newly acquired map trace of the San Diego Trough Fault (as was currently being refined by Conrad, J.E.) with the Astiz and Shearer (2000) relocated epicenters of the 1986 Oceanside events indicates the earthquakes very clearly match a right step in the San Diego Trough Fault, which clearly explains the oblique thrust focal mechanisms in this earthquake sequence rather than the model presented in Rivero et al. (2000) and Rivero (2004).

Shaw, J.H., and Plesch, A., 2010, Appendix A, Attachment A-3, Seismic source characteristics of Inner California Borderland's blind thrust fault systems, for GeoPentech, Inc., 15 pp.

STRUCTURAL

- 1986 Oceanside thrust earthquake and "extensive research of hundreds of proprietary oil industry marine geophysical seismic reflection survey lines, lead us to infer the presence of two distinct, active thrust fault systems located offshore of southern Orange County and San Diego County."
- The "OBT extends at least from Laguna Beach to the Mexican border and may dip under the shoreline."
- "The slip rate was estimated for the OBT based on measures of fault offsets and uplift using the marine geophysical seismic reflection survey data and estimates of the ages of the deformed geologic formations."
- "We recognize that others believe that right-lateral strike slip faults (model 1) dominate the tectonics off-shore of Orange and San Diego Counties. However, based on the currently available data, we would assign a weight of '0' to rupture model 1 [as it] is not kinematically compatible with the large amount of displacement we document on the OBT."
- "[I]t is unclear whether the shallow dipping thrust faults (such as the OBT) are primary seismic source faults, with the steeply dipping, right-lateral, strike-slip faults, such as the NI or RC faults, being subsidiary, or whether the steep, strike-slip faults are the primary seismic sources, and the thrust faults are subsidiary."
- "Association of the OBT and the San Joaquin Hills thrust, combined with the patterns of uplifted coastal marine terraces, further support fault activity."
- "At the depths and locations where data is necessary to resolve the uncertainty...regarding the intersection between the NI/RC and the OBT, the faults are within the basement rocks and the velocity contrast/acoustic impedance of the basement rocks either side of where these faults are inferred to be interacting is not likely to be significant enough to produce adequate reflectors in the marine geophysical seismic reflection surveys."
- "[I]t is doubted whether high energy, deep penetrating 2-D or 3-D seismic surveys can retrieve the necessary data to be able to unequivocally resolve this particularly important uncertainty."

SEISMOLOGY

- “[R]everse/thrust focal mechanism solution tied to the offshore 1986 Oceanside (M_L 5.3) Earthquake demonstrated that active blind thrust faults also exist in Southern California’s inner Continental Borderland.”

GEODETIC

- Research and analysis considered “GPS data from the SCEC Crustal motion Map that Kier and Mueller (1999) used...our sense is that these geodetic data are poorly constrained....Thus, there is a large uncertainty with this rate deformation, but at present we simply lack another means to estimate this rate.”

Wetmore, P.H., Malservisi, R., Fletcher, J., Alsleben, H., Callihan, S., Springer, A., and González-Yajimovich, O., 2010, in review, Transtension within a restraining bend domain of a transform plate boundary: the role of block rotations and the reactivation of preexisting crustal structures: Geological Society of America Lithosphere, submitted for consideration of publication 2010, 17 pp.

STRUCTURAL

- “Given its structural context the ABF should be characterized by a significant component of contractional dip-slip motion. However, the ABF is uniquely characterized by nearly pure strike-slip displacements along the east-west trending eastern portion and an increasing normal component of dip-slip motion along western segments where its trend becomes more northwesterly.”
- “The net effect is to connect regions of high extension in the Gulf of California with those in the northern Continental Borderlands.”
- “However, the kinematics and distribution of faults that accommodate the plate motion exhibit profound along-strike variations and the margin can be separated into three distinct tectonic domains.”
- “The Gulf of California forms the southern segment of the plate margin where a system of en echelon transform and spreading centers accommodate integrated transtensional shearing across a relatively narrow deformation belt along the axis of the gulf.”
- “In the northern plate-boundary segment, most of the shearing is accommodated by the San Andreas Fault system. Dextral strike-slip faults in this domain are kinematically coordinated with folds and thrust faults to produce strongly transpressional shearing.”
- In the central domain of the plate margin, shearing is marked by the “Big Bend” of the San Andreas Fault, which “[l]inks plate-margin shearing along coastal California with that in the Gulf of California. In many ways the central domain is a transitional region between the two radically different domains to the north and south. However is also has unique pattern of faulting that is distinct from the other two domains. Although thrust faults and folds are present throughout the northern half of the central domain (Zoback and Zoback, 1980; Bartley et al., 1993) horizontal contraction is largely accommodated by conjugate strike-slip faults.”
- Major late Miocene normal faults form an important kinematic component of deformation in the southern half of the central domain, but extreme crustal thinning is partially compensated by north-south shortening associated with detachment folds and conjugate strike-slip faults.

APPENDIX A – ATTACHMENT A-2

**SEISMIC SOURCE CHARACTERISTICS OF
ONSHORE ROSE CANYON FAULT**

By

**Dr. Thomas Rockwell
San Diego State University**

INTRODUCTION

The following document has been prepared at the request of Southern California Edison (SCE) in consultation with technical members of their Seismic Hazard Assessment Program (SHAP).

The onshore traces of the Rose Canyon (RC) Fault Zone, as currently mapped through San Diego, are shown on Figure A2-1 (Rockwell, 2010a). The onshore evidence for the presence and recent activity of the Rose Canyon Fault Zone is abundant, with tectonic geomorphic expression of the active traces clearly evident in early aerial photography (Treiman, 1993; Lindvall and Rockwell, 1995, Rockwell, 2010a). As presented in Rockwell (2010a), 3-D trench data suggest that the most recent earthquake on the fault that resulted in surface rupture occurred sometime between AD 1523 and 1769. These 3-D trenching data further suggest that about 3 m of right-lateral, strike-slip surface displacement occurred during this event, with a 1:10 ratio of vertical to horizontal displacement.

Although the evidence for onshore rupture of the RC fault is not specific to the fault traces offshore of SONGS, these onshore data are some of the only available to address the size and frequency of earthquakes that may be expected from the Newport-Inglewood-Rose Canyon (NI/RC) Fault System, and therefore supports its seismic source characteristics. In particular, the onshore data supports the argument that the high-angle, right-lateral, strike-slip NI/RC Fault System is a primary seismic source fault whereas the nearby, shallow-dipping normal, oblique, and reverse faults are subsidiary.

The following sections of this appendix provide more information regarding:

1. How the onshore RC data supports the conclusion that the high-angle, right-lateral, strike-slip NI/RC Fault System is the primary seismic source fault, as was concluded during the 1980s licensing of the plant, and as was recently incorporated into the preparation of the current version of the National Seismic Hazard Map (USGS, 2009);
2. Why these data are appropriate to use to define the current model of the NI/RC Fault System for incorporation into the update of the plant's Probabilistic Seismic Hazard Assessment, and the update of its deterministic tsunami assessment with a Probabilistic Tsunami Hazard Assessment; and
3. The identification of recommended future research that will further strengthen our understanding of the potential hazards associated with the NI/RC Fault System.

PRESENCE AND LEVEL OF ACTIVITY

The active surface trace of the RC fault can clearly be mapped southward from the La Jolla coastline, up over Mount Soledad, down through Rose Canyon, across the San Diego River Valley, through Old Town San Diego and downtown San Diego, and across Coronado Island based on analysis of early aerial

photography (Treiman, 1993, Lindvall and Rockwell, 1995, Rockwell, 2010a). The location of the fault is marked by the presence of scarps, deflected drainages, a sag and several pressure ridges, all of which attest to its recent activity (Figure A2-2). Most of these features also demonstrate that the fault has been repeatedly active throughout the late Quaternary with essentially the same kinematic motion. The traces beneath San Diego Bay have been imaged by shallow seismic techniques, where several strands of the fault clearly cut Holocene marine sediments (Kennedy and Clarke, 1996), also indicating that the Rose Canyon fault is young and active. Surprisingly, an early (Glover, 1876) artist's rendition of Newtown (present day downtown San Diego) shows the trace of the fault as a scarp and several deflected drainages precisely where recent trenching has determined to be the main traces of the fault (see Figure A2-3), and supports the recency of displacement that has been demonstrated in the trenching studies (Lindvall and Rockwell, 1995; Rockwell, 2010a).

The linearity of the fault trace across hilly topography argues that the fault maintains a steep dip through much of San Diego, except in the Mount Soledad area, where the fault appears to dip to the southwest beneath the uplift. The fault strike in this area is also more westerly, consistent with a restraining bend geometry that has resulted in the uplift of the mount. Marine terraces on the southwest flank of the uplift (Kern, 1977; Kern and Rockwell, 1992), along with the presence of the Linda Vista Formation marine terrace alluvium capping Mount Soledad, attest to the higher rate of uplift of the restraining bend area (0.25 mm/yr) relative to the surrounding coastal plain (0.13 mm/yr) (Kern and Rockwell, 1992), with the background regional uplift attributed to rift-flank uplift from extension in the Gulf (Mueller et al., 2009).

The level of late Quaternary fault activity is indicated by both the relatively large lateral deflections of stream channels that are incised into low marine terraces (Figure A2-4), and by the results of the three-dimensional trenching. These observations suggest a lateral slip rate of about 2 mm/yr during the late Quaternary (Rockwell, 2010a).

SEISMIC CHARACTERISTICS

The expected length of a future rupture on the Rose Canyon fault may be limited by structural controls, such as steps, bends, and changes in strike that may be large enough to terminate dynamic rupture. For the southern termination, the right-step between the Rose Canyon and Descanso faults forms the depression occupied by San Diego Bay (Figure A2-1), and is likely large enough to arrest dynamic slip. This step exceeds 5 km in step-over width (Figure A2-5), which is more than the largest releasing step that has been ruptured through in historical, well-documented strike-slip earthquakes (Wesnousky, 2008). Based on this, the southern termination of future large earthquakes on the Rose Canyon fault is expected to be in San Diego Bay.

For the northern termination, there are several structural features that may play a role, but none are as large as the step across San Diego Bay. The left bend in the Rose Canyon fault that facilitated the uplift of Mt. Soledad is only on the order of a couple kilometers in cross-fault dimension (Figure A2-5) and many historical earthquakes have ruptured through bends and steps of such dimensions (Wesnousky, 2008) (cf. the 1968 Mw6.4 Borrego Mountain earthquake ruptured across the 1.5-2 km wide Ocotillo Badlands with less than a half meter of displacement, Clark, 1972). Thus, the Mt. Soledad bend and uplift is not likely to be large enough to define a rupture segment boundary, especially if the Rose Canyon fault has 3 m of displacement in Rose Creek. Furthermore, it is a continuous surface fault

through the region of this bend based on the geomorphology and extensive local trenching (Lindvall and Rockwell, 1995; Rockwell and Murbach, 1999).

Farther north, the Rose Canyon fault steps to the right (releasing step) near Oceanside, but the dimensions of the step are only on the order of 2-3 km or so (Figure A2-5). This can be a significant barrier to rupture in moderate earthquakes, but is less likely to stop a large dynamic displacement. More significantly, however, the Rose Canyon fault has a more westerly strike to the northwest of this step, and the change in azimuth is on the order of 15 degrees from the average strike of the fault between Oceanside and San Diego Bay. The combination of the releasing step plus a change in fault strike make the Oceanside step a likely termination zone for ruptures, although a through-going rupture cannot be precluded.

The SONGS sits along the coast between Oceanside and the San Joaquin Hills uplift, and there are no major, obvious structural complexities that can be used to segment the Rose Canyon fault along this stretch. However, the San Joaquin Hills may represent uplift associated with a step from the northern termination of the Rose Canyon to the Newport- Inglewood fault zone. Grant et al. (2002) consider the uplift as the consequence of slip on a blind thrust, but likely structurally linked to the Newport- Inglewood fault zone (Grant et al., 1999, 2000). A closely related model is that the Rose Canyon fault bends northward and steps left across the hills to the Newport Inglewood fault, producing uplift by slip on the low-angle accommodation fault. An alternative model is that the San Joaquin uplift is related to a blind thrust system, the Oceanside thrust, that accommodates shortening in the Borderland (Rivero et al., 2000). In any case, the San Joaquin uplift is a structural complexity and may serve to segment the offshore zone of faulting.

An approach to shedding light on this problem, and to better constrain the likely sizes and termination zones for future earthquakes associated with the Rose Canyon and Newport-Inglewood faults, is to assess the current paleoseismic data in terms of whether they support co-seismic rupture of these faults together in the past. Grant and Rockwell (2002) documented the occurrence of a sequence of large earthquakes that ruptured the coastal zone of faults in the past few hundred years, but was pre-historical in age. This sequence involved the onshore Agua Blanca fault in northern Baja California, as well as the onshore Rose Canyon fault in San Diego and the San Joaquin Hills fault beneath Newport Bay, and was succeeded by the 1933 rupture of the Newport- Inglewood fault in Los Angeles Basin (Figure A2-6). Based on radiocarbon dating of the most recent earthquakes on these three faults, this sequence appears to have propagated northward, because rupture of the Agua Blanca fault is apparently the oldest of the events. In actuality, the dates of these three events all overlap to some degree, but there is the appearance that events to the north are younger than those to the south. Furthermore, it is unlikely that an earthquake ruptured both the Agua Blanca- Descanso and Rose Canyon faults simultaneously because of the large step-over at San Diego Bay. Combined with the occurrence of the 1933 event, which is clearly the youngest, the interpretation presented by Grant and Rockwell (2002) seems reasonable. Alternatively, as the most recent event on the Rose Canyon fault overlaps with the interpreted uplift of Newport Bay, it is possible that the entire Rose Canyon fault ruptured in a large earthquake just prior to the Mission period, and that the Newport Bay uplift is a consequence of this event. Because of the inherent problems in precise radiocarbon dating in this time period, this question may be difficult to resolve. Nevertheless, the occurrence of the sequence (or single event) supports the idea that the San Joaquin uplift is structurally tied to the coastal system of strike-slip faults.

There is a clearer difference in timing between Rose Canyon and onshore Newport- Inglewood fault ruptures (Figure A2-6; compiled from Grant et al., 1997; Grant and Rockwell, 2002; Leon, et al., 2009), which argues against the likelihood of a very long rupture. Although the timing is similar, Grant and Rockwell argue that the pre-Mission sequence of ruptures represent multiple events, and likely propagated northward, culminating in the relative small M6.4 1933 Long Beach earthquake. It is noteworthy that the 1933 earthquake is not known to have ruptured the surface, and there were plenty of people around who should have noticed a significant rupture. Grant et al. (1997) use this observation to argue that the Holocene events identified for the Newport-Inglewood fault at Bolsa Chica likely represent larger earthquakes than that which occurred in 1933.

The pre-historic Newport-Inglewood and Compton-Los Alamitos events are nearly indistinguishable in timing (Figure A2-6), considering their large uncertainties. Nevertheless, they both have a similar return period for large earthquakes – those that can be identified by CPT and core correlation techniques, which implies that they are larger than 1933. One could argue that the Compton Los Alamitos and Newport- Inglewood faults ruptured together in the largest earthquakes, suggesting that they are kinematically linked. This may support Wright’s (1991) interpretation of the Compton fault as a high angle oblique splay of the Newport-Inglewood fault. In any case, it is clear that the 1933 earthquake is smaller, and it was not associated with a large event on the Compton structure. Barrows (1974) does, however, document that the area between the Los Alamitos and Newport-Inglewood faults was uplifted in the 1933 earthquake (Figure A2-7), again indicating a structural tie between these structures.

Rose Canyon fault has a very different paleoseismic record of past earthquakes than those faults to the north. The Rose Canyon fault experienced a cluster of events in the early Holocene, followed by a hiatus of several thousand years (Figures A2-6)(Rockwell, 2010a). Although one could argue that the mid-Holocene event documented at Bolsa Chica on the Newport-Inglewood fault could correlate to one of the mid-Holocene Rose Canyon events, it is clear that the others do not, as there are no other recognized events during this cluster at Bolsa Chica. Unfortunately, the San Joaquin Hills record is too short (one event) to assess whether there is a correlation between Rose Canyon events and uplift at Newport Bay. Nevertheless, it appears that the Rose Canyon earthquake history is generally dissimilar to that of the Newport-Inglewood fault, which likely means that these faults do not typically rupture together.

In summary, the Rose Canyon fault is interpreted as a distinct seismic source that does not likely rupture with the Newport-Inglewood fault to the north, nor the Agua Blanca-Descanso fault to the south. If the Oceanside step-over is a barrier to rupture propagation, it would divide the Rose Canyon fault into two roughly similar-length sections: a 65 km segment from San Diego Bay to Oceanside, and a 55 km segment from Oceanside to the San Joaquin Hills. From the short paleoseismic record at Newport Bay, it is not possible to test long-term patterns of recurrence between these two segments. Further, due to the overlap in ages between the most recent ruptures inferred for these two segments (assuming the Newport Bay uplift is associated with a northern Rose Canyon rupture that involved the San Joaquin Hills), one cannot preclude rupture of the entire Rose Canyon fault for a distance of more than 100 km. However, I consider this model a lower likelihood than rupture of individual segments and weight it at 25%, versus 75% for the more segmented rupture behavior.

For PSHA and PTHA seismic source characterization model, I suggest using the maximum slip rate range of 1.1 to 2.5 mm/yr, with the best estimate of 1.5-2.5 mm/yr, with the following weights:

0.5 (0% weight)

- 1.0 (10% weight)
- 1.5 (30% weight)
- 2.0 (40% weight)
- 2.5 (20% weight)
- 3.0 (0% weight)

For calculations that involve lapse time since the most recent event (time-based probabilities), you may want to consider that the Rose Canyon fault apparently behaves in a clustered mode, where the time between events within a cluster is shorter than the average long-term recurrence interval. This can be viewed, in effect, as variations in short term slip rate, with the period between about 10-5 ka having a higher rate than the long term average (Figure A2-8), the rate from 5-0.5 ka being essentially zero, and the current rate somewhat uncertain. Considering that the fault experienced a recent large earthquake after several thousand years of quiescence, and if it is reasonable to assume that we have entered another cluster which reflects a short-term increase in slip rate, then it follows that the time to the next event will be shorter than that inferred from the long-term average. Rockwell (2010a) inferred the intra-cluster recurrence interval to be less than 1 ka, with five events between 9.3 and 5 ka. This yields a recurrence interval of about 900 years within that cluster. If each event was as large as the most recent event, about 3 m, this would suggest a slip rate of more than 3 mm/yr for this interval. Considering that short and long-term fault behavior of faults is somewhat enigmatic and a current topic of debate within the scientific community (see Rockwell, 2010b), I would suggest using the long-term rate with an 80% weight, and consider using an alternative weighting scheme for slip rate (in mm/yr) with a 20% overall weight as follows:

- 0.5 (0% weight)
- 1.0 (10% weight)
- 1.5 (30% weight)
- 2.0 (30% weight)
- 2.5 (20% weight)
- 3.0 (10% weight)

KEY REMAINING UNCERTAINTIES

There are two key uncertainties that need to be resolved. For understanding the short and long-term pattern of earthquakes on the Rose Canyon fault, and their implications for future activity, it is critical to test the cluster model of Rockwell (2010a) by resolving whether there were any surface ruptures between about 5 and 0.5 ka. There was no deposition at the Rose Creek site during this period, and the inference of no ruptures is based on the strength of a soil that is developed across the earlier Holocene fault strands (Rockwell, 2010a), so it is possible that an event was missed or not well-recorded. Paleoseismic investigations in mid-late Holocene sediments across the Rose Canyon fault could resolve

whether other events may have occurred, as well as potentially determine their amount of displacement. This may affect our perception of recurrence and earthquake magnitude along the Rose Canyon Fault.

The other remaining major question relates to the nature of the inferred shortening deformation suggested by Rivero et al. (2000) in the offshore region, and its relationship to the Rose Canyon fault. Geodetic observations clearly see significant right-lateral shear between San Clemente Island and Monument Peak, but there is no observable shortening or extension (figure A2-9). In fact, the right-lateral nature of the Agua Blanca fault in Baja California, along with its westerly strike, could be interpreted that there should be a small amount of continuing extension in the Borderland region (Wetmore et al., 2010 in review). Therefore, the cause of the apparent folding in the offshore Inner Borderland Region (Rivero et al., 2000) remains open to interpretation.

There are other areas where similar patterns of deformation have been observed, and it may prove valuable to assess these areas in terms of their overall structural style and seismic potential. One area that appears to have slip partitioned between strike-slip and convergence is in central California. In this area, the San Andreas fault (at 35 mm/yr) is the undisputed dominant seismic source, both in terms of magnitude and frequency. Nevertheless, a small component of shortening, estimated at no more than 3 mm/yr from geodetic data, is partly expressed as a series of folds and blind thrust faults to the east of the San Andreas fault (Coalinga anticline, Kettleman Hills, etc.: Yerkes, 1990, Wentworth, 1990). In this case, these secondary seismic sources are clearly seismically active, having produced several earthquakes in the M5.5- M6.5 range during the instrumental period, but are subordinate to the San Andreas fault. However, in comparison to the Inner Borderland, the central California example is clearly different because 1) there are clearly-defined folds that overlie blind thrusts; 2) these folds have significant structural relief and fold Holocene terraces; 3) there is a clear geodetic signal to the shortening; 4) there are earthquakes with thrust mechanisms clearly associated with these structures.

In the Inner Borderland Region, the association is not nearly as clear. There is a Miocene detachment surface, above which there has apparently been some folding (Rivero et al., 2000). However, there is no recognizable geodetic signal of shortening, nor is the seismicity clearly associated with this inferred detachment surface. An analogous situation is present in the western Salton Trough along the southern San Jacinto fault zone.

The West Salton Detachment-San Jacinto Example: The West Salton Detachment underlies much of the western Salton Trough east of the Peninsular Ranges from Borrego Valley and to the south to the Mexican Border (Axen and Fletcher, 1998). In this area, the high-angle, right-lateral San Jacinto fault cuts and offsets the West Salton Detachment and is clearly the dominant structure. Of note is the ubiquitous presence of extensive folding in the Borrego Badlands, San Filipe Hills, and Fish Creek Badlands, all of it post-detachment in age and all of it related to the continuing development of the southern San Jacinto fault zone (Dorsey and Janecke, 2002; Lutz et al., 2006).

There are many similarities between the western Salton Trough and the Inner Borderland Region. First, there is young folding above the Miocene-Pliocene detachment system, with the folding in the western Salton Trough being of substantially greater magnitude and significance than the folding in the offshore region. Furthermore, the folding is not only associated with bends in the strike-slip faults, but rather, appears to be more regionally scaled and related to secondary space accommodation above the detachment surface driven by the dominant strike-slip faulting. Second, neither region shows a geodetic signal of convergence, but rather, GPS and InSAR show virtually pure strike slip at the regional scale for

the southern San Jacinto fault zone (see Fialko, 2006). Third, at least one fold grew during the 1987 Superstition Hills earthquake sequence in the western Salton Trough (Klinger and Rockwell, 1989), so there is a demonstrable association between strike-slip faulting and fold growth in this area. These and other similarities warrant a thorough examination and comparison between these two structural domains, in part because the western Salton Trough is well-studied and easily accessible.

RECOMMENDATIONS TOWARD RESOLVING REMAINING UNCERTAINTIES

For the Rose Canyon Fault itself, there are potential paleoseismic study sites to resolve whether the fault sustained displacement between about 5 and 0.5 ka. The sediments within and adjacent to the San Diego River are of the appropriate age, as river aggradation probably ceased about the time sea level rose to its present level at about 5-6 ka, and after that, sedimentation on the flood plain has locally preserved alluvium of various ages in the 0.5 to 5 ka timeframe. One area that may preserve such a record is in Old Town, where the landscape is only minimally altered. One potential site is in a golf course that essentially preserved the original topography; the fault is still expressed as a linear depression. The golf course property is owned by the City of San Diego, although it is currently under lease. Another potential site is close to the Lindvall and Rockwell (1995) trench site where a closed depression (sag) is observed in the 1928 and 1941 aerial photography. This is on private land, so access will likely be an issue. A third general site is in the flood plain of the San Diego River in Mission Valley. The fault is expressed in the 1928 aerial photographs, so the fault location can be determined with some work. The fault location may be better determined with CPT or geophysical means, once it is approximately located by interpretation of the old aerial photography. It may be possible to trench along a street, once the fault is well located.

To assess and understand the significance of the folding above the detachment surface in the offshore region, I also recommend that we thoroughly document the structural styles, rates of folding and faulting, etc. for the analogous Western Salton Trough and compare to that of those observed for the Inner Borderland Region. We need to better understand the relationship between the strike-slip faulting and the folding in the Borderland, and the western Salton Trough is far more open to study and analysis because it is sub-aerial and easily accessible. In the southern San Jacinto fault zone, we can better understand how, and when, the folding occurred, and how it relates to the dominant strike-slip faulting, perhaps even to individual events. We should also reanalyze the geodetic signals of these two areas for a component of convergence and test whether a small shortening component can be precluded or accepted.

REFERENCES

- Axen, G. J., and Fletcher, J. M. 1998. Late Miocene-Pleistocene extensional faulting, northern Gulf of California, Mexico and Salton Trough, California. *Int. Geol. Rev.* 40:217–244.
- Barrows, A.G., 1974, A review of the geology and earthquake history of the Newport- Inglewood structural zone, southern California: California Division of Mines and Geology Special Report 114, 115 p.
- Clark, M.M., 1972, Surface Rupture Along the Coyote Creek Fault, USGS Professional Papers, 787, 55-86.
- Dorsey, R. J., and Janecke, S. U. 2002. Late Miocene to Pleistocene West Salton detachment fault and basin evolution, southern California: new insights. *Geol. Soc. Am. Abstr. Program* 34:248.
- Fialko, Y., 2006, Interseismic strain accumulation and the earthquake potential on the southern San Andreas fault system, *Nature* v. 441, 968- 971.10.1038/nature04797.
- Glover, E.S., 1876, Bird's Eye View of San Diego, California. Map published by Schneider and Kueppers, San Diego.
- Grant, L.B., Waggoner, J.T., Rockwell, T.K., and von Stein, C., 1997, Paleoseismicity of the north branch of the Newport-Inglewood fault in Huntington Beach, California: *Bulletin of the Seismological Society of America*, v. 87, pp. 277-293.
- Grant, L. B., K. J. Mueller, E. M. Gath, H. Cheng, R. L. Edwards, R. Munro and G. L. Kennedy, Late Quaternary Uplift and Earthquake Potential of the San Joaquin Hills, southern Los Angeles Basin, California, *Geology*, v. 27, no. 11, p. 1031-1034, 1999.
- Grant, L. B. L. J. Ballenger, and E. E. Runnerstrom. Coastal uplift of the San Joaquin Hills, Southern Los Angeles basin, California, by a large earthquake since 1635 A.D. *Bulletin Seismological Society of America*, v. 92, no. 2, p.590-599, 2002.
- Grant L. B. and Rockwell, T. K., 2002, A northward propagating earthquake sequence in coastal southern California?: *Seismological Research Letters*, v. 73, no. 4, p. 461-469.
- Kennedy, M. P. and Clarke, S.H., 1996, Analysis of late Quaternary faulting in San Diego Bay and hazard to the Coronado Bridge, prepared for Caltrans.
- Kern, J.P., 1977, Origin and history of upper Pleistocene marine terraces, San Diego, California, *Geological Society of America Bulletin*, v. 88, p. 1553-1566.
- Kern, J.P. and Rockwell, T.K., 1992, Chronology and deformation of Quaternary marine shorelines, San Diego County, California: in *Quaternary Coasts of the United States: Marine and Lacustrine Systems: Society of Economic Paleontologists and Mineralogists Special Publication.No. 48*, p. 377-382.
- Klinger, R.E. and Rockwell, T.K., 1989, Flexural-slip folding along the eastern Elmore Ranch fault in the Superstition Hills earthquake sequence of November 1987: *Bulletin of the Seismological Society of America*, v. 79, no. 2, p. 297-303.

**SAN ONOFRE NUCLEAR GENERATING STATION
SEISMIC HAZARD ASSESSMENT PROGRAM
2010 PROBABILISTIC SEISMIC HAZARD ANALYSIS REPORT**

Leon, L.A., Dolan, J.F., Shaw, J.H., and Pratt, T.L., 2009, Evidence for large Holocene earthquakes on the Compton-Los Alamitos fault, Los Angeles, California. *Journal of Geophysical Research*, v. 114, B12305, doi:10.1029/2008JB006129.

Lindvall, S. and Rockwell, T.K., 1995, Holocene activity of the Rose Canyon fault, San Diego, California: *Journal of Geophysical Research*, v. 100, no. B12, p. 24121- 24132.

Lutz, A. T.; Dorsey, R. J.; Housen, B. A.; and Janecke, S.U. 2006. Stratigraphic record of Pleistocene faulting and basin evolution in the Borrego Badlands, San Jacinto fault zone, southern California. *Geol. Soc. Am. Bull.* 118:1377–1397.

Mueller, K., Kier, G., Rockwell, T. and Jones, C. 2009, Quaternary Rift-Flank Uplift of the Peninsular Ranges in Baja and Southern California by Removal of Mantle Lithosphere. *Tectonics*, v. 28, 17 p. doi:10.1029/207TC002227.

Rivero, C., Shaw, J.H., and Mueller, K.J., 2000, Oceanside and Thirty Mile Bank blind thrusts: Implications for earthquake hazards in coastal southern California. *Geology*, v 28, p. 891-894.

Rockwell, T., 2010a, The Rose Canyon Fault Zone in San Diego; Proceeding of Fifth International Conference on Recent Advances in Geotechnical Earthquake Engineering and Soil Dynamics and Symposium in Honor of Professor I.M. Idriss; Paper No. EQ 5, 9pgs.

Rockwell, T., 2010b, The non-regularity of earthquake recurrence in California: Lessons from long paleoseismic records from the San Andreas and San Jacinto faults in southern California, and the north Anatolian fault in turkey, Proceeding of Fifth International Conference on Recent Advances in Geotechnical Earthquake Engineering and Soil Dynamics and Symposium in Honor of Professor I.M. Idriss; Paper No. EQ 5, 9pgs.

Rockwell, T.K. and Murbach, M., 1999, Holocene earthquake history of the Rose Canyon fault zone. USGS Final Technical Report for Grant No. 1434-95-G-2613, 36 p + App.

Treiman, J., 1993, The Rose Canyon fault zone, southern California, California Div. of Mines and Geology, Open File Report 93-02, 45 p.

USGS, 2009, Personal Communication.

Wentworth, C.M., 1990, Structure of the Coalinga region and thrust origin of the earthquake, in The Coalinga, California earthquake of May 2, 1983. U.S. Geological Survey Professional Paper 1487, p. 41-68.

Wetmore et al., 2010 in review, The Agua Blanca Fault in Baja California, submitted to *Tectonics*.

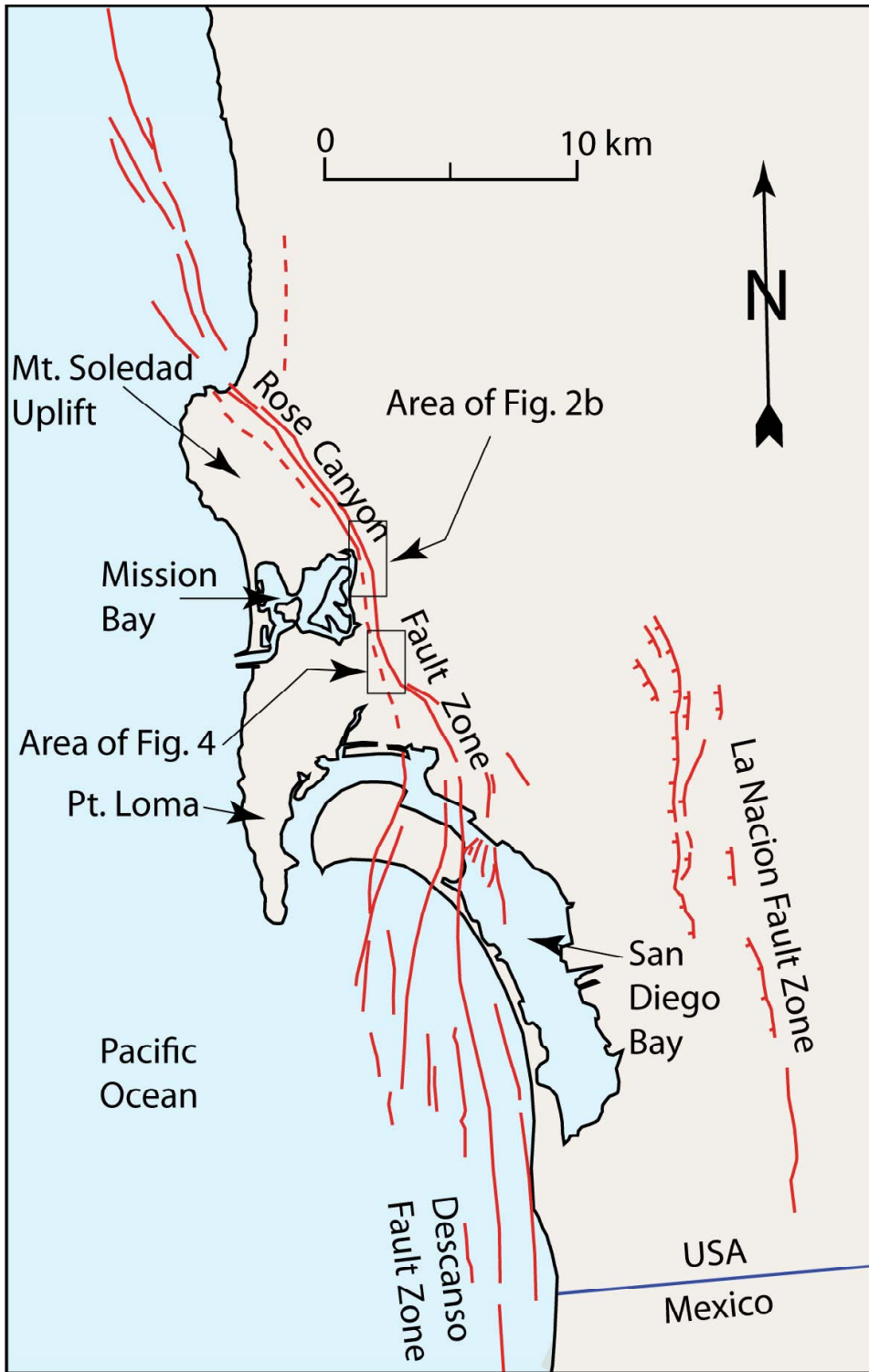
Wesnousky, S.G., 2008, Displacement and geometrical characteristics of earthquake surface ruptures: Issues and implications for seismic-hazard analysis and the process of earthquake rupture. *Bull. Seismological Society of America*, v. 98, p. 1609-1632.

Wright, T.L., 1991, Structural geology and tectonic evolution of the Los Angeles basin, California. In *Am. Assoc. Petroleum Geologists Memoir* 52, p. 35-134.

**SAN ONOFRE NUCLEAR GENERATING STATION
SEISMIC HAZARD ASSESSMENT PROGRAM
2010 PROBABILISTIC SEISMIC HAZARD ANALYSIS REPORT**

Yerkes, R.F., 1990, Tectonic setting, in The Coalinga, California earthquake of May 2, 1983. U.S. Geological Survey Professional Paper 1487, p. 13-22.





MAP OF THE MAIN ELEMENTS OF
THE ROSE CANYON FAULT IN SAN DIEGO

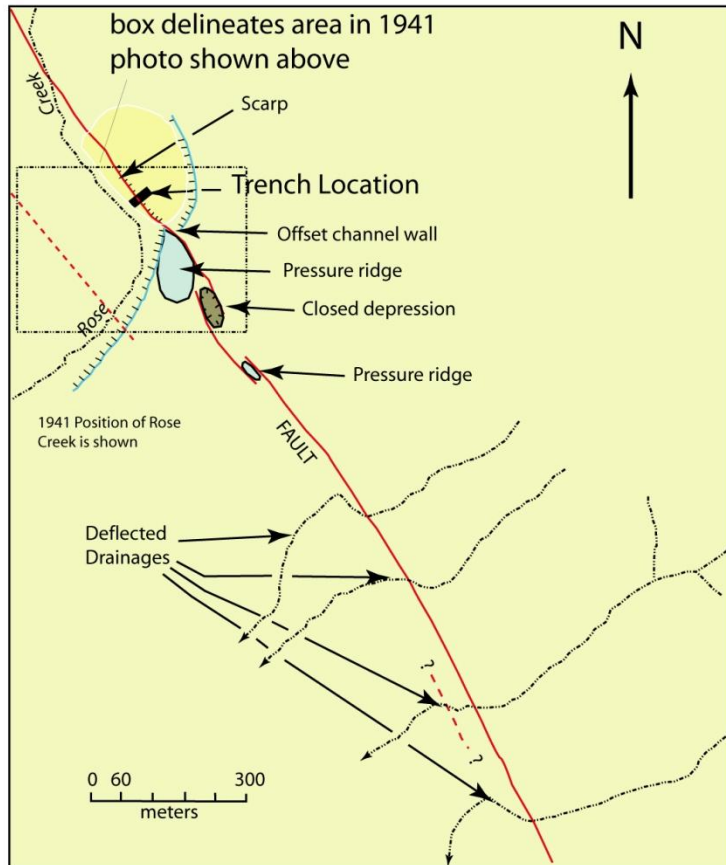
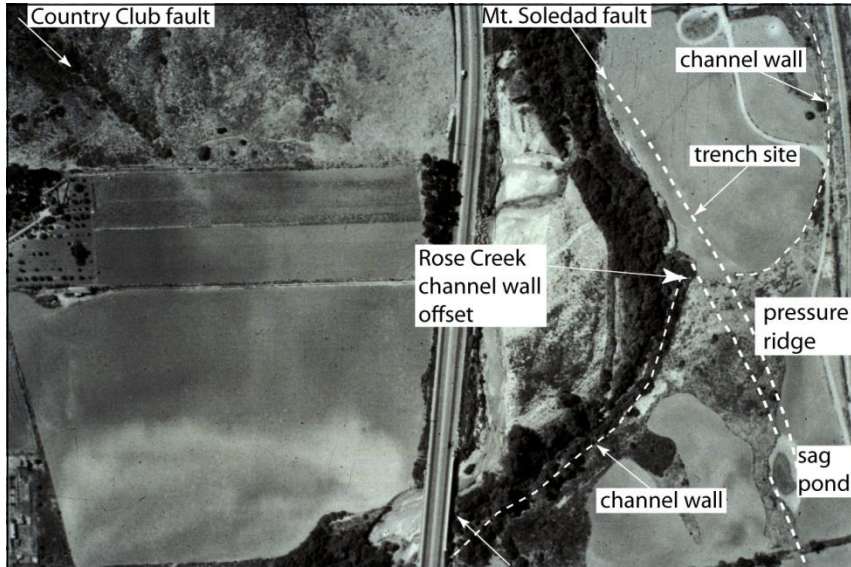
FIGURE
A2-1



GeoPentech
Geotechnical & Geoscience Consultants

By Rockwell (2010)

SAN ONOFRE NUCLEAR GENERATING STATION
SEISMIC HAZARD ASSESSMENT PROGRAM



NOTE: Annotated air photo (upper) shows detail of area in the box in the lower diagram (from Lindvall and Rockwell, 1995, Rockwell, 2010).



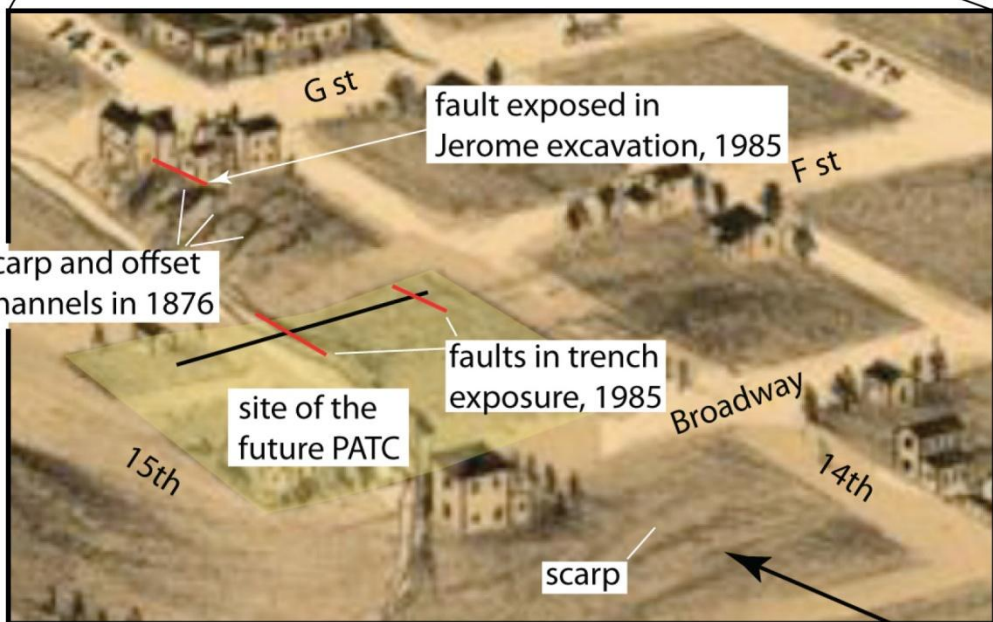
GeoPentech
Geotechnical & Geoscience Consultants

By Rockwell (2010)

**INTERPRETIVE MAP OF TECTONIC GEOMORPHIC
FEATURES IN THE ROSE CREEK AREA**

**FIGURE
A2-2**

**SAN ONOFRE NUCLEAR GENERATING STATION
SEISMIC HAZARD ASSESSMENT PROGRAM**



NOTE: Remarkably, the artist's eye picked out and drew scarps and deflected drainages along the Rose Canyon fault: the location of the fault in this area was determined by excavations in 1985 for the new Police headquarters building (PATC) and for a foundation excavation for a Jerome's warehouse.



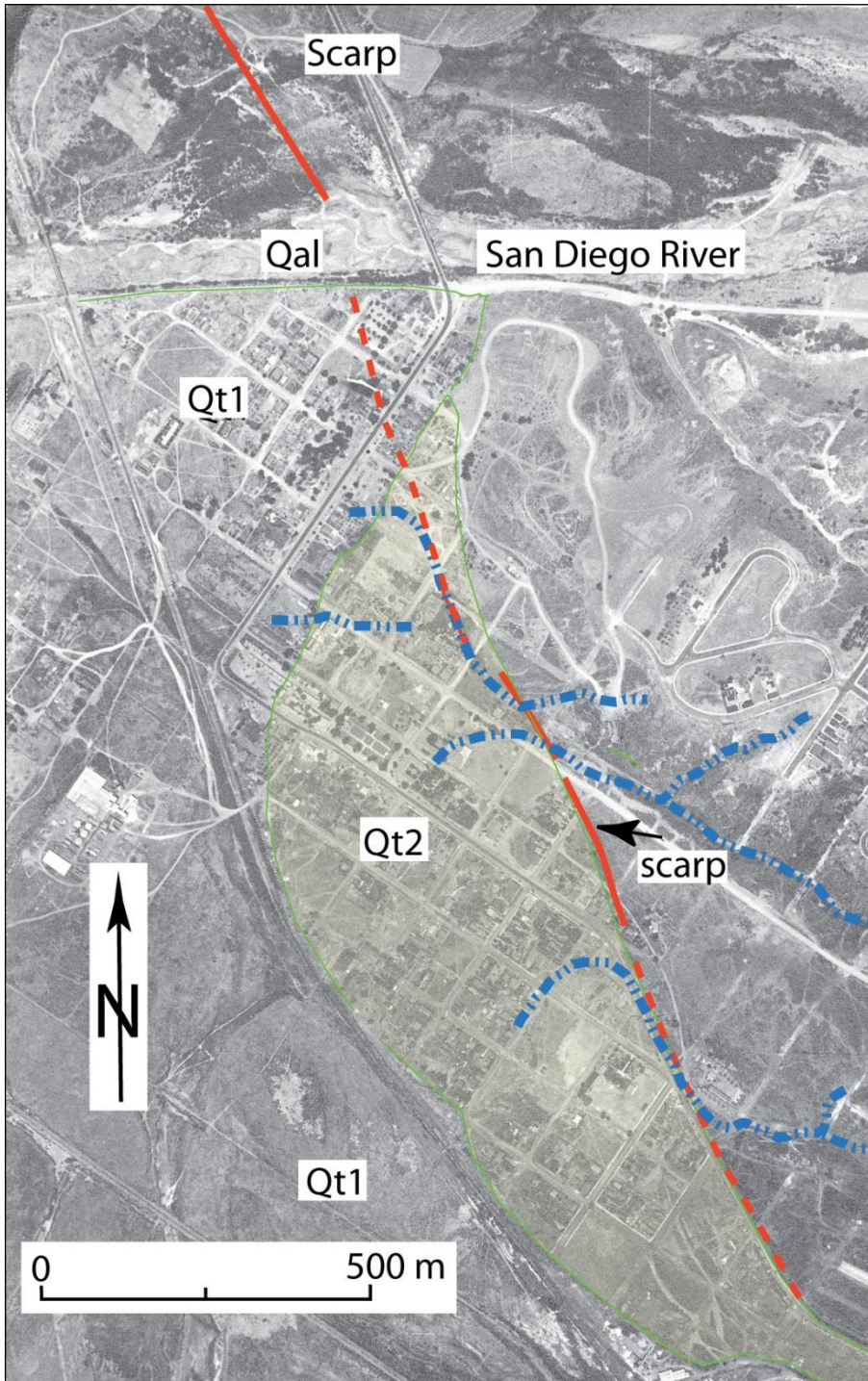
GeoPentech
Geotechnical & Geoscience Consultants

By Rockwell (2010)

ANNOTATED ARTIST'S RENDITION
OF DOWNTOWN SAN DIEGO IN 1876

FIGURE
A2-3

SAN ONOFRE NUCLEAR GENERATING STATION
SEISMIC HAZARD ASSESSMENT PROGRAM



NOTE: Note the deflected channels incised into the Qt2 surface, which is interpreted to be last the interglacial terrace based on its elevation (from Rockwell, 2010).



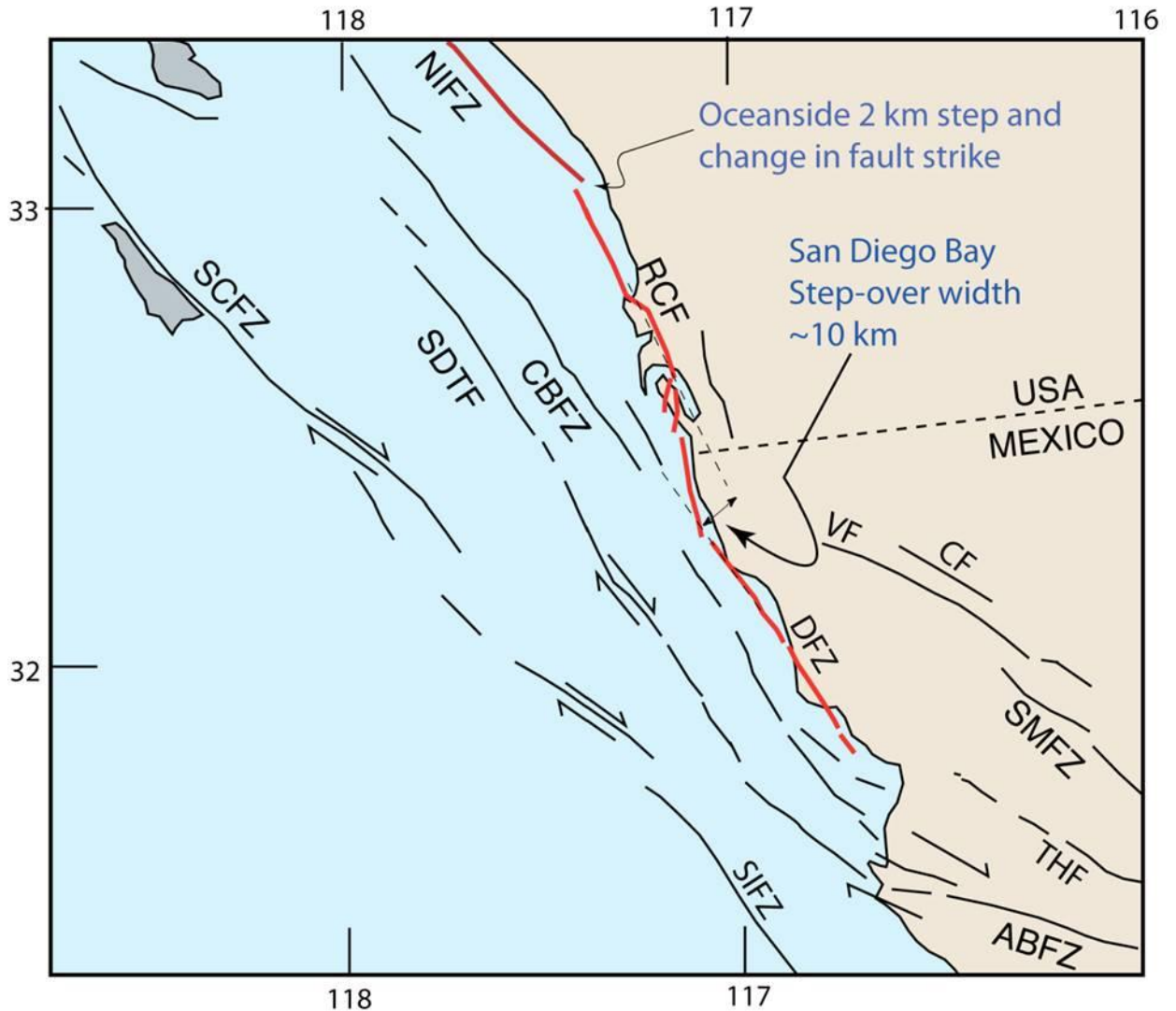
GeoPentech
Geotechnical & Geoscience Consultants

By Rockwell (2010)

**INTERPRETED 1941 AERIAL PHOTOGRAPHY
OF THE OLD TOWN AREA OF SAN DIEGO**

**FIGURE
A2-4**

**SAN ONOFRE NUCLEAR GENERATING STATION
SEISMIC HAZARD ASSESSMENT PROGRAM**



NOTE: Also shown is the smaller step at Oceanside with the change in fault strike. SAFZ - San Andreas fault zone; SJFZ - San Jacinto fault zone; IF - Imperial fault; CPF - Cerro Prieto fault; LSF - Laguna Salada fault; NIFZ - Newport- Inglewood fault zone; RCF - Rose Canyon fault; CF - Calabazas fault; VF - Vallecitos fault; SMFZ - San Miguel fault zone; THF - Tres Hermanes fault; ABFZ - Agua Blanca fault zone; CBFZ - Coronado Bank fault zone; DFZ - Descanso fault zone; SDTF - San Diego Trough fault; SCFZ - San Clemente fault zone; SIFZ - San Isidro fault zone.



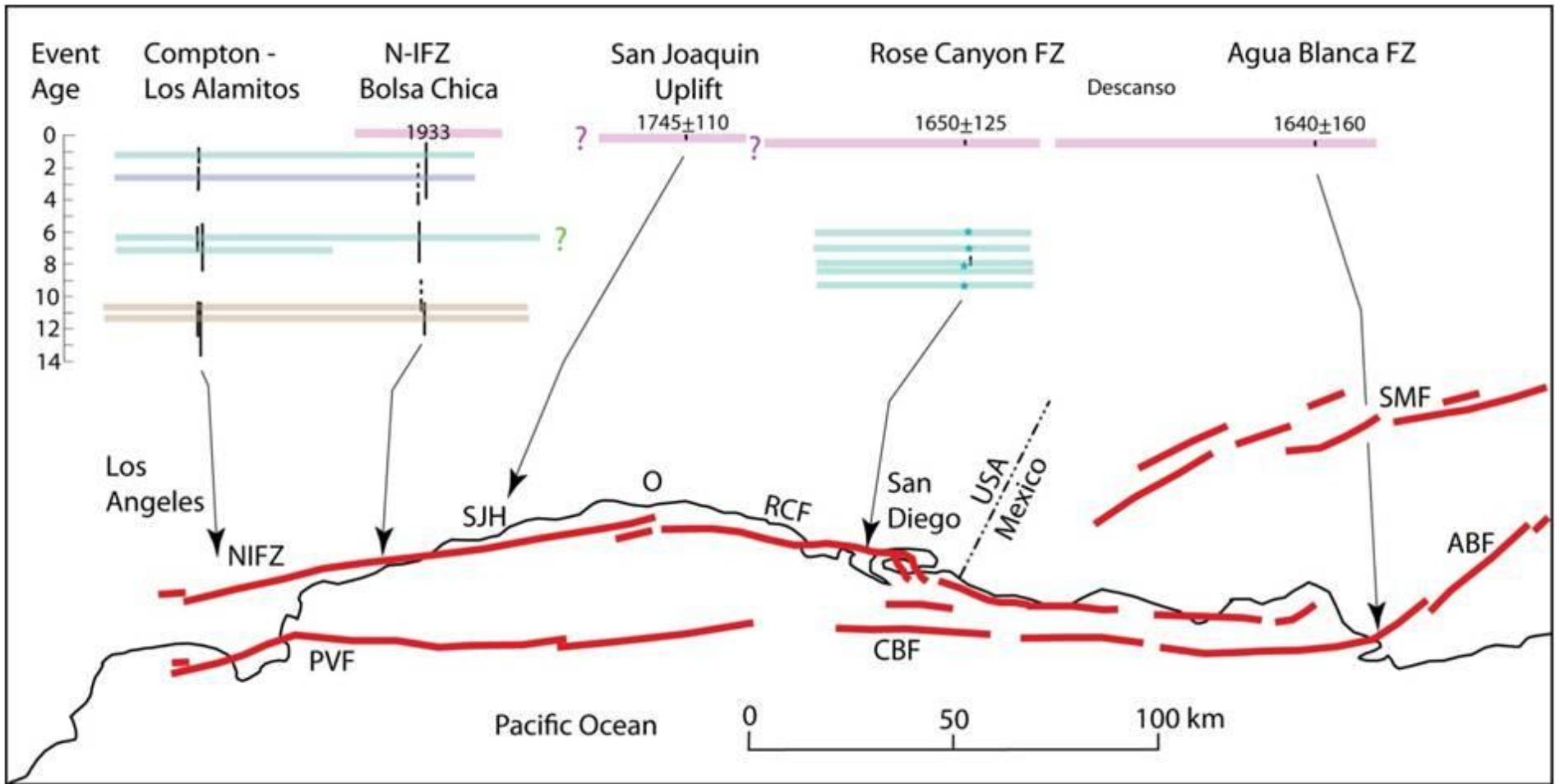
GeoPentech
Geotechnical & Geoscience Consultants

By Rockwell (2010)

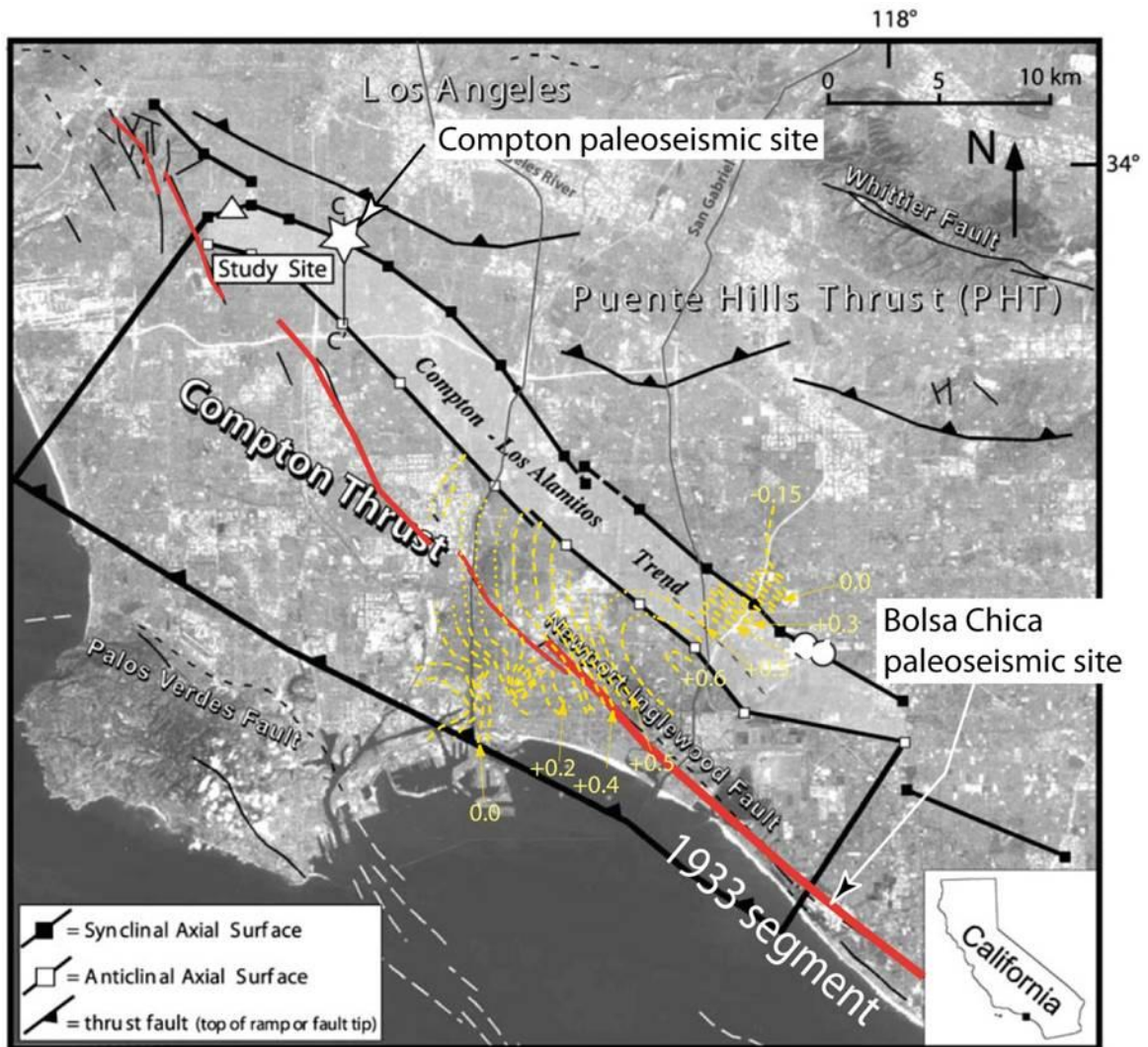
MAP SHOWING HOW STEP-OVER WIDTH WAS MEASURED FOR THE SAN DIGEO BAY STEP

FIGURE A2-5

SAN ONOFRE NUCLEAR GENERATING STATION
SEISMIC HAZARD ASSESSMENT PROGRAM



NOTE: Results from paleoseismic studies for the Agua Blanca, Rose Canyon, San Joaquin Hills, Newport-Inglewood, and Compton faults (from Grant and Rockwell, 2002; Grant et al., 1997, Leon et al., 2009).



NOTE: Location figure from Leon et al. (2009), showing their Compton paleoseismic site. The bolded red line is the inferred segment that ruptured in 1933 (Barrows, 1974), along with the area that sustained uplift in the 1933 earthquake, based on leveling data (Barrows, 1974). Maximum uplift was documented as more than 60 cm, with the locus between the Newport-Inglewood and Los Alamitos structures, supporting Wright's (1991) interpretation that the Compton-Los Alamitos trend is deformation associated with an oblique, high-angle fault.



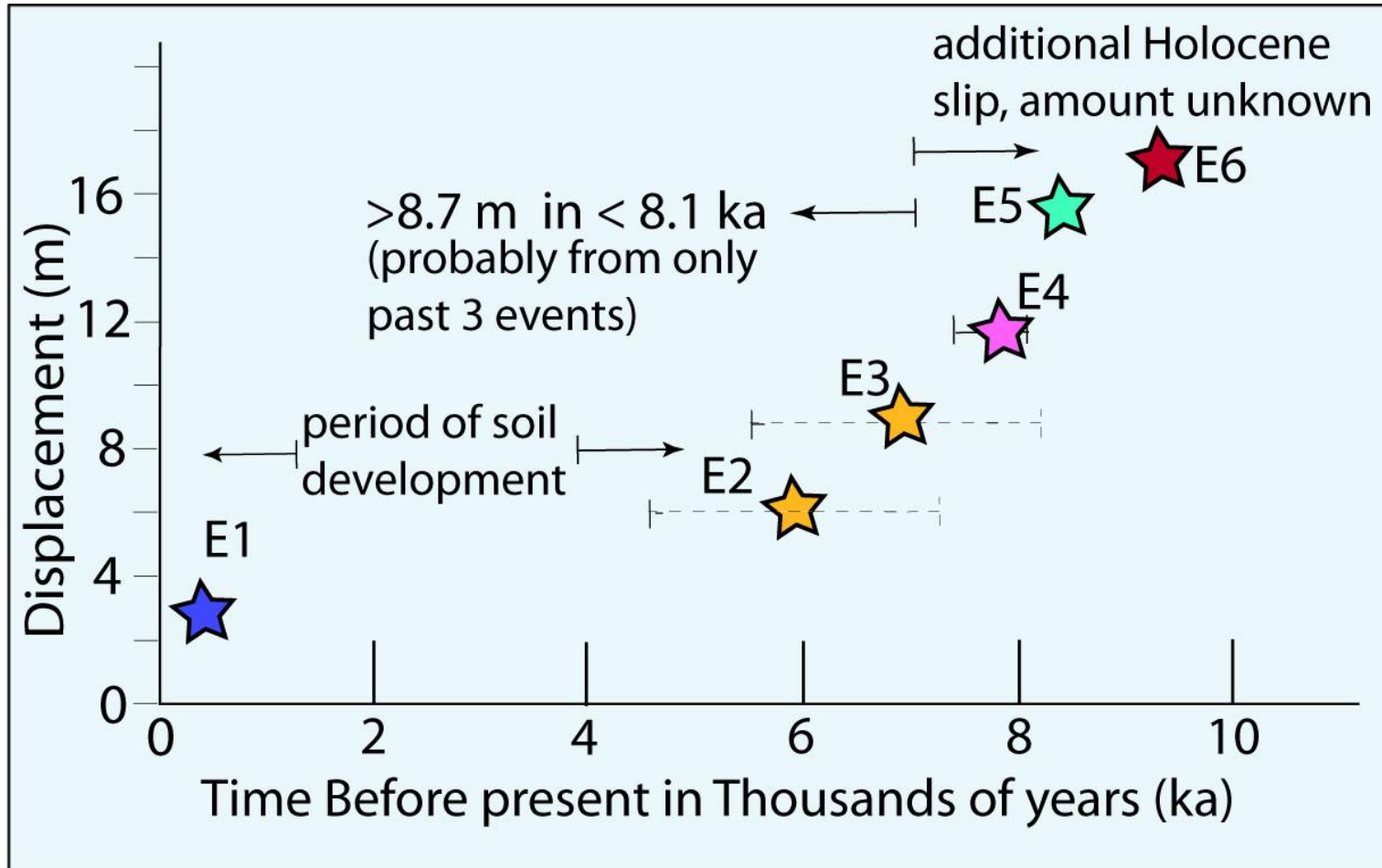
GeoPentech
Geotechnical & Geoscience Consultants

By Rockwell (2010)

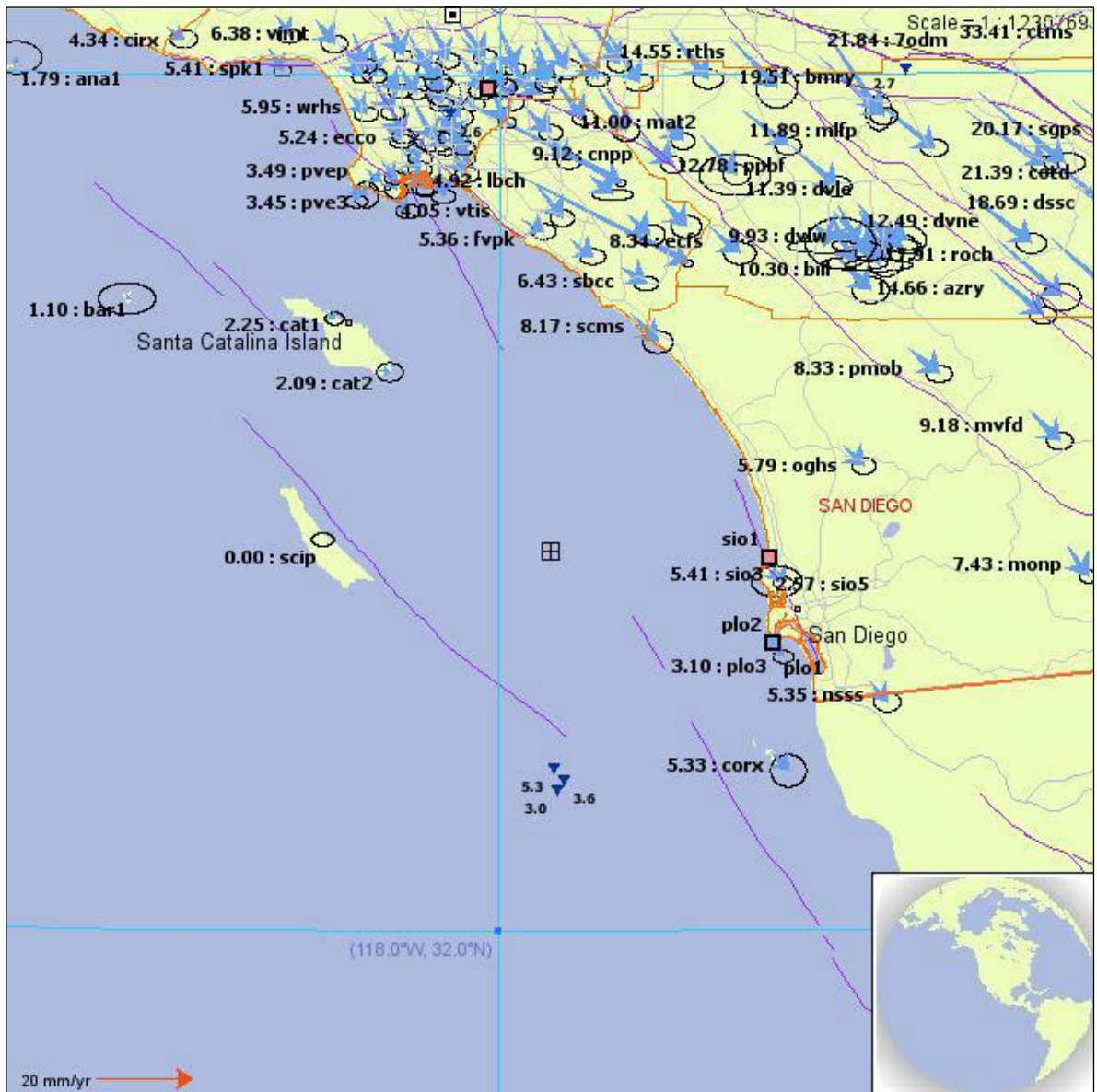
LOCATION FIGURE FROM LEON ET AL. (2009)

FIGURE
A2-7

SAN ONOFRE NUCLEAR GENERATING STATION
SEISMIC HAZARD ASSESSMENT PROGRAM



NOTE: Timing of surface ruptures at Rose Creek, assuming that the strong soil development across the early Holocene fault splays accurately represents a lack of activity for several thousand years (from Rockwell, 2010a).



NOTE: GPS velocity field of the southern California Borderland, plotted with San Clemente Island as the reference frame (plotted in 2005 from the SCIGN web page).

APPENDIX A – ATTACHMENT A-3

**SEISMIC SOURCE CHARACTERISTICS OF
INNER CALIFORNIA BORDERLAND'S BLIND THRUST FAULT SYSTEMS**

By

Dr. John Shaw and Dr. Andreas Plesch

Department of Earth and Planetary Sciences Harvard University, Cambridge, MA

INTRODUCTION

The following document has been prepared at the request of Southern California Edison (SCE) in consultation with technical members of their Seismic Hazard Assessment Program (SHAP).

Active thrust faults have long been known to exist in southern California, particularly in the Transverse Range Province. Awareness of the seismic risk associated with these thrust faults was heightened by the 1971 San Fernando (M_w 6.6) Earthquake, which resulted from slip on the San Fernando segment of the Sierra Madre Thrust Fault System; slip that ruptured the ground surface. Later, the 1987 Whittier Narrows (M_L 5.9) and the 1994 Northridge (M_w 6.7) earthquakes demonstrated the seismic hazards posed by these 'blind' thrust faults; slip that does not rupture the ground surface. The lack of surface ruptures on 'blind' thrust faults hinders our ability to locate them and assess their level of seismic activity.

The reverse/thrust focal mechanism solution tied to the offshore 1986 Oceanside (M_L 5.3) Earthquake demonstrated that active blind thrust faults also exist in southern California's Inner Continental Borderland. This offshore earthquake, combined with our extensive research of hundreds of proprietary oil industry marine geophysical seismic reflection survey lines, lead us to infer the presence of two distinct, active thrust fault systems located offshore of southern Orange County and San Diego County (Rivero et.al., 2000). As shown on Figure A3-1, the Oceanside Blind Thrust (OBT) extends at least from Laguna Beach to the Mexican border and may dip under the shoreline. The smaller Thirty-mile Bank Blind Thrust (TMBT) lies to the west, farther offshore.

Following is a brief discussion of our current understanding of the seismic source characteristic of the OBT and the TMBT developed since Rivero et.al. (2000). This briefing also summaries our current understanding of the relationship between the OBT and the TMBT with other thrust, reverse, normal, and strike-slip faults in southern California's Inner Continental Borderland. Most of what is presented herein is derived from what has been described in Rivero (2004) and Rivero and Shaw (in press).

Specifically, in this briefing we summarize:

- 1) Constraints on the location of the OBT and TMBT and our assessment of their level of seismic activity;
- 2) Our current understanding and weightings of the seismic characteristics of these two fault systems;

**SAN ONOFRE NUCLEAR GENERATING STATION
SEISMIC HAZARD ASSESSMENT PROGRAM
2010 PROBABILISTIC SEISMIC HAZARD ANALYSIS REPORT**

- 3) The logic tree developed to facilitate incorporating, particularly the OBT fault systems into SCE's Probabilistic Seismic Hazard Assessment (PSHA) and Probabilistic Tsunami Hazard Assessment (PTHA) updates for the San Onofre Nuclear Generating Station (SONGS);
- 4) The key remaining uncertainties regarding each fault's seismic source characteristics; and
- 5) Our recommendations for future efforts to resolve these key remaining uncertainties. A list of the references flagged herein is included at the end of this briefing document.

PRESENCE AND LEVEL OF ACTIVITY

In Rivero (2004) and Rivero and Shaw (in press) we supplemented the information provided in Rivero et.al., (2000) with more details on the various data supporting the presence and activity of the OBT and TMBT and their connections with the offshore high-angle, strike slip faults; the latter including the Newport-Inglewood (NI), Rose Canyon (RC), and San Diego Trough (SDT) faults.

These data include:

- a) High-resolution seismic reflection data that image the OBT and TMBT. These faults are defined by deep, shallow dipping, seismic reflections off the coast of southern California underlying folded and faulted sediments. The youngest of these sediments are inferred to be at least Plio-Pleistocene in age (some apparently displacing the sea floor).
- b) Balanced and restored cross sections that document significant contraction or shortening on these structures since the Pliocene (such as the ~2.2 to 2.7 km across the OBT within the last ~1.8 – 2.4 million years).
- c) Earthquake epicenter/hypocenter/focal mechanisms, particularly the Oceanside 1986 M_L 5.3 event, which occurred between San Clemente Island and Oceanside, CA and ruptured the TMBT. In addition, the 1986 Coronado Bank earthquake events, max M_L 3.7, which occurred offshore of Point Loma in August 1986 (Astiz and Shearer, 2000), were incorporated in our analysis;
- d) Elevated marine terraces along the Orange/San Diego County's shoreline; and
- e) GPS data from the SCEC Crustal Motion Map that Kier and Mueller (1999) used to calculate the components of motion perpendicular to the offshore thrust fault traces. Rivero 2005 used the maximum of these station values, minus the slip rate derived for the OBT, to bracket the slip rate on the Thirty-mile Bank fault. Our sense is that these geodetic data are poorly constrained, largely due to the lack of offshore data coverage. Thus, there is a large uncertainty associated with this rate determination, but at present we simply lack another means to estimate this rate.

SEISMIC CHARACTERISTICS

Figure A3-1 provides a map of the OBT and TMBT and their associated hanging wall and footwall subsidiary faults, as modified from Rivero (2004). Also modified from Rivero (2004), Figure A3-2 summarizes the various rupture models considered for these faults. Figure A3-3 provides a more simplified version of the fault map presented on Figure A3-1. This more simplified map was used to obtain the representative three dimensional coordinates for the OBT, TMBT and their associated splay faults relative to the location of the SONGS for input into the PSHA program (Abrahamson, 2010).

**SAN ONOFRE NUCLEAR GENERATING STATION
SEISMIC HAZARD ASSESSMENT PROGRAM
2010 PROBABILISTIC SEISMIC HAZARD ANALYSIS REPORT**

The table presented in Figure A3-4 provides a complete listing of our current estimates of the OBT's and TMBT's seismic source characteristics. In addition, we provide seismic source characteristics of other thrust, reverse, normal, and strike-slip faults in the region that may rupture in conjunction with the OBT and TMBT Fault Systems. Each row of the table represents different individual or multi-segment combinations of plausible rupture scenarios, keyed to the schematic drawings of the four alternative rupture models presented in Figure A3-2.

The rupture area (km²) for each plausible rupture scenario listed in Figures A3-3 and A3-4 was estimated based on the 3-D mapping of the fault in the SCEC Community Fault Model that we have developed (Plesch et al., 2007), assuming a seismogenic depth > 5 km and <17 km. The resulting maximum magnitude earthquake was then calculated using the rupture area versus magnitude relationships developed by Wells and Coppersmith (1994).

The slip rate was estimated for the OBT based on measures of fault offsets and uplift using the marine geophysical seismic reflection survey data and estimates of the ages of the deformed geologic formations. Using the estimated slip rates we then calculated recurrence intervals of the maximum magnitude earthquake for each particular rupture scenario using Wells & Coppersmith (1994) and Shaw and Suppe (1996).

The slip rate for the TMBT was estimated from limited GPS data, as discussed above. We have no constraints on the slip rate of the SDT fault, although it appears to be active based on offsets of near seafloor horizons.

The slip rate on the Carlsbad Fault was estimated by Rivero (2004) based on a range of dip-slip values (0.4 to 0.6 km) using two alternative structural models. The rates are derived using maximum and minimum ages (2.4 and 1.8 mya, respectively) for the initiation of faulting and folding, as defined by patterns of syntectonic (growth) sediments.

Slip rate estimates for the offshore extensions of the NI and RC right-lateral strike-slip faults were based on slip rates assigned to the on-shore traces of these faults from CGS (2002).

LOGIC TREE FOR PSHA/PTHA

Our sense is that these alternative rupture models represent a range of possible scenarios. In reality, however, some may not occur. If more than 1 of these alternatives does occur (which seems plausible), it implies that various fault segment rupture in different types of earthquakes. Thus, the alternatives attempt to capture both epistemic and aleatory uncertainty.

The first step in utilizing the above seismic source characterization of the OBT, TMBT and related subsidiary faults in the SONGS PSHA involved the preparation of the logic tree presented on Figure A3-5. This logic tree was used to accommodate both the epistemic and aleatory uncertainty in the seismic source characteristics (SSC) of the various alternative rupture models. A digital file of this logic tree is also provided in the attached CD.

In terms of our confidence in the reality of the various branches of the logic tree presented on Figure A3-5, we feel it is acceptable to apply equal weights to accommodate the epistemic uncertainty in both model 3 and 4, and a reduced weight for model 2. Although this is a subjective assessment, we would suggest that model 2 should be weighted substantially lower than model 3 or 4 (by a factor 4 or more).

Our reasoning for this weighting is that no viable structural model has been presented to explain the observed slip on the Oceanside thrust is driven by motion on the strike-slip faults. Therefore on a percentage basis, in terms of our best guess, something like 45% for model 3, 45% for model 4, and 10% for model 2, would be a reasonable fit.

We recognize that others believe that right-lateral strike slip faults (model 1) dominate the tectonics off-shore of Orange and San Diego Counties. However, based on the currently available data, we would assign a weight of '0' to rupture model 1 on Figure A3-5. As we stated above, rupture model 1 is not kinematically compatible with the large amount of displacement we document on the OBT Fault. Thus, we believe that the seismogenic potential of the strike-slip faults is represented most effectively in models 2, 3, or 4.

Our percentage weightings applied to the alternative linkage hypotheses for both single and complex strike-slip and thrust earthquake sources in rupture models 3 and 4, are also shown on Figure A3-5. These best guess percentages also reflect on the current epistemic uncertainty of the existing data regarding the connection of the various possible rupture linkages within a seismogenic depth > 5 km and <17 km.

Based on the available data and interpretations there are 67 combinations of fault rupture segments as shown on Figure A3-5. Those branches of the logic tree that reflect the "either/or" epistemic uncertainty of the data are highlight with blue colored lines. The "sometime this way/ sometimes that way" aleatory uncertainty in the data is highlighted in the logic tree by orange line boxes.

Model 1 (0% weighting) focuses the remaining portion of this Appendix on the remaining three OBT models. The possibility of Model 1 as a likely seismic source is discussed in more detail in the other subsections of Appendix A.

Model 2 (10% weighting) reflects two separate alternative seismic sources, i.e., the high angle, strike-slip NI and RC faults. Either these two sources is reflected as 'sometimes' rupturing only on a single segment and 'sometimes' rupturing on multisegments, both onshore and offshore. Model 2 also accommodates the aleatory possibility that the OBT will rupture as a southwest vergent subsidiary fault off of either the NI or the RC faults' rupture. Using the magnitude and slip rate calculations listed in Figure A3-4, the resulting earthquake recurrence was calculated using the Wells and Coppersmith, (1994) Maximum Magnitude recurrence models.

Model 3 (45% weighting) reflects three separate alternative seismic sources, i.e., the onshore/near shore segments of the NI and RC strike-slip faults and the OBT. The OBT has two epistemic branches reflecting the uncertainty as to its extent on-shore to the north of Dana Point and under the San Joaquin Hills. This uncertainty impacts the source area/maximum magnitude calculation, but otherwise the make-up of the logic tree is the same for the branch "North of Dana Point" as is for the branch "South of Dana Point". Using the "South of Dana Point" branch as an example for Model 3, the 4 "linkage" options, i.e., 3a, 3b₁, 3b₂, and 3c and their corresponding epistemic weightings are considered. Then under each of these four linkage alternatives, the single and multiple thrust fault/hanging and footwall subsidiary fault aleatory randomness is accommodated. Then, as was explained in the Model 2 discussion, for each of these rupture models the corresponding slip rates and recurrence calculations are provided.

Model 4 (45% weighting) reflects a similar logic three as Model 3, but with fewer branches to reflect the lack of a footwall faults in Model 4 in comparison with Model 3. However, two differences exist between Model 3 and Model 4 rupture scenarios. The first of these differences is reflected by “linkage 4b” were no seismogenic links exist between the high-angle strike-slip fault in the hanging wall above the OBT because of its depth below the seismic zone (> 17 km). In this situation the hanging wall, high angle, strike-slip fault ruptures as an independent source in addition to the thrust fault source. The second Model 4 versus Model 3 variation was to accommodate the presence of the Carlsbad Thrust Fault in the hanging wall above the OBT. The Carlsbad fault rupture scenario was not part of Model 3 because it presence only in the hanging wall was clearly supported by the marine seismic reflection data, thus only fitting Model 4.

KEY REMAINING UNCERTAINTIES

The key uncertainties associated with representing these potential seismic sources in the SONGS’s PSHA result from the lack of good constraints on the fault slip rates and the inability to distinguish between the several single and multi-segment rupture scenarios that are considered. Specifically, it is unclear whether the shallow dipping thrust faults (such as the OBT) are the primary seismic source faults, with the steeply dipping, right-lateral, strike-slip faults, such as the NI or the RC faults, being subsidiary, or whether the steep, strike-slip faults are the primary seismic sources, and the thrust faults are subsidiary.

Unfortunately this uncertainty continues to exist. The TMBT fault is locally imaged in the seismic reflection to the east of its intersection of the San Diego Trough strike-slip fault. This, combined with the location and focal mechanism of the 1986 Oceanside earthquake, imply that the TMBT is a continuous, active structure. This favors models 3 and 4. None of the seismic reflection profiles we examined, however, clearly imaged subsurface conditions at the depths and locations necessary to resolve the critical interactions of the OBT and NI-RC system. The OBT is not imaged in these locations because it juxtaposes basement on top of basement rocks. Thus, no significant impedance boundary exists, and the fault cannot be imaged by the seismic data.

Regarding fault activity and slip rates, the TMBT is clearly active based on the 1986 Oceanside earthquake. However, its recent (Holocene) slip rate is largely unconstrained, as is the slip rate for the San Diego Trough strike-slip fault. We simply lack the ability to measure direct fault offsets and/or to have constraints on the ages of offset horizons given the lack of well data in this area. The evidences for activity of the OBT are more indirect. Perhaps the best constrains on recent activity of the OBT come from folded and offset horizons at or near the seafloor. However, lacking direct age control for these young sediments limits our ability to constrain how recently the fault has rupture and its slip rate. Association of the OBT and the San Joaquin Hills thrust, combined with the patterns of uplifted coastal marine terraces, further support fault activity.

RECOMMENDATIONS TOWARDS RESOLVING REMAINING UNCERTAINTIES

At the depths and locations where data is necessary to resolve the uncertainty discussed above regarding the intersection between the NI/RC and the OBT, the faults are within the basement rocks and the velocity contrast/acoustic impedance of the basement rocks either side of where these faults are inferred to be interfacing is not likely to be significant enough to produce adequate reflectors in the marine geophysical seismic reflection surveys. As such, even if environmental hurdles to future deep seismic surveys are overcome, it is doubted whether high energy, deep penetrating 2-D or 3-D seismic

**SAN ONOFRE NUCLEAR GENERATING STATION
SEISMIC HAZARD ASSESSMENT PROGRAM
2010 PROBABILISTIC SEISMIC HAZARD ANALYSIS REPORT**

surveys can retrieve the necessary data to be able to unequivocally resolve this particularly important uncertainty.

In lieu of this data, the following is recommended to better define the extent of the OBT and the TMBT and to more precisely estimate their late Pleistocene and Holocene activity.

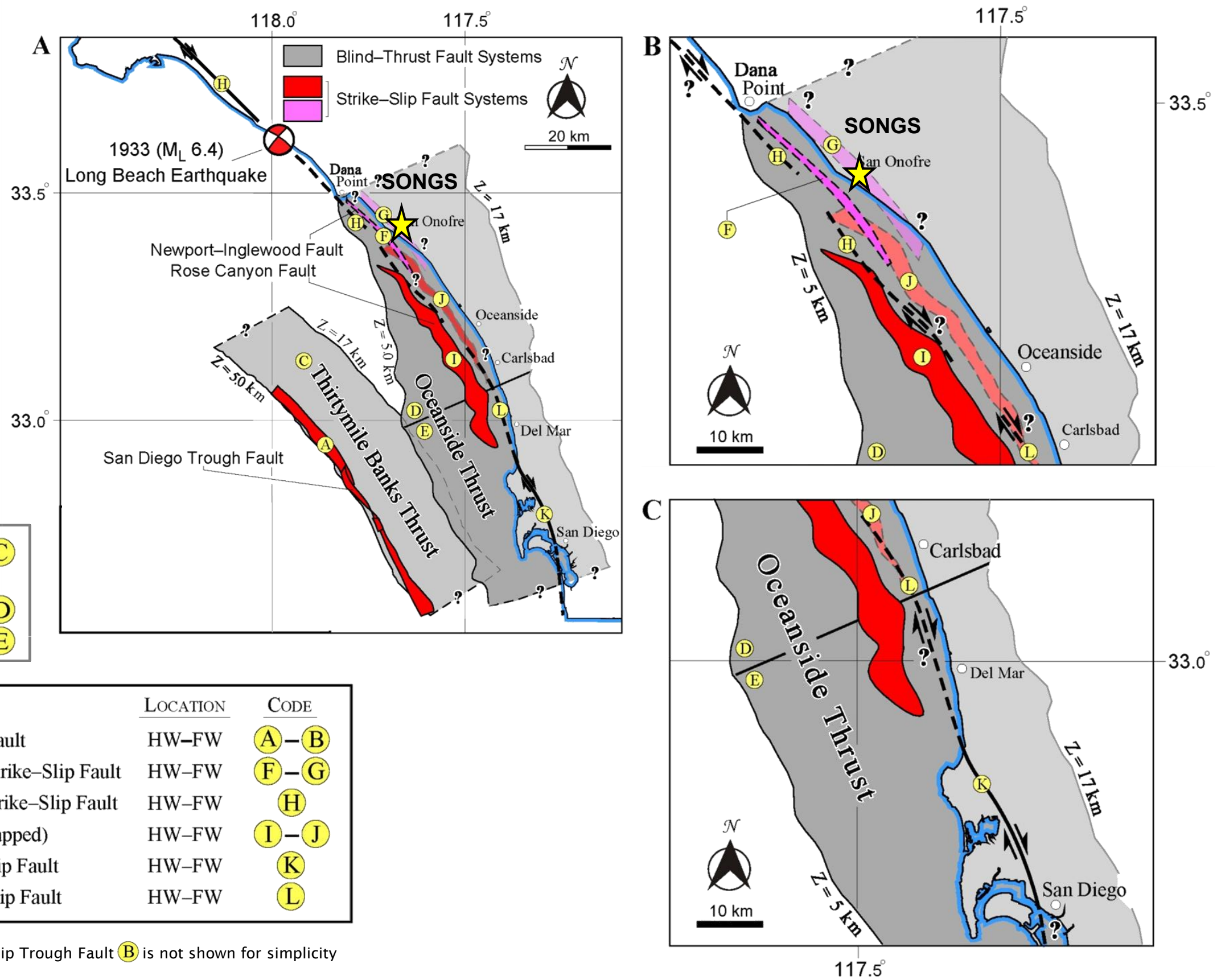
- High-resolution side-scan sonar and seismic reflection imaging of seafloor deformation combined with sediment sampling and dating, would likely provide better constraints on activity and slip rates for the OBT, TMBT, and San Diego Trough strike-slip fault (highest priority). Regarding recommended sites of future studies, Figure A3-6 highlights three possible study regions. Clearly, we would need to do a more thorough evaluation of current data to confirm the appropriateness of each site, and the particular types of data (side-scan sonar, high-res seismic) that would be most useful. Nevertheless, region 1 would target improving our understanding of the along strike continuity of the Oceanside and San Joaquin Hills structures, as well as the offshore Newport-Inglewood fault. Region 2 would target defining a slip rate on the Carlsbad fault based on the discrete near-surface fold, as well as perhaps a slip rate on the offshore Rose Canyon fault system. Region 3 would target the San Diego Trough fault in a releasing bend, thereby constraining the fault slip rate.
- Precise relocation of offshore seismicity using newly available 3D velocity models for the region and advanced relocation methods. Better earthquake locations will improve our ability to establish which fault segments are active, and to define better their subsurface geometries.
- Evaluation of current geodetic observations to improve constraints on shortening and strike-slip rates.

**SAN ONOFRE NUCLEAR GENERATING STATION
SEISMIC HAZARD ASSESSMENT PROGRAM
2010 PROBABILISTIC SEISMIC HAZARD ANALYSIS REPORT**

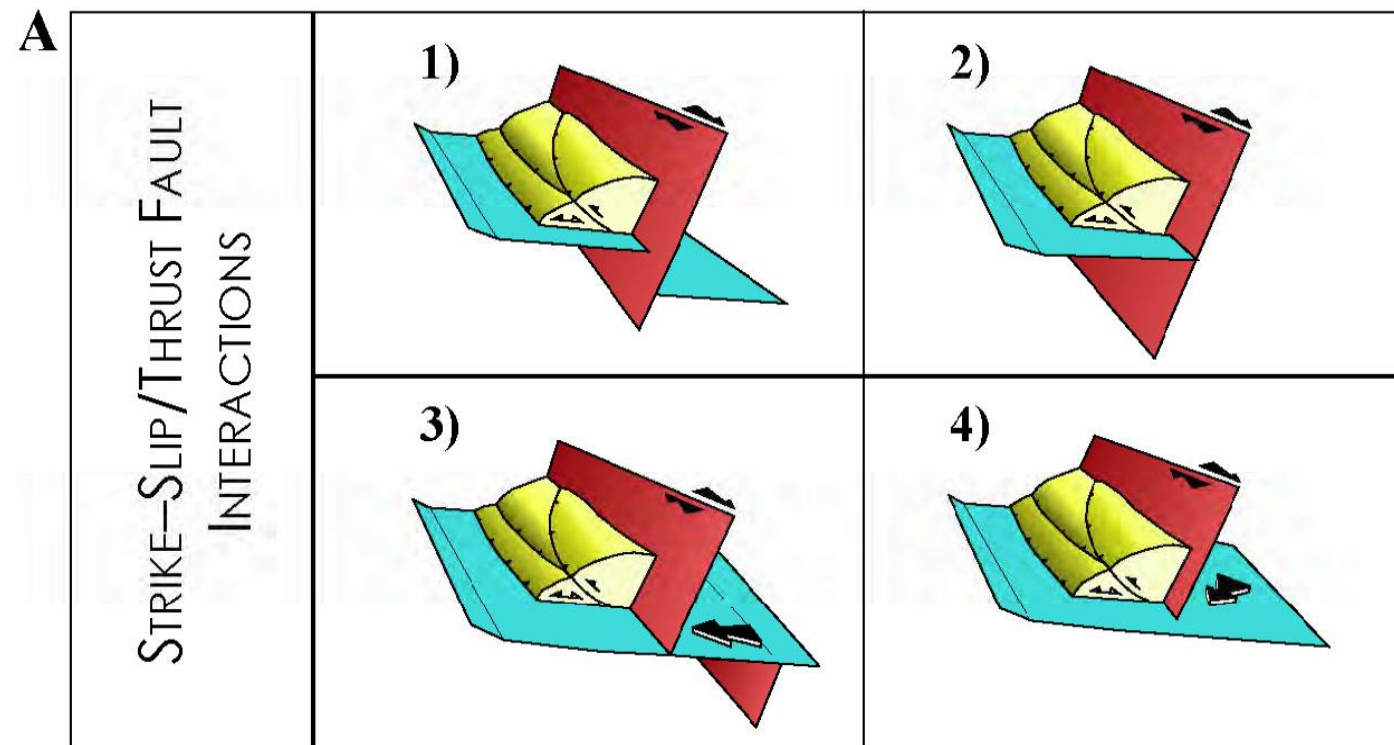
REFERENCES

- Abrahamson, Norm A. (personal communication, 2010)
- Astiz, Luciana, and Shearer, Peter (2000). Earthquake Locations in the Inner Continental Borderland, Offshore Southern California, *Bulletin of the Seismological Society of America*, v. 90, no. 2. 425-449.
- California Geological Survey (2002). California fault parameters-Interactive fault parameter map of California,
http://www.consrv.ca.gov/cgs/rghm/psha/fault_parameters/htm/Pages/index.aspx.
- Kier, Grant, and Mueller, Karl (1999). Flexural modeling of the northern Gulf of California Rift: Relating marine terrace uplift to the forebulge on a subsiding plate, *Southern California Earthquake Center 1999 internship final report*, 11p.
- Plesch, Andreas, et. al. (2007). Community Fault Model (CFM) for Southern California, *Bulleting of the Seismological Society of America*, v. 97, no. 6, 1793-1802.
- Rivero, Carlos, et. al. (2000). Oceanside and Thirty-mile Bank blind thrusts: Implications for earthquake hazards in coastal southern California, *Geology*, v. 28, no. 10, 891-894.
- Rivero-Ramirez, Carlos Alberto (2004). Origin of Active Blind-Thrust Faults in the southern Inner California Borderlands, thesis, *Department of Earth and Planetary Sciences, Harvard University, Cambridge, Massachusetts, 176 p.*
- Rivero, Carlos, and Shaw, John H. (2005). Fault related folding in reactivated offshore basins, California, *Interpretation of Contractional Fault-Related Folds, An AAPG Seismic Atlas, Studies in Geology*, no. 53, 3 p.
- Rivero, Carlos, and Shaw, John H. (in press). Active Folding and Blind-thrust Fault Induced by Basin Inversion Processes, Inner California Borderlands, *AAPG*.
- Shaw, John H. and Suppe, John (1996). Earthquake Hazards of Active Blind-thrust Faults Under the Central Los Angeles Basin, California: *Journal of Geophysical Research* 101, B4, p. 8623-8642.
- Wells, D.L., and Coppersmith, K. J., (1994). New empirical relationships among the Magnitude, Rupture Length, Rupture Width, Rupture Area, and Surface Displacement: *Bulletin of the Seismological Society of America*, v. 84, p. 974-1002.

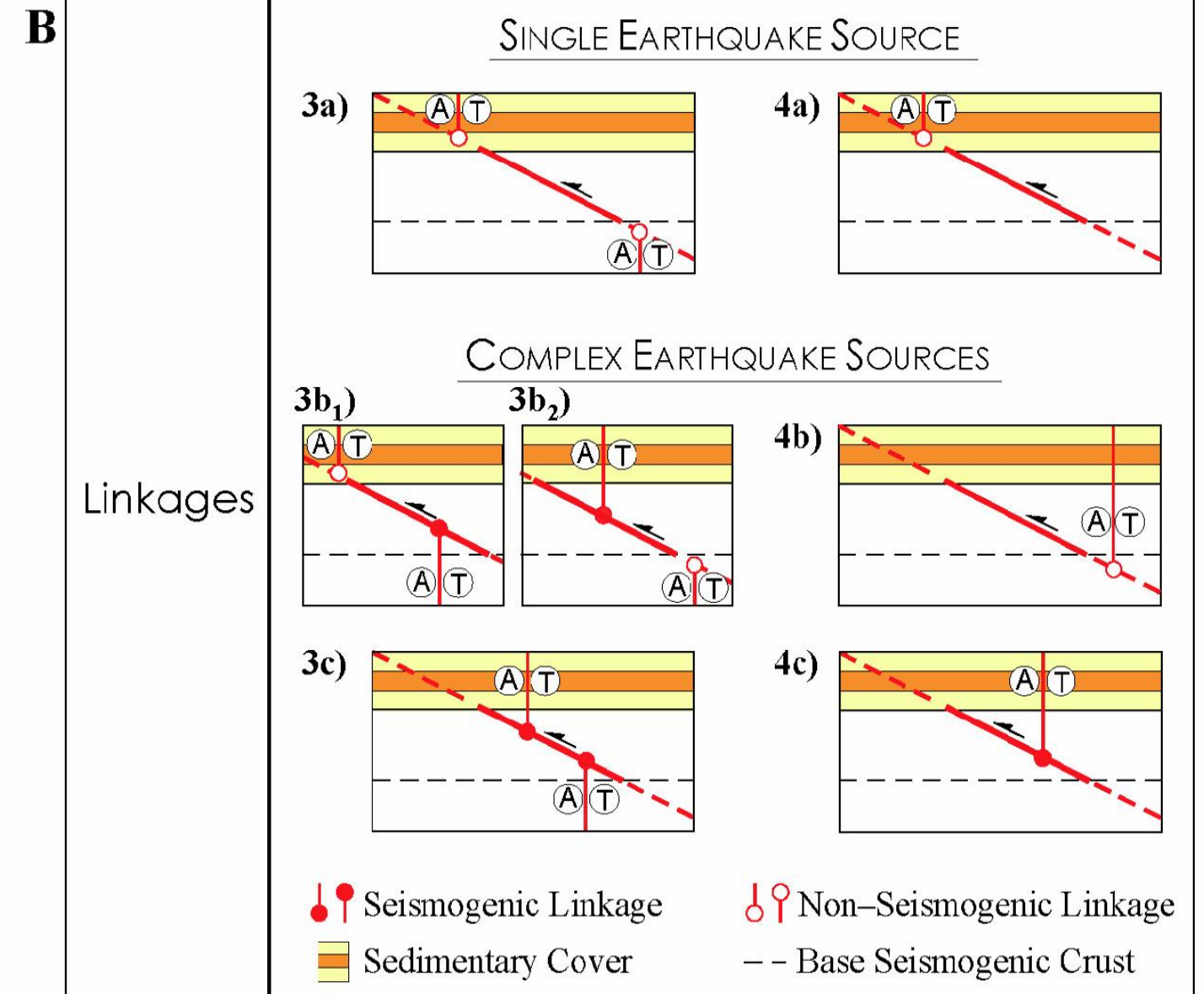




Notes: (1) Modified from Rivero (2004)
 (2) Footwall segment of the San Diego Strike-Slip Trough Fault (B) is not shown for simplicity
 (3) Latitude and longitude approximate

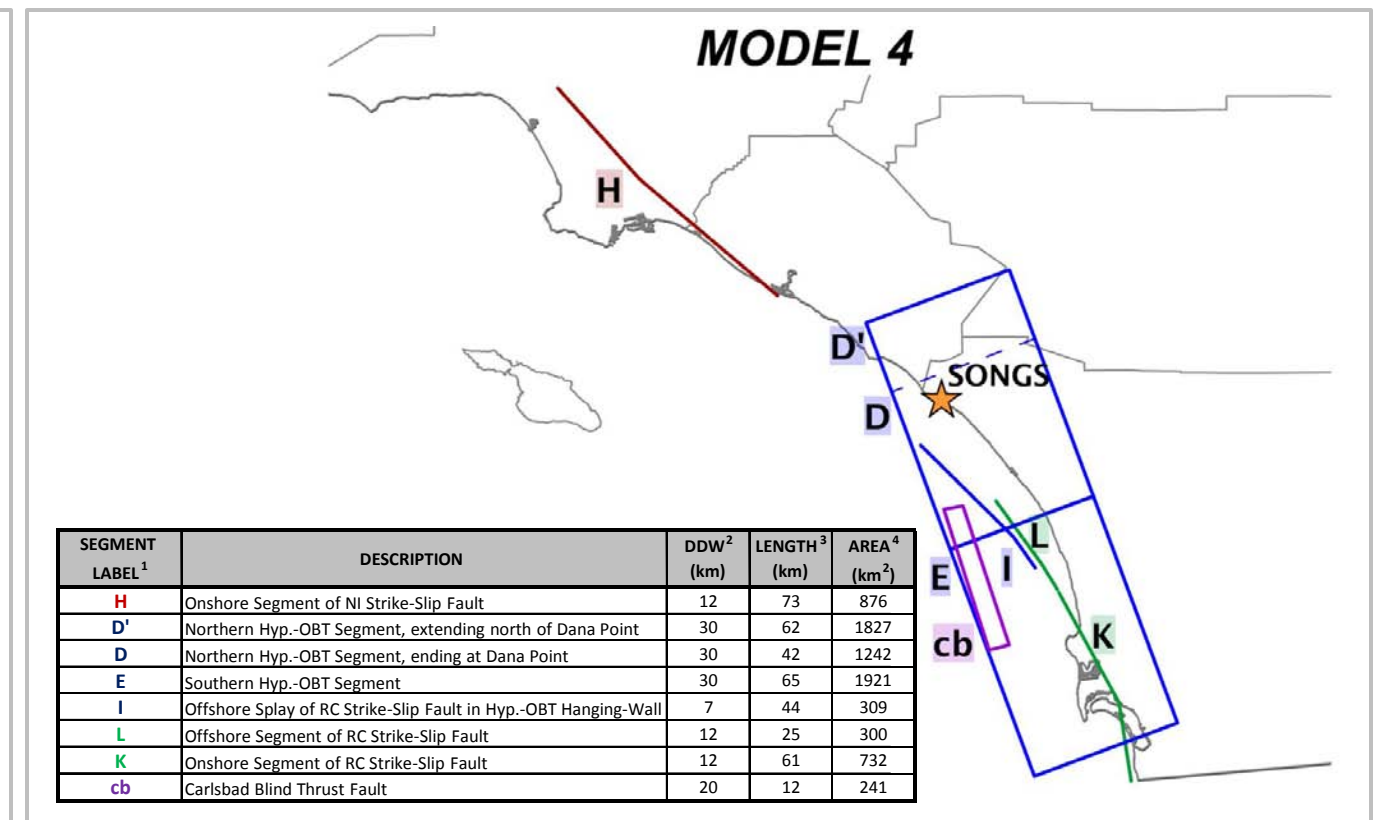
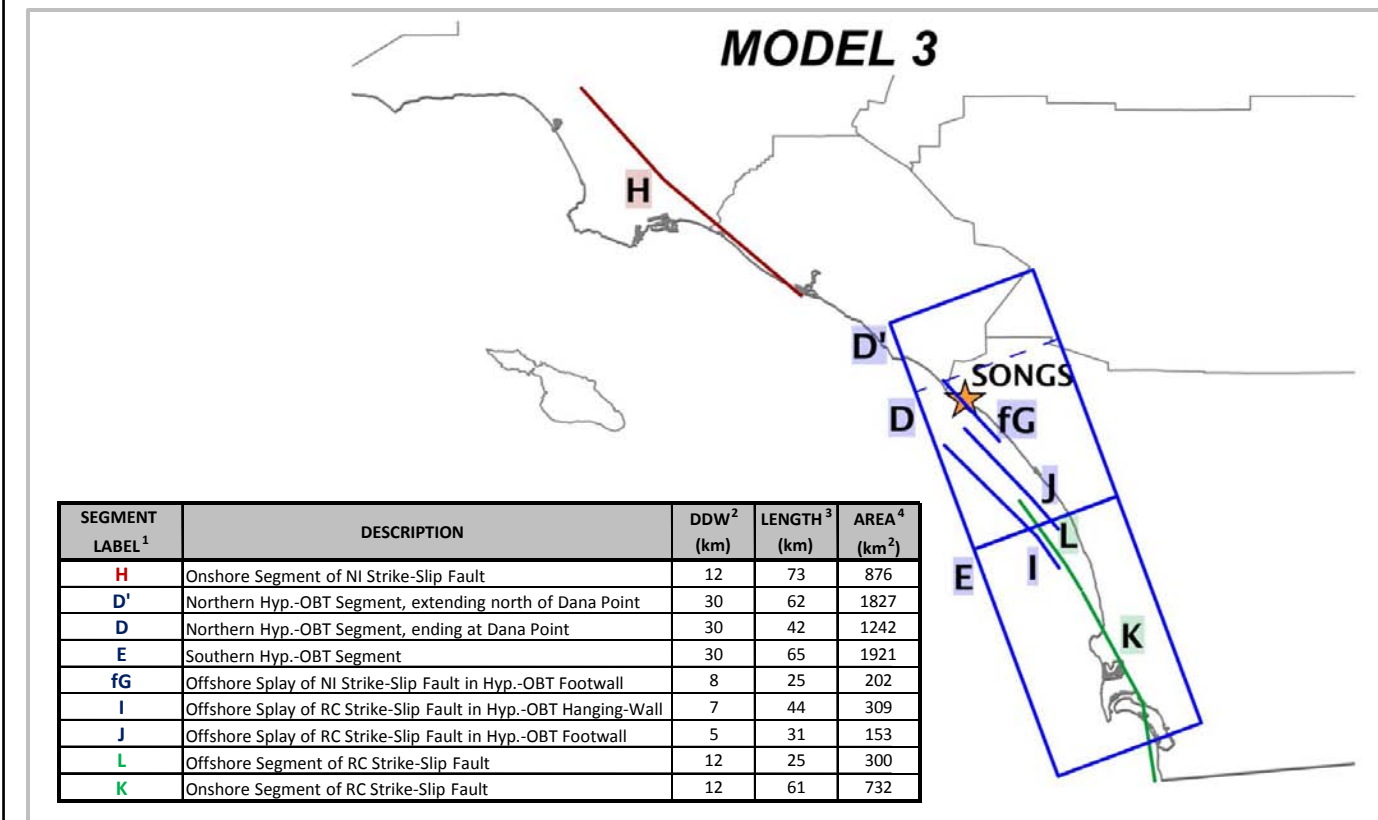
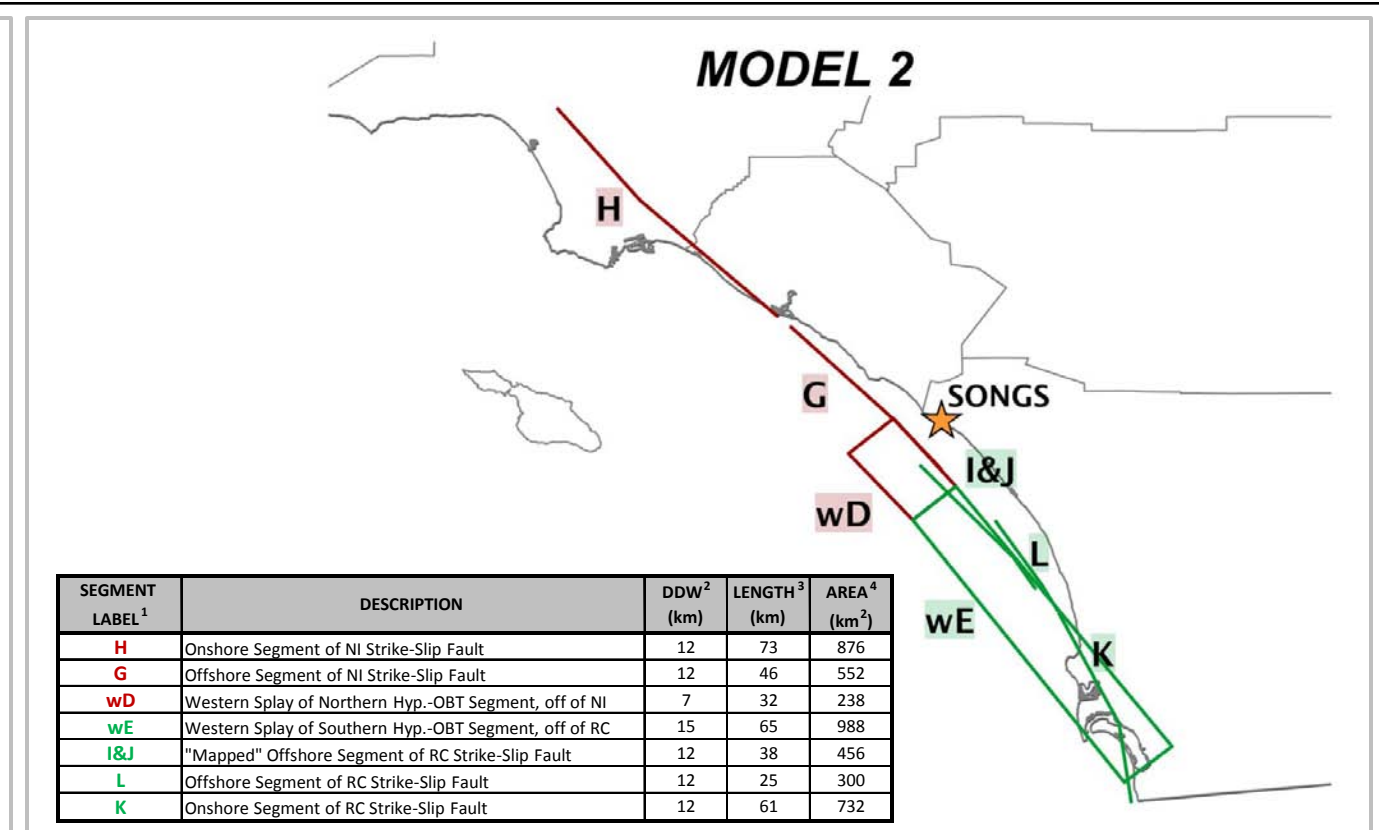
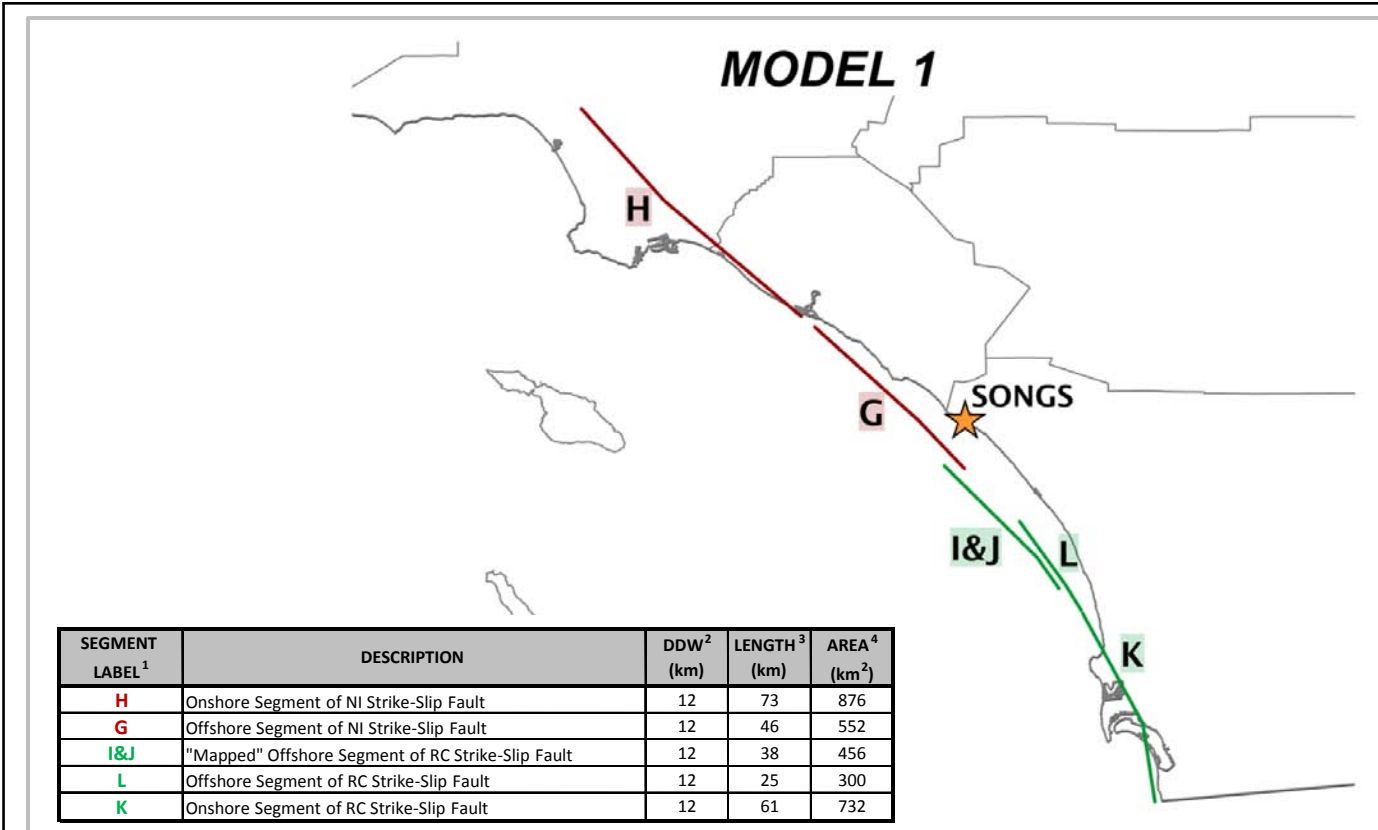


- 3a) NON-SEISMOGENIC LINKAGES WITH 1 EARTHQUAKE SOURCE
- 3b) HYBRID SEISMOGENIC LINKAGES WITH 2 EARTHQUAKE SOURCES
- 3c) SEISMOGENIC LINKAGES WITH 3 EARTHQUAKE SOURCES
- 4a) NON-SEISMOGENIC LINKAGE WITH 1 EARTHQUAKE SOURCE
- 4b) NON-SEISMOGENIC LINKAGE WITH 2 EARTHQUAKE SOURCES
- 4c) SEISMOGENIC LINKAGE WITH 2 EARTHQUAKE SOURCES



(A) Schematic representation of different structural scenarios considered in this study for strike-slip and blind-thrust fault interactions [modified from Rivero *et al.*, 2000]. (B) Geometric linkages between strike-slip and blind-thrust faults defined for preferred structural scenarios 3.25A₃ and 3.25A₄. The type of geometric linkage and their position relative to the depth of the sediments and the seismogenic crust determine the seismogenic potential of the faults and the type of earthquake source.

Notes: Modified from Rivero (2004)

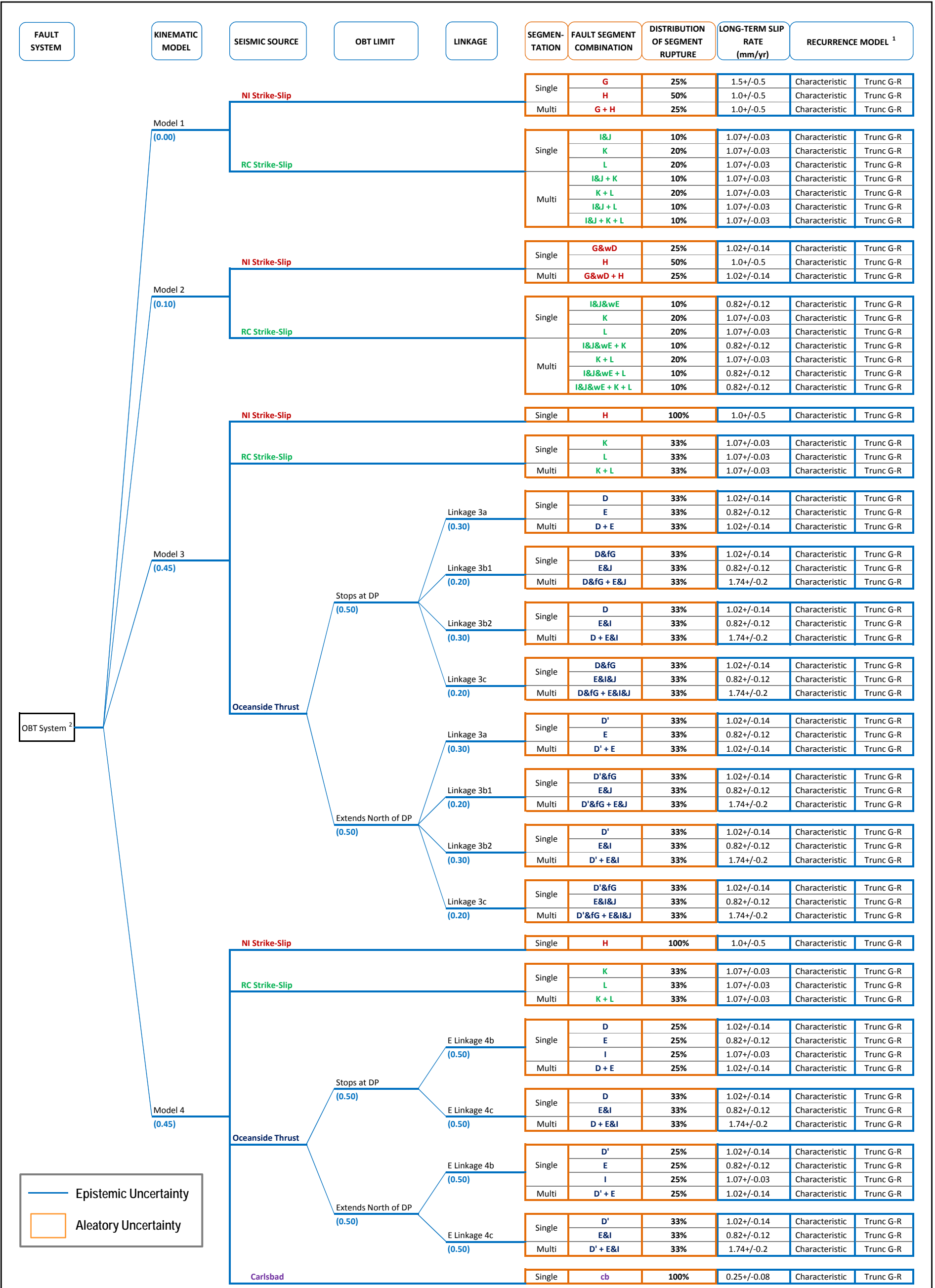


Notes:

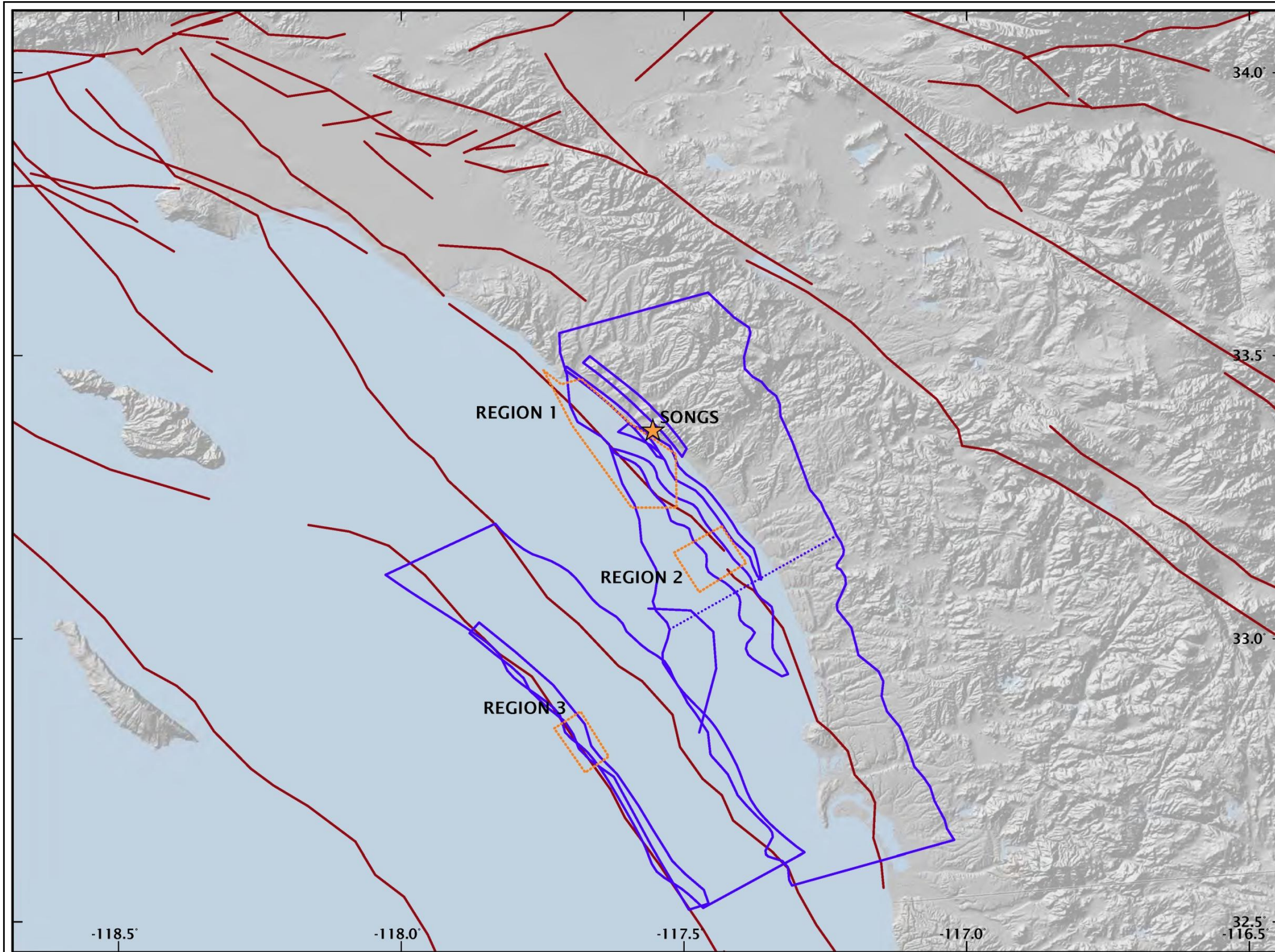
- ¹ Labels modified from Figure A-2-1
- ² Assuming 5km to 17km Seismogenic Depth
- ³ Based on Rivero (2004)
- ⁴ Calculated based on DDW and Length

KINEMATIC MODEL	SEISMIC SOURCE	OBT LIMIT	LINKAGE	SINGLE SEGMENT					MULTI SEGMENT						
				SEGMENTS	RUPTURE AREA (KM ²)	MAX MAG ¹ (M)	SLIP RATE ² (mm/yr)	RECURRENT ³ (yr)	SEGMENTS	RUPTURE AREA (KM ²)	MAX MAG ¹ (M)	SLIP RATE ² (mm/yr)	RECURRENT ³ (yr)		
1)	NI Strike-Slip			G	552	6.8	1.5+/-0.5	390 - 780	G + H	1428	7.2	1+/-0.5	980 - 2940		
				H	876	7.0	1+/-0.5	710 - 2140							
	RC Strike-Slip			I&J	456	6.7	1.07+/-0.03	600 - 640	I&J + K	1188	7.1	1.07+/-0.03	1140 - 1210		
				K	732	6.9	1.07+/-0.03	830 - 880	K + L	1032	7.0	1.07+/-0.03	970 - 1030		
				L	300	6.5	1.07+/-0.03	440 - 470	L + I&J	756	6.9	1.07+/-0.03	830 - 880		
-	-	-	-	-	I&J + K + L	1488	7.2	1.07+/-0.03	1340 - 1420						
2)	NI Strike-Slip			G&wD	790	6.9	1.02+/-0.14	790 - 1040	G&wD + H	1666	7.2	1.02+/-0.14	1270 - 1670		
				H	876	7.0	1+/-0.5	710 - 2140							
	RC Strike-Slip			I&J&wE	1444	7.2	0.82+/-0.12	1570 - 2100	I&J&wE + K	2176	7.3	0.82+/-0.12	1840 - 2470		
				K	732	6.9	1.07+/-0.03	830 - 880	K + L	1032	7.0	1.07+/-0.03	970 - 1030		
				L	300	6.5	1.07+/-0.03	440 - 470	L + I&J&wE	1744	7.2	0.82+/-0.12	1570 - 2100		
-	-	-	-	-	I&J&wE + K + L	2476	7.4	0.82+/-0.12	2150 - 2890						
3)	NI Strike-Slip			H	876	7.0	1+/-0.5	710 - 2140	-	-	-	-	-		
				RC Strike-Slip	K	732	6.9	1.07+/-0.03	830 - 880	K + L	1032	7.0	1.07+/-0.03	970 - 1030	
	L				300	6.5	1.07+/-0.03	440 - 470							
	Oceanside Thrust				Ends at Dana Point (D)	3a	D	1242	7.1	1.02+/-0.14	1080 - 1430	D + E	3163	7.5	1.02+/-0.14
				E		1921	7.3	0.82+/-0.12	1840 - 2470						
				3b1		D&fG	1444	7.2	1.02+/-0.14	1270 - 1670	D&fG + E&J	3518	7.6	1.74+/-0.2	1430 - 1810
				E&J		2074	7.3	0.82+/-0.12	1840 - 2470						
				3b2		D	1242	7.1	1.02+/-0.14	1080 - 1430	D + E&I	3472	7.5	1.74+/-0.2	1220 - 1540
				E&I		2230	7.4	0.82+/-0.12	2150 - 2890						
				3c	D&fG	1444	7.2	1.02+/-0.14	1270 - 1670	D&fG + E&I&J	3827	7.6	1.74+/-0.2	1430 - 1810	
				E&I&J	2383	7.4	0.82+/-0.12	2150 - 2890							
				Extends North of Dana Point (D')	3a	D'	1827	7.3	1.02+/-0.14	1490 - 1960	D' + E	3748	7.6	1.02+/-0.14	2400 - 3160
					E	1921	7.3	0.82+/-0.12	1840 - 2470						
					3b1	D'&fG	2029	7.3	1.02+/-0.14	1490 - 1960	D'&fG + E&J	4103	7.6	1.74+/-0.2	1430 - 1810
					E&J	2074	7.3	0.82+/-0.12	1840 - 2470						
3b2	D'	1827	7.3		1.02+/-0.14	1490 - 1960	D' + E&I	4057	7.6	1.74+/-0.2	1430 - 1810				
E&I	2230	7.4	0.82+/-0.12		2150 - 2890										
3c	D'&fG	1444	7.2	1.02+/-0.14	1270 - 1670	D'&fG + E&I&J	4412	7.6	1.74+/-0.2	1430 - 1810					
E&I&J	2383	7.4	0.82+/-0.12	2150 - 2890											
4)	NI Strike-Slip			H	876	7.0	1+/-0.5	710 - 2140	-	-	-	-	-		
				RC Strike-Slip	K	732	6.9	1.07+/-0.03	830 - 880	K + L	1032	7.0	1.07+/-0.03	970 - 1030	
	L				300	6.5	1.07+/-0.03	440 - 470							
	Oceanside Thrust				Ends at Dana Point (D)	4b	D	1242	7.1	1.02+/-0.14	1080 - 1430	D + E	3163	7.5	1.02+/-0.14
				E		1921	7.3	0.82+/-0.12	1840 - 2470						
				4c		D	1242	7.1	1.02+/-0.14	1080 - 1430	D + E&I	3472	7.5	1.74+/-0.2	1220 - 1540
				E&I		2230	7.4	0.82+/-0.12	2150 - 2890						
				Extends North of Dana Point (D')	4b	D'	1827	7.3	1.02+/-0.14	1490 - 1960	D' + E	3748	7.6	1.02+/-0.14	2400 - 3160
					E	1921	7.3	0.82+/-0.12	1840 - 2470						
					4c	D'	1827	7.3	1.02+/-0.14	1490 - 1960	D' + E&I	4057	7.6	1.74+/-0.2	1430 - 1810
E&I	2230	7.4	0.82+/-0.12	2150 - 2890											
Carlsbad Thrust	cb	241	6.4	0.25+/-0.08	1250 - 2430	-	-	-	-	-	-				

Notes:
¹Maximum Magnitude based on Wells & Coppersmith (1994)
²Value estimated by Rivero (2004) or Shaw & Plesch (2010)
³Recurrence Interval based on Shaw & Suppe (1996)



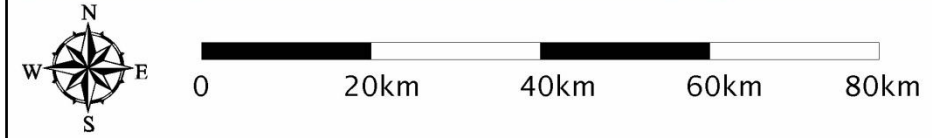
Notes:
¹ Recurrence based on 2/3 Characteristic Model and 1/3 Truncated Gutenberg-Richter Distribution
² See Appendix A, Attachment A-3 for details



- Legend**
- ★ SONGS Facility Location
 - Fault Systems from Rivero (2004)
 - Fault Traces from USGS (2009)
 - ▭ Areas Recommended for Future Study

Region	Approx. Area
Region 1	250 km ²
Region 2	90 km ²
Region 3	50 km ²

Notes:
 Base map is shaded relief of southern California based on SRTM model prepared by ESRI, 2009.



APPENDIX B

2010 PSHA GROUND MOTION CHARACTERIZATION



APPENDIX B OUTLINE

- B1.0 INTRODUCTION**
- B2.0 QA/QC OF HAZ4.2 PSHA COMPUTER PROGRAM**
- B3.0 SHEAR WAVE VELOCITY PARAMETERS USED IN NGA RELATIONSHIPS**
- B4.0 GROUND MOTION PREDICTION EQUATION EPISTEMIC UNCERTAINTY**
- B5.0 RECURRENCE RELATIONSHIPS**



**APPENDIX B
2010 PSHA GROUND MOTION CHARACTERIZATION**

B1.0 INTRODUCTION

This Appendix provides further discussions on selected PSHA-related issues addressed in the main report. The selected issues consist of QA/QC work done on the PSHA computer program HAZ4.2 (Abrahamson, 2010); characterization of the site shear wave velocity parameters used in the attenuation relationships; epistemic uncertainty associated with the attenuation relationships used; and recurrence relationships for the hypothesized OBT source.

B2.0 QA/QC OF HAZ4.2 PSHA COMPUTER PROGRAM

The PSHA computer program HAZ4.2, developed by Dr. Norman Abrahamson (2010) as the newest version of his PSHA program, was selected for use in the 2010 PSHA. This latest version enabled SHAP to implement the NSHM 2009 (USGS, 2009, PC) seismic source model and adopt the UCERF 2 (WGCEP, 2008) time independent model for conducting PSHA. However, because HAZ4.2 had not yet gone through a QA/QC process, SHAP, guided by Dr. Norman Abrahamson, followed the PSHA Validation Project methodology described in Thomas et al. (2010) to initiate this QA/QC process. The process was completed for the elements of HAZ4.2 pertinent to this study, but not others. The resulting QA/QC'd portion of the HAZ4.2 computer program will be considered an interim version of HAZ4.2 on the 2010 PSHA. The actual process in completing the QA/QC'd portion of HAZ4.2 involved interactions of SHAP with Dr. Nicholas Gregor who works with Dr. Norman Abrahamson in developing the program. SHAP and Dr. Nicholas Gregor completed a series of computer runs followed by identifications and modification resolutions on various aspects of the computer program.

The purpose of the PSHA Validation Project (Thomas et al., 2010) was to develop a consistent method for testing several aspects of the PSHA calculation process for various, widely-used PSHA computer programs in the engineering community. The validation process consisted of test cases using strike-slip, reverse, and areal sources along with various site locations as illustrated on Figure B-1. Figure B-1 also shows the sites used in the validation. The test cases were designed to address calculation of site distance, rate, ground motion attenuation, hanging wall effects, earthquake recurrence, ground motion variability, and rupture area variability against hand-calculations whenever available. The test case results for each computer program were validated by comparing them to Pacific Earthquake Engineering Research (PEER) reported results by Thomas et al. (2010) for each test case.

SHAP compared the HAZ4.2 results for all test cases against the PEER reported results from Thomas et al. (2010). Figures B-2 and B-3 compare the HAZ4.2 results with the PEER reported results for two different cases as example results. As shown on Figures B-2 and B-3, the HAZ4.2 results match with the PEER reported results from Thomas et al. (2010). The comparisons of results shown on Figures B-2 and B-3 are representative of the remaining 104 cases considered. The final results for all test cases of the QA/QC process, when eventually completed, will be presented in a report titled "QA/QC of HAZ4.2 PSHA Computer Program."

B3.0 SHEAR WAVE VELOCITY PARAMETERS USED IN NGA RELATIONSHIPS

**SAN ONOFRE NUCLEAR GENERATING STATION
SEISMIC HAZARD ASSESSMENT PROGRAM
2010 PROBABILISTIC SEISMIC HAZARD ANALYSIS REPORT**

Table B-1 shows the attenuation relationships from the NGA models used in the PSHA. These attenuation relationships are called the NGA relationships herein and consist of the following:

- Abrahamson and Silva (2008)
- Boore and Atkinson (2008)
- Campbell and Bozorgnia (2008)
- Chiou and Youngs (2008)
- Idriss (2008)

Table B-1 also summarizes the estimated shear-wave velocity parameters for SONGS used in the NGA relationships, including 1) the average shear-wave velocity from the ground surface to a depth of 30 m (V_{S30}), 2) the approximate depth to 1 km/s shear-wave velocity material ($Z_{1.0}$), and 3) the approximate depth to 2.5 km/s shear-wave velocity material ($Z_{2.5}$). These shear wave velocity parameters, not all of them used by all five relationships listed above, were based on relevant data compiled from past reports documenting previous site investigations. Figures B-4 and B-5 present compilations of the site seismic velocity data from the ground surface to a depth of 30 m and 4,000 m, respectively. These figures show both shear- and pressure-wave data that was either directly measured in the site vicinity (colored solid lines) or was estimated based on other data (colored dashed lines). Also, a generalized stratigraphic column showing the geologic units is presented between the shear- and pressure-wave graphs on Figures B-4 and B-5. This geologic interpretation is based on data presented in Dames & Moore (1970) and SCE (2001).

As shown on Figures B-4 and B-5, the pressure-wave velocities at the site were directly measured from 1) a surface seismic velocity survey by Dames & Moore (1970), 2) an acoustic velocity survey of borehole B-1 by Dames & Moore (1970), 3) a downhole seismic velocity survey by Weston Geophysical (1971), 4) an offshore seismic reflection survey by Western Geophysical (1972), and 5) geophysical data compiled by Dames & Moore (1970) to the base of the San Onofre Breccia (Tso) or to a depth of approximately 1,525 m (5,000 ft). Below the base of the San Onofre Breccia, the pressure-wave data was estimated by Dames & Moore (1970) based on measurements performed within the deeper rock units in the region by others.

As shown on Figures B-4 and B-5, the shear-wave velocities at the site were directly measured from 1) a surface seismic velocity survey by Dames & Moore (1970), 2) a downhole seismic velocity survey by Weston Geophysical (1971), 3) Rayleigh wave tests by Woodward-McNeill (1974), and 4) geophysical data compiled by Dames & Moore (1970) to the base of the Monterey Formation Tm (see Figure B-5) or to a depth of approximately 760 m (2,500 ft).

Shear-wave velocities at the site were also estimated based on pressure-wave velocities, Poisson's ratio, and shear modulus relationships. As shown on Figures B-4 and B-5, shear-wave velocities below the base of the Monterey Formation were computed by Dames & Moore (1970) from pressure-wave velocities and estimates of the Poisson's ratio measured in similar materials. Estimates of the shear-wave velocity were also calculated from the acoustic velocity log within B1 shown on Figures B-4 and B-5 (Dames & Moore, 1970) and the offshore seismic pressure-wave data (Western Geophysical, 1972) using the

Poisson's ratio values presented in Dames & Moore (1970). Lastly, shear-wave velocities estimates were calculated based on shear modulus relationships presented in Woodward-McNeill (1972). These estimates were calculated for the San Mateo Formation to a depth of 285 m (935 ft).

The San Mateo Formation sandstone comprises the first 30 m of geologic material beneath SONGS. As shown on Figure B-4, the shear-wave velocities measured or estimated within the first 30 m below the site are relatively similar to each other with the widest spread in values in the near-surface between approximately 0 and 12 m. The V_{s30} values based on Dames & Moore (1970) data (solid yellow and red lines on Figure B-4) and estimated based on offshore data by Western Geophysical (1972) (dashed green line on Figure B-4) are approximately 670 m/s and 730 m/s, respectively. These V_{s30} values were based on widely spaced survey data and pressure-wave velocity measurements that resulted in poor resolution of the near-surface shear-wave velocity values. Investigations resulting in a higher resolution of near-surface shear-wave velocities were performed by Weston (1971) (solid magenta line on Figure B-4) and Woodward-McNeill (1974) (solid purple line on Figure B-4). The V_{s30} based on the Weston (1971) data is approximately 500 m/s. The V_{s30} value was also calculated by combining the Woodward-McNeill (1974) data (solid purple line), which had a maximum exploration depth of about 4.5 m, with the shear-wave velocity estimated based on the San Mateo Formation's shear modulus relationship developed by Woodward-McNeill (1972) (dashed cyan line on Figure B-4). As shown on Figure B-4, this combined V_{s30} is about 500 m/s, which is the same as the V_{s30} based on the Weston (1971) data. Since the Weston and Woodward-McNeill data provided the best resolution of shear-wave velocities within the first 30 m of the San Mateo Formation, the V_{s30} within the San Mateo Formation at the site is estimated to be 500 m/s for the NGA relationships in Table B-1.

As shown on Figure B-5, the estimated $Z_{1.0}$ varies depending on the source of the shear-wave velocity data. The upper bound of $Z_{1.0}$ is approximately 135 m and is based on the San Mateo Formation shear modulus relationship developed by Woodward-McNeill (1972) (dashed cyan line on Figure B-5). The $Z_{1.0}$ based on the Dames and Moore (1970) data (solid red line on Figure B-5) and Western Geophysical (1972) data (dashed green line on Figure B-5) is approximately 610 m and 305 m, respectively. This puts the $Z_{1.0}$ at the top of the Monterey Formation, which varies between the two sources. It is noted that the top of the Monterey Formation at the site, as shown on the geology log on Figure B-5, is based on the Western Geophysical (1972) offshore seismic data presented in SCE (2001), and includes the latest geologic interpretation. This latest geologic interpretation together with the idea that the $Z_{1.0}$ depth occurs at the top of the Monterey Formation leads to a $Z_{1.0}$ depth of approximately 305 m, which was used in the NGA relationships in Table B-1. This value is similar to the average of all $Z_{1.0}$ sources, which is approximately 350 m.

Dames and Moore (1970) provides the only site-specific shear-wave data below the base of the Monterey Formation (dashed red lines on Figure B-5). As shown on Figure B-5, the $Z_{2.5}$ is estimated to occur at approximately 3,350 m, which corresponds to the approximate top of the crystalline basement igneous and metamorphic rocks.

B4.0 GROUND MOTION PREDICTION EQUATION EPISTEMIC UNCERTAINTY

The attenuation relationships associated with the NGA work are often referred to as the GMPE. In using attenuation relationships, their epistemic uncertainty should be considered. In the past, this epistemic

**SAN ONOFRE NUCLEAR GENERATING STATION
SEISMIC HAZARD ASSESSMENT PROGRAM
2010 PROBABILISTIC SEISMIC HAZARD ANALYSIS REPORT**

uncertainty was often accommodated by using multiple attenuation relationships. However, given the coordinated process used to develop the NGA relationships, it should not be adequate to address this epistemic uncertainty by just using multiple NGA relationships. An epistemic GMPE uncertainty in addition to the use of five NGA relationships was reflected in the PSHA herein as described below.

The additional epistemic uncertainty follows USGS (2008) as summarized below:

The USGS applies the epistemic uncertainty d_{gnd} symmetrically (USGS, 2008) so that the weights for $(\ln(gnd)+d_{gnd})$ and $(\ln(gnd)-d_{gnd})$ are the same at 0.185 and the unmodified $\ln(gnd)$ has a weight of 0.63. Here, $\ln(gnd)$ stands for the natural logarithm of the median peak or spectral acceleration, “gnd”, for a given attenuation relationship. The term “ d_{gnd} ” stands for the median or spectral acceleration uncertainty for any given attenuation relationship.

Due to the limitations of the data (particularly for large earthquakes) used in developing the NGA relationships and the considerable interactions that took place among the NGA modelers (USGS, 2008), NGA modelers suggested that the NGA relationships should also incorporate epistemic uncertainty (beyond using multiple relationships). Following the NGA modelers' suggestion, the USGS partitioned the source space into nine (9) bins determined by three partitions in the distance space (0 to 10 km, 10 to 30 km, and larger than 30 km) and three partitions in the magnitude space (5 to 6, 6 to 7, and larger than 7) as shown in Table B-2. However, of all the attenuation relationships considered by the USGS, only Campbell and Bozorgnia (2008) and Chiou and Youngs (2008) provided sufficient information to estimate the epistemic uncertainty within the nine bins considered. Based on an average epistemic uncertainty, Table B-2 shows the resulting epistemic uncertainty within each of the 9 bins considered by the USGS (2008).

As in the USGS evaluation, the space was divided into 9 bins (3 ranges in the magnitude space and 3 ranges in the distance space). Within each bin, an average value of the range was used to compute the peak or spectral accelerations for all 5 attenuation relationships considered. For example, in the case of the magnitude range 6 to 7, and distance the range 0 to 10 km, an average magnitude value of 6.5 and an average rupture distance of 5 km was used to compute the spectral ordinates from all 5 attenuation relationships. Figures B-6 and B-7 show the computed spectral ordinates for strike-slip and reverse faulting mechanism, respectively. Next, the ratio of the maximum to minimum calculated spectral accelerations was computed for each frequency. Figure B-8 shows the resulting ratios for each of the two styles of faulting mechanism considered, as well as their average values within the range of frequencies of interest. In general, the average ratio for the reverse faulting mechanism tends to be larger than that of the strike-slip faulting mechanism. In the present evaluation, average ratios obtained from the reverse faulting mechanism were used.

The epistemic uncertainty from the attenuation relationships can be compared to the epistemic uncertainty values provided by the USGS by noting that the minimum and maximum spectral accelerations are provided by $(\ln(gnd)-d_{gnd})$ and $(\ln(gnd)+d_{gnd})$, respectively. Therefore, in the USGS case, the ratio of maximum (“max”) to minimum (“min”) response spectra is provided by:

$$Sa_{Max,USGS}/Sa_{Min,USGS} = \exp[\ln(gnd) + d_{gnd}] / \exp[\ln(gnd) - d_{gnd}]$$

$$Sa_{Max,USGS}/Sa_{Min,USGS} = \exp(2 \times d_{gnd})$$



where $Sa_{Max,USGS}/Sa_{Min,USGS}$ is the ratio of the maximum and minimum USGS spectral acceleration. Conversely, for a given average ratio value, the corresponding epistemic $dgnd$ term can also be computed as follows:

$$dgnd = \ln(Sa_{Max,USGS}/Sa_{Min,USGS})/2$$

In the example case cited above, the comparison of the USGS epistemic uncertainty ratio and the attenuation relationship epistemic uncertainty is shown on Figure B-9. The computed $dgnd$ term obtained from the attenuation relationship epistemic uncertainty is provided in Table B-3.

A comparison of the $dgnd$ terms provided by the USGS listed in Table B-2 and the attenuation relationship epistemic uncertainty listed in Table B-3 is also shown in graphical form on Figure B-10.

The results from the use of the five attenuation relationships already reflect some epistemic uncertainty from the attenuation relationships. In order to account for the “full” GMPE epistemic uncertainty due to the lack of data, the difference between the two $dgnd$ values for each of the nine bins above needs to be considered. The final epistemic uncertainty included in the current study is provided in Table B-4.

In this study, the events controlling the shaking condition at the site were mainly magnitude 6 to 7 events with a distance range of less than 10 km. Therefore, the epistemic uncertainty for this magnitude range and distance range is the only one that was used for all five attenuation relationships considered in the PSHA evaluation.

B5.0 RECURRENCE RELATIONSHIPS

The recurrence relationships used for the NI/RC Fault Zone source were based on the time-independent part of the UCERF 2 and followed the UCERF 2 methodology (WGCEP, 2008). Following this methodology, a characteristic recurrence relationship (Youngs and Coppersmith, 1985) was assigned a weight of 2/3, and a truncated exponential relationship (Youngs and Coppersmith, 1985) was assigned a weight of 1/3. For the hypothesized OBT source, which was not based on the UCERF 2, appropriate recurrence relationships to be used were guided in part by available historic seismicity data.

Figure B-11 shows 1) the limited observed historic main shock seismicity evaluated for completeness in the area of SONGS and 2) a region generally within 10 km of the hypothesized OBT used in the evaluation of historic seismicity data for the hypothesized OBT source. The historic seismicity catalog and general methodologies used to process this catalog are from UCERF2 (WGCEP, 2008). Figure B-12 shows the hypothesized OBT earthquake recurrence based on the observed historic earthquakes within the hypothesized OBT region (five total, as shown on Figure B-11). The historic seismicity model shown on Figure B-12 includes: 1) the cumulative annual frequency of occurrence of various magnitude or greater observed earthquakes (shown as open circles) and 2) the upper and lower standard deviation recurrence bounds based on Weichert (1980) (shown as vertical bars). Figure B-12 also shows the earthquake recurrence relationship developed using the seismic source parameters for the hypothesized OBT source (Section 2.0 and Appendix B) and assuming only the characteristic recurrence model by Youngs and Coppersmith (1985). As shown on Figure B-12, the use of only the characteristic recurrence relationship to represent the hypothesized OBT source results in the recurrence relationship that is reasonably consistent with the historic seismicity in the hypothesized OBT region. On the basis of

**SAN ONOFRE NUCLEAR GENERATING STATION
SEISMIC HAZARD ASSESSMENT PROGRAM
2010 PROBABILISTIC SEISMIC HAZARD ANALYSIS REPORT**

the results shown on Figure B-12, only the characteristic recurrence relationship was used to represent the hypothesized OBT source.



TABLE B-1
NGA Relationships and Shear-wave Velocity Parameters

NGA	Epistemic Weight	Shear-Wave Velocity Parameters†		
		V _{s30} *	Z _{1.0} **	Z _{2.5} ***
Abrahamson and Silva (2008)	0.20	500-m/s	0.31-km	3.35-km
Boore and Atkinson (2008)	0.20			
Campbell and Bozorgnia (2008)	0.20			
Chiou and Youngs (2008)	0.20			
Idriss (2008)	0.20			

†Used as needed in each NGA relationship

*V_{s30} = the average shear wave velocity from the ground surface to a depth of 30-m

**Z_{1.0} = the approximate depth to 1.0 km/s shear wave velocity material

***Z_{2.5} = the approximate depth to 2.5 km/s shear wave velocity material

TABLE B-2
Epistemic Uncertainty in the GMPE (natural log term)

Magnitude Range	Rupture Distance Range	Average <i>dgnd</i> Term
5 to 6	0 to 10km	± 0.375
	10 to 30km	0.21
	≥ 30 km	0.245
6 to 7	0 to 10km	0.23
	10 to 30km	0.225
	≥ 30 km	0.23
≥ 7	0 to 10km	0.40
	10 to 30km	0.36
	≥ 30 km	0.31

TABLE B-3
Epistemic Uncertainty in the Attenuation Relationships (natural log term)

Magnitude Range	Rupture Distance Range	Average <i>dgnd</i> Term
5 to 6	0 to 10km	±0.285
	10 to 30km	0.252
	≥30km	0.293
6 to 7	0 to 10km	0.157
	10 to 30km	0.15
	≥30km	0.208
≥7	0 to 10km	0.17
	10 to 30km	0.154
	≥30km	0.147

TABLE B-4
Epistemic Uncertainty (natural log term) Used in the Current Study

Magnitude Range	Rupture Distance Range	Average <i>dgnd</i> Term
5 to 6	0 to 10km	±0.090
	10 to 30km	0.0*
	≥30km	0.0*
6 to 7	0 to 10km	0.073
	10 to 30km	0.075
	≥30km	0.022
≥7	0 to 10km	0.230
	10 to 30km	0.206
	≥30km	0.163

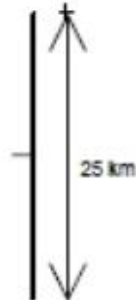
* signifies that when the *dgnd* value from the attenuation relationships exceeds the USGS *dgnd* value, an epistemic uncertainty value of 0.0 was conservatively used.

FAULT 1



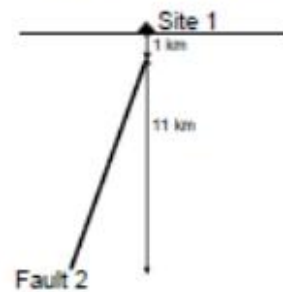
Fault Type: Strike Slip
 Dip: 90 degrees
 Fault Plane Depths: 0 - 12 km

FAULT 2

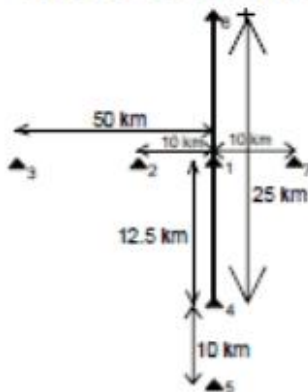


Fault Type: Reverse
 Dip: 60 degrees west
 Fault Plane Depths: 1 - 12 km

Cross-sectional view of Fault 2

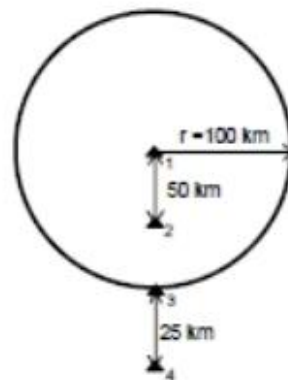


SITES FOR FAULTS 1 & 2



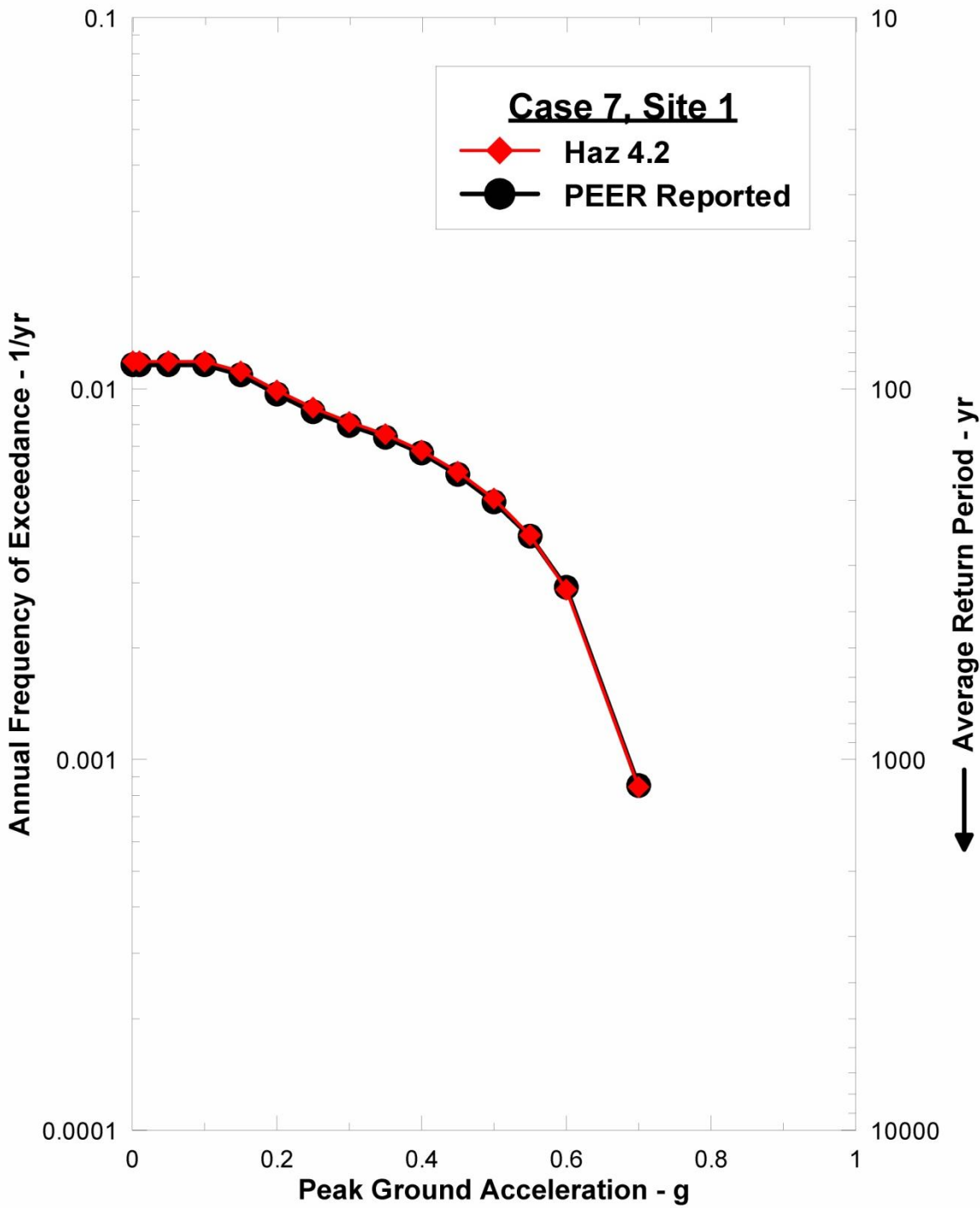
- Site 1: On fault, at midpoint along strike
- Site 2: 10 km west of fault, at midpoint along strike
- Site 3: 50 km west of fault, at midpoint along strike
- Site 4: On fault, at southern end
- Site 5: 10 km south of fault along strike
- Site 6: On fault, northern end
- Site 7: 10 km east of fault, at midpoint along strike

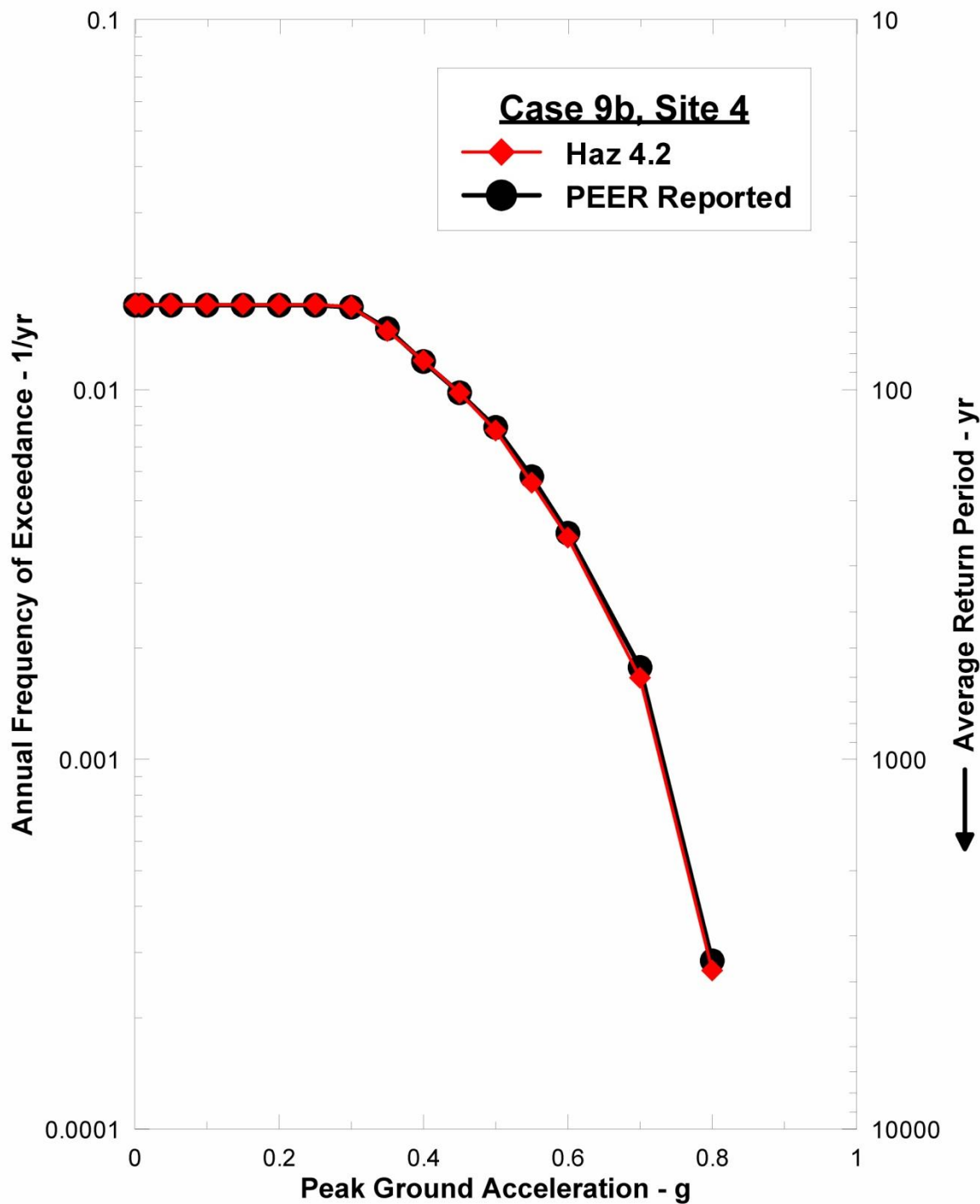
AREA 1 WITH SITES

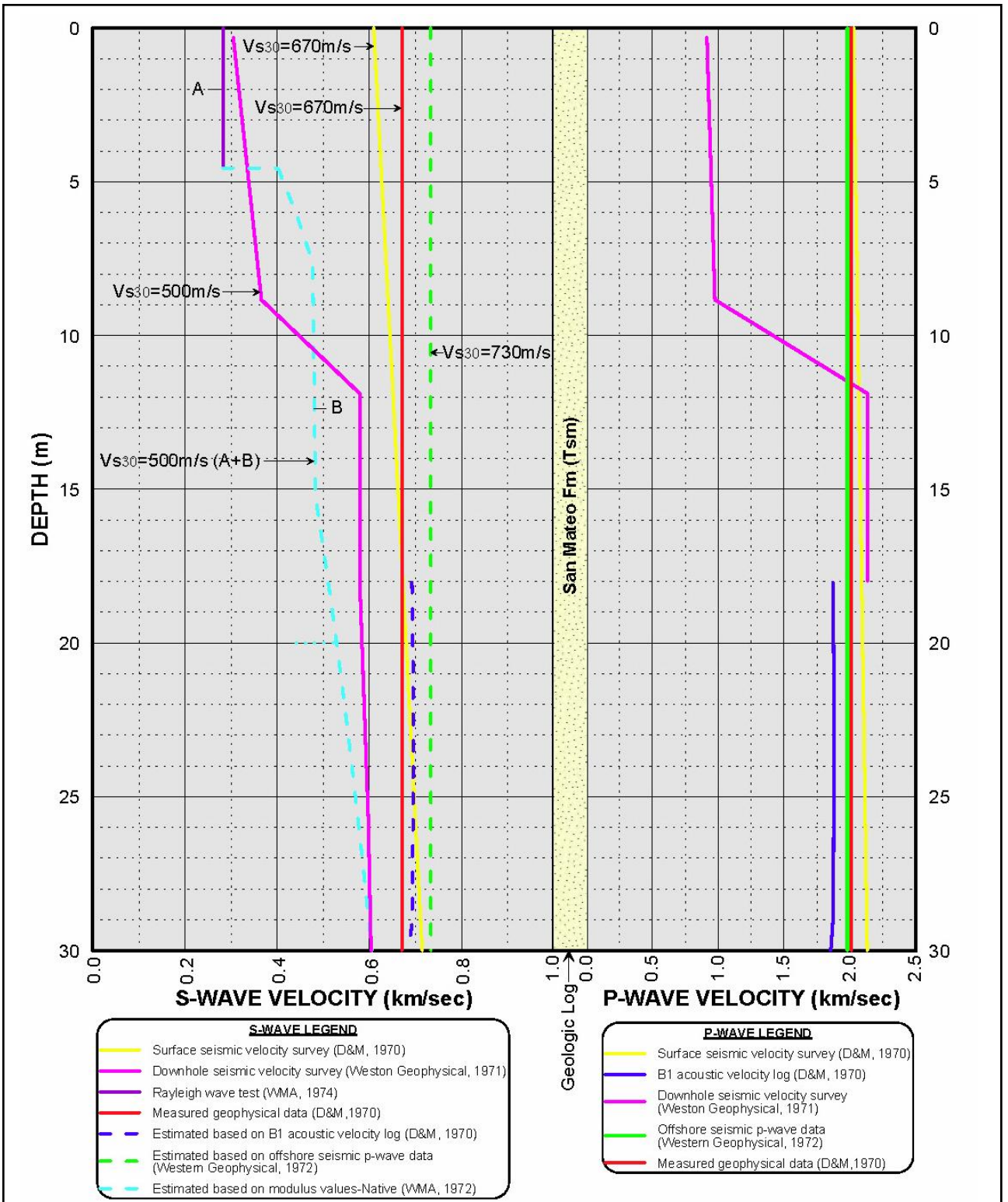


- Site 1: At center of area
- Site 2: 50 km from center (radially)
- Site 3: On area boundary
- Site 4: 25 km from boundary







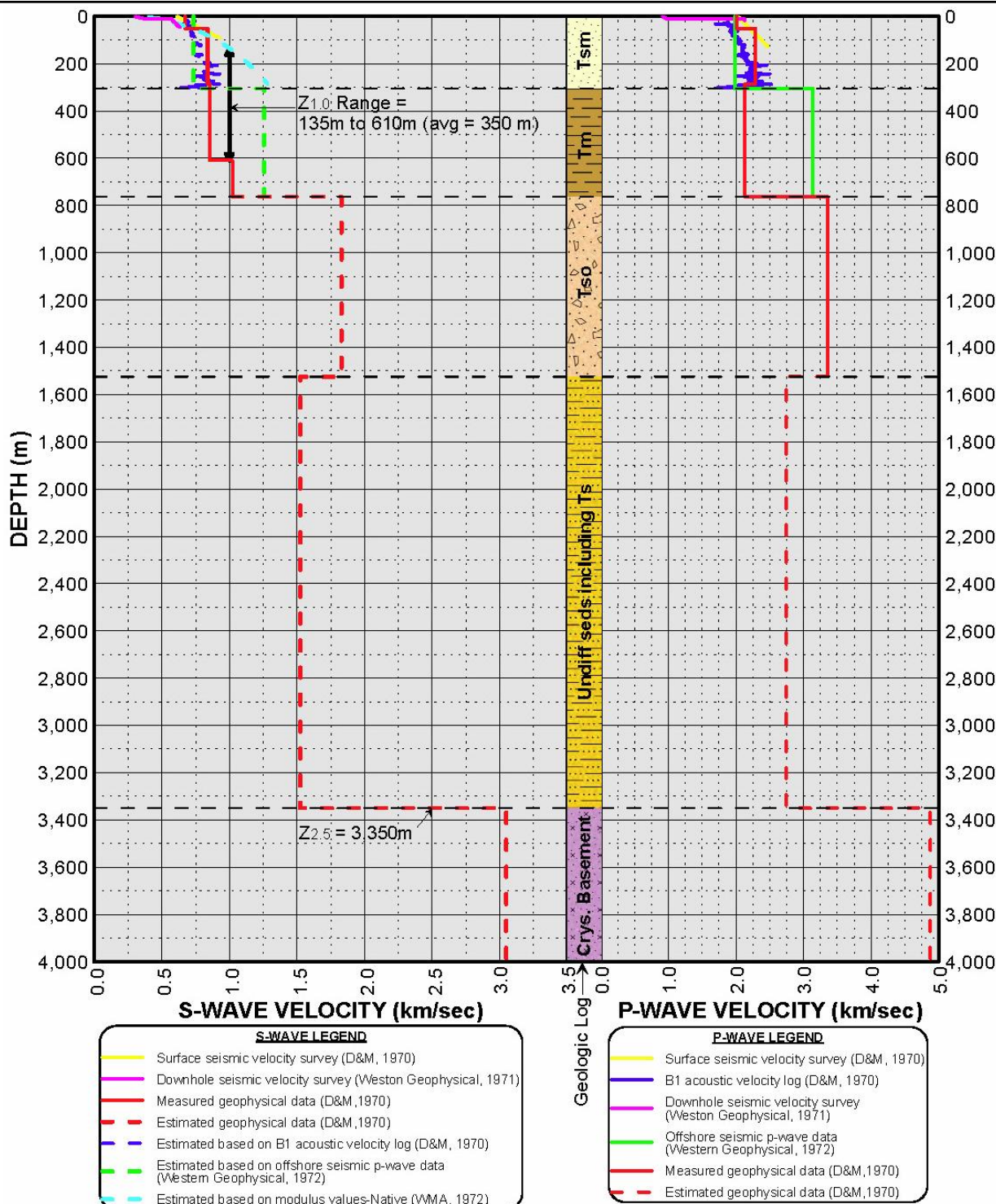


SHEAR- WAVE AND PRESSURE- WAVE VELOCITY SUMMARY (0 to 30 m)

FIGURE B-4

SAN ONOFRE NUCLEAR GENERATING STATION SEISMIC HAZARD ASSESSMENT PROGRAM





NOTE: Geology based on D&M (1970) and SCE (2001).

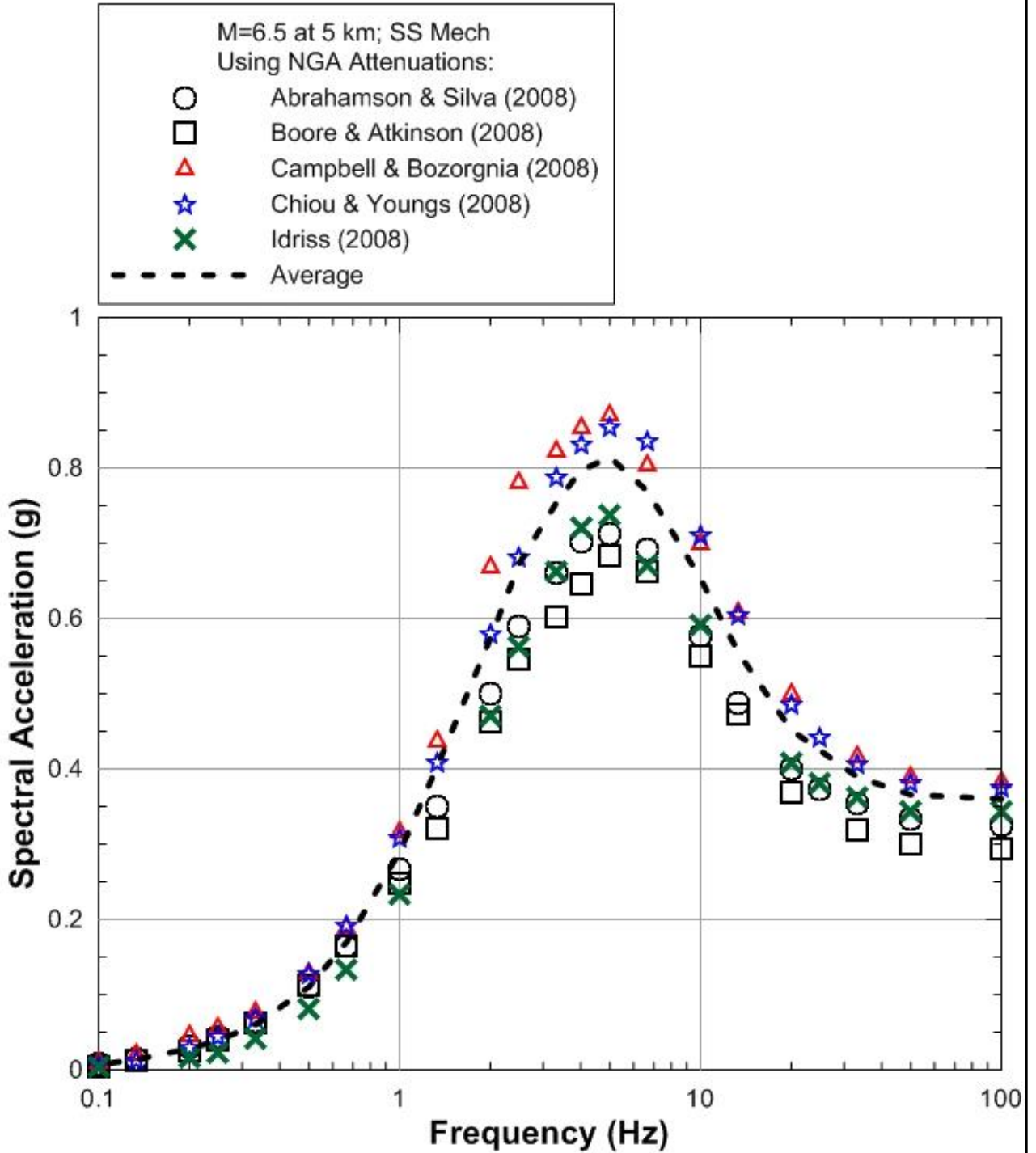
Tsm= San Mateo Fm.; Tso=San Onofre Breccia; Ts=Santiago Fm.



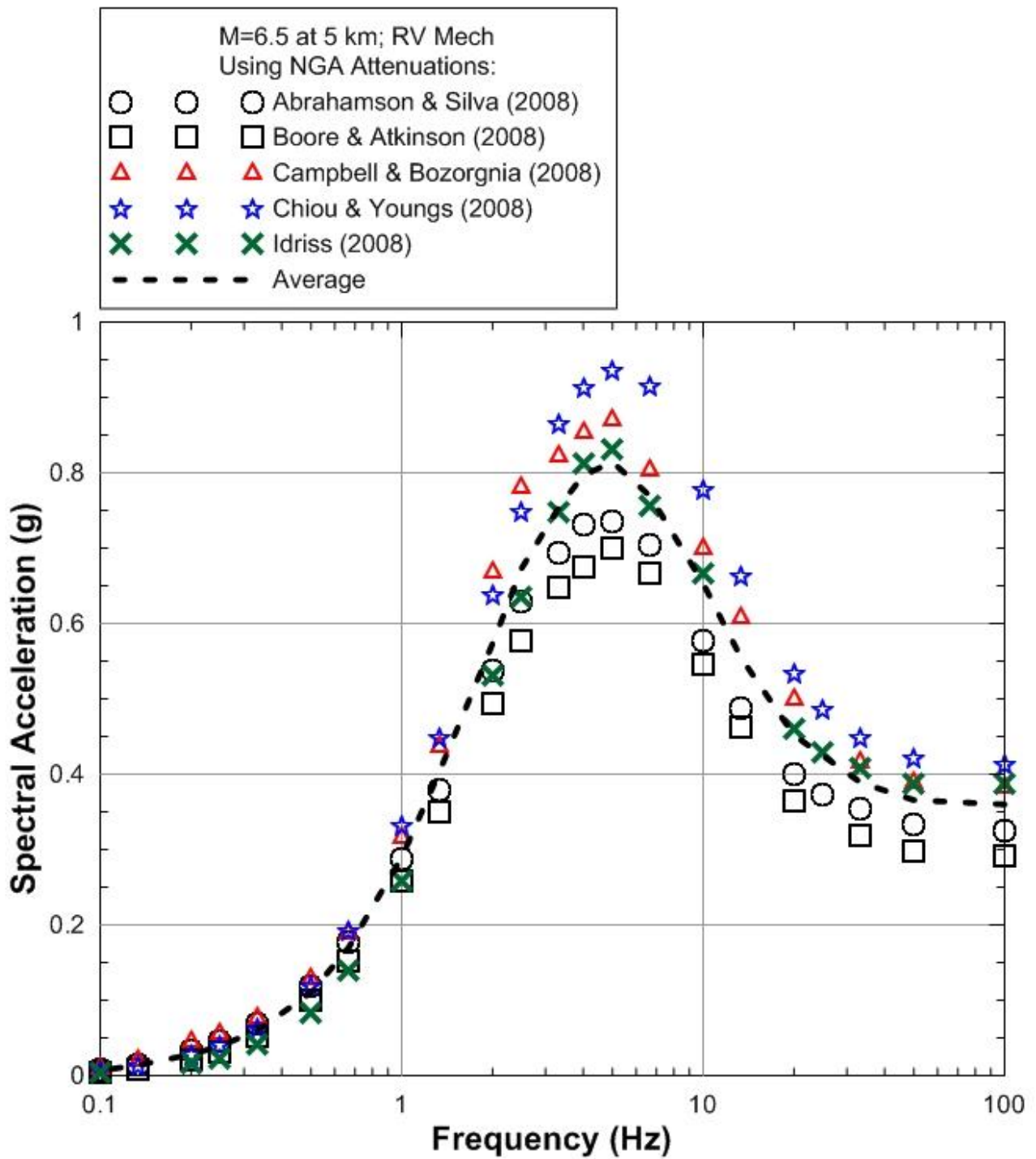
**SHEAR- WAVE AND PRESSURE- WAVE VELOCITY
SUMMARY (0 to 4,000 m)**

**FIGURE
B-5**

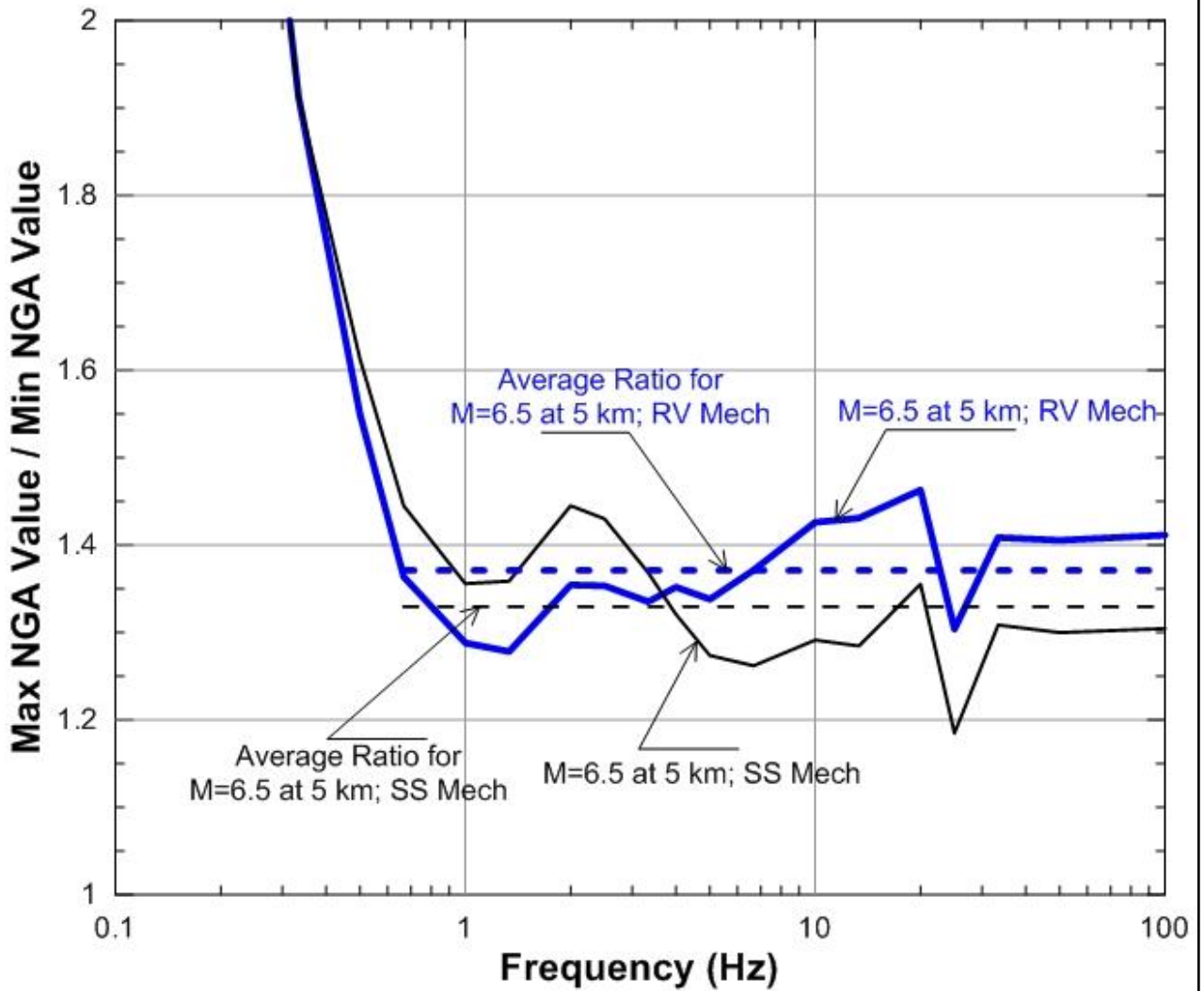
**SAN ONOFRE NUCLEAR GENERATING STATION
SEISMIC HAZARD ASSESSMENT PROGRAM**



NOTE: Mw=6.5 at 5 km for strike-slip faulting mechanism



NOTE: Mw=6.5 at 5 km for reverse faulting mechanism



NOTE: Mw=6.5 at 5 km for strike-slip and reverse faulting mechanism

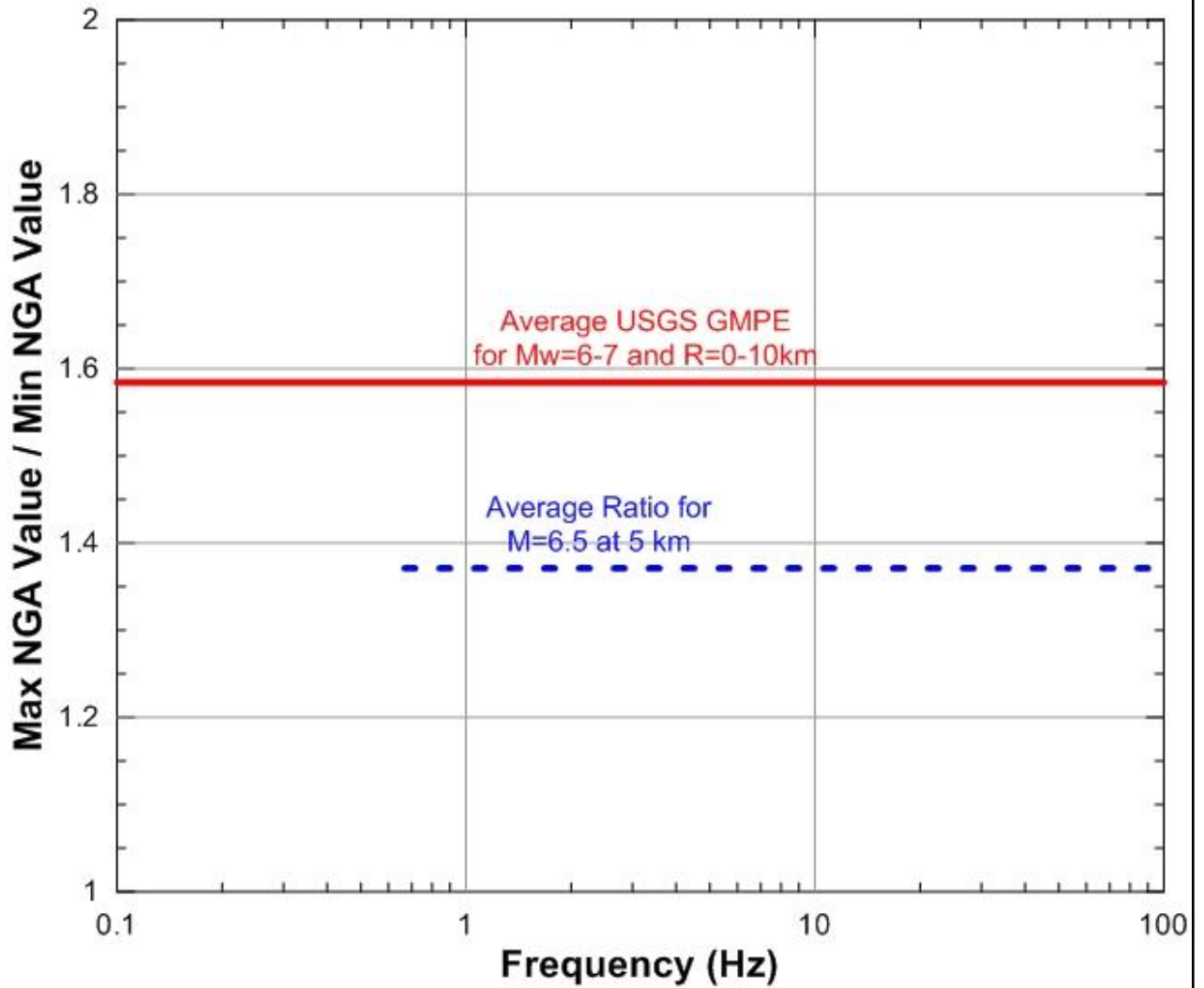


GeoPentech
Geotechnical & Geoscience Consultants

**RATIOS OF MAXIMUM TO MINIMUM
SPECTRAL ACCELERATIONS**

**FIGURE
B-8**

**SAN ONOFRE NUCLEAR GENERATING STATION
SEISMIC HAZARD ASSESSMENT PROGRAM**



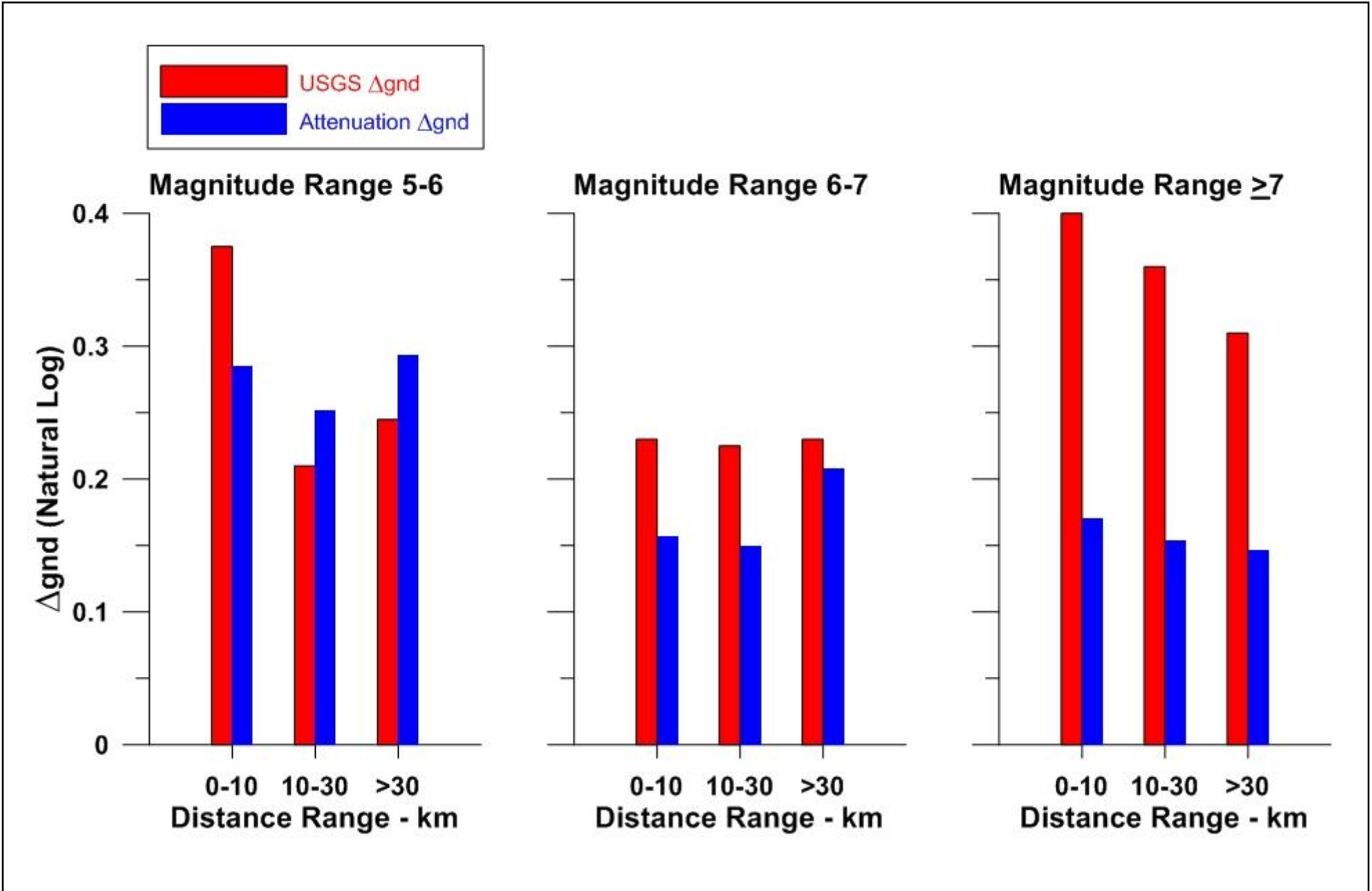
NOTE: Mw=6-7, R=0-10 km

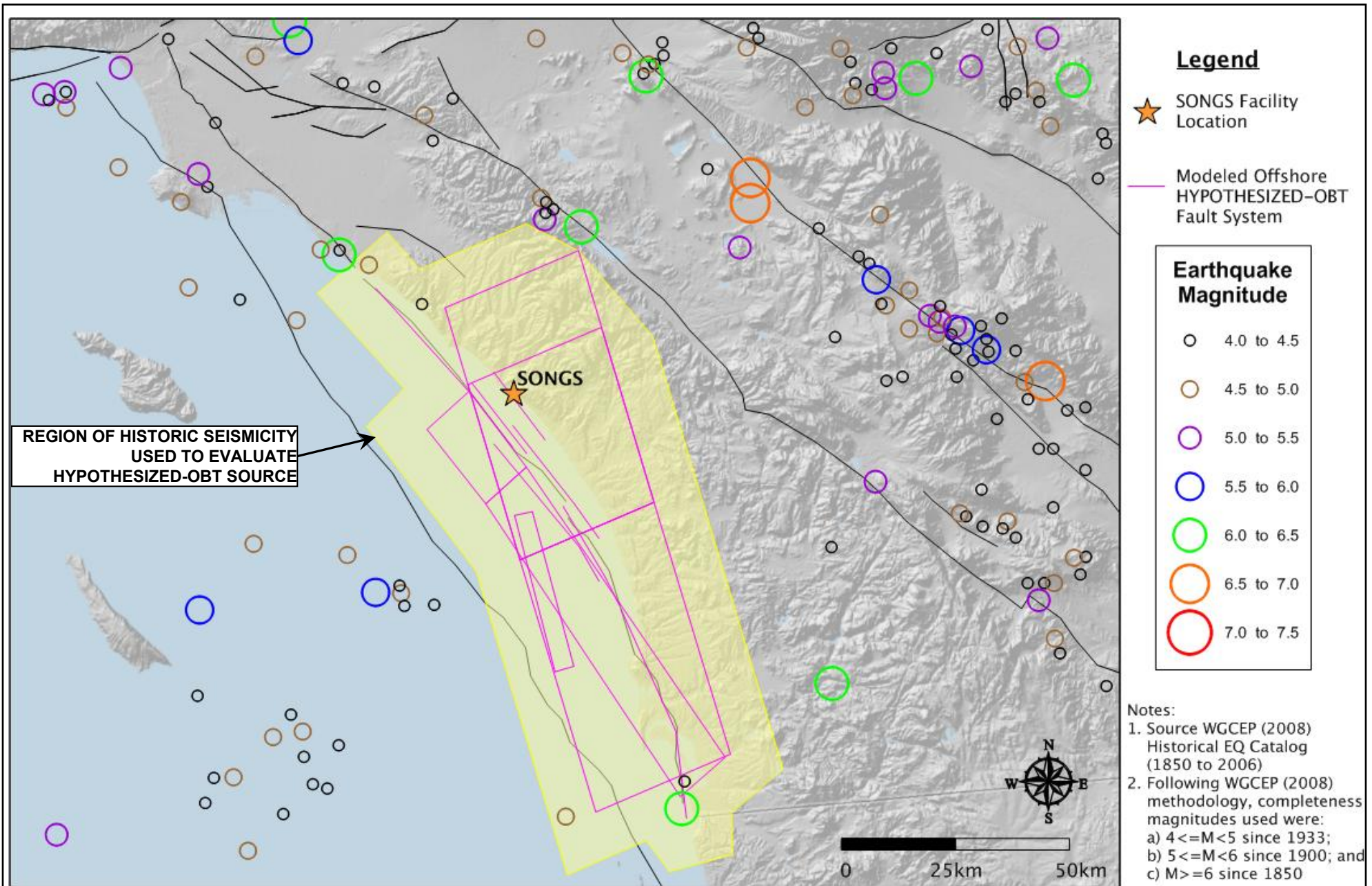


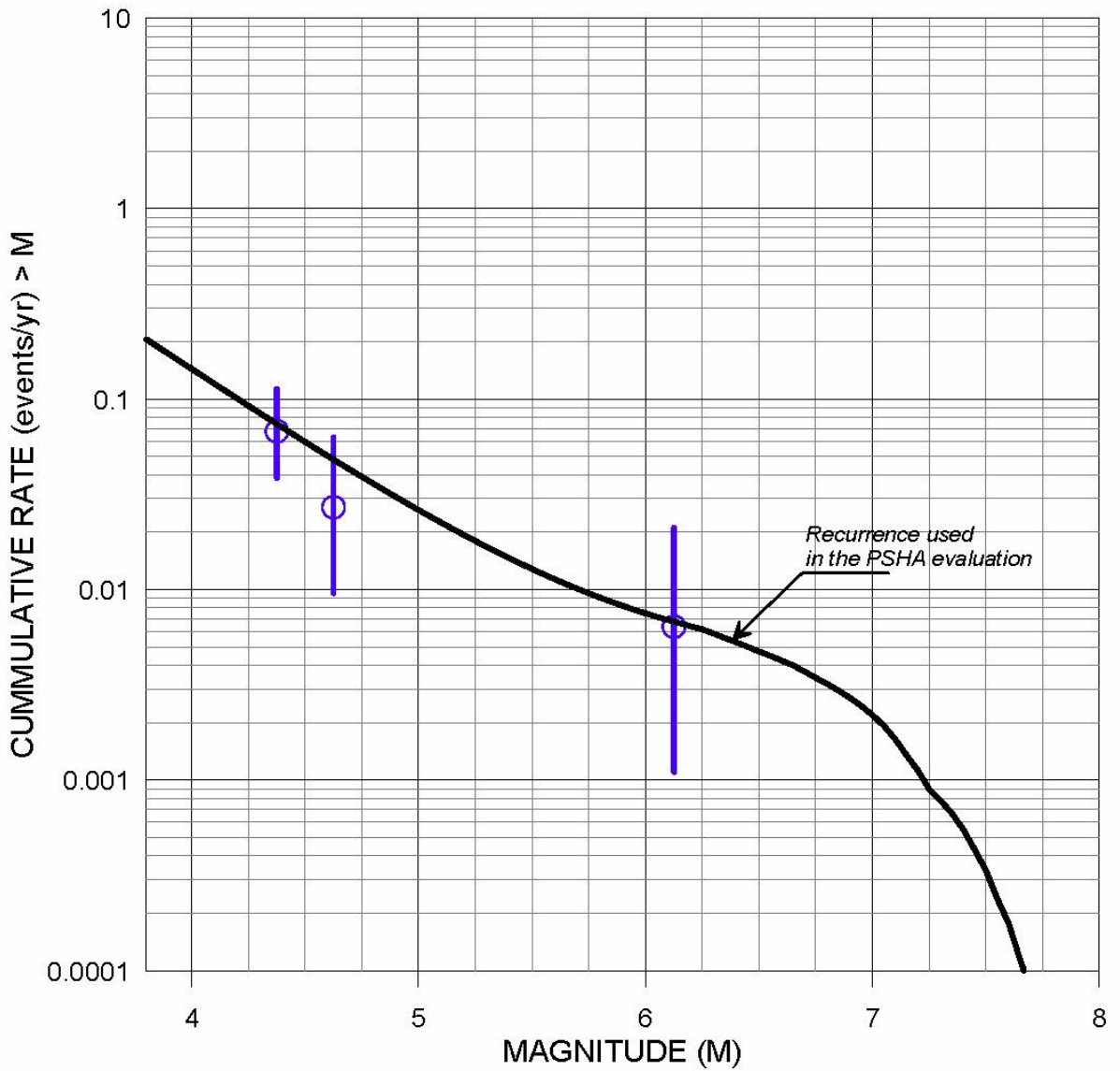
COMPARISON OF USGS EPISTEMIC UNCERTAINTY AND ATTENUATION RELATIONSHIP EPISTEMIC UNCERTAINTY

FIGURE B-9

SAN ONOFRE NUCLEAR GENERATING STATION
SEISMIC HAZARD ASSESSMENT PROGRAM

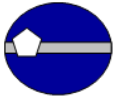






Appendix 2

Tsunami Hazard Evaluation



TSUNAMI HAZARD EVALUATION

PURPOSE

A tsunami hazard evaluation was performed to evaluate tsunami vulnerability at the San Onofre Nuclear Generating Station (SONGS) in light of the recently published tsunami inundation maps as discussed below.

The “Tsunami Inundation Map for Emergency Planning,” which was published June 1, 2009, for southern California’s coastline in southern Orange County and northern San Diego County, was prepared jointly by the State of California Office of Emergency Services, the California Geologic Survey, the University of Southern California Tsunami Research Center, and the National Oceanic and Atmospheric Administration. A copy of this map is presented as Figure 1 and can be downloaded from the California Geological Survey’s Website on tsunami information at http://www.conservation.ca.gov/cgs/geologic_hazards/Tsunami/Inundation_Maps/Pages/index.aspx.

EVALUATION

As indicated on Figure 1, the red line shows a potential maximum tsunami inundation elevation of 17 to 20 feet (ft) above mean sea level (msl) or an equivalent elevation of 19.9 to 22.9 ft mean lower low water (mllw).

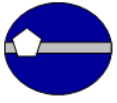
The tsunami inundation elevation shown on Figure 1 was created by the State of California (State) to identify a “credible upper bound” to the potential tsunami inundation at any location along the coastline. It was created by combining the ensemble of source events affecting the region, as summarized in Table 1 on Figure 1. In identifying the inundation elevation as a “credible upper bound,” the State “adjusted the near shore bathymetric grids in their model to ‘mean high water’ sea level conditions (*which is higher than mean sea level by 2.6 ft*)⁽¹⁾, representing a conservative sea level for the tsunami modeling and mapping.” This conservatism is reflected in the end result of the inundation map and shows the maximum elevation of the tsunami wave to be between elevations of 17 to 20 ft msl or the equivalent elevations of 19.9 to 22.9 ft mllw.

The top of the existing seawall at SONGS Units 2 and 3 is at an elevation of 30 ft mllw and, in the North Industrial Area, the top of the existing seawall is at an elevation of 28.2 ft mllw. The ground surface elevation of the site at SONGS Units 2 and 3 is the same as the top of the seawall so the State’s map correctly represents the potential tsunami inundation, and there is no flooding at the location of SONGS Units 2 and 3. Utilizing the elevation at the top of the existing seawall and the estimated inundation elevations by the State, the existing seawall provides 7.1 to 10.1 ft of freeboard at SONGS Units 2 and 3.

As indicated on Figure 1, the North Industrial Area adjacent to and northwest of SONGS Units 2 and 3, is incorrectly shown as being inundated. As highlighted in the notes on Figure 1, under “Method of Preparation,” the topography in the gridded area used to prepare the inundation map was enhanced by utilizing high-resolution digital topography from coastal interferometric data

Notes:

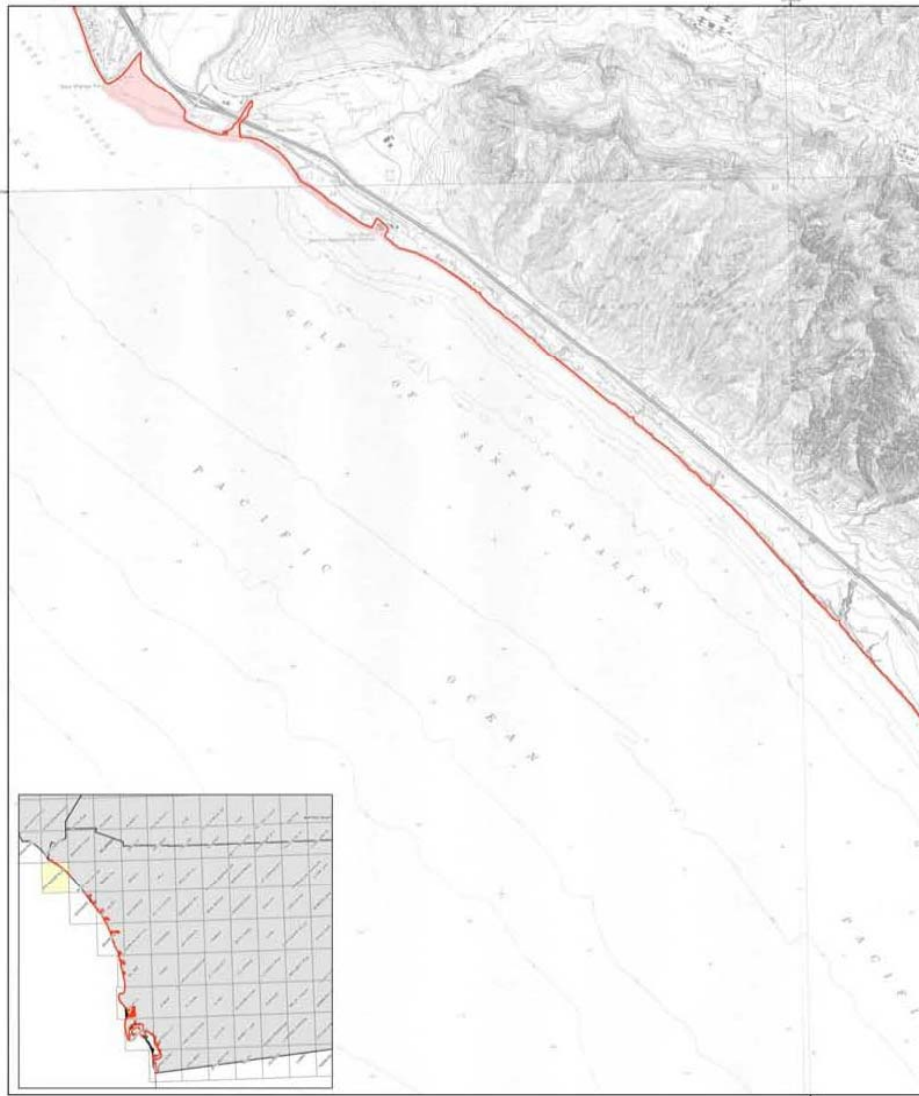
⁽¹⁾ *Italicized note added to quote.*



(circa 2003). This method did not detect the seawall due to its narrow profile. Therefore, during the preparation of the “Tsunami Inundation Map for Emergency Planning,” the North Industrial Area seawall was inadvertently excluded and the inundation map erroneously indicated the potential for flooding. The existing seawall in the North Industrial Area will actually preclude flooding and provides 5.3 to 8.3 ft of freeboard above the State’s estimated tsunami inundation elevations. To accurately reflect the actual layout of SONGS, Figure 2 was developed by showing the State’s tsunami inundation line as it should be drawn in the vicinity of SONGS.

CONCLUSION

The estimated tsunami elevations shown on Figure 1, “Tsunami Inundation Map for Emergency Planning,” do not identify any potential tsunami impacts or flooding to the SONGS site. The maximum elevation of the tsunami is about 23 ft mllw and the tops of the seawalls are at elevations of 30 ft mllw and 28.2 ft mllw for Units 2 and 3 and the North Industrial Area, respectively.



METHOD OF PREPARATION

Initial tsunami modeling was performed by the University of Southern California (USC) Tsunami Research Center funded through the California Emergency Management Agency (CEMMA) by the National Tsunami Hazard Mitigation Program. The tsunami modeling project obtained the MOST (Model of Simulating Tsunami) computational program (Owens et al., which allows the model execution from a remote workstation and subsequently used for the inundation mapping (Thom and Guntenspergen, 1997; Thom and Synalaska, 1998).

The bathymetric/topographic data that were used in the tsunami model consisted of a series of nested grids. Resolution grids with a 30-second (75 to 90-centimeter) resolution in height were adjusted to "Mean High Water" sea level conditions. Interpolating a conventional sea level for the intended use of the tsunami modeling and mapping.

A list of tsunami source events was selected for modeling, representing realistic local and distant earthquakes and hypothetical volcanic eruptions, near-shore tsunamis (Table 1). Local tsunami sources that were considered include offshore faults along the Pacific coast, including faults on either side of the coast and large submarine landslides adjacent to agricultural waterways. Distant tsunami sources that were considered include great subduction zone events that are known to have occurred historically (1960 Chile and 1964 Alaska earthquakes) and others which have not occurred since the Pacific Ocean "Ring of Fire".

In order to enhance the result from the 75 to 90-meter resolution grid data, a model was developed utilizing higher-resolution digital topographic data (2 to 10 meters resolution) that better defines the location of the maximum inundation line (U.S. Geological Survey, 1982; reference: 2002, NOAA, 2005). The location of the maximum inundation line was determined by using digital imagery and terrain data on a GIS platform with coordinates given to known inundation information (Lander et al., 1993). This information was used, where possible, to fill gaps coordinated with local survey personnel.

The accuracy of the inundation line shown on these maps is subject to limitations in the accuracy and completeness of available source and inundation information, and the current understanding of tsunami generation and propagation mechanisms as expressed in models. This accuracy of inundation line is not a result of a specific tsunami event.

This map does not represent inundation from a single tsunami event. It was created by combining inundation results for an ensemble of source events affecting a given region (Table 1). For this reason, all of the inundation region in a particular area will not likely be inundated during a single tsunami event.

References:
Lander, J.P., Laska, P.A., and Kishor, M.J., 1993. Tsunami affecting the West Coast of the United States, 1960-1992. National Oceanic and Atmospheric Administration Technical Report 92, NOAA, NESDIS, NGDC, 242 p.

National Atmospheric and Oceanic Administration (NOAA), 2004. Interferometric Synthetic Aperture Radar (SAR) Digital Elevation Models from Synthetic Aperture Radar (SAR) Interferometry data.

Thom, V.V., and Synalaska, C.E., 1997. Implementation and Testing of the Method of Simulating Tsunami (MOST). NOAA Technical Memorandum ERL PMEL-115, 11 p.

Thom, V.V., and Synalaska, C.E., 1998. Numerical modeling of tidal wave surge. Journal of Atmospheric, Plan. Coastal and Ocean Engineering, ASCE, 124 (4), pp 183-191.

U.S. Geological Survey, 1982. Digital Elevation Models. National Mapping Program, National Instructions, Data Users Guide 1, 8 p.

TSUNAMI INUNDATION MAP FOR EMERGENCY PLANNING

State of California - County of San Diego
SAN ONOFRE BLUFF QUADRANGLE

June 1, 2009



MAP EXPLANATION

- Tsunami Inundation Line
- Tsunami Inundation Area

PURPOSE OF THIS MAP

This tsunami inundation map was prepared for local cities and counties in identifying their tsunami hazard. It is intended for local governmental, coastal emergency planning only. This map, and the information presented herein, is not a legal document and does not meet disclosure requirements for real estate transactions, nor for any other regulatory purpose.

The inundation map has been compiled with best currently available scientific information. The inundation line represents the maximum inundation range from a number of events, yet neither, tsunami source, inundation line, nor results, but to a lack of tsunami occurrence in the historical record. This map includes no information about the probability of any tsunami affecting any area within a specific period of time.

Please refer to the following website for additional information on the construction and intended use of the tsunami inundation map:

State of California Emergency Management Agency, Earthquake and Tsunami Program
http://www.sos.ca.gov/EMAP/Programs/Earthquake%20and%20Tsunami%20Program.htm

University of Southern California - Tsunami Research Center
http://www.usc.edu/ep/tsunami2009/index.php

National Oceanic and Atmospheric Administration (NOAA) Tsunami Research (MOST) model
http://hmi.pmel.noaa.gov/most/background/index.html

MAP BASE

Topographic base maps prepared by U.S. Geological Survey as part of the 7.5-minute Quadrangle Map Series (topography 1:24,000 scale). Tsunami inundation line boundaries may differ slightly from contour lines on the base map.

DISCLAIMER

The California Emergency Management Agency (CEMMA), the University of Southern California (USC), and the California Geological Survey (CGS) make no representation or warranty regarding the accuracy of this inundation map or the data from which the map was derived. Neither the State of California nor USC, shall be liable under any circumstances for any direct, indirect, special, incidental or consequential damages with respect to any claim by any user or any third party on account of or arising from the use of this map.

Table 1. Tsunami source modeled for the San Diego County coastline

Source ID	Name of Inundation Map Coverage and Event	Area of Inundation Map Coverage and Event		
		Phase	Subduction	Vol. Erupt.
Local Sources	Carlsbad Thrust Fault	X	X	X
	Caliente Fault	X	X	X
	Coronado Fault	X	X	X
	San Onofre Fault	X	X	X
	San Onofre Fault Segment	X	X	X
	San Mateo Thrust Fault	X	X	X
	Conchita Fault	X	X	X
	Conchita Subduction Zone #1 (S1)	X	X	X
	Conchita Subduction Zone #2 (S2)	X	X	X
	Conchita Subduction Zone #3 (S3)	X	X	X
	Conchita Subduction Zone #4 (S4)	X	X	X
	Conchita Subduction Zone #5 (S5)	X	X	X
	Conchita Subduction Zone #6 (S6)	X	X	X
	Conchita Subduction Zone #7 (S7)	X	X	X
	Conchita Subduction Zone #8 (S8)	X	X	X
	Conchita Subduction Zone #9 (S9)	X	X	X
	Conchita Subduction Zone #10 (S10)	X	X	X
	Conchita Subduction Zone #11 (S11)	X	X	X
	Conchita Subduction Zone #12 (S12)	X	X	X
	Conchita Subduction Zone #13 (S13)	X	X	X
	Conchita Subduction Zone #14 (S14)	X	X	X
	Conchita Subduction Zone #15 (S15)	X	X	X
	Conchita Subduction Zone #16 (S16)	X	X	X
	Conchita Subduction Zone #17 (S17)	X	X	X
	Conchita Subduction Zone #18 (S18)	X	X	X
	Conchita Subduction Zone #19 (S19)	X	X	X
	Conchita Subduction Zone #20 (S20)	X	X	X
	Conchita Subduction Zone #21 (S21)	X	X	X
	Conchita Subduction Zone #22 (S22)	X	X	X
	Conchita Subduction Zone #23 (S23)	X	X	X
	Conchita Subduction Zone #24 (S24)	X	X	X
	Conchita Subduction Zone #25 (S25)	X	X	X
	Conchita Subduction Zone #26 (S26)	X	X	X
	Conchita Subduction Zone #27 (S27)	X	X	X
	Conchita Subduction Zone #28 (S28)	X	X	X
	Conchita Subduction Zone #29 (S29)	X	X	X
	Conchita Subduction Zone #30 (S30)	X	X	X
	Conchita Subduction Zone #31 (S31)	X	X	X
	Conchita Subduction Zone #32 (S32)	X	X	X
	Conchita Subduction Zone #33 (S33)	X	X	X
	Conchita Subduction Zone #34 (S34)	X	X	X
	Conchita Subduction Zone #35 (S35)	X	X	X
	Conchita Subduction Zone #36 (S36)	X	X	X
	Conchita Subduction Zone #37 (S37)	X	X	X
	Conchita Subduction Zone #38 (S38)	X	X	X
	Conchita Subduction Zone #39 (S39)	X	X	X
	Conchita Subduction Zone #40 (S40)	X	X	X
	Conchita Subduction Zone #41 (S41)	X	X	X
	Conchita Subduction Zone #42 (S42)	X	X	X
	Conchita Subduction Zone #43 (S43)	X	X	X
	Conchita Subduction Zone #44 (S44)	X	X	X
	Conchita Subduction Zone #45 (S45)	X	X	X
	Conchita Subduction Zone #46 (S46)	X	X	X
	Conchita Subduction Zone #47 (S47)	X	X	X
	Conchita Subduction Zone #48 (S48)	X	X	X
	Conchita Subduction Zone #49 (S49)	X	X	X
	Conchita Subduction Zone #50 (S50)	X	X	X
	Conchita Subduction Zone #51 (S51)	X	X	X
	Conchita Subduction Zone #52 (S52)	X	X	X
	Conchita Subduction Zone #53 (S53)	X	X	X
	Conchita Subduction Zone #54 (S54)	X	X	X
	Conchita Subduction Zone #55 (S55)	X	X	X
	Conchita Subduction Zone #56 (S56)	X	X	X
	Conchita Subduction Zone #57 (S57)	X	X	X
	Conchita Subduction Zone #58 (S58)	X	X	X
	Conchita Subduction Zone #59 (S59)	X	X	X
	Conchita Subduction Zone #60 (S60)	X	X	X
	Conchita Subduction Zone #61 (S61)	X	X	X
	Conchita Subduction Zone #62 (S62)	X	X	X
	Conchita Subduction Zone #63 (S63)	X	X	X
	Conchita Subduction Zone #64 (S64)	X	X	X
	Conchita Subduction Zone #65 (S65)	X	X	X
	Conchita Subduction Zone #66 (S66)	X	X	X
	Conchita Subduction Zone #67 (S67)	X	X	X
	Conchita Subduction Zone #68 (S68)	X	X	X
	Conchita Subduction Zone #69 (S69)	X	X	X
	Conchita Subduction Zone #70 (S70)	X	X	X
	Conchita Subduction Zone #71 (S71)	X	X	X
	Conchita Subduction Zone #72 (S72)	X	X	X
	Conchita Subduction Zone #73 (S73)	X	X	X
	Conchita Subduction Zone #74 (S74)	X	X	X
	Conchita Subduction Zone #75 (S75)	X	X	X
	Conchita Subduction Zone #76 (S76)	X	X	X
	Conchita Subduction Zone #77 (S77)	X	X	X
	Conchita Subduction Zone #78 (S78)	X	X	X
	Conchita Subduction Zone #79 (S79)	X	X	X
	Conchita Subduction Zone #80 (S80)	X	X	X
	Conchita Subduction Zone #81 (S81)	X	X	X
	Conchita Subduction Zone #82 (S82)	X	X	X
	Conchita Subduction Zone #83 (S83)	X	X	X
	Conchita Subduction Zone #84 (S84)	X	X	X
	Conchita Subduction Zone #85 (S85)	X	X	X
	Conchita Subduction Zone #86 (S86)	X	X	X
	Conchita Subduction Zone #87 (S87)	X	X	X
	Conchita Subduction Zone #88 (S88)	X	X	X
	Conchita Subduction Zone #89 (S89)	X	X	X
	Conchita Subduction Zone #90 (S90)	X	X	X
	Conchita Subduction Zone #91 (S91)	X	X	X
	Conchita Subduction Zone #92 (S92)	X	X	X
	Conchita Subduction Zone #93 (S93)	X	X	X
	Conchita Subduction Zone #94 (S94)	X	X	X
	Conchita Subduction Zone #95 (S95)	X	X	X
	Conchita Subduction Zone #96 (S96)	X	X	X
	Conchita Subduction Zone #97 (S97)	X	X	X
	Conchita Subduction Zone #98 (S98)	X	X	X
	Conchita Subduction Zone #99 (S99)	X	X	X
	Conchita Subduction Zone #100 (S100)	X	X	X



TSUNAMI INUNDATION MAP



PROJECT: SONGS	DATE: OCT 2010	FIG: 1
PROJECT #: 09024A		



Area near Unit 1 was modified based on plant specific topography and the approximate plant footprint for Units 2 and 3.

Appendix 3

Lessons Learned from Kashiwazaki-Kariwa Nuclear Power Plant

Lessons Learned from Kashiwazaki-Kariwa Nuclear Power Plant

Prepared by: Southern California Edison and Simpson Gumpertz & Heger
December 2010

LESSONS LEARNED FROM KASHIWAZAKI-KARIWA (KK) NUCLEAR PLANT

Table of Contents

1.	INTRODUCTION	1
2.	BACKGROUND ON NCO EARTHQUAKE AT KK.....	1
3.	FINDINGS, LESSONS LEARNED AND IMPLICATIONS FOR SONGS.....	1
	3.1 INPO Significant Event Notice SEN 269	2
	3.2 EPRI Independent Review of the TEPCO Evaluation of KK	2
	3.3 IAEA Findings and Lessons Learned at KK.....	4
4.	CONCLUSION	5
5.	REFERENCES	6

Appendices

Appendix A: Assessment of INPO Findings

Appendix B: Assessment of EPRI Findings

Appendix C: Assessment of IAEA Findings

LESSONS LEARNED FROM KASHIWAZAKI-KARIWA (KK) NUCLEAR PLANT

1. INTRODUCTION

This report summarizes the lessons learned from the Kashiwazaki-Kariwa (KK) nuclear power plant following the 2007 Niigataken-Chuetsu-Oki (NCO) earthquake that occurred near the plant. The purpose of studying the lessons learned from the NCO earthquake near KK nuclear plant is to evaluate the potential for additional pre-planning or mitigation actions that could minimize plant outage times following a major seismic event at San Onofre Nuclear Generating Station (SONGS). This report identifies both the lessons learned from the KK nuclear plant following the NCO earthquake near the plant and the implications of those lessons learned to SONGS.

2. BACKGROUND ON THE NCO EARTHQUAKE AT KK

Based on the net electrical power rating, the KK plant is the largest nuclear generation facility in the world, with a total output of 7,965 megawatts (MW). This electrical output is sufficient to provide electricity to about 16 million households. The KK nuclear plant is located in the Niigata prefecture, on the northwest coast of Japan, and is operated by Tokyo Electric Power Company (TEPCO). The KK site has seven nuclear power units. Five reactors are of the boiling water reactor (BWR) type with a net installed capacity of 1,067 MW each. Two reactors are of the advanced boiling water reactor (ABWR) type with a net installed capacity of 1,315 MW each. The five BWR units commenced commercial operation between 1985 and 1994 and the two ABWRs commenced commercial operation in 1996 and 1997, respectively.

The KK nuclear plant is 16 kilometers away from the epicenter of the 2007 Niigataken-Chuetsu-Oki (NCO) earthquake (magnitude 6.6) that occurred on July 16, 2007. Ground motion recordings at the KK nuclear plant revealed that the NCO earthquake exceeded the seismic design level over a broad frequency range. Units 3, 4, and 7 automatically shutdown from 100 percent power when the units exceeded their seismic high-level shutdown set points. Unit 2 also automatically shut down during startup operations. Units 1, 5, and 6 were already shut down for planned outages at the time of the earthquake.

3. FINDINGS, LESSONS LEARNED AND IMPLICATIONS FOR SONGS

Since the occurrence of the NCO earthquake, extensive studies have been carried out by different organizations. These studies have resulted in a very broad range of lessons learned on the effects of the earthquake. Southern California Edison (SCE) has reviewed the following three reports that document the effects of the NCO earthquake on the KK nuclear plant:

- Institute of Nuclear Power Operations (INPO) Significant Event Notification SEN 269 on the Earthquake at Kashiwazaki-Kariwa, dated October 24, 2007 (INPO, 2007).
- Electric Power Research Institute (EPRI) Independent Peer Review of the TEPCO Seismic Walkdown and Evaluation of the Kashiwazaki-Kariwa Nuclear Power Plants, dated December 2007 (EPRI, 2007).

- International Atomic Energy Agency (IAEA) Mission Report on the Findings and Lessons Learned from the 16 July 2007 Earthquake at Kashiwazaki-Kariwa NPP, dated January 2009 (IAEA, 2009).

Some of the lessons learned in the referenced reports identified activities that were necessary since the NCO earthquake ground motions exceeded KK nuclear plant's seismic design basis. Activities associated with the exceedance of the design basis earthquake are not included in this SONGS study because the probability of an earthquake ground motion exceeding the SONGS design basis is extremely unlikely. SCE already had an established process to assure the complete evaluation of the impact to plant structures, systems and components (SSCs) in the remote event that an earthquake exceeded the design basis earthquake at SONGS. Additionally, during the initial design and licensing for SONGS, SCE performed extensive studies to identify and characterize faults near SONGS. These studies were used to determine the appropriate conservative ground motions from the nearby Newport–Inglewood/Rose Canyon (NI/RC) fault zone that were then factored into the plant's design.

3.1 INPO Significant Event Notice SEN 269

INPO routinely investigates events occurring at nuclear plants with the objective of identifying lessons learned from the events for the benefit of the entire nuclear power industry in the United States. INPO investigated the effects that the NCO earthquake had on the KK nuclear plant and documented the effects and lessons learned in the referenced report (INPO, 2007). Appendix A contains the detailed list of findings from the INPO report along with an assessment of how each of these findings, if applicable, relates to SONGS.

The key lessons learned from the INPO report are that:

- An integrated emergency response strategy and alternate methods of communication can improve the response to site wide events with multiple challenges.
- Fire protection capability for earthquakes should be assessed.
- Unintentional radiological liquid releases may occur following an earthquake.
- Seismic events can impact the integrity of radioactive waste storage drums or other items that are stacked without restraints.
- Items such as lighting fixtures, ventilation diffusers, cabinets, and materials should be seismically fastened in important operating spaces, such as in the main control room, to prevent falling objects from interfering with plant operations. use

3.2 EPRI Independent Review of the TEPCO Evaluation of KK

EPRI conducted an independent peer review to analyze various aspects related to the effects that the NCO earthquake had on the KK nuclear plant. The objective of EPRI's review was to assess the TEPCO seismic walkdown and evaluation program for the KK nuclear plant. The peer review used experts from the United States who possessed experience in conducting post-earthquake investigations, determining earthquake effects on power plants, and performing seismic qualifications (analysis and testing) for

nuclear plant SSCs. The findings from EPRI's review, along with how those findings relate to SONGS, are documented in Appendix B.

The scope of EPRI's review consisted of the following tasks:

- Reviewing with TEPCO cognizant engineers the performance of the KK plant systems and equipment, during and following the July 16, 2007 earthquake.
- Completing a peer review on the key elements of the TEPCO program plan to assess the damage, assure continued safe shutdown, and assess a potential restart of the KK nuclear plant units.
- Completing peer review walkdowns on selected portions of the KK plant.
- Documenting the results of the peer review and walkdowns in an EPRI report.

The peer review included a "vertical slice" assessment of the KK nuclear plant's seismic review program, and involved sampling select elements of the TEPCO program. The areas that were peer reviewed included:

- Locations that exceeded the seismic design basis where the response had been measured.
- Critical safety-related (SR) SSCs that sustained visible damage based on a peer review walkdown as well as TEPCO's records that documented TEPCO's walkdowns, inspections and non-destructive examinations.

Specific peer review focus areas included:

- Damage and degraded conditions to SR equipment and structures.
- Damage to non-safety-related (NSR) equipment and structures.
- Results of the TEPCO post-earthquake evaluations, inspections and tests.
- Recommended additional inspections, non-destructive examinations and tests, if considered necessary.
- Recommended additional analyses, if considered necessary.
- Recommended supplemental in-service inspections and surveillance tests, if considered necessary.

The key lessons learned from the EPRI independent review are as follow:

- Comprehensive programs / procedures are required in order to address the effects of major seismic events at nuclear power plants.

- Instances of damage occurred to NSR SSCs at the KK nuclear plant as a result of the NCO earthquake.

3.3 IAEA Findings and Lessons Learned at KK

Following the NCO earthquake, the government of Japan through the Japanese Nuclear and Industrial Safety Agency (NISA) invited the IAEA to assess the preliminary findings and lessons learned from the NCO earthquake in order to share them with the international nuclear community. The assessment was completed from August 6, to August 10, 2007. In January 2008, six months following the earthquake event, a second IAEA assessment was conducted. The second assessment considered the results from the investigations and studies that were performed at KK nuclear plant up to that time, as well as any corrective actions that were implemented. Following an invitation from the Japanese government, an IAEA-led team of international experts conducted an additional review from December 1, to December 5, 2008, with their purpose being to discuss and share the lessons learned from the effects of the NCO earthquake on the KK nuclear plant. The team focused its efforts on Unit 7. The results from the IAEA's assessment and follow-up effort are documented in the IAEA report, dated January 29, 2009 (IAEA, 2009). Appendix C provides a summary of the IAEA findings related to the NCO earthquake, along with a discussion of the implications to SONGS.

The scope of the IAEA's assessment and follow-up efforts were as follows:

- To review the general approach and organizational structure used by the Japanese organizations (i.e., NISA, JNES, TEPCO) that were involved in responding to the earthquake.
- To assess of the results obtained from the inspection plan performed on the SSCs at the KK nuclear plant. Specifically, the status and final results of the integrity and functional inspections / investigations (i.e., documentation, reporting, etc.) performed on the SSCs for Unit 7 were reviewed to evaluate the behavior and response to the NCO earthquake.
- To review seismic safety. The following were obtained from seismic hazard investigations:
 - Status and results from the studies and investigations conducted as a follow up to the lessons that were learned during previous geophysical, geological, seismological studies and investigations performed on-shore and off-shore. This includes results associated with determining the new seismic hazard at the site, which is necessary for evaluating the seismic safety of the plant.
 - Status and results from the assessment of the seismic response of the SSCs to the NCO earthquake, including:
 - a. An analytical simulation of the structural building response to the recorded ground motions from the NCO earthquake.
 - b. A comparison with design values and assessment of margins;
 - c. A comparison between the "original design seismic loads," "real seismic loads," and "limit state loads" for SSCs (analysis and / or tests).

- d. A comparison between the “originally calculated” and “actually recorded / evaluated” response (i.e. floor response spectra).
- Status and results from the re-evaluation of the seismic safety based on the newly defined seismic hazard, including:
- a. The criteria that were selected for the re-evaluation of the seismic safety.
 - b. Structural analyses of buildings and equipment.
 - c. Seismic qualifications of the SSCs (e.g. analysis, testing, comparison, earthquake experience data).
 - d. Results of the application of the evaluation criteria and decision and design on upgrades (if any).

The key lessons learned from the IAEA report are summarized below:

- TEPCO performed a re-evaluation of the seismic hazard at the site, which involved properly defining the ground motion that can result from a nearby fault.
- TEPCO evaluated the ground deformations. Results indicated that large ground deformations did not affect SR SSCs, but did affect road accessibility, water intakes, underground piping and facilities, electric switchyards, etc.
- TEPCO evaluated their fire protection response. As a result of the evaluation, a dedicated site fire brigade was established to be available at all times. New diverse water sources (underground tanks), water distribution piping above ground, and fire suppression upgrades in buildings were needed to improve response capabilities.

4. CONCLUSION

There are many lessons learned as a result of the NCO earthquake event and the impact it had on the KK nuclear plant. One key lesson is the need to properly determine the plant’s seismic hazard and to revalidate the plant’s design basis as new information becomes available. SCE has and continues to confirm the adequacy of the SONGS seismic design basis relative to the site’s seismic setting. While the lessons to be learned from the three independent reports of the NCO earthquake near the KK nuclear plant are applicable to SONGS, a review of SONGS’ design, processes and procedures confirmed that SONGS is properly designed and well prepared for a seismic event. The primary reason for SONGS being so well prepared for an earthquake is because SCE properly characterized the SONGS seismic hazard for its location in southern California and the plant was designed accordingly.

SCE determined the appropriate conservative ground motions from the nearby NI/RC fault zone when SONGS was originally designed and licensed. At that time, extensive studies were conducted to determine the existence and location of faults near SONGS in defining the seismic hazard at SONGS. In 1995, the validity of the original design in terms of the seismic hazard was confirmed to quantify the plant’s seismic risk. This 1995 assessment included the review of relevant and updated earthquake information for the SONGS site. This assessment affirmed the adequacy of SONGS seismic design.

SCE has an active on-going seismic program to assess the seismic hazard for the SONGS site. This program reviews new seismic data and new developments in seismic research that are relevant to SONGS. The purpose of the program is to continually assess the seismic hazards that could affect the safe operation of SONGS.

The probability of earthquake ground motions exceeding the SONGS design basis is extremely unlikely. In the remote event that an earthquake exceeded the design basis earthquake at SONGS, SCE has an established process to assure that a complete assessment is conducted to evaluate the impact that an earthquake would have on the plant's SSCs.

SONGS operators have been and are trained to use written instructions on the actions to be taken when earthquake ground motions occur at the site. These actions include determining the earthquake accelerations so that the appropriate activities will be performed to ensure plant safety.

Much of the damage to the KK nuclear plant was caused by large ground deformations. The SONGS site will not have large ground deformations because the San Mateo soil, which was studied and tested prior to constructing SONGS, is not prone to liquefaction or large soil settlement during a seismic event.

Fire protection issues at KK nuclear plant have already been addressed at SONGS. SCE maintains a full-time dedicated fire department on-site and there are multiple alternative fire protection systems available to respond to fires.

The potential for unmonitored releases of radioactive liquids to the environment from the SONGS spent fuel pools was reviewed from the KK nuclear plant. In addition, the plant was reviewed under the Ground Water Protection Initiative that included the identification of possible radiological sources, the potential for system leakage, early detection techniques, spill containment features and mitigation measures. SCE has taken actions to minimize the potential for an unintended release.

As a result of the lessons learned review, one outstanding action was identified, which involves further evaluating the offshore discharge conduits for soil liquefaction and the potential effect on plant operation.

5. REFERENCES

EPRI Independent Peer Review of the TEPCO Seismic Walkdown and Evaluation of the Kashiwazaki-Kariwa Nuclear Power Plants: *A Study in Response to the July 16, 2007, NCO Earthquake*, EPRI Report 1016317, released for public August 6, 2009.

IAEA Mission Report on the Findings and Lessons Learned from the 16 July 2007 Earthquake at Kashiwazaki-Kariwa NPP, January 29, 2009.

GeoPentech, *San Onofre Nuclear Generating Station, Seismic Hazard Assessment Program, 2010 Probabilistic Seismic Hazard Report*; December 2010.

INPO Significant Event Notification SEN 269, *Earthquake at Kashiwazaki-Kariwa*, October 24, 2007.

San Onofre Nuclear Generating Station, Units 2 and 3, Updated Final Safety Analysis Report (UFSAR); Section 2.5, Geology, Seismology and Geotechnical Engineering.

Simpson, Gumpertz & Heger, *Seismic Reliability Study for San Onofre Nuclear Generating Station*; December 2010.

Southern California Edison, *Individual Plant Examination of External Events for San Onofre Nuclear Generating Station, Units 2 & 3*; December 1995 (contains the details of the SONGS probabilistic seismic hazard assessment and the seismic probabilistic risk assessment).

APPENDIX A - Assessment of INPO Findings	
INPO – KK Findings	Discussion of Implications to SONGS
<p>1) An overall strategy is needed for managing site wide events resulting from multiple challenges. This strategy should be embedded in emergency response plans, processes, procedures, and training. Basic public services and systems lost during earthquakes or other natural disasters require strategies, contingencies, and prioritization schemes to respond to multiple challenges. The recommendations in SOER 02-1, Severe Weather, provide insights to consider in responding to a natural disaster. For natural disasters that cannot be predicted, such as earthquakes, the following lessons were identified:</p>	<p>SCE has an overall emergency response plan and procedures that consider the loss of basic public services from an emergency event and has contingencies and disaster strategies documented that address a wide range of emergencies that could occur at SONGS. Specific earthquake response plans and strategies are defined below.</p>
<p>a) Personnel resources and materials may be difficult to obtain immediately after natural disasters and need to be factored into emergency recovery plans, with realistic time frames for obtaining these resources.</p>	<p>The SONGS Emergency Response Organization (ERO) onsite at the time of the event would staff the Emergency Response Facilities, and a recall would be initiated for ERO members. Plant personnel responding to the event would work with local authorities, identifying themselves as SONGS ERO members, in order to access the site.</p> <p>Assigned members of the ERO are responsible for coordinating provisions for transportation, food, and other logistic support. They also act as a liaison with vendors to obtain additional resources such as manpower, equipment, supplies, transportation, and technical assistance to support recovery actions. Emergency procedures include the necessary actions for ERO members to take.</p>

APPENDIX A - Assessment of INPO Findings	
INPO – KK Findings	Discussion of Implications to SONGS
<p>b) Emergency recovery needs following natural disasters include near- and intermediate-term food supplies, temporary housing, drinking and domestic water, sewage treatment facilities, computer power supplies, and communication equipment alternatives and repair (such as mobile telephones and technicians capable of repairing communication equipment). These lessons were also identified during the Katrina hurricane in 2005.</p>	<p>There are emergency food and water supplies stored at various locations at SONGS, including the control area of the auxiliary building. Assigned members of the ERO would address other recovery needs. The SCE Information Technology department provides telecommunications technicians (as part of the SONGS' ERO) to repair damaged equipment. In addition, SONGS has at least six satellite phones on-site, and one at each of the California Highway Patrol (CHP) offices in San Juan Capistrano and Oceanside. There are also cell phones available, and a number of key SONGS' personnel have been issued Government Emergency Telecommunications Service (GETS) cards that give the user higher priority access to available communication circuits, whether land-line, cell phone or satellite phone. The SONGS computer servers are provided with backup power if offsite power is lost.</p>

APPENDIX A - Assessment of INPO Findings	
INPO – KK Findings	Discussion of Implications to SONGS
<p>2) Seismic events can create vulnerabilities for station fire protection systems, support equipment, and fire-fighting personnel response. Fire system piping and tanks situated throughout the station can be damaged and local fire-fighting response may be delayed, requiring contingency plans. For example, the loss of fire protection water systems may require the use of dry chemical fire trucks, tanker trucks, or other backup contingencies.</p>	<p>SCE maintains a full-time "state registered" professional fire department on-site. In addition to plant fire suppression equipment, the San Onofre Fire Department (SOFD) is equipped with two fire engines (Type 1 fully equipped) with water and foam firefighting capabilities. The SOFD maintains post seismic readiness utilizing the North Industrial Area demineralized water storage tank (DWST), which is a 150,000 gallon seismically qualified water source with a seismically qualified mobile skid mounted pump. Water can be distributed to plant areas with fire hoses. Procedures are in place to implement this system and perform visual inspections of the plant should an earthquake occur.</p> <p>In addition, there are multiple alternate water sources available, including plant systems and non-plant city water. Multiple pumping sources are also available. Over and above these sources, the SOFD maintains mutual aid agreements with the Camp Pendleton Fire and Emergency Services (CPF&ES), located on the adjacent property, and with San Diego County. These agreements provide a large number of emergency resources (i.e., fire engines, foam crash trucks, tanker trucks, and air support) to SONGS in a timely manner. Further, the SOFD has a communication plan to ensure the ability to effectively communicate with all off-site responding agencies (including law enforcement, fire, and medical), using multiple radio frequencies. The SOFD conducts routine fire drills to verify that SONGS can effectively communicate with off-site responding agencies.</p>

APPENDIX A - Assessment of INPO Findings	
INPO – KK Findings	Discussion of Implications to SONGS
<p>3) Items such as lighting fixtures, ventilation diffusers, cabinets, and materials should be securely fastened in offices and important operating spaces, such as in the main control room, to prevent falling objects from interfering with plant operations or injuring people.</p>	<p>Safe plant operation will not be affected by falling objects during and after an earthquake because SONGS seismic design criteria requires SR SSCs and NSR SSCs that could impact SR components to be designed to withstand a design basis earthquake. For example, the SONGS control room is seismically designed to ensure components like lights and ceiling panels do not fall during an earthquake. Furniture and office equipment are restrained accordingly to prevent movement and overturning. The operators have rules associated with good housekeeping for seismic considerations in the control room.</p> <p>Similarly, NSR plant office areas have a seismic design requirement to anchor or restrain items for earthquake to preclude personnel injuries.</p>
<p>4) Alternate methods of evacuating personnel from radiological controlled areas may need to be established, including designating backup locations for personnel contamination and alternate exit path monitoring.</p>	<p>Emergency Planning implementation procedures provide the methods for evacuating personnel from radiological controlled areas and the SONGS site. The procedure includes alternate locations for the site assembly areas, the use of unaffected pathways, and directing personnel to offsite reception centers when contamination is likely. The offsite Orange County reception center uses mobile showers for decontamination. San Diego has fixed showers for their reception center but also have mobile decontamination shower assets available if the fixed showers are unusable.</p>

APPENDIX A - Assessment of INPO Findings	
INPO – KK Findings	Discussion of Implications to SONGS
<p>5) Radioactive waste storage drums and other portable radioactive waste containers need to be properly restrained if stacked.</p>	<p>Drums and low specific activity (LSA) boxes containing solid low level radioactive waste are stored in the SONGS Multipurpose Handling Facility (MPHF) and may be double-stacked. Limiting the stacking height will minimize the possibility of movement and overturning of the containers. The radioactive drums at the KK nuclear plant were stacked up to three levels which increased their seismic instability. Even if the containers were to fall during an earthquake, the MPHF is designed to preclude waste from being unintentionally released to the environment.</p> <p>Stacked cargo containers or radioactive equipment material storage (REMS) boxes are located outdoors and are procedurally required to be seismically secured to prevent overturning.</p>

APPENDIX A - Assessment of INPO Findings	
INPO – KK Findings	Discussion of Implications to SONGS
<p>6) Leaks occurring during a seismic event could result in an unplanned discharge of contaminated liquid to the environment through unmonitored release paths. Guidance may be required to monitor and control these paths during seismic events. Sump pumps located adjacent to radiological controlled areas that could provide unmonitored discharge to the environment should be turned off if unexplained inputs are encountered. Alternatively, sumps with the p</p> <p>The potential for unmonitored releases should be considered for monitoring and processing through radioactive waste processing systems.</p>	<p>The potential for unmonitored releases of radioactive liquids to the environment was reviewed. Specifically, the potential for water spillage from the spent fuel pool was considered in the design of the Fuel Handling Buildings. In the unlikely event that water were to spill out of the spent fuel pool, it would go to the building sump and be managed consistent with station procedures for the control of radioactive liquids. In addition, as part of SCE's implementation of the industry Ground Water Protection Initiative, SCE evaluated the potential for unintended releases due to equipment leakage or human error. The review included the identification of possible radiological sources, the potential for system leakage, early detection techniques, spill containment features and mitigation measures. SCE has taken actions to minimize the potential for unintended releases and to enhance its groundwater protection program.</p>

APPENDIX A - Assessment of INPO Findings	
INPO – KK Findings	Discussion of Implications to SONGS
<p>7) Transformer structures, designed to contain oil leaks, may become compromised during a seismic event. Methods of mitigating the spread of transformer oil into the environment, such as the use of temporary berms or the blocking of alternate oil release paths, should be considered.</p>	<p>If a transformer leaked oil, the transformer berm would contain and prevent the oil from going into the surrounding soil and the groundwater below the site. Mitigation of any oil spill beyond the berm would be accomplished by hazmat responders, who are trained to use temporary containment measures.</p> <p>If the valve or the drain line was broken, the hazmat emergency response rig has the capability to plug drain lines. It also has the capability to either pump liquids from one berm to another if the integrity of a berm was degraded or transfer the oil to the oily waste system within the plant. This could be done by simply utilizing a diesel pump to transfer the oil to the oily waste system. To enable the use of another drain pathway in an emergency is an option that could be completed with the existing hazmat emergency response teams' equipment, and within the incident command structure. The hazmat emergency response team also has portable tanks, as well as an empty tanker that could be utilized in an emergency.</p> <p>Vacuum trucks are available through subcontractors and can be brought on-site.</p>
<p>8) Seismic events can result in the actuation of blowout panels and tornado dampers that may adversely affect secondary containment or other important ventilation systems. Station procedures should provide guidance for these potential conditions.</p>	<p>SONGS has a pressurized water reactor system and there is no secondary containment as in BWR systems. Thus, there are no blowout panels and tornado dampers inside the containment structure and this finding is not applicable to SONGS.</p>

APPENDIX B - Assessment of EPRI Findings	
EPRI – KK Findings	Discussion of Implications to SONGS
<p>1) Comprehensive programs / procedures are required in order to address the effects of significant earthquakes at nuclear power plants. These procedures should include three fundamental areas (as defined in ANSI/ANS Standard 2.23):</p> <ul style="list-style-type: none"> – Visual inspections – Operability reviews and assessments – Detailed inspections, testing, and analyses 	<p>SCE has an operating instruction for responding to earthquakes and the instruction requires operator actions, visual inspections, testing, and evaluations as specified in ANSI/ANS Standard 2.23. The amount of detailed inspections, testing, and evaluations to be performed is dependent on the level of the ground motions recorded at SONGS.</p>
<p>2) SR structures at the KK nuclear plant performed well during and following the NCO Earthquake. Based on the sampling visual inspections performed as a part of this peer review, KK SR SSCs performed very well in response to the NCO earthquake. No significant damage was detected by visual inspection on the representative SR SSCs reviewed.</p>	<p>SR SSCs have been designed to the design basis earthquake level and have seismic margin beyond those levels at SONGS.</p>
<p>3) Instances of damage occurred to NSR SSCs at the KK nuclear plant as a result of the NCO earthquake. The key examples of NSR damage noted in the EPRI study included:</p>	<p>A discussion of the implications to SONGS is provided for each of the NSR SSCs listed below.</p>
<p>a) House transformer fire</p>	<p>The house transformer fire was the result of ground settlement following the earthquake. Studies have verified that the SONGS site is not vulnerable to liquefaction or large soil settlement. The studies are documented in the Section 2.5 of the SONGS Updated Final Safety Analysis Report (UFSAR) (SONGS, UFSAR).</p>

APPENDIX B - Assessment of EPRI Findings

EPRI – KK Findings	Discussion of Implications to SONGS
<p>b) Outside tank failures (e.g., buckling, attached piping failures, and tank wall ruptures)</p>	<p>Large unanchored vertical tanks are vulnerable to buckling damage and attached piping failures. The SONGS large vertical tanks were reviewed in the SONGS seismic reliability study. Only the unanchored makeup demineralized water tanks were found to be vulnerable to a major earthquake. SCE has a backup plan to bring in portable tanks and pumps in order to maintain a demineralized water source and to continue generating electricity in the event that the makeup demineralized water tank fails.</p>
<p>c) Underground fire suppression piping failures</p>	<p>The underground fire water piping failures at the KK nuclear plant were induced by soil settlement and liquefaction. Studies have verified that the SONGS site is not vulnerable to liquefaction or large soil settlement. Even if there were to be fire water piping failures, there are multiple alternative water and pumping sources available to the SONGS fire fighters.</p>
<p>d) Yard structure foundation failures and subsidence (liquefaction induced)</p>	<p>The yard structure failures at the KK nuclear plant were induced by soil settlement and liquefaction. Studies have verified that the SONGS site is not vulnerable to liquefaction or large soil settlement.</p>

APPENDIX B - Assessment of EPRI Findings	
EPRI – KK Findings	Discussion of Implications to SONGS
e) Stack and transmission tower damage	<p>The damaged exhaust stack and steel transmission tower are both tall structures with large aspect ratios at the KK nuclear plant. The steel transmission tower damage was a single brace failure which did not result in power disruption. Since the single damaged brace was the only damaged element found among numerous towers at the KK nuclear plant site, it was concluded that there may have been a defect in the damaged brace connection. Transmission towers at SONGS are designed for greater than building code force levels and have a large ductility that provides a high seismic margin. Other SCE towers similar to the SONGS towers have sustained base damage in prior earthquakes, however, the towers remained functional and the damage was repaired in a very short time.</p> <p>The SONGS units, being pressurized water reactors, do not have a large exhaust stack similar to the ones at the KK nuclear plant, which are BWR units.</p>
f) Pump house foundation and structure failures	<p>The pump house at the KK nuclear plant failed due to an improperly designed foundation which separated when the soil foundation subsided during the earthquake. The foundation for this pump house was expanded two separate times using different foundation designs and were improperly tied together. This unique modified building foundation is not an issue at SONGS because building foundations have not been expanded and significant soil settlements will not occur in an earthquake at the SONGS site.</p>

APPENDIX B - Assessment of EPRI Findings	
EPRI – KK Findings	Discussion of Implications to SONGS
g) Water treatment component anchorage failures	The anchorage for NSR SSCs was reviewed in the SONGS seismic reliability study. SONGS mechanical components are anchored for loadings that exceed building code requirements.
h) Falling control room ceiling items (e.g., light fixtures and ceiling diffusers)	Safe plant operation will not be affected by falling objects during and after an earthquake because SONGS seismic design criteria requires SR SSCs and NSR SSCs that could impact SR components to be designed to withstand a design basis earthquake. For example, the SONGS control room is seismically designed to ensure components like lights and ceiling panels do not fall during an earthquake. Furniture and office equipment are restrained accordingly to prevent movement and overturning. The operators have rules associated with good housekeeping for seismic considerations in the control room.
4) The KK turbines exhibited some anomalies during the NCO earthquake. The main turbines in Unit 7 were reviewed by EPRI and resulted indicated that a high vibration alarm occurred during the earthquake, but tripped as a result of the automatic scram signal. TEPCO reported that was possible cause was due to the turbine shafts showing some shifting and bearing damage.	During the TEPCO post-earthquake evaluation, the turbines were disassembled and inspected for damage. While several bearings had light contact marks (including turbine bearings that were not in operation during the earthquake), there were no anomalies that would have prevented post-earthquake operation of the turbines. The SONGS turbines have been evaluated in the SONGS seismic reliability study and found to have a high seismic capability. Turbine damage due to direct shaking during a seismic event is unlikely. See the SONGS Seismic Reliability Study report for additional details (Simpson, Gumpertz & Heger, 2010).

APPENDIX B - Assessment of EPRI Findings	
EPRI – KK Findings	Discussion of Implications to SONGS
<p>5) Unanchored and poorly anchored components failed in the earthquake. In the control rooms of Units 6 and 7, several overhead lighting fixtures fell, an unanchored copy machine toppled over, one or more HVAC diffusers fell to the floor, and documents on shelves typically fell out. No significant damage was apparent and reportedly no operators were injured.</p>	<p>Safe plant operation will not be affected by falling objects during and after an earthquake because SONGS seismic design criteria requires SR SSCs and NSR SSCs that could impact SR components to be designed to withstand a design basis earthquake. For example, the SONGS control room is seismically designed to ensure components like lights and ceiling panels do not fall during an earthquake. Furniture and office equipment are restrained accordingly to prevent movement and overturning. The operators have rules associated with good housekeeping for seismic considerations in the control room.</p>
<p>6) TEPCO operators followed proper procedures following the earthquake by responding to alarms, verifying safe and stable conditions, and implementing a formal earthquake response procedure.</p>	<p>SONGS has an earthquake response procedure for earthquakes. The operators are trained on the procedure and demonstrate their proficiency during drills.</p>
<p>7) Emergency Communications had problems following the earthquake. The access door to the Technical Support Center in the Administrative Building was stuck shut for about 45 minutes following the earthquake, preventing access of personnel to the instrumentation and communication equipment in the Technical Support Center.</p>	<p>SCE maintains an emergency offsite facility (EOF) which is designed for Uniform Building Code (UBC) levels of seismic loading. The heavy shielding doors of the SONGS EOF are always propped open so access will not be an issue like the binding door scenario that the KK nuclear plant experienced. Also, the doors can be closed if required to protect the occupants of the facility due to the robust structural strength of the reinforced concrete walls.</p>

APPENDIX B - Assessment of EPRI Findings

EPRI – KK Findings	Discussion of Implications to SONGS
<p>8) The general yard area and roadways showed relatively extensive ground ruptures and subsidence due to liquefaction.</p>	<p>Studies have verified that the SONGS site is not vulnerable to liquefaction or large soil settlement.</p>
<p>9) The switchyard in the KK nuclear plant performed extremely well given the very large accelerations from the NCO earthquake. The main components of the NSR switchyard are founded on a single foundation. This foundation and the anchorages of main components were said to be designed for a static acceleration of 0.2g and appeared to be capable of withstanding significantly larger loads. Two of the four power feeds continued to supply power throughout the earthquake. The two which were not available were disconnected by protective relaying due to off-site transmission and distribution problems (i.e., power line slapping, insulator failures, and relay malfunctions).</p> <p>The only anomalies reported in the actual switchyard components were a control cabinet (mounted next to, but not on the engineered foundation) which tipped slightly but continued to function and damage to a termination plate at the top of a bushing stack which broke an oil seal.</p>	<p>The SONGS switchyard was reviewed as part of the SONGS seismic reliability study. While the power circuit breakers have been designed to withstand earthquakes, the SONGS standard dead end tower configuration and line drops to switches may sustain damage to the suspended components and the adjacent switches. Such earthquake damage is common to substation apparatus and can be quickly repaired.</p>

APPENDIX C - Assessment of IAEA Findings	
IAEA – KK Findings	Discussion of Implications to SONGS
<i>Specific Lessons Learned</i>	
1) A re-evaluation of the seismic hazard at the site is necessary. This entails properly defining the ground motion that can result from a nearby fault. Also, it is necessary to perform a probabilistic analysis of the ground motion and fault displacements.	During initial licensing SCE had already determined the appropriate conservative ground motions from the nearby NI/RC fault zone. At that time, extensive studies were conducted to identify faults near SONGS and define the seismic hazard at SONGS. These studies and evaluations are documented in the Section 2.5 of the UFSAR (SONGS, UFSAR). In 1995, a probabilistic seismic hazard assessment was performed to quantify the plant's seismic risk and the assessment included the review of relevant updated earthquake information for the SONGS site. The SONGS' seismic probabilistic risk assessment is updated accordingly to reflect any new seismic information that becomes available.
2) Large ground deformations did not affect SR SSCs, but did affect road accessibility, water intakes, underground piping and facilities, electric switchyards, etc.	The SONGS site will not have large ground deformations because the San Mateo soil was studied and tested to not be vulnerable to liquefaction or large soil settlement. The studies are documented in the Section 2.5 of the SONGS UFSAR (SONGS, UFSAR).
3) SR anchorages performed very well during the intensive seismic shaking.	The SONGS equipment is anchored as required by the SONGS seismic design criteria and will withstand seismic events without loss of function.

APPENDIX C - Assessment of IAEA Findings

IAEA – KK Findings	Discussion of Implications to SONGS
<p>4) Dedicated site fire brigade was available at all times. New diverse water sources (i.e., underground tanks), above ground water distribution piping, and fire extinguishing upgrades in buildings were needed to improve response capabilities.</p>	<p>SCE maintains a full-time "state registered" professional fire department on-site. In addition to plant fire suppression equipment, the SOFD is equipped with two fire engines (Type 1 fully equipped) with water and foam firefighting capabilities. The SOFD maintains post seismic readiness utilizing the North Industrial Area DWST, which is a 150,000 gallon seismically qualified water source with a seismically qualified mobile skid mounted pump. Water can be distributed to plant areas with fire hoses. Procedures are in place to implement this system and perform visual inspections of the plant should an earthquake occur.</p> <p>In addition, there are multiple alternate water sources available, including plant systems and non-plant city water. Multiple pumping sources are also available. Over and above these sources, the SOFD maintains mutual aid agreements with the CPF&ES, located on the adjacent property, and with San Diego County. These agreements provide a large number of emergency resources (i.e., fire engines, foam crash trucks, tanker trucks, and air support) to SONGS in a timely manner. Further, the SOFD has a communication plan to ensure the ability to effectively communicate with all off-site responding agencies (including law enforcement, fire, and medical), using multiple radio frequencies. The SOFD conducts routine fire drills to verify that SONGS can effectively communicate with off-site responding agencies.</p>

APPENDIX C - Assessment of IAEA Findings	
IAEA – KK Findings	Discussion of Implications to SONGS
<i>Lessons Learned from Findings Sheets</i>	
<i>Finding A.1-01 Exceedance of the Design Basis Ground Motion by the Earthquake</i>	
<p><i>Fault Mechanism and Directivity</i> Near source fault effects are to be considered in the seismic hazard.</p>	<p>These effects were evaluated in the probabilistic seismic hazard assessment for SONGS in 2001. The result of adding these effects was an insignificant change to the seismic risk of the plant.</p>
<p><i>Local Geological Conditions</i> Differences in the site geology need to be considered for all units.</p>	<p>Site geology is the same for SONGS Unit 2 and Unit 3. Both are underlain with San Mateo formation to the same depth as documented in Section 2.5 of the UFSAR (SONGS, USFAR).</p>
<p><i>Attenuation Relationships</i> Attenuation relationships play an important part in seismic hazard assessments and there has been new equations developed from the recent available earthquake records. When seismic sources are present near the site vicinity, it is necessary to take into consideration the recent records obtained in the near field.</p>	<p>Since the construction of SONGS, there have only been small ground motions recorded due to distant earthquakes, like the Northridge and Landers earthquakes. There are no recent earthquake records near SONGS that can be used to determine a specific attenuation relationship for SONGS. The latest developed attenuation relationships are used for the probabilistic seismic hazard updates for SONGS.</p>
<p><i>Accounting for Uncertainties</i> Identification and quantification of aleatory (random) and epistemic (modeling) uncertainties are very important and is usually not straightforward. The data used needs to be qualified in terms of its reliability and the methods need to allow for alternative models.</p>	<p>The SONGS probabilistic seismic hazard incorporates both the aleatory and the epistemic uncertainties. These uncertainties are documented in the SONGS seismic hazard report.</p>

APPENDIX C - Assessment of IAEA Findings	
IAEA – KK Findings	Discussion of Implications to SONGS
<p><i>Importance of Seismic Instrumentation</i> Immediate indication to the operator of the severity of earthquake needs to be considered.</p>	<p>The SONGS seismic instrumentation provides the data to the operators and engineers when an earthquake occurs. SONGS earthquake procedure describes the analysis requirements for determining the seismic accelerations when an earthquake’s ground motions are recorded at the plant.</p>
<i>Finding A1-02 Re-Evaluation of the Seismic Hazard</i>	
<p><i>Need for Strengthening of the Database to Decrease Uncertainties</i> Investigations both on land and offshore would significantly enhance the geological database and help in reducing uncertainties regarding fault existence, location, and characterization.</p>	<p>SCE determined the appropriate conservative ground motions from the nearby NI/RC fault zone when the plant was licensed. At that time, extensive studies were conducted in looking for faults near SONGS and defining the seismic hazard at SONGS. These studies and evaluations are documented in the Section 2.5 of the UFSAR. In 1995, a probabilistic seismic hazard assessment was performed to quantify the plant's seismic risk and the assessment included the review of relevant updated earthquake information for the SONGS site. This assessment affirmed the adequacy of the SONGS seismic design. An on-going seismic program is in place to review the seismic setting in the vicinity of SONGS as seismic understanding evolves and new data becomes available.</p>
<p><i>Use of Deterministic and Probabilistic Methods</i> Probabilistic seismic hazard will be needed to quantify the variety of seismotectonic settings and their uncertainties. This would be used in a probabilistic seismic hazard analysis of the plant.</p>	<p>SCE conducted a probabilistic seismic hazard assessment in 1995. The probabilistic seismic hazard assessment is updated to incorporate new seismic information as part of an on-going seismic program that continually reviews the seismic hazard at SONGS.</p>

APPENDIX C - Assessment of IAEA Findings	
IAEA – KK Findings	Discussion of Implications to SONGS
<p><i>Faults in Near Region</i> Fault mechanisms and directivity can play an important role in a near fault ground motion.</p>	<p>The SONGS seismic hazard uses attenuation relationships which incorporate these concepts. These effects were evaluated in the probabilistic seismic hazard assessment for SONGS in 2001. The result of adding these effects was an insignificant change to the seismic risk of the plant.</p>
<p><i>Local Geological Conditions</i> The variation of the geological conditions both in terms of age and depth played a role in the damage patterns to NSR items at the KK nuclear plant.</p>	<p>Site local geology is the same for SONGS Unit 2 and Unit 3. Both are underlain with San Mateo formation to the same depth as documented in Section 2.5 of the UFSAR (SONGS, UFSAR).</p>
<p><i>Construction of Seismotectonic Model</i></p>	<p>Seismic hazard for SONGS includes the proper characterization of uncertainties, and different seismic source models, such as fault lengths and fault capabilities, in predicting the probabilistic seismic hazard.</p>
<p><i>Treatment of Uncertainties</i></p>	<p>The SONGS probabilistic seismic hazard incorporates both the aleatory and the epistemic uncertainties. These uncertainties are documented in the SONGS seismic hazard report.</p>
<p><i>Ground Motion Characterization</i></p>	<p>The latest attenuation relationships are being used for the current probabilistic seismic hazard update for SONGS.</p>
<p><i>Assessment of Potential Surface Faulting at the Site</i></p>	<p>Not applicable to SONGS. Based on-site excavations at the time of the plant construction, no credible surface faulting exists or was found within the plant boundary.</p>

APPENDIX C - Assessment of IAEA Findings	
IAEA – KK Findings	Discussion of Implications to SONGS
<i>Soil Failures at the Site</i>	Studies have verified that the SONGS site is not vulnerable to liquefaction or large soil settlement. The studies are documented in the Section 2.5 of the SONGS UFSAR (SONGS, UFSAR).
<i>Probabilistic Seismic Hazard Analysis</i>	SCE conducted a probabilistic seismic hazard assessment in 1995. The probabilistic seismic hazard assessment is updated to incorporate new seismic information as part of an on-going seismic program that continually reviews the seismic hazard at SONGS.
<i>Finding A2-01 Offsite Power</i>	
The loss of offsite power for earthquake events greater than 0.25g may be conservative in countries like Japan where seismic design of electric facilities is relatively advanced.	The finding acknowledges the conservatism of assuming an earthquake will cause the loss of offsite power. However, SCE has and will continue to conservatively assume the loss of offsite power in its accident scenarios in response to a seismic event.
<i>Finding A2-02 Seismic System Interactions</i>	
Diligence is required in the design, construction, and operation of all plants to ensure seismic system interaction issues are minimized.	SCE performed a system interaction review as part of the seismic probabilistic risk assessment in 1995, which remains valid today. The system interactions included seismic induced fire and flooding, and seismic interaction of NSR components.

APPENDIX C - Assessment of IAEA Findings	
IAEA – KK Findings	Discussion of Implications to SONGS
Plant walkdowns performed to evaluate conditions for potential seismic vulnerabilities should extensively consider the potential consequences of failures due to non-seismic conditions.	Plant walkdowns were conducted by experienced and trained engineers in doing the system interaction review for the seismic probabilistic risk assessment in 1995. The walkdowns identified some potential vulnerabilities such as closely spaced electrical panels and a non SR ammonia tank. These vulnerabilities were addressed to preclude failure during a design basis earthquake event.
A seismic system interaction program for spray and flooding hazards should be implemented to verify the lack of failure of sources of water and / or verify that no negative consequences to SR equipment if leaks or failures occur.	SCE performed a system interaction review as part of the seismic probabilistic risk assessment in 1995, which remains valid today. The system interactions included seismic induced fire and flooding, and seismic interaction of NSR components.
The capacities of non SR SSCs should be verified when considering the new seismic hazard for seismic evaluation of existing nuclear power plants.	The review of NSR SSCs is documented in the SONGS seismic reliability report.
<i>Finding A2-03 Fire Protection</i>	
Seismically induced fires are frequent events after an earthquake in urbanized areas, but are relatively rare at a nuclear power plant.	A seismic / fire interaction review and walkdown were conducted as a part of the seismic probabilistic risk assessment in 1995 at SONGS. The review did not reveal any vulnerability that would have significantly increased the plant's seismic / fire risk.

APPENDIX C - Assessment of IAEA Findings

IAEA – KK Findings	Discussion of Implications to SONGS
<p>Common cause failure should be avoided. Failure of the fire fighting system (including tanks, pumps, piping, and distribution systems) and its consequences can be minimized by providing adequate seismic capacity, redundancy, and diversification of the systems.</p>	<p>SCE maintains a full-time "state registered" professional fire department on-site. In addition to plant fire suppression equipment, the SOFD is equipped with two fire engines (Type 1 fully equipped) with water and foam firefighting capabilities. The SOFD maintains post seismic readiness utilizing the North Industrial Area DWST, which is a 150,000 gallon seismically qualified water source with a seismically qualified mobile skid mounted pump. Water can be distributed to plant areas with fire hoses. Procedures are in place to implement this system and perform visual inspections of the plant should an earthquake occur.</p> <p>In addition, there are multiple alternate water sources available, including plant systems and non-plant city water. Multiple pumping sources are also available. Over and above these sources, the SOFD maintains mutual aid agreements with the CPF&ES, located on the adjacent property, and with San Diego County. These agreements provide a large number of emergency resources (i.e., fire engines, foam crash trucks, tanker trucks, and air support) to SONGS in a timely manner. Further, the SOFD has a communication plan to ensure the ability to effectively communicate with all off-site responding agencies (including law enforcement, fire, and medical), using multiple radio frequencies. The SOFD conducts routine fire drills to verify that SONGS can effectively communicate with off-site responding agencies.</p>

APPENDIX C - Assessment of IAEA Findings

IAEA – KK Findings	Discussion of Implications to SONGS
<p>Large soil settlements can cause piping failure. Flexible joints, flexible penetrations, protective buried channels, and other means could be used to minimize the probability of failure.</p>	<p>Not applicable to SONGS. Large settlements are not expected at SONGS due to the competent soil. In addition, alternate sources of fire suppression exist at SONGS if the underground fire water piping were to fail. These alternate sources include foam fire fighting as well as additional water sources (alternate water tanks and pumps with hoses are part of the emergency fire fighting plan).</p>
<p>For nuclear power plants located in coastal areas, corrosion problems could affect the resistance of fire protection systems exposed to the exterior environment. The use of corrosion resistant material and the implementation of an adequate inspection program will be important to prevent unexpected failures due to earthquake occurrence.</p>	<p>SCE has a maintenance program which inspects fire protection equipment for degradation including the effects of corrosion. Also, SCE maintains cathodic protection for underground piping, and has a program to evaluate the condition of underground piping. Since fire protection systems are quality affecting at SONGS, nonconforming or degraded conditions are identified and placed in the plant’s corrective action program. Therefore, the SONGS fire protection system is maintained and monitored to preclude unexpected failures.</p>

APPENDIX C - Assessment of IAEA Findings	
IAEA – KK Findings	Discussion of Implications to SONGS
<p>It would be helpful to give due consideration to important aspects, such as secondary effects of fire suppression systems, spurious operation of automatic fire protection systems, and fire related explosions.</p>	<p>Consideration of these aspects was given with respect to their effects on the SR systems at SONGS. The lessons learned from KK nuclear plant on fire protection system failures and fires from the earthquake identified soil failure and the resulting large deformations imposed on the system equipment. SONGS has studied the potential for soil failures as a result of a large earthquake and found those soil related failure modes to not be applicable to SONGS because the San Mateo soil will not have significant soil settlements or soil liquefaction. The studies are documented in the Section 2.5 of the SONGS UFSAR (SONGS, USFAR).</p>
<p>The confirmation of appropriate staffing of the in-house fire brigade including addressing the scenarios involving the occurrence of multiple fires should be completed.</p>	<p>SCE maintains a full-time "state registered" professional fire department on-site. A required minimum staffing level is maintained at all times that is sufficient to respond to events involving multiple fires.</p>
<p>Communications with the local authorities, media, and the public during emergency situations can be made easier by establishing a permanent dialogue between stakeholders, the regulators, and the licensees.</p>	<p>SONGS emergency response team has a thorough set of procedures which include communication requirements with all affected stakeholders and regulators in the event of an emergency such as an earthquake. Also see above for more details about the communication plan.</p>

APPENDIX C - Assessment of IAEA Findings	
IAEA – KK Findings	Discussion of Implications to SONGS
First responders to fires from a major natural disaster should not be restrained from performing their functions due to failure of their systems.	The fire protection systems at SONGS have multiple sources to ensure that even if a particular system were to fail, that there are backup systems to ensure fire protection capability. These backup systems include alternate water sources and a fire pump that can use hoses for obtaining water from tanks.
Seismic design of fire brigade building should be similar to the seismic design criteria used for other critical portions of the nuclear plant and should not collapse.	SONGS has a fire protection system that has the capability to withstand the design basis earthquake. The system is located outdoors and includes a water storage tank and diesel powered pump with the use of fire hoses. The fire fighters are housed in a portion of the AWS Building that would not collapse during a design basis earthquake.
<i>Finding A2-04 Soil Deformation</i>	
In case of large seismic shaking, large ground deformations are frequently inevitable. Nevertheless, measures to limit their effects could be taken.	Not applicable to SONGS because the San Mateo soil will not have significant soil settlements or soil liquefaction. Studies have verified that the SONGS site is not vulnerable to liquefaction or large soil settlement. The studies are documented in the Section 2.5 of the SONGS UFSAR (SONGS, UFSAR).

APPENDIX C - Assessment of IAEA Findings	
IAEA – KK Findings	Discussion of Implications to SONGS
Backfilling measures could be taken including the use of proper soil materials for backfill and proper soil compacting, the protection of the penetration by expansion joints that can allow large displacements and/or concrete channels to protect the underground piping, lowering groundwater levels, etc.	SONGS backfill requirements used only San Mateo soil or a cement-sand slurry mix. These materials provided similar soil properties to the native San Mateo soil and thus will not have significant soil settlements or soil liquefaction.
Although the observed large ground deformations did not affect SR SSCs, these ground deformations had an influence on the overall performance of the plant including impeding the ability to carry out immediate actions following an earthquake. Road accessibility, water intakes, underground piping and facilities, electrical switchyards, etc. could be significantly and adversely affected by large ground deformations.	Not applicable to SONGS because the San Mateo soil is not subject to significant soil settlements or soil liquefaction. Studies have verified that the SONGS site (onshore) is not vulnerable to liquefaction or large soil settlement. The studies are documented in the Section 2.5 of the SONGS UFSAR (SONGS, UFSAR). The NSR offshore discharge conduits may be affected by soil liquefaction offshore as identified in the SONGS Seismic Reliability Study report (Simpson, Gumpertz & Heger, 2010). The offshore conduits will be evaluated to determine the potential effect on plant operations.
<i>Finding A2-05 Anchorage Behavior</i>	
The long term behavior of anchorages should be guaranteed by a proper aging management program.	SCE conducts structural inspection activities as part of a Nuclear Regulatory Commission (NRC) required maintenance program that includes the periodic review of anchorages for SR equipment.

APPENDIX C - Assessment of IAEA Findings	
IAEA – KK Findings	Discussion of Implications to SONGS
<p>Anchorage of SR SSCs at the KK nuclear plant performed very well. Specific details and design practice presented by TEPCO will contribute to increasing the seismic safety of anchorages.</p>	<p>The SONGS SR equipment is anchored as required by the SONGS seismic design criteria and will withstand seismic events without loss of function.</p>
<i>Finding A2-06 Basic Integrity Assessment Policy</i>	
<p>Basic policy to assess the integrity of the KK nuclear plant due to an earthquake exceeding the plant’s design basis. This basic policy uses a methodology based on the combination of inspections and analyses to determine the integrity of SSCs.</p> <p>The KK nuclear plant inspection plan is recommended to be made available to the nuclear community.</p>	<p>The basic integrity assessment policy provides a comprehensive inspection / evaluation plan for a plant that has experienced seismic ground motions which have exceeded the plant’s design basis.</p> <p>The details of the policy are provided in Appendix IV of the IAEA report and are useful to SONGS for the purpose stated above (IAEA, 2009).</p>

APPENDIX C - Assessment of IAEA Findings	
IAEA – KK Findings	Discussion of Implications to SONGS
<i>Findings A3-01 Operational Safety Management Response After Shutdown</i>	
The accident management of the event in all units was successfully carried out with respect to the operation of the reactor safety systems. The availability of both operating and safety systems and the existence of applicable accident procedures ensured the safety of the units and demonstrated the strength of maintaining several levels of defenses in depth.	SONGS has an operating instruction for earthquakes and includes specific operator actions, visual inspections, testing, and evaluations. The amount of detailed inspections, testing and evaluations to be performed is dependent on the level of the ground motion recorded at SONGS.
Verification of readiness for operation of the safety systems that were not activated was carried out through visual inspection. It should be carefully analyzed if this procedure is sufficient or if it should be the accepted practice to test with full activation of safety systems without substantial delay after the occurrence of an earthquake.	Not applicable for SONGS since no extreme event has occurred at the site. If a major seismic event were to occur, SONGS has an operating instruction for earthquakes and includes specific operator actions, visual inspections, testing, and evaluations. The amount of detailed inspections, testing and evaluations to be performed is dependent on the level of the ground motion recorded at SONGS.
There was a time delay in reporting the leakage of radioactive material to the authorities. Information from the plant should have been issued more promptly. It is of key importance to report information on releases of radioactive material to the authorities as soon as possible to provide guidance for off-site emergency organizations, even if no significant releases have occurred or are expected to occur as a result of the event.	SONGS emergency planning procedures have specific reporting requirements and schedules for the unintended release of radioactive materials from the plant. In addition, there is a voluntary communication protocol for the Ground Water Protection Initiative which applies to unintended releases. The voluntary communication protocol is made to designated stakeholders and the NRC.

APPENDIX C – Assessment of IAEA Findings	
IAEA – KK Findings	Discussion of Implications for SONGS
<i>Finding A3-02 Releases</i>	
<p>Although no releases of radioactive material from the reactor core due to the earthquake were detected, careful attention should be paid to other possible sources of releases, even if the releases are of limited low amounts.</p>	<p>The potential for unmonitored releases of radioactive liquids to the environment was reviewed. SCE evaluated the potential for unintended releases due to equipment leakage or human error. The review included the identification of possible radiological sources, the potential for system leakage, early detection techniques, spill containment features, and mitigation measures. SONGS has taken actions in accordance with the Ground Water Protection Initiative to minimize the potential for an unintended release and to enhance its groundwater protection program.</p>

Appendix 4

**Seismic Reliability Study of San Onofre Generating Station Non-Safety-Related
Structures, Systems, and Components**



Seismic Reliability
Study of San Onofre
Nuclear Generating
Station Non-Safety
Related Structures,
Systems, and
Components

San Onofre Nuclear
Generating Station
San Onofre, California
January 2011

SGH Project 108036

SIMPSON GUMPERTZ & HEGER



Engineering of Structures
and Building Enclosures

PREPARED BY:

Southern California Edison
5000 Pacific Coast Highway
San Clemente, CA

and

Simpson Gumpertz & Heger Inc.
4000 MacArthur Boulevard
Seventh Floor, Suite 710
Newport Beach, CA
Tel: 949.930.2500
Fax: 949.885.0456

Table of Contents

1.	OBJECTIVE	1
2.	PLANT INFORMATION	2
2.1	Plant Location and Configuration	2
2.2	SONGS Seismic Design Basis	3
3.	STUDY METHODOLOGY	5
3.1	Phase I – Identify Important-to-Reliability NSR SSCs	6
3.2	Phase II – Identify Seismic Capacity Screening Criteria	7
3.3	Phase III – Determine SONGS Review Level Earthquake	8
3.4	Phase IV – Evaluate Seismic Capacity of Important-to-Reliability NSR SSCs	10
3.5	Phase V – Develop Repair / Replacement Duration Estimates and Mitigation Plans	13
3.6	Screening Process for NSR Buildings that House Important-to-Reliability SSCs	14
4.	RELIABILITY STUDY RESULTS	15
4.1	SONGS Important-to-Reliability NSR SSCs	15
4.2	Capacity Evaluation Results	17
4.2.1	SSCs with Seismic Capacity Greater Than the SONGS Review Level Earthquake	18
4.2.2	SSCs with Seismic Capacity Less Than the SONGS Review Level Earthquake	21
4.2.3	SSCs Requiring Additional Analysis for Seismic Capacity Assessment	24
4.3	Repair and Replacement Duration Estimates	24
4.3.1	Plant Yard Electrical Components	26
4.3.2	Switchyard Components	27
4.3.3	Makeup Demineralized Water Tanks	27
4.4	Mitigation Plans	27
5.	CONCLUSIONS	28
6.	REFERENCES	29

APPENDICES

Appendix A	List of Acronyms
Appendix B	Equipment Classification List
Appendix C	Electrical Equipment List
Appendix D	Mechanical Equipment List
Appendix E	Evaluation of Important-to-Reliability NSR Building Structures

1. OBJECTIVE

The objective of this study is to identify important-to-reliability, non-safety-related (NSR) structures, systems, and components (SSCs) at the San Onofre Nuclear Generating Station (SONGS) that could be the cause of a prolonged outage due to a major seismic event. Specifically, the study evaluates NSR SSCs that are required for power generation, including the switchyard, which are, for the purposes of this study, identified as important-to-reliability.

2. PLANT INFORMATION

2.1 Plant Location and Configuration

SONGS consists of two nuclear reactor units, San Onofre Unit 2 and San Onofre Unit 3, which are each capable of generating approximately 1,100 megawatts (MW) of electrical power. Each unit is a separate and independent power plant with no common support equipment required for power generation, with the exception of the site fire protection, carbon dioxide (CO₂) and nitrogen (N₂) supply, and instrument air. The power generation portions of each plant are virtually identical.

SONGS is located along the Pacific coastline south of San Clemente and west of Interstate Highway 5. The plant is located entirely within the boundaries of the U.S. Marine Corps Camp Pendleton Base in northern San Diego County. An aerial view of the site is shown on Figure 2-1. The site was created by excavating the original bluff to remove the terrace deposits and create a level area for the plant on what is known as the San Mateo Sandstone Formation, which consists of very dense sand approximately 900 feet (ft) deep with an average shear wave velocity of approximately 1,900 feet per second (ft/sec) in the top 100 to 150 ft depth. The site soils directly supporting the plant structures were extensively investigated during plant construction and found not to be susceptible to liquefaction. The switchyard is located on a slope that rises to the original bluff level. There are two benches cut into the slope that provide the access roads for the two bus lines that comprise the switchyard. There are offices and shop / storage buildings adjacent to the plant's operational structures. The buildings shown on Figure 2-1, which are east of Interstate 5, are additional offices and warehouse facilities that support the plant's operations.

The SONGS units use ocean water to condense the pressurized steam that has expanded through the turbines and to provide cooling of other plant water systems through heat exchangers. The ocean water for each unit is channeled from offshore intake structures through buried conduit systems to the on-shore intake structure where it is channeled to the circulating water pumps of each unit. The water from each unit is then discharged back to the ocean through separately buried offshore discharge conduits.

SONGS is licensed by the U.S. Nuclear Regulatory Commission (NRC), which issues policies and regulations governing the initial construction, modifications, and operations of nuclear power reactors.



Figure 2-1 Aerial Site View of Both Units

2.2 SONGS Seismic Design Basis

Each of the two units contains safety-related (SR) SSCs and NSR SSCs. The plant's SR SSCs include, but are not limited to, the reactor, nuclear steam supply system (NSSS), containment, and associated emergency equipment. The NRC regulates the design parameters and operation of SR SSCs, which have been designed to allow for the safe-shutdown of a nuclear power plant in the event of a large seismic event, specifically the design-basis earthquake (DBE). The DBE, also known as the safe-shutdown earthquake by the NRC, is associated with an extremely low probability of occurrence.

The SONGS Updated Final Safety Analysis Report (UFSAR), (UFSAR, Current) identifies three categories of SSCs that have specific seismic design criteria.

- **Seismic Category I (SC I).** All SC I SSCs are SR and are, therefore, not evaluated as part of this study¹. SC I SSCs are designed to remain functional and / or retain structural integrity if a DBE occurs. SC I SSCs must meet the DBE design conditions, as mandated by the NRC and specified in the Code of Federal Regulations (CFR) (10CFR100AppA, Current). The design requirements for SC I SSCs are determined by using a design spectrum shape that has a peak ground acceleration (PGA) value of 0.67g.

¹ SC I SSCs are not evaluated as part of this study (CEC, 2008) because they are designed to withstand a safe-shutdown earthquake without damage.

- **Seismic Category II (SC II).** All SC II SSCs are NSR and were evaluated as part of this study. SONGS SC II SSCs include equipment whose limited damage could interrupt power generation. SC II SSCs, with the exception of the switchyard, were designed to meet an effective static seismic design loading of 0.20g horizontal and 0.13g vertical with no increase factor on allowable stress values. In addition, the design involved verifying that the effective static seismic design loading was not lower than the building code requirements at the time of the design. This was the general seismic design criteria for all Southern California Edison (SCE) power plant structures and equipment anchorage which were in use at the time of plant design.

The 230 kilovolt (kV) switchyard SSCs were designed to meet the SCE transmission facility effective static seismic design loading of 0.50g horizontal, which was the SCE transmission facility design criterion in use at the time of plant design. This SCE substation design criterion was adopted following the 1971 San Fernando earthquake.

- **Seismic Category III (SC III).** SC III SSCs are NSR SSCs that are not SC I or SC II SSCs but whose failure could inconvenience normal plant operations. Only a few of these SC III SSCs were considered within the scope and evaluated as part of this study. These SSCs were designed to meet the building code requirements at the time of design.

In addition to the three SC categories, there is an additional classification for those SC II SSCs that are located in close proximity to SC I SSCs. These SSCs are required to maintain their structural integrity, including the anchorage at a DBE loading level. This special case of SC II SSCs is denoted as seismic interaction (SI) II/I and is defined as equipment that is not SC I but whose collapse or failure could result in the loss of the safety functions of SC I SSCs.

The design criteria for the plant are viewed as minimum allowable values per the applicable codes and standards that are associated with the SSCs. These standard allowable values have a built-in seismic margin, although there is often a significant seismic margin beyond the built-in margin due to conservatism that are integrated in the design process.

3. STUDY METHODOLOGY

The following five-phase approach was developed to address the important-to-reliability NSR SSCs.

- 1) Phase I – Identify important-to-reliability NSR SSCs
- 2) Phase II – Identify seismic capacity screening criteria
- 3) Phase III – Determine SONGS review level earthquake
- 4) Phase IV – Evaluate seismic capacity of important-to-reliability NSR SSCs
- 5) Phase V – Develop repair / replacement duration estimates and mitigation plans

Figure 3-1 provides an overview of these sequential phases. A similar phased approach is used for NSR buildings that house important-to-reliability SSCs. A different methodology is used for Phase IV to evaluate the capacity of NSR buildings that house important-to-reliability SSCs. This methodology is summarized separately in Section 3.6.

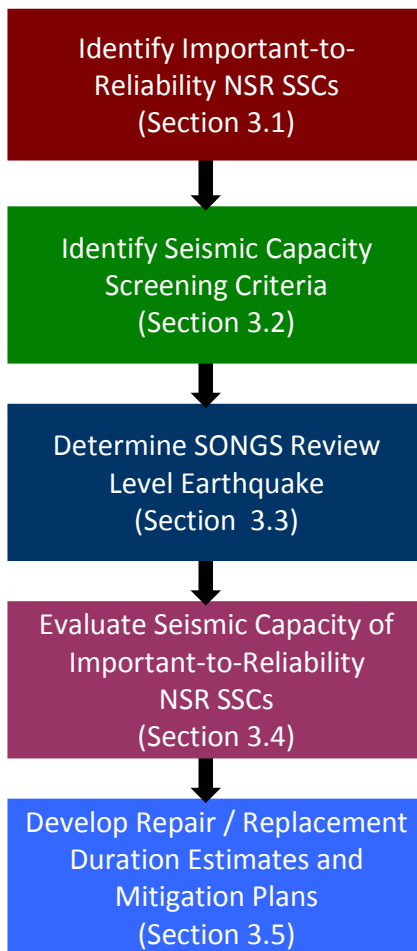


Figure 3-1 Methodology Overview

3.1 Phase I – Identify Important-to-Reliability NSR SSCs

The first phase of this process involves identifying the important-to-reliability NSR SSCs. Figure 3-2 shows the general logic flow that is used to identify the important-to-reliability NSR SSCs. Only NSR SSCs that are required for power generation are included in the final list. The first step involves reviewing the SCE Quality and Classification List (SCE Document No. 90034), which is a list that contains the SSCs at SONGS and their seismic category (SCE, 2009). The next step consists of removing the SSCs in the SCE Quality and Classification List that are outside the scope of this study. First, the SC I SSCs are identified and removed from consideration given that they are outside of the scope. Then, the SSCs not required for power generation are identified and removed from consideration because these SSCs do not impact the power generation reliability. The SSCs remaining on the list constitute the important-to-reliability NSR SSCs (see Appendix B).

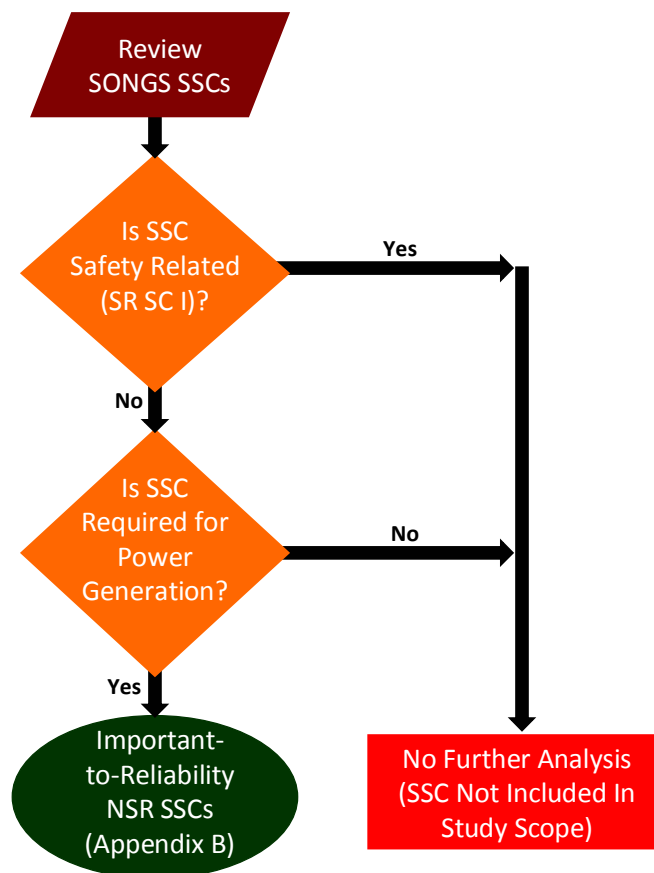


Figure 3-2 Important-to-Reliability NSR SSCs Identification Process

3.2 Phase II – Identify Seismic Capacity Screening Criteria

The next phase involves identifying the seismic capacity screening criteria. NSR SSCs are, at a minimum, designed to meet the building code seismic requirements at the time that they were designed. However, historical earthquake performance has shown that such equipment typically has inherent seismic capacity much greater than the minimum building code seismic requirements. Over the past 20 years, a group known as the Seismic Qualification Utility Group (SQUG)² has collected data and documented the results about the performance of various SSCs at large power / industrial plants during and following an earthquake (referred to as earthquake experience data) (SQUG, 1991). SQUG averaged the earthquake response spectra³ of sites having facilities with representative SSCs that experienced strong ground motion seismic events to determine a ground motion level for which power plant SSCs have survived without damage. This ground motion level is described by a seismic capacity spectrum (referred to as the “reference spectrum” by SQUG). The 5% damping seismic capacity spectrum is characterized by a spectral acceleration level of 1.2g over a frequency range of 2.5 to 7.5 hertz (Hz) and a PGA of 0.5g, which is depicted on Figure 3-3 as the bold line.

² SQUG was formed in the early 1980s to develop a generic methodology to resolve Unresolved Safety Issue (USI) A-46, which was concerned with verifying the seismic adequacy of equipment that was already installed in operating nuclear power plants. Working in conjunction with the regulatory authorities and industry, SQUG developed a methodology and procedure to apply earthquake experience data to demonstrate the seismic capacity of electrical and mechanical equipment for resolution of USI A-46. SQUG developed the "Generic Implementation Procedure (GIP) for Seismic Verification of Nuclear Plant Equipment" which provided a generic means of applying this experience data to evaluate the seismic adequacy of mechanical equipment, electrical equipment, distributive systems (i.e., ducting, cable trays, conduit, etc.) and passive items (i.e., tanks, heat exchangers, etc.) that are typically part of the balance of plant at a nuclear power plant (SQUG, 1991). The GIP implements this SQUG approach and includes the technical approach, generic procedures, and engineering guidance. The NRC embraced the use of experience-based methods for resolution of USI A-46 in Generic Letter (GL) 87-02, "Verification of Seismic Adequacy of Mechanical and Electrical Equipment in Operating Reactors, Unresolved Safety Issue (USI) A-46" (NRC, 1987).

³ A response spectrum is defined as a plot of the maximum response of an array of single-degree-of-freedom systems of different natural frequencies, each having a damping value expressed as a percentage of critical damping.

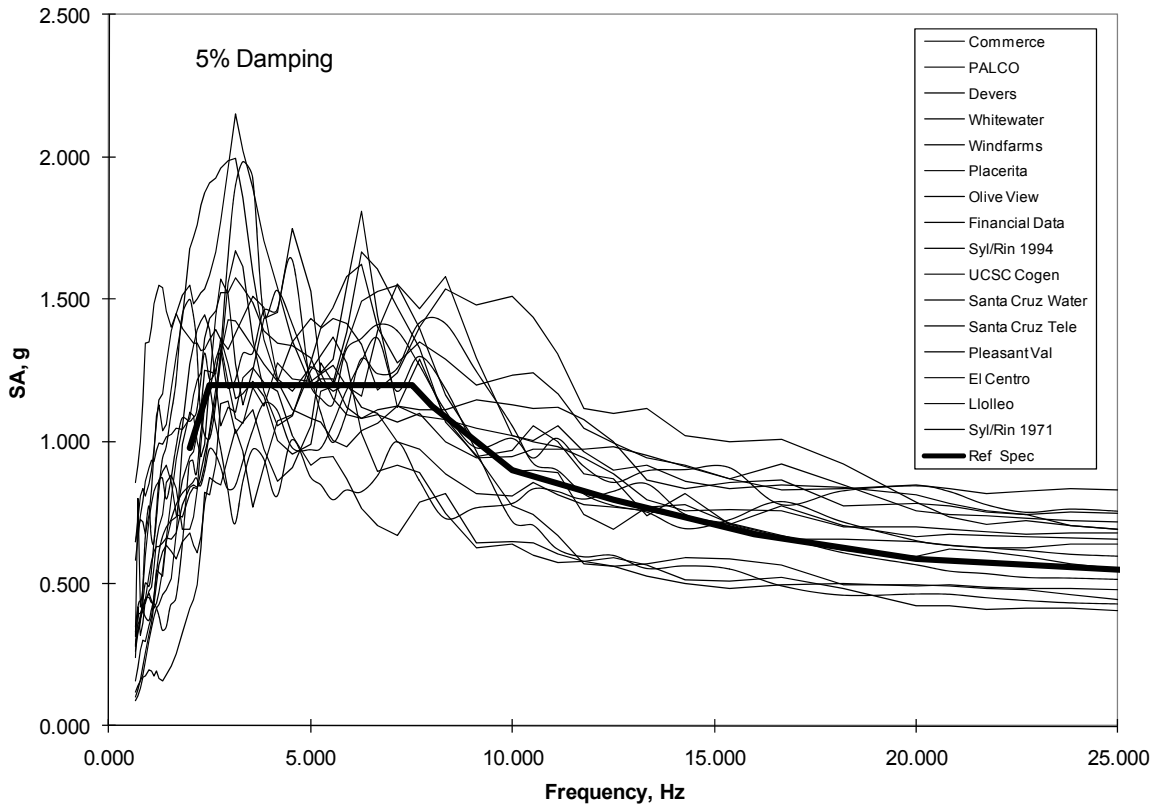


Figure 3-3 Average Horizontal Response Spectra for SQUG Database Sites Compared to the Seismic Capacity Spectrum (also known as the Reference Spectrum)

Based on the number and diversity of SSCs that have survived the motion level represented by the seismic capacity spectrum, this motion level was established as a high confidence of a low probability of failure (HCLPF) (EPRI, 1994, 2002 and 2009). As such, the seismic capacity spectrum does not represent a failure level but rather a level for which there is a high confidence that failure of the SSCs will not occur. The data contained in the SQUG database demonstrate that the actual mean failure level, otherwise known as fragility, is typically at least 2 to 3 times the seismic capacity spectrum (EPRI, 2002 and 2009). This failure margin allows the seismic capacity spectrum to be used as a conservative measure of seismic capacity to screen the important-to-reliability NSR SSCs for the site-specific seismic demand conditions.

3.3 Phase III – Determine SONGS Review Level Earthquake

The seismic capacity spectrum was derived using actual earthquake experience data and represents a conservative measure of seismic capacity for the important-to-reliability NSR SSCs. To understand if this capacity is sufficient to demonstrate adequate reliability for power generation, the seismic demand that is bound by the seismic capacity needs to be determined considering the location and the site-specific conditions at SONGS. Site-specific earthquake

ground motion conditions are described by the SONGS probabilistic seismic hazard analysis (PSHA) that was recently updated in 2010 (SCE, 2010).

The SONGS 2010 PSHA determined each spectral acceleration value associated with a given oscillator frequency as a function of annual return period. The annual return period is the number of years it may take for the spectral acceleration value to occur (i.e., a 1,000-year return signifies that the value may occur once in 1,000 years). These sets of functions are denoted as hazard curves. For a given annual return period, a uniform hazard spectrum (UHS) can be plotted to provide the expected spectral content of the motion associated with that annual return period.

The seismic motion that is used for assessing the seismic capacity of the important-to-reliability NSR SSCs is referred as the SONGS review level earthquake. A UHS with a 1,000-year period was chosen for the SONGS review level earthquake. This is a highly unlikely event having an annual probability of exceedance of 0.1%. If SONGS operates through 2042 (assuming that its current license, which expires in 2022, is renewed for an additional 20 years), this motion level corresponds to about a 3.1% probability of occurring over the plant's remaining 31 years of operation.

The SONGS review level earthquake is shown on Figure 3-4. This motion is characterized by a maximum spectral acceleration level of 0.75g at a frequency of 5 Hz and a PGA of 0.32g at 5% damping.

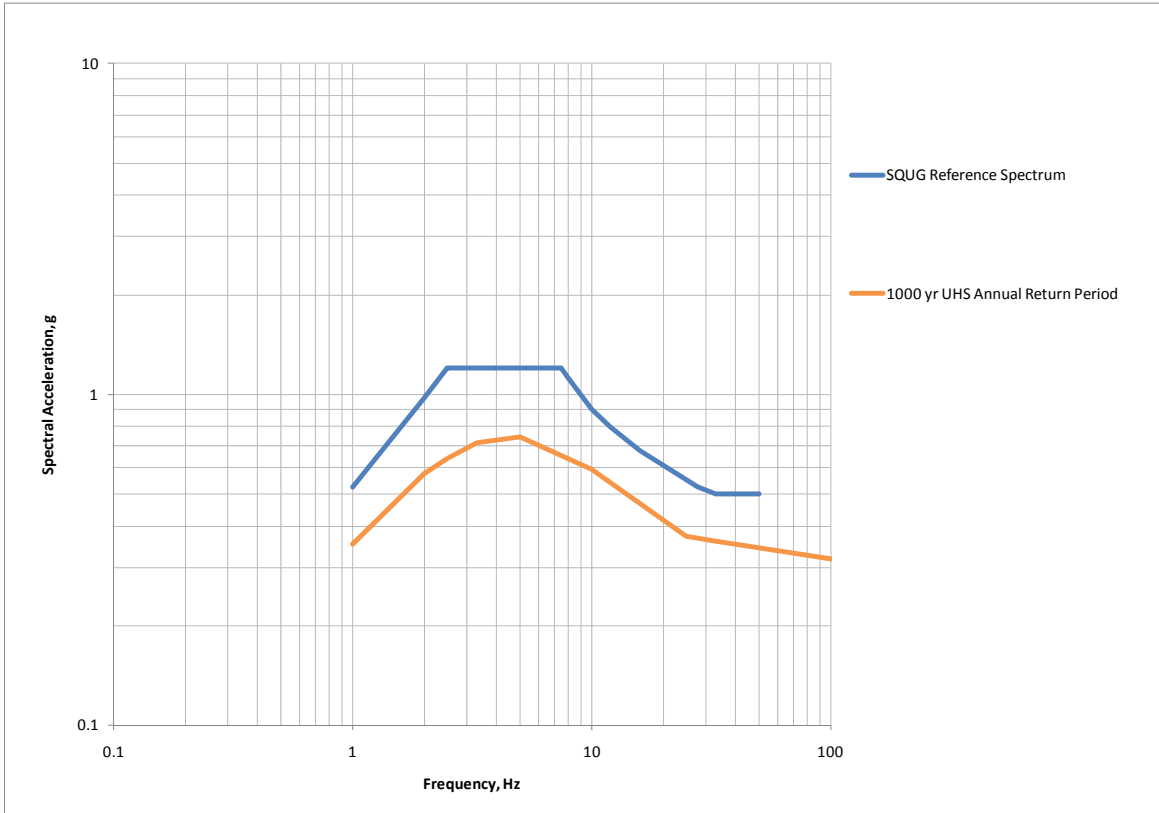


Figure 3-4 Comparison of the Seismic Capacity Spectrum with SONGS Review Level Earthquake (Using a 1,000-Year UHS Annual Return Period)

3.4 Phase IV – Evaluate Seismic Capacity of Important-to-Reliability NSR SSCs

Using the important-to-reliability NSR SSCs list that was generated during Phase I and included in Appendix B, the next phase involves the screening of these SSCs to determine the important-to-reliability NSR SSCs that have a seismic capacity greater than the SONGS review level earthquake.

The seismic capacity screening is accomplished by reviewing plant design documents, conducting walkdowns, and using the SQUG database. Three specific criteria are used in the seismic capacity screening:

- Anchorage
- Spatial Interaction
- Functionality

SI II/I SSCs are screened only for the spatial interaction and functionality criteria given that their anchorages were already designed to the DBE loading. Figure 3-5 shows the general logic flow used to accomplish the screening.

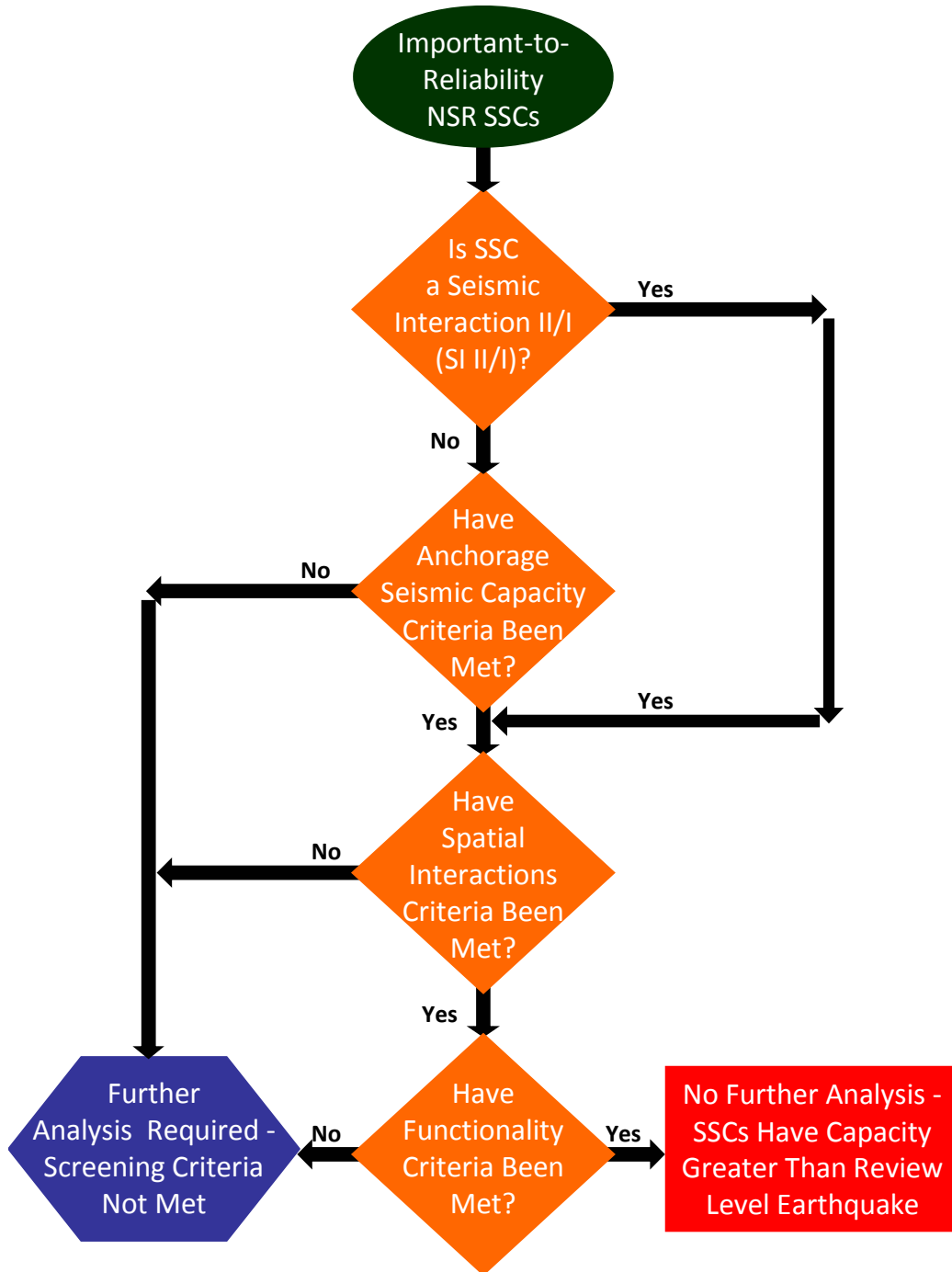


Figure 3-5 Seismic Capacity Screening Process

The anchorage seismic capacity screening involves verifying that the anchorage can withstand a SONGS review level earthquake. In performing the anchorage evaluation, the plant's existing documentation, including drawings, specifications, calculations, and typical details are reviewed. In addition, the anchorage is visually inspected during a walkdown to check for adequate installation and to determine if the anchorage load path is sufficient. Specifically, the strength of the equipment is assessed to verify that it is able to effectively transfer the loads to the anchorage. Base isolation systems for equipment must also be evaluated for seismic adequacy.

The spatial interactions screening involves performing the following interaction evaluations:

- Proximity – Determine the impact from adjacent equipment due to relative motion.
- Structural failure and falling – Determine the impact from the failure of overhead and adjacent equipment, structures, or architectural features.
- Flexibility – Determine the impact of attached lines due to relative displacements.

The functionality screening involves determining if the candidate SSC is similar to SSCs in the existing seismic experience database. This screening consists of examining the design documentation (e.g., specifications and drawings) to determine similarity to the actual SSCs contained in the seismic experience SQUG database. If the SQUG seismic experience database does not include similar SSCs, a specific evaluation is performed.

SSCs whose seismic capacity is greater than the SONGS review level earthquake (i.e., SSCs that demonstrate no seismic vulnerabilities at the SONGS review level earthquake level) are screened out, and no further analysis is required. For those SSCs that are not screened out, a more rigorous evaluation of seismic capacity is necessary. A fragility evaluation is conducted to determine the probable failure modes of the SSC. If the SSC seismic capacity is shown to be higher than the SONGS review level earthquake, then no further evaluation is needed. If the SSC seismic capacity is shown to be lower than the SONGS review level earthquake, then this SSC is added to the subset of SSCs that require repair / duration estimates. Figure 3-6 shows the general logic flow used for this further seismic evaluation.

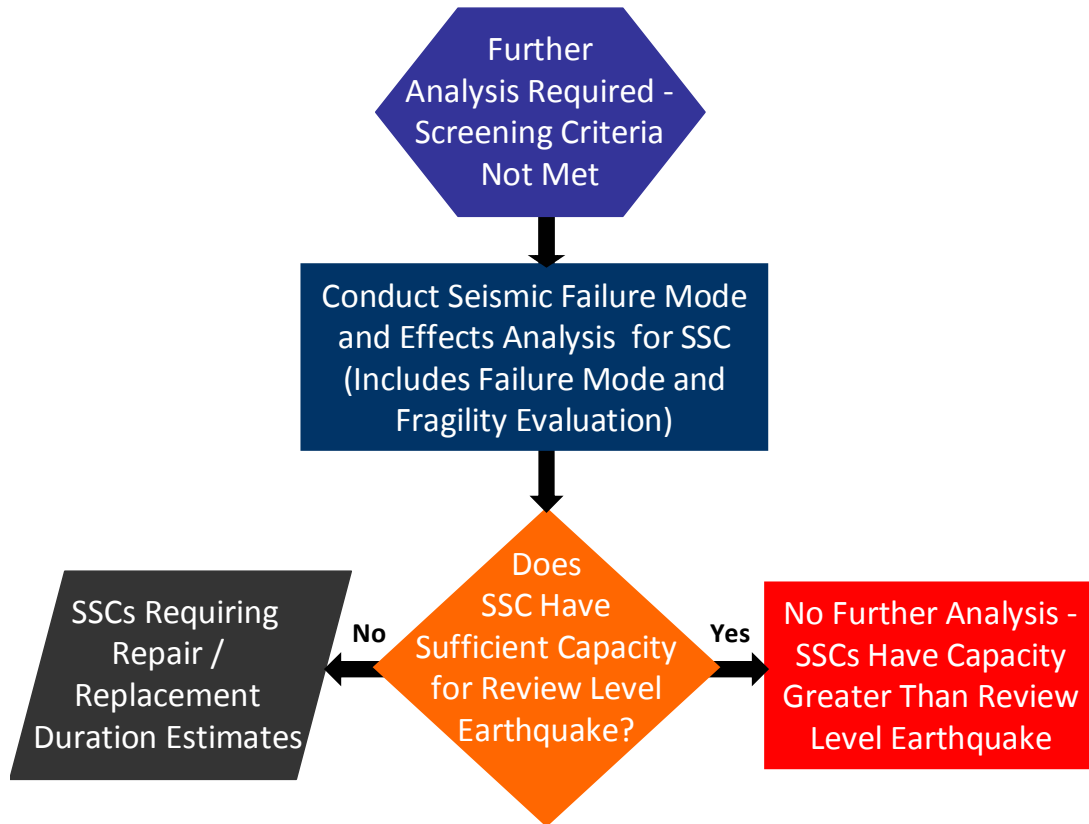


Figure 3-6 Further Seismic Evaluation Process

3.5 Phase V – Develop Repair / Replacement Duration Estimates and Mitigation Plans

Having established the probable failure modes and likely extent of damage to those SSCs that do not have seismic capacity equivalent to the SONGS review level earthquake, the next phase is to determine the conceptual level repair / replacement time duration estimates for those SSCs. The repair / replacement time duration estimates are evaluated to determine whether they represent the possibility of a prolonged outage following a major seismic event. For any SSCs identified as requiring a prolonged outage under those circumstances, mitigation plans are developed by SCE. The general logic flow used for this final phase is shown on Figure 3-7.

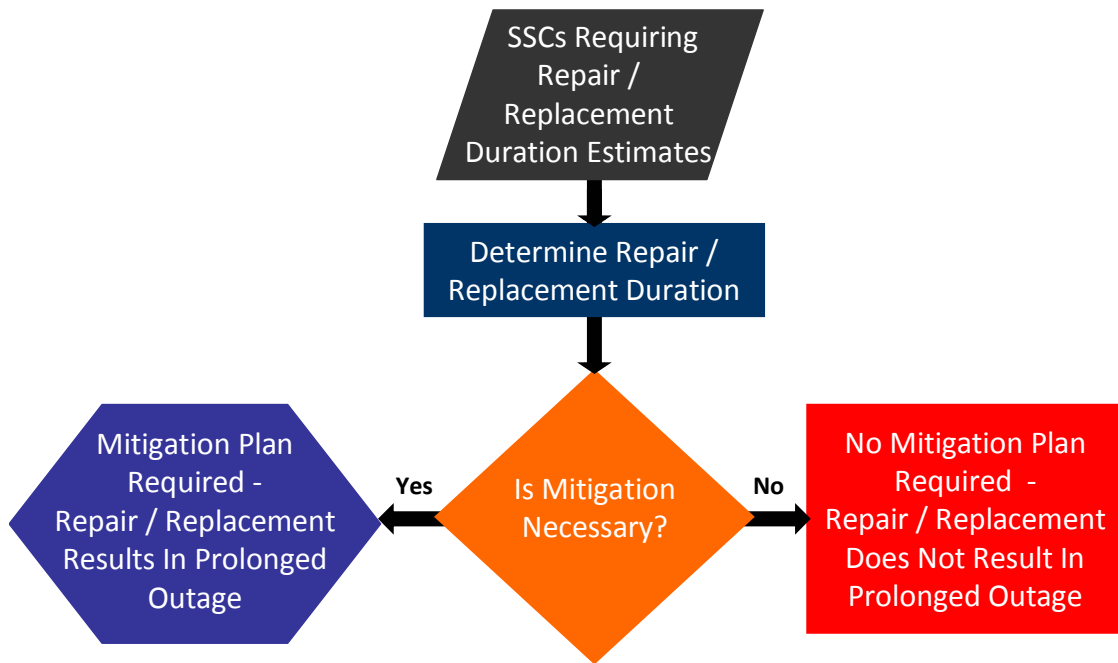


Figure 3-7 Repair / Replacement Duration Estimate and Mitigation Plan Development Process

3.6 Screening Process for NSR Buildings that House Important-to-Reliability SSCs

This seismic capacity screening process described in Section 3.4 is not applicable for NSR buildings that house important-to-reliability NSR SSCs. Instead, a commonly accepted methodology developed by the Federal Emergency Management Agency (FEMA) (FEMA, 2000, 2006) is used. This methodology is used by design professionals to assess building safety following earthquakes and is contained in national consensus software designated as HAZards United States (HAZUS). Within the HAZUS methodology are seismic capacity functions for different model building types that can be used to assess the risk of earthquake damage to these traditional commercial structures. Using the HAZUS methodology, the capacity can be estimated for the selected NSR buildings that house important-to-reliability NSR SSCs, considering the acceptable damage state and type of construction. These procedures are discussed in detail in Appendix E.

4. RELIABILITY STUDY RESULTS

4.1 SONGS Important-to-Reliability NSR SSCs

Using the five-phase methodology described in Section 3.0, important-to-reliability NSR SSCs were identified. An initial list, provided in Appendix B, of important-to-reliability NSR SSCs was generated following a review of SCE's Quality and Classification List. However, this equipment classification list could not be used to complete seismic capacity evaluation because it only considered general component types within a system and did not specify the individual component identification and location. Separate lists were prepared for the electrical equipment (see Appendix C) and the mechanical equipment (See Appendix D). These lists provide the identification and location of each specific important-to-reliability NSR SSC. In addition, Table 4-1 lists the plant's systems associated with power generation that were identified during this process. In order to prepare these lists, plant system documentation and the process and instrumentation diagrams (P&ID) or one-line electrical drawings were reviewed to identify specific components.

The primary SSCs associated with power generation are housed in the turbine building, the main steam isolation valve (MSIV) area, the control area of the auxiliary building, the tank building, and the intake structure. Additional SSCs used for the distribution of the generated power are located in the plant yard. While the turbine buildings were classified as SC II, the turbine buildings are designed for SI II/I to resist the DBE loading. Additionally, while the mechanical, electrical, and distribution system components housed within the turbine buildings were classified as SC II, their anchorages would be able to resist DBE loading. This was confirmed by a walkdown and review of plant design documentation.

Table 4-1 Plant Systems Associated with Power Generation

<p>Steam and Power Conversion Systems</p> <ul style="list-style-type: none"> • Steam System • Feedwater and Condensate Systems • Turbine Lube System • Condenser Air Removal System • Main Condenser System • Generator Seal Oil System • Electro Hydraulic Oil System
<p>Balance-of-Plant Water Systems</p> <ul style="list-style-type: none"> • Circulating Water System • Turbine Plant Cooling Water System • Main Generator Cooling System • Demineralized Water Systems
<p>HVAC Systems</p> <ul style="list-style-type: none"> • Control Area-Auxiliary Building • Turbine Building
<p>Electrical Systems</p> <ul style="list-style-type: none"> • 22,000 V AC System • 6,900 V AC System • 4,160 V AC System • 480 V System • DC System • AC Control Power System • Lighting System • Excitation System • 230 kV Switchyard
<p>Fire Protection System</p>
<p>Auxiliary Systems</p> <ul style="list-style-type: none"> • Instrument Air System • N₂ Gas Supply System • H₂ Gas Supply System

Explanation:

1. V = volts
2. AC = alternating current
3. DC = direct current
4. N₂ = nitrogen
5. H₂ = hydrogen

There are only two non-power block NSR buildings – the SCE switchyard relay building and the San Diego Gas & Electric (SDG&E) switchyard relay building – that house operational important-to-reliability NSR SSCs. Both are separate single-story buildings that house relay racks. In addition, the Mesa warehouse is a NSR building that houses spare parts that can be

used for repairing important-to-reliability NSR SSCs. These spare parts may be needed to repair the NSR SSCs that may sustain damage during a major seismic event.

The list of NSR buildings selected for evaluation is shown in Table 4-2.

Table 4-2 SONGS NSR Buildings Selected for Evaluation

Mesa Warehouse - Pre-engineered Steel Structure
Switchyard Relay Houses - Reinforced Masonry
<ul style="list-style-type: none">• SCE – Single-Story Separate Building• SDG&E – Single-Story Separate Building

4.2 Capacity Evaluation Results

The equipment lists provided in Appendices C and D were used to perform the walkdown of the SONGS important-to-reliability NSR SSCs required for power generation as part of the seismic capacity evaluation. The walkdown was conducted by qualified seismic capability engineers who were certified as having successfully completed the SQUG training course⁴ on seismic evaluation methods and who met the requisite education and engineering experience requirements. Since Units 2 and 3 are virtually identical in layout and components, Unit 2 was selected for the walkdown.

Within the SONGS plant's systems, some SSCs were identified as requiring a more rigorous analysis. The more rigorous analysis involved conducting a detailed seismic capacity evaluation that identified failure modes and fragilities. The NSR building structures identified as important-to-reliability were also evaluated using the HAZUS procedures and screened against the SONGS review level earthquake.

The SSCs were categorized as 1) having seismic capacity greater than the SONGS review level earthquake, 2) having seismic capacity less than the SONGS review level earthquake, or 3) requiring further review. A discussion of each of these categories is provided in the following sections.

⁴ SQUG offers training courses to help users properly apply the various guidelines and tools developed by SQUG. This training is needed since the criteria and guidelines in the GIP included new methods and approaches as compared to the traditional methods for seismic qualification of equipment.

4.2.1 SSCs with Seismic Capacity Greater Than the SONGS Review Level Earthquake

The majority of the important-to-reliability NSR SSCs were determined to have a seismic capacity greater than the SONGS review level earthquake. A discussion is provided below for select power generation components.

4.2.1.1 Turbine / Generator Support Systems

The turbine / generator are the primary components for power generation. The primary mechanical support systems necessary to ensure turbine function are the steam / reheat system, the feedwater / condensate system including the condensate and feedwater pumps, the circulating water system, the condenser, the turbine plant cooling system, the lube oil system, the seal oil system, the stator cooling water system, and the hydrogen cooling system. These systems comprise pumps, valves, and the associated piping distribution systems. The primary electrical power support systems necessary to ensure turbine function are the medium voltage AC power system, the low voltage AC power systems, the DC power systems, and the associated cable tray and conduit distribution systems. The mechanical and electrical systems are controlled by various control interfaces and instrumentation systems, and associated wiring and cable distribution systems. The bulk of these components are housed within the turbine building of each unit and the auxiliary building with other components housed within the respective MSIV areas and tank buildings of each unit. The turbine building is mainly an open structure that has only local fans to promote air movement. The auxiliary building and portions of the turbine buildings have heating, ventilation, and air conditioning (HVAC) systems and the associated distribution ducts for air movement and heat removal. The important-to-reliability NSR SSCs of these mechanical, electrical, control / instrumentation, and HVAC support systems are of a similar type and configuration as non-nuclear power plant SSCs and are therefore similar to those found in SQUG's seismic experience database. The important-to-reliability NSR SSCs within these buildings were found to have anchorages able to withstand the DBE. Additionally, they were determined to be similar to the SSCs that performed well during and after an earthquake, based on earthquake experience. Thus, these SSCs were found to have a capacity greater than the SONGS review level earthquake.

4.2.1.2 Turbine / Generator

The rotating turbine shaft is supported and rides on 11 journal bearings, and longitudinal movements of the shaft are prevented using a single Kingsbury-type thrust bearing. These bearings use high oil pressure maintained by the lube oil system to prevent excessive

movement of the shaft and metal-to-metal contact at the bearings. The Kingsbury-type of thrust bearing is designed to sustain very high thrust loads and remain functional.

The turbine / generator were considered to be special components requiring a more in-depth review. In general, turbo-machinery has high seismic capacity, and the earthquake experience with turbine generators is good. For an operating turbine, the most common issue has been associated with the loss of lube oil pressure during turbine coast-down caused by the loss of offsite power following an earthquake. The SSCs that comprise the turbine / generator coast-down lube oil system must maintain the necessary oil pressure required for the journal and thrust bearing to function during turbine / generator coast-down following the trip of a unit. If any disruption of the oil supply and pressure occurs during the coast-down period, then the journal and / or thrust bearings could be damaged. This type of failure mode, however, is associated with the design of the lube oil system and not the turbine / generator itself. The SONGS lube oil and seal oil systems were recently upgraded with redundant pumps and battery-backed power sources to prevent this failure mode from occurring. These components are anchored for the DBE loading, and their functionality will not be impacted after a SONGS review level earthquake event.

Except for a few isolated cases, earthquake damage to turbine components has otherwise not occurred. In one case, turbine / generator alignment was disturbed by the shifting of alignment shims during an aftershock. The SONGS turbine generator is not aligned in this manner.

It is important to note that a nuclear plant turbine is larger and operates at lower temperatures and pressures than a fossil-fired plant turbine. Until recently, the earthquake experience with larger nuclear plant turbines was limited. However, the turbine generators for the nuclear units at the Kashiwazaki-Kariwa Nuclear Power Plant were disassembled and inspected following the offshore magnitude 6.8 Niigataken-Chuetsu-Okai (NCO) earthquake that occurred near the plant in 2007. Four of the turbine generators were in operation at the time the earthquake occurred. While contact marks were found on the bearing surfaces, no issues that would have prevented turbine operation following the earthquake were discovered. The thrust bearings for the turbines were not the Kingsbury-type like those found at SONGS, but rather simple parallel plane-type bearings, which are not as rugged. Minor contact marks were found on the turbine bearing surface of all of the units, even those that had not been in operation during the earthquake. This suggests that the contact marks on the bearing surfaces were not earthquake-caused, but rather occurred during normal operation and start-up procedures. Some partially fractured turbine blades were also found in two of the units. However, these

fractures were concluded to not be earthquake-related, but rather due to the over-speed test of the turbines during the initial unit start-up period. The plant's units had been operating with the partially fractured blades prior to the earthquake. This experience suggests that nuclear turbines have substantial seismic capacity and that functional performance following an earthquake is limited by the support system components and not the turbine generator itself. Consequently, the seismic capacity of the turbine generator exceeds the SONGS review level earthquake.

4.2.1.3 Offshore Intake Conduit and Main Intake Structure

The buried offshore intake conduit is SC I, with the exception of the segment from the auxiliary intake structure to the main offshore intake structure, which is SC II. However, the SC II segment of the offshore intake conduit has the same design as the SC I segment. In addition, controlled gravel that is not susceptible to liquefaction was used as backfill material for the entire length of the conduit. As a result, offshore intake conduits were determined as having a seismic capacity greater than SONGS review level earthquake.

The offshore intake structure, although SC II, was designed to withstand DBE loading and therefore has a seismic capacity greater than the SONGS review level earthquake.

4.2.1.4 Switchyard Relay Houses

There are two one-story relay houses located in the SONGS switchyard that contain relay racks. The relay racks were determined as having a capacity greater than the SONGS review level earthquake. These two buildings were evaluated with the HAZUS procedure, and the results indicated that they were likely to sustain moderate damage following a SONGS review level earthquake. This would result in the building being green tagged, which would allow continued unrestricted entry and access to the structure.

4.2.1.5 Spare Parts for Important-to-Reliability SSCs Stored in the Mesa Warehouse Building

The 100,000 square foot (sq. ft) warehouse is located in the Mesa area east of Interstate 5. The warehouse stores spare parts that may be required for repairing the transformer and switchyard important-to-reliability NSR SSCs. These spare parts are generally packed in crates and are stored either on the ground or on the lower shelves of the storage racks. The racks in the Mesa warehouse building are anchored to the concrete slab and are braced. Additionally, the racks have adequate moment connections between the horizontal members of the shelves and the rack legs. Although the racks may sustain moderate deformations and distortions during a SONGS review level earthquake, the access to and retrieval of the items stored on the shelves

will not be difficult. However, some of the items, mainly those located on the top shelves, may slide or fall off the shelves during an earthquake. These would likely fall into the aisles between the racks, but would not impact the items that are stored on the lower shelves in the racks. Thus the damage to the stored spare parts required for repairing important-to-reliability NSR SSCs would be limited following a SONGS review level earthquake. The building was evaluated using the HAZUS methodology, and the results indicated that it would sustain extensive damage following a SONGS review level earthquake yet allow for access to the building contents. However, any debris that results from the extensive damage would come from the light roof elements. This debris would not affect the spare parts since they are crated and stored within the racks at ground level or on lower shelves.

4.2.2 SSCs with Seismic Capacity Less Than the SONGS Review Level Earthquake

The walkdown and the subsequent detailed analyses identified the following SSCs as having capacities below the SONGS review level earthquake:

- Main, Auxiliary, and Reserve Auxiliary Transformers
- Line Dead End Towers, Downcomers, and Switches
- Transmission Breakaway Towers
- Makeup Demineralized Water Tanks

For each of the important-to-reliability NSR SSCs above, a detailed analysis was conducted to identify the probable failure modes and the likely extent of damage that might be sustained during a SONGS review level earthquake. Table 4-3 provides a summary of the failure modes identified for each SSC.

Table 4-3 Components that Have Capacities Below SONGS Review Level Earthquake

Component	Location	Failure Mode
<i>Main, Unit Auxiliary, and Reserve Auxiliary Transformers</i>		
Main Transformer	Yard	Anchorage Failure
Main Transformer Phase Bus	Yard	Expansion Joint Boot Damage
Main Transformer 230 kV Bushings	Yard - Main Transformers	Shifting of Porcelain
Main Transformer Surge Arresters	Yard - Main Transformers	Porcelain Failure
Main Transformer Radiator Headers	Yard - Main Transformers	Gasket Joint Failure
Unit Auxiliary Transformers	Yard	Anchorage Failure
Reserve Auxiliary Transformers	Yard	Anchorage Failure
Reserve Auxiliary Transformers 230 kV Bushings	Yard – Reserve Auxiliary Transformers	Shifting of Porcelain
Reserve Auxiliary Transformer Surge Arresters	Yard - Reserve Auxiliary Transformers	Porcelain Failure
Reserve Auxiliary Transformers Radiator Headers	Yard - Reserve Auxiliary and Unit Auxiliary Transformers	Gasket Joint Failure
<i>Line Dead End Towers, Downcomers, and Switches</i>		
Line Dead End Towers	Switchyard	Base Plate Connection Weld Cracking
Downcomers	Switchyard	Tether Post Anchorage Failure
Disconnect Switches	Switchyard	Switch Misalignment and Base Bearing Deformation
<i>Transmission Breakaway Towers</i>		
Main Transformer - Transmission Breakaway Tower	Yard - Main Transformers	Base Plate Connection Weld Cracking
Reserve Auxiliary Transformers - Transmission Breakaway Tower	Yard – Reserve Auxiliary Transformers	Base Plate Connection Weld Cracking
Tall Pedestal Mounted Disconnect Switches	Yard – Reserve Auxiliary Transformer	Switch Misalignment, Base Bearing Deformation, and Porcelain Failure
<i>Makeup Demineralized Water Tanks</i>		
Makeup Demineralized Water Tanks	South Tank Area	Base Uplift and Shell Buckling

4.2.2.1 Main, Auxiliary, and Reserve Auxiliary Transformers

The output of the 22 kV generators is routed to the main transformer of each unit using phase bus structures that were designed using the 0.2g NSR seismic design criterion. Earthquake joints were incorporated in the phase bus design, but the sealing boots are expected to pull apart in an earthquake. Because the phase bus is air cooled, the loss of the joint seals will reduce the current capacity in the phase bus until it is repaired.

The anchorage of the main transformers was also designed for the 0.2g NSR seismic design criterion. An analysis of the anchorage load path using American Concrete Institute (ACI) 349 criteria indicates that the anchorage capacity is below the SONGS review level earthquake. The supports of the conservator tank mounted on the main transformer are judged to be vulnerable at the same earthquake level.

A similar anchorage analysis was performed for the smaller auxiliary transformers and the reserve auxiliary transformers, and results indicated that the anchorage capacities of the transformers are less than the SONGS review level earthquake.

Past earthquake experience indicates that the transformer oil radiator piping has the potential to leak. In addition, the transformer bushings may shift and the mounted surge arresters may fail. Fragility data compiled by California utilities (Eidinger, et al, 1995) indicate that capacities are below the SONGS review level earthquake.

The disconnect switches supported on the tall pedestal frames adjacent to the reserve auxiliary transformers may also become misaligned. In addition, the base bearings may deform and the porcelain may become damaged.

4.2.2.2 Line Dead End Towers, Downcomers, and Switches (Switchyard) and Transmission Breakaway Towers (Yard)

In the SONGS switchyard, the 0.5g SCE transmission facility (1975) seismic design criterion was utilized for the anchorage of the power apparatus and design of the support structures.

The SONGS line dead end towers, as well as the transmission getaway towers located in the plant yard adjacent to the transformers, use the same configuration and fabricated tube type that was extensively damaged in the 1994 Northridge earthquake at the SCE Pardee Substation, which was designed at approximately the same time as SONGS. The Pardee dead end towers experienced two basic failure modes: 1) the flexibility of the towers contributed to the lateral displacement of the suspended potential transformers (PTs) incorporated in the conductor downcomers that resulted in the failure of the downcomer post supports and also caused damage to the adjacent disconnect switches; and 2) weld cracking that occurred in the base plate connection of the tower tubular sections. The weld failures were similar to the unanticipated brittle weld fractures that occurred in many building connections subjected to the 1994 Northridge earthquake. The cause of such weld cracking was determined to not be a design issue but rather the result of fabrication issues, such as the lack of control of base metal properties, the use of weld filler materials with low toughness, and the lack of proper preheat

and welding procedures (FEMA, 2000). The towers were designed for 0.5g loading; however, the tower base connection weld detail had a unique configuration (i.e., a full penetration weld of a tubular structural member to a very thick base plate) which produced welds that were susceptible to brittle cracking. This unique configuration was only specific to the tower base welded connections and was not present in any other location at SONGS. Furthermore, the rest of the tower structure behaved as expected in conformance with the design. The Pardee towers were still functional following the Northridge earthquake but required re-welding of the base details and the addition of gusset plates to the base plate connections. The measured ground motion at the Pardee substation was used to provide the basis for the capacity evaluation of the line dead end towers, the transmission breakaway towers, the conductor downcomers and suspended PTs, and the adjacent disconnect switches.

4.2.2.3 Makeup Demineralized Water Tanks

The makeup demineralized water tanks consist of unanchored 535,000 gallon tanks that were designed in accordance with the American Petroleum Institute (API) Standard 620 seismic design criteria. These types of tanks have historically been damaged due to base uplift and shell buckling that would ultimately lead to a loss of contents.

4.2.3 SSCs Requiring Additional Analysis for Seismic Capacity Assessment

4.2.3.1 Offshore Discharge Conduits

The offshore discharge conduits were identified as potentially unable to withstand the SONGS review level earthquake; thus, a detailed analysis is required. Some of the backfill used for the discharge conduits was sand. Thus, soil liquefaction of the backfill is possible during an earthquake, which could cause the discharge conduits to become buoyant and come apart at the joints. A detailed analysis is in progress to evaluate the capacity of the offshore discharge conduits to withstand a SONGS review level earthquake.

4.3 Repair and Replacement Duration Estimates

Table 4-4 of this study presents conceptual repair / replacement time duration estimates to restore function of the important-to-reliability NSR SSCs that may sustain damage during a SONGS review level earthquake. Procurement, design, and construction times were evaluated and provided by SCE. The conceptual repair / replacement time duration estimates assumed the following:

- Only one unit is required to be put back to service following a SONGS review level earthquake as the SCE transmission system is designed to operate reliably with one SONGS unit out-of-service.
- When groups of common SSCs were considered, they were assumed to have a 50% failure rate. Based on the recovery efforts for power system damage caused by prior earthquakes (Eidinger, et al, 1995), a failure rate of 40 to 50% for a 230 kV substation power apparatus has been observed for ground motion levels having PGA values within the range 0.4 to 0.5g. Thus, a 50% failure rate is an upper bound estimate for earthquake damage to yard and switchyard equipment due to a SONGS review level earthquake.
- The other unit can be a source for replacement parts, which may eliminate the need of procurement for some parts that have a long lead time.

Table 4-4 Conceptual Repair and Replacement Estimates

Repair / Replacement Area	Component	Estimated Time to Restore Function (Months)
Plant Yard Electrical Components	Main, Unit Auxiliary, and Reserve Auxiliary Transformer <ul style="list-style-type: none"> • Phase Bus • 230 kV Bushings • Surge Arresters • Radiator Headers • Anchorages 	≤ 3
	Transmission Breakaway Towers <ul style="list-style-type: none"> • Tower Bases • Tall Pedestal Mounted Disconnect Switches 	
Switchyard Components	Line Dead End Towers Base Plates	≤ 3
	Downcomers	
	Disconnect Switches	
Makeup Demineralized Water Tanks	-	≤ 4

4.3.1 Plant Yard Electrical Components

The scope of work to repair / replace the plant yard electrical components includes:

- Repair of 50% of the transformer anchorages (including anchor bolt replacements, concrete repairs, and weld repairs).
- Replacement of 50% of the transformer bushings and arresters.
- Repair of 50% of the transformer radiator oil piping supporting the radiators.
- Repair of the conservator tank supports.
- Repair of 50% of the isophase joints (the outer casing joints will need to be resealed).
- Repair of 50% of the breakaway transmission tower base plate connections.

This work is estimated to take 3 months.

4.3.2 Switchyard Components

The scope of work to repair / replace the switchyard components includes:

- Repair of the base plate weld connection on 50% of the dead end transmission towers.
- Repair of 50% of the downcomer tethers.
- Replacement of 50% of the disconnect switch bases.

This work is estimated to take 3 months.

4.3.3 Makeup Demineralized Water Tanks

There are three 535,000 gallon makeup demineralized water tanks that, if damaged during an earthquake, will require replacement. The scope of this work includes:

- Demolition.
- Removal of the existing tanks.
- Installation of a new foundation.
- Supply and installation of new tanks.
- Replacement of the connection pipes.

A complete replacement of the tanks is estimated to take 4 months.

4.4 Mitigation Plans

The initial repair / replacement estimates have not identified any component that could cause a prolonged outage due to a seismic event. Therefore, mitigation plans were not developed.

5. CONCLUSIONS

This study has not identified any important-to-reliability NSR SSCs that could be the cause of a prolonged outage due to a seismic event. The offshore discharge conduits are currently undergoing further specialized evaluations (soil laboratory testing and time history soil structure interaction analyses) to assess their seismic capacity.

6. REFERENCES

- 10CFR100AppA, Current, Seismic and Geologic Siting Criteria for Nuclear Power Plant, Title 10, Code of Federal Regulations, Part 100, Appendix A.
- CEC, 2008, AB 1632 Assessment of California's Operating Nuclear Plants, prepared by California Energy Commission, CEC-100-2008-005-F, October 2008.
- Eidinger, J. et al, 1995, High Voltage Electric Substation Performance in Earthquakes, Lifeline Earthquake Engineering, Monograph No. 6, Technical Council on Lifeline Earthquake Engineering, August 1995.
- EPRI, 1994, Methodology for Developing Seismic Fragilities, prepared by Electric Power Research Institute, TR-103959, June 1994.
- EPRI, 2002, Seismic Fragility Application Guide, prepared by Electric Power Research Institute, Report 1002988, December 2002.
- EPRI, 2009, Seismic Fragility Applications Guide Update, prepared by Electric Power Research Institute, Report 1019200, December 2009.
- FEMA, 2006, Multi-hazard Loss Estimation Methodology, Earthquake Model, prepared by Federal Emergency Management Agency, HAZUS-MH MR4, Technical Manual.
- FEMA, 2000, Recommended Specifications and Quality Assurance Guidelines for Steel Moment-frame Construction for Seismic Applications, prepared by Federal Emergency Management Agency, FEMA 653.
- NRC, 1987, Verification of Seismic Adequacy of Mechanical and Electrical Equipment in Operating Reactors, Unresolved Safety Issue (USI) A-46, prepared by the U.S. Nuclear Regulatory Commission, Generic Letter 87-02.
- SCE, 2009, San Onofre Nuclear Generating Station, Q-List, Classification of Structures, Systems, and Components, Document 90034, Rev. 10, 2009.
- SCE, 2010, San Onofre Nuclear Generating Station, Seismic Hazard Assessment Program, 2010 Probabilistic Seismic Hazard Analysis Report.
- SCE, 1995, Seismic Hazard at San Onofre Nuclear Generating Station.

SQUG, 1991, Generic Implementation Procedure (GIP) for Seismic Verification of Nuclear Plant Equipment, prepared by Seismic Qualification Utility Group, Revision 2.

UFSAR, Current, San Onofre Nuclear Generating Station, Units 2 and 3, Current, prepared by Updated Final Safety Analysis Report.

Appendix A
List of Acronyms

AC	Alternating Current
ACI	American Concrete Institute
AEBM	Advanced Engineering Building Module
AISC	American Institute of Steel Construction
AMCA	Air Movement and Control Association
ANSI	American National Standards Institute
API	American Petroleum Institute
ASCE	American Society of Civil Engineers
ASME	American Society of Mechanical Engineers
CEC	California Energy Commission
CBC	California Building Code
CFR	Code of Federal Regulations
CMAA	Construction Management Association of America
CO ₂	Carbon Dioxide
DBE	Design-Basis Earthquake
DC	Direct Current
UFSAR	Updated Final Safety Analysis Report
EPRI	Electric Power Research Institute
FCC	Federal Communications Commission
FEMA	Federal Emergency Management Agency
ft	Feet
ft/sec	Feet per Second
GIP	Generic Implementation Procedure
GL	Generic Letter
H ₂	Hydrogen
HAZUS	HAZards United States
HCLPF	High Confidence of Low Probability of Failure
HEI	Heat Exchange Institute
HVAC	Heating, Ventilation, and Air Conditioning
Hz	Hertz
IEEE	Institute of Electrical and Electronics Engineers
IES	Illuminating Engineering Society
in.	Inch
kV	Kilovolts
kVA	Kilovolts-Amperes
MSIV	Main Steam Isolation Valves

MW	Megawatts
N ₂	Nitrogen
NCO	Niigataken-Chuetsu-Oki
NEMA	National Electrical Manufacturers Association
NFPA	National Fire Protection Association
NSR	Non-Safety-Related
NSSS	Nuclear Steam Supply System
NRC	Nuclear Regulatory Commission
ORNL	Oak Ridge National Laboratory
o.c.	On Center
P&ID	Process and Instrumentation
PGA	Peak Ground Acceleration
PSHA	Probabilistic Seismic Hazard Analysis
PT	Potential Transformer
SCE	Southern California Edison
SC I	Seismic Category I
SC II	Seismic Category II
SC III	Seismic Category III
SDG&E	San Diego Gas & Electric
SI II/I	Seismic Interaction II/I
SMACNA	Sheet Metal and Air Conditional Contractors' National Association
SONGS	San Onofre Nuclear Generating Station
sq. ft	Square Foot
SQUG	Seismic Qualification Utility Group
SR	Safety-Related
SSCs	Structures, Systems, and Components
UBC	Uniform Building Code
UFSAR	Updated Final Safety Analysis Report
UHS	Uniform Hazard Spectrum
USI	Unresolved Safety Issue
UL	Underwriters Laboratory
V	Volts

Appendix B
Equipment Classification List

Equipment Classification						
UFSAR Section	Principal Component	Principal Design and Construction Code or Standard ⁽¹⁾	Seismic Category	Location ⁽²⁾	In/Out of Scope	Comment
1.2.6.3	Lightning Protection					
	Lightning rods, associated cables and fasteners	U.L. 96A,NFPA 78	II	C	Out	Does not affect power generation ⁽⁴⁾
2.4 & 2.5	HYDROLOGIC ENGINEERING/GEOLOGY, SEISMOLOGY, AND GEOTECHNICAL ENGINEERING (SITE-RELATED HAZARDS AND PROTECTION)					
2.4.5.5	Seawall	ACI 318	II	O	Out	Does not affect power generation ⁽⁴⁾
2.5.6	PROBABLE MAXIMUM FLOOD (PMF) BERM AND CHANNEL		II	M/O	Out	Does not affect power generation ⁽⁴⁾
3.2	CLASSIFICATION OF STRUCTURES, COMPONENTS, AND SYSTEMS					
	Consumables (including lubricants/greases) not important to the functional capacity and performance of SR SSCs		II,III	All	Out	Readily replaced
3.4.1	FLOOD PROTECTION					
3.4.1.1	Waterstops, bellows	————	II ⁽³⁾	All	Out	Designed for II/I ⁽⁵⁾ ; Does not affect power generation ⁽⁴⁾
	SEISMIC CATEGORY I STRUCTURES					
3.8.3	CONTAINMENT INTERNAL STRUCTURES					
	Jib Crane	CMAA	II ⁽³⁾	C	Out	Designed for II/I ⁽⁵⁾ ; Does not affect power generation ⁽⁴⁾
4	REACTOR					
4.2	REACTOR FUEL SYSTEM					
	Neutron source	None	II	C	Out	Does not affect power generation ⁽⁴⁾
5	REACTOR COOLANT SYSTEM (RCS) AND CONNECTED SYSTEMS					
5.4.1	REACTOR COOLANT PUMPS (RCPS)					
	Motors	NEMA MG-1	II ⁽³⁾	C	In	Designed for II/I ⁽⁵⁾
	Operating and backup oil lift pumps		II ⁽³⁾	C	In	Designed for II/I ⁽⁵⁾
	Operating and backup oil lift pump motors		II ⁽³⁾	C	In	Designed for II/I ⁽⁵⁾
	Operating and backup anti-reverse rotation device (ARRD) pumps		II ⁽³⁾	C	In	Designed for II/I ⁽⁵⁾
	Operating and backup ARRD pump motors		II ⁽³⁾	C	In	Designed for II/I ⁽⁵⁾
	RCP seal heat exchangers					
	<i>CCW side</i>	B31.1	II	C	In	Internal design of heat exchanger - unit anchored for II/I ⁽⁵⁾
	Motor heat exchangers		II ⁽³⁾	C	In	Designed for II/I ⁽⁵⁾
5.4.10	PRESSURIZER					
	Heaters and cables	III-1	I, II	C	Out	Internal subcomponents of Category I component
5.4.11	PRESSURIZER RELIEF DISCHARGE SYSTEM					
	Quench tank	VIII	II ⁽³⁾	C	In	Designed for II/I ⁽⁵⁾
	Piping					
	<i>Downstream of safety valve</i>	B31.1	II	C	In	
	Valves associated with quench tank	B31.1	II	C	In	
6	ENGINEERED SAFETY FEATURES					
6.3	SAFETY INJECTION SYSTEM					
	Piping and valves					

Equipment Classification						
UFSAR Section	Principal Component	Principal Design and Construction Code or Standard ⁽¹⁾	Seismic Category	Location ⁽²⁾	In/Out of Scope	Comment
	<i>Drain lines</i>	B31.1	II	C	Out	Does not affect power generation ⁽⁴⁾
6.5	FISSION PRODUCT REMOVAL AND CONTROL SYSTEMS					
	Iodine removal system					
	<i>Tank</i>	III-2	II ⁽³⁾	S	Out	Designed for II/I ⁽⁵⁾ ; System deactivated
	<i>Piping and valves</i>	III-2	II ⁽³⁾	C/S	Out	Designed for II/I ⁽⁵⁾ ; System deactivated
	<i>Supports</i>	ASME	II ⁽³⁾	C	Out	Designed for II/I ⁽⁵⁾ ; System deactivated
7	INSTRUMENTATION AND CONTROL SYSTEMS					
7.5	SR DISPLAY INSTRUMENTATION					
7.5.1.6	<i>Control element assembly position indication</i>	IEEE 279	II	A/C	Out	Does not affect power generation ⁽⁴⁾
7.6	ALL OTHER INSTRUMENTATION SYSTEMS REQUIRED FOR SAFETY(Z)					
7.6.1.7	<i>Anticipated Transient Without Scram (ATWS) System</i>					
	Diverse Scram System (DSS) Cabinet and Cabling		II ⁽³⁾	A/C/P	Out	Designed for II/I ⁽⁵⁾ ; Does not affect power generation ⁽⁴⁾
	Diverse Turbine Trip (DTT) Cabling		II	A	Out	Does not affect power generation ⁽⁴⁾
	Diverse Emergency Feedwater Actuation System (DEFAS) Cabinet and Cabling		II ⁽³⁾	A/C	Out	Designed for II/I ⁽⁵⁾ ; Does not affect power generation ⁽⁴⁾
7.6.1.10	<i>Data Acquisition System (DAS)</i>					
			II	A	Out	Does not affect power generation ⁽⁴⁾
7.7	CONTROL SYSTEMS NOT REQUIRED FOR SAFETY					
7.7.1.1.1	<i>Boron control system</i>					
			II	A/C	Out	Does not affect power generation ⁽⁴⁾
7.7.1.2.1	<i>Pressurizer pressure control system</i>					
			II	A/C	Out	Does not affect power generation ⁽⁴⁾
7.7.1.2.2	<i>Pressurizer level control system</i>					
			II	A/C	Out	Does not affect power generation ⁽⁴⁾
7.7.1.3	<i>Feedwater control system</i>					
			II	A/C/T/ MSIV	In	
7.7.1.4	<i>Steam bypass control system</i>					
			II	A/C/T	In	
7.7.1.7	<i>In-core instrumentation system</i>					
			II	A/C	Out	Does not affect power generation ⁽⁴⁾
7.7.1.8	<i>Ex-core instrumentation system (startup and control channels)</i>					
			II	A/C	Out	Does not affect power generation ⁽⁴⁾
7.7.1.10	<i>Drain Down Level Monitoring System (DLMS)</i>					
	Cable and incontainment junction boxes		II ⁽³⁾	A/C/P	Out	Designed for II/I ⁽⁵⁾ ; Does not affect power generation ⁽⁴⁾
7.7.3.1	<i>Refueling Water Level Instrument (RWLI)</i>					
	Transmitters		II	C	Out	Does not affect power generation ⁽⁴⁾
	Indicators		II ⁽³⁾	A	Out	Designed for II/I ⁽⁵⁾ ; Does not affect power generation ⁽⁴⁾
8	ELECTRIC POWER SYSTEMS					
8.2	OFFSITE POWER SYSTEM					
	Main transformers	ANSI C57.12	II	O	In	
	Auxiliary transformers	ANSI C57.12	II	O	In	
	Reserve auxiliary transformers	ANSI C57.12	II	O	In	
	220 kV disconnect switches	ANSI C57.30	II	O	In	
	Electrical equipment (220 kV switchyard)		II	O	In	

Equipment Classification						
UFSAR Section	Principal Component	Principal Design and Construction Code or Standard ⁽¹⁾	Seismic Category	Location ⁽²⁾	In/Out of Scope	Comment
8.3	ONSITE POWER SYSTEMS					
8.3.1	AC POWER SYSTEMS					
	Non-class 1E equipment		II, II ⁽³⁾	All	In	Designed for II/I ⁽⁵⁾
8.3.2	DC POWER SYSTEMS					
	Non-class 1E equipment		II, II ⁽³⁾	All	In	Designed for II/I ⁽⁵⁾
9	AUXILIARY SYSTEMS					
9.1.3	SPENT FUEL POOL COOLING AND CLEANUP SYSTEM					
	Pumps					
	<i>Makeup and purification pumps</i>		II	F	Out	Does not affect power generation ⁽⁴⁾
	Pump motors					
	<i>Makeup and purification pump motors</i>		II	F	Out	Does not affect power generation ⁽⁴⁾
	Piping and valves					
	<i>Purification subsystem</i>					
	Other	B31.1	II	C/F/P	Out	Does not affect power generation ⁽⁴⁾
	<i>Makeup subsystem (backup)</i>	B31.1	II	F/O/TK	Out	Does not affect power generation ⁽⁴⁾
	<i>Other</i>					
	<i>Ion-exchangers</i>	VIII	II	F	Out	Does not affect power generation ⁽⁴⁾
	<i>Filters and strainers</i>	VIII	II	F	Out	Does not affect power generation ⁽⁴⁾
9.1.4	FUEL HANDLING SYSTEM					
	Refueling machine including auxiliary hoist	CMAA/AISC	II ⁽³⁾	C	Out	Designed for II/I ⁽⁵⁾ ; Does not affect power generation ⁽⁴⁾
	Spent fuel handling machine	CMAA/AISC	II ⁽³⁾	F	Out	Designed for II/I ⁽⁵⁾ ; Does not affect power generation ⁽⁴⁾
	Control element assembly change machine	AISC	II ⁽³⁾	C	Out	Designed for II/I ⁽⁵⁾ ; Does not affect power generation ⁽⁴⁾
	Fuel transfer equipment set	CMAA/AISC	II	F/C	Out	Does not affect power generation ⁽⁴⁾
	Reactor vessel head lifting rig		II ⁽³⁾	C	Out	Designed for II/I ⁽⁵⁾ ; Does not affect power generation ⁽⁴⁾
	Reactor internals lifting rig		II ⁽³⁾	C	Out	Designed for II/I ⁽⁵⁾ ; Does not affect power generation ⁽⁴⁾
	Refueling pool seal assembly		II	C	Out	Does not affect power generation ⁽⁴⁾
	Containment polar crane	CMAA	II ⁽³⁾	C	Out	Designed for II/I ⁽⁵⁾ ; Does not affect power generation ⁽⁴⁾
	<i>Mechanical Operation</i>					
	Bridge structure		II ⁽³⁾	C	Out	Designed for II/I ⁽⁵⁾ ; Does not affect power generation ⁽⁴⁾
	Trolley		II ⁽³⁾	C	Out	Designed for II/I ⁽⁵⁾ ; Does not affect power generation ⁽⁴⁾
	Main hoist and auxiliary hoist		II ⁽³⁾	C	Out	Designed for II/I ⁽⁵⁾ ; Does not affect power generation ⁽⁴⁾
	Main hoist and auxiliary hoist brakes		II ⁽³⁾	C	Out	Designed for II/I ⁽⁵⁾ ; Does not affect power generation ⁽⁴⁾
	<i>Electrical Control</i>					
	DC Power/PLC		II ⁽³⁾	C	Out	Designed for II/I ⁽⁵⁾ ; Does not affect power generation ⁽⁴⁾
	Trolley drive and brakes		II ⁽³⁾	C	Out	Designed for II/I ⁽⁵⁾ ; Does not affect power generation ⁽⁴⁾
	Bridge drive and brakes		II ⁽³⁾	C	Out	Designed for II/I ⁽⁵⁾ ; Does not affect power generation ⁽⁴⁾
	Main hoist and auxiliary hoist drives		II ⁽³⁾	C	Out	Designed for II/I ⁽⁵⁾ ; Does not affect power generation ⁽⁴⁾
	Rotate drive (main hook)		II ⁽³⁾	C	Out	Designed for II/I ⁽⁵⁾ ; Does not affect power generation ⁽⁴⁾
	Limit switches and resolvers		II ⁽³⁾	C	Out	Designed for II/I ⁽⁵⁾ ; Does not affect power generation ⁽⁴⁾

Equipment Classification						
UFSAR Section	Principal Component	Principal Design and Construction Code or Standard ⁽¹⁾	Seismic Category	Location ⁽²⁾	In/Out of Scope	Comment
	<i>Platforms and Jib Hoist</i>		II ⁽³⁾	C	Out	Designed for II/I ⁽⁵⁾ ; Does not affect power generation ⁽⁴⁾
	Cask handling crane	CMAA	II ⁽³⁾	F	Out	Designed for II/I ⁽⁵⁾ ; Does not affect power generation ⁽⁴⁾
	New fuel elevator	CMAA/AISC	II ⁽³⁾	F	Out	Designed for II/I ⁽⁵⁾ ; Does not affect power generation ⁽⁴⁾
	New fuel crane	CMAA	II ⁽³⁾	F	Out	Designed for II/I ⁽⁵⁾ ; Does not affect power generation ⁽⁴⁾
9.2.3	DEMINEALIZED WATER MAKEUP SYSTEM					
	Demineralized water storage system	API 620	II	O	In	
9.2.5	ULTIMATE HEAT SINK					
	Main offshore intake structure	ACI 318	II ⁽³⁾	O	In	Per UFSAR designed to withstand DBE
	Intake conduit					
	<i>From one pipe section beyond auxiliary intake structure to main offshore intake structure</i>	ACI 318	II ⁽³⁾	O	In	Per UFSAR designed to withstand DBE
	Outfall conduit					
	<i>West end box conduit seaward</i>		II	O	In	
9.2.6	CONDENSATE STORAGE FACILITY					
	Portion associated with turbine plant					
	<i>Condensate storage tank 2(3)T-120</i>	API 650	II	TK	In	
	<i>Pumps</i>		II	O	In	
	<i>Piping and valves</i>	B31.1	II	O	In	
9.2.7	NUCLEAR SERVICE WATER SYSTEM					
	Storage tank	API 620	II	Y	In	
	Pumps and motors	HI/NEMA MG-1	II	Y	In	
	Piping and valves					
	<i>Other</i>	B31.1	II	A/C/F/P/S/Y	In	
9.2.8	TURBINE PLANT COOLING WATER SYSTEM					
	Tanks	API 620	II	O	In	
	Pumps and motors		II	O	In	
	Piping and valves	B31.1	II	T/O	In	
	Heat exchangers	VIII	II	O	In	
	Filters		II	T/O	In	
9.3.1	COMPRESSED AIR SYSTEM					
	Receivers	VIII	II	T	In	
	Compressors	VIII	II	T	In	
	Piping and valves					
	<i>Other</i>	B31.1	II	All	In	
	Aftercoolers	VIII	II	T	In	
	Dryers	VIII	II	T	In	
	Filters	VIII	II	T	In	
9.3.2	PROCESS SAMPLING SYSTEMS					
	Nuclear plant sampling system					

Equipment Classification						
UFSAR Section	Principal Component	Principal Design and Construction Code or Standard ⁽¹⁾	Seismic Category	Location ⁽²⁾	In/Out of Scope	Comment
	Sample vessels	VIII	II	A	Out	Does not affect power generation ⁽⁴⁾
	Sample blowers	VIII	II	A	Out	Does not affect power generation ⁽⁴⁾
	Piping and valves					
	Coolant chemical and volume control system sample lines	III-2	II	A	Out	Does not affect power generation ⁽⁴⁾
	Volume control tank sample lines up through the first normally shut valve	III-2	II	A	Out	Does not affect power generation ⁽⁴⁾
	Waste gas system sample lines	B31.1	II	A	Out	Does not affect power generation ⁽⁴⁾
	Other	B31.1	II	C/P/A	Out	Does not affect power generation ⁽⁴⁾
	Coolers	VIII	II	A	Out	Does not affect power generation ⁽⁴⁾
	Filters	VIII	II	A	Out	Does not affect power generation ⁽⁴⁾
	Turbine plant sampling system coolers	VIII	II	A	Out	Does not affect power generation ⁽⁴⁾
9.3.3	EQUIPMENT AND FLOOR DRAINAGE SYSTEM					
	Nonradioactive sump and drain systems					
	Piping and valves/pumps					
	Auxiliary building	UPC	II, III	A	Out	Does not affect power generation ⁽⁴⁾
	Diesel generator building	UPC	II	D	Out	Does not affect power generation ⁽⁴⁾
	East and west turbine plant area	UPC	II, III	T	Out	Does not affect power generation ⁽⁴⁾
	North Industrial Area	UPC	II, III	Y	Out	Does not affect power generation ⁽⁴⁾
	Radioactive sump and drain systems					
	Piping and valves/pumps					
	Component cooling water	B31.1	II	S	Out	Does not affect power generation ⁽⁴⁾
	Containment area	B31.1	II	C	Out	Does not affect power generation ⁽⁴⁾
	Fuel handling building	B31.1	II	F	Out	Does not affect power generation ⁽⁴⁾
	Penetration area	B31.1	II	P	Out	Does not affect power generation ⁽⁴⁾
	Safety injection area	B31.1	II	S	Out	Does not affect power generation ⁽⁴⁾
	Storage tank area	B31.1	II	TK	Out	Does not affect power generation ⁽⁴⁾
	Radwaste area	B31.1	II	A	Out	Does not affect power generation ⁽⁴⁾
	Liner plate for safety equipment building sumps, fuel handling building sump, penetration area sump, and radwaste area sump	AISC/ASME	II	A/F/P/S	Out	Does not affect power generation ⁽⁴⁾
9.3.4	CHEMICAL AND VOLUME CONTROL SYSTEM					
	Tanks					
	Volume control tank	III-2	II	A	In	
	Pumps					
	Primary plant makeup pumps		II	A	In	Needed to make power in reactor
	Motors					
	Primary plant makeup pump motors		II	A	In	Needed to make power in reactor
	Piping and valves					

Equipment Classification						
UFSAR Section	Principal Component	Principal Design and Construction Code or Standard ⁽¹⁾	Seismic Category	Location ⁽²⁾	In/Out of Scope	Comment
	<i>Letdown portion (from letdown backpressure control valve to radwaste diversion valve)</i>	III-2	II	A	In	
	<i>Volume control tank (between isolation valves)</i>	III-2	II	A	In	
	<i>Letdown heat exchanger</i>					
	<i>Purification ion-exchanger</i>	III-2	II	A	In	
	<i>Delithiating ion-exchanger</i>	III-2	II	A	In	
	<i>Deborating ion-exchanger</i>	III-2	II	A	Out	Not required for power operation
	<i>Purification filter</i>	III-2	II	A	In	
9.4.1	CONTAINMENT BUILDING VENTILATION SYSTEMS					
9.4.1.1	Normal Operation--Containment Building Ventilation Systems					
	Containment normal cooling units					
	<i>Air handling units</i>	ARI/AMCA	II	C	In	
	<i>Ductwork and dampers</i>	SMACNA	II ⁽³⁾	C	In	Designed for II/I ⁽⁵⁾
	<i>Chillers</i>	ARI	II	A	In	
	<i>Chilled water pumps</i>		II	A	In	
	<i>Compression tanks</i>	ASME Section VIII	II	A	In	
	<i>Piping and valves</i>					
	<i>Other (inside containment)</i>	B31.1	II ⁽³⁾	C	In	Designed for II/I ⁽⁵⁾
	<i>Other (outside containment)</i>	B31.1	II	P/A	In	
	<i>Strainers</i>		II	A	In	
	Purge recirculation cleanup system					
	<i>Purge supply units</i>	AMCA	II	A	Out	Does not affect power generation ⁽⁴⁾
	<i>Purge exhaust units</i>	AMCA	II	A	Out	Does not affect power generation ⁽⁴⁾
	<i>Recirculation cleanup unit (HEPA filters)</i>	HSI-306/MIL-F-51068C	II	C	Out	Does not affect power generation ⁽⁴⁾
	<i>Ductwork and dampers</i>					
	<i>Other</i>	ORNL-65/SMACNA	II ⁽³⁾	C/P/A	Out	Designed for II/I ⁽⁵⁾ ; Does not affect power generation ⁽⁴⁾
	CEDM cooling system					
	<i>Cooling coils</i>		II	C	In	
	<i>Fans and motors</i>	AMCA	II	C	In	
	<i>Ductwork and dampers</i>	SMACNA	II ⁽³⁾	C	In	Designed for II/I ⁽⁵⁾
	Reactor cavity cooling system					
	<i>Fans and motors</i>	AMCA	II	C	In	
	<i>Ductwork and dampers</i>	SMACNA	II ⁽³⁾	C	In	Designed for II/I ⁽⁵⁾
	MSIV enclosure and penetration area cooling system					
	<i>Supply fans</i>	AMCA	II	MSIV	In	Only need penetration fans, not penetration area cooling.
	<i>Exhaust fans</i>	AMCA	II	MSIV	Out	Does not affect power generation ⁽⁴⁾
	<i>Duct work and dampers</i>	SMACNA	II	MSIV	In	
9.4.1.2	Emergency Operation--Containment Building Ventilation Systems					

Equipment Classification						
UFSAR Section	Principal Component	Principal Design and Construction Code or Standard ⁽¹⁾	Seismic Category	Location ⁽²⁾	In/Out of Scope	Comment
	Hydrogen purge supply and exhaust units					
	<i>Prefilters</i>		II ⁽³⁾	P	Out	Designed for II/I ⁽⁵⁾ ; Does not affect power generation ⁽⁴⁾
	<i>HEPA filters</i>	HSI-306/MIL-F-51068C	II ⁽³⁾	P	Out	Designed for II/I ⁽⁵⁾ ; Does not affect power generation ⁽⁴⁾
	<i>Charcoal filters</i>	CS-8T	II ⁽³⁾	P	Out	Designed for II/I ⁽⁵⁾ ; Does not affect power generation ⁽⁴⁾
	<i>Electric heating coils</i>		II	P	Out	Does not affect power generation ⁽⁴⁾
	<i>Fans and motors</i>	AMCA	II	P	Out	Does not affect power generation ⁽⁴⁾
	<i>Ductwork</i>					
	Other	ORNL-65/SMACNA	II ⁽³⁾	C/P	Out	Designed for II/I ⁽⁵⁾ ; Does not affect power generation ⁽⁴⁾
	<i>Valves</i>					
	Other	B31.1	II	P	Out	Does not affect power generation ⁽⁴⁾
	Dome air circulating units					
9.4.2	AUXILIARY BUILDING VENTILATION SYSTEMS					
9.4.2.1	Normal Operation--Auxiliary Building Ventilation Systems					
	Control room system					
	<i>Air handling units</i>	AMCA/ARI	II	A	In	
	<i>Fan coil units</i>	AMCA/ARI	II	A	In	
	<i>Control room smoke removal fan</i>	AMCA/NFPA	II	A	Out	Does not affect power generation ⁽⁴⁾
	<i>Electric duct heaters</i>		II	A	In	
	<i>Exhaust fans</i>	AMCA	II	A	In	
	<i>Transfer fans</i>	AMCA	II	A	In	
	<i>Ductwork and dampers</i>	SMACNA	I, II ⁽³⁾	A	In	Designed for II/I ⁽⁵⁾
	Radwaste area system					
	<i>Air handling units</i>	AMCA	II	A	Out	Does not affect power generation ⁽⁴⁾
	<i>Exhaust fans</i>	AMCA	II	A	Out	Does not affect power generation ⁽⁴⁾
	<i>CEDMCS room fan coil units</i>		II	A	In	
	<i>Electric duct heaters</i>		II	A	Out	Does not affect power generation ⁽⁴⁾
	<i>Ductwork and dampers</i>	SMACNA	II	A	Out	Does not affect power generation ⁽⁴⁾
	ESF switchgear room systems					
	<i>Air handling units</i>	AMCA/ARI	II	A	In	
	<i>Exhaust fans</i>	AMCA	II	A	In	
	<i>Electric duct heaters</i>		II	A	In	
	<i>Ductwork and dampers</i>	SMACNA	II	A	In	
	Cable spreading and electrical room systems					
	<i>Air handling units</i>	AMCA	II	A	Out	Does not affect power generation ⁽⁴⁾
	<i>Return fans</i>	AMCA	II	A	Out	Does not affect power generation ⁽⁴⁾
	<i>Ductwork and dampers</i>	SMACNA	II	A	Out	Does not affect power generation ⁽⁴⁾
	Chiller room systems					
	<i>Air handling unit</i>	AMCA	II	A	In	
	<i>Exhaust fan</i>	AMCA	II	A	In	

Equipment Classification						
UFSAR Section	Principal Component	Principal Design and Construction Code or Standard ⁽¹⁾	Seismic Category	Location ⁽²⁾	In/Out of Scope	Comment
	<i>Electric duct heater</i>		II	A	Out	Does not affect power generation ⁽⁴⁾
	<i>Ductwork and dampers</i>	SMACNA	II	A	In	
	Battery room systems					
	<i>Air handling unit</i>	AMCA	II	A	In	
	<i>Exhaust fan</i>	AMCA	II	A	In	
	<i>Ductwork and dampers</i>	SMACNA	II	A	In	
	Continuous exhaust system					
	<i>Fans</i>	AMCA	II	A	In	Need at least 1 of these 3 fans
	<i>Ductwork and dampers</i>	SMACNA	II	A/O	In	
	<i>Plant vent stacks</i>		II ⁽³⁾	O	In	Designed for II/I ⁽⁵⁾
9.4.3	SUPPORT BUILDING VENTILATION SYSTEMS					
9.4.3.1	Fuel Handling Building Ventilation System					
	Normal supply and exhaust system					
	<i>Prefilters</i>		II	F	Out	Does not affect power generation ⁽⁴⁾
	<i>Fans and motors</i>	AMCA	II	F	Out	Does not affect power generation ⁽⁴⁾
	<i>Ductwork and dampers</i>	SMACNA	II	F	Out	Does not affect power generation ⁽⁴⁾
9.4.3.2	Safety Equipment Building Ventilation System					
	Pump room normal cooling systems					
	<i>Fan coil units</i>	AMCA/ARI	II	S	Out	Can operate with only Emergency Room coolers
	Heat exchanger room normal cooling systems					
	<i>Fan coil units</i>	AMCA/ARI	II	S	Out	Does not affect power generation ⁽⁴⁾
	<i>Ductwork and dampers</i>	SMACNA	II	S	Out	Does not affect power generation ⁽⁴⁾
	Air conditioning equipment room normal cooling system					
	<i>Fan coil units</i>	AMCA/ARI	II	S	Out	Does not affect power generation ⁽⁴⁾
	<i>Ductwork and dampers</i>	SMACNA	II	S	Out	Does not affect power generation ⁽⁴⁾
	Lobby area air conditioning system					
	<i>Fan coil units</i>	AMCA/ARI	II	S	Out	Does not affect power generation ⁽⁴⁾
	<i>Ductwork and dampers</i>	SMACNA	II	S	Out	Does not affect power generation ⁽⁴⁾
	<i>Electric duct heaters</i>		II	S	Out	Does not affect power generation ⁽⁴⁾
9.4.3.3	Turbine Building Ventilation System					
	Steam air ejector exhaust system					
	<i>Exhaust filtration unit</i>	HSI-306/MIL-F-51068C	II	T	Out	Don't require to operate
	<i>Piping and valves</i>	ANSI B31.1	II	T	In	
	Main generator isophase bus connection enclosure ventilation system					
	<i>Exhaust fans and motors</i>		III	T	In	The Iso-Phase Bus has a current rating of 36.3 kA with forced cooling provided, and 21.2 kA if self-cooled.
	<i>Ductwork</i>	SMACNA	III	T	In	
	D7 Battery and Battery Charger Rooms (El. 56')					

Equipment Classification						
UFSAR Section	Principal Component	Principal Design and Construction Code or Standard ⁽¹⁾	Seismic Category	Location ⁽²⁾	In/Out of Scope	Comment
	Supply Air Units	AMCA	II	T	In	
	Exhaust fans and motors	AMCA	II	T	In	
	Ductwork and dampers	SMACNA	II	T	In	
	Electric duct heaters		II	T	In	
9.4.3.4	Diesel Generator Building Ventilation System					
	Normal ventilation system					
	Fans and motors	AMCA	II	D	Out	Does not affect power generation ⁽⁴⁾
	Ductwork	SMACNA	II	D	Out	Does not affect power generation ⁽⁴⁾
9.4.3.5	Penetration Building and Electric and Piping Tunnels Ventilation System					
	Penetration building system					
	Air conditioning and ventilation supply units	AMCA/ARI	II	P	Out	Does not affect power generation ⁽⁴⁾
	Prefilters		II	P	Out	Does not affect power generation ⁽⁴⁾
	Transfer fans	AMCA	II	P	Out	Does not affect power generation ⁽⁴⁾
	Ductwork and dampers	SMACNA	II	P	Out	Does not affect power generation ⁽⁴⁾
	Electric and piping tunnel system					
	Ventilation supply units	AMCA	II	All	Out	Does not affect power generation ⁽⁴⁾
	Exhaust fans	AMCA	II	All	Out	Does not affect power generation ⁽⁴⁾
	Ductwork and dampers	SMACNA	II	All	Out	Does not affect power generation ⁽⁴⁾
9.4.3.7	Auxiliary Feedwater Pump Room Ventilation System					
	Normal heating and ventilation system					
	Electrical unit heater		II	TK	Out	Does not affect power generation ⁽⁴⁾
9.4.3.8	Safety Equipment Building Elevator Machine Room and Condensate Storage Tank Area Ventilation System					
	Safety Equipment Building Elevator Machine Room Ventilation System					
	Exhaust fan	AMCA	II	S	Out	Does not affect power generation ⁽⁴⁾
	Condensate Storage Tank Area Ventilation System					
	Electrical unit heater		II	TK	Out	Does not affect power generation ⁽⁴⁾
9.5.1	FIRE PROTECTION SYSTEM					
	Water System					
	Tanks	NFPA/API 650	II	O	In	Required by the Technical Specifications
	Pumps and motors	NFPA/NMR	II	O	In	
	Piping and valves					
	Suppression system	NFPA	II	All	In	
	Gaseous system (Halon)	NFPA/VIII	II	A	In	Not needed to start
	Gaseous system (CO ₂)					
	Other	NFPA	II	T/O	In	Not needed to start
	Fire Barrier					
	Rated doors, walls	ACI-318, NFPA	II, III	A/C/D/F/MS IV/S/T/TK	Out	Does not affect power generation ⁽⁴⁾

Equipment Classification						
UFSAR Section	Principal Component	Principal Design and Construction Code or Standard ⁽¹⁾	Seismic Category	Location ⁽²⁾	In/Out of Scope	Comment
	<i>Penetration seals</i>	ASTM E119	II,III	A/C/D/F/MS IV/S/T/TK	Out	Does not affect power generation ⁽⁴⁾
	<i>Fire resistant wrap</i>	NFPA/ASTM E119	II ⁽³⁾	A/C/D/F/S/T /TK	Out	Designed for II/I ⁽⁵⁾ ; Does not affect power generation ⁽⁴⁾
	<i>Conduits and cable trays</i>		I, II ⁽³⁾	All	Out	Designed for II/I ⁽⁵⁾ ; Does not affect power generation ⁽⁴⁾
	<i>Fire dampers</i>	NFPA	II, III	A/C/D/F/S/T /TK	Out	Does not affect power generation ⁽⁴⁾
	Fluid diversion structure (RCP lube oil collection system)	ANSI B31.1, ASME VIII, and AISC	II	C	Out	Designed for II/I ⁽⁵⁾ ; Does not affect power generation ⁽⁴⁾
9.5.2	COMMUNICATIONS SYSTEM					
	Reservoir Thunderbolt Siren	FCC	II	O	Out	Does not affect power generation ⁽⁴⁾
9.5.3	LIGHTING SYSTEMS					
	Lighting components integral to control room ceiling		II ⁽³⁾	A	Out	Designed for II/I ⁽⁵⁾ ; Does not affect power generation ⁽⁴⁾
	Control room emergency lights		II ⁽³⁾	A	Out	Designed for II/I ⁽⁵⁾ ; Does not affect power generation ⁽⁴⁾
	8-hour emergency lights	UL924, IES	II/III	All	Out	Does not affect power generation ⁽⁴⁾
9.5.6	DIESEL GENERATOR STARTING AIR SYSTEM					
	Compressors		II	D	Out	Does not affect power generation ⁽⁴⁾
	Air dryers		II	D	Out	Does not affect power generation ⁽⁴⁾
	Filters, intake		II	D	Out	Does not affect power generation ⁽⁴⁾
10	STEAM AND POWER CONVERSION SYSTEM					
10.2	TURBINE-GENERATOR					
	Turbine: High, low pressure		II	T	In	
	Control and protective valve system	B31.1	II	T	In	
	Turbine drains	B31.1	II	T	In	
	Exhaust hood spray system	B31.1	II	T	In	
	Lube oil system					
	<i>Components</i>	VIII	II	T	In	
	Turbine control system		II	T	In	Per high pressure and low pressure valve
	Turbine control panel		II	T	In	
	Turbine supervisory system		II	T	In	
	Turbine protective devices		II	T	In	
	Turbine overspeed protection	IEEE 279	II	A/T	In	
	Turbine monitoring equipment		II	T	In	
	Turbine support accessories		II	T	In	
	Generator		II	T	In	
	Seal oil system	VIII	II	T	In	
	Hydrogen coolers	VIII	II	T	In	
	Generator H ₂ /CO ₂ system		II	T	In	
	Stator water system	VIII	II	T	In	

Equipment Classification						
UFSAR Section	Principal Component	Principal Design and Construction Code or Standard ⁽¹⁾	Seismic Category	Location ⁽²⁾	In/Out of Scope	Comment
	Exciter switchgear and voltage regulator		II	T	In	
	Exciter		II	T	In	
	Piping and valves	B31.1	II		In	
	Turbine gantry crane	CMAA	II	T/O	Out	Does not affect power generation ⁽⁴⁾
10.3	MAIN STEAM SUPPLY SYSTEM					
	Steam traps		II	S/T/TK	Out	Does not affect power generation ⁽⁴⁾
	Reheaters	VIII	II	T	In	
	Moisture separator-reheater drain tanks	VIII	II	T	In	
	Main steam tube bundle drain tanks	VIII	II	T	In	
	Bled steam tube bundle drain tanks	VIII	II	T	In	
	Y-strainers	VIII	II	T	In	
	Piping and valves					
	Other	B31.1	II	MSIV/T	In	
10.4.1	MAIN CONDENSER					
	Main condensers	HEI	II	T	In	
	Vent and drain system	B31.1	II	T	In	
	Piping and valves	B31.1	II	T	In	
10.4.2	MAIN CONDENSER EVACUATION SYSTEM					
	Seal water heat exchanger	VIII/HEI	II	T	In	
	Air ejector condenser	VIII	II	T	In	
	Air ejectors	VIII/HEI	II	T	In	
	Condenser vacuum pump	VIII	II	T	In	
	Seal water pumps		II	T	In	
	Separator tanks		II	T	In	
10.4.3	TURBINE GLAND SEALING SYSTEM					
	Gland steam condenser exhaust fan		II	T	In	
	Gland steam condenser	VIII	II	T	In	
	Piping and valves	B31.1	II	T	In	
10.4.4	TURBINE BYPASS SYSTEM					
	Piping and valves	B31.1	II	T	In	
10.4.5	CIRCULATING WATER SYSTEM					
	Pumps and motors		II	IN	In	
	Piping and valves	B31.1	II	IN	In	
	Expansion joints		II	IN	In	
	Strainers	VIII	II	IN	In	
	Traveling rakes and bar screens		II	IN	In	
	Gates #4, 5, and 6		II ⁽³⁾	IN	In	Designed for II/I ⁽⁵⁾
	Gate operators and accessory equipment		II ⁽³⁾	IN	In	Designed for II/I ⁽⁵⁾
10.4.6	CONDENSATE CLEANUP SYSTEM (FULL FLOW CONDENSATE POLISHING DEMINERALIZER)					

Equipment Classification						
UFSAR Section	Principal Component	Principal Design and Construction Code or Standard ⁽¹⁾	Seismic Category	Location ⁽²⁾	In/Out of Scope	Comment
	Seal water heat exchangers	VIII	II	FFCPD	Out	Does not affect power generation ⁽⁴⁾
	Tanks	VIII	II	FFCPD/O	Out	Does not affect power generation ⁽⁴⁾
	Pumps		II	FFCPD/O	Out	Does not affect power generation ⁽⁴⁾
	Polishers					
	<i>Fines filter</i>		II	FFCPD	Out	Does not affect power generation ⁽⁴⁾
	<i>Sample coolers</i>		II	O	Out	Does not affect power generation ⁽⁴⁾
	<i>Air blower package</i>		II	FFCPD	Out	Does not affect power generation ⁽⁴⁾
	<i>Resin hopper</i>		II	FFCPD	Out	Does not affect power generation ⁽⁴⁾
	Piping and valves	ANSI B31.1	II	FFCPD/O	Out	Does not affect power generation ⁽⁴⁾
10.4.7	CONDENSATE AND FEEDWATER SYSTEM (ALSO REFER TO CONDENSATE STORAGE SYSTEM, SUBSECTION 9.2.6)					
	Tanks					
	<i>Heater drain tanks</i>	VIII	II	T	In	
	<i>Feedwater pump seal drain tanks</i>	VIII	II	T	In	
	<i>Feedwater pump turbine drain tanks</i>	VIII	II	T	In	
	Pumps and motors					
	<i>Condensate transfer pumps</i>		II	T	In	
	<i>Condensate pumps</i>		II	T	In	
	<i>Heater drain pumps</i>		II	T	In	
	<i>Feedwater pumps</i>		II	T	In	
	<i>Feedwater pump turbine drain pumps</i>		II	T	In	
	Piping and valves					
	<i>Other</i>	B31.1	II	T	In	
	Feedwater heaters	VIII	II	T	In	
10.4.8	STEAM GENERATOR BLOWDOWN SYSTEM					
	Tanks					
	<i>Blowdown flash tank</i>	VIII	II	T	Out	Can bypass tank
	<i>Demineralizer acid storage tanks</i>	VIII	II	T	Out	Not used
	<i>Demineralizer caustic storage tanks</i>	VIII	II	T	Out	Not used
	Pumps and motors					
	<i>Acid metering pumps</i>	VIII	II	T	Out	Not used
	<i>Caustic metering pumps</i>	VIII	II	T	Out	Not used
	Piping and valves					
	<i>Other</i>	B31.1	II	MSIV/T	In	
	Blowdown heat exchanger	VIII	II	T	In	
	Demineralizer hot water heat exchanger	VIII	II	T	Out	Not used
	Mixed bed demineralizers	VIII	II	T	Out	Not used
10.4.10	TURBINE PLANT CHEMICAL ADDITION SYSTEM					
	Pumps and motors					
	<i>Amine feed pumps</i>		II	T	In	

Equipment Classification						
UFSAR Section	Principal Component	Principal Design and Construction Code or Standard ⁽¹⁾	Seismic Category	Location ⁽²⁾	In/Out of Scope	Comment
	Piping and valves	B31.1	II	T	In	
11	RADIOACTIVE WASTE MANAGEMENT SYSTEMS					
11.2	LIQUID WASTE MANAGEMENT SYSTEM (COOLANT RADWASTE, MISCELLANEOUS LIQUID WASTE, AND BORIC ACID RECYCLE SYSTEMS)					
	Tanks, atmospheric (except primary plant makeup storage tank)	API 650	II	A	Out	Does not affect power generation ⁽⁴⁾
	Tanks, pressure	VIII	II	C	Out	Does not affect power generation ⁽⁴⁾
	Pumps and motors		II	A	Out	Does not affect power generation ⁽⁴⁾
	Piping and valves					
	<i>Other</i>	B31.1	II	A/C/P	Out	Does not affect power generation ⁽⁴⁾
	Ion-exchangers	VIII	II	A	Out	Does not affect power generation ⁽⁴⁾
	Filters and strainers	VIII	II	A	Out	Does not affect power generation ⁽⁴⁾
	Tank heaters	NEMA 4	II	A	Out	Does not affect power generation ⁽⁴⁾
	Gas strippers	VIII	II	A	Out	Does not affect power generation ⁽⁴⁾
	Evaporators					
	<i>Process and cooling water side</i>	III-3	II	A	Out	Does not affect power generation ⁽⁴⁾
	<i>Steam side</i>	VIII	II	A	Out	Does not affect power generation ⁽⁴⁾
11.3	GASEOUS WASTE MANAGEMENT SYSTEM (WASTE GAS SYSTEM)					
	Tanks					
	<i>Surge tank</i>	VIII	II	A	Out	Does not affect power generation ⁽⁴⁾
	<i>Decay tanks</i>	VIII	II	A	Out	Does not affect power generation ⁽⁴⁾
	Pumps and motors					
	<i>Surge tank drain pump</i>		II	A	Out	Does not affect power generation ⁽⁴⁾
	<i>Compressor assembly</i>					
	<i>Compressor</i>	VIII	II	A	Out	Does not affect power generation ⁽⁴⁾
	<i>Motor</i>		II ⁽³⁾	A	Out	Designed for II/I ⁽⁵⁾ ; Does not affect power generation ⁽⁴⁾
	Piping and valves					
	<i>Waste gas surge tank drain</i>	B31.1	II	A	Out	Does not affect power generation ⁽⁴⁾
	<i>Waste gas discharge header</i>	B31.1	II	A	Out	Does not affect power generation ⁽⁴⁾
	<i>Vent gas collection header</i>	B31.1	II	A	Out	Does not affect power generation ⁽⁴⁾
	<i>Other</i>	B31.1	II	A/C/P	Out	Does not affect power generation ⁽⁴⁾
	Y-strainer	VIII	II	A	Out	Does not affect power generation ⁽⁴⁾
11.5	PROCESS AND EFFLUENT RADIOLOGICAL MONITORING AND SAMPLE SYSTEMS					
	All other airborne radiation monitors		II	A/T	Out	Does not affect power generation ⁽⁴⁾
	Liquid radiation monitors	VIII	II	A/P/T/Y	Out	Does not affect power generation ⁽⁴⁾
	Sample piping and tubing	B31.1	II	T	Out	Does not affect power generation ⁽⁴⁾
	Normal sample lab isolation monitor	IEEE 279/323/338/383	II	A	Out	Does not affect power generation ⁽⁴⁾
12	RADIATION PROTECTION					
12.3	AREA RADIATION MONITORING SYSTEM					
	Area radiation monitors		II	A/C/F/S	Out	Does not affect power generation ⁽⁴⁾

Explanation:

1. Principal Design and Construction Code or Standard includes: ACI = America Concrete Institute, AISC = American Institute of Steel Construction, AMCA = Air Movement and Control Association, ANSI = American National Standards Institute, ASME = American Society of Mechanical Engineers, CMAA = Construction Management Association of America, FCC = Federal Communications Commission, HEI = Heat Exchange Institute, IEEE = Institute of Electrical and Electronics Engineers, IES = Illuminating Engineering Society, ORNL = Oak Ridge National Laboratory, NEMA = National Electrical Manufacturers Association, NFPA = National Fire Protection Association, SMACNA = Sheet Metal and Air Conditional Contractors' National Association, and U.L. = Underwriters Laboratory,
2. The location was assigned to one of the following categories: A = Auxiliary Building, C = Containment Building, D = Diesel Generator Building, F = Fuel Handling Building, FFCPD = Full Flow Condensate Polishing Demineralizer Area, IN = Intake Structure, MSIV = Main Steam Isolation Valve Area, O = Outdoor Yard Area, P = Penetration Area, S = Safety Equipment Building, T = Turbine Building, TK = Tank Building
3. Signifies that the Category II component is anchored for the DBE loading to prevent interaction with Category I components.
4. Signifies that the Category II component may be need to be functional during power operation but does not affect power generation capability and is easily replaceable / repairable.
5. II/I = seismic interaction II/I

Appendix C
Electrical Equipment List

Electrical Equipment							
Tag	Item	Description	Comment	Location	Anchorage Satisfactory?	Free From Known Seismic Vulnerabilities?	Free From Seismic Interaction?
2XM	Main Transformer	Power Transformer 22 kV/220 kV	Anchorage Capacity	Yard	No	No	Yes
	Surge Arrester	Mounted Subcomponent	Porcelain Capacity	Yard	No	No	No
	Bushings	Mounted Subcomponent	Porcelain Shift	Yard	No	No	No
	Radiators	Mounted Subcomponent	Not Braced	Yard	No	No	Yes
	Conservator	Mounted Subcomponent	Weak Lateral Load Path	Yard	No	No	Yes
	Sudden Pressure Relay	Mounted Subcomponent	Recoverable if Tripped	Yard	Yes	Yes	Yes
	Intermediate Structure	Tower	Pardee Type Structure-II/I Design	Yard	Yes	No	Yes
	Dead End Structure	Tower	Pardee Type Structure-II/I Design	Yard	Yes	No	Yes
2XU1	Unit Auxiliary Transformer	Power Transformer 22 kV/4.16 kV	Anchorage Capacity	Yard	No	No	Yes
2XU2	Unit Auxiliary Transformer	Power Transformer 22 kV/6.9 kV	Anchorage Capacity	Yard	No	No	Yes
	Radiators	Mounted Subcomponent	Not Braced	Yard	No	No	Yes
	Sudden Pressure Relay	Mounted Subcomponent	Recoverable If Tripped	Yard	Yes	Yes	Yes
IPB	Isophase Bus	Bus 22 kV	Outer Casing Boot	Yard	No	No	Yes
	Isophase Bus Cooling Unit			Yard	Yes	Yes	Yes
2XR1	Reserve Auxiliary Transformer	Power Transformer 220 kV/4.16 kV	Anchorage Capacity	Yard	No	No	Yes
2XR2	Reserve Auxiliary Transformer	Power Transformer 220 kV/4.16 kV	Anchorage Capacity	Yard	No	No	Yes
2XR3	Reserve Auxiliary Transformer	Power Transformer 220 kV/6.9 kV	Anchorage Capacity	Yard	No	No	Yes
	Surge Arresters	Mounted Subcomponent	Porcelain Capacity	Yard	No	No	No
	Bushings	Mounted Subcomponent	Porcelain Shift	Yard	No	No	No
	Radiators	Mounted Subcomponent	Not Braced	Yard	No	No	Yes
	Sudden Pressure Relay	Mounted Subcomponent	Recoverable If Tripped	Yard	Yes	Yes	Yes
	Dead End Structure	Tower	Pardee Type Structure-II/I Design	Yard	Yes	No	No
	Electrical Tunnel			Yard	Yes	Yes	Yes

Electrical Equipment							
Tag	Item	Description	Comment	Location	Anchorage Satisfactory?	Free From Known Seismic Vulnerabilities?	Free From Seismic Interaction?
2A01	Bus 2A01	Medium Voltage Switchgear 6.9 kV	Reactor Coolant Pumps	45' Penetration Building	Yes	Yes	Yes
2A02	Bus 2A02	Medium Voltage Switchgear 6.9 kV	Reactor Coolant Pumps	63' Penetration Building	Yes	Yes	Yes
2XR1DSA03	Disconnect Switch	Medium Voltage Switchgear 4.16 kV			Yes	Yes	Yes
2XR1DSA08	Disconnect Switch	Medium Voltage Switchgear 4.16 kV			Yes	Yes	Yes
2XR2DSA07	Disconnect Switch	Medium Voltage Switchgear 4.16 kV			Yes	Yes	Yes
2XR2DSA09	Disconnect Switch	Medium Voltage Switchgear 4.16 kV			Yes	Yes	Yes
2A03	Bus 2A03	Medium Voltage Switchgear 4.16 kV		30' Turbine Building	Yes	Yes	Yes
2A07	Bus 2A07	Medium Voltage Switchgear 4.16 kV		30' Turbine Building	Yes	Yes	Yes
2A08	Bus 2A08	Medium Voltage Switchgear 4.16 kV		85' Control Building	Yes	Yes	Yes
2A09	Bus 2A09	Medium Voltage Switchgear 4.16 kV		85' Control Building	Yes	Yes	Yes
2B01	2B01 Bus	Low Voltage Switchgear 480 V			Yes	Yes	Yes
2B01X	Loadcenter Transformer	Transformer 4.16 kV/480 V			Yes	Yes	Yes
2B02	2B02 Bus	Low Voltage Switchgear 480 V	Pressurizer Heaters		Yes	Yes	Yes
2B02X	Loadcenter Transformer	Transformer 4.16 kV/480 V			Yes	Yes	Yes
2B03	2B03 Bus	Low Voltage Switchgear 480 V		30' Turbine Building	Yes	Yes	Yes
2B03X	Loadcenter Transformer	Transformer 4.16 kV/480 V		30' Turbine Building	Yes	Yes	Yes
2B07	2B07 Bus	Low Voltage Switchgear 480 V		30' Turbine Building	Yes	Yes	Yes
2B07X	Loadcenter Transformer	Transformer 4.16 kV/480 V	SCE Switchyard Relay House	30' Turbine Building	Yes	Yes	Yes

Electrical Equipment							
Tag	Item	Description	Comment	Location	Anchorage Satisfactory?	Free From Known Seismic Vulnerabilities?	Free From Seismic Interaction?
2B08	2B08 Bus	Low Voltage Switchgear 480 V	Pressurizer Heaters		Yes	Yes	Yes
2B08X	Loadcenter Transformer	Transformer 4.16 kV/480 V			Yes	Yes	Yes
2B09	2B09 Bus	Low Voltage Switchgear 480 V			Yes	Yes	Yes
2B09X	Loadcenter Transformer	Transformer 4.16 kV/480 V			Yes	Yes	Yes
2B10	2B10 Bus	Low Voltage Switchgear 480 V		85' Control Building	Yes	Yes	Yes
2B11	2B11 Bus	Low Voltage Switchgear 480 V		30' Turbine Building	Yes	Yes	Yes
2B11X	Loadcenter Transformer	Transformer 4.16 kV/480 V		30' Turbine Building	Yes	Yes	Yes
2B12	2B12 Bus	Low Voltage Switchgear 480 V		30' Turbine Building	Yes	Yes	Yes
2B12X	Loadcenter Transformer	Transformer 4.16 kV/480 V		30' Turbine Building	Yes	Yes	Yes
2B13	2B13 Bus	Low Voltage Switchgear 480 V		30' Turbine Building	Yes	Yes	Yes
2B13X	Loadcenter Transformer	Transformer 4.16 kV/480 V		30' Turbine Building	Yes	Yes	Yes
2B14	2B14 Bus	Low Voltage Switchgear 480 V		30' Turbine Building	Yes	Yes	Yes
2B14X	Loadcenter Transformer	Transformer 4.16 kV/480 V		30' Turbine Building	Yes	Yes	Yes
2B15	2B15 Bus	Low Voltage Switchgear 480 V		85' Control Building	Yes	Yes	Yes
2B15X	Loadcenter Transformer	Transformer 4.16 kV/480 V		85' Control Building	Yes	Yes	Yes
2B16	2B16 Bus	Low Voltage Switchgear 480 V		85' Control Building	Yes	Yes	Yes
2B16X	Loadcenter Transformer	Transformer 4.16 kV/480 V		85' Control Building	Yes	Yes	Yes
2B18	2B18 Bus	Low Voltage Switchgear 480 V			Yes	Yes	Yes
2B18X	Loadcenter Transformer	Transformer 4.16 kV/480 V			Yes	Yes	Yes

Electrical Equipment							
Tag	Item	Description	Comment	Location	Anchorage Satisfactory?	Free From Known Seismic Vulnerabilities?	Free From Seismic Interaction?
2B19	2B19 Bus	Low Voltage Switchgear 480 V		HFMUD	Yes	Yes	Yes
2B24	2B24 Bus	Low Voltage Switchgear 480 V		50' Control Building	Yes	Yes	Yes
2B26	2B26 Bus	Low Voltage Switchgear 480 V		50' Control Building	Yes	Yes	Yes
2/3B58	2/3B58 Bus	Low Voltage Switchgear 480 V		N Industrial Area	Yes	Yes	Yes
2B1611BP	Panel	480 V		56' Control Building	Yes	Yes	Yes
B10X-A	Loadcenter Transformer	Transformer 4.16 kV/480 V			Yes	Yes	Yes
L01X-A	Transformer	Transformer 4.16 kV/208V/120 V	Lighting		Yes	Yes	Yes
L02X-A	Transformer	Transformer 4.16 kV/208V/120 V	Lighting		Yes	Yes	Yes
B10	B10 Bus	Low Voltage Switchgear 480 V	Common Unit Bus		Yes	Yes	Yes
L01	L01 Bus	Low Voltage Switchgear 480 V	Common Unit Lighting Bus		Yes	Yes	Yes
L02	L02 Bus	Low Voltage Switchgear 480 V	Common Unit Lighting Bus		Yes	Yes	Yes
2BX	Motor Control Center	Motor Control Center		50' Control Building	Yes	Yes	Yes
2BA	Motor Control Center	Motor Control Center		45' Penetration Area	Yes	Yes	Yes
2BC	Motor Control Center	Motor Control Center		34' Turbine Building	Yes	Yes	Yes
2BDX	Motor Control Center	Motor Control Center		30' Diesel Generator	Yes	Yes	Yes
2BMX	Motor Control Center	Motor Control Center		30' Turbine Building	Yes	Yes	Yes
2BLX	Motor Control Center	Motor Control Center		30' Turbine Building	Yes	Yes	Yes
2BV	Motor Control Center	Motor Control Center		34' Turbine Building	Yes	Yes	Yes
2BF	Motor Control Center	Motor Control Center		30' Aux FW	Yes	Yes	Yes

Electrical Equipment							
Tag	Item	Description	Comment	Location	Anchorage Satisfactory?	Free From Known Seismic Vulnerabilities?	Free From Seismic Interaction?
2BB	Motor Control Center	Motor Control Center		7' Turbine Building	Yes	Yes	Yes
2BK	Motor Control Center	Motor Control Center		7' Intake Structure	Yes	Yes	Yes
2BL	Motor Control Center	Motor Control Center		30' Turbine Building	Yes	Yes	Yes
2BDX	Motor Control Center	Motor Control Center		30' Diesel Generator	Yes	Yes	Yes
2BHX	Motor Control Center	Motor Control Center		30' Aux FW	Yes	Yes	Yes
2BW	Motor Control Center	Motor Control Center		7' Turbine Building	Yes	Yes	Yes
2BI	Motor Control Center	Motor Control Center		34' Turbine Building	Yes	Yes	Yes
2BM	Motor Control Center	Motor Control Center		7' Turbine Building	Yes	Yes	Yes
DM	Motor Control Center	Motor Control Center			Yes	Yes	Yes
2BRC	Motor Control Center	Motor Control Center		34' Turbine Building	Yes	Yes	Yes
2BN	Motor Control Center	Motor Control Center		63' Penetration Area	Yes	Yes	Yes
2Q086	Motor Control Center	Motor Control Center			Yes	Yes	Yes
BO	Motor Control Center	Motor Control Center	Common Between Units		Yes	Yes	Yes
BP	Motor Control Center	Motor Control Center	Common Between Units		Yes	Yes	Yes
BG	Motor Control Center	Motor Control Center	Common Between Units		Yes	Yes	Yes
BT	Motor Control Center	Motor Control Center	Common Between Units		Yes	Yes	Yes
BU	Motor Control Center	Motor Control Center	Common Between Units		Yes	Yes	Yes
BQ	Motor Control Center	Motor Control Center	Common Between Units	50' Control Building	Yes	Yes	Yes
BRD	Motor Control Center	Motor Control Center		HFMUD	Yes	Yes	Yes
BRE	Motor Control Center	Motor Control Center		HFMUD	Yes	Yes	Yes
BS	Motor Control Center	Motor Control Center	Common Between Units	50' Control Building	Yes	Yes	Yes

Electrical Equipment							
Tag	Item	Description	Comment	Location	Anchorage Satisfactory?	Free From Known Seismic Vulnerabilities?	Free From Seismic Interaction?
2T011	Transformer	Transformer 4.16 kV/120 V	UPS		Yes	Yes	Yes
2T014	Transformer	Transformer 4.16 kV/120 V	UPS		Yes	Yes	Yes
2B011	125 V Battery Set		Normal 125 V		Yes	Yes	Yes
2B005	125 V Battery Charger				Yes	Yes	Yes
2D1	125 V Distribution Switchboard			50' Room 310A	Yes	Yes	Yes
2D1P1	125 V Distribution Switchboard			50' Room 310A	Yes	Yes	Yes
2D2	125 V Distribution Switchboard			50' Room 310D	Yes	Yes	Yes
2D2P1	125 V Distribution Switchboard			50' Room 310D	Yes	Yes	Yes
2D3	125 V Distribution Switchboard			50' Room 310B	Yes	Yes	Yes
2D3P1	125 V Distribution Switchboard			50' Room 310B	Yes	Yes	Yes
2D4	125 V Distribution Switchboard			50' Room 310C	Yes	Yes	Yes
2D4P1	125 V Distribution Switchboard			50' Room 310C	Yes	Yes	Yes
2D5	125 V Distribution Switchboard				Yes	Yes	Yes
2Y005	120 V Inverter				Yes	Yes	Yes
2D5P1	125 V Distribution Panel				Yes	Yes	Yes
2D5P2	125 V Distribution Panel				Yes	Yes	Yes
2D5P3	125 V Distribution Panel				Yes	Yes	Yes
2D5P4	125 V Distribution Panel				Yes	Yes	Yes
BA1	125 V Battery Set		Switchyard House		Yes	Yes	Yes
BA2	125 V Battery Set		Switchyard House		Yes	Yes	Yes
BC1	125 V Battery Charger		Switchyard House		Yes	Yes	Yes

Electrical Equipment							
Tag	Item	Description	Comment	Location	Anchorage Satisfactory?	Free From Known Seismic Vulnerabilities?	Free From Seismic Interaction?
BC2	125 V Battery Charger		Switchyard House		Yes	Yes	Yes
DP1	125 V Distribution Switchboard		Switchyard House		Yes	Yes	Yes
DP2	125 V Distribution Panel		Switchyard House		Yes	Yes	Yes
DP3	Distr SWBD		Switchyard House		Yes	Yes	Yes
DP4	Distr Panel		Switchyard House		Yes	Yes	Yes
2B012	250 V Battery Set		Turbine Oil Pressure		Yes	Yes	Yes
2B006A	250 V Battery Charger				Yes	Yes	Yes
2B006	250 V Battery Charger		Standby		Yes	Yes	Yes
2D6	250 V Distribution Switchboard				Yes	Yes	Yes
2B019	250 V Battery Set		Turbine Oil Pressure		Yes	Yes	Yes
2B018E	250 V Battery Charger				Yes	Yes	Yes
2B018W	250 V Battery Charger				Yes	Yes	Yes
2D7	250 V Distribution Switchboard				Yes	Yes	Yes
2B016	250 V Battery Set		UPS		Yes	Yes	Yes
2B015	250 V Battery Charger				Yes	Yes	Yes
2Y012	120 V Inverter				Yes	Yes	Yes
2Y010	120 V Inverter			Turbine Building	Yes	Yes	Yes
2Y011	120 V Inverter			Turbine Building	Yes	Yes	Yes
2B005S	Single Cell Chargers				Yes	Yes	Yes
2B006S	Single Cell Chargers				Yes	Yes	Yes

Electrical Equipment							
Tag	Item	Description	Comment	Location	Anchorage Satisfactory?	Free From Known Seismic Vulnerabilities?	Free From Seismic Interaction?
2B015S	Single Cell Chargers				Yes	Yes	Yes
2B018S	Single Cell Chargers				Yes	Yes	Yes
2Q017	Q Panel			45' Penetration Building	Yes	Yes	Yes
2Q018	Q Panel			7' Turbine Building	Yes	Yes	Yes
2Q019	Q Panel			34' Turbine Building	Yes	Yes	Yes
2Q026	Q Panel			30' Turbine Building	Yes	Yes	Yes
2Q027	Q Panel			7' Turbine Building	Yes	Yes	Yes
2Q028	Q Panel			63' Penetration Building	Yes	Yes	Yes
2Q031	Q Panel			50' Control Building	Yes	Yes	Yes
2/3Q032	Q Panel			50' Control Building	Yes	Yes	Yes
2/3Q033	Q Panel			50' Control Building	Yes	Yes	Yes
2/3Q035	Q Panel			50' Control Building	Yes	Yes	Yes
2Q038	Q Panel			34' Turbine Building	Yes	Yes	Yes
2Q039	Q Panel			50' Control Building	Yes	Yes	Yes
2Q040	Q Panel			56' Turbine Building	Yes	Yes	Yes
2Q041	Q Panel			50' Control Building	Yes	Yes	Yes
2Q042	Q Panel			7' Turbine Building	Yes	Yes	Yes
2Q060	Q Panel			30' Control Building	Yes	Yes	Yes
2Q062	Q Panel			50' Control Building	Yes	Yes	Yes
2Q063	Q Panel			50' Control Building	Yes	Yes	Yes

Electrical Equipment							
Tag	Item	Description	Comment	Location	Anchorage Satisfactory?	Free From Known Seismic Vulnerabilities?	Free From Seismic Interaction?
2Q065	Q Panel			50' Control Building	Yes	Yes	Yes
2Q069	Q Panel			7' Turbine Building	Yes	Yes	Yes
2Q070	Q Panel			7' Turbine Building	Yes	Yes	Yes
2Q071	Q Panel			50' Control Building	Yes	Yes	Yes
2/3Q072	Q Panel			50' Control Building	Yes	Yes	Yes
2Q074	Q Panel			50' Control Building	Yes	Yes	Yes
2Q075	Q Panel			50' Control Building	Yes	Yes	Yes
2/3Q076	Q Panel			70' Control Building	Yes	Yes	Yes
2Q077	Q Panel			30' Turbine Building	Yes	Yes	Yes
2Q078	Q Panel			30' Turbine Building	Yes	Yes	Yes
2Q079	Q Panel			34' Turbine Building	Yes	Yes	Yes
2Q080	Q Panel			34' Turbine Building	Yes	Yes	Yes
2Q083	Q Panel			30' Control Building	Yes	Yes	Yes
2/3Q084	Q Panel			9' Control Building	Yes	Yes	Yes
2/3Q085	Q Panel			HFMUD	Yes	Yes	Yes
2Q0611	Q Panel			7' Turbine Building	Yes	Yes	Yes
2Q0612	Q Panel			50' Control Building	Yes	Yes	Yes
2Q800N				50' Control Building	Yes	Yes	Yes
2Q800S				50' Control Building	Yes	Yes	Yes

Electrical Equipment							
Tag	Item	Description	Comment	Location	Anchorage Satisfactory?	Free From Known Seismic Vulnerabilities?	Free From Seismic Interaction?
2Q809				9' Control Building	Yes	Yes	Yes
2Q870				70' Control Building	Yes	Yes	Yes
NE Bus	Bus Support Structures			Switchyard	Yes	Yes	Yes
NW Bus	Bus Support Structures			Switchyard	Yes	Yes	Yes
CC (6 each)	Bus Coupling Capacitor	Phase to Ground Coupling Capacitor		Switchyard	Yes	Yes	Yes
"A" Section Bus Disconnect (2 each)	3 Phase Disconnect Switch	Center Break Disconnect Switch 200 kV		Switchyard	Yes	Yes	Yes
Bus Ground Disconnect (2 each)	3 Phase Disconnect Switch	Center Break Disconnect Switch 200 kV		Switchyard	Yes	Yes	Yes
PT (6 each)	Potential Transformer			Switchyard	Yes	Yes	Yes
CCVT (6 each)	Coupling Capacitor Voltage Transformer			Switchyard	Yes	Yes	Yes
CB-4022	Feed Power Circuit Breaker	Dead Tank Gas Circuit Breaker 220 kV	IEEE 693 Qualified	Switchyard	Yes	Yes	Yes
CB-6022	Feed Power Circuit Breaker	Dead Tank Gas Circuit Breaker 220 kV	IEEE 693 Qualified	Switchyard	Yes	Yes	Yes
Bus Disconnect (2 each)	3 Phase Disconnect Switch	Center Break Disconnect Switch 200 kV		Switchyard	Yes	Yes	Yes
Line Disconnect (2 each)	3 Phase Disconnect Switch	Center Break Disconnect Switch 200 kV	Downcomer Interaction	Switchyard	Yes	No	No
Ground Disconnect	3 Phase Disconnect Switch	Center Break Disconnect Switch 200 kV		Switchyard	Yes	Yes	Yes
CCVT (4 each)	Coupling Capacitor Voltage Transformer		Downcomer Interaction	Switchyard	No	No	No
Transmission Line Position 2	Dead End Structure		Pardee Type Structure	Switchyard	Yes	No	No

Electrical Equipment							
Tag	Item	Description	Comment	Location	Anchorage Satisfactory?	Free From Known Seismic Vulnerabilities?	Free From Seismic Interaction?
CB-4042	Feed Power Circuit Breaker	Dead Tank Gas Circuit Breaker 220 kV	IEEE 693 Qualified	Switchyard	Yes	Yes	Yes
CB-6042	Feed Power Circuit Breaker	Dead Tank Gas Circuit Breaker 220 kV	IEEE 693 Qualified	Switchyard	Yes	Yes	Yes
Bus Disconnect (2 each)	3 Phase Disconnect Switch	Center Break Disconnect Switch 200 kV		Switchyard	Yes	Yes	Yes
Line Disconnect (2 each)	3 Phase Disconnect Switch	Center Break Disconnect Switch 200 kV	Downcomer Interaction	Switchyard	Yes	No	No
Ground Disconnect	3 Phase Disconnect Switch	Center Break Disconnect Switch 200 kV		Switchyard	Yes	Yes	Yes
CCVT (3 each)	Coupling Capacitor Voltage Transformer		Downcomer Interaction	Switchyard	No	No	No
CT (3 each)	Current Transformer		Downcomer Interaction	Switchyard	No	No	No
Unit 2 Overhead Line Position 4	Dead End Structures (2 each)		Pardee Type Structure	Switchyard	Yes	No	No
CB-4052	Feed Power Circuit Breaker	Dead Tank Gas Circuit Breaker 220 kV	IEEE 693 Qualified	Switchyard	Yes	Yes	Yes
CB-6052	Feed Power Circuit Breaker	Dead Tank Gas Circuit Breaker 220 kV	IEEE 693 Qualified	Switchyard	Yes	Yes	Yes
Bus Disconnect (2 each)	3 Phase Disconnect Switch	Center Break Disconnect Switch 200 kV		Switchyard	Yes	Yes	Yes
Line Disconnect (2 each)	3 Phase Disconnect Switch	Center Break Disconnect Switch 200 kV	Downcomer Interaction	Switchyard	Yes	No	No
Ground Disconnect	3 Phase Disconnect Switch	Center Break Disconnect Switch 200 kV		Switchyard	Yes	Yes	Yes
CCVT (4 each)	Coupling Capacitor Voltage Transformer		Downcomer Interaction	Switchyard	No	No	No
Transmission Line Position 5	Dead End Structure		Pardee Type Structure	Switchyard	Yes	No	No
CB-4062	Generator Power Circuit Breaker	Dead Tank Gas Circuit Breaker 220 kV	IEEE 693 Qualified	Switchyard	Yes	Yes	Yes

Electrical Equipment							
Tag	Item	Description	Comment	Location	Anchorage Satisfactory?	Free From Known Seismic Vulnerabilities?	Free From Seismic Interaction?
CB-6062	Generator Power Circuit Breaker	Dead Tank Gas Circuit Breaker 220 kV	IEEE 693 Qualified	Switchyard	Yes	Yes	Yes
Bus Disconnect (2 each)	3 Phase Disconnect Switch	Center Break Disconnect Switch 200 kV		Switchyard	Yes	Yes	Yes
Line Disconnect (2 each)	3 Phase Disconnect Switch	Center Break Disconnect Switch 200 kV	Downcomer Interaction	Switchyard	Yes	No	No
Ground Disconnect	3 Phase Disconnect Switch	Center Break Disconnect Switch 200 kV		Switchyard	Yes	Yes	Yes
CCVT (3 each)	Coupling Capacitor Voltage Transformer		Downcomer Interaction	Switchyard	No	No	No
CT (6 each)	Current Transformer		Downcomer Interaction	Switchyard	No	No	No
Unit 2 Overhead Line Position 6	Dead End Structures (2 each)		Pardee Type Structure	Switchyard	Yes	No	No
CB-4072	Feed Power Circuit Breaker	Dead Tank Gas Circuit Breaker 220 kV	IEEE 693 Qualified	Switchyard	Yes	Yes	Yes
CB-6072	Feed Power Circuit Breaker	Dead Tank Gas Circuit Breaker 220 kV	IEEE 693 Qualified	Switchyard	Yes	Yes	Yes
Bus Disconnect (2 each)	3 Phase Disconnect Switch	Center Break Disconnect Switch 200 kV		Switchyard	Yes	Yes	Yes
Line Disconnect (2 each)	3 Phase Disconnect Switch	Center Break Disconnect Switch 200 kV	Downcomer Interaction	Switchyard	Yes	No	No
Ground Disconnect	3 Phase Disconnect Switch	Center Break Disconnect Switch 200 kV		Switchyard	Yes	Yes	Yes
CCVT (3 each)	Coupling Capacitor Voltage Transformer		Downcomer Interaction	Switchyard	No	No	No
Unit 2 Overhead Line position 7	Dead End Structure		Pardee Type Structure	Switchyard	Yes	No	No
CB-4082	Feed Power Circuit Breaker	Dead Tank Gas Circuit Breaker 220 kV	IEEE 693 Qualified	Switchyard	Yes	Yes	Yes
CB-6082	Feed Power Circuit Breaker	Dead Tank Gas Circuit Breaker 220 kV	IEEE 693 Qualified	Switchyard	Yes	Yes	Yes

Electrical Equipment							
Tag	Item	Description	Comment	Location	Anchorage Satisfactory?	Free From Known Seismic Vulnerabilities?	Free From Seismic Interaction?
Bus Disconnect (2 each)	3 Phase Disconnect Switch	Center Break Disconnect Switch 200 kV		Switchyard	Yes	Yes	Yes
Line Disconnect (2 each)	3 Phase Disconnect Switch	Center Break Disconnect Switch 200 kV	Downcomer Interaction	Switchyard	Yes	No	No
Ground Disconnect	3 Phase Disconnect Switch	Center Break Disconnect Switch 200 kV		Switchyard	Yes	Yes	Yes
CCVT (3 each)	Coupling Capacitor Voltage Transformer		Downcomer Interaction	Switchyard	No	No	No
Unit 2 Overhead Line Position 8	Dead End Structure		Pardee Type Structure	Switchyard	Yes	No	No
CB-4112	Cross-Tie Power Circuit Breaker	Dead Tank Gas Circuit Breaker 220 kV	IEEE 693 Qualified	Switchyard	Yes	Yes	Yes
CB-6112	Cross-Tie Power Circuit Breaker	Dead Tank Gas Circuit Breaker 220 kV	IEEE 693 Qualified	Switchyard	Yes	Yes	Yes
CT (6 each)	Current Transformer			Switchyard	Yes	Yes	Yes
2L-002	Turbine Protection Cubicle			Control Building El.30	Yes	Yes	Yes
2L-014	Unitized Actuator Panel			Control Building El.30	Yes	Yes	Yes
2L-015	Turbine Supervisory Equipment Panel			Control Building El.30	Yes	Yes	Yes
2L-017	Electric Governor Cubicle			Control Building El.30	Yes	Yes	Yes
2L-048	Feedwater Control System Rack 1			Control Building El.30	Yes	Yes	Yes
2L-049	Feedwater Control System Rack 2			Control Building El.30	Yes	Yes	Yes
2L-120	Steam Bypass System Rack			Control Building El.30	Yes	Yes	Yes
2L-4	Gen. Gas Control Cubicle			Turbine Building El. 15	Yes	Yes	Yes
2/3L-104	Air Compressor Panel			Turbine Building El. 15	Yes	Yes	Yes
2L-12	Turbine Protection Cubicle			Turbine Building El. 45	Yes	Yes	Yes
2L-08	Excitation Control Cubicle			Turbine Building El. 45	Yes	Yes	Yes

Electrical Equipment							
Tag	Item	Description	Comment	Location	Anchorage Satisfactory?	Free From Known Seismic Vulnerabilities?	Free From Seismic Interaction?
2L-70	Generator Protective Relay Panel			Control Building El.15	Yes	Yes	Yes
2L-73	Turbine Auxillary Control Relay Panel			Control Building El.15	Yes	Yes	Yes
Pos. 1-17	Relay Panels			Switchyard Relay House	Yes	Yes	Yes

Explanation:

1. IEEE = Institute of Electrical and Electronics Engineers
2. kV = kilovolts
3. V = volts

Appendix D
Mechanical Equipment List

Mechanical Equipment					
System	Item/Subsystem	Description/Breakdown	Anchorage Satisfactory?	Free From Known Seismic Vulnerabilities?	Free From Seismic Interaction?
Reactor Coolant Pumps	Pump Motor		Yes	Yes	Yes
	Oil Lift Pumps	Operating and Backup	Yes	Yes	Yes
	Other	Anti-Reverse Rotation Pumps	Yes	Yes	Yes
		ARRP Motor	Yes	Yes	Yes
	Motor and Seal Heat Exchangers	Yes	Yes	Yes	
Pressurizer Relief Discharge System	Quench Tank		Yes	Yes	Yes
	Valves		Yes	Yes	Yes
Demineralized Water Makeup System	Demineralized Water Storage System	Makeup Demineralized Water Tanks	No	No	No
Ultimate Heat Sink	Main Offshore Intake Structure		Yes	Yes	Yes
	Intake Conduit	From One Pipe Section Beyond Auxiliary Intake Structure to Main Offshore Intake Structure	Yes	Yes	Yes
	Outfall Conduit	West End Box Conduit Seaward	No	No	No
Condensate Storage Facility	Condensate Storage Tank T-120		Yes	Yes	Yes
	Pumps		Yes	Yes	Yes
	Piping and Valves		Yes	Yes	Yes
Nuclear Service Water System	Storage Tank		Yes	Yes	Yes
	Pumps and Motors		Yes	Yes	Yes
	Piping and Valves		Yes	Yes	Yes
	Other		Yes	Yes	Yes
Turbine Plant Cooling Water System	Tanks		Yes	Yes	Yes
	Pumps and Motors		Yes	Yes	Yes
	Piping and Valves		Yes	Yes	Yes
	Heat Exchangers		Yes	Yes	Yes

Mechanical Equipment					
System	Item/Subsystem	Description/Breakdown	Anchorage Satisfactory?	Free From Known Seismic Vulnerabilities?	Free From Seismic Interaction?
	Filters		Yes	Yes	Yes
Compressed Air System	Receivers		Yes	Yes	Yes
	Compressors		Yes	Yes	Yes
	Piping and Valves		Yes	Yes	Yes
	Aftercoolers		Yes	Yes	Yes
	Dryers		Yes	Yes	Yes
	Filters		Yes	Yes	Yes
Chemical and Volume Control System	Tanks	Volume Control Tank	Yes	Yes	Yes
		Boric Acid Batching Tank	Yes	Yes	Yes
	Pumps	Primary Plant Makeup Pumps	Yes	Yes	Yes
	Motors	Primary Plant Makeup Pump Motors	Yes	Yes	Yes
	Piping and Valves	Letdown Portion (From Letdown Back Pressure Control Valve to Radwaste Diversion Valve)	Yes	Yes	Yes
		Volume Control Tank (Between Isolation Valves)	Yes	Yes	Yes
	Letdown Heat Exchanger		Yes	Yes	Yes
	Purification Ion-Exchanger		Yes	Yes	Yes
	Delithiating Ion-Exchanger		Yes	Yes	Yes
Purification Filter		Yes	Yes	Yes	
Normal Operation--Containment Building Ventilation Systems	Containment Normal Cooling Units	Air Handling Units	Yes	Yes	Yes
		Ductwork and Dampers	Yes	Yes	Yes
		Chillers	Yes	Yes	Yes
		Chilled Water Pumps	Yes	Yes	Yes
		Compression Tanks	Yes	Yes	Yes
	Piping and Valves		Yes	Yes	Yes

Mechanical Equipment						
System	Item/Subsystem	Description/Breakdown	Anchorage Satisfactory?	Free From Known Seismic Vulnerabilities?	Free From Seismic Interaction?	
	Strainers		Yes	Yes	Yes	
	CEDM Cooling System	Cooling Coils	Yes	Yes	Yes	
		Fans and Motors	Yes	Yes	Yes	
		Ductwork and Dampers	Yes	Yes	Yes	
	Reactor Cavity Cooling System	Fans and Motors	Yes	Yes	Yes	
		Ductwork and Dampers	Yes	Yes	Yes	
	MSIV Enclosure and Penetration Area Cooling System	Supply Fans	Yes	Yes	Yes	
		Ductwork and Dampers	Yes	Yes	Yes	
	Normal Operation--Auxiliary Building Ventilation Systems	Control Room System	Air Handling Units	Yes	Yes	Yes
			Fan Coil Units	Yes	Yes	Yes
Computer Room Fan Coil Units			Yes	Yes	Yes	
Electric Duct Heaters			Yes	Yes	Yes	
Exhaust Fans			Yes	Yes	Yes	
Transfer Fans			Yes	Yes	Yes	
Ductwork and Dampers			Yes	Yes	Yes	
Radwaste Area System		CEDMCS Room Fan Coil Units	Yes	Yes	Yes	
ESF Switchgear Room Systems		Air Handling Units	Yes	Yes	Yes	
		Exhaust Fans	Yes	Yes	Yes	
		Electric Duct Heaters	Yes	Yes	Yes	
		Ductwork and Dampers	Yes	Yes	Yes	
Non-Class 1E Switchgear Room Systems		Exhaust Fans	Yes	Yes	Yes	
		Ductwork and Dampers	Yes	Yes	Yes	
		Prefilters	Yes	Yes	Yes	
Chiller Room Systems		Air Handling Unit	Yes	Yes	Yes	

Mechanical Equipment						
System	Item/Subsystem	Description/Breakdown	Anchorage Satisfactory?	Free From Known Seismic Vulnerabilities?	Free From Seismic Interaction?	
		Exhaust Fan	Yes	Yes	Yes	
		Ductwork and Dampers	Yes	Yes	Yes	
	Battery Room Systems	Air Handling Unit	Yes	Yes	Yes	
		Exhaust Fan	Yes	Yes	Yes	
		Ductwork and Dampers	Yes	Yes	Yes	
	Normal Chilled Water System	Chillers	Yes	Yes	Yes	
		Pumps and Motors	Yes	Yes	Yes	
		Air Separator	Yes	Yes	Yes	
		Compression Tank	Yes	Yes	Yes	
		Piping and Valves	Yes	Yes	Yes	
	Continuous Exhaust System	Fans	Yes	Yes	Yes	
		Ductwork and Dampers	Yes	Yes	Yes	
		Plant Vent Stacks	Yes	Yes	Yes	
	Turbine Building Ventilation System	Switchgear Room and D6 Battery (Elevation 7') Room Systems	Supply Air Units	Yes	Yes	Yes
			Exhaust Fans and Motors	Yes	Yes	Yes
Ductwork and Dampers			Yes	Yes	Yes	
Electric Duct Heaters			Yes	Yes	Yes	
Lube Oil Room System		Supply Air Units	Yes	Yes	Yes	
		Exhaust Fans and Motors	Yes	Yes	Yes	
		Ductwork and Dampers	Yes	Yes	Yes	
Steam Air Ejector Exhaust System		Piping and Valves	Yes	Yes	Yes	
Main Generator Iso-Phase Bus Connection Enclosure Ventilation System		Exhaust Fans and Motors	Yes	Yes	Yes	
		Ductwork	Yes	Yes	Yes	
D7 Battery and Battery Charger		Supply Air Units	Yes	Yes	Yes	

Mechanical Equipment						
System	Item/Subsystem	Description/Breakdown	Anchorage Satisfactory?	Free From Known Seismic Vulnerabilities?	Free From Seismic Interaction?	
	Rooms (Elevation 56')	Exhaust Fans and Motors	Yes	Yes	Yes	
		Ductwork and Dampers	Yes	Yes	Yes	
		Electric Duct Heaters	Yes	Yes	Yes	
Fire Protection System	Tanks		Yes	Yes	Yes	
	Pumps and Motors		Yes	Yes	Yes	
	Piping and Valves		Yes	Yes	Yes	
Turbine-Generator	Turbine: High, Low Pressure		Yes	Yes	Yes	
	Control and Protective Valve System		Yes	Yes	Yes	
	Turbine Drains		Yes	Yes	Yes	
	Exhaust Hood Spray System		Yes	Yes	Yes	
	Lube Oil System	Components		Yes	Yes	Yes
		Piping		Yes	Yes	Yes
	Electric Turning Gear		Yes	Yes	Yes	
	Turbine Control System		Yes	Yes	Yes	
	Turbine Control Panel		Yes	Yes	Yes	
	Turbine Supervisory System		Yes	Yes	Yes	
	Turbine Protective Devices		Yes	Yes	Yes	
	Turbine Overspeed Protection		Yes	Yes	Yes	
	Turbine Monitoring Equipment		Yes	Yes	Yes	
	Turbine Support Accessories		Yes	Yes	Yes	
	Generator		Yes	Yes	Yes	
	Seal Oil System		Yes	Yes	Yes	
Hydrogen Coolers		Yes	Yes	Yes		
Generator H ₂ /CO ₂ System		Yes	Yes	Yes		

Mechanical Equipment					
System	Item/Subsystem	Description/Breakdown	Anchorage Satisfactory?	Free From Known Seismic Vulnerabilities?	Free From Seismic Interaction?
	Stator Water System		Yes	Yes	Yes
	Exciter Switchgear and Voltage Regulator		Yes	Yes	Yes
	Exciter		Yes	Yes	Yes
	Piping and Valves		Yes	Yes	Yes
Main Steam Supply System	Reheaters		Yes	Yes	Yes
	Moisture Separator-Reheater Drain Tanks		Yes	Yes	Yes
	Main Steam Tube Bundle Drain Tanks		Yes	Yes	Yes
	Bled Steam Tube Bundle Drain Tanks		Yes	Yes	Yes
	Y-Strainers		Yes	Yes	Yes
	Piping and Valves		Yes	Yes	Yes
Main Condenser	Main Condensers		Yes	Yes	Yes
	Vent and Drain System		Yes	Yes	Yes
	Piping and Valves		Yes	Yes	Yes
Main Condenser Evacuation System	Seal Water Heat Exchanger		Yes	Yes	Yes
	Air Ejector Condenser		Yes	Yes	Yes
	Air Ejectors		Yes	Yes	Yes
	Condenser Vacuum Pump		Yes	Yes	Yes
	Seal Water Pumps		Yes	Yes	Yes
	Separator Tanks		Yes	Yes	Yes
Turbine Gland Sealing System	Gland Steam Condenser Exhaust Fan		Yes	Yes	Yes
	Gland Steam Condenser		Yes	Yes	Yes
	Piping and Valves		Yes	Yes	Yes
Turbine Bypass System	Piping and Valves		Yes	Yes	Yes
Circulating Water System	Pumps and Motors		Yes	Yes	Yes

Mechanical Equipment					
System	Item/Subsystem	Description/Breakdown	Anchorage Satisfactory?	Free From Known Seismic Vulnerabilities?	Free From Seismic Interaction?
	Piping and Valves		Yes	Yes	Yes
	Expansion Joints		Yes	Yes	Yes
	Strainers		Yes	Yes	Yes
	Traveling Rakes and Bar Screens		Yes	Yes	Yes
	Gates #4, 5, and 6		Yes	Yes	Yes
	Gate Operators and Accessory Equipment		Yes	Yes	Yes
Condensate and Feedwater System	Tanks	Heater Drain Tanks	Yes	Yes	Yes
		Feedwater Pump Seal Drain Tanks	Yes	Yes	Yes
		Feedwater Pump Turbine Drain Tanks	Yes	Yes	Yes
	Pumps and Motors	Condensate Transfer Pumps	Yes	Yes	Yes
		Condensate Pumps	Yes	Yes	Yes
		Heater Drain Pumps	Yes	Yes	Yes
		Feedwater Pumps	Yes	Yes	Yes
		Feedwater Pump Turbine Drain Pumps	Yes	Yes	Yes
	Piping and Valves		Yes	Yes	Yes
	Other		Yes	Yes	Yes
Feedwater Heaters		Yes	Yes	Yes	
Steam Generator Blowdown System	Piping and Valves		Yes	Yes	Yes
	Blowdown Heat Exchanger		Yes	Yes	Yes
Turbine Plant Chemical Addition System	Pumps and Motors	Amine Feed Pumps	Yes	Yes	Yes
	Piping and Valves		Yes	Yes	Yes

Explanation:

- | | |
|--|-------------------------------------|
| 1. CEDM = Control Element Drive Mechanism | 4. H ₂ = Hydrogen |
| 2. CEDMCS = Control Element Drive Mechanism Control system | 5. CO ₂ = Carbon Dioxide |
| 3. MSIV = Main Steam Isolation Valve | |

Appendix E
Evaluation of Important-to-Reliability NSR Building Structures

E.1 INTRODUCTION

E.1.1 Objective

The objective of this assessment was to determine if any of the non-power block NSR buildings that house important-to-reliability NSR SSCs could cause a prolonged outage due to a seismic event.

E.1.2 Scope of Work

The scope of work involved 1) identifying the NSR buildings that house important-to-reliability NSR SSCs and 2) evaluating the extent of damage of the selected buildings in the event of a SONGS review level earthquake. This assessment was achieved by:

- Reviewing available structural and architectural drawings and calculations to form engineering opinions of the expected seismic performance of each building relative to other similar buildings of the same vintage located in the same seismic environment.
- Selecting an appropriate corresponding HAZUS model building type for each building based on the building's characteristics.
- Modifying the HAZUS fragility curves for the appropriate model building types using engineering judgment.
- Estimating the probable damage of each building in the event of a SONGS review level earthquake.

The description of each selected building and the basis of the HAZUS building fragility evaluations are summarized in this appendix.

E.2 NSR BUILDINGS THAT HOUSE IMPORTANT-TO-RELIABILITY NSR SSCs

The buildings included in the scope of this study were constructed between the 1970s and 1990s. Three SONGS buildings were identified as housing important-to-reliability NSR SSCs:

- Mesa Warehouse.
- SCE Switchyard Relay House.
- SDG&E Switchyard Relay House.

The Mesa warehouse was selected because it houses replacement parts that may be required to repair important-to-reliability NSR SSCs following the occurrence of an earthquake. The SCE

and SDG&E switchyard relay houses contain switchyard control instrumentation that is required for the transmission of the power generated at the plant.

E.3 ASSESSMENT PROCESS

E.3.1 Field Observations

As part of the assessment, a walk-through was completed at the Mesa warehouse and switchyard. The purpose of the walk-through was to become familiar with the buildings, observe the general conformance of the actual constructed facilities to the original drawings, and take representative photographs of the buildings' gravity and lateral load carrying systems.

E.3.2 Document Review

In addition to the walk-throughs, the structural, civil, and architectural drawings, as available, were reviewed for all three buildings. The SONGS structural design calculations were also examined. In many cases, the drawings available were not complete sets and / or information about the seismic details was lacking, which is important when making decisions about the quality factors (defined in Section E.4.6). The drawings were reviewed to develop an engineering opinion about the quality of the seismic design features and were compared with drawings of similar buildings of the same vintage and seismic zone (which were still in the Uniform Building Code (UBC) and in use at the time these buildings were designed). Summaries of the reviews are provided below.

E.3.3 Mesa Warehouse Building

E.3.3.1 Information Reviewed

The following drawings and calculations were reviewed in association with the Mesa warehouse:

- Drawing C-1: General Notes, March 30, 1982.
- Civil Drawing C-2: Offsite Warehouses Sections and Details, March 30, 1982.
- Structural Drawing S-6: 100,000 sq. ft Warehouse Foundation Sections and Details, March 30, 1982.
- Structural Drawings S-9, S-10: 100,000 sq. ft Warehouse Miscellaneous Sections and Details, September 14, 1983.

- Structural Drawing S-11: 100,000 sq. ft Warehouse Office Area Framing Plans, December 19, 1983.
- Structural Drawings S-12, S-13: 100,000 sq. ft Warehouse Office Area Framing Sections and Details, December 19, 1983.
- Structural Calculations for building frame and lateral bracing performed by Capitol Metal Buildings, Stockton, California, May 21, 1982 and June 11, 1982.
- Structural Calculations for building foundation and slab-on-grade performed by Engineering Department of S.C. Edison Co., March 11, 1982.

E.3.3.2 Building Description

The Mesa warehouse consists of three interconnected structures. The warehouse is a single-story prefabricated metal building with dimensions of 400 ft by 250 ft. The adjacent office building has plan dimensions of 240 ft by 75 ft. The adjacent flammable material storage space has dimensions of 150 ft by 250 ft. The buildings were constructed circa 1982 using the seismic provisions of the 1979 UBC.

E.3.3.2.1 Gravity Load-Resisting System

The gravity load-resisting systems of the three buildings consist of gable type portal frames placed at 25 ft on center (o.c.). Eight inch (in.) deep gage metal Z purlins span between the frames and support the metal deck roofs that complete the gravity load-resisting system. The steel columns are supported by isolated footings. The reinforced concrete slab-on-grade is 6 in. thick.

E.3.3.2.2 Lateral Load-Resisting System

The lateral load-resisting systems of the three buildings consist of gable type portal frames in the transverse direction and X-braced frames in the longitudinal direction. The frames in the transverse direction are spaced at 25 ft o.c. and consist of tapered girders and columns with fully welded moment connections. The column base connection at the transverse moment frame columns was designed as a pinned connection. It includes four 1-1/8 in. diameter anchor rods embedded approximately 22 in. into the foundation. The X-braced frames consist of single-angle members. Lateral load from the roofs is accumulated along the purlins and transferred to the longitudinal bracing through a system of horizontal rod X bracing, whose location coincides with the location of the braced frame bays.

A gravity load-carrying column is located in the warehouse at the center of the bay that breaks up the span of the girders into two identical spans of 125 ft each. There are four bays of longitudinal bracing on each end bay.

The office building relies on the continuation of the frames from the warehouse for its lateral support in the transverse direction. Along the longitudinal direction, it has three bays of diagonal steel angle bracing.

A similar system exists in the flammable materials storage space as well. It has five bays of transverse frames and two bays of longitudinal bracing.

Using the terminology of HAZUS, the Mesa warehouse is a S3 – Steel Light Frame Structure.

E.3.3.3 Discussion

Although prefabricated metal buildings do not typically have a robust lateral system, they have performed relatively well in past earthquakes. Based on the review of the moment connections, it is expected that they will have a performance similar to pre-Northridge earthquake connections of similar vintage. However, due to the relatively large spans of the girders, it is likely that the building has inadequate lateral stiffness to prevent damage due to seismic loads in the transverse direction. In the longitudinal direction, the resistance is provided by ordinary single angle tension braces only, since the compression braces are expected to buckle and provide negligible lateral resistance. In addition to these deficiencies, past experience with these types of buildings has indicated that the rod bracing at the roof diaphragm level will likely not be adequate to prevent damage, thereby providing an indirect load path for the seismic loads.

E.3.3.4 Recommendations

It is recommended that a quality factor (see Section E.4.6) of 1.2 be used both for transverse loading and longitudinal loading relative to buildings similar to the vintage of the Mesa warehouse.

E.3.4 Switchyard Relay Houses

E.3.4.1 Information Reviewed

The following calculation was used to perform this review:

- Structural Calculations for San Onofre Generating Station, 220 kilovolt (kV) Switchyard, October 14, 1975 performed by Bechtel.

E.3.4.2 Building Description

The two switchyard relay houses are referred to as the SCE building and the SDG&E building. Both are roughly of equal size, rectangular in plan with major dimensions of 35 ft by 28 ft. The roof of each is about 11 ft above the finished floor. One edge of each of the buildings is buried into the sloping ground with the concrete wall acting as a retaining wall. The remaining walls of the buildings are of reinforced masonry. The buildings were constructed circa 1974 using the provisions of the 1973 UBC. However, the design calculations point out that an internal SCE criterion requiring the structures to be designed for a base shear capacity of 0.5g was used. Due to similar construction, a single assessment was applied to the two switchyard relay houses.

E.3.4.2.1 Gravity Load-Resisting System

Structural and architectural drawings of the buildings were unavailable. Design calculations show that the perimeter walls along with an open-steel, open-web joist system and the 1-1/2 in. deep metal deck with 3 in. concrete topping constitute the gravity load-resisting system.

E.3.4.2.2 Lateral Load-Resisting System

The lateral load-resisting systems of the switchyard relay houses include the perimeter reinforced masonry walls along with the concrete shear wall that also acts as the retaining wall. The masonry walls are grouted at 32 in. o.c. with a #5 bar in the cell. Remaining cells are also grouted with Zonolite masonry fill up to the bond beam level. The roof diaphragm of each structure is a 1-1/2 in. deep metal deck with 3 in. deep concrete topping.

E.3.4.3 Discussion

The switchyard relay houses have been designed to a high level of base shear, even compared to the current 2007 California Building Code (CBC). The steel deck roof diaphragm is positively attached (through welding) to the masonry walls with steel angles that are connected to the masonry walls with 7/8 in. diameter cast in place bolts placed at 16 in. o.c. These structures are expected to behave in a superior fashion in an earthquake.

Using the terminology of HAZUS, the switchyard relay houses can be classified as a C2L – Low Rise Concrete Shear Wall Building. The other possible classification as a RM2L – Reinforced Masonry Bearing Wall with Precast Concrete Diaphragms is not applicable.

E.3.4.4 Recommendations

As a result of reviewing the calculations, it is recommended that a quality factor (see Section E.4.6) of 0.8 be used for the HAZUS analysis of the switchyard relay houses.

E.4 BUILDING FRAGILITY

E.4.1 HAZUS Fragility Data

HAZUS is national consensus software developed by the FEMA to help estimate damage to the built environment as the result of future scenario earthquakes (FEMA, 2003, 2005). One of its primary purposes of the software is to help government agencies evaluate risks, and the software includes national databases embedded within. This software is described in the Technical Manual. There is also an Advanced Engineering Building Module (AEBM) Manual, which is an extension of the general methods in HAZUS intended for use in estimating individual building losses.

In developing HAZUS, fragility curves for different model building types (e.g., steel light frame buildings) were determined. An example of a fragility curve is shown on Figure E.4-1. Generally the cumulative probability of reaching a damage state for a given level of deformation (drift) or severity of shaking (e.g., PGA) is plotted. This plot is usually generated assuming a lognormal distribution of damage, with a corresponding median and beta (logarithmic standard deviation).

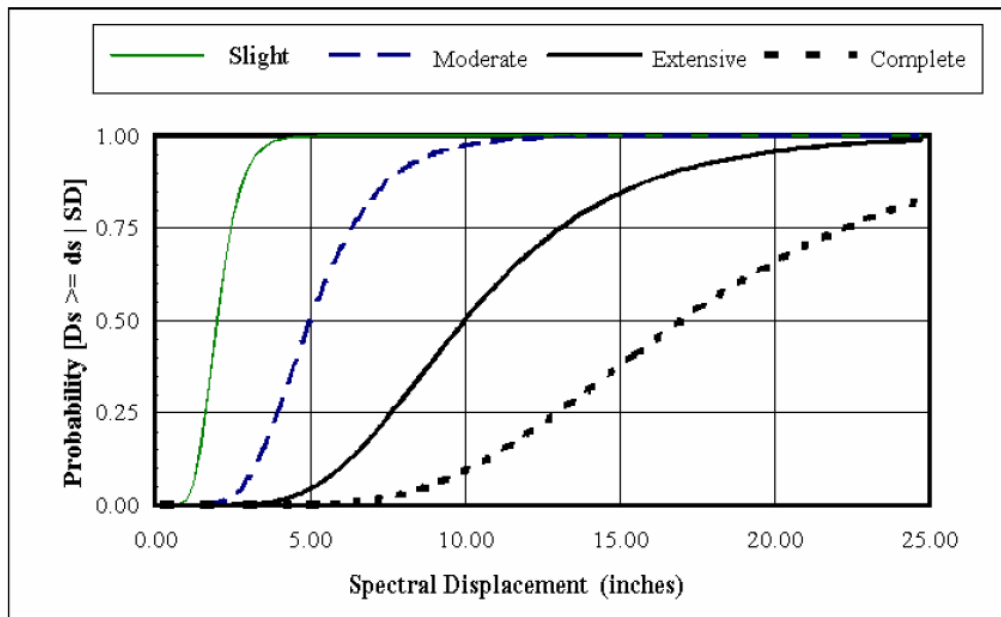


Figure E.4-1 Sample Fragility Curves

E.4.2 Displacement vs. PGA

While most of the fragility data in the HAZUS Technical Manual is based on building displacements, an alternate procedure that is based on PGA data is also presented. This alternate procedure was used in this evaluation.

E.4.3 Damage States

In the case where different damage states are defined for a building, fragility curves can be developed for each damage state. In HAZUS, the damage states defined are slight, moderate, extensive, and complete. HAZUS fragility functions are provided for each damage state.

The HAZUS Technical Manual indicates that the moderate damage state has 5 to 25% damage, and that it corresponds with a green tag after an earthquake. Moderate damage may be localized. A green tag means that the building has been inspected and that no significant weakening of the structure has occurred. Thus, there are no restrictions on occupancy.

Furthermore, the HAZUS Technical Manual indicates that the extensive damage state has 25 to 100% damage, and corresponds with a yellow tag after an earthquake. A yellow tag means occupancy is restricted but that sufficient reserve capacity exists and that collapse is not expected if an aftershock were to occur. The building cannot be occupied as it was before the earthquake occurred unless some action is taken. Some portion of the building may be unsafe. Generally occupants are permitted to remove important belongings through brief visits until the damage is mitigated, or until the likelihood of a significant aftershock decreases.

Finally, the HAZUS Technical Manual indicates that the complete damage state corresponds with 100% damage, which corresponds with a red tag. A red tag indicates that the building is unsafe and that there is a risk of collapse on its own or due to an aftershock. No entry into the building is permitted, even to conduct repairs or remove important belongings. However, the complete damage state does not necessarily correspond with the physical collapse of a building. In general, the complete damage state implies that building repair costs exceed the cost of building replacement. The HAZUS collapse rates for the various building types are not uniform and range from 3% (wood frame buildings) to 15% (un-reinforced buildings).

As indicated above, fragility curves for different model building types are included in the HAZUS documentation. Model building types of relevance for this study are concrete shear wall buildings (C2) and steel light frame buildings (S3). HAZUS also differentiates between low-rise,

mid-rise, and high-rise buildings. All the buildings included in this study qualify as low-rise buildings.

For each model building type, HAZUS also provides fragility data corresponding to different seismic design levels. The fragility data was developed in the 1990s when seismic zones defined in the UBC were still in use. High-Code is intended to reflect design practice in Seismic Zone 4 after 1975; Moderate-Code is representative of the design practice in Seismic Zone 2B after 1975; and Low-Code is intended to reflect design practice in Seismic Zone 1 after 1975. The AEBM Manual indicates that for buildings constructed between 1941 and 1975 the appropriate design levels should be reduced by one. Only the switchyard relay houses fall into this category. However, the switchyard relay houses were designed for an elevated base shear capacity appropriate for High-Code classification. Buildings constructed prior to 1941 are considered pre-Code and have a different set of fragility data. Thus, there are fragility data for four seismic design levels included in HAZUS.

E.4.4 Design Level

At the time these three buildings were constructed (1970 to 1990), the region that SONGS is located in was considered Seismic Zone 4, according to the UBC. The switchyard relay houses, on the other hand, although designed per 1973 UBC, used the internal SCE guideline of 0.5g base shear coefficient for seismic design qualifying it for the High-Code seismic design level. Based on this information, it was determined that the fragility data associated with the High-Code seismic design level is appropriate for all the buildings.

E.4.5 Fragility Data for Generic Building Types

The median PGA provided in the HAZUS Technical Manual for the fragility curves is given in Table E.4-2. As noted above, these values correspond to High-Code Design.

Table E.4-2 Fragility Data for Generic Building Types

Building Type	Damage State			
	Slight	Moderate	Extensive	Complete
	PGA Median, g	PGA Median, g	PGA Median, g	PGA Median, g
C2L	0.24	0.45	0.90	1.55
S3	0.15	0.26	0.54	1.00

E.4.6 Quality Factor

HAZUS fragility data are intended to represent the average building type of a certain height and age, and are designed using specific building code provisions. However, not all buildings designed under such conditions will perform equally in an earthquake. Based on the drawing review, an assessment was made on whether a building was better or worse than the average building. A quality factor that is used to scale the median of the fragility data was used. In this study, quality factors ranged from 0.8 to 1.2, with 1.2 representing a building with a median that is 1/1.2 lower than the average. Quality factors assigned for each building were presented in Section E.3.

The quality factor not only is used to reflect the superior or inferior detailing or configurations, it also incorporates what was learned by reviewing the drawings or design criteria about the importance factors used in the design. Thus, the quality factor for the switchyard relay houses was decreased to account for the high design base shear coefficient.

E.4.7 Expected Building Fragility Levels

E.4.7.1 Moderate Damage

The fragility level for each of the three structures being in the moderate damage state is listed in Table E.4-3. The generic fragility values of Table E.4-2 are modified by dividing them by the quality factor.

Table E.4-3 Fragility Corresponding with Moderate Damage State

Building	HAZUS Building Type	Quality Factor	Median Fragility, g
Mesa Warehouse	S3	1.2	0.22
Switchyard Relay Houses (2)	C2L	0.8	0.56

Note: Fragilities for all buildings assume High-Code Design.

E.4.7.2 Extensive Damage

The fragility level for each of the three structures in the extensive damage state is listed in Table E.4-4. The generic fragility values of Table E.4-2 are modified by dividing them by the quality factor.

Table E.4-4 Fragility Corresponding with Extensive Damage State

Building	HAZUS Building Type	Quality Factor	Median Fragility, g
Mesa Warehouse	S3	1.2	0.45
Switchyard Relay Houses (2)	C2L	0.8	1.13

Note: Fragilities for all buildings assume High-Code Design.

E.4.7.3 Complete Damage

The fragility level for each of the three structures in the complete damage state is listed in Table E.4-5. The generic fragility values of Table E.4-2 are modified by dividing them by the quality factor.

Table E.4-5 Fragility Corresponding with Complete Damage State

Building	HAZUS Building Type	Quality Factor	Median Fragility, g
Mesa Warehouse	S3	1.2	0.83
Switchyard Relay Houses (2)	C2L	0.8	1.94

Note: Fragilities for all buildings assume High Code Design.

E.5 CONCLUSIONS

For the SONGS review level earthquake, the two switchyard relay houses will sustain only moderate damage and will be green tagged after the earthquake and thus will remain functional. However, the Mesa warehouse will sustain extensive damage and will be yellow tagged following a SONGS review level earthquake and access to the building will be restricted.

The HAZUS damage states used in this evaluation correspond with the structural damage states. Nonstructural components within the building were not directly evaluated; however, they were observed during the walk-through of each building. The relay panels and equipment within the switchyard relay houses are all anchored and braced to the ceiling joists. These components were screened for the SONGS review level earthquake during the equipment walkdowns.

E.6 REFERENCES

FEMA, 2003, Department of Homeland Security and Response Directorate, Federal Emergency Management Agency, Mitigation, Division, Multi-hazard Loss Estimation Methodology, Earthquake Model, HAZUS-MH MR1, Advanced Engineering Building Module, Washington, D.C..

FEMA, 2005, Department of Homeland Security and Response Directorate, Federal Emergency Management Agency, Mitigation, Division, Multi-hazard Loss Estimation Methodology, Earthquake Model, HAZUS-MH MR4, Technical Manual, Washington, D.C..

Appendix 5

Building Codes and Seismic Design Standards

BUILDING CODES AND SEISMIC DESIGN STANDARDS

1 Objective

This report summarizes the evaluation of the San Onofre Nuclear Generating Station (SONGS) non-safety-related (NSR) systems, structures, and components (SSCs) as compared to the current building codes and seismic design standards for non-nuclear power plants. Additionally, a review of the seismic design standards changes was performed to determine if there are any implications to the SONGS NSR SSCs.

2 Building Code Requirements for Power Plant Construction

The original seismic design criteria for SONGS NSR components were specified in the "Project Design Criteria Manual for the San Onofre Nuclear Generation Stations Units 2 & 3." The Seismic Category II equipment was to be designed using an equivalent static seismic load of 0.2g horizontally and 0.13g vertically, applied simultaneously, with no increase in allowable stress levels (a one-third increase in allowable stress levels was a common design practice during the period of SONGS design). This was the general design criteria in use for all SCE power plant structures and equipment anchorages at the time of plant design. In general, the 0.20g lateral loading had been in use for at least two decades prior to the design of SONGS. This 0.20g design criteria had been used for many California power plants and was greater or equal to that required by Uniform Building Code (UBC) of the same vintage. SONGS Seismic Category III SSCs were designed in accordance with the UBC in effect at the time of actual design (mostly 1973-1984).

The switchyard had a 0.50g lateral force design criteria which was an SCE interim substation design criteria adopted after the 1971 San Fernando Earthquake.

Historically, the post-1971 San Fernando Earthquake time period saw major changes in the UBC. Figure 2-2 shows the development of UBC/IBC design levels for non-structural components and equipment from 1933-2006. In the 1979 UBC, force levels were specified for non-structural components and equipment as 0.3g. Prior to 1979, the non-structural loading had been 0.2g. In 1997, the UBC was changed to allow both Load Resistance Factor Design (LRFD) and Allowable Stress Design (ASD), thus the code lateral force coefficients have to be appropriately factored for the chosen design criteria. Also, in 1997, the code lateral force coefficient was made a function of site soil type, component type, and elevation within a structure. In 2000, the International Building Code (IBC) was published, with other revisions following in subsequent years. Figure 2-1 assumes ASD, Zone 4, Site Condition C, and a building elevation ratio, $z/h = 0.55$. As can be noted from Figure 2-1, the effective lateral force factor specified for SONGS NSR seismic design is very close to the design value required in the current 2007 California Building Code (CBC) that is based on the 2006 IBC and ASCE 7-2005.

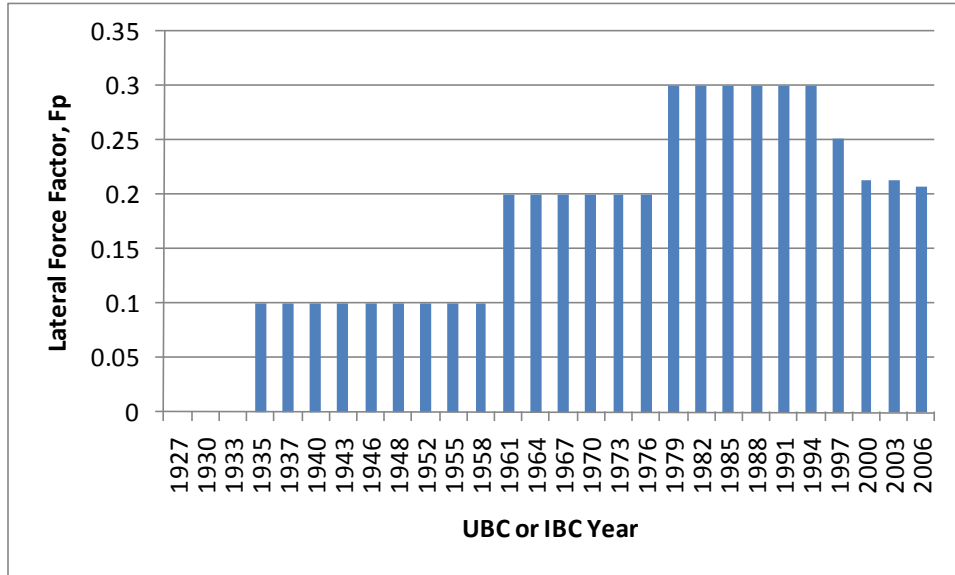


Figure 2-1. Comparison of Building Code Lateral Force Coefficient for Components (Adjusted for Allowable Stress Design and Soil Classification C for 1997-2006)

Seismic anchor loads calculations of a component located within a SONGS Turbine Building (TB) for both the original SONGS design criteria and the current CBC code are provided in Section 3 to illustrate the comparison between the design codes. The 2007 CBC horizontal design loading is about 4% higher than the original design loading. The 2007 CBC vertical design loading is less than the original SONGS design loading. Thus, the anchor loads for both the original design criteria and the current building code are essentially the same.

3 Current Code Anchor Design Comparison

The current code specified for power plant design by the CEC is 2007 California Building Code (CBC) that is based on 2006 IBC and ASCE 7-2005. For LRFD, the horizontal seismic design force for nonstructural components and equipment is calculated, as follows:

$$F_{ph} = \frac{0.4 \cdot a_p \cdot S_{DS} \cdot W_p}{\left(\frac{R_p}{I_p}\right)} \left(1 + 2 \frac{z}{h}\right), \text{ however, } F_{ph} \text{ shall not be less than } F_{ph} = 0.3 \cdot I_p \cdot S_{DS} \cdot W$$

For ASD, the horizontal seismic design force is:

$$F'_{ph} = (0.7) \cdot F_{ph}$$

Where

F_p = seismic design force for LRFD

F'_p = seismic design force for ASD

S_{DS} = short period spectral acceleration (0.2 sec or $f=5$ Hz)

a_p = Component amplification factor (from code table)

I_p = component importance factor (from code table)

W_p = operating weight

R_p = component response modification factor

z = height in structure of point of attachment with respect to the base

h = average roof height structure with respect to the base

For LRFD the vertical seismic design force is: $F_{pv} = 0.20 \cdot S_{DS} \cdot W$

For ASD the vertical seismic design force is: $F'_{pv} = (0.7) \cdot F_{pv}$

Seismic anchor loads calculations for a 150KVA transformer located at Elevation 43 ft in the SONGS TB for the original design criteria and the current code are provided to illustrate the comparison between the design codes.

$W_p = 4450$ lbs

3.1 Original SONGS Design Criteria

$$F'_{ph, original} = 0.2 \cdot W_p = 0.2 \cdot 4450 = 890 \text{ lbs}$$

$$F'_{pv, original} = 0.13 \cdot W_p = 0.13 \cdot 4450 = 579 \text{ lbs}$$

3.2 2007 California Building Code

S_{DS} = 0.882 g (from USGS web site for SONGS longitude and latitude; Site Class C)
 a_p = 1.0
 I_p = 1.0
 R_p = 2.5
 z = 36 ft (approximately 80% of all turbine support equipment is at this level (TB elev. 43') or lower)

h = 65.5 ft (TB height)

$$F_{ph} = \frac{0.4 \cdot 1.0 \cdot 0.882 \cdot W_p}{\left(\frac{2.5}{1.0}\right)} \left(1 + 2 \frac{36}{65.5}\right) = 0.296 \cdot W_p$$

F_p shall not be less than $F_p = 0.3 \cdot S_{DS} \cdot I_p \cdot W_p = 0.265 \cdot W_p$

For Allowable Stress Design load combination, the seismic loads are multiplied by a factor of 0.7

$$F'_{ph, 2007\text{ CBC}} = 0.7 (0.296) 4450 = 922\text{lbs}$$

$$F'_{pv, 2007\text{ CBC}} = 0.7 (0.2) (0.882) (4450) = 549\text{lbs}$$

3.3 Comparison

The 2007 CBC horizontal design loading is about 4% higher than the original design loading. The 2007 CBC vertical design loading is less than the original SONGS design loading. Thus, the anchor loads for both the original design criteria and the current building code are essentially the same.

4 Seismic Design Standards Changes

The seismic standard design changes from the original design to the present time have been reflected in the building code changes throughout this period. These changes are primarily related to the magnitude of calculated earthquake lateral and vertical forces. Sections 2 and 3 of this report show more details about changes in earthquake forces. The 2003 IAEA Safety Guide for the Seismic Design and Qualification of Nuclear Plants (NS-G-1.6) covers primarily safety-related SSCs. The standard looks at the potential of non-safety related SSCs interacting with safety-related SSCs. For this case, the standard prescribes that the non-safety-related SSCs to be designed at the same high level of earthquake as the safety-related SSCs. SONGS non-safety related SSCs whose collapse or failure could result in the loss of the safety functions of safety-related SSCs are designed at the same level earthquake as the safety-related SSCs. Since the above referenced IAEA Safety Guide and SONGS design of non-safety related are very similar, there are no seismic design implications for the SONGS non-safety related SSCs.

5 Conclusion

The report shows that the changes in building codes and associated seismic design standards from the original design to present time does not have any implications for the SONGS NSR SSCs. These SSCs were designed to seismic loads comparable to the current building code.

The 2003 IAEA Safety Guide for the Seismic Design and Qualification of Nuclear Plants (NS-G-1.6) is similar to the requirements of the SONGS design basis and it does not reveal any potential weakness in the SONGS NSR SSCs seismic design.

Appendix 6

San Onofre Nuclear Generating Station Evacuation Time Evaluation Final Report

FINAL REPORT

San Onofre Nuclear Generating Station (SONGS) Evacuation Time Evaluation (ETE)

Prepared for:
Southern California Edison
P.O. Box 700
Rosemead, CA 91770
Tel: 949.368.8345

Prepared by:



Wilbur Smith Associates
900 Wilshire Boulevard, Suite 930
Los Angeles, CA 90017
Tel: 213.627.3855
Fax: 213.627.3859

A31392
June 12, 2007

Table of Contents

	<u>Page</u>
Executive Summary	E-1
Chapter 1 Evacuation Time Estimates for Protective Action Zones	1-1
1.1 Evacuation Time Estimates	1-5
Chapter 2 Data Collection	2-1
2.1 Study Area	2-1
2.2 Emergency Response Plans	2-2
2.3 Transportation Facilities	2-5
2.4 Demographic/Employment Data	2-5
2.5 Schools and Special Institutions	2-6
Chapter 3 Simulation Model	3-1
3.1 The Network	3-1
3.2 General Assumptions	3-2
3.3 Earthquake Assumptions	3-4
3.4 Network Assumptions	3-6
3.5 Centroids	3-8
Chapter 4 Evacuation Scenarios	4-1
4.1 Time Frame Variations	4-1
4.2 I-5 Management Variations	4-2
4.3 Variations in Other Conditions	4-3
Chapter 5 Evacuation Network	5-1
5.1 Major Evacuation Routes	5-1
5.2 Planned Improvements to the Major Roadway Network	5-4
5.3 Designated Evacuation Routes and Reception Centers	5-4
5.4 Evacuation Route Link/Node Network	5-5
5.5 Roadway Characteristics for Evacuation Network	5-5
Chapter 6 Demand Estimates	6-1
6.1 Public Evacuation Time Components	6-1
6.2 Mobilization Rates	6-1
6.3 Evacuation Population Elements	6-3
Chapter 7 Results – Evacuation Time Estimates	7-1
7.1 Emergency Evacuation Time Estimates	7-1
7.2 Evacuation Time Estimates for Protective Action Zone (PAZ) Structure	7-4

7.3	Range of Certainty	7-13
-----	--------------------------	------

Appendices

A.	Appendix A.....	A-1
B.	Public and Private School Enrollment	A-2
C.	Retirement Homes and Hospitals.....	A-4
D.	Appendix D.....	A-5
E.	Contra-Flow Implementation.....	A-11
F.	Sub-Zone Descriptions	A-12

Acronyms		Acr-1
-----------------------	--	-------

Tables

<u>Table</u>		<u>Page</u>
1.1	EPZ Permanent and Transient Population Summary 2011 by Protective Action Zone (PAZ)	1-1
1.2	Estimated 2011 Household Vehicle Ownership and Occupancy Summer Weekend/Weekday and Night	1-4
1.3	2011 PAZ Vehicles Evacuated by Scenario	1-4
1.4a	Summary of Total ETE for All Scenarios Tested Using PAZ Structure (Total Hours to Evacuate EPZ)	1-5
1.4b	Summary of Sensitivity Tests of Total ETE on Daytime Summer Weekday Conditions Using PAZ Structure (Total Hours to Evacuate EPZ).....	1-6
3.1	List of Non-Retrofitted Bridge Structures in the EPZ	3-5
6.1	EPZ Permanent and Transient Population Summary 2006.....	6-7
6.2	EPZ Permanent and Transient Population Summary 2011.....	6-11
6.3	Estimated 2010 Household Vehicle Ownership and Occupancy Summer Weekend/Weekday	6-13
6.4	Evacuation Vehicles Generated by Sub-Zone 2011	6-15
6.5	Number of Bus Loads Needed to Transport Residents without an Auto	6-16
6.6	Number of Needed Bus Loads to Transport Transients without Autos	6-17
6.7	Estimated Year 2011 Transportation Assistance Requirements for Hospitals and Assisted Living Population Requiring Special Assistance	6-18
6.8	Estimated Year 2011 Transportation Assistance Requirements for Homebound Population Requiring Special Assistance	6-19
6.9	Estimated Number of Vehicle used by Evacuating SONGS Workers.....	6-19
6.10	Estimated Population and Transportation Requirements for Camp Pendleton.....	6-21
7.1a	Summary of Total ETE for All Scenarios Tested Using PAZ Structure (Total Hours to Evacuate EPZ).....	7-5
7.1b	Percent of Weekday Time Estimate for All Scenarios Tested Using PAZ Structure.....	7-5
7.2a	Summary of Sensitivity Tests of Total ETE on Daytime Summer Weekday Conditions Using PAZ	

Structure (Total Hours to Evacuate EPZ)	7-6
7.2b Percent of Weekday Time Estimate for All Sensitivity Tests Using PAZ Structure.....	7-6

Figures

<u>Figure</u>		<u>Page</u>
1.1	2011 PAZ Population	1-2
1.2	2011 PAZ Employment	1-3
2.1	Regional Location	2-3
2.2	Study Area	2-4
2.3	Schools	2-7
2.4	Assisted Living and Hospitals	2-8
3.1	Sub-Zones	3-10
5.1	Evacuation Routes.....	5-3
6.1	NUREG-0654 Samples of Time to Complete Evacuation Phases	6-2
6.2	Mobilization Rates	6-3
6.3	2006 Population	6-5
6.4	2006 Employment	6-6
6.5	2011 Population	6-9
6.6	2011 Employment	6-10
7.1	Total Vehicles Evacuated Under I-5 Management Approaches.....	7-1
7.2	Difference between Expected Mobilization and Delayed Mobilization	7-2
7.3	Average Throughput of an I-5 Lane During Evacuation Scenarios	7-3
7.4	Relative Share of Evacuation Traffic on I-5 and Non-Freeway Routes.....	7-4
7.5	Total Vehicles Evacuated Using PAZ Structure PAZ 1 and 2 Evacuation	7-8
7.6	Total Vehicles Evacuated Using PAZ Structure PAZ 1 and 3 Evacuation	7-9
7.7	Total Vehicles Evacuated Using PAZ Structure PAZ 1 and 4 Evacuation	7-10
7.8	Total Vehicles Evacuated Using PAZ Structure PAZ 1, 3 and 4 Evacuation	7-11
7.9	Total Vehicles Evacuated Using PAZ Structure PAZ 1, 4 and 5 Evacuation	7-12

EXECUTIVE SUMMARY

The Nuclear Regulatory Commission has requested that licensees of nuclear power plants provide information regarding time estimates for evacuation of the resident and transient population within a radius of about 10 miles from the nuclear reactor sites. This area is called the Emergency Planning Zone (EPZ). The evacuation time estimates are for use by those emergency response personnel charged with recommending and deciding on protective actions during an emergency.

The recommendations of NUREG-0654, Rev. 1 and NUREG/CR-6863 suggest that the evacuation time estimates should be updated as local conditions change.

The San Onofre Nuclear Generating Station (SONGS) is located in San Diego County, California, approximately four miles southeast of San Clemente and 15 miles north of Oceanside. The station is situated between Interstate 5 and the Pacific Ocean. The Southern California Edison Company, operator of SONGS, began generating electricity from Unit 1 in January 1968, from Unit 2 in August 1982, and from Unit 3 in April 1983. Unit 1 ceased generating electricity in 1992.

The previous evacuation time estimates for the SONGS area were prepared in 2000, with results documented in a 2001 study report.¹ The study included evacuation time estimates for projected 2006 area population.

Moderate population growth has occurred in the area since the 2001 evacuation time analysis. Current developer activities and plans indicate that slightly more than expected new development has occurred since the 2006 projections were prepared in 2000.

Evacuation Time Estimates for Protective Action Zones

The following table summarizes the Evacuation Time Estimates (ETE) for Protective Action Zones (PAZ) within the EPZ.

A brief description of the PAZs and the associated population follows:

- PAZ 1: SONGS facility, San Onofre State Beach, San Mateo Campground, San Onofre Bluffs Campground, and Camp Pendleton housing (5,702 people)
- PAZ 2: Pacific ocean (0 people)
- PAZ 3: Marine Corps Base Camp Pendleton (10,061 people)
- PAZ 4: San Clemente, portion of Marine Corps Base Camp Pendleton and parts of Southern Orange County (78,363 people)
- PAZ 5: Dana Point and San Juan Capistrano (90,821 people)

¹ Analysis of Time Required to Evacuate Transient and Permanent Population from Various Areas within the Emergency Planning Zone, San Onofre Nuclear Generating Station, Update for 2000-2006, prepared for Southern California Edison Company by Wilbur Smith Associates, July 2001.

SUMMARY OF TOTAL ETE FOR ALL SCENARIOS TESTED USING PAZ STRUCTURE
EVACUATION TIME ESTIMATE (ETE) TOTAL HOURS TO EVACUATE

	WEEKDAY	WEEKEND	NIGHT	ADVERSE WEATHER	WEEKDAY EARTHQUAKE
PAZ 1 & PAZ 2	3.0	3.3	1.5	4.0	11.0
PAZ 1 & PAZ 3	3.1	3.3	1.5	4.0	11.0
PAZ 1 & PAZ 4	7.3	6.8	6.3	8.3	14.3
PAZ 1 & PAZ 3 & PAZ4	7.3	7.0	6.3	9.0	16.3
PAZ 1 & PAZ 4 & PAZ5	9.5	9.2	8.2	10.3	18.0

Source: Wilbur Smith Associates, 2006

The estimates range from 1.5 hours for the least populated areas under the most favorable of circumstances to 18 hours for the most populated areas under earthquake conditions. If the earthquake scenario is not considered, then the less populated portions could evacuate in 4 hours or less and the more populated areas in 10.3 hours or less. The range of certainty for evacuation of the EPZ is plus or minus 2 hours.

Chapter 1

EVACUATION TIME ESTIMATES FOR PROTECTIVE ACTION ZONES

An Emergency Planning Zone (EPZ) structure was developed based on prevailing wind direction at the SONGS facility and grouped large areas of population and employment for evacuation time estimates. These areas are identified as Protective Action Zones (PAZs). The EPZ was subdivided into five (5) PAZs, as summarized below:

- PAZ 1: SONGS facility, San Onofre State Beach, San Mateo Campground, San Onofre Bluffs Campground, and Camp Pendleton housing (5,702 people)
- PAZ 2: Pacific ocean (0 people)
- PAZ 3: Marine Corps Base Camp Pendleton (10,061 people)
- PAZ 4: San Clemente, portion of Marine Corps Base Camp Pendleton and parts of Southern Orange County (78,363 people)
- PAZ 5: Dana Point and San Juan Capistrano (90,821 people)

The estimates for population, employment, and vehicles within each PAZ were developed using the data described in the remaining chapters of this report. An estimate of population and employment by PAZ is provided in **Table 1.1**.

Table 1.1:
EPZ PERMANENT AND TRANSIENT POPULATION SUMMARY 2011
BY PROTECTIVE ACTION ZONE (PAZ)

PAZ	RESIDENTS (ALL SCENARIOS)	NON-RESIDENTS						GRAND TOTALS		
		SUMMER WEEKEND		SUMMER WEEKDAY		NIGHT		SUMMER WEEKEND	SUMMER WEEKDAY	NIGHT
		WORKER	BEACH/ VISITOR	WORKER	BEACH/ VISITOR	WORKER	BEACH/ VISITOR			
1	5,702	62	14,760	2,225	7,380	8	1,476	20,524	15,307	7,186
2*	0	0	0	0	0	0	0	0	0	0
3	10,061	0	0	0	0	0	0	10,061	10,061	10,061
4	78,363	5,636	16,468	13,851	9,166	949	1,711	100,467	101,380	81,023
5	90,821	8,334	19,560	19,713	9,956	987	1,206	118,715	120,491	93,014
TOTAL:	184,947	14,032	50,788	35,789	26,503	1,944	4,393	249,767	247,239	191,284

Source: Wilbur Smith Associates, November 2006

Note:

1. PAZ 2 is the Pacific Ocean. It is not possible to estimate the number of ocean going vessels that may occupy this PAZ under Year 2011 conditions; however, it is assumed that in an emergency situation the appropriate evacuation notice would be provided to any vessels within the EPZ and evacuation times would be within the total estimates ETE as summarized in the subsequent sections.

Figure 1.1 shows the population estimates by PAZ and **Figure 1.2** shows the employment estimates by PAZ.



- PAZ 1
- PAZ 2
- PAZ 3
- PAZ 4
- PAZ 5

San Onofre Nuclear Generating Station Evacuation Time Estimate 2011 PAZ Population

0 0.5 1 2 3 4 Miles



Figure 1.1



San Onofre Nuclear Generating Station
Evacuation Time Estimate
2011 PAZ Employment

- PAZ 1
- PAZ 2
- PAZ 3
- PAZ 4
- PAZ 5

0 0.5 1 2 3 4 Miles



Figure 1.2

SAN ONOFRE NUCLEAR GENERATING STATION (SONGS) EVACUATION TIME EVALUATION (ETE) STUDY
FINAL REPORT

Table 1.2 shows the calculation of vehicles by PAZ based on household vehicle ownership and occupancy.

Table 1.2:
ESTIMATED 2011 HOUSEHOLD VEHICLE OWNERSHIP AND OCCUPANCY SUMMER WEEKEND/WEEKDAY AND NIGHT

PAZ	RESIDENT POPULATION	PEOPLE/ HH	TOTAL HH	% HH NO VEHICLE	% HH W/ 1 VEHICLE	% HH W/ 2 VEHICLES	% HH W/ 3 OR MORE VEHICLE	HH W/0	HH W/1	HH W/2	HH W/3	VEHICLES OWNED	VEHICLES USED	VEHICLE OCCUPANCY
1	5,702	-	-	NA	NA	NA	NA	NA	NA	NA	NA	NA	1,426	4.00
2	-	-	-	NA	NA	NA	NA	NA	NA	NA	NA	NA	0	NA
3	10,061	-	-	NA	NA	NA	NA	NA	NA	NA	NA	NA	2,515	4.00
4	78,363	2.37	33,025	2.3%	25.2%	46.5%	26.0%	773	8,326	15,347	8,578	69,102	44,207	1.77
5	90,821	2.37	38,292	3.3%	29.3%	44.3%	23.1%	1,252	11,213	16,977	8,851	76,143	48,771	1.86
Total/Ave	184,947		71,317	2.8%	27.4%	45.3%	24.5%	2,025	19,539	32,324	17,429	145,245	96,919	1.91

Source: Wilbur Smith Associates, November 2006

Table 1.3 shows the resultant summary of vehicles by PAZ and evacuation scenario:

Table 1.3:
2011 PAZ VEHICLES EVACUATED BY SCENARIO

PAZ	RESIDENTS VEHICLES (ALL SCENARIOS)	NON-RESIDENTS VEHICLES						GRAND TOTAL VEHICLES		
		SUMMER WEEKEND		SUMMER WEEKDAY		NIGHT		SUMMER WEEKEND	SUMMER WEEKDAY	NIGHT
		WORKER	BEACH/ VISITOR	WORKER	BEACH/ VISITOR	WORKER	BEACH/ VISITOR			
1	1,426	52	5,216	2,184	2,608	8	522	6,694	6,218	1,955
2	0	0	0	0	0	0	0	0	0	0
3	2,515	0	0	0	0	0	0	2,515	2,515	2,515
4	44,207	4,696	5,819	11,542	3,239	791	604	54,722	58,988	45,602
5	48,771	6,945	6,911	16,427	3,518	822	425	62,627	68,717	50,019
Total	96,919	11,693	17,946	30,153	9,365	1,621	1,552	126,558	136,438	100,091

Source: Wilbur Smith Associates, November 2006

Evacuation estimates were prepared for the following combinations of PAZs:

- PAZ 1 and 2
- PAZ 1 and 3
- PAZ 1 and 4
- PAZ 1, 3, and 4
- PAZ 1, 4, and 5

These groupings reflect communities and areas affected based on their distance from SONGS and wind direction.

Each of the five combinations of PAZ evacuations shown above were tested for the following

scenarios:

- Daytime summer weekday
- Daytime summer weekend
- Night
- Adverse weather conditions
- Earthquake conditions

In addition to the scenarios described above, sensitivity tests were run for the following conditions under the daytime summer weekday condition:

- Contra-flow on I-5
- Incident on I-5
- Delayed mobilization
- 20% shadow demand
- 80% population under earthquake conditions
- Aggressive access control on I-5

1.1 Evacuation Time Estimates

Tables 1.4a and 1.4b summarize the evacuation time results by PAZ. Data in Table 1.4a provides a summary of all simulations, while Table 1.4b provides a summary of the sensitivity tests performed against the daytime summer weekday evacuation condition.

Table 1.4a:
SUMMARY OF TOTAL ETE FOR ALL SCENARIOS TESTED USING PAZ STRUCTURE
(TOTAL HOURS TO EVACUATE EPZ)

	WEEKDAY	WEEKEND	NIGHT	ADVERSE WEATHER	WEEKDAY EARTHQUAKE
PAZ 1 & PAZ 2	3.0	3.3	1.5	4.0	11.0
PAZ 1 & PAZ 3	3.1	3.3	1.5	4.0	11.0
PAZ 1 & PAZ 4	7.3	6.8	6.3	8.3	14.3
PAZ 1 & PAZ 3 & PAZ 4	7.3	7.0	6.3	9.0	16.3
PAZ 1 & PAZ 4 & PAZ 5	9.5	9.2	8.2	10.3	18.0

Source: Wilbur Smith Associates, 2006

Table 1.4a indicates that the combination of PAZs 1, 4 and 5 take the longest time to evacuate. These regions include southern Orange County, San Clemente, Dana Point, San Juan Capistrano, and the SONGS facility. It requires 9.5 hours to evacuate these areas on a weekday. This is more than three times the evacuation time for PAZs 1 and 3, the facility and Camp Pendleton. The fact that PAZ 4 and PAZ 5 are more populated than the other PAZs is a significant contributing factor to this trend.

PAZs 1 and 4, and PAZs 1, 3 and 4 take the same amount of time to evacuate both on a weekday and during night; each taking more than seven and six hours respectively. PAZs 1 and 2, and PAZs 1 and 3, take the same amount of time to evacuate under different scenarios.

Table 1.4b:
SUMMARY OF SENSITIVITY TESTS OF TOTAL ETE ON DAYTIME SUMMER WEEKDAY
CONDITIONS USING PAZ STRUCTURE (TOTAL HOURS TO EVACUATE EPZ)

	CONTRA-FLOW ON I-5	INCIDENT ON I-5	DELAYED MOBILIZATION	20% SHADOW DEMAND	80% POPULATION UNDER EARTHQUAKE CONDITIONS	AGGRESSIVE ACCESS CONTROL ON I-5
PAZ 1 & PAZ 2	2.3	5.1	3.1	3.3	5.0	3.0
PAZ 1 & PAZ 3	3.0	5.1	3.1	3.3	5.1	3.0
PAZ 1 & PAZ 4	6.4	8.0	7.4	7.3	10.2	6.5
PAZ 1 & PAZ 3 & PAZ 4	6.5	8.2	7.5	9.0	10.2	6.5
PAZ 1 & PAZ 4 & PAZ 5	7.5	11.0	8.5	11.2	12.3	8.2

Source: Wilbur Smith Associates, 2006

Table 1.4b describes the Sensitivity Tests on a summer weekday for the different combination of PAZs. In summary:

- Contra-flow operations on I-5 would reduce the time required to evacuate all combinations of PAZ evacuations, with the greatest reduction occurring for the combination of PAZ 1, 4, and 5 of approximately two hours.
- An incident on I-5 could increase the evacuation times by nearly two hours.
- Delayed mobilization has a negligible effect for the majority of PAZ evacuation combinations; however, for the combination of PAZ 1, 4, and 5 the total evacuation time actually reduces by approximately one hour. This is assumed to be a result of the dense populations within these PAZs and the benefits of delayed mobilization as compared to available capacity on the EPZ roadway network: The roadway network does not reach capacity as quickly and therefore can move more vehicles faster out of the EPZ when the mobilization is delayed.
- When shadow demand is assumed to be at 20%, the effects are proportional to the volume evacuating the EPZ. Therefore, the effect of increased shadow demand is minimal for the PAZ evacuation combinations of lower populations. Under the combination of PAZ 1, 4, and 5, the increased shadow demand would potentially increase evacuation times by almost two hours.
- If only 80% of the population evacuates under earthquake conditions, the total evacuation time for each PAZ combination reduces substantially. The greatest reduction occurs for the PAZ combinations with the smallest populations (PAZ 1 and 2).
- Aggressive access control on I-5 will have the greatest reduction in evacuation times for those PAZ combinations with the highest total volume of evacuating population.

Chapter 7 provides graphical representation of vehicles moved beyond the EPZ boundary for the 5 combinations of PAZ evacuations.

Chapter 2

DATA COLLECTION

The Southern California Edison Company requested that the evacuation time estimates reflect resident and transient populations anticipated for the area in mid-2010. For the purposes of this study, the Year 2011 was identified for future estimates. This would provide emergency response personnel with evacuation time estimates that would continue to be useful as the anticipated new development occurs within the area. The evacuation time study includes:

1. The identification of resident and transient population within the area in 2006, based upon available information, and the estimated numbers and distribution of population by 2011.
2. Identification of existing institutions which require special evacuation assistance, as well as those known new institutions planned for construction.
3. An evaluation of the evacuation routes relative to their traffic-carrying capacity during an evacuation.
4. Estimation of evacuation time requirements for the resident and transient population, and special institutions, under normal and adverse weather conditions.
5. The assessment of evacuation time requirements if major damage occurs to the primary evacuation routes as a result of an earthquake (or similar disruptive event) occurring prior to, or during, the evacuation.
6. Review and inclusion of new NUREG elements where appropriate.

Data collection includes the following efforts:

1. Establish a study area;
2. Review Emergency Response Plans for the various jurisdictions and agencies within the EPZ;
3. Inventory existing highway facilities, including roadway facility type, number of lanes, operating speeds, and traffic controls;
4. Review available demographic data, employment data, recreational facility usage and future plans and forecasts; and
5. Assemble information for schools, and special institutions within the area.

All spatially referenced data was compiled and referenced to a Geographic Information System (GIS) database. Included in this GIS database are all the features obtained or created by the project team.

2.1 Study Area

The San Onofre Nuclear Generating Station (SONGS) is located in San Diego County, California, approximately four miles southeast of San Clemente and 15 miles north of Oceanside. **Figure 2.1**

presents the regional context of SONGS.

The Nuclear Regulatory Commission stipulates that the EPZ must include land areas within 10 miles of the SONGS site². **Figure 2.2** shows the 10-mile radius EPZ boundary which encompasses all of the cities of San Clemente, San Juan Capistrano, Dana Point, and a large portion of the United States Marine Corps Base, Camp Pendleton. San Juan Capistrano, Dana Point, and the Ortega area have been included in the EPZ evacuation time estimates although the 10-mile radius actually bisects these communities. This expanded planning area, or geopolitical EPZ, is here after referred to as simply the EPZ or study area.

2.2 Emergency Response Plans

Contacts were made with local and regional planning agencies, County and State transportation departments, and local and county officials responsible for emergency response planning. Appendix A provides the agencies contacted, information received, and approximated date.

The principal emergency response plans include:

- County of Orange Nuclear Power Plant Emergency Plan for the San Onofre Nuclear Generating Station, January 2005;
- City of San Juan Capistrano Emergency Operations Plan, February 2004; San Onofre Nuclear Generating Station Emergency Response Plan, June 2004.
- City of Dana Point Emergency Plan, January 2004;
- City of San Clemente Multi-hazard Emergency Response Plan, December 2003;
- Marine Corps Camp Pendleton Force Protection Plan, Annex C (Operations), July 2004;
- Department of California Highway Patrol, Border Division Nuclear Response Plan for the San Onofre Nuclear Generating Station, March 2005;
- Capistrano Unified School District Emergency Guide, San Onofre Nuclear Power Plant, October 2005;

² NUREG/CR-6863 p.4



**San Onofre Nuclear Generating Station
Evacuation Time Estimate**

Study Area

 EPZ/Study Area



Figure 2.2

2.3 Transportation Facilities

One interstate route (I-5) and two state routes (SR-1 and SR-74) currently serve the area within the EPZ limits. Interstate 5 (San Diego Freeway) is the primary north-south route serving traffic between Orange and San Diego Counties.

State Route 1 (Pacific Coast Highway) provides secondary north-south access within the northern part of the EPZ. State Route 74 (Ortega Highway) is the only regional east-west roadway within the study area. The Ortega Highway is a winding, mountain-area roadway which connects the area to Interstate 15, approximately 32 miles to the east.

State Route 73 (The San Joaquin Hills Transportation Corridor), a north-south toll roadway which connects to I-5 approximately 3 miles north of SR-74, was opened to traffic in late November, 1996. This six-lane roadway, which connects to SR-55 and State Route 405 in Costa Mesa, significantly increases the capacity for northbound evacuation traffic.

These major corridors are shown in **Figure 2.2**

2.4 Demographic/Employment Data

The numbers of evacuating persons and vehicles from the area were obtained by applying the estimated growth in each area since the 2000 census, and anticipated growth up to 2011. The 2006 and 2011 resident and transient estimates were made as follows:

1. The estimated number of 2006 residents for San Clemente, San Juan Capistrano, and Dana Point was obtained from the California State University, Fullerton (CSUF) Center for Demographic Research and from local planning agencies.
2. The geographic distribution of population increases was based on development project plans identified by local agencies; CSUF demographic data; and recent demographic information obtained from the Cities of San Clemente, San Juan Capistrano, and Dana Point planning agencies.
3. Population projections for 2011 in the Cities of San Clemente, San Juan Capistrano, and Dana Point were based on estimates provided by the local planning agencies and by CSUF. The distribution of new residents within each City was based on information provided by the local planning agencies which reflects developer proposals and/or building permit projections and CSUF demographic projections.
4. State Park Beach usage was based on peak visitation records for the 2005 summer season. According to the State Parks, beach capacity will not increase because it is limited by the amount of parking.
5. The 2006 and 2011 employment for the three cities was estimated using employment information compiled from CSUF projections. Then percentages of people that work and live in the same city were subtracted from the total employment so as to not double count people within the vicinity. This was obtained from the 2000 census.
6. Average household size and vehicle ownership statistics obtained from the 2000 census were applied to each community to estimate the number of vehicles per households and persons in households without vehicles in 2006 and 2011.

2.5 Schools and Special Institutions

Several population segments require special evacuation consideration. These segments include members of the residential population not having access to an automobile, special needs citizens, and special institutions such as schools, nursery schools, hospitals, and assisted living facilities.

2.5.1 Schools

A summary of student enrollment in public and private schools within the EPZ is presented in **Appendix B** and shown on **Figure 2.3**. Current school enrollments within the study area are approximately 19,944 students in public schools and 5,648 students in private schools.

2.5.2 Special Populations

There are three types of institutions within the EPZ that would require assistance in relocation. These are hospitals, assisted living facilities, and homebound persons with special needs.

Assisted living facilities located within the EPZ are provided in Appendix C and shown on **Figure 2.4**. Health care center and hospital population figures were furnished by institutional staffs, except where noted.

One hospital is located within the EPZ: Saddleback Memorial Medical Center, San Clemente Campus; shown on **Figure 2.4**

There are no civilian detention facilities within the EPZ.



**San Onofre Nuclear Generating Station
Evacuation Time Estimate
Schools**

 School



Figure 2.3



-  Assisted Living Facility
-  Hospital

**San Onofre Nuclear Generating Station
Evacuation Time Estimate
Assisted Living and Hospitals**

0 0.5 1 2 3 4 Miles



Figure 2.4

Chapter 3

SIMULATION MODEL

This study does not rely on specific evacuation route maps that unnecessarily imply the public should take routes which may not be the most ideal for the duration of the evacuation. Instead it relies on individual decisions of route selection that comply with traffic control points, access management plans, and actions coordinated through a supervisor.

The evacuation time assessment was conducted using DYNASMART-P. DYNASMART-P is a state-of-the-art dynamic route assignment model sponsored by the Federal Highway Administration and developed at the University of Maryland. This software package provides a blend of four step regional models and corridor level micro-simulation models.

Individual driver behavior is considered in selecting available routes, and the model attempts to route them in the most efficient manner possible. This model represents intersections on the arterial system, and ramp merges on freeways as significant constraining points. Its dynamic assignment capability allows each vehicle to determine its best path out of the area.

On the freeway system, it represents the stop-and-go conditions when there is overwhelming demand. Conversely, it shows that both speeds and throughput are increased when an aggressive access management plan is in place. DYNASMART-P tracks the performance of individual links, as well as reports minute by minute the number of vehicles that have successfully crossed the EPZ boundary line.

3.1 The Network

The DYNASMART-P software evaluates travel on a specific network. The evacuation route roadways are defined as a series of links and nodes. Each link represents a specific segment of roadway with common geometric features and operational characteristics. A pair of nodes identifies the limits of each link. Nodes are located wherever evacuation routes intersect, change geometric characteristics, or change operational characteristics.

Links are defined as arterials, highways, and freeways. Freeways include High Occupancy Vehicle (HOV) lanes where these facilities exist. The number of through lanes, turn lanes, link speed, maximum service flow rate, saturation flow rate and grade are defined at nodes as well as the type of control (stop sign, traffic light, etc.).

The traffic characteristics of each link and node in the evacuation network were determined through field review, aerial photos, and traffic engineering analyses. A listing of the link characteristics was prepared identifying the roadway name, the length of link, the operating speed, and the link capacity (the number of lanes multiplied by the assigned capacity per lane). The operating speeds and lane capacities reflect average operating conditions.

Sub-zones were used to define centroids. Sub-zone boundaries generally follow readily identifiable natural or man-made features, census tracts, and Southern California Association of Government

Transportation Analysis Zones (TAZ).

Trips from origin centroids were generated on various links within the EPZ. The destination was a single large area beyond the EPZ encompassing all possible evacuation routes.

Trip creation occurs at the rate which the public mobilizes. The route selected to get beyond the EPZ depends on the trip start and previous demand on the routes. Mobilization time is the combination of time to receive the warning, travel home (if necessary), and make preparations to leave.

The model evaluation information includes the total evacuation time and a distribution of trip percentages reaching the EPZ boundary from the start of evacuation. The distributions may also be produced for trips from any specified subarea. Average travel time and delay time is calculated by time increment for trips exiting the EPZ by time increment.

3.2 General Assumptions

Various assumptions were necessary in the estimation of the numbers of persons and vehicles which would evacuate and the analysis of evacuation times. All assumptions are consistent with NUREG guidance.

3.2.1 Public Information and Notification

All residents and employees in the EPZ have been provided with information regarding evacuation instructions and preferred or required evacuation routes. The community alert siren system is used to alert the EPZ population, followed by instructions through radio, television, and public address systems.

3.2.2 Evacuations Prior to General Evacuation

This estimate assumes a single point in time when there is a general notification to evacuate and all evacuations start from that point. This is a requirement of the DYNASMART-P software.

The evacuation time evaluation assumes a slow escalation of the emergency, so reality may well deviate from this single point notification for reasons such as the following:

- ◆ San Onofre State Beach authorities may evacuate the park and campgrounds as a precautionary measure.
- ◆ Individuals may voluntarily decide to evacuate before a general evacuation is issued.

Substantial pre-notification evacuation will reduce the number of individuals evacuating to the north and would logically reduce the estimates in this document. Estimates have been created for sets of PAZs. The estimates for evacuation of PAZs 1 and 2 and PAZs 1 and 3 could be applied to a site area emergency as they primarily contain populations within and immediately surrounding the SONGS facility, where the general emergency condition would include PAZs 4 and 5.

3.2.3 Traffic Controls

It is assumed that the freeway network within the EPZ is isolated from external traffic. Diversion of freeway traffic away from the affected area is assumed to begin within 30 minutes. Most traffic control officers and barricades for directing traffic are assumed to be in place within 60 to 90 minutes.

3.2.4 Number of People and Vehicles Evacuating

This ETE assumes an average auto usage of 1.3 vehicles per household even though a higher number of eligible drivers and autos exist³. This number is in part the result of public information efforts that educate residents about the reasons for avoiding unnecessary vehicles.

More specific calculations and assumptions are outlined below.

1. Estimates of vehicle usage are as follows:
 - a. One-vehicle households would evacuate as a single unit generating one evacuating vehicle
 - b. On average two-vehicle households will use 1.3 vehicles.
 - c. Three (or more)-vehicle households would generate 1.75 vehicles. This recognizes that many 3 vehicle households only have 2 drivers.
2. All persons, residents and transients, evacuate.
3. The majority of the EPZ labor force (non-military) work outside of the EPZ, with almost all commuting to work by personal automobile.
 - a. For estimating the number of vehicles evacuating, it was assumed that a minimum of one vehicle would be evacuated for every auto-owning household. This reflects in part that the majority of households have a second vehicle available.
 - b. This also conservatively assumes that commuters from one-vehicle households would be able to return to their homes to evacuate their family.
 - c. To ensure that there is sufficient bus transportation, the estimates of persons requiring transportation assistance assume that none of the residents who commute to work outside the EPZ would be able to return to evacuate their family.
4. The number of non-resident vehicles evacuating reflects the following occupancy level assumptions:
 - a. Non-resident beach visitors average 3.0 to 3.5 persons per vehicle, based on statistics for each park area.
 - b. Non-resident workers would average 1.2 persons per vehicle.
 - c. Persons staying at area hotels/motels and visitors to areas other than the beaches would average 2.0 persons per vehicle.
 - d. Because determining whether visitors are at the beach or are visiting other places is difficult, an average of 2.8 persons per vehicle is assumed for those categories.
5. Transportation capacities for those needing special assistance are:
 - a. 2 persons per ambulance.
 - b. 6 persons per wheelchair van.
 - c. 36 persons per bus (for those in assisted living centers).

³ Sorensen and Voght, "Interactive Emergency Evacuation Guidebook: Prepared for the Protective Action IPT, "February 2006, Oak Ridge National Laboratory <<http://emc.ornl.gov/CSEPPweb/evac-files/index.htm>>

- d. 70 persons per bus (for those who do not have auto transportation).
- e. 60 persons per bus for schools and daycares.
6. The total number of people needing to be evacuated in each of the scenarios (summer weekend, summer weekday, and nighttime) assumes all the residents are present during each of these times. Only the transient population changes for each scenario.
7. The ratio of residents who live and work within an EPZ city over the total number of workers in each EPZ city was obtained from the 2000 Census data as follows:
 - a. 43% of San Clemente workers live within San Clemente.
 - b. 25% of San Juan Capistrano workers live within San Juan Capistrano.
 - c. 36% of Dana Point workers live within Dana Point.
 - d. 20% of workers from any given EPZ city reside in a neighboring EPZ city.

3.2.5 Evacuation Route Conditions

A set of evacuation time estimates was developed for the area based on all existing evacuation routes being available.

Additional time estimates were made for adverse weather and earthquakes. Adverse weather conditions in this area would most likely be heavy rain or fog. Such weather conditions are assumed to reduce roadway capacities by 15 percent.

Assumptions regarding potential evacuation route blockages due to an earthquake event are below.

3.3 Earthquake Assumptions

This scenario could also assume any situation where the use of bridge structures is impeded. Caltrans has identified older bridges in the study area that have not been retrofitted to current seismic design standards. These locations are shown on **Table 3.1**. Locations for potential landslides are not shown; these locations exist along existing routes adjacent to cliffs (e.g. PCH and portions of I-5).

**Table 3.1:
 LIST OF NON-RETROFITTED BRIDGE STRUCTURES IN THE EPZ**

ROUTE	DISTRICT	PM	BR. NO.	CITY	ROAD/WATERWAY OVERPASSED	LENGTH (M)	YEAR BUILT/ YEAR WID. EXT.
5	12	2.31	550204	SCLE	Avenida Presido	43.6	1960\1981
5	12	2.66	550205	SCLE	Avenida Palizada	49.7	1960\1981
5	12	3.39	550207	SCLE	Avenida Pico	42.7	1960\1981
5	12	4.97	550223	SCLE	Avenida Vaquero	53.0	1981
5	12	6.69	550226	DAPT	S.R. 1 \ Camino Las Ramblas	69.8	1960\1973
5	12	10	550230	SJCP	El Horno St	54.2	1958\1969
5	12	10.91	550231	SJCP	Junipero Serra Rd	38.1	1958\1969
5	12	11.45	550289	SJCP	Trabuco Creek	72.8	1959\1969

Source: Caltrans District 12, Wilbur Smith Associates, 2006

Notes:

- DAPT – City of Dana Point
- OCN - City of Oceanside
- SJCP – City of San Juan Capistrano
- SCLE – City of San Clemente

For purposes of testing a potential earthquake scenario, the following approach was taken:

1. Where landslides spill onto the I-5 mainline, one through lane will be possible.
2. I-5 Bridges identified by Caltrans that have not been retrofitted will fail. Where the bridge is part of an interchange, vehicles can go down the off-ramp and back up the on-ramp.
3. When ramps are used for rerouting the mainline, three travel lanes can be accommodated regardless of the normal striping on the ramp.
4. Traffic from the west that would normally access I-5 at that point must use an alternative path since they cannot cross under/over I-5 to the northbound ramps.
5. Pacific Coast Highway is assumed to be essentially unusable due to high potential for landslides.
6. The at-grade arterial system remains largely in-tact and available for evacuation with the exception of PCH and roadways crossing I-5 at vulnerable bridges.
7. Two sensitivity tests were tried. The first test assumes that 100% of the vehicles in a normal evacuation would be used, and the second 80% of normal evacuation vehicles. The second scenario reflects that officials are able to reduce vehicles through public awareness of the gravity of unnecessarily consuming remaining capacity.
8. All scenarios are timed beginning at first public notice to evacuate although it may take longer to order an evacuation due to officials assessing evacuation routes.

9. Modeling does not account for minor debris removal, law enforcement mobilization, and organizing rerouting (as in traffic control for the off- and on-ramps) that may be necessary before vehicles can move as the model expects. An extra hour is added to both scenarios to account for this.

3.4 Network Assumptions

The assumptions utilized in developing the link travel times and capacities are discussed in the following sections.

3.4.1 Directional Flow

All roadways will operate as they do under present conditions. Under normal conditions on a four-lane, two-way roadway, only the two outbound lanes would be utilized for evacuation.

3.4.2 Travel Speeds

In accordance with the Highway Capacity Manual 2000 (HCM 2000) procedures, starting speeds (or uncongested average traversing speeds) were assigned to each link according to the character of the roadway. Freeway free flow speeds begin at 65 miles per hour with ramp speeds at 25 miles per hour. Four-lane roadways were generally assigned speeds ranging from 25 miles per hour to 45 miles per hour depending on posted speed limits, roadway quality, and access control. Congested speeds are then calculated by DYNASMART-P.

3.4.3 Roadway Conditions

Capacities assigned to each roadway are consistent with recommendations in HCM 2000. For the purpose of this analysis, the following capacities by roadway type were assigned:

- Freeway - An average 2,200 vphpl was estimated for all freeways in the area.
- Interchange Ramps - 1,200 vphpl for on-ramps.
- At-grade arterials – Typically two and four-lane roadways were assigned capacities between 1,000 - 1,400 vehicles per lane per hour along the primary evacuation path. This is higher than normal conditions, which are attempting to serve demands in all directions. Instead, green time at the traffic signals is governed by officers and flashing yellow lights which increase the flow in the major direction. Such an increase is supported by HCM 2000 procedures.
- Capacity constraints: Receiving capacity outside the EPZ boundary was reduced on at-grade arterials for the first several hours due to competition from shadow demand.

The average lane capacities summarized above are consistent with those used in standard traffic engineering and planning studies.

3.4.4 Roadway Closures and Management Plans

A review of California Highway Patrol (CHP) plans, Orange County Sheriff plans, and local management plans indicate that within the first 30 minutes of notice to evacuate:

- ◆ I-5 will be closed to northbound traffic at SR-78 and Harbor Drive. This measure will also reduce the effects of shadow demand.
- ◆ I-5 will be closed to southbound traffic just north of the El Toro "Y".
- ◆ Between the EPZ boundary and the El Toro "Y", all access ramps – northbound and southbound – are to be closed to all but emergency vehicles.
- ◆ Southbound at-grade arterial streets entering the EPZ will remain open to allow family members who were beyond the EPZ at first notice to return and assist their families with evacuating.

Local plans do not call for closing or even metering access to northbound I-5 from within the EPZ. Rather, officers are instructed to assist with orderly loading of ramps, but there is no intention to slow the rate of entry to the mainline if it begins to fail.

Traffic generated entirely within the EPZ may be sufficient to cause I-5 to fail, and it is not uncommon for freeways to be reduced to 65-75% of their maximum throughput when this happens. Model scenarios were constructed to reflect the existing plans and to reflect limited or metered access to I-5 insuring maximum throughput.

For a description of the traffic control points, please see Appendix D.

3.4.5 Northbound – Southbound Split

Plans suggest that all vehicles north of SONGS will be required to evacuate north, and those south will be required to evacuate to the south. Due to population distributions more than 90% of all evacuating vehicles will travel northbound. The work presented here focuses on northbound evacuation unless otherwise specified.

3.4.6 Shadow Demand Characteristics

This ETE assumes as a baseline condition that there will be no significant demand on evacuation routes from the shadow ring (0% shadow evacuation assumed). In the event that a significant shadow evacuation does occur, a sensitivity test was conducted to reveal the implications that a 20% shadow demand may have on at-grade evacuation routes.

3.4.7 Background Traffic Characteristics

In this modeling, we assume access will be denied to both northbound and southbound I-5 for all background and shadow demand between the EPZ boundary and the El Toro "Y", and the only non-EPZ vehicles allowed on freeway evacuation routes are mainline southbound trips being rerouted northbound.

While shadow demand will have little impact on I-5, it will have significant impact on at-grade

evacuation routes. To estimate the effects of all these factors on the evacuating traffic, the following approach was taken:

1. Assume that 100% of normal day-to-day traffic activities occur in the first 30 minutes, dropping to 75% in the 31-60 minute range, 50% in the 61-120 minute range, 25% in the 121-240 range, and finally no significant contribution to northbound movements from background traffic beyond this point.
2. Assume that 6% of the Average Daily Traffic on I-5, I-405, and SR-73 is southbound in a typical hour, as per Caltrans data.
3. Assume that the first 30 minutes of southbound freeway traffic does not have a chance to react to media warnings to avoid southbound travel.
4. Assume that in the 31-60 minute range, about half of the normal flow will receive notice to avoid southbound freeway travel toward the area.
5. Assume in the 61-120 minute range, only 10% of normal flow becomes queued in the southbound direction and rerouted to northbound movement.
6. Beyond 2 hours, there is no longer a significant entry of southbound vehicles that must be rerouted onto northbound evacuation routes.

For modeling the effects of 20% shadow demand:

1. Identify 2011 population and employment in first five miles beyond the geopolitical EPZ.
2. Assume that 20% of this population (shadow demand) would mobilize for evacuation along the same curve used within the EPZ, but delayed by 60 minutes (as they would take extra reaction time to conclude that they are sufficiently at risk to evacuate).
3. All shadow demand is excluded from using I-5, in all scenarios, except for one sensitivity test in which no restrictions are made to accessing I-5 other than officer-assisted, orderly access.

3.4.8 Traffic Signals

This modeling assumes that traffic signals on the approaches to I-5, as well as at significant intersections within the EPZ and the shadow ring, will at a minimum be set to flash mode, with the flashing yellow supporting a primary evacuation path. Ideally, officers would aid at these intersections to occasionally break the stream and allow secondary movements to enter. The agency-specific evacuation plans specify instructions for manual traffic signal control at key locations, and these locations are summarized in Appendix D.

3.4.9 Contra-Flow on I-5

One model run of the highest demand scenario allows for two contra-flow lanes on I-5. Access to and egress from the contra-flow lanes is not significant in the model, but in practice there are some redundant considerations included in the recommendations section.

There are several issues to consider in designing the access to and egress from contra-flow lanes. Some of these are noted in Appendix E.

3.5 Centroids

The DYNASMART-P requires that a trip, in this case the evacuation trip, be loaded into the network

from a point. The point is called a centroid. Sub-zones were used to define these centroids, as shown in **Figure 3.1**.

Specific sub-zones were developed to encompass existing population concentrations and easily identifiable land uses. Sub-zones were delineated to follow existing political, natural, and manmade boundaries and features, or other readily recognizable features such as the Southern California Association of Governments (SCAG) TAZ boundaries. The approximate areas of habitation were outlined as the sub-zone boundary for those areas comprised of family military housing or barracks concentrations.

A brief description of the area encompassed by each sub-zone is presented in Appendix F.



**San Onofre Nuclear Generating Station
Evacuation Time Estimate
Sub-Zones**



Figure 3.1

Chapter 4

EVACUATION SCENARIOS

4.1 Time Frame Variations

The time of day at which an evacuation is initiated would affect the number of persons to be evacuated and the time interval required to respond to the evacuation warning. Both of these factors would affect the total time interval required to evacuate the area. Three common time periods were selected for the development of evacuation time estimates.

- 1a: Daytime on a summer weekday;
- 1b: Daytime on a peak summer weekend;
- 1c: Night, either on a weekend or weekday

4.1.1 Summer Weekday Evacuation (1a – Base for comparison)

The first scenario represents the event that an evacuation takes place during a summer weekday during work hours with many residents working outside the EPZ, and a significant number of workers within the EPZ who reside outside the EPZ. This condition would include a substantial number of non-resident workers and tourists. Recreation usage at State Parks and beaches would be moderately heavy, consistent with current park usage statistics.

The evacuation times for schools in the EPZ have also been included in the weekday time estimate for special institutions. The time estimates reflect normal school year attendance.

4.1.2 Summer Weekend Evacuation (1b)

The second case is the condition where an evacuation takes place on a summer weekend, where a significant portion of the populace would be non-residents who are in the area as workers and tourists, or for recreational purposes. Weekend resident population in the area would be higher than on a weekday when many residents would be out of the area at their place of work. Estimates of beach visitors are based on data for the July 4th holiday, which is usually one of the peak visitor days in the year. The number of visitors to most beach areas is limited by the available parking areas on this day.

4.1.3 Night Evacuation (1c)

In the event that an evacuation takes place at night, the maximum resident population and the minimum non-resident population would be in the EPZ. This scenario assumes evacuation warning would occur in the late evening when most people would be at their permanent or temporary place of residence.

4.2 I-5 Management Variations

All traffic management variants center around management of I-5. I-5 is the most significant facility available for evacuation and the most practical facility for implementing various management strategies. Four operating strategies were modeled:

- 1a: Moderate management of I-5 (Current local plans: Traffic from San Diego denied use of I-5, and northbound on ramps north of the EPZ boundary are closed to shadow demand and background traffic).
- 2a: No significant restrictions on I-5 (Same as 1a, but ramps north of EPZ boundary remain open).
- 2b: Aggressive traffic management of I-5 (Same as 1a, but officers meter ramp entry to ensure more efficient 50-60 mph speeds).
- 2c: Same as 2b, but with northbound contra-flow implemented on two southbound lanes.

4.2.1 Moderate Management of I-5 (1a Baseline)

The existing I-5 management plan calls for barricading all north-bound on ramps between the EPZ boundary and the El Toro "Y". This will eliminate competition from shadow demand and background traffic to ensure that the receiving capacity of I-5 is reserved exclusively for evacuating vehicles. This operating plan is considered a "baseline assumption" because it is the plan that local officials are prepared to implement at present. This plan is applied to the above weekday, weekend, and night evacuations. It is also applied to other sensitivity tests where noted.

While this plan is an effective strategy to ensure that receiving capacity beyond the EPZ boundary will be sufficient, it does not consider the potential for overloading the freeway (collapsing speeds are reducing throughput to just 65-75% of normal capacity) with traffic generated entirely within the EPZ. Existing plans are hence dubbed a "moderate" management plan, since it has effective elements, but also misses out on some efficiency that more aggressive plans could obtain.

4.2.2 No Significant Restrictions on I-5 (2a)

This sensitivity test is designed to reveal the benefit of the moderate management plan. In other words, what would happen if officials simply closed I-5 for through trips to and from San Diego, and still allowed unfettered northbound access for non-evacuating traffic between the EPZ boundary and the El Toro "Y"?

4.2.3 Aggressive Management of I-5 (2b)

This sensitivity test is designed to reveal additional benefit that could be realized if maximum throughput is maintained on I-5 for the duration of the evacuation. This "maximum efficiency" can be achieved by coordination with a central supervisor that has a birds-eye view of the system and can enforce actions that will improve efficiency, and if officers will slow the rate of entry if speeds are below the 50-60 mph range.

4.2.4 Aggressive Management of I-5 (2b) with Contra-Flow on I-5 (2c)

Heavy demand on I-5 northbound is expected to last nearly the entire evacuation. However, I-5 southbound may have significant ability to help move vehicles northward. This sensitivity test uses the assumptions of the aggressive management plan, but in addition assumes that where I-5 southbound has four and five lanes, two lanes could be used for northbound evacuating vehicles.

4.3 Variations in Other Conditions

Several other conditions may coincide with an evacuation. It is also possible that variation in a few critical assumptions may have an effect. The following sensitivity tests were modeled to establish the expected range of ETEs should certain conditions exist, or for the expected range of variance in major assumptions. All these use weekday moderate I-5 management but for the noted differences.

- 3a. Longer mobilization times than expected.
- 3b. Adverse weather conditions (rain or fog).
- 3c. Incident on northbound I-5 reduces capacity.
- 3d. Up to 20% shadow demand.
- 3e. Earthquake event, with associated bridge, structure, and slope failures.

4.3.1 Delayed Mobilization Sensitivity Test (3a)

There is reason to believe that even if the time consumed in mobilization is significantly higher than estimated, the overall evacuation time may be only minimally affected. The significant question is how quickly roadway capacity will be consumed by those who are first to mobilize. Once the roads are full those not yet mobilized may be able to take their time since they would only be entering gridlock.

A sensitivity test using a longer than expected mobilization time distribution, was used to test this situation.

4.3.2 Adverse Weather (3b)

Several adverse weather conditions occur in the EPZ which could potentially coincide with and impede an evacuation. The most probable would be the effects of heavy rainfall or dense fog. Heavy rainfall is used for this analysis.

HCM 2000 suggests that the affect of rain/fog is to reduce freeway speeds by 16%, and capacities by 15%. Arterials can be expected to see a 10% reduction in speed, and a 6% reduction in capacity. Once the effects of these reductions are modeled, the resulting percent change (or sensitivity) in overall ETE between the normal day and the adverse weather conditions can then be applied to weekend and night scenarios.

4.3.3 Unexpected Incident on Northbound I-5 (3c)

There is significant potential for an event to occur on northbound I-5 during the evacuation (vehicle collisions or breakdowns). This scenario assumes an incident occurs near the EPZ boundary which closes all lanes on I-5 for 45 minutes.

4.3.4 Up to 20% Shadow Demand (3d)

This scenario was developed to quantify the range of uncertainty that exists in the assessment of evacuation time should shadow demand reach 20% instead of the anticipated negligible amount (0%). Calculations suggest that 20% shadow demand, combined with background demand and demand from rerouting, would consume 75% of at-grade arterial roadway capacity during the first 120 minutes. With time, conditions improve so that 50% of at-grade capacity is available to the target population until the 240 minute mark. Shadow demand will not affect freeway capacity due to

restricted access.

4.3.5 Earthquake Event (3e and 3f)

This scenario assumes that an earthquake event has compromised the SONGS facilities resulting in the need to evacuate and possible landslides and bridge failures have rendered many roadway sections unusable. This scenario could also apply to any situation where the use of bridge structures is impeded.

Chapter 5

EVACUATION NETWORK

Evacuation plans identify the area roadways to be used as evacuation routes by each community. The major roadway system and the principal evacuation routes within the EPZ sectors are depicted in Figure 5.1.

5.1 Major Evacuation Routes

Major roadways in the area which were examined for use as evacuation routes are described in the following paragraphs.

- ◆ Interstate 5 (San Diego Freeway) is the principal north-south roadway and passes just east of SONGS. I-5 is an eight- to ten-lane freeway. Four northbound lanes are available for evacuation use south of Camino Las Ramblas and five lanes are available north of this point. Four lanes are available in the southbound direction, south of State Route 1.
- ◆ The San Joaquin Hills Transportation Corridor (State Route 73) extends from State Route 55 in Costa Mesa to I-5 between Junipero Serra Road and Avery Parkway. The two-lane connector ramp from northbound I-5 to northbound San Joaquin Hills Transportation Corridor adds one additional evacuation lane between Ortega Highway and Junipero Serra Road and two additional evacuation lanes from Junipero Serra Road north to the SR-73 connector ramp.
- ◆ Basilone Road is a two-lane road which intersects I-5 approximately two miles north of SONGS and runs in a southeasterly direction into the interior of Camp Pendleton.
- ◆ Old Highway 101 was originally a four-lane roadway, but has been narrowed to two lanes in some areas to provide shoulder-area parking for visitors to the State Beach areas. This highway parallels I-5 from the Basilone Road interchange past the SONGS facility, with a southern connection to I-5 at the Las Pulgas interchange approximately seven miles south of the SONGS site.
- ◆ El Camino Real (State Route 1) is a four-lane undivided roadway which generally parallels I-5 from the Orange County line northward to the Avenida Pico area in northern San Clemente.
- ◆ State Route 1 continues north of Avenida Pico as the Pacific Coast Highway between Avenida Pico and Doheny Park Road. North of Del Obispo Street, Pacific Coast Highway operates as a three-lane, one-way street couple to Street of the Blue Lantern and then narrows to a four-lane (two-way) roadway and generally parallels the coastline.
- ◆ Avenida Pico is a four-lane arterial within the City of San Clemente west of I-5, with its western terminus at El Camino Real (State Route 1) near the Pacific Ocean. It is generally six-lanes east of I-5.

- ◆ Ortega Highway (State Route 74) is a generally four-lane, east-west roadway from Camino Capistrano to east of Hunt Club Road, which is located near the eastern city limits. Ortega Highway then narrows to two lanes and continues across the San Juan Creek channel to the Lake Elsinore area in Riverside County. Though it has limited capacity, it is expected to be fully utilized in an evacuation.
- ◆ Antonio Parkway is a four-lane north-south arterial which runs from Ortega Highway (SR-74) in the south, at La Pata Avenue, to Crown Valley Parkway in the north. From Crown Valley Parkway to Oso Parkway, Antonio widens to six lanes. At this point just east of the Mission Viejo city limit it continues as a six-lane arterial and runs in a northeasterly direction to connect with the Foothill Transportation Corridor (SR-241).
- ◆ Camino Capistrano begins as a two-lane arterial at its intersection with Pacific Coast Highway in northern San Clemente, and parallels the Pacific Coast Highway through the Capistrano Beach residential areas of Dana Point. At Camino Las Ramblas, it turns northward and parallels I-5 through San Juan Capistrano. At its junction with Doheny Park Road, Camino Capistrano widens to a four-lane cross-section to Del Obispo Street. From Del Obispo Street to Ortega Highway, Camino Capistrano operates as a two-lane roadway. The roadway extends north of Ortega Highway as a four-lane roadway to a point near Oso Road, where it tapers down to a two-lane roadway.
- ◆ Rancho Viejo Road extends from Calle Arroyo in the south, across Ortega Highway. Most of the roadway is four lanes wide.
- ◆ Street of the Golden Lantern is generally a six-lane arterial which extends from Pacific Coast Highway north beyond the limits of Dana Point and becomes Moulton Parkway north of Crown Valley Parkway in Laguna Niguel.
- ◆ Niguel Road is a four-lane roadway which extends from Pacific Coast Highway north beyond the limits of Dana Point and connects with Alicia Parkway immediately north of Crown Valley Parkway in Laguna Niguel.
- ◆ Crown Valley Parkway is generally a six-lane arterial which extends north through Dana Point, then northeasterly through Laguna Niguel to I-5.



Evacuation Routes

San Onofre Nuclear Generating Station Evacuation Time Estimate Evacuation Routes



Figure 5.1

5.2 Planned Improvements to the Major Roadway Network

Near-term/on-going, medium-term, and long-term planned roadway improvements were identified through contact with responsible agencies. These are described below.

5.2.1 Near-Term/On-Going Roadway Projects

Antonio Parkway is currently a four- and six- lane arterial paralleling east of I-5 between Oso Parkway and Ortega Highway (SR-74). The road has been planned to extend south along La Pata Avenue and connect Avenida Pico near Avenida Vista Hermosa, thus providing a bypass route to the communities living east of I-5.

Currently, the La Pata Avenue Extension of Antonio Parkway extends as a two-lane road one mile south of Ortega Highway to the County Landfill site. Further extension of this road to Avenida Vista Hermosa has been deferred and is not anticipated to be completed before 2011. The potential impact of this improvement on evacuation routing and evacuation time will not be included as part of this study.

5.2.2 Long-Term Roadway Projects

There are several regional arterials being considered, in the long term and in or near the study area. Those which could ultimately increase available evacuation route capacity are summarized below:

The extension of Antonio Parkway as a high-capacity two-lane arterial along the alignment of La Pata Avenue from the County Landfill to Avenida Pico (as described above).

The Foothill-South Transportation Corridor (FSTC, or SR-241), runs between I-5 at the Orange County/San Diego County line and Oso Parkway. This roadway, if completed, would be aligned along the northern boundary of Camp Pendleton Marine Corps Base and northeast of San Clemente, providing additional capacity to the north.

SR-241 currently connects Oso Parkway near Santa Rancho Margarita to SR-91 in Santa Ana Canyon. The project construction may be anticipated to begin in 2007-2008 and may be completed by 2011. Since its earliest completion is the last year of the study, it is assumed that it will not be available during the study time frame. Antonio Parkway, an existing arterial, could be utilized as an alternate route to SR-241 and is included in the modeling network for the ETE analyses.

Thus, these projects do not anticipate their full completion before 2011, or at best near the very end of the horizon period. As such, none of the above-mentioned long-range regional arterial improvements were reflected in terms of available new evacuation roadway capacity for this evaluation time analysis.

5.3 Designated Evacuation Routes and Reception Centers

The principal northbound evacuation routes are I-5 and the Pacific Coast Highway, with Camino Capistrano, Street of the Golden Lantern, Niguel Road, Crown Valley Parkway, and Antonio Parkway as secondary routes. These are preferred routes only.

Population from within the U.S. Marine Corps Base, Camp Pendleton and San Onofre State Park have been assigned evacuation routes leading to the south. The principal routes to the south are Basilone Road and I-5. Basilone Road is primarily for evacuation of Camp Pendleton.

Nonessential SONGS personnel and visitors will be directed to evacuate north or south via I-5, depending on the safest prevailing conditions at the time.

The Orange County Fairgrounds is the assigned reception center identified in the Offsite Emergency Response Plan for those who evacuate north. Carlsbad High School is the reception center for those who evacuate to the South. Reception centers are more accurately called Reception and Decontamination Centers. These are referred to in most of this document as reception centers for ease of use.

5.4 Evacuation Route Link/Node Network

The designated evacuation routes were translated into a link/node network for input to a Dynamic Assignment Simulation Program.

5.5 Roadway Characteristics for Evacuation Network

Each roadway has an observed free flow speed and capacity that must be coded as a starting point for simulation. A brief description of these attributes is given below:

- **Speed:** The normal speed limit or observed speed is provided as a starting point for the simulation. The length of each link is also computed to determine average time to traverse the link. Note that this speed is not the normal peak hour observed speeds, which are typically much lower than the posted speed limit on congested arterials and freeways.
- **Capacity:** Capacity in vehicles per hour per lane (vphpl) identifies the number of vehicles which can traverse a typical intersection for that class of roadway. Link capacity is then simply lane capacity multiplied by the number of lanes.

Chapter 6

DEMAND ESTIMATES

6.1 Public Evacuation Time Components

For the general population, the time required to evacuate is comprised of several individual time components. The following time components during an evacuation are expected from the majority of the population:

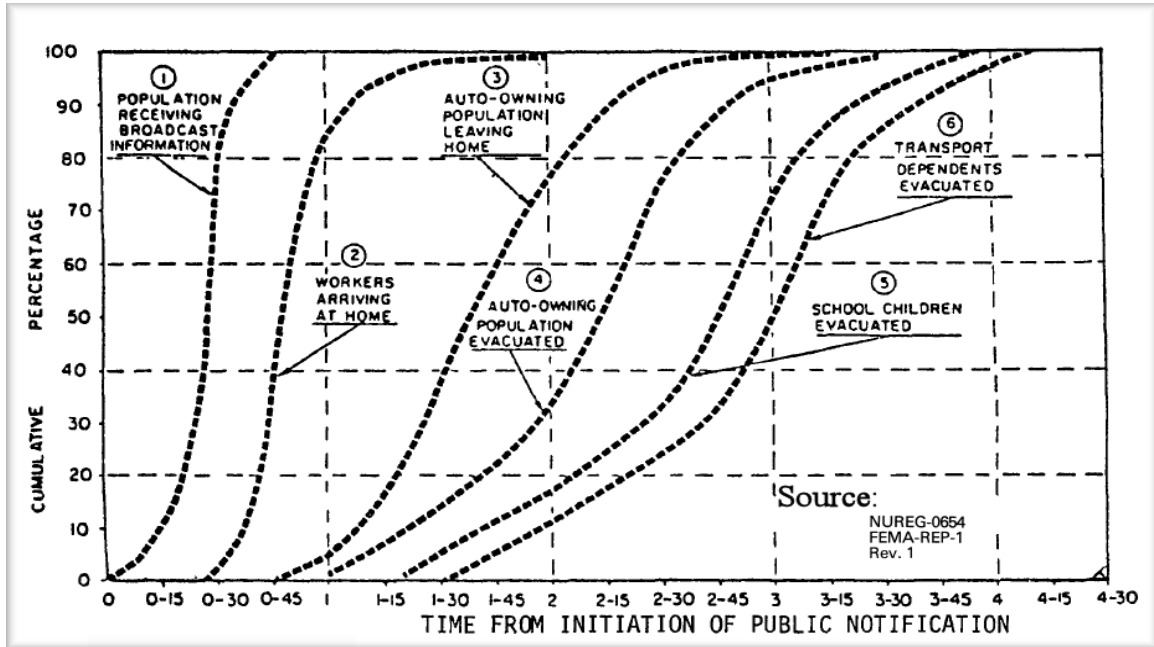
1. Receipt of Notification - The time required for the general population to receive notification of evacuation once public warning is initiated.
2. Return to Home - The time required for persons to return to their homes. This reflects the time required to close up businesses and places of work.
3. Departure from Home - The time required to assemble family members, pack essential items for the evacuation, and secure the home prior to leaving.
4. Evacuation Travel Time - The time required for the population to travel out of the affected area.

The transient population (visitors and workers who reside outside the EPZ) would skip steps two and three, mobilizing much faster than the resident population.

6.2 Mobilization Rates

Each evacuation time component can be expressed graphically as a distribution curve of the percent of population completing a public response component over time (**Figure 6.1**). Mobilization time is that period between the initial evacuation notification and the time that people leave home. In **Figure 1** this is line 3, Auto-Ownning Population Leaving Home. The mobilization time distribution controls the rate at which vehicles enter onto the evacuation network.

Figure 6.1:
 NUREG-0654 SAMPLES OF TIME TO COMPLETE EVACUATION PHASES

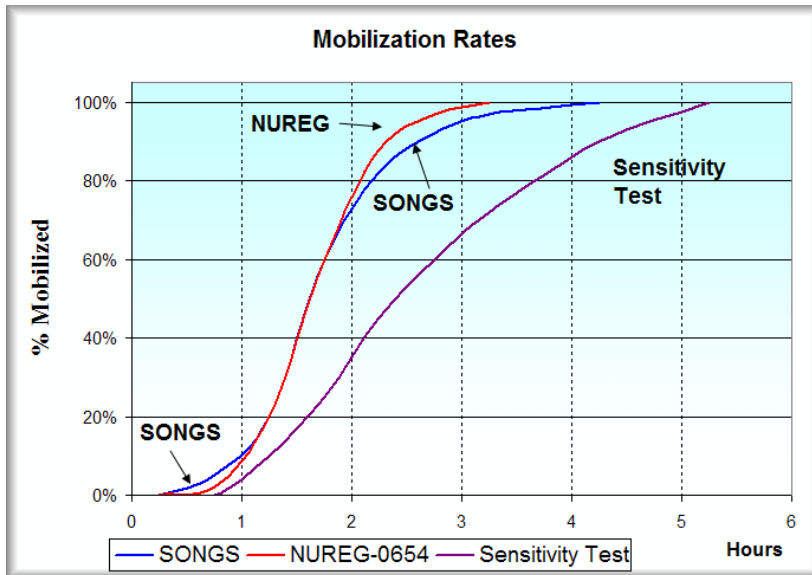


Source: NUREG-0654, Rev. 1

Visitors and people who work in the EPZ but live outside the EPZ are able to mobilize to leave the EPZ much more quickly than those who live within the EPZ. Mobilization rates of beach visitors or SONGS employees follow a curve between Figure 6.1 curves 1 and 2 (receiving notice, and workers arriving at home). Curves 5 and 6 were used to account for schools and transport-dependent individuals. Curve 4 is an example of a final ETE.

A blending of the relevant NUREG curves applied to SONGS is shown in Figure 6.2. This is compared with the NUREG curve 3 which encompasses the majority of evacuees.

Figure 6.2:
 MOBILIZATION RATES



Source: Wilbur Smith Associates, 2006

The mobilization rate in the first few minutes is far more important than in latter minutes. Roadway capacity is largely unused in the first few minutes. Once demand begins to overwhelm capacity it may be irrelevant whether the remainder of evacuees mobilize quickly.

A sensitivity test was conducted of a far more pessimistic mobilization rate than that recommended by NUREG-0654. The test concluded that the slower mobilization rate did not change the overall ETE in a meaningful way. The analysis is presented in Chapter 7.

6.3 Evacuation Population Elements

The populace within the EPZ has been classified into two main groups and a total of six sub-groups. The groups are:

1. Persons Evacuating By Personal Vehicle
 - a. Residents who own automobiles; and
 - b. Transients (visitors and non-resident workers) who have automobiles available.
2. Persons Requiring Evacuation Assistance
 - a. Residents without automobiles;
 - b. Transients without automobiles;
 - c. School children; and
 - d. Special needs populations having restricted mobility.

Projections received from CSUF and local planning agencies were used to estimate population for 2006. The evacuation time estimates reflect the 2006 demographic forecasts.

The following sections identify the population segments, the vehicle volumes, and transportation

requirements.

6.3.1 Resident and Transient Population Estimates

The estimated resident and transient population which would evacuate reflects the following:

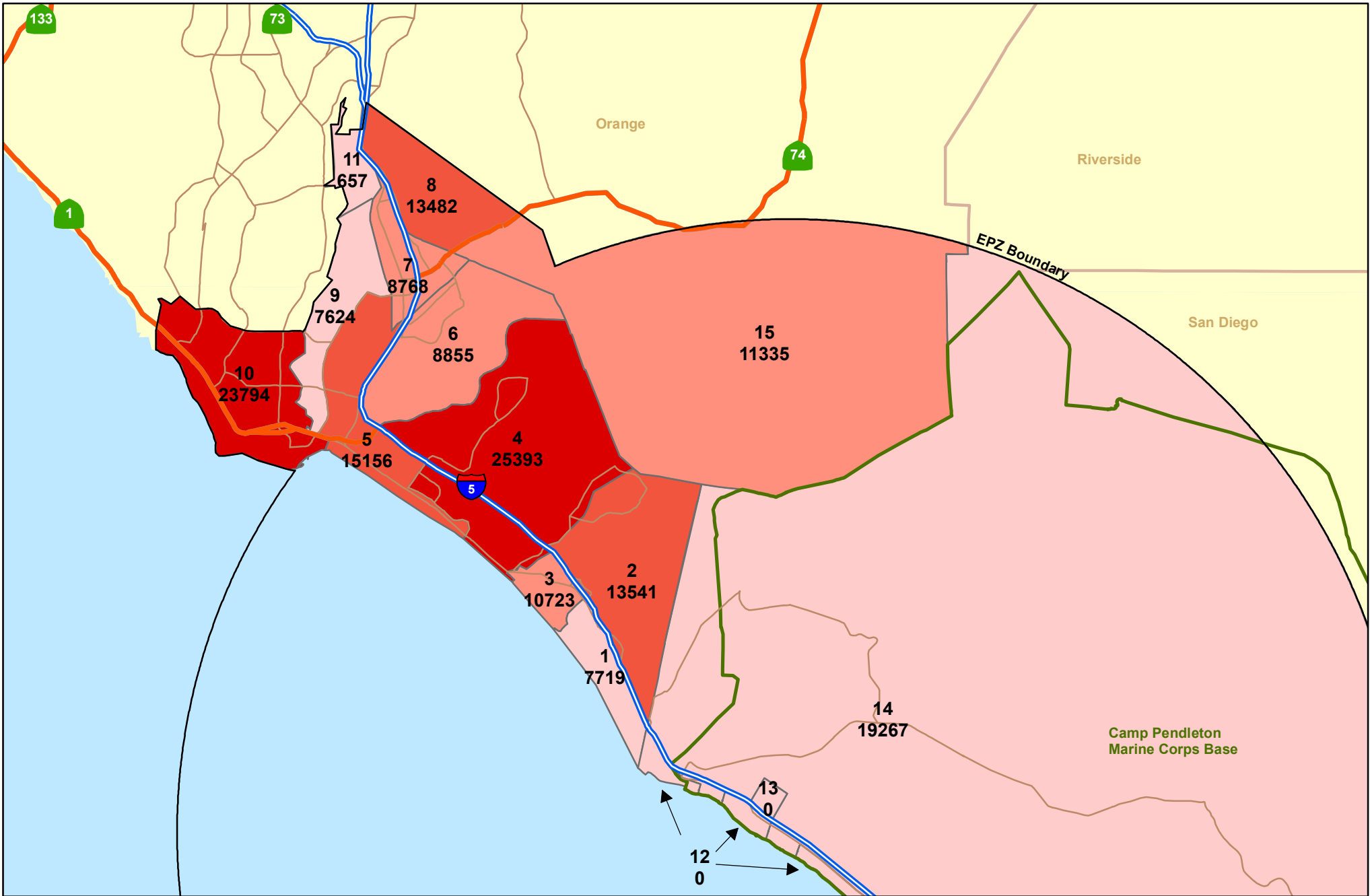
1. The resident population reflects the total number of persons estimated to reside within each zone.
2. The workers represent the estimated total number of non-resident persons (transients) employed within each zone or visiting the zone for business purposes.
3. The tourist and beach populations reflect the estimated number of recreational visitors (non-residents) within the zone.

6.3.1.1 2006 Resident and Transient Population

The estimated number of Year 2006 residents and transients who would evacuate is summarized by scenario in **Table 6.1** and shown geographically on **Figures 6.3 2006 Population and 6.4 2006 Employment**. On **Figure 6.3**, Camp Pendleton population is not shown in the legend in the highest category, as this population will evacuate to the south and not influence the modeling of populations evacuating north. **Figure 6.4** is summer weekday employment.

The maximum population which may be within the area at any one time would occur for the Summer Weekend scenario. The evacuees, which total 221,078 persons, include 166,314 permanent residents, 12,703 transient workers, and 42,061 recreational visitors. This assumes that all permanent residents are present in the area at the time of peak visitor accumulation at the beaches and parks. The estimated total number of persons evacuating for the three scenarios is:

Summer Weekend	221,078 persons
Summer Weekday	220,563 persons
Night	172,453 persons



- 0 - 8000 people
- 8001 - 12000 people
- 12001 - 16000 people
- greater than 16000 people

San Onofre Nuclear Generating Station Evacuation Time Estimate 2006 Population

Note: Population of Camp Pendleton not modeled

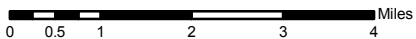
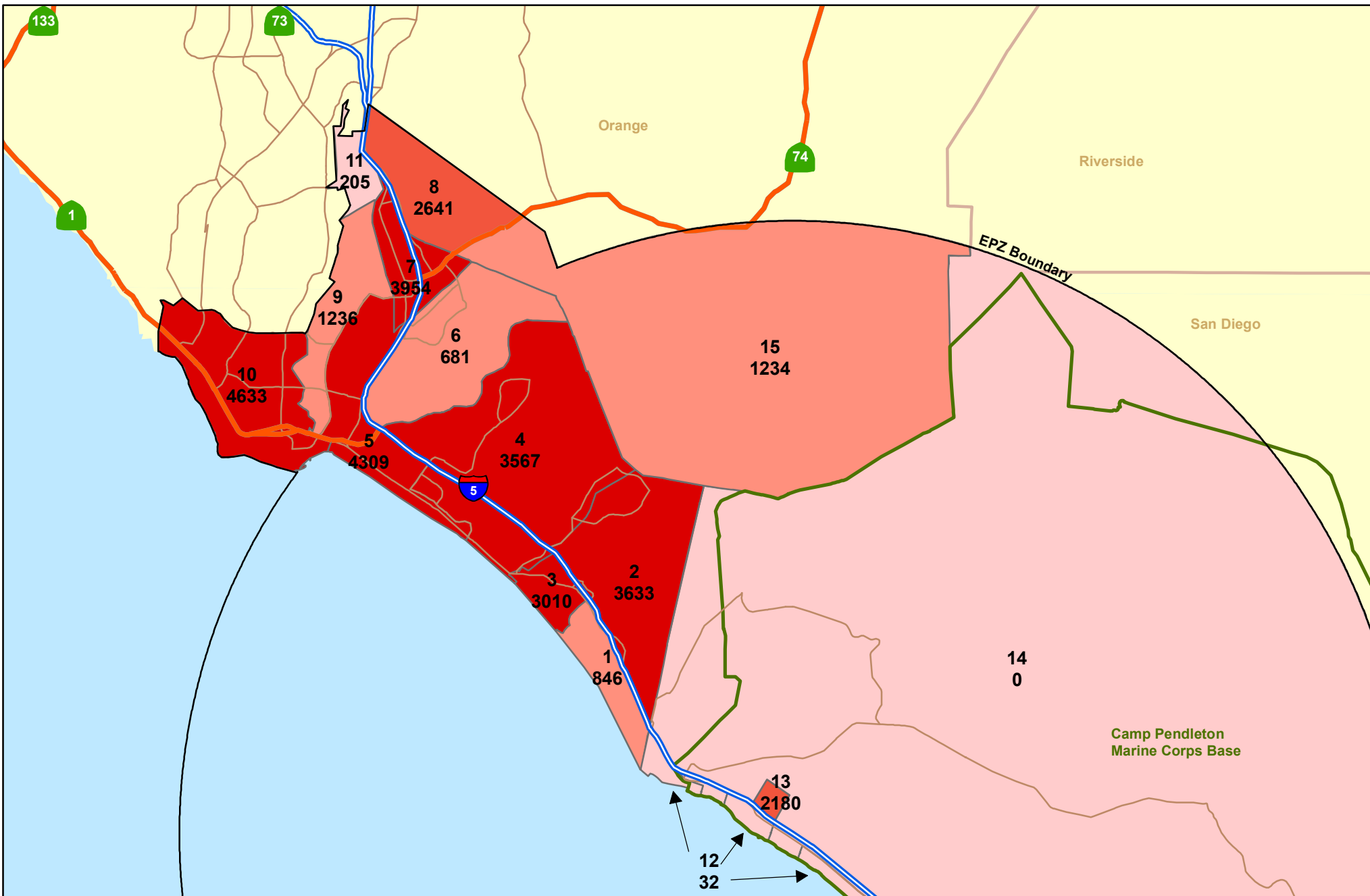


Figure 6.3



- 0 - 500 jobs
- 501 - 1500 jobs
- 1501 - 3000 jobs
- greater than 3000 jobs

San Onofre Nuclear Generating Station Evacuation Time Estimate 2006 Employment



Figure 6.4

Table 6.1:
EPZ PERMANENT AND TRANSIENT POPULATION SUMMARY 2006

Sub-zone	Residents (All Scenarios)	Non-Residents						Grand Totals		
		Summer Weekend		Summer Weekday		Night		Summer Weekend	Summer Weekday	Night
		Worker	Beach/ Visitor	Worker	Beach/ Visitor	Worker	Beach/ Visitor			
1	7,719	666	3,180	846	2,095	82	960	11,565	10,660	8,761
2	13,541	1,211	280	3,633	249	171	95	15,032	17,423	13,807
3	10,723	1,904	10,060	3,010	5,030	301	270	22,687	18,763	11,294
4	25,393	863	40	3,567	220	182	88	26,296	29,180	25,663
5	15,156	2,028	12,480	4,309	6,240	285	420	29,664	25,705	15,861
6	8,855	187	177	681	115	34	40	9,219	9,651	8,930
7	8,768	1,318	175	3,954	114	198	40	10,261	12,836	9,005
8	13,482	998	277	2,641	219	844	77	14,757	16,341	14,402
9	7,624	778	267	1,236	211	74	74	8,669	9,071	7,772
10	23,794	2,214	2,714	4,633	1,357	172	339	28,722	29,784	24,305
11	657	78	21	205	17	21	6	756	879	684
12	0	48	12,300	32	6,150	8	1,230	12,348	6,182	1,238
13	0	0	0	2,180	0	0	0	0	2,180	0
14	19,267	0	0	0	0	0	0	19,267	19,267	19,267
15	11,335	410	90	1,234	71	103	25	11,835	12,641	11,463
TOTAL:	166,314	12,705	42,061	32,161	22,088	2,475	3,664	221,078	220,563	172,453

Source: Wilbur Smith Associates, 2006

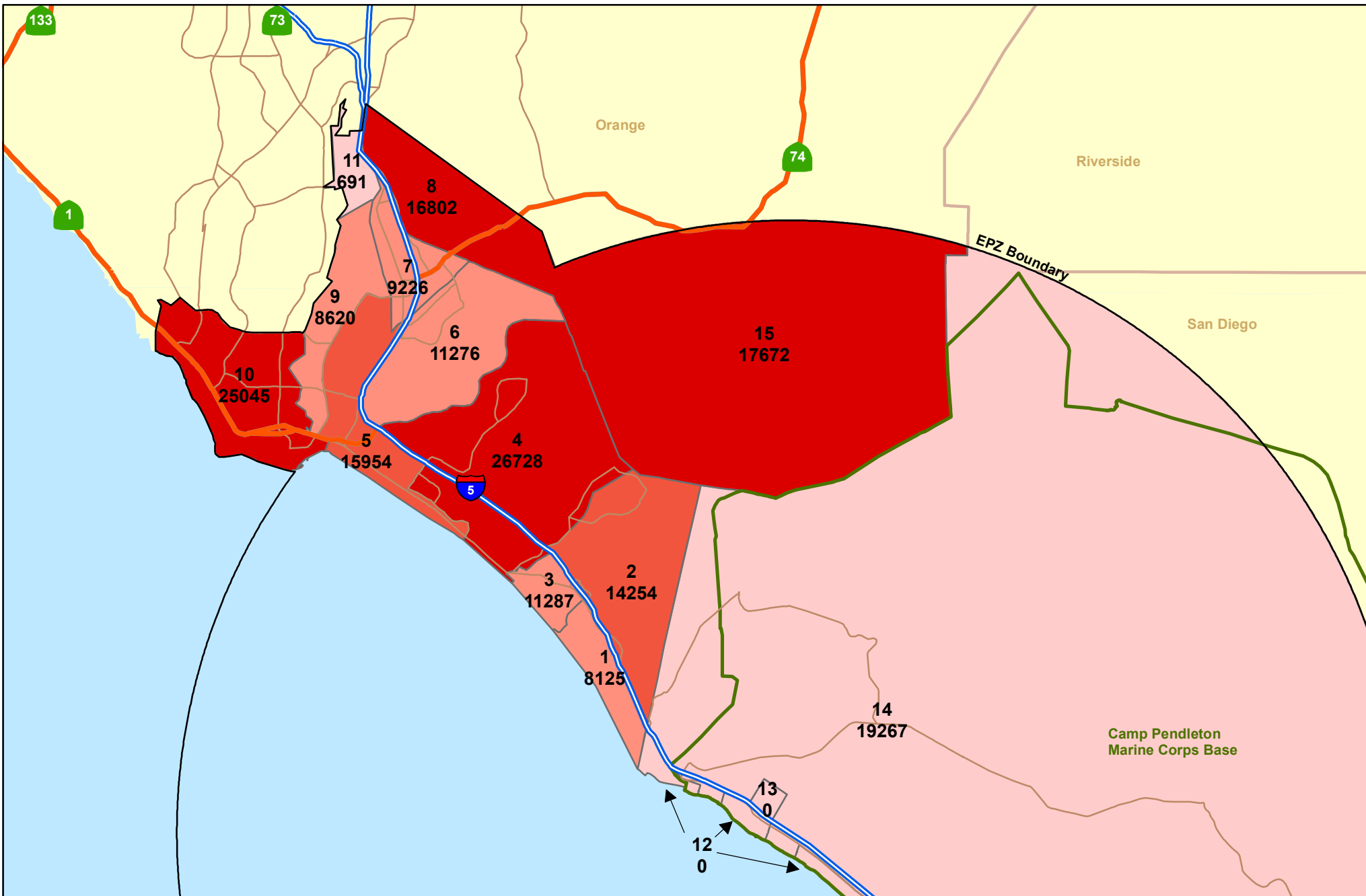
Note:

Sub-zone 13 is SONGS and only workers are counted for this sub-zone .
Sub-zone 14 is Camp Pendleton, the number stated is peak population not distinguishing between workers and residents.

6.3.1.2 2011 Resident and Transient Population

Estimated resident and transient populations for 2011 are summarized in **Table 6.2** for each evacuation scenario, and shown on **Figures 6.5 2011 Population and 6.6 2011 Employment**. Camp Pendleton population was treated in **Figure 6.5** as it was in 2006. Employment is also summer weekday employment. The total number of persons included in each scenario is as follows:

Summer Weekend	249,767 persons
Summer Weekday	247,239 persons
Night	191,284 persons



- 0 - 8000 people
- 8001 - 12000 people
- 12001 - 16000 people
- greater than 16000 people

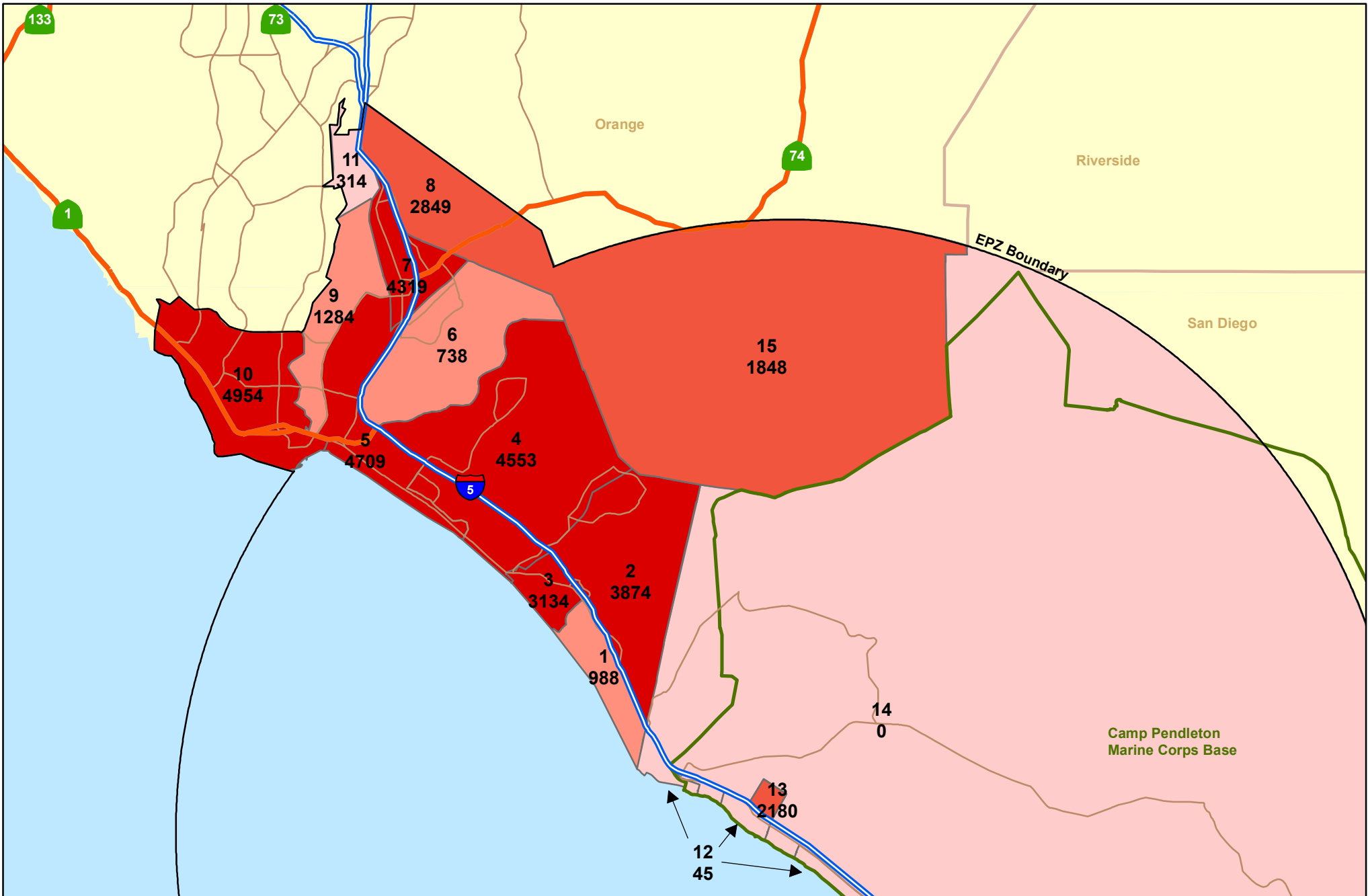


San Onofre Nuclear Generating Station Evacuation Time Estimate 2011 Population

Note: Population of Camp Pendleton not modeled



Figure 6.5



**San Onofre Nuclear Generating Station
Evacuation Time Estimate
2011 Employment**

- 0 - 500 jobs
- 501 - 1500 jobs
- 1501 - 3000 jobs
- 3001 - 4954 jobs



Figure 6.6

Table 6.2:
EPZ PERMANENT AND TRANSIENT POPULATION SUMMARY 2011

SUB-ZONE	RESIDENTS (ALL SCENARIOS)	NON-RESIDENTS						GRAND TOTALS		
		SUMMER WEEKEND		SUMMER WEEKDAY		NIGHT		SUMMER WEEKEND	SUMMER WEEKDAY	NIGHT
		WORKER	BEACH/ VISITOR	WORKER	BEACH/ VISITOR	WORKER	BEACH/ VISITOR			
1	8,125	779	3,816	988	2,514	95	1,152	12,720	11,627	9,372
2	14,254	1,291	240	3,874	299	182	113	15,785	18,427	14,549
3	11,287	1,982	12,072	3,134	6,036	314	324	25,341	20,457	11,925
4	26,728	1,102	264	4,553	264	232	106	28,094	31,545	27,066
5	15,954	2,216	14,976	4,709	7,488	312	504	33,146	28,151	16,770
6	11,276	203	94	738	138	38	48	11,573	12,152	11,362
7	9,226	1,440	524	4,319	136	216	47	11,190	13,681	9,489
8	16,802	1,077	332	2,849	262	108	92	18,211	19,913	17,002
9	8,620	809	321	1,284	253	77	89	9,750	10,158	8,786
10	25,045	2,367	3,256	4,954	1,628	184	406	30,668	31,627	25,635
11	691	90	25	314	20	24	7	806	1,025	722
12	0	62	14,760	45	7,380	8	1,476	14,822	7,425	1,484
13	0	0	0	2,180	0	0	0	0	2,180	0
14	19,267	0	0	0	0	0	0	19,267	19,267	19,267
15	17,672	614	108	1,848	85	154	29	18,394	19,605	17,855
TOTAL:	184,947	14,032	50,788	35,789	26,503	1,944	4,393	249,767	247,239	191,284

Source: Wilbur Smith Associates, 2006

Note:

Sub-zone 13 is SONGS and only workers are counted for this sub-zone.
Sub-zone 14 is Camp Pendleton, the number stated is peak population not distinguishing between workers and residents.

6.3.2 Evacuation Vehicles Used by Resident Population

6.3.2.1 Resident Population

The projected 184,947 persons in 2011 residing in sections of the EPZ which would evacuate north are estimated at 71,317 households. Household automobile ownership information from the 2000 Census was used to estimate the number of households in 2011 that own one or more automobiles (68,950 households). This information is displayed in **Table 6.3**.

Household automobile ownership information from the 2000 Census was used to estimate the number of households that own zero, one, two, and three or more vehicles. Based on vehicle per family assumptions the number of vehicles taken by residents was calculated. **Table 6.3** shows the process of figuring the total number of vehicles used by residents for Summer Weekend/Weekday and Nighttime scenarios.

**Table 6.3:
ESTIMATED 2010 HOUSEHOLD VEHICLE OWNERSHIP AND OCCUPANCY SUMMER WEEKEND/WEEKDAY**

SUB-ZONE	RESIDENT POPULATION	PEOPLE/ HH	TOTAL HH	% HH NO VEHICLE	% HH W/ 1 VEHICLE	% HH W/2 VEHICLE	% HH W/ 3 OR MORE VEHICLE	HH W/0	HH W/1	HH W/2	HH W/3	TOTAL VEHICLES OWNED	TOTAL VEHICLES USED	AVERAGE VEHICLE OCCUPANCY
1	8,125	2.08	3,905	2%	26%	51%	21%	91	998	1,984	831	7,876	5,032	1.61
2	14,254	2.34	6,095	2%	25%	52%	21%	128	1,515	3,148	1,304	12,375	7,890	1.81
3	11,287	2.19	5,158	6%	45%	35%	14%	333	2,331	1,792	702	8,372	5,889	1.92
4	26,728	2.27	11,749	2%	30%	46%	22%	234	3,537	5,387	2,591	23,381	15,075	1.77
5	15,954	2.41	6,631	6%	34%	40%	19%	392	2,283	2,684	1,272	12,102	7,998	1.99
6	11,276	2.56	4,404	5%	27%	48%	20%	202	1,190	2,134	878	8,530	5,500	2.05
7	9,226	2.98	3,097	6%	35%	37%	22%	193	1,084	1,136	685	5,752	3,759	2.45
8	16,802	2.23	7,541	2%	29%	43%	25%	176	2,169	3,276	1,919	15,440	9,788	1.72
9	8,620	2.40	3,599	1%	17%	49%	33%	40	603	1,757	1,199	8,314	4,986	1.73
10	25,045	2.22	11,277	2%	30%	46%	22%	216	3,385	5,176	2,500	22,487	14,489	1.73
11	691	2.07	333	1%	22%	50%	26%	5	74	168	86	712	444	1.56
12	-	-	-	NA	NA	NA	NA	NA	NA	NA	NA	NA	-	NA
13	-	-	-	NA	NA	NA	NA	NA	NA	NA	NA	NA	-	NA
14	19,267	-	-	NA	NA	NA	NA	NA	NA	NA	NA	NA	4,817	NA
15	17,672	2.35	7,528	0%	5%	49%	46%	15	370	3,682	3,462	19,904	11,254	1.57
Total/Ave	184,947		71,317	3%	30%	45%	22%	2,025	19,539	32,324	17,429	145,245	96,919	1.91

Source: Wilbur Smith Associates, 2006

The 2011 resident population would use an estimated 96,919 vehicles to evacuate. The number of resident vehicles is summarized by sub-zone in **Table 6.4**.

6.3.2.2 Transient Population

Virtually all travel of the transient population within the area occurs via private automobile. The number of vehicles used by these transient groups was derived by applying the following average vehicle occupancy factors to the estimated number of visitors within the area represented by each population centroid:

Transient Workers	1.2 persons/vehicle
Transient Beach-Goers	3.0 persons/vehicle
Campers	3.5 persons/vehicle
Other Business, Shopping, Recreational Visitors	2.0 persons/vehicle
Beach-Goers, Campers, and Other Average	2.8 persons/vehicle

The number of vehicles used by transients in an evacuation is presented by sub-zone in **Table 6.4**.

Table 6.4:
EVACUATION VEHICLES GENERATED BY SUB-ZONE 2011

SUB-ZONE	RESIDENTS	NON-RESIDENTS						GRAND TOTAL VEHICLES		
	ALL SCENARIOS	SUMMER WEEKEND		SUMMER WEEKDAY		NIGHT		SUMMER WEEKEND	SUMMER WEEKDAY	NIGHT
		WORKER	BEACH/ VISITOR	WORKER	BEACH/ VISITOR	WORKER	BEACH/ VISITOR			
1	5,032	649	1,348	823	888	79	407	7,030	6,744	5,519
2	7,890	1,076	85	3,228	106	152	40	9,050	11,223	8,081
3	5,889	1,652	4,266	2,612	2,133	261	114	11,807	10,634	6,265
4	15,075	918	93	3,794	93	193	37	16,086	18,962	15,306
5	7,998	1,847	5,292	3,924	2,646	260	178	15,136	14,568	8,436
6	5,500	169	33	615	49	31	17	5,702	6,163	5,548
7	3,759	1,200	185	3,599	48	180	17	5,144	7,406	3,955
8	9,788	897	117	2,374	93	90	32	10,802	12,254	9,910
9	4,986	674	113	1,070	90	64	31	5,773	6,145	5,081
10	14,489	1,973	1,151	4,128	575	154	144	17,612	19,192	14,786
11	444	75	9	262	7	20	2	527	712	466
12	0	52	5,216	38	2,608	7	522	5,267	2,646	528
13	0	0	0	2,146	0	0	0	0	2,146	0
14	4,817	0	0	0	0	0	0	4,817	4,817	4,817
15	11,254	511	38	1,540	30	129	10	11,804	12,825	11,393
TOTAL:	96,919	11,693	17,946	30,153	9,365	1,621	1,552	126,558	136,438	100,091

Source: Wilbur Smith Associates, 2006

Note:

* Resident vehicle estimates were computed in Table 6.3.

The largest number of transient vehicles would be included in an evacuation occurring on a summer weekday, when the combination of transient workers and a relatively large number of beach visitors would increase the number of transient vehicles to 39,519. This compares to 29,757 transient vehicles for a summer weekend and 3,171 vehicles for a nighttime evacuation. The evacuation time estimates assume that all transient vehicles will leave the EPZ.

6.3.2.3 Total Number of Vehicles Evacuating EPZ (Unassisted Population)

The combined number of permanent resident and transient vehicles included within the evacuation time estimate is as follows:

Summer Weekday	136,438 vehicles
Summer Weekend	126,558 vehicles
Night	100,091 vehicles

6.3.3 General Population Requiring Evacuation Assistance

A portion of the population in the EPZ will not have an automobile available to use in an evacuation. Groups which may require transportation assistance would include households which do not own an automobile, households where the family vehicles are unavailable at the time of evacuation, homebound special needs population, and persons in institutions (for example schools, hospitals and assisted living facilities). The demand for public transit is figured by estimating the number of bus loads needed to evacuate this portion of the population. These numbers are not necessarily the number of buses required, because one bus can make several trips reducing the number of buses needed and vehicles on the road at the time of the evacuation.

6.3.3.1 Residents without Automobiles

The 2000 Census reveals that between two and five percent of the households within the EPZ do not own an automobile. Applying the average household size to the number of 2011 households without autos in each community yields an estimated 4,916 residents who may require transportation assistance. In **Table 6.5** the total weekend and night population needing evacuation assistance without an auto is 4,916.

**Table 6.5:
 NUMBER OF BUS LOADS NEEDED TO TRANSPORT RESIDENTS WITHOUT AN AUTO**

SCENARIO	PERSONS	BUS LOADS
Weekend	4,916	71
Weekday	13,597	195
Night	4,916	71

Source: Wilbur Smith Associates, 2006

This estimate includes many school-age children of no auto households who would be provided transportation through the school authorities if an evacuation occurs on a school day. A weekday scenario would drop the population of no auto households to 4,129 by excluding school children, but would include households with one vehicle that may not be available at the household.

Census data indicates that between 17 and 45 percent of the households in the various areas has access to only one vehicle. Based upon regional work trip patterns, it is estimated that approximately

25 percent of these one-car households have workers who commute more than 20 miles from home and would be beyond the traffic control/diversion perimeter.

Applying the average number of persons per household (less the driver of the absent vehicle) to the one-car households without an available auto would result in as many as 9,468 persons. The total weekday population potential requiring assistance is 13,597.

The average seating capacity of the current bus fleet is approximately 36 persons per bus. In an emergency situation standees would be accommodated therefore 70 persons per bus was used to determine bus load demand.

The permanent residents without autos produce a potential need for up to 195 bus loads under summer weekday conditions.

School children and residents of assisted living facilities are not included in the above weekday scenario. They are addressed as a separate institution requirement on weekdays.

6.3.3.2 Transients without an Automobile

Most of the non-resident workers and recreational visitors would be expected to have an automobile available for use in an evacuation. An individual dropped off at work or at the beach by someone who then travels out of the EPZ could create a transient without an automobile. The analysis assumes that two percent of transient visitors do not have a vehicle available at the time of evacuation. The number of persons and bus loads is provided in **Table 6.6**.

**Table 6.6:
NUMBER OF NEEDED BUS LOADS TO TRANSPORT TRANSIENTS WITHOUT AUTOS**

SCENARIO	PERSONS	BUS LOADS
Weekend	1296	19
Weekday	1246	18
Night	127	2

Source: Wilbur Smith Associates, 2006

6.3.4 Schools

The primary means of transport for children in school evacuating the EPZ would be by bus.

The evaluation of transportation requirements for school children assumes that the majority of students attending public schools would be transported outside the affected area by school district or public transit bus.

Current information obtained from the CUSD indicates that the school district has sufficient capacity to transport approximately 5,000 students at one time. OCTA advises that the average capacity of their current public transit fleet is 36 seated adult passengers. Recognizing that somewhat more pupils could be accommodated, an average capacity of 60 pupils per bus was used.

Local emergency response plans envision that many of the children attending private schools would be picked up by their parents prior to evacuating the area. For the purpose of this estimate, only

private school students who take the bus to school would be evacuated by bus. Approximately 1,275 students take buses to private school⁴.

Using the approximate school district bus fleet lift capacity, it is estimated that as many as 352 public transit bus loads could be required to evacuate all public and private schools within the EPZ.

6.3.5 Special Populations Having Restricted Mobility

There are three types of institutions within the EPZ that would require assistance in relocation. These are hospitals, retirement homes, and homebound persons with special needs. These persons would be relocated to hospitals, assisted living facilities, and other appropriate facilities outside the affected area.⁵

6.3.5.1 Hospitals, Assisted Living Facilities, and Retirement Homes

Saddleback Memorial Medical Center, San Clemente Campus is the only hospital located in the EPZ. The 68 patients in this facility would be transported by ambulance and wheelchair van. Of the 68 patients, 42 would be accommodated by seven wheelchair vans, while 26 would be accommodated by 13 ambulances. Transportation requirements are based on assessments made by officials representing the hospital.

Based on information provided by facility staffs, a total of 822 of the assisted living residents were assessed to be ambulatory. Assuming a seated capacity of 36 per bus, some 23 transit bus loads would be required for evacuation. The estimated total of 309 wheelchair-bound persons would require 52 wheelchair vans having an average capacity of six chairs each.

Hospital and assisted living vehicle requirements are listed in **Table 6.7** below.

Table 6.7:
ESTIMATED YEAR 2011 TRANSPORTATION ASSISTANCE REQUIREMENTS FOR HOSPITALS AND ASSISTED LIVING POPULATION REQUIRING SPECIAL ASSISTANCE

ITEM	AMBULANCES	WHEELCHAIR VANS	BUS LOADS	TOTAL
Persons	26	351	822	1199
Vehicles	13	59	23	95

Source: Wilbur Smith Associates, 2006

Note:

Assumed vehicle capacities: Ambulances (2 per unit); wheelchair vans (6 per unit); bus loads (36 passengers per bus).

6.3.5.2 Homebound Populations Requiring Special Transportation Assistance

The County of Orange maintains a Special Assistance population list of persons who live at home and have chronic disabilities that may limit their mobility. Transportation assistance for homebound persons who are members of this program would have to be assigned on an individual basis. The type of transportation required would depend on the nature of the person's disability.

⁴ Per discussions with Orange County Sheriffs Department (OCSD)

⁵ County of Orange Nuclear Power Plant Emergency Plan for San Onofre Nuclear Generating Station, coordinated by Orange County Sheriff-Coroner Emergency Management Division, Interjurisdictional Procedures #8, #9, and #18. p. V-14.

The current number of persons enrolled in the Special Assistance program requiring transportation assistance is 529. Based on current program participants, approximately 54 of the total would require ambulances and 164 wheelchair vans. The remaining 311 are ambulatory and could be transported by bus, with some minor assistance. This resulted in the estimated transportation assistance requirements that are summarized on **Table 6.8** below.

**Table 6.8:
 ESTIMATED YEAR 2011 TRANSPORTATION ASSISTANCE REQUIREMENTS FOR
 HOMEBOUND POPULATION REQUIRING SPECIAL ASSISTANCE**

ITEM	AMBULANCES	WHEELCHAIR VANS	BUS LOADS	TOTAL
Persons	54	164	311	529
Vehicles	27	27	9	63

Source: Wilbur Smith Associates, 2006

Note:

Assumed vehicle capacities: Ambulances (2 per unit); wheelchair vans (6 per unit); bus loads (36 passengers per bus).

6.3.5 SONGS Workers and Visitors

The number of on-site workers and visitors present at the SONGS facility depends upon the time of the week and whether or not a generation unit is shut down for maintenance or refueling purposes. During routine shut-downs or outages there is a large increase in the number of contract personnel on site. Each of the two generating units is scheduled for shut-down once every 18 to 24 months for refueling, with the outages scheduled to avoid the summer period when demand is greatest.

Southern California Edison would mandate an evacuation of the plant upon declaration of a General Emergency. Approximately 150 essential personnel would remain on site. **Table 6.10** presents the estimated number of workers and visitor vehicles that would exit the site.

SONGS workers would evacuate either north or south depending upon the safest direction of travel at the time.

**Table 6.9:
 ESTIMATED NUMBER OF VEHICLE USED BY EVACUATING SONGS WORKERS**

CONDITION	WEEKDAY	WEEKEND	NIGHTTIME
Total Vehicle Evacuating			
During Normal Operations	2146	0	0
During Outage Operations	2514	341	341

Source: SONGS SCE, 2006

6.3.8 U.S. Marine Corps Base, Camp Pendleton

Peak population in those base areas included within the EPZ is estimated at 19,267 persons, as shown on **Table 6.11**. The estimated number of persons that would be evacuated would total 16,665 persons for an evacuation occurring during normal work hours, and 17,698 persons if the evacuation occurs outside of normal work hours.

Transportation resources used to evacuate these areas will include privately-owned vehicles and government vehicles.⁶ Estimated evacuation demand has been expressed only in terms of persons requiring transportation.

⁶ Annex C (Operations) to MCP FP Plan 04, July 2004

**Table 6.10:
 ESTIMATED POPULATION AND TRANSPORTATION REQUIREMENTS FOR CAMP
 PENDLETON**

AREA	ESTIMATED PEAK POPULATION FOR CAMP PENDLETON	NUMBER OF PERSONNEL TO BE EVACUATED	
		NORMAL WORK HOURS	AFTER NORMAL WORK HOURS
San Onofre Recreation Beach	200	100	50
San Onofre Family Housing	4,712	2,500	3,500
Mobile Home Park (248 Trailers)	500	300	500
San Onofre	3,000	3,000	3,000
San Mateo	3,197	3,197	3,197
San Mateo Pt. Housing	290	200	290
Horno	3,245	3,245	3,245
Talega	307	307	100
Las Flores	930	930	930
Las Pulgas	2,886	2,886	2,886
TOTAL	19,267	16,665	17,698

Source: Camp Pendleton Housing, 2005

Chapter 7

RESULTS – EVACUATION TIME ESTIMATES

7.1 EMERGENCY EVACUATION TIME ESTIMATES

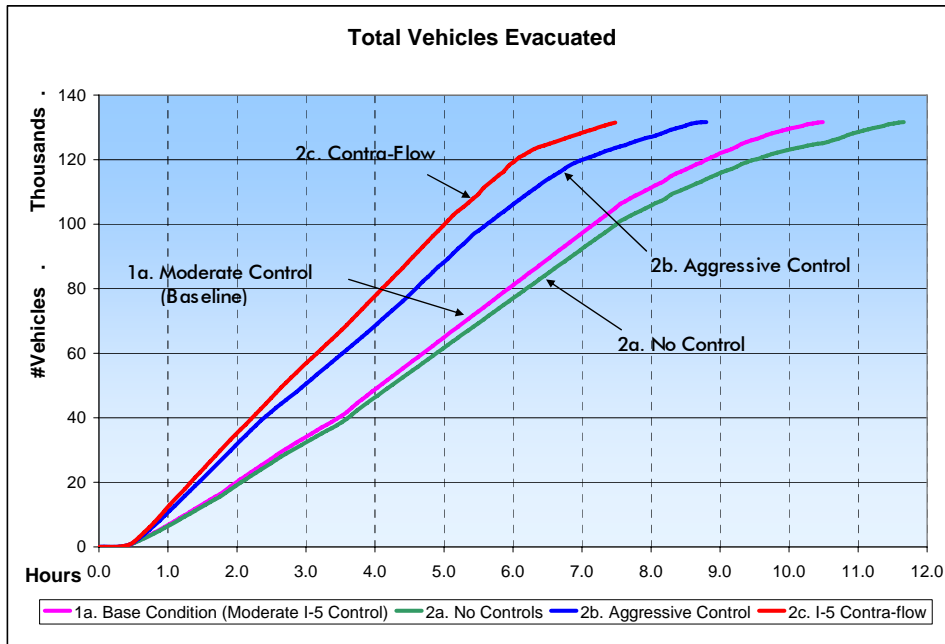
Emphasis was placed on the more densely populated areas within the northern sector in the development of evacuation time estimates. Approximately 90 percent of the total resident population within the EPZ is located in Orange County, north of SONGS. Evacuation to the South is expected to experience no capacity constraints, and will be affected only by the mobilization time.

7.1.1 Graphical Analysis of Evacuation Elements

Figure 7.1 shows how many vehicles have moved beyond the EPZ boundary at each hour for several I-5 control scenarios. The point at the upper-right of each curve represents the total ETE for the respective scenario.

Compared to the no controls alternative, the existing I-5 management plan (1a) is effective at improving the ETE. The procedural action of ensuring that I-5 operates at maximum throughput improves the estimates dramatically. The addition of two contra-flow lanes is also significant but has implementation and operational issues.

Figure 7.1:
 TOTAL VEHICLES EVACUATED UNDER I-5 MANAGEMENT APPROACHES



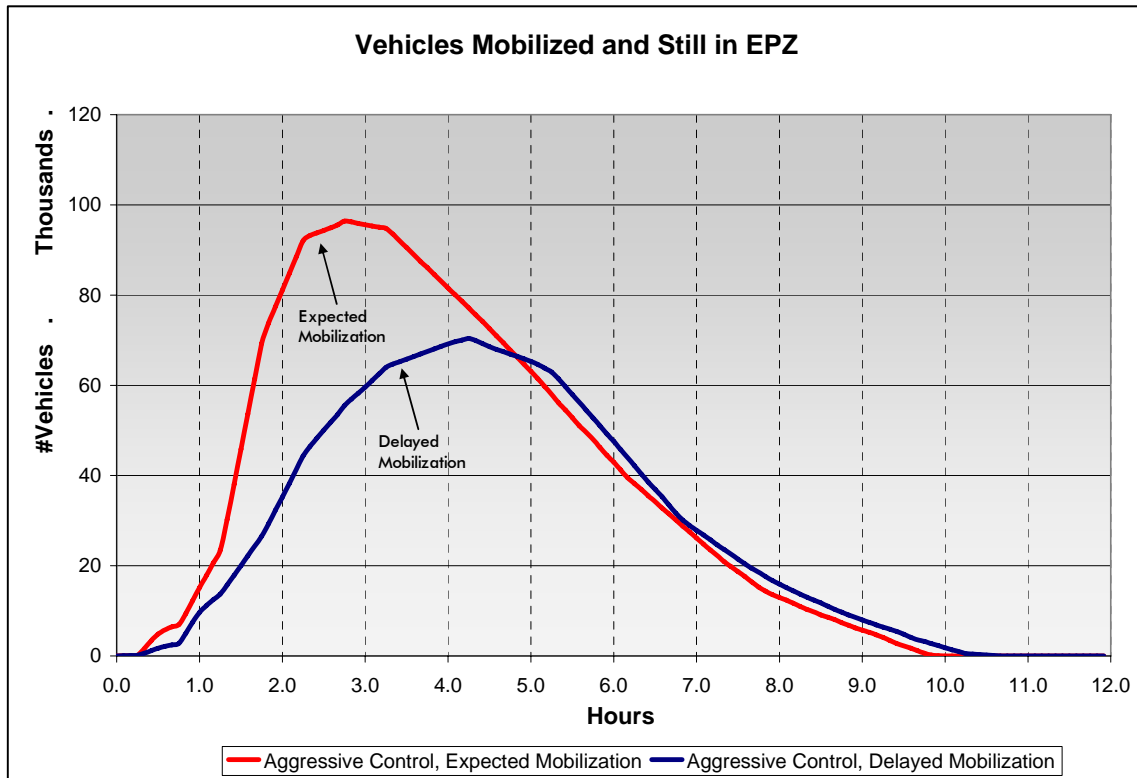
Source: Wilbur Smith Associates, 2006

Figure 7.2 shows how many vehicles have been mobilized, but are still in the EPZ over time. The highest curve has a lot more people stuck in traffic, while the bottom curve lets them stay at home a little longer. All vehicles from the bottom curve are fully mobilized in the fifth hour, at which point

they enter congestion the same as if they had been sitting in their vehicles the whole time. The slight differences after hour 5 are not meaningful and can be considered noise.

Potential negative outcomes of extreme congestion may be worth considering when determining a mobilization plan. Vehicles running out of fuel, aggressive driving, and shoulder commandeering could add significant time to the evacuation and are typical of extreme congestion. Staged mobilization can reduce the potential for these negatives. While it makes no difference in the total ETE, it would make a difference to each individual.

Figure 7.2:
 DIFFERENCE BETWEEN EXPECTED MOBILIZATION AND DELAYED MOBILIZATION



Source: Wilbur Smith Associates, 2006

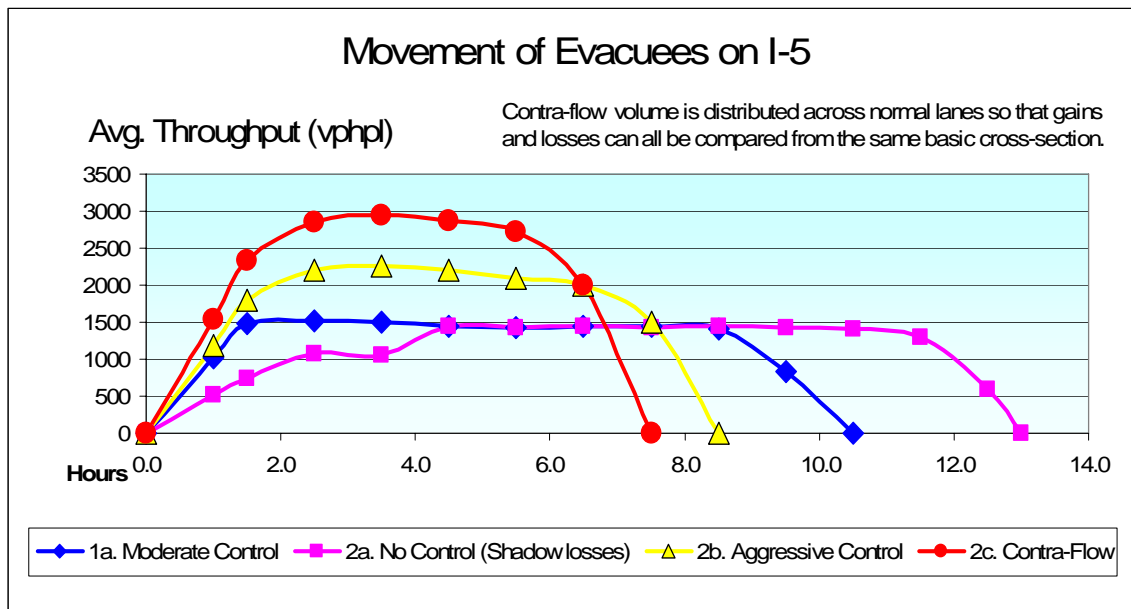
Figure 7.3 is an analysis of I-5 with various levels of access management. The second highest line (yellow) shows that aggressive I-5 access control would likely move nearly 2,200 vehicles per hour per lane until nearly the 7th hour, where demand starts to dissipate.

The base case line (1a, blue) will move evacuees at about 1,500 vphpl (about 30% loss) until nearly the 9th hour, at which point demand falls off.

The no-control line (2a) shows what occurs when shadow demand can access I-5 beyond the EPZ. For the first several hours I-5 carries less than 1,500 vphpl. In reality I-5 will still move 1,500 vphpl, but many of them are not evacuees. This figure shows only evacuees. No-control would stretch the evacuation out to nearly 13 hours.

In the contra-flow scenario, the lanes do not actually carry 3,000 vphpl each. This is theoretically impossible. The total volume from contra lanes is added to the original number of lanes to make it comparable with the other scenarios.

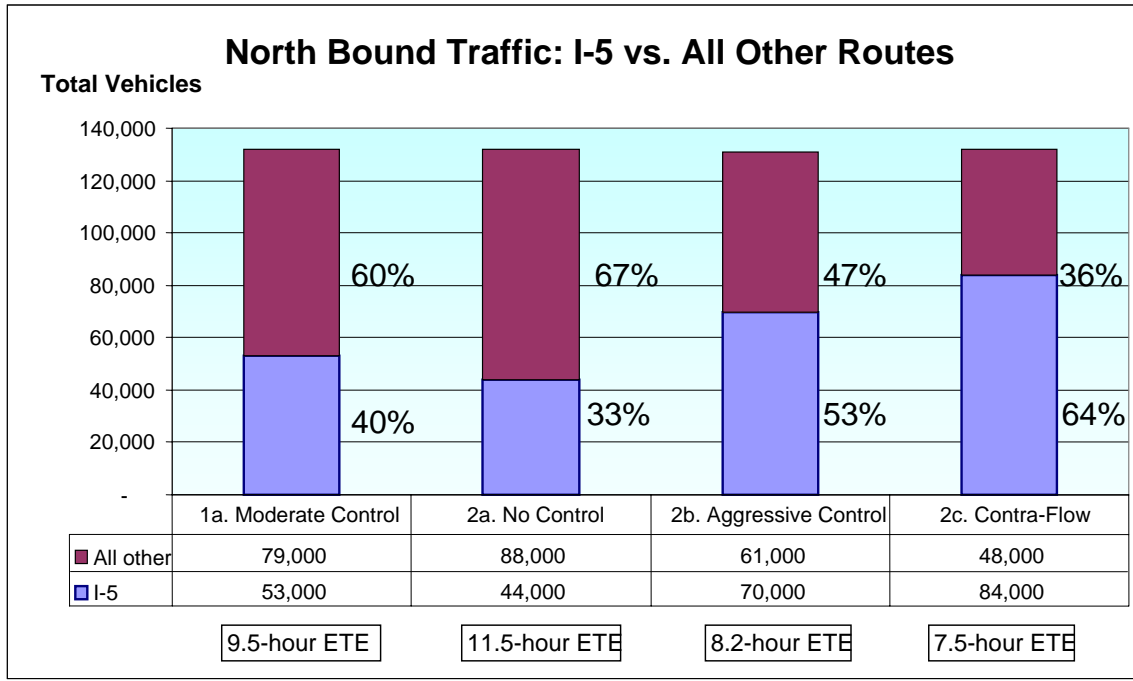
Figure 7.3:
 AVERAGE THROUGHPUT OF AN I-5 LANE DURING EVACUATION SCENARIOS



Source: Wilbur Smith Associates, 2006

Figure 7.4 is a depiction of how much of the evacuation occurs on I-5 as opposed to all other roadways for the different management scenarios. In each case there are 132,000 vehicles. In the base case 40% of the traffic is moved on I-5, while in the contra-flow case up to 64% of the traffic would use I-5.

Figure 7.4:
 RELATIVE SHARE OF EVACUATION TRAFFIC ON I-5 AND NON-FREEWAY ROUTES



Source: Wilbur Smith Associates, 2006.

7.1.2 Special Institutions

Special institutions, such as schools, hospitals, retirement and assisted living facilities, are expected to require significantly more mobilization time than the general public. It could take as long as four hours to mobilize these populations. The analysis has demonstrated that in most cases, the time required to dissipate queued vehicles is longer than the mobilization time, so these special institutions would still evacuate with the general public, but likely at the tail end of the queues.

7.2 Evacuation Time Estimates for Protective Action Zone (PAZ) Structure

7.2.1 Tabular Analysis of PAZ Evacuation Elements

Chapter 1 has already presented the time estimates from the analysis. The evacuation time summary Tables 1.4a and 1.4b are reproduced as 7.1a and 7.2a. Tables 7.1b and 7.2b represent relative percentage change from the baseline for each scenario.

Table 7.1a:
SUMMARY OF TOTAL ETE FOR ALL SCENARIOS TESTED USING PAZ STRUCTURE
(TOTAL HOURS TO EVACUATE EPZ)

	WEEKDAY	WEEKEND	NIGHT	ADVERSE WEATHER	WEEKDAY EARTHQUAKE
PAZ 1 & PAZ 2	3.0	3.3	1.5	4.0	11.0
PAZ 1 & PAZ 3	3.1	3.3	1.5	4.0	11.0
PAZ 1 & PAZ 4	7.3	6.8	6.3	8.3	14.3
PAZ 1 & PAZ 3 & PAZ 4	7.3	7.0	6.3	9.0	16.3
PAZ 1 & PAZ 4 & PAZ 5	9.5	9.2	8.2	10.3	18.0

Source: Wilbur Smith Associates, 2006

Table 7.1b:
PERCENT OF WEEKDAY TIME ESTIMATE
FOR ALL SCENARIOS TESTED USING PAZ STRUCTURE

	WEEKDAY	WEEKEND	NIGHT	ADVERSE WEATHER	WEEKDAY EARTHQUAKE
PAZ 1 & PAZ 2	---	110%	50%	133%	367%
PAZ 1 & PAZ 3	---	106%	48%	129%	355%
PAZ 1 & PAZ 4	---	93%	86%	114%	196%
PAZ 1 & PAZ 3 & PAZ 4	---	96%	86%	123%	223%
PAZ 1 & PAZ 4 & PAZ 5	---	97%	86%	108%	189%

Source: Wilbur Smith Associates, 2006

PAZs 1/2 and 1/3 have a higher beach population on weekends reflected in the increased weekend relative ETE percentage. The increase in workers on weekdays offset the weekend recreational population. The weekend ETE percentage of the base is therefore less than 1.

As expected, adverse weather slows the evacuation. The relative impact is not related to population. It is related to available evacuation routes and distance required to leave the EPZ. The network is very restricted until PAZ 5. PAZs 1, 3 and 4 are restricted to I-5 and PCH for most of the distance in a northern evacuation. The distance and limited opportunities compound to make the evacuation of these areas more inefficient relative to the scenario's base.

This is even more evident in an earthquake scenario where the actual time it takes to evacuate a relatively small population is longer than the evacuation of a population 22 times that size on a summer weekday. PAZ combination 1/4/5 evacuates 123,812 vehicles, while the PAZ combination 1/2 evacuates 5605 vehicles. It takes these 5605 vehicles 11 hours to evacuate, while under normal circumstances the 123,812 vehicles in 1/4/5 evacuate in 9.5 hours.

Under earthquake conditions the length and number of facilities impacted compound evacuation difficulty for those PAZs located the furthest from the EPZ boundary. This results in the most significant increase in EPZ evacuation percentage relative to the base. An earthquake is essentially multiple incidents compounding the distance and limited opportunities to evacuate the population closer to SONGS.

Tables 7.2a and 7.2b continue this examination for the sensitivity tests.

**Table 7.2a:
SUMMARY OF SENSITIVITY TESTS OF TOTAL ETE ON DAYTIME SUMMER WEEKDAY
CONDITIONS USING PAZ STRUCTURE (TOTAL HOURS TO EVACUATE EPZ)**

	CONTRA- FLOW ON I-5	INCIDENT ON I-5	DELAYED MOBILIZATION	20% SHADOW DEMAND	80% POPULATION UNDER EARTHQUAKE CONDITIONS	AGGRESSIVE ACCESS CONTROL ON I-5
PAZ 1 & PAZ 2	2.3	5.1	3.1	3.3	5.0	3.0
PAZ 1 & PAZ 3	3.0	5.1	3.1	3.3	5.1	3.0
PAZ 1 & PAZ 4	6.4	8.0	7.4	7.3	10.2	6.5
PAZ 1 & PAZ 3 & PAZ 4	6.5	8.2	7.5	9.0	10.2	6.5
PAZ 1 & PAZ 4 & PAZ 5	7.5	11.0	8.5	11.2	12.3	8.2

Source: Wilbur Smith Associates, 2006

**Table 7.2b:
PERCENT OF WEEKDAY TIME ESTIMATE
FOR ALL SENSITIVITY TESTS USING PAZ STRUCTURE**

	CONTRA- FLOW ON I-5	INCIDENT ON I-5	DELAYED MOBILIZATION	20% SHADOW DEMAND	80% POPULATION UNDER EARTHQUAKE CONDITIONS	AGGRESSIVE ACCESS CONTROL ON I-5
PAZ 1 & PAZ 2	77%	170%	103%	110%	167%	100%
PAZ 1 & PAZ 3	97%	165%	100%	106%	165%	97%
PAZ 1 & PAZ 4	88%	110%	101%	100%	140%	89%
PAZ 1 & PAZ 3 & PAZ 4	89%	112%	103%	123%	140%	89%
PAZ 1 & PAZ 4 & PAZ 5	79%	116%	89%	118%	129%	86%

Source: Wilbur Smith Associates, 2006

Contra-flow and aggressive access control on I-5 are two positive scenarios. Aggressive access control has no influence on PAZ 1. Since PAZ 1 will enter the network at the start, there isn't any need for access control. The ramp queue will be the access control.

Contra-flow and access control help the most with PAZ combination 1/4/5. Increasing the efficiency of the main evacuation route has its greatest impact on the scenario with the most population. Increasing the efficiency of I-5 makes the less efficient alternative evacuation opportunities less inviting.

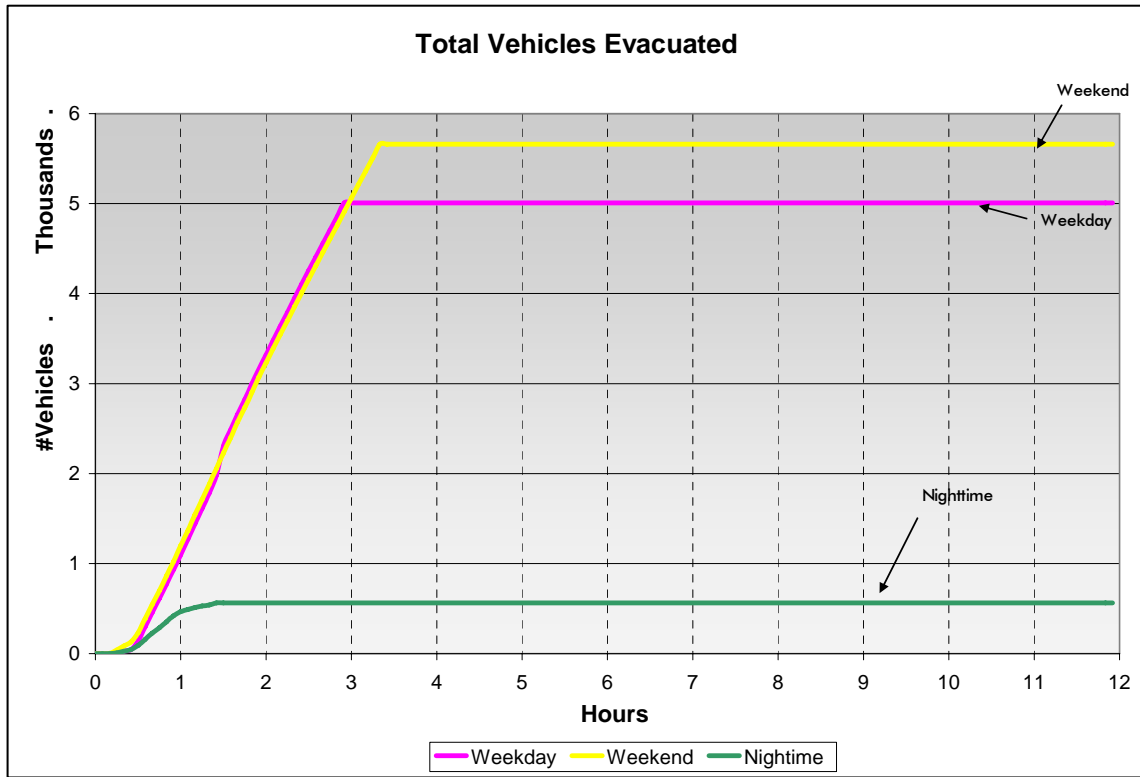
An incident on I-5 has the greatest relative impact on the PAZ combinations with the most reliance and greatest distance on I-5. The evacuation time on these PAZ combinations is also relatively small so an equivalent delay will have a greater relative impact.

Delayed mobilization was discussed in detail above in the graphical analysis of section 7.1.1. The positive impact of delayed mobilization on PAZ combination 1/4/5 further demonstrates that maintaining efficiency in the network has a positive influence on evacuation.

7.2.2 Graphical Analysis of PAZ Evacuation Elements

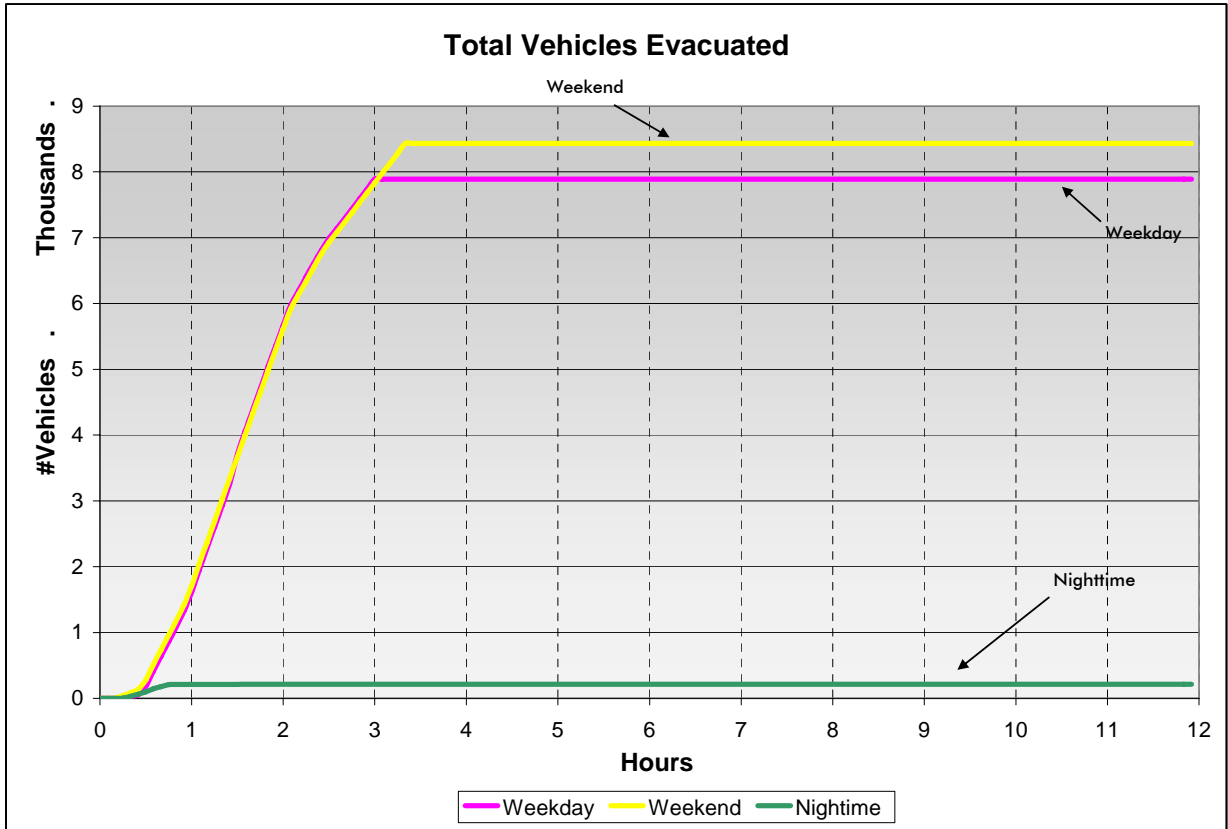
Figures 7.5 through 7.9 show how many vehicles have moved beyond the EPZ boundary at each hour for the five combinations of PAZ evacuations.

Figure 7.5:
TOTAL VEHICLES EVACUATED USING PAZ STRUCTURE PAZ 1 AND 2 EVACUATION



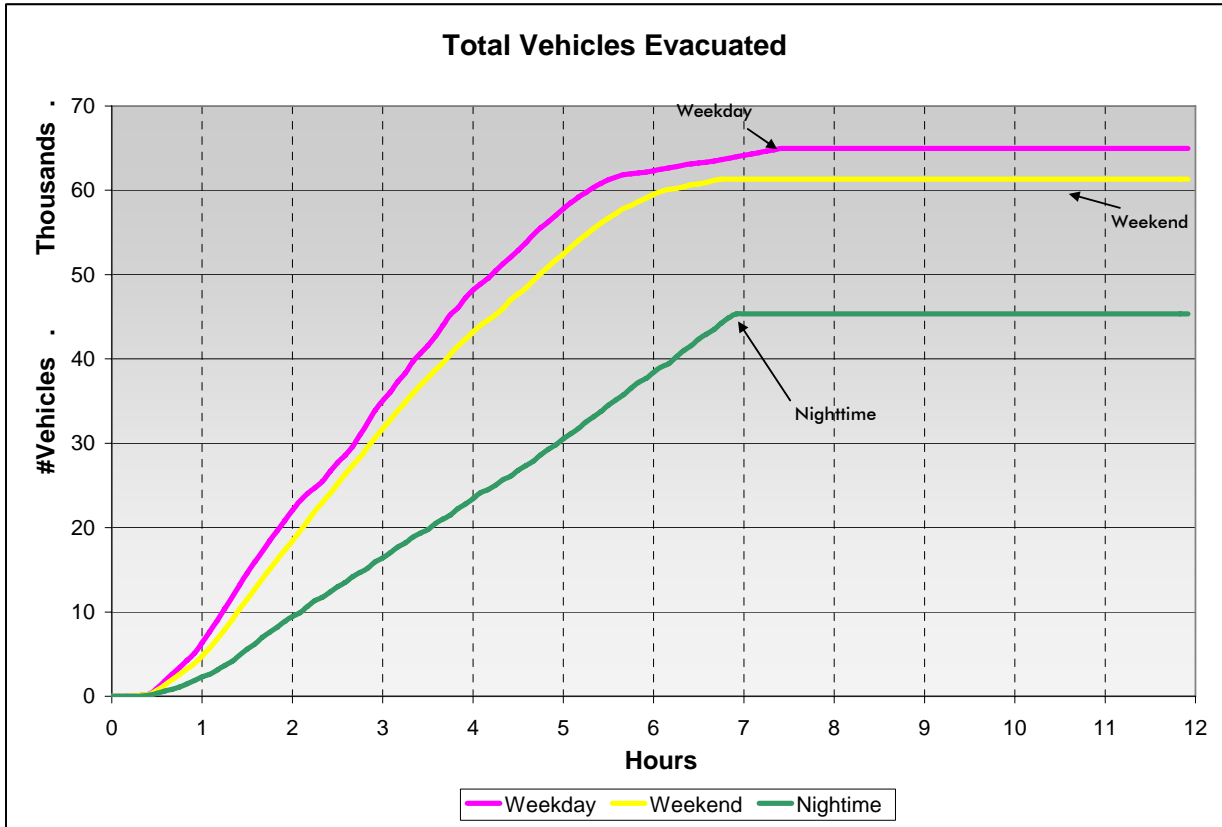
Source: Wilbur Smith Associates, 2006

Figure 7.6:
TOTAL VEHICLES EVACUATED USING PAZ STRUCTURE PAZ 1 AND 3 EVACUATION



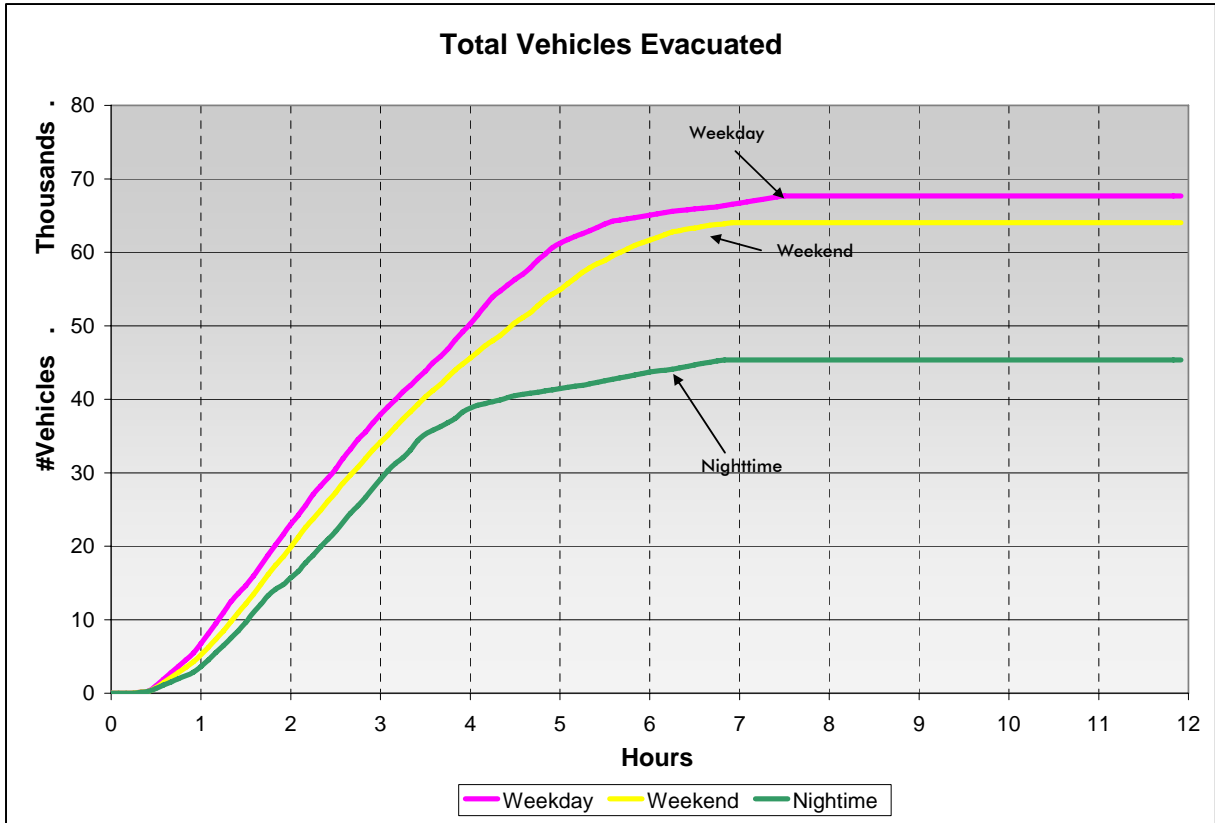
Source: Wilbur Smith Associates, 2006

Figure 7.7:
TOTAL VEHICLES EVACUATED USING PAZ STRUCTURE PAZ 1 AND 4 EVACUATION



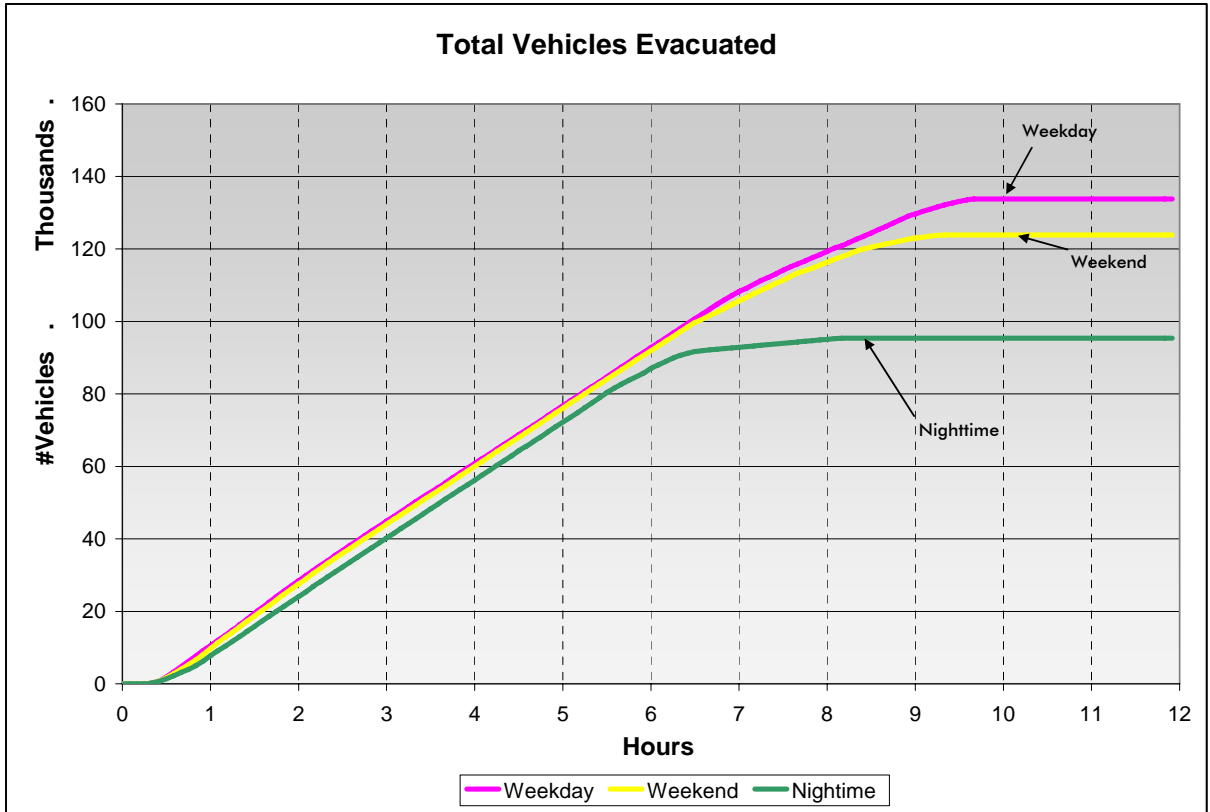
Source: Wilbur Smith Associates, 2006

Figure 7.8:
TOTAL VEHICLES EVACUATED USING PAZ STRUCTURE PAZ 1, 3 AND 4 EVACUATION



Source: Wilbur Smith Associates, 2006

Figure 7.9:
TOTAL VEHICLES EVACUATED USING PAZ STRUCTURE PAZ 1, 4 AND 5 EVACUATION



Source: Wilbur Smith Associates, 2006

7.3 Range of Certainty

There are both positive and negative factors that could influence the ETE.

1. **Shadow Demand:** Shadow demand as high as 20% could add as much as 1.7 hours to the total evacuation even if shadow demand traffic is prohibited from I-5. The effect of increased shadow demand is minimal for the PAZ evacuation combinations of lower populations.
2. **Incidents:** An incident on I-5 could add more than two hours to the total ETE.
3. **Adverse Weather:** Adverse weather could add 1.7 hours, and would increase the likelihood of an incident.
4. **Inefficiency:** No significant management of I-5 is a possibility if the existing plans for I-5 traffic management are not adhered to. Likewise, simple inefficiency or miscommunication in the execution of any critical elements could add time to the ETE.
5. **Combination of Events:** It is conceivable that all these time-adding events could coincide to produce a "worst case" scenario adding perhaps an additional 4-6 hours to the ETE. The earthquake condition is an extreme example of event combination and it increases the ETE by up to 9 hours.
6. **Total Population/Vehicles:** We have assumed a relatively low vehicle usage of 1.3 vehicles per household. If this assumption proved to be too low or high, the ETE would follow suite.
7. **Rate of Escalation:** There are varying levels of emergency classification. Should an incident progress gradually, certain population may be ordered to evacuate earlier than general evacuation. Individuals may also voluntarily evacuate under such situations. Should a general emergency evacuation eventually be declared, less people would be left to evacuate. This would improve the ETES.
8. **Contra-Flow:** Local adoption of the use of contra-flow lanes and a more aggressive approach to managing I-5 improves the ETE by as much as 2.0 hours.
9. **Daytime Population:** Modeling conducted here for a weekday assumes that the majority of those who work north of the EPZ would desire to and be successful at re-entering to assist their families. The number of evacuating vehicles for the weekday condition is slightly over-estimated if fewer individuals return from work locations outside the EPZ.
10. **Evacuation Sooner Than 2011:** If a full-scale evacuation occurs before 2011, fewer people will reside in the area than are estimated in this analysis lowering the ETE.
11. **SR-241 Extension:** It is possible that the Foothill-South Transportation Corridor, or SR-

241, could be completed in 2010 or 2011. This would provide significant additional capacity to the area and would significantly improve expected ETEs.

Based on the items identified above, and the fact that any live event would unfold somewhat differently than expected, WSA is confident that an ETE following one of the scenarios presented here would likely be within plus or minus two hours.

FINAL REPORT

San Onofre Nuclear Generating Station (SONGS) Evacuation Time Evaluation (ETE)

APPENDIX A

Appendices

Appendix A

AGENCY CONTACTED	INFORMATION PROVIDED	APPROX. DATE
Cal State Fullerton Center for Demographic Research	Demographic Information	10-7-05
City of San Clemente	City Emergency Plan	8-31-05
City of San Juan Capistrano	City Emergency Plan & Private Schools Emergency Plan	9-14-05
City of Dana Point	City Emergency Plan	9-14-05
California Highway Patrol	CHP Emergency Plan	8-31-05
Caltrans District 12	Traffic Data, Roadway Characteristics, and Infrastructure Plans	8-31-05
Southern California Edison SONGS	Schools and Daycare Info. & SONGS Worker Info.	8-18-05 12-21-05
Orange County Sheriffs Department	County Emergency Plan, Private School Travel Survey	9-14-05
United States Marine Corps, Camp Pendleton	Camp Pendleton Population & Emergency Plan	11-7-05
SCAG	Model Information	9-22-05
SANDAG	Model Information	9-22-05
Capistrano Unified School District	School Populations, Emergency Plan, & Bus System Capacity	9-22-05
Orange County Transportation Authority	Bus Capacity	12-13-05
State Parks	Beach Capacity	9-22-05
Dana Point Visitors Bureau	Orange County Visitors Information	9-30-05

FINAL REPORT

San Onofre Nuclear Generating Station (SONGS)

Evacuation Time Evaluation (ETE)

APPENDIX B: PUBLIC AND PRIVATE SCHOOL ENROLLMENT

Appendix B: PUBLIC AND PRIVATE SCHOOL ENROLLMENT

Public Schools	Address	SUB-ZONE	Teachers	Students
Palisades Elementary School	26462 Via Sacramento, Capistrano Beach, CA 92624	5	28	600
Dana Hills High School	33333 Golden Lantern, Dana Point, CA 92629	10	160	2900
R.H. Dana Elementary School	24242 La Cresta Drive, Dana Point, CA 92629	10	17	397
R.H. Dana Exceptional Needs Facility	24242 La Cresta Drive, Dana Point, CA 92629	10	15	120
Adult Education	31431 El Camino Real, San Juan Capistrano, CA 92675	7	100	1000
Junipero Serra High School & Fresh Start	31422 Camino Capistrano, San Juan Capistrano, CA 92675	7	18	200
San Juan Elementary	31642 El Camino Real, San Juan Capistrano, CA 92675	7	29	630
Harold Ambuehl Elementary School	28001 San Juan Creek Road, San Juan Capistrano, CA 92675	6	30	620
Marco Forster Middle School	25601 Camino del Avion, San Juan Capistrano, CA 92675	9	85	1600
Del Obispo Elementary School	25591 Camino del Avion, San Juan Capistrano, CA 92675	9	21	500
Kinoshita Elementary School	2 Via Positiva, San Juan Capistrano, CA 92675	6	35	720
Marblehead Elementary School	2410 Via Turqueza, San Clemente, CA 92673	4	26	600
Vista Del Mar Elementary and Middle School	1130 Avenida Talega, San Clemente, CA 92673	15	64	1300
Clarence Lobo Elementary School	200 Avenida Vista Montana, San Clemente, CA 92672	2	26	500
San Clemente High School & Upper Campus	700 Avenida Pico, San Clemente, CA 92673	2	120	3200
Shorecliffs Middle School	240 Via Socorro, San Clemente, CA 92672	4	49	1300
Truman Benedict Elementary School	1251 Sarmientoso, San Clemente, CA 92673	4	31	762
Concordia Elementary School	3120 Avenida del Presidente, San Clemente, CA 92672	1	30	660
Bernice Ayer Middle School	1271 Sarmientoso, San Clemente, CA 92673	4	31	730
Las Palmas Elementary School	1101 Calle Puente, San Clemente, CA 92672	3	30	660
Private Schools				
Capistrano Beach Calvary School	25975 Domingo Avenue, Capistrano Beach, CA 92624	5	40	200
St. Edward's Parish School	33866 Calle La Primavera, Dana Point, CA 92629	9	56	550
Saint Michael's Academy	107 West Marquita, San Clemente, CA 92672	3	11	145
Monarch Bay Montessori Academy	32920 Pacific Coast Highway, Dana Point, CA 92629	10	4	140
Mission Parish School	31641 El Camino Real, San Juan Capistrano, CA 92675	7	25	350
Our Lady of Fatima Elementary School	105 N. La Esperanza, San Clemente, CA 92672	2	14	280
JSerra High School	26351 Junipero Serra Road, San Juan Capistrano, CA 92672	7	30	300
Capistrano Valley Christian School	32032 Del Obispo St., San Juan Capistrano, CA 92675	5	90	700
St. Margaret's Episcopal School	31641 La Novia Ave., San Juan Capistrano, CA 92675	7	210	1230
StoneyBrooke Christian School	26300 Via Escolar, San Juan Capistrano, CA 92692	8	41	660
Saddleback Valley Christian Elementary School	26333 Oso Road, San Juan Capistrano, CA 92675	7	13	350
Saddleback Valley Christian Jr High/High School	26333 Oso Road, San Juan Capistrano, CA 92675	7	25	150
Our Savior's Lutheran Elementary and Preschool	200 E. Avenida San Pablo, San Clemente, CA 92672	2	13	238
Pre-schools and Daycares				
Saddleback Valley Christian Preschool	26333 Oso Road, San Juan Capistrano, CA 92675	7	5	90
Nobis Children's Center	26153 Victoria Blvd., Capistrano Beach, CA 92624	5	10	50
Wee Can Preschool	34240 Camino Capistrano, Capistrano Beach, CA 92624	5	7	60
Palisades United Methodist Preschool & Kinder.	27002 Camino de Estrella, Capistrano Beach, CA 92624	4	15	110

St. Edward's Parish Preschool	33926 Calle La Primavera, Dana Point, CA 92629	9	14	78
South Shores Christian Preschool	32712 Crown Valley Parkway, Dana Point, CA 92629	10	14	116
Gloria Dei Lutheran Preschool	33501 Stonehill Drive, Dana Point, CA 92629	9	13	75
Happy Campers Preschool	33501 Del Obispo, Dana Point, CA 92629	9	4	20
Dana Preschool	34052 Street of the Violet Lantern, Dana Point, CA 92629	10	4	30
Broderick Montessori School	24292 Del Prado Ave, Dana Point, CA 92629	10	4	60
Appletree Day Care	33061 Elisa Drive, Dana Point, CA 92629	10	3	15
KinderCare Learning Center	1141 Puerta Del Sol, San Clemente, CA 92673	15	17	80
Early Explorations	2015 Calle Frontera, San Clemente, CA 92673	4	25	200
San Clemente Presbyterian Preschool	119 Avenida De La Estrella, San Clemente, CA 92672	3	14	166
La Cristianita Preschool	35522 Camino Capistrano, San Clemente, CA 92672	4	9	125
Serra Preschool	1005 Calle Puente, San Clemente, CA 92672	3	6	25
St. Michael's Infant/Toddler Center	702 N. Ave De La Estrella, San Clemente, CA 92672	3	10	40
Saint Michael's Preschool	107 West Marquita, San Clemente, CA 92672	3	8	50
Stepping Stone Preschool	130 Avenida Granada, San Clemente, CA 92672	3	3	18
Boys & Girls Club of San Clemente	1304 Calle Valle, San Clemente, CA 92672	3	15	600
Garden Gate Childcare	207 Ave. San Pablo, San Clemente, CA 92672	2	1	6
Chris's Corner	213 Calle Tinaja, San Clementem, CA 92672	4	2	18
San Clemente Preschool	163 Avenida Victoria, San Clemente, CA 92672	1	10	60
San Clemente Montessori Preschool	189 Avenida La Questa, San Clemente, CA 92672	1	5	48
Evelyn Lobo Villegas Head Start	32204 Del Obispo, San Juan Capistrano, CA 92675	5	6	68
Childbridge Preschool	31113 Rancho Viejo Rd., San Juan Capistrano, CA 92675	7	13	130
Community Presbyterian Preschool	32202 Del Obispo, San Juan Capistrano, CA 92675	5	14	200
Capistrano Valley Head Start	31485 El Camino Real, San Juan Capistrano, CA 92675	7	9	88
Stonebridge Day School	32091 Alipaz, San Juan Capistrano, CA 92675	5	3	21
San Juan Preschool	26891 Spring Street, San Juan Capistrano, CA 92675	7	2	
San Juan Montessori Preschool	32143 Alipaz, San Juan Capistrano, CA 92675	5	5	50
Rancho Capistrano Schools	29251 Camino Capistrano, San Juan Capistrano, CA 92675	11	20	160
Aunty Jody's Childcare	27701 Paseo Esteban, San Juan Capistrano, CA 92675	7	3	12
Family Day Care	33061 Elisa Drive, Dana Point, CA 92629	10	3	7
Family Day Care	207 San Pablo, San Clemente, CA 92672	2	1	6
Capistrano Valley Christian Preschool	32032 Del Obispo, San Juan Capistrano, CA 92675	5	4	28
Total Enrollment			1,818	27,202

Source: Southern California Edison, www.dexonline.com, 2006, Interjurisdictional Planning Committee: Model Nuclear Power Plant Emergency Plan for Private Schools and Childcare Facilities, August 2004

FINAL REPORT

San Onofre Nuclear Generating Station (SONGS)

Evacuation Time Evaluation (ETE)

APPENDIX C: RETIREMENT HOMES AND HOSPITALS

Appendix C: RETIREMENT HOMES AND HOSPITALS

RETIREMENT HOMES AND HOSPITALS	ADDRESS	SUB-ZONE	RESIDENTS/PATIENTS		
			AMBULATORY	NON-AMBULATORY	TOTAL
Dana Point					
Bay Side Terrace	23031 Java Sea Dr.	10	3	1	4
Palmera Terrace	24622 Jeremiah Dr.	10	6	0	6
The Fountains at Sea Bluffs	25411 Sea Bluffs Dr.	9	98	2	100
Seaside Terrace	32591 Seven Seas Dr.	10	3	3	6
San Clemente					
Pacific Breeze Home	113 Avenida Del Reposo	3	0	6	6
Wycliffe Casa De Seniors	105 Avenida Presidio	2	75	2	77
Saddleback Memorial Medical Center	654 Camino De Los Mares	4	11	8	19
San Clemente Villas by the Sea	660 Camino De Los Mares	4	31	123	154
Accent on Seniors	273 Via Ballena	4	4	2	6
San Juan Capistrano					
Capistrano Beach Extended Care	35410 Del Rey	4	15	62	77
Mirabel by the Sea	26961 Calle Granada	5	0	6	6
Aegis of Dana Point	26922 Camino De Estrella	4	50	20	70
Aegis of Laguna Niguel	32170 Niguel Rd.	10	54	20	74
ARV Assisted Living	32200 Del Obispo St.	5	75	20	95
Atria Chateau San Juan	32353 San Juan Creek Rd.	6	105	0	105
Brighton Gardens	31741 Rancho Viejo Rd.	7	15	10	25
Casa de Amma	27231 Calle Arroyo	7	17	0	17
Silverado Senior Living	30311 Camino Capistrano	7	57	20	77
Villa Paloma Senior Apartment	27221 Paseco Espada	9	97	3	100
Seasons Senior Apartments	31641 Rancho Viejo Rd.	7	102	1	103
Tessie's Place	27642 Rosedale Dr.	8	4	0	4
Total Residents/Patients			822	309	1,131

Source: www.dexonline.com, 2006

FINAL REPORT

San Onofre Nuclear Generating Station (SONGS) Evacuation Time Evaluation (ETE)

APPENDIX D

Appendix D

City of San Clemente

- SC-1. Location: Cristianitos Road at I-5 Interchange.
Control: Direct traffic from Cristianitos Road onto northbound I-5 on-ramp.
- SC-2. Location: Avenida Del Presidente and Avenida Calafia- Southbound I-5 Ramps.
Control: Direct traffic northbound on Avenida del Presidente.
- SC-3. Location: South El Camino Real at Northbound I-5 Ramps.
Control: Direct traffic from northbound Avenida del Presidente onto Avenida Mendocino overpass and then northbound El Camino Real. Direct traffic from south El Camino Real onto northbound I-5 on-ramp.
- SC-4. Location: South El Camino Real at I-5 Interchange (S. El Camino Real underpass).
Control: Direct traffic from El Camino Real onto northbound I-5 on ramp.
- SC-5. Location: South El Camino Real and Avenida Presidio.
Control: Direct traffic from El Camino Real onto eastbound Avenida Presidio (towards I-5 interchange northbound on-ramp).
- SC-6. Location: Avenida Presidio at I-5 Interchange.
Control: Direct traffic from Avenida Presidio onto northbound I-5 on ramp.
- SC-7. Location: Avenida Palizada at I-5 Interchange.
Control: Direct traffic from Avenida Palizada and Avenida Caballeros onto northbound I-5 on-ramp.
- SC-8. Location: Avenida Pico at I-5 interchange.
Control: Direct traffic from Avenida Pico onto northbound I-5 on-ramp.
- SC-9. Location: North El Camino Real and Avenida Pico.
Control: Direct traffic to the north on El Camino Real.
- SC-10. Location: Camino De Estrella at I-5 interchange.
Control: Direct traffic from Camino De Estrella onto northbound I-5 on-ramps. Since the volume of evacuation traffic is projected to be greater from the east than the west, one of the westbound lanes could be directed onto the south-side

northbound I-5 on-ramp until eastside evacuation traffic has dissipated.

SC-11. Location: Pacific Coast Highway (North El Camino Real) and Camino Capistrano.
Control: Direct traffic to the north on Pacific Coast Highway.

SC-12 Location: Vista Hermosa at the I-5 Interchange and the Vista Hermosa Interchange and Calle Frontera
Control: Direct traffic from Frontera onto the northbound I-5 onramp to the freeway; if they cross over the I-5 from the southbound lanes of the freeway, just redirect them right back on to the northbound side of the I-5.

City of San Juan Capistrano

- SJC-1. Location: Via California and Camino Los Ramblas.
Control: Direct traffic west on Camino Las Ramblas (towards I-5 on-ramp).
- SJC-2. Location: U.S.1-Camino Las Ramblas at I-5 Interchange.
Control: Direct traffic from U.S. 1- Camino Las Ramblas onto northbound I-5 on ramps. Since the vast majority of evacuation traffic would approach from the east, traffic using one of the westbound lanes could be directed to the south-side northbound I-5 on-ramp (loop ramp).
- SJC-3. Location: Alipaz Street and Del Obispo Street.
Control: Direct traffic onto eastbound Del Obispo Street.
- SJC-4. Location: Camino Capistrano and Del Obispo Street.
Control: Direct eastbound Del Obispo Street traffic in left lane onto northbound Camino Capistrano. Direct eastbound Del Obispo Street traffic in right lane to continue east on Del Obispo Street (towards I-5 on-ramp at Ortega Highway interchange. Direct traffic from northbound Camino Capistrano onto eastbound Del Obispo Street.
- SJC-5. Location: Camino Capistrano and I-5 Southbound Ramps (South of San Juan Creek Road).
Control: Direct traffic northbound on Camino Capistrano.
- SJC-6. Location: San Juan Creek Road and Valle Road.
Control: Direct traffic from San Juan Creek Road onto southbound Valley Road (towards the northbound I-5 on-ramp at La Novia Avenue).
- SJC-7. Location: La Novia Avenue and San Juan Creek Road.
Control: Direct traffic to the north on La Novia Avenue (towards Ortega Highway).
- SJC-8. Location: La Novia Avenue at Ortega Highway
Control: As conditions permit, direct from La Novia to eastbound out Ortega to Antonio Parkway, or direct westbound on Ortega to Rancho Viejo Road.
- SJC-9. Location: Ortega Highway and Rancho Viejo Road.
Control: Direct traffic to the north on Rancho Viejo Road.
- SJC-10. Location: Ortega Highway at I-5 Interchange.

- Control: Direct traffic from eastbound Ortega Highway onto the northbound I-5 on-ramp.
- SJC-11. Location: Camino Capistrano and Junipero Serra Road.
Control: Direct traffic to continue northbound on Camino Capistrano. As conditions at the Junipero Serra Road/northbound I-5 on ramp permit, divert a portion of the northbound on Camino Capistrano Traffic to the freeway interchange on-ramp.
- SJC-12. Location: Junipero Serra Road at I-5 Interchange.
Control: Direct traffic from Junipero Serra Road onto the northbound I-5 on-ramp.
- SJC-13. Location: Rancho Viejo Road and Junipero Serra Road.
Control: Direct the majority of northbound traffic on Rancho Viejo Road to continue north on Rancho Viejo Road. As conditions at the Junipero Serra Road/northbound I-5 on-ramp permit, divert a portion of the northbound Rancho Viejo Road traffic to the freeway interchange on-ramp

City of Dana Point

- DP-1. Location: Pacific Coast Highway and Doheny Park Road
Control: Direct traffic north on Doheny Park Road (towards Camino Capistrano).
- DP-2. Location: Pacific Coast Highway and Del Obispo Street
Control: Direct traffic onto northwest-bound Pacific Coast Highway.
- DP-3. Location: Pacific Coast Highway and Selva Road
Control: Direct traffic northbound on Pacific Coast Highway.
- DP-4. Location: Street of the Golden Lantern and Camino Del Avion
Control: Direct traffic northbound on Street of the Golden Lantern.
- DP-5. Location: Del Obispo Street and Stonehill Drive
Control: Direct traffic northbound on Del Obispo Street.
- DP-6. Location: Del Prado at Golden Lantern
Control: Direct southbound Del Prado northbound on Golden Lantern.
- DP-7. Location: PCH and Golden Lantern
Control: Route Southbound Golden Lantern traffic north on PCH.
Do not allow traffic to proceed to southbound Del Prado.
- DP-8. Location: PCH and Niguel Road
Control: Direct all traffic northbound.
- DP-9. Location: PCH and Crown Valley Parkway
Control: Direct all traffic northbound.
- DP-10. Location: Niguel Road at Camino Del Avion
Control: Prevent traffic from traveling south on Niguel Road.
- DP-11. Location: Pacific Coast Highway at Palisades Drive.
Control: Block Palisades Drive on the north of Coast Highway to prevent traffic from interfering with neighborhood evacuations.
- DP-12. Location: Palisades Drive at Doheny Place
Control: Block Palisades Drive at Doheny Place to prevent neighborhood traffic from

bottlenecking at Coast Highway.

- DP-13 Location: Las Ramblas at Interstate 5
 Control: Block the southbound on-ramp to prevent traffic from traveling southbound on Interstate 5.
- DP-14 Location: Victoria Road at Camino Capistrano
 Control: Block Victoria Road so as to keep Capistrano Beach residential traffic flowing north on Camino Capistrano.
- DP-15 Location: Doheny Park Road at Pacific Coast Highway
 Control: Block on-ramp to southbound Pacific Coast Highway (Las Ramblas). Route Doheny Park Road traffic toward Camino Capistrano or to northbound Pacific Coast Highway.
- DP-16 Location: Pacific Coast Highway at San Juan Creek. Block southbound Pacific Coast Highway at the San Juan Creek cut-off to prevent southbound traffic from bottlenecking at Coast Highway.

FINAL REPORT

San Onofre Nuclear Generating Station (SONGS)

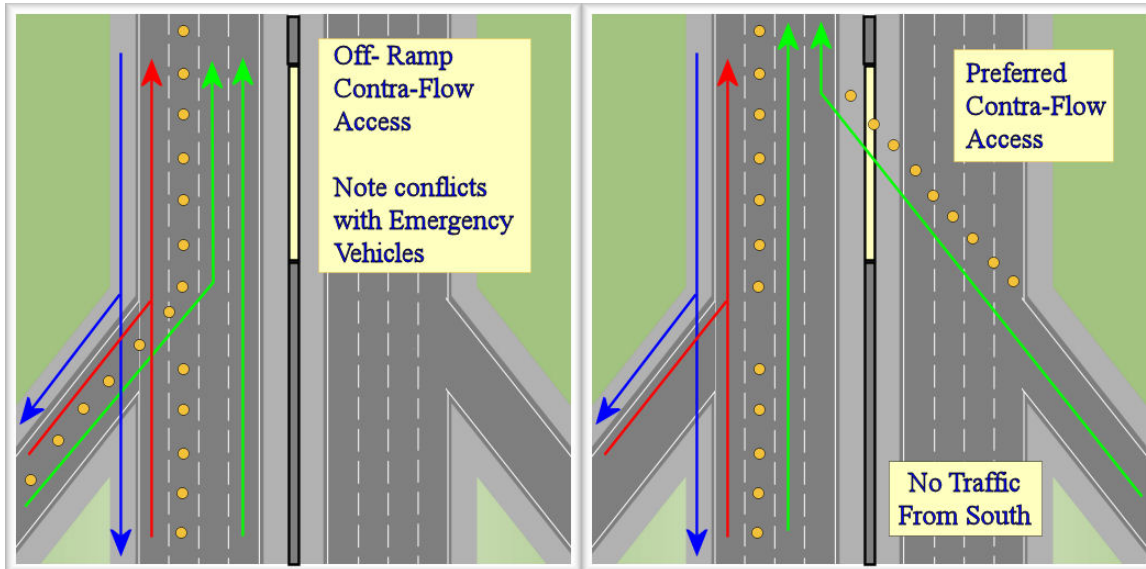
Evacuation Time Evaluation (ETE)

APPENDIX E: CONTRA-FLOW IMPLEMENTATION

Appendix E: CONTRA-FLOW IMPLEMENTATION

Two methods of accessing and managing contra-flow lanes are presented in the figure below along with practical steps that should be taken to help contra-flow succeed safely:

POTENTIAL CONTRA-FLOW ACCESS METHODS



The image on the left shows a means of accessing the lanes by converting an off-ramp into an on ramp. One mainline lane is consumed by cones to create separation from emergency vehicles which would be moving both directions on the shoulder and outer-most lane (shown in red and blue). Note that the green traffic stream conflicts with emergency vehicle paths. If there are large gaps between emergency vehicles, this approach can work well if officers halt the flow of traffic while emergency vehicles pass.

Contra-flow could be implemented on both I-5 and SR-73 up to the point at which southbound traffic has been rerouted. A mirror arrangement would need to be made at ramps near the barricade point to allow contra-flow vehicles to exit down on-ramps and safely transition to cross-streets.

The diagram on the right removes conflicts, and as such is a more ideal way of accessing contra-flow lanes. The approach in the image would have no traffic on the mainline from the south if it is applied at the first several interchanges nearest to SONGS. Cones would channel all traffic across the mainline through a removable barrier into the lanes. Traffic from three of the southernmost interchanges could be routed into contra-flow lanes without overloading the lanes.

Exiting the lanes outside the EPZ should be done by going down an on-ramp rather than trying to re-enter the regular northbound lanes through removable barriers. This is because outside the EPZ I-5 northbound will be running full, and trying to bring two contra-flow lanes back into an already full freeway will cause a long bottleneck that will impede the evacuation. If three ramps are used to load the flow, at least three ramps should be used to disperse the flow also.

Though well separated from emergency vehicles, driving the reverse direction on a freeway may be awkward for many, so speeds in contra-flow lanes should be restricted.

FINAL REPORT

San Onofre Nuclear Generating Station (SONGS)

Evacuation Time Evaluation (ETE)

APPENDIX F: SUB-ZONE DESCRIPTIONS

Appendix F: SUB-ZONE DESCRIPTIONS

SUB-ZONE 1 - Sub-zone 1 includes all residential, commercial, and recreational (San Clemente State Beach) areas west of I-5, south of Victoria Avenue and north of the Orange County/San Diego County boundary.

SUB-ZONE 2 - Sub-zone 2 includes all residential, commercial, and recreational areas east of I-5, north of the Orange County/San Diego County line and south of Avenida Pico.

SUB-ZONE 3 - Sub-zone 3 includes all residential, commercial, and recreational areas west of I-5, north of Victoria Avenue and south of Avenida Pico.

SUB-ZONE 4 - Sub-zone 4 includes all residential, commercial, and recreational areas north of Avenida Pico, east of Pacific Coast Highway, and south of Camino Las Ramblas.

SUB-ZONE 5 - Sub-zone 5 includes portions of San Juan Capistrano, Capistrano Beach residential, commercial, and recreational areas of Dana Point which lie west of I-5 and north between Del Obispo and I-5 in the north.

SUB-ZONE 6 - Sub-zone 6 includes all residential, commercial, and recreational areas west of La Mancha Avenue, south of San Juan Creek, north of Las Ramblas and east of I-5.

SUB-ZONE 7 - Sub-zone 7 includes the residential, commercial, and recreational areas within San Juan Capistrano which lie north of San Juan Creek, west of I-5, east of Trabuco Creek and also includes area east of I-5 to Sundance Drive.

SUB-ZONE 8 - Sub-zone 8 includes the residential, commercial, and recreational areas within San Juan Capistrano which lie north of SR-74 and east of I-5.

SUB-ZONE 9 - Sub-zone 9 includes the residential, commercial, and recreational areas of San Juan Capistrano and Dana Point which lie west of Trabuco Creek, north of Del Obispo, ½ mile east of Golden Lantern, and south of San Juan Canyon. The boundary to the west aligns with the City boundary line.

SUB-ZONE 10 - Sub-zone 10 includes the residential, commercial, and recreational areas which lie ½ mile west of Del Obispo, south of Camino Del Avion and east of Salt Creek. Boundaries to the north and west align with Dana Point City boundaries.

SUB-ZONE 11 - Sub-zone 11 includes the residential, commercial, and recreational areas which lie north of Junipero Sierra, west of I-5, west of Golden Lantern, and south of Avery Parkway.

SUB-ZONE 12 - Sub-zone 12 includes the recreational areas which comprise San Onofre State Beach.

SUB-ZONE 13 - Sub-zone 13 includes all areas which comprise San Onofre Nuclear Generating Station (SONGS).

SUB-ZONE 14 - Sub-zone 14 includes all areas in Camp Pendleton Marine Corps Base that are within the 10-mile EPZ boundary.

SUB-ZONE 15 - Sub-zone 15 includes all areas which are North of Avenida Pico, South of SR-74, East of sub-zones 4 and 6, and West of County Line.

FINAL REPORT

San Onofre Nuclear Generating Station (SONGS) Evacuation Time Evaluation (ETE)

ACRONYMS

Acronyms

CHP - California Highway Patrol
CSUF - California State University, Fullerton
CUSD - Capistrano Unified School District
DYNASMART-P - a state-of-the-art dynamic route assignment model sponsored by the Federal Highway Administration and developed at the University of Maryland.
ETE - Evacuation Time Estimates
FSTC - Foothill-South Transportation Corridor
HCM 2000 - Highway Capacity Manual 2000
HOV - High Occupancy Vehicle
I - Interstate Highway
OCTA Orange County Transportation Authority
PAZ - Protective Action Zone
PCH - Pacific Coast Highway (California 1)
SCAG - Southern California Association of Governments
SONGS - San Onofre Nuclear Generating Station
SR - State Route (California Highway)
TAZ - Traffic Analysis Zones
vphpl - vehicles per hour per lane
WSA - Wilbur Smith Associates

Appendix 7

**Annual Assessment of the San Onofre Nuclear Generating Station Evacuation Time
Evaluation, dated August 23, 2010**

Memorandum for File
August 23, 2010

Subject

Annual Assessment of the San Onofre Nuclear Generating Station Evacuation Time Evaluation Background

Background

On June 12, 2007, Wilbur Smith Associates produced the San Onofre Nuclear Generating Station (SONGS) Evacuation Time Evaluation (ETE) for Southern California Edison. The purpose of this memorandum is to review current information to determine if the 2007 ETE accurately reflects conditions in the Emergency Planning Zone

References used

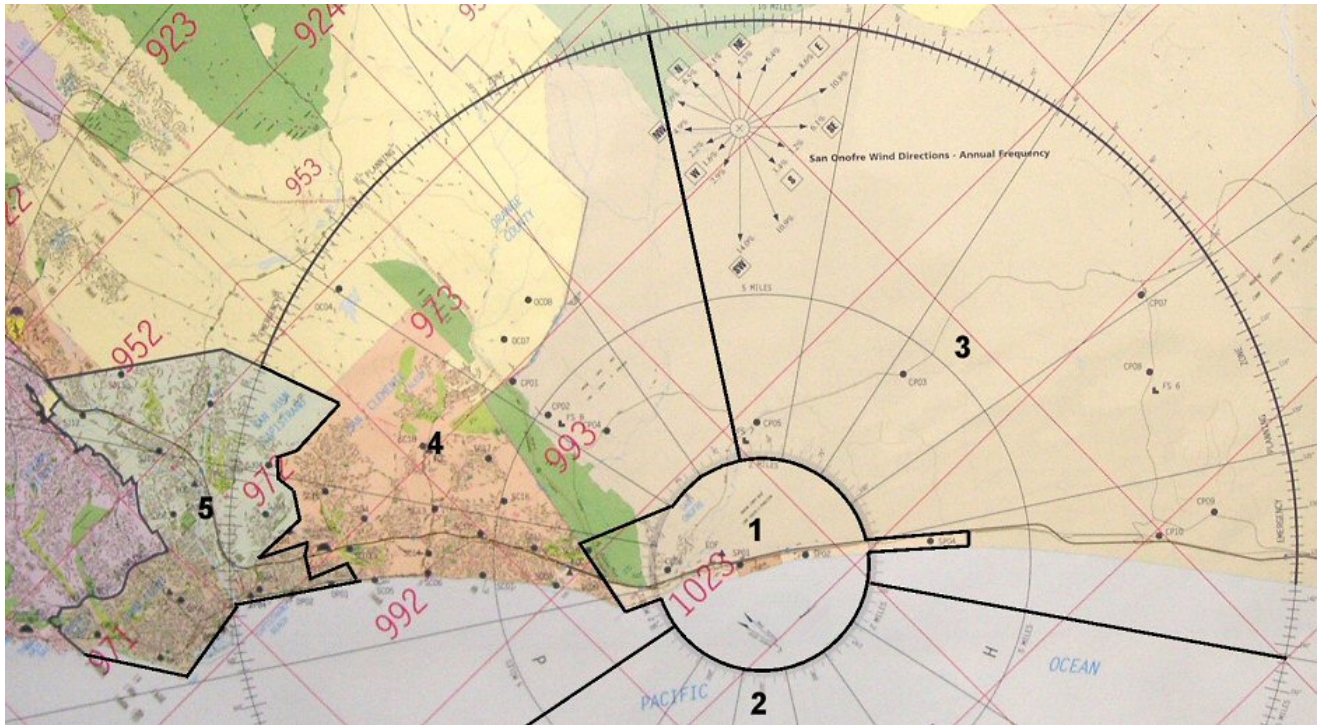
1. San Onofre Nuclear Generating Station (SONGS) Evacuation Time Evaluation, Prepared for Southern California Edison by Wilbur Smith Associates, dated June 12, 2007
2. NUREG/CR-6863 "Development of Evacuation Time Estimate Studies for Nuclear Power Plants"
3. Center for Demographic Research, Orange County City Demographics, August 2009, <http://www.fullerton.edu/cdr/city.asp>
4. Camp Pendleton Base Housing 2009
5. Southern California Edison - Nuclear Organization Chart, updated August 12, 2010
6. Orange County Sheriffs Long Term Care Population 2010
7. California Department of Transportation ITS Architecture and System Plan, Final Report, dated November 3, 2004

Basis for Annual Assessment

In accordance with Reference 2, the primary elements of the Evacuation Time Study, population and roadway capacity, should be periodically evaluated to assess whether there is an impact to the Evacuation Time Estimate. The evaluation of the population should address increases in the population, changes in age demographics, and changes to the special needs population. Evaluation of the roadways should address improvements, constraints, traffic flow and changes to the transient traffic flow through the Emergency Planning Zone. Additionally, an increase in the number of special needs facilities or special events, implementation of intelligent transportation systems, or jurisdictional changes in response authority, should also be considered

Population Demographics

The permanent population was assessed for San Clemente, Dana Point, San Juan Capistrano, and Camp Pendleton located in Protective Action Zones (PAZ) 1, 3, 4 and 5 (see map next page). As shown, there is no permanent population located in PAZ 2 which is the Pacific Ocean.



According to Reference 3, the population for San Clemente, Dana Point, and San Juan Capistrano is 142,268. According to Reference 4, Camp Pendleton reports their 2009 population as 23,380. Using this data, the total population for PAZ 1, 3, 4 and 5 is 165,648.

Table 1.1 of SONGS 2007 ETE projects the population in the same area as 184,947. Since estimates are within 10% of the projected estimates listed in Reference 3, the current SONGS ETE is considered to be a valid and conservative assessment of evacuation times.

Reference 1 lists the SONGS evacuating vehicles as 2514. The SONGS 2007 ETE assumes this population has 1.2 persons per vehicle. This works out to 3017 persons being evacuated. Reference 4 lists the SONGS population as 4,139. Using the same assumptions as above, the number of vehicles exiting SONGS during an evacuation is 3449.

The population remains within the bounds of the total population estimate contained in the 2007 SONGS ETE.

Special Needs Population

The current evacuation time study lists 21 facilities with 1131 long term care residents living in the Emergency Planning Zone. For 2010, a new assessment was conducted by Orange County Sheriffs Emergency Management and SONGS staff (Reference 5). That assessment identifies 50 facilities with a long term care population of 1313.

The population remains within the bounds of the total population estimate contained in the 2007 SONGS ETE.

Roadway Assessment

As noted in the Reference 1, Antonio Parkway is currently a four- and six- lane arterial paralleling east of I-5 between Oso Parkway and Ortega Highway (SR-74). The road has been planned to extend south along La Pata Avenue and connect Avenida Pico near Avenida Vista Hermosa, thus providing a bypass route to the communities living east of I-5. As of this date, this roadway is still under construction.

As noted in Reference 1, The planned Foothill-South Transportation Corridor (FSTC, or SR-241), if completed would run between I-5 at the Orange County/San Diego County line to Oso Parkway and provide additional roadway capacity for the EPZ. This roadway project is no longer being considered in its current form.

These projects are not anticipated to be completed before 2011. As such, the existing roadway capacity noted in Reference 1 is unchanged.

New Special Facilities

Based on feedback from city contacts, there have been no new special facilities such as entertainment venues, office complexes and hospitals constructed in the EPZ that would adversely affect the evacuation times noted in Reference 1.

New Special Events

Based on feedback from city contacts, there have been no new special events (concerts, holiday events and festivals) staged in the EPZ that would adversely affect the evacuation times noted in Reference 1.

Implementation of intelligent transportation systems

Reference 7 describes the implementation of California's intelligent transportation system. Although the SONGS 2007 ETE is silent on intelligent transportation systems, the California current system was in place at the time of this evacuation time study.

Jurisdictional Changes in Response Authority

Based on feedback from city contacts, there have been no jurisdictional changes in response authority that would adversely affect the EPZ evacuation times noted in Reference 1.

Summary

There has been no significant changes in the SONGS EPZ that would adversely affect the information contained in the San Onofre Nuclear Generating Station (SONGS) Evacuation Time Evaluation, Prepared for Southern California Edison by Wilbur Smith Associates, dated June 12, 2007.



Richard A. Garcia
Offsite Emergency Planning and External Affairs
San Onofre Nuclear Generating Station

Appendix 8

**Economic Impacts of the San Onofre Nuclear Generating Station on the California
Economy**

Economic Impacts of the San Onofre Nuclear Generating Station on the California Economy

Prepared by IHS Global Insight
U.S. Regional Services
800 Baldwin Tower
Eddystone, PA 19022

Impacts of the San Onofre Nuclear Generating Station

Introduction

The purpose of this analysis is to estimate the impacts of the San Onofre Nuclear Generating Station (SONGS) on the California economy. This will be assessed over a five-year period from 2010 through 2014 using expenditure estimates provided by the Southern California Edison Company (SCE). The information provided by SCE for use in the impact evaluation consists of workers directly employed by the plant, employee compensation, material purchases, fixed costs, and other service expenditures needed to maintain and operate the facility. The analysis here is limited to estimating the macroeconomic impact of operations and maintenance of SONGS on the California economy. The impact estimate will show how many jobs are directly created by operation and maintenance of the nuclear plant and the macroeconomic impact associated with indirect and induced effect on other economic sectors in California. The impact results will provide an estimate of output, value added, taxes and earnings generated in the California economy. Under the SCE proposal, annual spending would range between \$712 million and \$862 million during the five-year period. Our computations revealed that operation and maintenance of SONGS have a significant impact on the California economy creating about 9,400 jobs and more than \$3.3 billion in output per year over the period under study. Each dollar spent on the operation and maintenance of SONGS produces \$1.35 of labor income in the California economy, the bulk of which (77%) is employee compensation.

Study Area

To assess the economic impacts of SONGS, IHS Global Insight defined the entire state of California as the study area. While SONGS is located in San Diego County, the economic activity generated by the plant will have significant impacts across California. Most of the labor and about half of the direct material inputs needed for SONGS operations and maintenance will be obtained in-state. California is the nation's largest state economy, accounting for 13% of gross domestic product and 12% of the population; California's 2008 gross state product of \$1,846.75 billion would make it about the eighth largest economy in the world, similar in size to Russia. Due to its heavy mix of high-paying service sector jobs, median household income is over \$60,000 or about 17% higher than the national average.

IHS Global Insight used the IMPLAN input/output (I/O) model to estimate the total economic impacts of SONGS because its high level of sector detail enables the final demand changes to be assigned to the appropriate economic sectors. An I/O model such as IMPLAN provides for an accounting of the effects that initial direct spending in one industry has on other sectors through the inter-industry relationships in the economy. IMPLAN contains a set of multipliers that produce estimates of the total regional increases in output, value added, employment, and income produced by direct spending. IMPLAN uses national inter-industry purchasing relationships, adjusted for the structure of the regional economy through the use of regional purchase coefficients, to derive a set of sector-specific multipliers that are unique to the regional economy being analyzed. The multipliers are used to derive indirect and induced effects, which are looked at along with the direct effects to obtain the total change in regional economic activity. The sizes of the multipliers are determined by the technical co-efficients of the

production functions in the affected final demand sectors, and on the number and types of industries that supply inputs to the directly affected sectors. The construction and maintenance of energy facilities with a high output value per worker has a relatively large economic multiplier effect because of the value of inputs and the consumer spending supported by the high-wage employees.

The key assumption in this type of economic impact study is the selection of the sectors where the final demand changes will occur. In the case of SONGS employees, the sectors are detailed later in the report, which were distributed using an employee mix provided by SCE. The spending for materials was also assigned as appropriate to IMPLAN sectors in accordance with NAICS classification based on a SCE detailed material-spending breakdown. The employee compensation generated by short-term service hires was applied to the model to capture the activity supported by the disposable income.

Measurement of Economic Impacts

The maintenance and operation activity at SONGS affects a large number of sectors in the California economy. In particular, the activities create direct, indirect, and induced demand for labor leading to a high employment multiplier. When a direct increase in regional spending occurs, there are two types of economic impacts generated through backward linkages that are considered by models such as IMPLAN:

- Indirect effects are generated when a business that receives an initial, direct increase in spending purchases additional inputs from their suppliers located in the region.
- Induced effects are produced by the increase in local spending of disposable income by the newly hired workers, including both the new direct workers hired by firms receiving the initial changes in final demand (e.g., the new construction workers) and by new workers in the supplying industries (e.g., firms who sell concrete or steel to the contractor and who, in turn, have to hire new workers to meet the increased demand.)

In terms of the modeling purposes for this study, the direct purchases are based on SCE's proposed and planned expenditures. The indirect purchases are determined from within the model and are calculated utilizing a combination of IMPLAN's industry specific production functions and regional purchase coefficients¹ (RPC). Based on information provided by the SCE, it is estimated that 50% of the direct material purchases will be made within California with the rest made outside the study area. The material spending will ultimately require non-labor inputs such as steel, machinery, and equipment, some of which will be purchased within the study area, indirectly supporting employment in those activities. Additionally, the wages supported by the plant generate activity for a multitude of other service and goods-producing sectors. The backward linkages for a producing firm in a regional economy consist of the other industries from which it buys the inputs needed to make the goods and services it sells.

The higher the share of inputs that are bought from suppliers located in the regional economy, the more complete the backward linkages, which will result in larger indirect and induced effects and higher economic multipliers. When evaluating the regional economic impacts of a project, it is important that the changes in all the primary measures of regional economic activity be considered. In other words, changes in levels of output, value added, and income should be examined along with changes in employment.

¹ This is the ratio representing the portion of regional demands purchased from local producers.

We have summarized the payroll, wage, material, and other direct California expenditures estimated to be needed to maintain and operate the plant. Any expenditures or activity generated outside the state will not be included in this study. SCE expects to spend close to \$4 billion from 2010 to 2014, averaging about \$770 million per year. During the five-year period, general spending is highest in 2010, the first year of this plan. Jobs related to contractor work and services will vary depending on the maintenance and capital improvements scheduled each year.

Wage, Employment and Material Expenditures Estimates for SONGS
Expenditure by Asset Class (Million Dollars)

Expenditure	2010	2011	2012	2013	2014	5-Year Avg.
SCE Salaries & Payroll Adds	410.54	408.18	395.53	410.48	427.04	410.35
Contrator Wages & Salaries	164.77	83.51	56.98	53.61	77.65	87.31
Service Wages & Salaries	107.81	82.17	86.48	99.51	97.88	94.77
Other Services	70.64	53.84	56.66	65.20	64.13	62.09
Material Purchases	36.08	37.82	42.06	46.43	41.67	40.81
General/Admin Expenses	25.47	20.57	21.28	22.40	23.29	22.60
Fixed Costs	23.58	24.15	24.88	25.56	26.22	24.88
Property Taxes & Insurance	22.82	25.79	28.35	29.87	30.69	27.50
Total	861.71	736.02	712.23	753.06	788.58	770.32

Job Estimates (Full Time Equivalent)

Job Type	2010	2011	2012	2013	2014	5-Year Avg.
SCE Permanent Staffing	2,439	2,439	2,314	1,939	1,939	2,214
SCE Temporary Staffing	52	36	36	34	43	40
Contractor Staffing	1,020	506	336	308	434	521
Total	3,511	2,981	2,686	2,281	2,416	2,775

The material purchases were distributed through the IMPLAN model utilizing a detailed spending list provided by SCE. The material breakdown was then applied to each year and is relevant from the point of view of how these expenditures affect the economy of California. Investment in each material-providing industry is distributed over the entire economy due to backward linkages. Industries have different strengths in terms of creating their impact on the economy.

Since we are analyzing an existing facility, much of the impacts will be related to the jobs it supports. While material spending is significant, the bulk of SCE spending plan is allocated to wage and salary expenditures. Over the study period the plant will employ an average of 2,214 full-time workers on-site and several hundred more through contract and temporary staffing with positions that range from high-paying nuclear operators to facility support and security services. How the employees are classified in the IMPLAN model is of particular importance in this study, as the impact on output and disposable income will vary greatly between employment types. Full-time SCE employees and contract workers were classified utilizing an employment mix provided by SCE. Note that employment estimates were provided only for staff that works at the site for an extended period. For short-term services, like an elevator repairman, we used the estimated service wages to calculate the impact that it has on disposable income spending in California. Direct employment related to material spending, fixed costs, and other services expenditures by SONGS is also not included in these job estimates but are reflected in the final results.

Distribution of SONGS Employment

Sectors	2010	2011	2012	2013	2014
Electric Power Generation, Transmission, and Distribution	2,106	1,779	1,599	1,359	1,442
Security Services	492	489	464	390	392
Management, Scientific, and Technical Services	405	314	273	233	256
Facilities Support Services	293	186	147	129	155
Accounting and Payroll Services	215	213	203	170	171
Total Employment	3,511	2,981	2,686	2,281	2,416

Results

The economic activity supported by SONGS is considerable. Outlining the results, indicates, for example, that the plant directly supports \$2.2-billion of output and a total output of \$3.3-billion. The employment multiplier is well above 2.0, meaning that for each direct job created by SONGS-related activity, indirect and induced impacts will produce more than one additional job in the study area; in total SONGS generates an average of 9,450 jobs per year (over 2010 to 2014) on a full-time equivalent basis (FTEs). In California, average annual wages in 2010 totaled \$56,000 and value added per employee is measured at about \$135,000 according to IHS Global Insights latest estimates. In comparison, SONGS generates jobs with annual average wages of \$84,000 and value added per employee of over \$243,000 per year, which is substantially more than the state average. The economic impact of SONGS operation and maintenance is significant, each dollar spent on operation and maintenance of the nuclear plant generates a total of \$4.3 in output and \$3.0 in value added in the California economy. Each dollar spent on the operation and maintenance of SONGS produces \$1.35 of labor income in the California economy, the bulk of which (77%) is employee compensation.

Economic Impacts of the San Onofre Nuclear Plant on California
(Millions of 2010 Dollars, Employment Full Time Equivalent)

	2010	2011	2012	2013	2014	5-Year Avg.
Expenditures	861.71	736.02	712.23	753.06	788.58	770.32
Employment						
Direct	4,442	3,801	3,631	3,436	3,444	3,751
Total	11,520	9,783	9,126	8,314	8,512	9,451
Multiplier	2.59	2.57	2.51	2.42	2.47	2.51
Output						
Direct	2,807.75	2,372.28	2,165.51	1,898.77	1,985.61	2,245.98
Total	4,123.93	3,485.22	3,187.50	2,805.20	2,927.69	3,305.91
Multiplier	1.47	1.47	1.47	1.48	1.47	1.47
Value Added						
Direct	2,125.83	1,799.07	1,635.16	1,420.29	1,489.31	1,693.93
Total	2,873.60	2,431.26	2,215.85	1,935.63	2,024.80	2,296.23
Multiplier	1.35	1.35	1.36	1.36	1.36	1.36
Labor Income						
Employee Compensation	984.32	835.07	769.06	684.92	708.23	796.32
Proprietor's Income	305.73	257.97	234.36	203.62	214.05	243.14
Total Labor Income	1,290.05	1,093.04	1,003.42	888.54	922.28	1,039.46
State and Local Taxes						
Personal Income taxes	43.19	36.59	33.55	29.65	30.81	34.76
Sales Taxes	149.28	126.13	114.28	98.72	103.98	118.48
Corporate Income Taxes	26.30	22.23	20.13	17.37	18.30	20.87
Other Taxes	91.49	77.19	69.55	59.44	63.02	72.14
Total State Taxes	310.26	262.13	237.51	205.18	216.10	246.24

Appendix 9

Letter from Peter Douglas, California Coastal Commission, dated February 4, 2010

CALIFORNIA COASTAL COMMISSION

45 FREMONT, SUITE 2000
SAN FRANCISCO, CA 94105-2219
VOICE (415) 904-5200
FAX (415) 904-5400
TDD (415) 597-5885



February 4, 2010

State Water Resources Control Board
1001 I Street
Sacramento, CA 95814

Re: Comments on "Draft Water Quality Control Policy on the Use of Coastal and Estuarine Waters for Power Plant Cooling"

Dear Chair Hoppin and Board Members:

I am writing to add to the comments Coastal Commission staff provided to you in September and December 2009 regarding the above-referenced proposed policy. The Board's proposed policy includes provisions that would allow Southern California Edison's San Onofre Nuclear Generating Station (SONGS) to continue using once-through cooling if it met several site-specific requirements.

Over the past several decades, the Coastal Commission has reviewed the facility's operations and its adverse impacts on marine life. Through approval of several coastal development permits and amendments, the Commission has required Edison to mitigate for those impacts by restoring coastal wetlands, constructing offshore reef habitat, operating a sea bass hatchery, and other measures. The Commission has also periodically reviewed the performance and success of these mitigation measures.

Should the Board determine that SONGS may continue to operate its once-through cooling system, it is the position of Commission staff that the facility's adverse effects on marine life have been fully mitigated and will continue to be mitigated as long as the mitigation measures continue to perform as required.

Please contact me at 415-904-5200 if you have any additional questions or comments regarding this issue.

Sincerely,

A handwritten signature in black ink, appearing to read "Peter Douglas".

PETER DOUGLAS
Executive Director

cc: Coastal Commissioners
James Boyd, Commissioner, California Energy Commission
Yakout Mansour, CEO, California Independent System Operator Corporation
Lester Snow, Secretary of Natural Resources
Michael Peevey, President, California Public Utilities Commission